

UNCLASSIFIED

AD NUMBER

AD900193

LIMITATION CHANGES

TO:

Approved for public release; distribution is unlimited. Document partially illegible.

FROM:

Distribution authorized to U.S. Gov't. agencies only; Test and Evaluation; DEC 1971. Other requests shall be referred to Air Force Rocket Propulsion Laboratory(STINFO), Edwards AFB, CA 93523.

AUTHORITY

AFRPL per ltr, 31 Jan 1974

THIS PAGE IS UNCLASSIFIED

✓  
AFRPL TR-72-45

FINAL REPORT

ORBIT-TO-ORBIT  
SHUTTLE ENGINE DESIGN STUDY

Contract F04611-71-C-0040

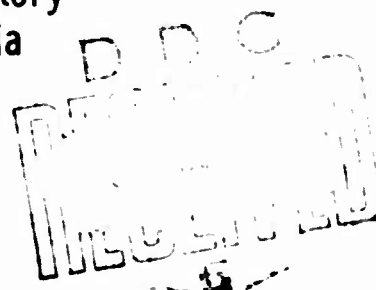
BOOK 4

W. P. Luscher, et. al.  
Aerojet Liquid Rocket Company  
Sacramento, California

Distribution limited to U.S. Government Agencies only. Data based on Test and Evaluation. December 1971. Other requests for this document must be referred to Air Force RPL. (STINFO) Edwards, California 93523

May 1972

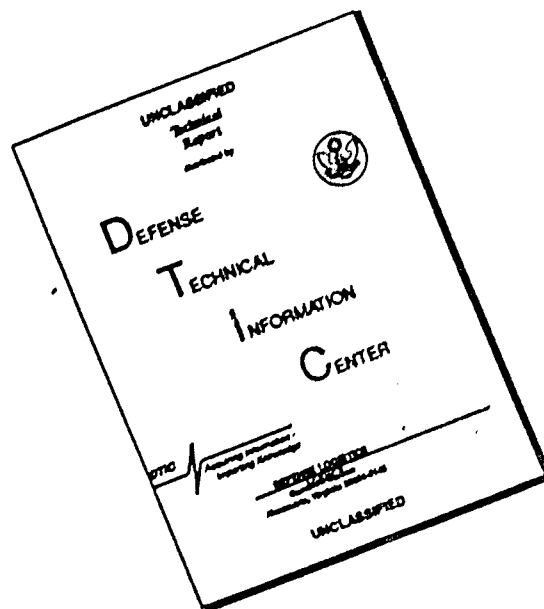
Air Force Rocket Propulsion Laboratory  
Edwards Air Force Base, California



AD900193



# DISCLAIMER NOTICE



THIS DOCUMENT IS BEST QUALITY AVAILABLE. THE COPY FURNISHED TO DTIC CONTAINED A SIGNIFICANT NUMBER OF PAGES WHICH DO NOT REPRODUCE LEGIBLY.

## INTRODUCTION

The intent of the Appendices is to present some of the material used to develop the data contained in Books 1, 2 and 3. Since this material is a backup, it is not edited and is presented as raw Engineering Data.

**Appendix A**

**NOZZLE CONTOUR AND  
TCA PERFORMANCE**

## NOZZLE CONTOUR

This Appendix provides documentation of initial calculations made regarding nozzle contours for the 8K to 50K parametric analysis. Included for use in preliminary engine cycle, thermodynamic, and payload optimization studies are surface area and length relationships for minimum length Rao contours for all overall area ratios. The information provided should allow computation of all weight and envelope factors required for preliminary engine optimization studies at mixture ratios 5, 6, and 7.

Iterations are being performed on all contour data provided herein. The included information should therefore be, in all cases, considered preliminary in nature and open for adjustment at a later date.

ALRC's Rao Optimum Nozzle Contour Program No. E21207 was utilized to design the study nozzle contours. This program utilizes the Method of Characteristics, the Hall Transonic Flow Model<sup>(1)</sup>, and a constant gamma perfect gas expansion to calculate the nozzle geometry. Contours were developed for the mixture ratio design point of 6.0:1 for area ratios from 140:1 to 500:1. A value of 1.22 was used for the ratio of specific heats (gamma) input to the program. This value was found to be representative of a mean value for gamma calculated from equilibrium expansion of  $O_2/H_2$  products to area ratios typical for this study. Nozzles of expansion ratios greater than 280 were developed with aid from information given in the final report for Contract NAS 7-136<sup>(2)</sup>.

---

(1) Hall, S. M., Transonic Flow in Two-Dimensional and Axially - Symmetric Nozzles, Quarterly Journal of Mechanics and Applied Mathematics, Vol. XV, Pt. 4, January 1962.

(2) Study of High Effective Area Ratio Nozzles for Space Craft Engines, AGC, Final Report for Contract NAS 7-136, June 1964.

100

90

80

70

60

50

40

30

20

10  
0

KAO MIN. LENGTH (NORMALIZED)  
VS. AREA RATIO M.R.=6.0

OVERALL

L/R<sub>t</sub>

C<sub>0</sub> - OVERALL AREA RATIO (R<sub>e</sub>/R<sub>t</sub>)<sup>2</sup>

100

200

300

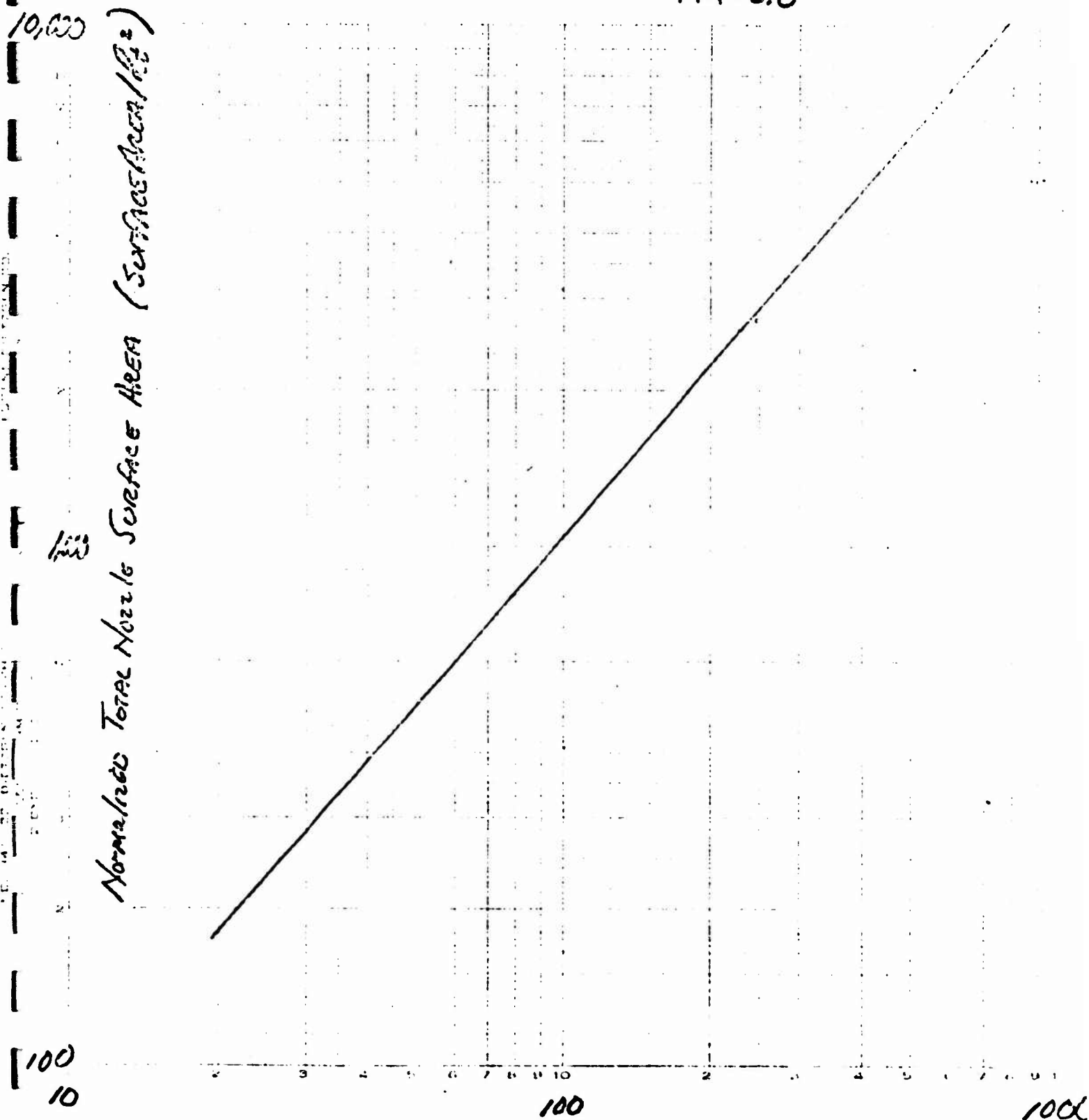
400

500

A-2

ENCL. (c)

Req. MIN. LENGTH CONTOURS  
NORMALIZED SURFACE AREA VS. AREA RATIO  
MR=6.0

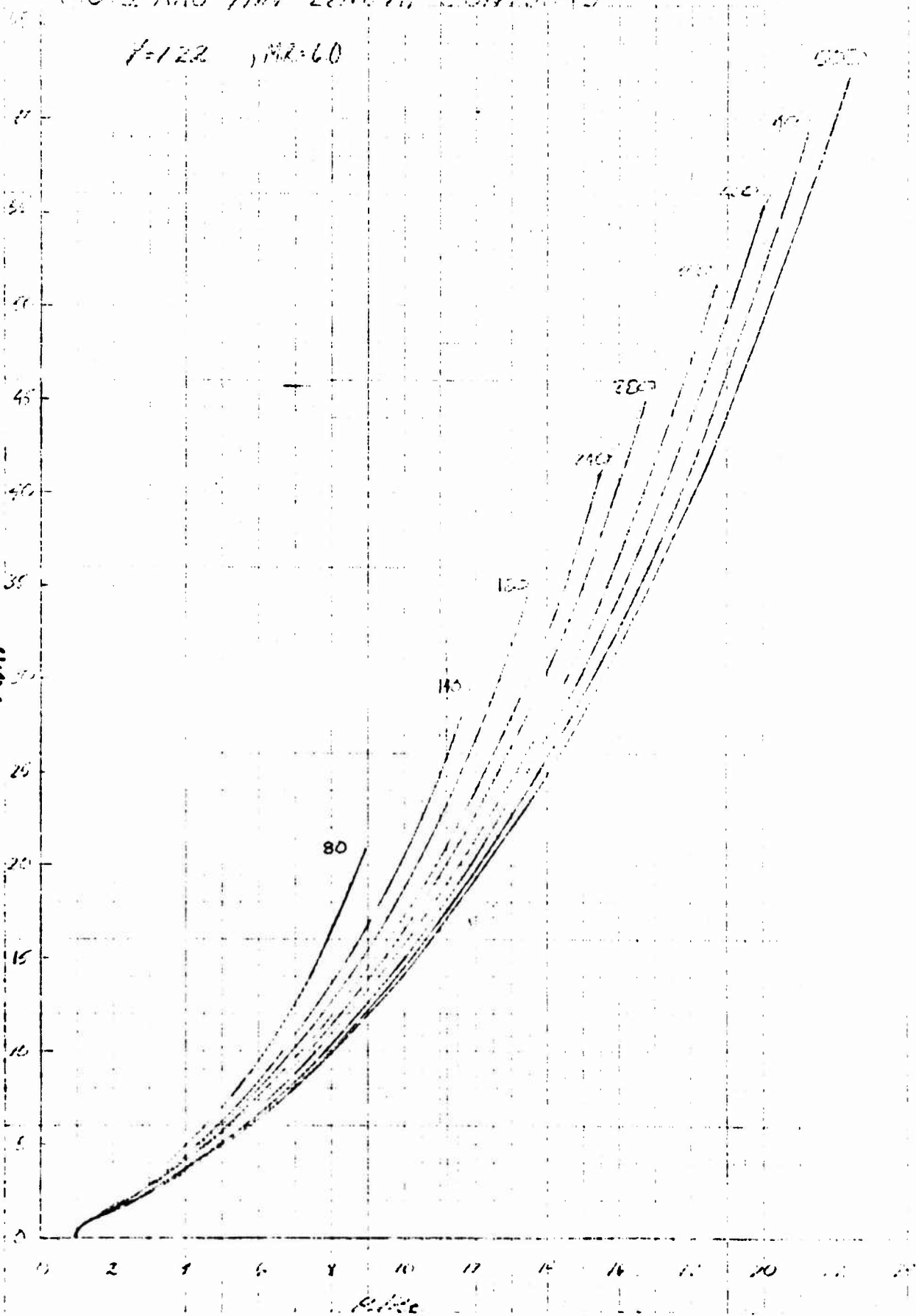


$E_o$ , OVERALL AREA RATIO  $(R_e/R_z)^2$

# O.O.S. RAO MIN LENGTH CONTOURS

$f=122$  ,  $M.R.=60$

X/10



Thrust (lbf)	$P_c$ (lbf/in. <sup>2</sup> )	$F/P_c$ (in. <sup>2</sup> )	$R_t$ (in.)	$L/R_t$ (L = 66 in.)	$\epsilon$ (@ L = 66 in.)	$\epsilon_{max}$ (@ L = 87 in.)
8K	300	26.7	2.09	31.58	158	433
	500	16.0	1.61	40.99	240	730
	1000	8.0	1.14	57.89	430	1456
	1500	5.3	0.92	71.74	614	2236
15K	300	50.0	2.88	22.90	93	228
	500	30.0	2.22	29.73	143	384
	1000	15.0	1.56	42.31	253	778
	1500	10.0	1.28	51.56	354	1155
	2500	6.0	0.98	67.35	555	1970
25K	300	83.3	3.73	17.69	62	136
	500	50.0	2.88	22.90	93	228
	1000	25.0	2.02	32.67	166	464
	1500	16.7	1.66	39.76	229	687
	2500	10.0	1.28	51.56	372	1155
50K	500	100.0	4.04	16.34	60	116
	1000	50.0	2.88	22.90	93	228
	1500	33.3	2.35	28.09	131	343
	2500	20.0	1.81	36.46	198	578

Note: area ratios of 350,400,450,500 will be included at all  $P_c$  and thrust levels except where envelope limited

O.O.S. Performance Analysis Study Matrix



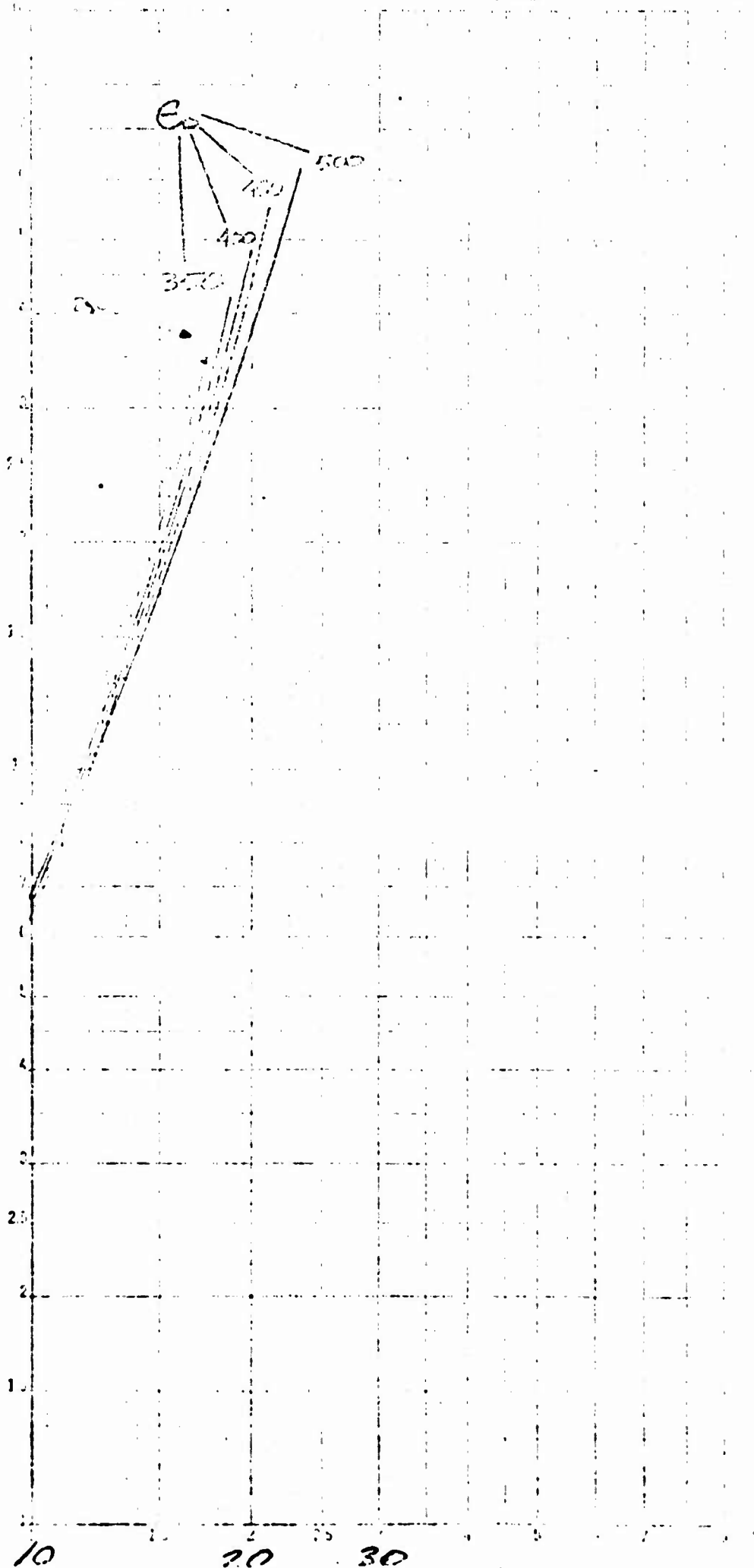
10000 SURFACE SURFACE FROM VO. LARS

CHC1. (1.1)

Surface Area 172

1000

100



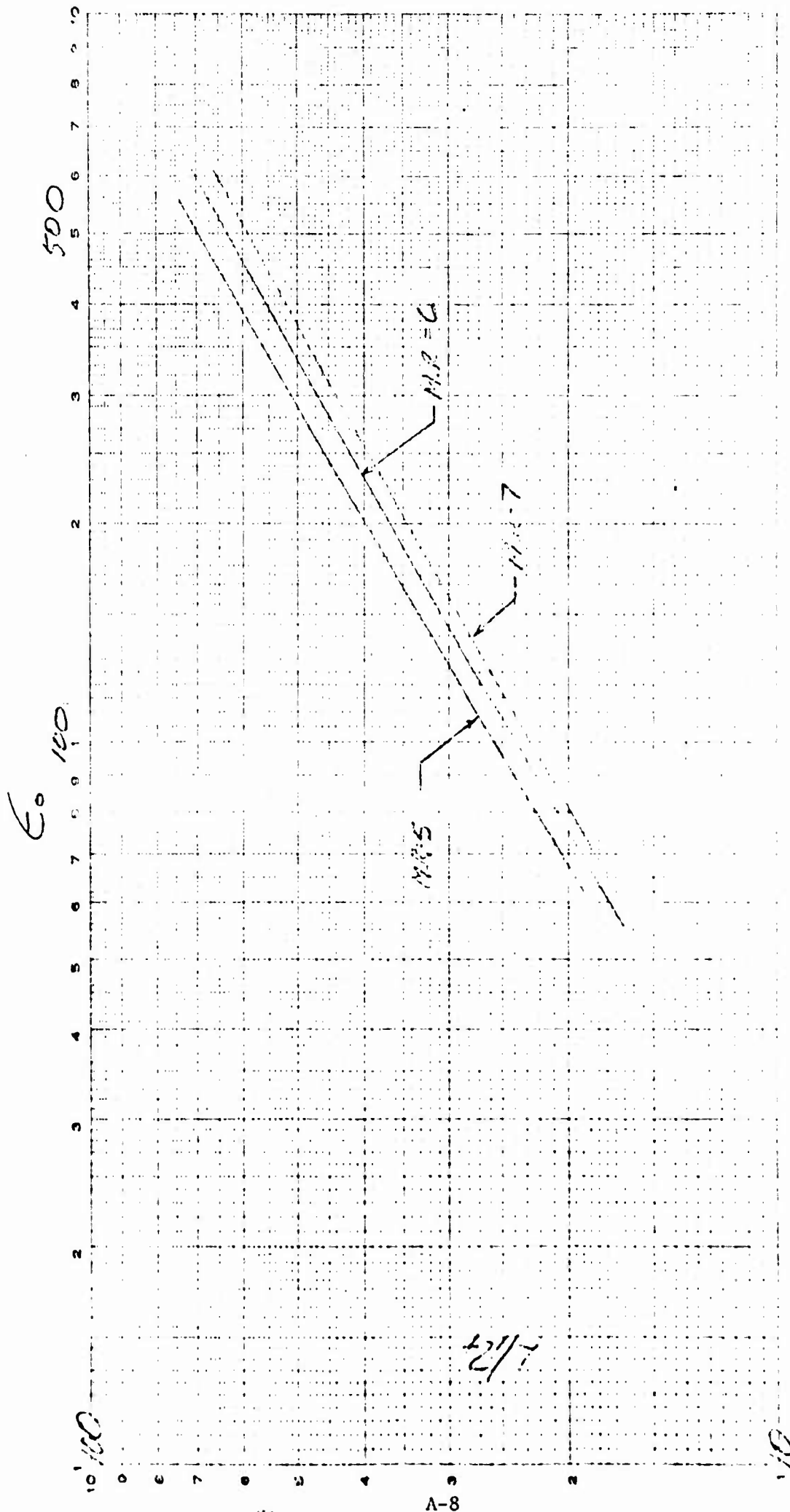
O.O.S. Task V  
Contour Info.

ALL MR CONTOUR INFO

	<u><math>\epsilon</math></u>	<u><math>(R/R_t)e</math></u>	<u><math>(L/R_t)e</math></u>	<u><math>SA/R_t^2</math></u>
MR 7				
	350	18.71	48.	3860
	400	20.	52.	4460
	450	21.21	55.6	5080
	500	22.36	59.0	5680
MR 5				
	350	18.71	56.1	4540
	400	20.	60.9	5250
	450	21.21	65.2	6000
	500	22.36	69.7	6740
MR 6				
	350	18.71	51.2	4150
	400	20.	55.3	4800
	450	21.21	59.4	5450
	500	22.36	63.2	6190

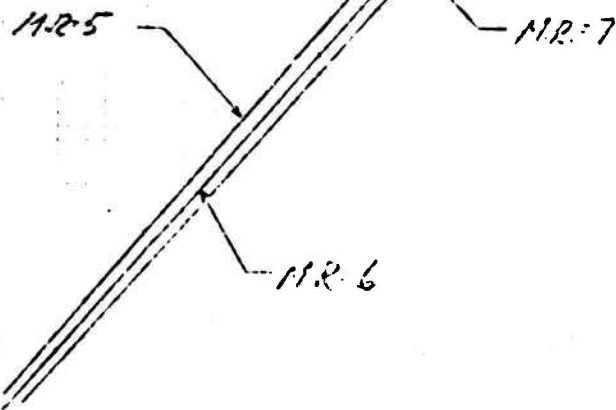
NO 340-L21 DIETZGEN DRAPP PAPER  
LOGARITHMIC  
2 CYCLES X 1 CYCLE

EUGENE DIETZGEN CO.  
MADE IN U.S.A.



10,000  
8000  
6000  
4000  
2000  
1000  
500  
250  
100

TOTAL SURFACE AREA / K<sub>T</sub><sup>2</sup>



$E_0$

A-9

0.05. TASK V

TANGENT POINT  
TANGENT POINT

5  
80.7

WALL CONDITIONS  
CF

R  
 $\frac{R}{R_1}$

Z  
 $\frac{Z}{R_1}$

$\frac{Z}{R_1}^2$

.10000+01	.00000	.12465+01	.00000
.11953+01	.59354+00	.13133+01	.42570+01
.11974+01	.59647+00	.13136+01	.42835+01
.12362+01	.64937+00	.13193+01	.47860+01
.12762+01	.70378+00	.13280+01	.53193+01
.13173+01	.75990+00	.13323+01	.58868+01
.13598+01	.81793+00	.13387+01	.64920+01
.14037+01	.87809+00	.13452+01	.71391+01
.14493+01	.94062+00	.13519+01	.78328+01
.14966+01	.10058+01	.13587+01	.85783+01
.15460+01	.10739+01	.13657+01	.93817+01
.15987+01	.11454+01	.13731+01	.10252+02
.16520+01	.12201+01	.13804+01	.11190+02
.17078+01	.12986+01	.13879+01	.12208+02
.17660+01	.13818+01	.13957+01	.13313+02
.18275+01	.14695+01	.14037+01	.14518+02
.18923+01	.15613+01	.14120+01	.15833+02
.19593+01	.16581+01	.14204+01	.17270+02
.20297+01	.17627+01	.14290+01	.18812+02
.21049+01	.18732+01	.14381+01	.20573+02
.21827+01	.19903+01	.14473+01	.22468+02
.22646+01	.21151+01	.14567+01	.24555+02
.23518+01	.22486+01	.14665+01	.26863+02
.24423+01	.23907+01	.14765+01	.29404+02
.25390+01	.25435+01	.14868+01	.32225+02
.26400+01	.27070+01	.14974+01	.35358+02
.27478+01	.28835+01	.15083+01	.38854+02
.31862+01	.36394+01	.15502+01	.55118+02
.35925+01	.43920+01	.15850+01	.73344+02
.39765+01	.51586+01	.16149+01	.93774+02
.43575+01	.59663+01	.16418+01	.11711+03
.47350+01	.68251+01	.16662+01	.14390+03
.51146+01	.77500+01	.16889+01	.17488+03
.54935+01	.87528+01	.17098+01	.21064+03
.58884+01	.98464+01	.17294+01	.25217+03
.62856+01	.11045+02	.17477+01	.30051+03
.66892+01	.12666+02	.17648+01	.35675+03

.68935+01	.13076+02	.17729+01	.38830+03
.72041+01	.14215+02	.17946+01	.44057+03
.75175+01	.15445+02	.17956+01	.49925+03
.77265+01	.16324+02	.18026+01	.54256+03
.80474+01	.17736+02	.18125+01	.61830+03
.83668+01	.19269+02	.18219+01	.69506+03
.85611+01	.20372+02	.18278+01	.75491+03
.89015+01	.22156+02	.18361+01	.85444+03
.89443+01	.22407+02	.18371+01	.86871+03

EXIT POINT

THROAT POINT  
TANGENT POINT

190:1

R  
 $\frac{R}{R_1}$

Z  
 $\frac{Z}{R_1}$

WALL CONDITIONS  
CF

S.A.  
 $\frac{S.A.}{R_1^2}$

.10000+01	.00000	.12465+01	.00000
.12140+01	.61827+00	.13181+01	.44914+01
.12391+01	.65022+00	.13197+01	.48046+01
.12825+01	.70572+00	.13257+01	.53637+01
.13273+01	.76301+00	.13319+01	.59603+01
.13735+01	.82229+00	.13382+01	.65986+01
.14213+01	.88379+00	.13446+01	.72830+01
.14708+01	.94777+00	.13511+01	.80188+01
.15224+01	.10145+01	.13578+01	.88117+01
.15761+01	.10843+01	.13647+01	.96686+01
.16321+01	.11574+01	.13717+01	.10597+02
.16908+01	.12343+01	.13790+01	.11605+02
.17522+01	.13153+01	.13864+01	.12703+02
.18167+01	.14007+01	.13941+01	.13902+02
.18861+01	.14914+01	.14022+01	.15217+02
.19579+01	.15872+01	.14103+01	.16655+02
.20319+01	.16882+01	.14186+01	.18229+02
.21099+01	.17952+01	.14271+01	.19953+02
.21931+01	.19130+01	.14360+01	.21669+02
.22794+01	.20329+01	.14450+01	.23563+02
.23708+01	.21652+01	.14544+01	.25291+02
.24675+01	.23025+01	.14640+01	.28866+02
.25690+01	.24514+01	.14738+01	.31717+02
.26770+01	.26115+01	.14840+01	.34895+02
.27906+01	.27834+01	.14945+01	.38435+02
.29115+01	.29690+01	.15053+01	.42400+02
.30492+01	.37687+01	.15170+01	.51085+02
.38756+01	.45733+01	.15318+01	.82356+02
.43234+01	.53989+01	.16119+01	.10654+03
.47675+01	.62721+01	.16301+01	.13451+03
.52142+01	.72076+01	.16540+01	.16701+03
.56682+01	.82214+01	.16871+01	.20498+03
.61323+01	.93270+01	.17087+01	.24942+03
.66086+01	.10539+02	.17290+01	.30156+03
.70992+01	.11877+02	.17482+01	.36292+03
.76045+01	.13357+02	.17662+01	.43516+03
.78628+01	.14158+02	.17748+01	.47602+03

.82585+01	.15444+02	.17872+01	.54419+03
.86623+01	.16840+02	.17990+01	.62140+03
.89369+01	.17840+02	.18066+01	.67878+03
.93561+01	.19455+02	.18175+01	.77463+03
.97822+01	.21215+02	.18278+01	.89351+03
.10071+02	.22486+02	.18344+01	.96483+03
.10511+02	.24549+02	.18438+01	.11012+04
.10953+02	.26805+02	.18525+01	.12562+04
.11251+02	.28450+02	.18580+01	.13729+04
.11700+02	.31133+02	.18657+01	.15690+04
.11832+02	.31985+02	.18679+01	.16328+04

EXIT POINT

100001 POINT  
TANGENT POINT

180:1

WALL CONDITIONS  
CF

$\frac{R}{R_1}$	$\frac{Z}{R_1}$		$\frac{S.A.}{R_1^2}$
.10000+01	.00000	.12465+01	.00000
.12233+01	.62993+00	.13174+01	.46057+01
.12399+01	.65045+00	.13196+01	.48102+01
.12851+01	.70649+00	.13256+01	.53821+01
.13317+01	.76433+00	.13317+01	.59935+01
.13798+01	.82420+00	.13379+01	.66480+01
.14295+01	.88634+00	.13443+01	.73511+01
.14811+01	.95101+00	.13507+01	.81079+01
.15347+01	.10185+01	.13574+01	.89245+01
.15905+01	.10390+01	.13641+01	.98081+01
.16488+01	.11631+01	.13711+01	.10767+02
.17098+01	.12409+01	.13783+01	.11809+02
.17737+01	.13208+01	.13857+01	.12945+02
.18408+01	.14039+01	.13933+01	.14187+02
.19113+01	.14911+01	.14011+01	.15547+02
.19856+01	.15835+01	.14091+01	.17041+02
.20639+01	.17016+01	.14175+01	.18686+02
.21463+01	.18115+01	.14260+01	.20497+02
.22379+01	.19295+01	.14353+01	.22514+02
.23287+01	.20540+01	.14442+01	.24721+02
.24244+01	.21869+01	.14534+01	.27164+02
.25261+01	.23293+01	.14630+01	.29879+02
.26327+01	.24815+01	.14727+01	.32887+02
.27462+01	.26453+01	.14828+01	.36248+02
.28658+01	.28213+01	.14932+01	.39999
.29931+01	.30114+01	.15039+01	.44202+02
.35189+01	.38324+01	.15454+01	.64116+02
.40131+01	.46608+01	.15801+01	.86919+02
.44897+01	.55131+01	.16101+01	.11299+03
.49640+01	.64172+01	.16373+01	.14330+03
.54436+01	.73891+01	.16623+01	.17662+02
.59326+01	.84426+01	.16856+01	.22022+03
.64345+01	.95956+01	.17074+01	.26907+03
.69521+01	.10663+02	.17280+01	.32664+03
.74875+01	.12265+02	.17474+01	.39472+03
.80415+01	.13820+02	.17657+01	.47521+03
.83258+01	.14662+02	.17745+01	.52091+03

.87629+01	.16018+02	.17872+01	.59740+03
.92107+01	.17491+02	.17993+01	.68434+03
.95167+01	.18550+02	.18071+01	.74916+03
.99853+01	.20259+02	.18184+01	.85777+03
.10464+02	.22127+02	.18291+01	.93162+03
.10791+02	.23478+02	.18359+01	.10744+04
.11290+02	.25674+02	.18457+01	.12366+04
.11794+02	.28080+02	.18548+01	.14069+04
.12138+02	.29838+02	.18606+01	.15436+04
.12658+02	.32710+02	.18689+01	.17710+04
.13175+02	.35870+02	.18764+01	.20308+04
.13417+02	.37469+02	.18797+01	.21600+04

EXIT POINT

TARGET POINT  
TANGENT POINT

5  
240:1

R	Z	WALL CONDITIONS	S.A.
$R_t$	$R_t$	CF	$R_t^2$
.10000+01	.00000	.12465+01	.00000
.12363+01	.64552+00	.13191+01	.47621+01
.12405+01	.65061+00	.13196+01	.48149+01
.12882+01	.70735+00	.13255+01	.54937+01
.13374+01	.76595+00	.13315+01	.60359+01
.13881+01	.82663+00	.13376+01	.67133+01
.14405+01	.88964+00	.13438+01	.74427+01
.14950+01	.95524+00	.13502+01	.82293+01
.15515+01	.10237+01	.13567+01	.90797+01
.16104+01	.10954+01	.13634+01	.10001+02
.16719+01	.11706+01	.13703+01	.11003+02
.17362+01	.12497+01	.13773+01	.12093+02
.18036+01	.13330+01	.13846+01	.13284+02
.18743+01	.14212+01	.13921+01	.14588+02
.19486+01	.15145+01	.13998+01	.16018+02
.20269+01	.16135+01	.14077+01	.17590+02
.21094+01	.17187+01	.14159+01	.19323+02
.21965+01	.18309+01	.14244+01	.21237+02
.22885+01	.19505+01	.14331+01	.23354+02
.23857+01	.20783+01	.14421+01	.25702+02
.24887+01	.22152+01	.14514+01	.28311+02
.25977+01	.23620+01	.14610+01	.31216+02
.27134+01	.25198+01	.14708+01	.34458+02
.28350+01	.26894+01	.14808+01	.38081+02
.29755+01	.28753+01	.14921+01	.42213+02
.31113+01	.30719+01	.15026+01	.46764+02
.36725+01	.39224+01	.15435+01	.62462+02
.42016+01	.47820+01	.15777+01	.92313+02
.47129+01	.56679+01	.16076+01	.12191+03
.52235+01	.66094+01	.16346+01	.15531+03
.57412+01	.76226+01	.16593+01	.19447+03
.62716+01	.87258+01	.16828+01	.24063+03
.68180+01	.99346+01	.17047+01	.29516+03
.73838+01	.11266+02	.17255+01	.35970+03
.79721+01	.12743+02	.17451+01	.43637+03
.85838+01	.14345+02	.17638+01	.52746+03
.88989+01	.15276+02	.17727+01	.57935+03

.93850+01	.16713+02	.17857+01	.66647+03
.98852+01	.18277+02	.17981+01	.76586+03
.10224+02	.19402+02	.18061+01	.84021+03
.10756+02	.21224+02	.18177+01	.96521+03
.11298+02	.23217+02	.18287+01	.11083+04
.11670+02	.24662+02	.18358+01	.12160+04
.12241+02	.27014+02	.18460+01	.13978+04
.12822+02	.29598+02	.18556+01	.16063+04
.13220+02	.31490+02	.18617+01	.17645+04
.13827+02	.34585+02	.18705+01	.20325+04
.14437+02	.38000+02	.18785+01	.23405+04
.14853+02	.40530+02	.18836+01	.25764+04
.15477+02	.44626+02	.18907+01	.28774+04
.15493+02	.44806+02	.18908+01	.28805+04

EXIT POINT



WALLOP POINT  
TANGENT POINT

5  
280.1

# WALL CONDITIONS

R	Z	CF	S.A.
$\frac{R}{R_+}$	$\frac{Z}{Z_+}$		$\frac{R}{R_+}$
.10000+01	.00000	.12465+01	.00000
.12498+01	.06119+00	.13207+01	.00238+01
.12909+01	.70803+00	.13254+01	.54213+01
.13427+01	.76740+00	.13254+01	.60752+01
.13963+01	.82891+00	.13373+01	.67780+01
.14517+01	.89282+00	.13434+01	.75357+01
.15092+01	.95938+00	.13496+01	.83548+01
.15689+01	.10289+01	.13560+01	.92413+01
.16310+01	.11017+01	.13626+01	.10204+02
.16960+01	.11781+01	.13693+01	.11252+02
.17638+01	.12586+01	.13763+01	.12396+02
.18349+01	.13434+01	.13834+01	.13646+02
.19096+01	.14331+01	.13908+01	.15017+02
.19880+01	.15281+01	.13984+01	.16524+02
.20706+01	.16289+01	.14062+01	.18182+02
.21576+01	.17354+01	.14143+01	.20013+02
.22494+01	.18487+01	.14226+01	.22036+02
.23464+01	.19688+01	.14313+01	.24279+02
.24488+01	.21053+01	.14401+01	.26767+02
.25572+01	.22431+01	.14493+01	.29535+02
.26718+01	.23930+01	.14587+01	.32618+02
.27934+01	.25542+01	.14685+01	.36064+02
.29215+01	.27276+01	.14784+01	.39916+02
.30638+01	.29165+01	.14892+01	.44263+02
.31706+01	.31102+01	.14970+01	.48925+02
.37899+01	.39951+01	.15393+01	.72199+02
.43953+01	.49029+01	.15769+01	.92611+02
.49297+01	.58168+01	.16052+01	.13049+03
.54627+01	.67860+01	.16317+01	.16649+03
.60022+01	.78277+01	.16563+01	.20860+03
.65550+01	.89510+01	.16793+01	.25850+03
.71251+01	.10203+02	.17011+01	.31694+03
.77160+01	.11571+02	.17217+01	.38635+03
.83315+01	.13069+02	.17413+01	.46865+03
.89723+01	.14776+02	.17600+01	.56692+03
.93033+01	.15692+02	.17690+01	.62263+03
.98144+01	.17171+02	.17820+01	.71677+03

.10341+02	.16782+02	.17946+01	.82406+03
.10704+02	.19943+02	.18026+01	.90438+03
.11262+02	.21821+02	.18144+01	.10396+04
.11337+02	.23379+02	.18256+01	.11946+04
.12232+02	.25373+02	.18323+01	.13114+04
.12840+02	.27806+02	.18432+01	.15089+04
.13462+02	.30482+02	.18530+01	.17358+04
.13889+02	.32443+02	.18593+01	.19883+04
.14542+02	.35656+02	.18682+01	.22011+04
.15202+02	.39206+02	.18765+01	.25364+04
.15654+02	.41640+02	.18818+01	.27975+04
.16336+02	.46183+02	.18897+01	.32392+04
.16739+02	.49008+02	.18932+01	.35357+04

EXIT POINT

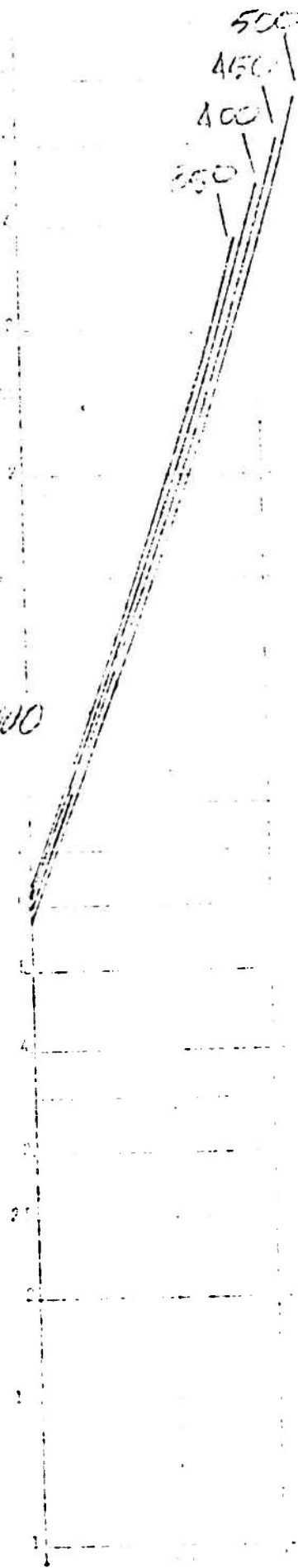
10,000

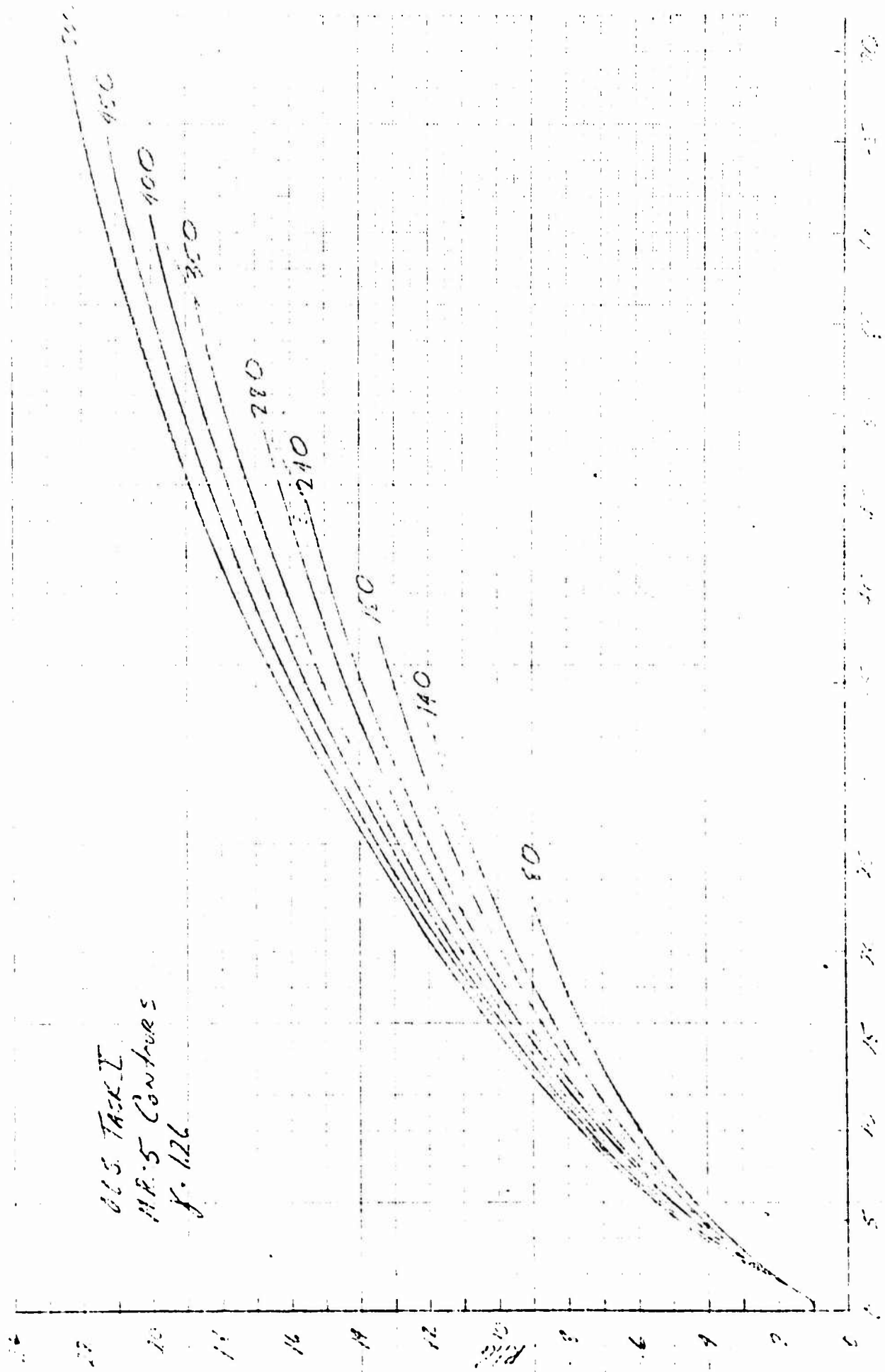
U.S. 1952 I 1100

Surface Area  $R_e$

1000

500  
450  
400  
350





THROAT POINT  
TANGENT POINT

*70:1*

R

*R<sub>1</sub>*

.10000+01  
.12262+01  
.12603+01  
.13044+01  
.13497+01  
.13966+01  
.14450+01  
.14953+01  
.15475+01  
.16019+01  
.16586+01  
.17183+01  
.17819+01  
.18462+01  
.19136+01  
.19841+01  
.20590+01  
.21372+01  
.22186+01  
.23043+01  
.23954+01  
.24896+01  
.25898+01  
.26953+01  
.28062+01  
.32583+01  
.36705+01  
.40592+01  
.44374+01  
.48110+01  
.51838+01  
.55582+01  
.59354+01  
.63171+01  
.67026+01  
.68969+01  
.71907+01

Z

*Z<sub>1</sub>*

.00000  
.63428+00  
.67521+00  
.72927+00  
.78511+00  
.84296+00  
.90304+00  
.96559+00  
.10369+01  
.10992+01  
.11708+01  
.12461+01  
.13255+01  
.14011+01  
.14772+01  
.15504+01  
.16295+01  
.17045+01  
.19058+01  
.20243+01  
.21510+01  
.22857+01  
.24300+01  
.25848+01  
.27510+01  
.34596+01  
.41553+01  
.48520+01  
.55801+01  
.63581+01  
.71781+01  
.80580+01  
.90061+01  
.10035+02  
.11152+02  
.11748+02  
.12694+02

WALL CONDITIONS  
OF

.12300+01  
.13152+01  
.13210+01  
.13277+01  
.13345+01  
.13415+01  
.13486+01  
.13559+01  
.13634+01  
.13711+01  
.13790+01  
.13873+01  
.13959+01  
.14045+01  
.14133+01  
.14224+01  
.14320+01  
.14418+01  
.14518+01  
.14621+01  
.14729+01  
.14838+01  
.14952+01  
.15070+01  
.15190+01  
.15558+01  
.16047+01  
.16385+01  
.16690+01  
.16970+01  
.17229+01  
.17473+01  
.17701+01  
.17916+01  
.18118+01  
.18215+01  
.18354+01

*70:1*

.00000  
.46489+01  
.50625+01  
.56250+01  
.62257+01  
.68686+01  
.75583+01  
.83000+01  
.90924+01  
.98631+01  
.10892+02  
.11915+02  
.13023+02  
.14226+02  
.15537+02  
.16969+02  
.18542+02  
.20265+02  
.22154+02  
.24232+02  
.26530+02  
.29055+02  
.31857+02  
.34965+02  
.38418+02  
.50418+02  
.72010+02  
.91501+02  
.11345+03  
.13831+03  
.16655+03  
.19885+03  
.23569+03  
.27793+03  
.32625+03  
.35304+03  
.39688+03

EXIT POINT

.74865+01  
.76852+01  
.79842+01  
.82833+01  
.84839+01  
.87837+01  
.89442+01

.13706+02  
.14423+02  
.15565+02  
.16790+02  
.17663+02  
.19058+02  
.19857+02

.18487+01  
.18572+01  
.18694+01  
.18810+01  
.18983+01  
.18988+01  
.19042+01

.44552+03  
.49097+03  
.53905+03  
.60351+03  
.65071+03  
.72813+03  
.77351+03

THROAT POINT  
TANGENT POINT

7  
140:1

$\frac{R}{R_+}$

$\frac{L}{R_+}$

WALL CONDITIONS  
CF

$\frac{S.A.}{R_+}$

.10000+01	.00000	.12380+01	.00000
.12499+01	.66128+00	.13192+01	.49247+01
.12625+01	.67570+00	.13209+01	.50764+01
.13105+01	.73074+00	.13274+01	.56690+01
.13605+01	.78757+00	.13341+01	.67341+01
.14118+01	.84668+00	.13409+01	.69863+01
.14650+01	.90803+00	.13479+01	.77208+01
.15201+01	.97196+00	.13550+01	.85133+01
.15775+01	.10388+01	.13623+01	.93705+01
.16372+01	.11087+01	.13698+01	.10300+02
.16996+01	.11821+01	.13776+01	.11310+02
.17648+01	.12594+01	.13856+01	.12409+02
.18331+01	.13400+01	.13938+01	.13610+02
.19045+01	.14270+01	.14023+01	.14923+02
.19800+01	.15201+01	.14110+01	.16363+02
.20591+01	.16148+01	.14201+01	.17904+02
.21446+01	.17178+01	.14297+01	.19691+02
.22337+01	.18273+01	.14395+01	.21613+02
.23247+01	.19432+01	.14493+01	.23723+02
.24208+01	.20667+01	.14594+01	.26054+02
.25230+01	.21990+01	.14700+01	.28641+02
.26292+01	.23399+01	.14808+01	.31498+02
.27423+01	.24913+01	.14920+01	.34680+02
.28613+01	.26538+01	.15036+01	.38223+02
.29875+01	.28288+01	.15156+01	.42183+02
.35041+01	.35790+01	.15621+01	.60729+02
.39798+01	.43210+01	.16009+01	.81433+02
.44328+01	.50756+01	.16349+01	.10468+03
.48778+01	.58646+01	.16657+01	.13117+03
.53220+01	.67018+01	.16942+01	.16153+03
.57696+01	.75984+01	.17208+01	.19643+03
.62231+01	.85657+01	.17459+01	.23667+03
.66847+01	.96134+01	.17696+01	.28309+03
.71567+01	.10756+02	.17922+01	.33684+03
.76387+01	.12003+02	.18135+01	.39897+03
.78837+01	.12671+02	.18238+01	.43367+03
.82571+01	.13734+02	.18387+01	.49080+03

.86363+01	.14876+02	.18529+01	.55465+03
.88931+01	.15636+02	.18622+01	.60148+03
.92836+01	.16982+02	.18755+01	.67874+03
.96789+01	.18378+02	.18882+01	.76515+03
.99463+01	.19375+02	.18964+01	.82861+03
.10351+02	.20974+02	.19081+01	.93399+03
.10758+02	.22702+02	.19192+01	.10517+04
.11033+02	.23946+02	.19263+01	.11389+04
.11446+02	.25949+02	.19364+01	.12833+04
.11832+02	.27991+02	.19453+01	.14353+04

EXIT POINT

7  
180!

17

下

124

10680+01	00000	12380+01	00000
10681+01	67384+00	13207+01	50679+01
10682+01	67576+00	13209+01	50735+01
10683+01	75126+00	13273+01	50858+01
10684+01	78658+00	13339+01	50879+01
10685+01	84823+00	13406+01	70396+01
10686+01	91017+00	13475+01	77003+01
10687+01	97474+00	13545+01	86181+01
10688+01	10422+01	13618+01	95002+01
10689+01	11130+01	13692+01	10462+02
10690+01	11873+01	13768+01	11509+02
10691+01	12655+01	13847+01	12651+02
10692+01	13480+01	13929+01	13900+02
10693+01	14352+01	14013+01	15268+02
10694+01	15276+01	14099+01	16770+02
10695+01	16257+01	14189+01	18422+02
10696+01	17299+01	14281+01	20242+02
10697+01	18409+01	14377+01	22253+02
10698+01	19594+01	14476+01	24477+02
10699+01	20860+01	14578+01	26945+02
10700+01	22223+01	14689+01	29793+02
10701+01	23664+01	14795+01	32732+02
10702+01	25213+01	14907+01	36111+02
10703+01	26877+01	15021+01	39681+02
10704+01	28670+01	15139+01	44101+02
10705+01	30671+01	15261+01	48951+02
10706+01	32808+01	15388+01	54241+02
10707+01	35088+01	15527+01	61141+03
10708+01	37513+01	15669+01	68231+03
10709+01	40088+01	15824+01	75594+03
10710+01	42813+01	15982+01	82170+03
10711+01	45688+01	16143+01	89006+03
10712+01	48713+01	16307+01	96143+03
10713+01	51888+01	16474+01	10353+04
10714+01	55213+01	16645+01	11191+04
10715+01	58688+01	16819+01	12066+04
10716+01	62313+01	16996+01	12986+04
10717+01	66088+01	17177+01	13951+04
10718+01	70013+01	17361+01	14961+04
10719+01	74088+01	17549+01	16016+04
10720+01	78313+01	17740+01	17116+04
10721+01	82688+01	17934+01	18261+04
10722+01	87213+01	18131+01	19451+04
10723+01	91888+01	18331+01	20686+04
10724+01	96713+01	18534+01	21966+04
10725+01	101688+01	18739+01	23291+04
10726+01	106913+01	18947+01	24661+04
10727+01	112288+01	19157+01	26076+04
10728+01	117813+01	19369+01	27536+04
10729+01	123488+01	19583+01	29051+04
10730+01	129313+01	19800+01	30621+04
10731+01	135288+01	20019+01	32246+04
10732+01	141413+01	20241+01	33926+04
10733+01	147688+01	20465+01	35661+04
10734+01	154113+01	20692+01	37451+04
10735+01	160688+01	20922+01	39296+04
10736+01	167413+01	21154+01	41196+04
10737+01	174288+01	21389+01	43151+04
10738+01	181313+01	21626+01	45161+04
10739+01	188488+01	21866+01	47226+04
10740+01	195813+01	22109+01	49346+04
10741+01	203288+01	22354+01	51521+04
10742+01	210913+01	22601+01	53751+04
10743+01	218688+01	22851+01	56036+04
10744+01	226613+01	23103+01	58376+04
10745+01	234688+01	23357+01	60771+04
10746+01	242913+01	23614+01	63221+04
10747+01	251288+01	23873+01	65726+04
10748+01	259813+01	24134+01	68286+04
10749+01	268488+01	24397+01	70901+04
10750+01	277313+01	24662+01	73571+04
10751+01	286		

.91925+01	.15424+02	.18533+01	.61139+03
.94780+01	.16279+02	.18628+01	.66427+03
.99134+01	.17647+02	.18765+01	.75172+03
.10356+02	.19123+02	.18897+01	.84984+03
.10657+02	.20180+02	.18982+01	.92234+03
.11115+02	.21876+02	.19104+01	.10825+04
.11577+02	.23711+02	.19221+01	.11774+04
.11891+02	.25035+02	.19295+01	.12777+04
.12365+02	.27168+02	.19402+01	.14443+04
.12838+02	.29453+02	.19501+01	.16313+04
.13158+02	.31168+02	.19565+01	.17714+04
.13416+02	.32612+02	.19614+01	.18938+04

A-19

INGOAL POINT 7  
 TANGENT POINT  
 240:1

WALL CONDITIONS

R	Z	CF	S.A.
$R_z$	$R_z$		$R_z$
.10000+01	.00000	.12380+01	.00000
.12759+01	.68967+00	.13225+01	.52303+01
.13158+01	.73177+00	.13272+01	.57633+01
.13705+01	.78980+00	.13337+01	.63780+01
.14272+01	.85094+00	.13403+01	.71957+01
.14858+01	.91272+00	.13470+01	.78923+01
.15467+01	.97812+00	.13539+01	.87443+01
.16100+01	.10465+01	.13610+01	.96690+01
.16760+01	.11182+01	.13683+01	.10676+02
.17449+01	.11936+01	.13758+01	.11774+02
.18170+01	.12730+01	.13836+01	.12974+02
.18926+01	.13569+01	.13916+01	.14283+02
.19719+01	.14456+01	.13999+01	.15731+02
.20553+01	.15395+01	.14084+01	.17318+02
.21430+01	.16395+01	.14172+01	.19067+02
.22355+01	.17458+01	.14264+01	.20993+02
.23330+01	.18595+01	.14358+01	.23135+02
.24358+01	.19799+01	.14456+01	.25503+02
.25445+01	.21092+01	.14556+01	.28133+02
.26590+01	.22477+01	.14660+01	.31058+02
.27809+01	.23962+01	.14768+01	.34318+02
.29096+01	.25560+01	.14879+01	.37961+02
.30460+01	.27283+01	.14994+01	.42046+02
.31920+01	.29146+01	.15113+01	.46639+02
.33792+01	.37156+01	.15279+01	.51865+02
.43352+01	.45078+01	.15461+01	.58810+02
.48560+01	.53171+01	.15698+01	.67554+03
.53707+01	.61668+01	.15904+01	.78240+03
.58882+01	.70725+01	.16190+01	.90925+03
.64129+01	.80424+01	.17156+01	.10719+04
.69494+01	.91020+01	.17413+01	.12763+04
.74996+01	.10250+02	.17655+01	.15340+04
.80665+01	.11508+02	.17887+01	.18682+04
.86509+01	.12887+02	.18108+01	.22543+04
.89501+01	.13627+02	.18214+01	.26960+04
.94084+01	.14610+02	.18370+01	.31972+04
.98720+01	.16084+02	.18520+01	.38500+04

.10198+02	.16991+02	.18618+01	.74566+03
.10688+02	.18445+02	.18759+01	.84626+03
.11188+02	.20016+02	.18896+01	.95957+03
.11529+02	.21141+02	.18984+01	.10435+04
.12051+02	.22952+02	.19112+01	.11831+04
.12580+02	.24915+02	.19233+01	.13404+04
.12942+02	.26332+02	.19312+01	.15177+04
.13491+02	.28621+02	.19424+01	.16531+04
.14044+02	.31109+02	.19530+01	.18735+04
.14420+02	.32923+02	.19598+01	.20392+04
.14986+02	.35862+02	.19694+01	.23157+04
.15492+02	.38743+02	.19774+01	.25958+04

EXIT POINT

THROAT POINT  
TANGENT POINT

7  
280:1

R  
R<sub>t</sub>  
.10000+01  
.12863+01  
.13171+01  
.13740+01  
.14328+01  
.14937+01  
.15570+01  
.16228+01  
.16914+01  
.17630+01  
.18380+01  
.19166+01  
.19992+01  
.20859+01  
.21772+01  
.22734+01  
.23749+01  
.24820+01  
.25952+01  
.27148+01  
.28414+01  
.29747+01  
.31226+01  
.32826+01  
.34534+01  
.44842+01  
.50269+01  
.55638+01  
.61034+01  
.66514+01  
.72124+01  
.77834+01  
.83837+01  
.89978+01  
.95130+01  
.97535+01  
.10293+02

Z  
R<sub>t</sub>  
.00000  
.70044+00  
.73201+00  
.79046+00  
.85117+00  
.91436+00  
.98032+00  
.10493+01  
.11217+01  
.11979+01  
.12781+01  
.13629+01  
.14527+01  
.15478+01  
.16430+01  
.17567+01  
.18715+01  
.19941+01  
.21253+01  
.22659+01  
.24153+01  
.25790+01  
.27553+01  
.29374+01  
.37636+01  
.45837+01  
.54129+01  
.62847+01  
.72115+01  
.82097+01  
.92921+01  
.10470+02  
.11762+02  
.13179+02  
.13941+02  
.15158+02  
.16471+02

WALL CONDITIONS  
CF  
.12389+01  
.15237+01  
.13272+01  
.15335+01  
.13400+01  
.13467+01  
.13755+01  
.15605+01  
.13677+01  
.13751+01  
.13828+01  
.13907+01  
.13989+01  
.14073+01  
.14160+01  
.14251+01  
.14344+01  
.14441+01  
.14540+01  
.14644+01  
.14750+01  
.14860+01  
.14978+01  
.15064+01  
.15552+01  
.15955+01  
.16278+01  
.16582+01  
.16865+01  
.17152+01  
.17326+01  
.17622+01  
.17861+01  
.18053+01  
.18190+01  
.18347+01  
.18499+01

S.A.  
R<sub>t</sub>  
.10000  
.53508+01  
.57127+01  
.64034+01  
.71500+01  
.72562+01  
.88351+01  
.97885+01  
.10828+02  
.11963+02  
.13205+02  
.14567+02  
.16065+02  
.17715+02  
.19536+02  
.21549+02  
.23773+02  
.26252+02  
.29002+02  
.32064+02  
.35082+02  
.38301+02  
.43619+02  
.49242+02  
.71296+02  
.97489+02  
.12698+03  
.16091+03  
.20016+03  
.24571+03  
.29474+03  
.35045+03  
.43268+03  
.51695+03  
.56437+03  
.64295+03  
.73149+03

EXIT POINT

.10631+02  
.11151+02  
.11682+02  
.12046+02  
.12602+02  
.13169+02  
.13557+02  
.14148+02  
.14745+02  
.15152+02  
.15768+02  
.16380+02  
.16735+02

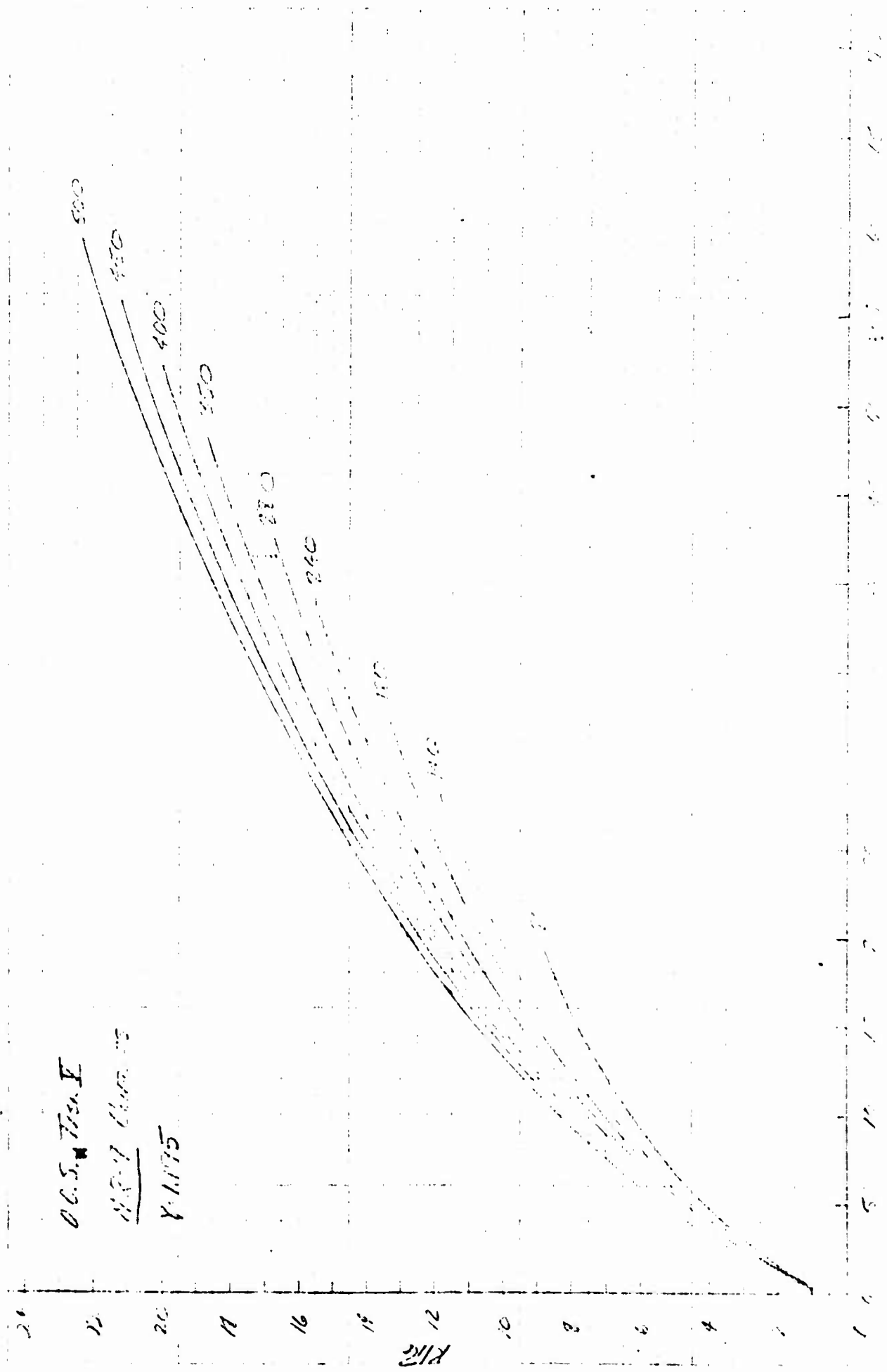
.17406+02  
.18905+02  
.20527+02  
.21690+02  
.23563+02  
.25594+02  
.27062+02  
.29435+02  
.32016+02  
.33960+02  
.36956+02  
.40291+02  
.42379+02

.18598+01  
.18742+01  
.18880+01  
.18969+01  
.19100+01  
.19224+01  
.19304+01  
.19420+01  
.19529+01  
.19599+01  
.19698+01  
.19790+01  
.19841+01

.70663+03  
.90539+03  
.10278+04  
.11186+04  
.12698+04  
.14406+04  
.15680+04  
.17808+04  
.20212+04  
.23023+04  
.26051+04  
.29474+04  
.30577+04







0.5.175

1.175

1.175

## PERFORMANCE

Thrust chamber performance data was developed for use in engine optimization studies and was conducted over the following parametric range:

- (1) Thrust level - 8,000 lbf to 50,000 lbf
- (2) Nominal engine mixture ratio - 6.0:1
- (3) Engine mixture ratio operating range - 5.5:1 to 6.5:1
- (4) Nozzle overall expansion ratio - 140:1 to 500:1
- (5) Engine Chamber Pressure - 300 psia to 2500 psia

Items (1), (2) and (3) were specified in the contract work statement. Item (4) was specified to include the optimum nozzle area ratio calculated at all combinations of thrust level and chamber pressure. The optimum area ratio was to be based on the following tradeoff factors furnished in the work statement:

(1)  $\Delta \text{payload} / \Delta I_{sp} = 157 \text{ lb/sec.}$  (2)  $\Delta \text{Payload} / \Delta \text{Weight at burnout} = 3.68.$   
The chamber pressure range in (5) was chosen so as to include possible design points for three basic engine cycles: (1) Staged Combustion, (2) Gas Generator Bleed Cycle, (3) Expander Cycle.

Figure 1 shows the OOS performance study matrix. Delivered specific impulse was evaluated for each configuration over the range of area ratios from 140:1 to 500:1. The analysis utilized the Rao minimum length nozzle configuration for all performance and weight calculations. For a given nozzle length, the Rao minimum length nozzle was considered to be thrust optimum; although this assumption may not be always correct, the resultant deviation from an optimum contour is small. The minimum length configuration is also the minimum surface area nozzle possessing a certain value for the thrust coefficient ( $C_F$ ), based on divergence loss considerations only. Engine envelope limitations specified were a maximum engine stowed length of 82 inches and a maximum engine diameter of 87 inches. The nozzle length

(throat to exit plane) limit was calculated to be 66 inches, leaving 16 inches from gimbal point to throat. In diameter limited cases, i.e., the optimum area ratio nozzle exit diameter exceeds 87 inches, it is possible that a nozzle of 87 inches exit diameter with length greater than the Rao minimum would prove to be optimum, if length increases could be afforded within the 66 inch nozzle stowed length limit.

#### PERFORMANCE METHODOLOGY

The performance evaluation technique for the OOS Design Study employed the simplified JANNAF Performance Evaluation Methodology<sup>(3)</sup> which formed the basis for the performance predictions of this study. The thrust chamber vacuum delivered specific impulse was calculated considering one-dimensional equilibrium (ODE) flow conditions to be the theoretical base line. All ODE calculations in this analysis include the effect of 0.5% by volume Argon impurity in the oxygen. This results in a performance degradation, compared to pure oxygen, of 1.0 to 1.5 sec of specific impulse depending upon the chamber pressure, mixture ratio and area ratio. ODE performance was evaluated using the JANNAF one-dimensional equilibrium computer program.<sup>(4)</sup> Delivered performance was calculated considering that real engine performance would be decreased by the sum of nozzle kinetics loss, divergence loss, boundary layer loss, and energy release loss.

These losses were calculated except for a simplification in determining the energy release loss (ERL), which was assumed to be one percent of ODE specific impulse over the engine mixture ratio operating range of 5.5:1 to 6.5:1. This assumption was made to speed calculation of preliminary performance values for engine optimization studies. The two-zone mass weighted stream tube distribution analysis described was utilized to refine the energy release loss analysis.

(3) Pieper, J. L., ICRPG Liquid Propellant Thrust Chamber Performance Evaluation Manual, CPIA Publication No. 178, Prepared for the ICRPG Performance Standardization Working Group, 30 September 1968.

(4) ICRPG One-Dimensional Equilibrium Reference Program, NASA-Lewis Research Center, Cleveland, Ohio, May 1968.

The kinetic performance loss (KL) was calculated with the JANNAF One-Dimensional Kinetic (ODK) Computer Program<sup>(5)</sup>. The kinetic performance loss accounts for the performance degradation due to chemical recombination lag during the gas expansion process. Normal boiling point oxygen and hydrogen properties were used as the pre-reaction conditions in the kinetic loss calculations.

The nozzle divergence loss (DL) is a measure of the performance which is lost due to non-axially directed momentum at the nozzle exit. Since a one-dimensional treatment of the nozzle kinetic expansion was used in the performance analysis the divergence loss was evaluated separately from the nozzle kinetics loss. ALRC's Frozen Flow Expansion Nozzle Program No. E21201 was used to calculate the nozzle divergence efficiency.

The boundary layer loss (BLL) calculated for the parametric study accounts for three separate boundary layer mechanisms. First, heat transfer and shear drag at the thrust chamber wall tends to reduce performance. Second, a portion of the total heat loss is recycled since a regeneratively cooled nozzle is expected to be used for the OOS engine to the nozzle extension attach point. Third, the effective nozzle area ratio is altered due to boundary layer growth; usually resulting in a small reduction in performance. The JANNAF Turbulent Boundary Layer Program (TBL)<sup>(6)</sup> was utilized to calculate the boundary layer losses as described here. The heat recycling effect on engine performance was evaluated by raising the hydrogen propellant inlet temperature and calculating the resulting performance increase with ODE<sup>(4)</sup>. The following wall temperature distribution was assumed for the boundary layer analysis: (1) injector to  $c = 6.0:1$ , 1000°F; (2) 6.0:1 to extension attach point, 1200°F; (3) extension attach point to nozzle exit, 2200°F.

(5) One Dimensional Kinetic Nozzle Analysis Computer Program, ICRPG Performance Standardization Working Group, AD 841201, 30 July 1968.

(6) Turbulent Boundary Layer Nozzle Analysis Computer Program, ICRPG Performance Standardization Working Group, AE 841202.

The three regimes represent, respectively, a regeneratively cooled slotted copper thrust chamber, a regeneratively cooled tube bundle nozzle, and a radiation cooled Columbian skirt extension. To simplify the boundary layer analysis for the parametric study it was assumed that all nozzle configurations analyzed would have an attach point area ratio for the nozzle skirt extension of 100:1. The error introduced by this assumption does not significantly affect the selection of an optimum area ratio for design purposes.

#### PERFORMANCE ANALYSIS RESULTS

Figures 2, 3 and 4 summarize the OOS Task IV performance analysis. Assuming a one percent energy release loss, performance was calculated for the mixture ratio design point of 6.0:1 and for the off-design operating points of 5.5:1 and 6.5:1. These performance evaluations were used in the engine optimization studies for the OOS Parametric Engine Analysis. Figures 5, 6, 7 and 8 show delivered specific impulse plotted versus area ratio for thrust levels of 8,000, 15,000, 25,000 and 50,000 lbf, respectively, at the nominal mixture ratio of 6.0:1.

Thrust (lbf)	$P_c$ (lbf/in. <sup>2</sup> )	$F/P_c$ (in. <sup>2</sup> )	$R_t$ (in.)	$L/R_t$ (L = 66 in.)	$\epsilon$ (@ L = 66 in.)	$\epsilon_{max}$ (D = 67 in.)
8K	300	26.7	2.09	31.58	158	433
	500	16.0	1.61	40.99	240	730
	1000	8.0	1.14	57.89	431	1456
	1500	5.3	0.92	71.74	614	2236
15K	300	50.0	2.88	22.90	93	228
	500	30.0	2.22	29.73	143	384
	1000	15.0	1.56	42.31	253	778
	1500	10.0	1.28	51.56	354	1155
	2500	6.0	0.98	67.35	555	1970
25K	300	83.3	3.75	17.69	62	136
	500	50.0	2.88	22.90	93	228
	1000	25.0	2.02	32.67	166	464
	1500	16.7	1.66	39.76	229	687
	2500	10.0	1.28	51.56	372	1155
50K	500	100.0	4.04	16.34	60	116
	1000	50.0	2.88	22.90	93	228
	1500	33.3	2.35	28.09	131	343
	2500	20.0	1.81	36.46	198	578

Figure 1. O.O.S. Performance Analysis Study Matrix

O.O.S. Task IV  
M.R. = 6

FIGURE 2 PERFORMANCE PRELIMINARY

P <sub>c</sub>	Type of	PK					25K					50K				
		300	500	1000	1500	2500	300	500	1000	1500	2500	300	500	1000	1500	2500
140	Top del	471.2	471.6	472.1	472.4	471.2	471.2	471.6	472.1	472.4	472.8	471.2	471.6	472.1	472.4	472.8
	200	10.2	6.9	4.0	2.8	9.3	6.2	3.5	2.5	3.1	2.2	1.5	4.8	2.7	1.9	1.0
	200	3.7	3.5	3.3	3.2	3.5	3.3	3.1	3.1	2.9	2.8	2.7	2.9	2.7	2.6	2.5
	200	4.7	4.7	4.8	4.8	4.7	4.8	4.8	4.8	4.8	4.8	4.8	4.8	4.8	4.8	4.8
	200	4.7	4.7	4.7	4.7	4.7	4.7	4.7	4.7	4.7	4.7	4.7	4.7	4.7	4.7	4.7
	200	4.7	4.7	4.7	4.7	4.7	4.7	4.7	4.7	4.7	4.7	4.7	4.7	4.7	4.7	4.7
160	Top del	447.9	451.8	455.3	456.9	449.0	452.6	455.9	457.4	458.8	459.1	459.1	459.1	457.2	458.4	459.8
	200	474.4	474.9	475.4	475.7	474.4	474.4	474.9	475.4	475.7	476.0	474.4	474.9	475.4	475.7	476.0
	200	10.6	7.2	4.3	3.0	9.6	6.5	3.8	2.7	1.8	2.4	1.6	5.1	2.9	2.0	1.1
	200	4.5	4.3	4.0	3.8	4.2	4.0	3.7	3.6	3.4	3.4	3.2	3.6	3.3	3.2	3.0
	200	4.3	4.4	4.4	4.4	4.3	4.4	4.4	4.4	4.4	4.4	4.4	4.4	4.4	4.4	4.4
	200	4.7	4.7	4.7	4.7	4.7	4.7	4.7	4.7	4.7	4.7	4.7	4.7	4.7	4.7	4.7
200	Top del	450.3	454.3	458.0	459.8	451.6	461.6	462.2	463.7	464.6	465.3	465.3	465.3	462.0	463.1	462.7
	200	478.0	478.4	478.8	479.1	478.0	478.4	478.8	479.1	479.4	479.7	478.0	478.4	478.8	479.1	479.4
	200	11.0	7.7	4.5	3.2	10.0	6.9	4.0	2.8	1.9	2.5	1.7	5.4	3.0	2.1	1.2
	200	5.4	5.2	4.8	4.6	5.1	4.8	4.5	4.3	4.1	4.1	3.9	4.3	4.0	3.8	3.6
	200	3.9	4.0	4.0	4.0	3.9	4.0	4.0	4.0	4.0	4.0	4.0	4.0	4.0	4.0	4.0
	200	4.8	4.8	4.8	4.8	4.8	4.8	4.8	4.8	4.8	4.8	4.8	4.8	4.8	4.8	4.8
350	Top del	452.9	456.7	460.7	462.5	454.2	464.6	465.3	466.1	467.8	468.2	468.2	468.2	466.2	467.7	469.2
	200	482.1	482.4	482.8	483.1	482.1	482.4	482.8	483.1	483.4	483.7	482.1	482.4	482.8	483.1	483.4
	200	11.8	8.4	4.9	3.6	10.7	7.5	4.3	3.2	2.0	2.8	1.8	5.9	3.3	2.4	1.2
	200	6.6	6.4	5.0	5.6	6.3	6.0	5.5	5.2	5.0	4.8	4.8	5.3	4.7	4.6	4.4
	200	3.6	3.6	3.6	3.6	3.6	3.6	3.6	3.6	3.6	3.6	3.6	3.6	3.6	3.6	3.6
	200	4.8	4.8	4.8	4.8	4.8	4.8	4.8	4.8	4.8	4.8	4.8	4.8	4.8	4.8	4.8
400	Top del	455.3	459.2	463.5	465.5	456.7	466.1	466.6	467.8	468.2	468.2	468.2	468.2	466.2	467.7	469.2
	200	483.4	483.6	484.1	484.3	483.4	483.6	484.1	484.3	484.6	484.9	483.4	483.6	484.1	484.3	484.6
	200	12.0	8.6	5.1	3.8	10.9	7.7	4.5	3.3	2.1	2.9	1.8	6.0	3.4	2.5	1.3
	200	7.1	6.8	6.4	6.0	6.7	6.4	5.9	5.7	5.4	5.1	5.1	5.7	5.3	4.9	4.7
	200	3.4	3.5	3.5	3.5	3.4	3.5	3.5	3.5	3.5	3.5	3.5	3.5	3.5	3.5	3.5
	200	4.8	4.8	4.8	4.8	4.8	4.8	4.8	4.8	4.8	4.8	4.8	4.8	4.8	4.8	4.8
450	Top del	484.5	484.8	485.2	485.4	484.5	484.8	485.2	485.4	485.7	485.7	485.7	485.7	485.2	485.4	485.7
	200	12.2	8.8	5.2	3.8	11.1	7.9	4.6	3.4	2.1	3.0	1.9	6.2	3.5	2.5	1.3
	200	7.5	7.2	6.8	6.4	7.1	6.8	6.3	6.0	5.7	5.4	5.4	6.0	5.6	5.2	5.0
	200	3.3	3.4	3.4	3.4	3.3	3.4	3.4	3.4	3.4	3.4	3.4	3.4	3.4	3.4	3.4
	200	4.8	4.8	4.8	4.8	4.8	4.8	4.8	4.8	4.8	4.8	4.8	4.8	4.8	4.8	4.8
	200	4.8	4.8	4.8	4.8	4.8	4.8	4.8	4.8	4.8	4.8	4.8	4.8	4.8	4.8	4.8
500	Top del	485.5	485.8	486.2	486.4	485.5	485.8	486.2	486.4	486.7	486.7	486.7	486.7	486.2	486.4	486.7
	200	12.4	8.9	5.3	3.9	11.3	8.0	4.7	3.5	2.1	3.1	1.9	6.3	3.6	2.6	1.3
	200	7.8	7.6	7.1	6.7	7.3	7.1	6.6	6.0	5.7	5.4	5.4	6.0	5.6	5.2	5.0
	200	3.2	3.2	3.2	3.2	3.2	3.2	3.2	3.2	3.2	3.2	3.2	3.2	3.2	3.2	3.2
	200	4.9	4.9	4.9	4.9	4.9	4.9	4.9	4.9	4.9	4.9	4.9	4.9	4.9	4.9	4.9
	200	4.9	4.9	4.9	4.9	4.9	4.9	4.9	4.9	4.9	4.9	4.9	4.9	4.9	4.9	4.9



FIGURE 3 PERFORMANCE PRELIMINARY

U.S. TASK IV  
W.R. 5.5

Task PC	PK					15K					25K					50K				
	300	500	1000	1500	2500	300	500	1000	1500	2500	300	500	1000	1500	2500	500	1000	1500	2500	500
120																				
Isode	472.1	472.5	472.8	473.0	472.1	472.1	472.5	472.8	473.0	473.2	472.1	472.5	472.8	473.0	473.2	472.5	472.8	473.0	473.2	473.2
3.R.L.	8.0	5.3	2.9	1.9	7.1	1.2	4.6	2.6	1.8	1.2	6.3	4.0	2.2	1.6	1.1	3.4	1.8	1.4	1.4	1.0
3.B.L.L.	3.5	3.3	3.1	3.0	3.3	2.6	3.1	2.9	2.8	2.6	3.1	2.9	2.7	2.6	2.6	2.7	2.6	2.5	2.4	2.4
3.D.L.	4.7	4.6	4.6	4.6	4.7	4.8	4.8	4.8	4.8	4.8	4.8	4.8	4.8	4.8	4.8	4.8	4.8	4.8	4.8	4.3
3.E.R.L.	4.7	4.7	4.7	4.7	4.7	4.7	4.7	4.7	4.7	4.7	4.7	4.7	4.7	4.7	4.7	4.7	4.7	4.7	4.7	4.7
1sp del	451.2	454.4	457.3	458.6	452.3	455.3	455.3	457.8	458.9	459.9	453.2	456.1	458.4	459.3	460.0	456.9	458.9	459.6	460.3	460.3
140																				
Isode	475.1	475.5	475.8	476.0	475.1	475.5	475.8	476.0	476.2	476.2	475.1	475.5	475.8	476.0	476.2	475.5	475.8	476.0	476.2	476.2
3.R.L.	8.2	5.5	3.1	2.0	7.3	1.2	4.8	2.7	1.9	1.2	6.6	4.2	2.4	1.8	1.1	3.6	1.9	1.5	1.5	1.0
3.B.L.L.	4.3	4.1	3.8	3.6	4.0	3.8	3.8	3.5	3.4	3.2	3.8	3.6	3.4	3.2	3.0	3.4	3.1	3.0	2.8	2.8
3.D.L.	4.3	4.4	4.4	4.4	4.4	4.4	4.4	4.4	4.4	4.4	4.4	4.4	4.4	4.4	4.4	4.4	4.4	4.4	4.4	4.4
3.E.R.L.	4.8	4.8	4.8	4.8	4.8	4.8	4.8	4.8	4.8	4.8	4.8	4.8	4.8	4.8	4.8	4.8	4.8	4.8	4.8	4.8
1sp del	453.5	456.7	459.7	461.2	454.6	457.7	460.4	461.5	462.6	463.5	455.5	458.5	460.8	461.8	462.9	459.3	461.5	462.3	463.2	463.2
160																				
Isode	478.3	478.6	478.9	479.1	478.3	478.6	478.9	479.1	479.3	479.3	478.3	478.6	478.9	479.1	479.3	478.6	478.9	479.1	479.3	479.3
3.R.L.	8.5	5.8	3.2	2.2	7.4	1.2	4.8	2.8	2.0	1.2	6.9	4.6	2.6	1.8	1.2	3.9	2.1	1.6	1.6	1.1
3.B.L.L.	5.1	4.9	4.5	4.3	4.8	4.5	4.3	4.1	4.1	3.9	4.5	4.4	4.1	3.9	3.7	4.1	3.8	3.5	3.4	3.4
3.D.L.	4.0	4.0	4.0	4.0	4.0	4.0	4.0	4.0	4.0	4.0	4.0	4.0	4.0	4.0	4.0	4.0	4.0	4.0	4.0	4.0
3.E.R.L.	4.8	4.8	4.8	4.8	4.8	4.8	4.8	4.8	4.8	4.8	4.8	4.8	4.8	4.8	4.8	4.8	4.8	4.8	4.8	4.8
1sp del	455.9	459.1	462.4	463.8	457.3	460.5	463.0	464.2	465.4	466.2	458.1	460.8	463.4	464.6	465.6	461.8	464.2	465.1	466.0	466.0
180																				
Isode	482.2	482.4	482.7	482.8	482.2	482.4	482.7	482.8	483.0	483.0	482.2	482.4	482.7	482.8	483.0	482.4	482.7	482.8	483.0	483.0
3.R.L.	9.0	6.2	3.5	2.4	8.1	1.3	5.5	3.0	2.2	1.3	7.4	4.8	2.7	2.0	1.3	4.2	2.4	1.8	1.2	1.2
3.B.L.L.	6.2	6.1	5.7	5.3	6.0	5.7	5.2	5.0	5.0	4.7	5.7	5.2	5.0	4.7	4.5	5.0	4.4	4.4	4.2	4.2
3.D.L.	3.6	3.6	3.6	3.6	3.6	3.6	3.6	3.6	3.6	3.6	3.6	3.6	3.6	3.6	3.6	3.6	3.6	3.6	3.6	3.6
3.E.R.L.	4.8	4.8	4.8	4.8	4.8	4.8	4.8	4.8	4.8	4.8	4.8	4.8	4.8	4.8	4.8	4.8	4.8	4.8	4.8	4.8
1sp del	458.6	461.7	465.1	466.7	459.7	462.8	466.1	467.2	468.5	469.3	460.7	464.0	466.6	467.7	468.7	464.8	467.5	468.1	469.1	469.1
200																				
Isode	483.4	483.5	483.8	484.0	483.4	483.5	483.8	484.0	484.2	484.2	483.4	483.5	483.8	484.0	484.2	483.5	483.8	484.0	484.2	484.2
3.R.L.	9.2	6.4	3.6	2.5	8.3	1.4	5.6	3.2	2.4	1.4	7.6	5.1	2.9	2.0	1.3	4.3	2.5	1.9	1.2	1.2
3.B.L.L.	6.7	6.4	6.1	5.7	6.3	6.1	5.6	5.4	5.4	5.1	6.1	5.6	5.4	5.1	4.8	5.4	5.1	4.5	4.4	4.4
3.D.L.	3.4	3.5	3.5	3.5	3.5	3.5	3.5	3.5	3.5	3.5	3.5	3.5	3.5	3.5	3.5	3.5	3.5	3.5	3.5	3.5
3.E.R.L.	4.8	4.8	4.8	4.8	4.8	4.8	4.8	4.8	4.8	4.8	4.8	4.8	4.8	4.8	4.8	4.8	4.8	4.8	4.8	4.8
1sp del	459.3	462.4	465.8	467.5	460.5	463.5	466.7	467.9	469.4	470.2	461.4	464.5	467.3	468.6	469.8	465.5	467.9	469.3	470.3	470.3
220																				
Isode	484.4	484.6	484.9	485.1	484.4	484.6	484.9	485.1	485.3	485.3	484.4	484.6	484.9	485.1	485.3	484.6	484.9	485.1	485.3	485.3
3.R.L.	9.3	6.5	3.7	2.6	8.4	1.4	5.6	3.2	2.4	1.4	7.7	5.2	2.9	2.2	1.4	4.5	2.6	1.9	1.3	1.3
3.B.L.L.	7.1	6.8	6.4	6.1	6.7	6.4	6.0	5.7	5.4	5.4	6.4	6.0	5.7	5.4	5.1	5.7	5.3	4.9	4.7	4.7
3.D.L.	3.4	3.4	3.4	3.4	3.4	3.4	3.4	3.4	3.4	3.4	3.4	3.4	3.4	3.4	3.4	3.4	3.4	3.4	3.4	3.4
3.E.R.L.	4.8	4.8	4.8	4.8	4.8	4.8	4.8	4.8	4.8	4.8	4.8	4.8	4.8	4.8	4.8	4.8	4.8	4.8	4.8	4.8
1sp del	459.8	463.1	466.6	468.1	461.1	464.4	467.5	468.7	469.9	470.7	462.1	465.2	468.1	469.2	470.5	466.2	468.8	470.0	471.0	471.0
240																				
Isode	485.3	485.5	485.7	485.9	485.3	485.5	485.7	485.9	486.1	486.1	485.3	485.5	485.7	485.9	486.1	485.5	485.7	485.9	486.1	486.1
3.R.L.	9.4	6.6	3.8	2.7	8.6	1.5	5.8	3.3	2.5	1.5	7.8	5.3	3.0	2.2	1.4	4.6	2.7	1.9	1.3	1.3
3.B.L.L.	7.4	7.2	6.7	6.3	7.1	6.7	6.3	6.1	5.7	5.7	6.7	6.3	6.0	5.7	5.4	6.0	5.6	5.2	5.0	5.0
3.D.L.	3.2	3.2	3.2	3.2	3.2	3.2	3.2	3.2	3.2	3.2	3.2	3.2	3.2	3.2	3.2	3.2	3.2	3.2	3.2	3.2
3.E.R.L.	4.9	4.9	4.9	4.9	4.9	4.9	4.9	4.9	4.9	4.9	4.9	4.9	4.9	4.9	4.9	4.9	4.9	4.9	4.9	4.9
1sp del	460.4	463.6	467.0	468.5	461.2	464.5	467.9	469.1	470.7	471.1	462.7	465.7	468.5	469.8	471.1	466.7	469.2	470.5	471.6	471.6

FIGURE 4 PERFORMANCE PRELIMINARY

C.O.S. TASA. IV  
M.R. = 6.5

Project P.C.	15K				23K				50K			
	300	500	1000	1500	300	500	1000	1500	300	500	1000	1500
140												
Tasce	460.2	469.9	470.7	471.1	469.2	469.9	470.7	471.1	469.2	469.9	470.7	471.1
T.K.L.	11.9	9.2	5.8	4.2	12.0	8.4	5.2	3.7	11.1	7.6	4.5	3.2
T.B.L.L.	3.9	3.7	3.5	3.4	3.7	3.5	3.3	3.2	3.5	3.3	3.1	3.0
T.D.L.	4.7	4.7	4.7	4.8	4.7	4.7	4.8	4.8	4.7	4.7	4.8	4.8
T.E.L.	4.7	4.7	4.7	4.7	4.7	4.7	4.7	4.7	4.7	4.7	4.7	4.7
Tsp del	463.0	447.6	452.0	454.0	444.1	448.6	452.7	454.7	445.2	449.6	453.6	455.4
180												
Tasce	472.8	473.4	474.1	474.5	472.8	473.4	474.1	474.5	472.8	473.4	474.1	474.5
T.K.L.	13.4	9.6	6.2	4.5	12.4	8.9	5.5	4.0	11.5	8.0	4.8	3.5
T.B.L.L.	4.7	4.5	4.2	4.0	4.4	4.2	3.9	3.6	4.2	4.0	3.6	3.4
T.D.L.	4.3	4.3	4.4	4.4	4.3	4.3	4.4	4.4	4.3	4.3	4.4	4.4
T.E.L.	4.7	4.7	4.7	4.7	4.7	4.7	4.7	4.7	4.7	4.7	4.7	4.7
Tsp del	465.7	450.3	454.6	456.9	447.0	451.3	455.6	457.6	448.1	452.4	456.4	458.3
240												
Tasce	476.6	477.2	477.7	478.1	476.6	477.2	477.7	478.1	476.6	477.2	477.7	478.1
T.K.L.	14.3	10.4	6.4	4.8	13.2	9.5	5.8	4.2	12.1	8.6	4.1	3.6
T.B.L.L.	5.7	5.5	5.1	4.8	5.4	5.1	4.7	4.5	5.1	4.8	4.5	4.3
T.D.L.	3.9	3.9	4.0	4.0	3.9	3.9	4.0	4.0	3.9	3.9	4.0	4.0
T.E.L.	4.8	4.8	4.8	4.8	4.8	4.8	4.8	4.8	4.8	4.8	4.8	4.8
Tsp del	468.2	452.6	457.4	459.7	449.3	453.9	458.4	460.6	450.7	455.1	459.3	461.4
350												
Tasce	481.0	481.6	482.2	482.4	481.0	481.6	482.2	482.4	481.0	481.6	482.2	482.4
T.K.L.	15.0	11.2	7.0	5.3	13.8	10.2	6.2	4.6	12.8	9.2	5.6	4.1
T.B.L.L.	7.0	6.7	6.3	5.9	6.6	6.3	5.8	5.6	6.3	5.8	5.6	5.3
T.D.L.	3.5	3.6	3.6	3.6	3.5	3.6	3.6	3.6	3.5	3.6	3.6	3.6
T.E.L.	4.8	4.8	4.8	4.8	4.8	4.8	4.8	4.8	4.8	4.8	4.8	4.8
Tsp del	450.7	455.3	460.5	462.8	452.3	456.7	461.8	463.8	453.6	458.2	462.5	464.6
400												
Tasce	482.4	482.9	483.5	483.8	482.4	482.9	483.5	483.8	482.4	482.9	483.5	483.8
T.K.L.	15.7	11.5	7.2	5.4	14.2	10.5	6.5	4.8	13.0	9.4	5.6	4.2
T.B.L.L.	7.5	7.2	6.7	6.3	7.1	6.3	6.2	6.0	7.2	6.2	6.0	5.7
T.D.L.	3.4	3.4	3.5	3.5	3.4	3.4	3.5	3.5	3.4	3.4	3.5	3.5
T.E.L.	4.8	4.8	4.8	4.8	4.8	4.8	4.8	4.8	4.8	4.8	4.8	4.8
Tsp del	451.1	456.0	461.3	463.8	452.9	457.9	462.5	464.7	454.5	459.1	463.6	465.6
450												
Tasce	483.6	484.1	484.7	485.0	483.6	484.1	484.7	485.0	483.6	484.1	484.7	485.0
T.K.L.	15.7	11.8	7.4	5.6	14.4	10.8	6.7	4.9	13.4	9.8	5.8	4.4
T.B.L.L.	7.9	7.6	7.2	6.7	7.5	7.2	6.6	6.3	7.2	6.6	6.3	6.0
T.D.L.	3.3	3.3	3.4	3.4	3.3	3.3	3.4	3.4	3.3	3.4	3.4	3.4
T.E.L.	4.8	4.8	4.8	4.8	4.8	4.8	4.8	4.8	4.8	4.8	4.8	4.8
Tsp del	451.9	456.6	461.9	464.4	453.6	458.0	463.2	465.5	454.9	459.5	464.4	466.3
500												
Tasce	484.8	485.2	485.8	486.1	484.8	485.2	485.8	486.1	484.8	485.2	485.8	486.1
T.K.L.	15.9	12.0	7.5	5.6	14.7	11.0	6.8	5.0	13.6	9.9	5.8	4.5
T.B.L.L.	8.2	8.0	7.5	7.1	7.9	7.5	7.1	6.7	7.5	7.1	6.6	6.2
T.D.L.	3.2	3.2	3.2	3.2	3.2	3.2	3.2	3.2	3.2	3.2	3.2	3.2
T.E.L.	4.8	4.8	4.8	4.8	4.8	4.8	4.8	4.8	4.8	4.8	4.8	4.8
Tsp del	452.7	457.1	462.7	465.2	454.2	458.6	463.3	466.2	455.7	460.1	465.0	467.1

C.O.S. TASK II DELIVERED SPECIFIC IMPULSE  
VERSUS RATIO

$F = 8 K$   
 $MR = 6.0$

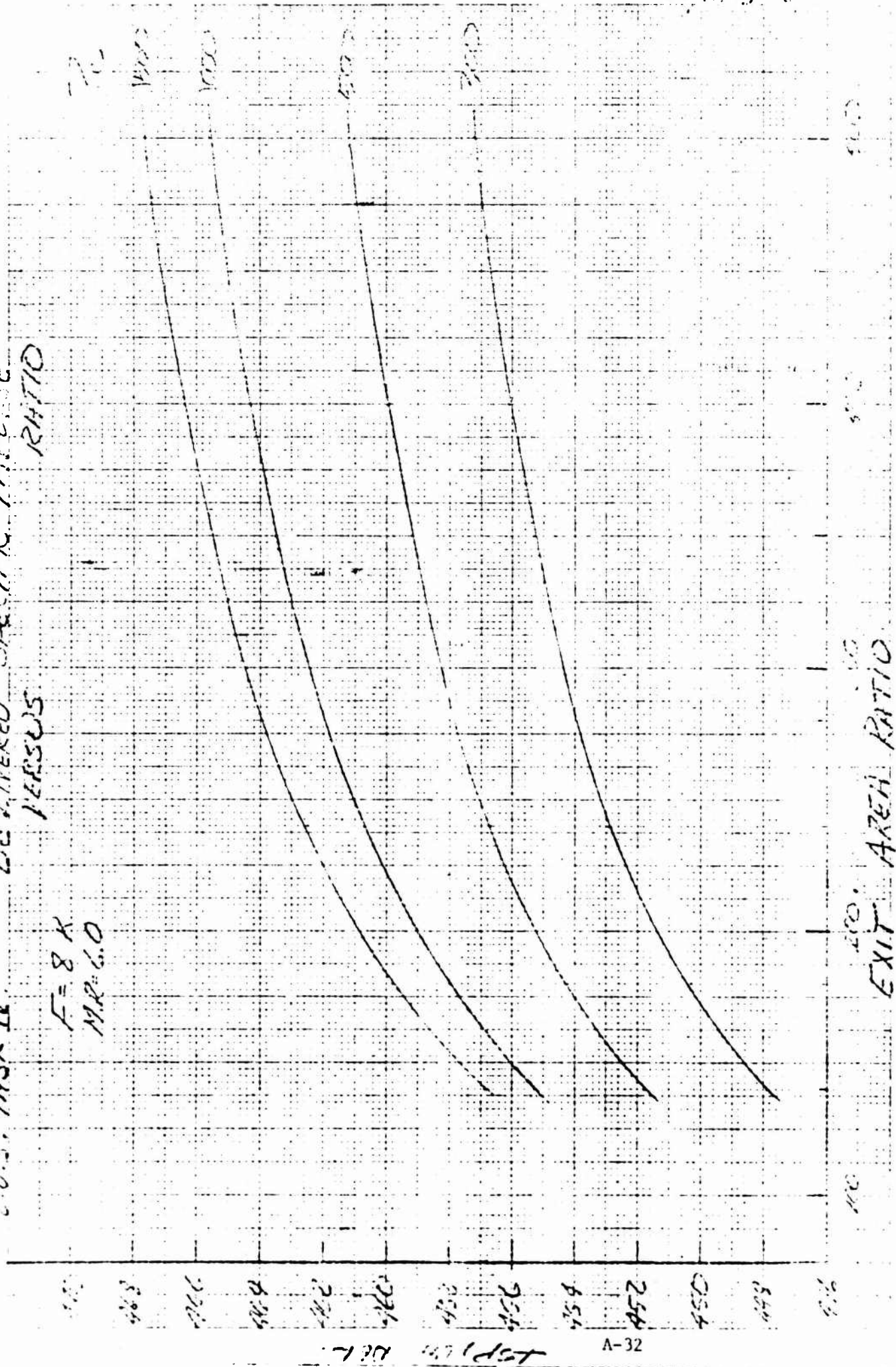


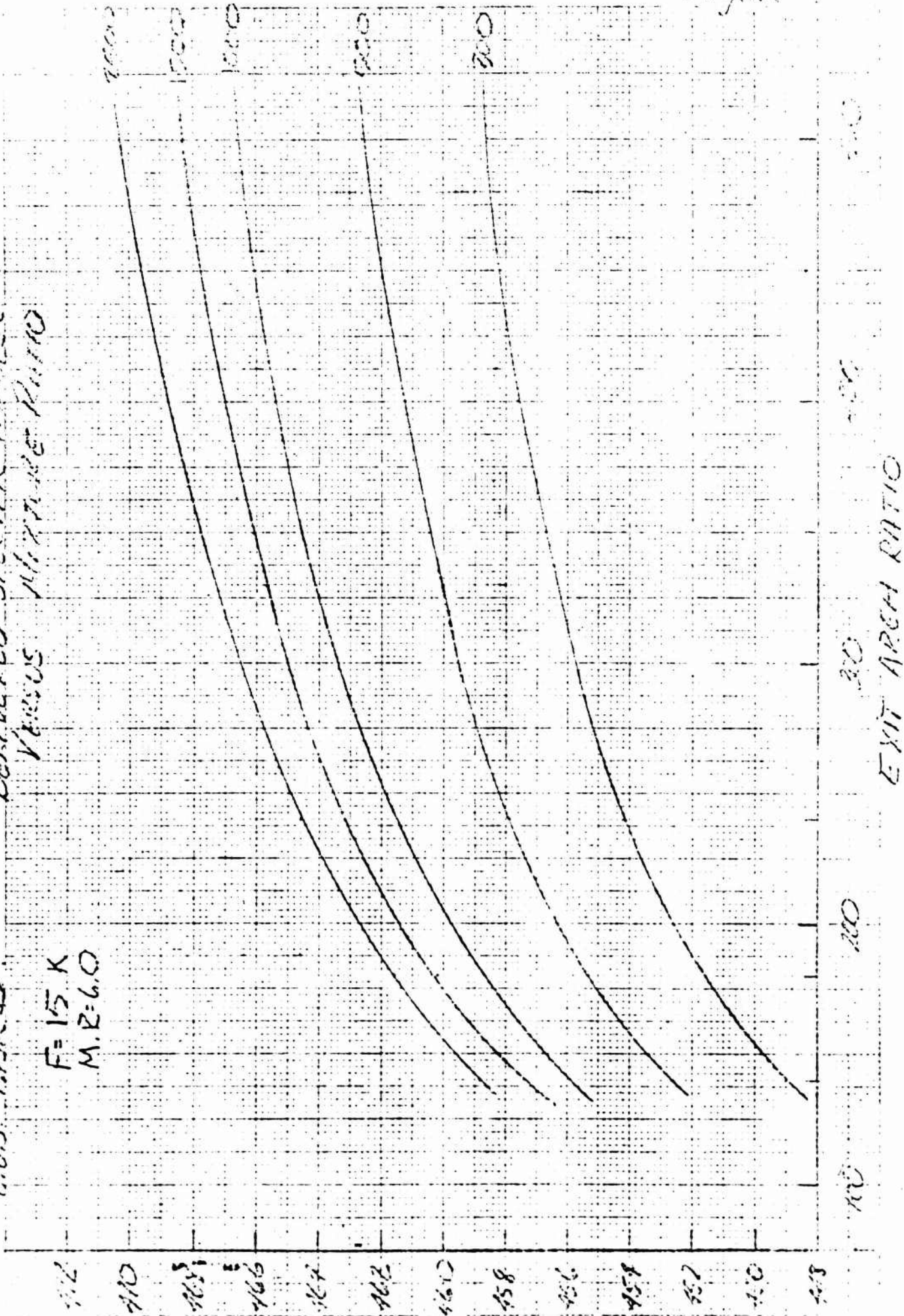
Figure 5

Figure 1

DELIVERED SPECIFIC IMPULSE  
VERSUS EXIT AREA RATIO

A.O.S. TASK II

$F = 15.5$   
 $M.R. = 6.0$

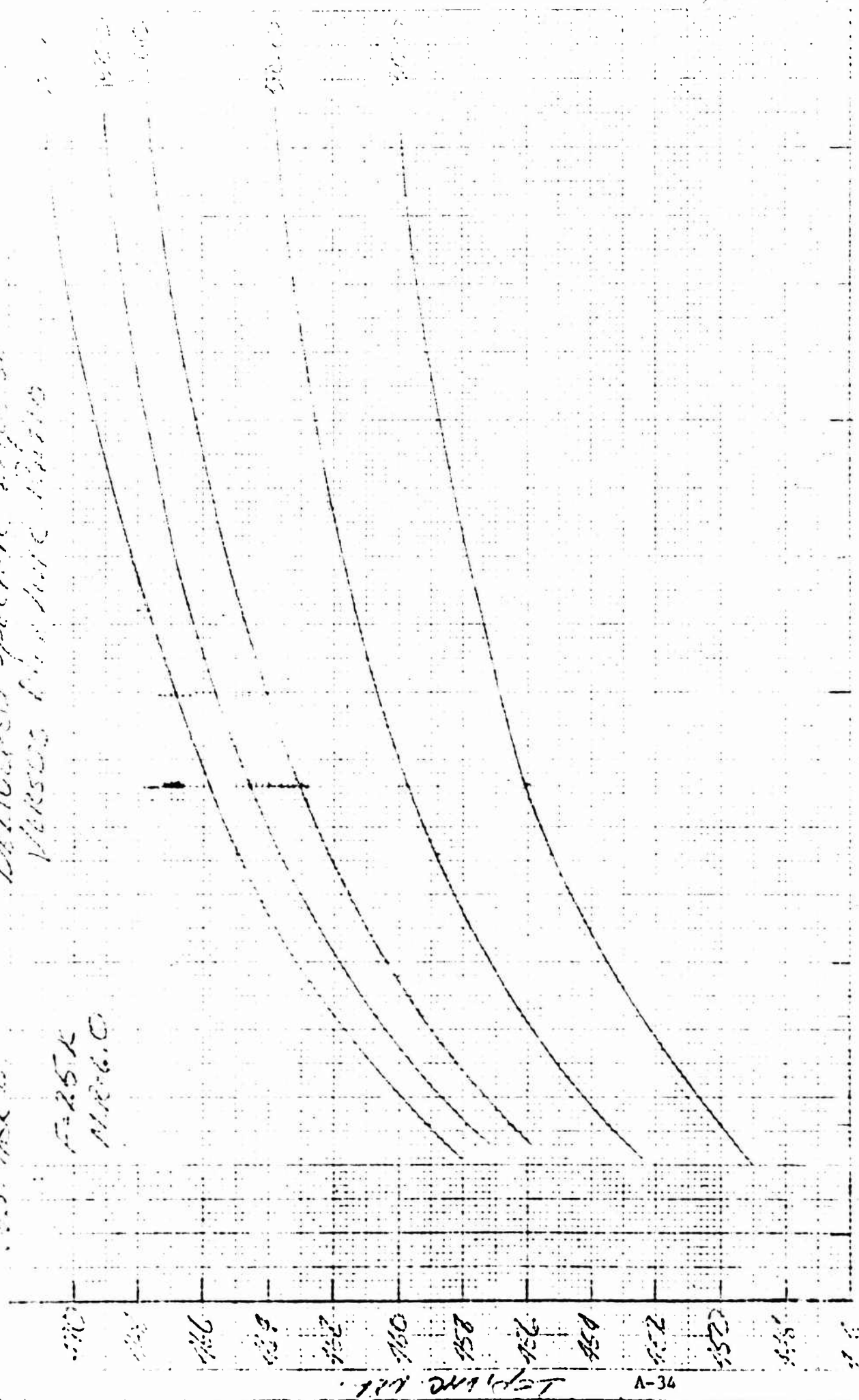




15. 15. 15.

Feb 25 1890

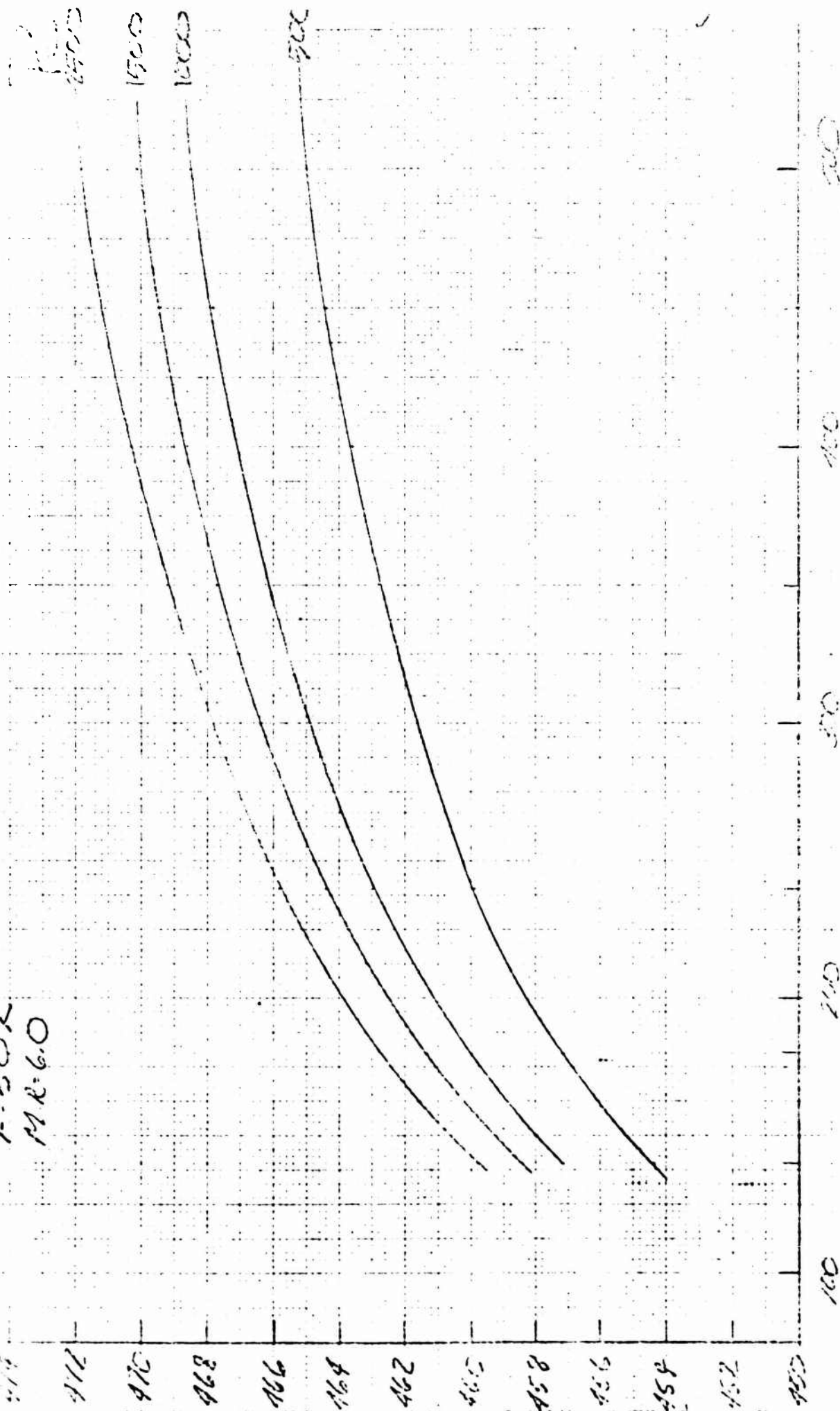
Derived specific fragments -  
Verses 1-4 and 10-11



2000

# C.O.S. TASK III. DELIVERED SPECIFIC IMPULSE VERSUS MIXTURE RATIO

F=50K  
MR=6.0



Exit Area Ratio

EFFECT OF DESIGN MIXTURE RATIO CHANGE  
ON 8K TO 25K THRUST LEVEL ENGINE PERFORMANCE

The purpose of the OOS changing mixture ratio performance evaluation effort was to extend the 8K to 25K parametric data to include nominal engine mixture ratios of 5.0:1 and 7.0:1 as requested in the Contract work statement. The analysis was conducted in a manner identical to that described under the Engine Performance Parametric Study for 8K to 50K thrust levels. The engine configurations analyzed covered the same chamber pressure and area ratio range as shown in the Study Matrix. This analysis essentially evaluated the effects of new design mixture ratio conditions on engine specific impulse, nozzle configuration, and nozzle dimensions.

As explained for the effort, nozzle contours were generated with ALRC computer program No. E21207, a method of characteristics, constant gamma expansion program. For the new design point mixture ratios of 5.0:1 and 7.0:1, an analysis was conducted to determine values for the program gamma input. It was determined that values of 1.26 and 1.195, for mixture ratios 5.0:1 and 7.0:1 respectively, were representative values for a mean gamma in an equilibrium  $O_2/H_2$  expansion to area ratios typical for the OOS Study. The effect of an increasing value of gamma on Rao nozzle geometry is to increase the minimum length and surface area for a given expansion ratio. This meant, in general, that an increase in the value for the design mixture ratio decreased nozzle weight and length. Figure 1 compares normalized lengths and surface areas for nozzles of all three nominal mixture ratios considered in the OOS Task IV and V performance analyses.

After determination of nozzle configurations for nominal engine mixture ratios of 5.0:1 and 7.0:1, a parametric performance analysis was conducted for each design point. The results of these analyses are tabulated in Figures 2 and 3, showing delivered vacuum specific impulse for the OOS performance study matrix. Figures 4, 5 and 6 show delivered specific impulse plotted versus

area ratio for thrust levels of 8,000, 15,000, and 25,000 lbf, respectively, for a nominal mixture ratio of 5.0:1. Figures 7, 8, and 9 are similar plots for a nominal mixture ratio of 7.0:1. The energy release loss for the Task V performance analysis was assumed to be one percent of one dimensional equilibrium performance. It is expected that a more refined analysis will show energy release loss increasing with an increasing nominal mixture ratio. As explained in the Performance Evaluation, a two stream tube analysis will be utilized in the study to more effectively predict energy release loss. Since the nozzle area ratio is expected to have a second-order effect on energy release loss, the preliminary assumption of one percent energy release loss will not affect appreciably the OOS area ratio optimization values. In the performance analyses the refined energy release loss calculation will affect primarily the predicted values of delivered specific impulse.



Figure 1

CO2 NOZZLE GEOMETRY FOR DESIGN MIXTURE  
RATIOS OF 5, 6, 7

Nominal Mixture Ratio		Overall Area Ratio						
		140	180	240	350	400	450	500
5.0	$(R/R_T)_e$	11.83	13.42	15.49	18.71	20.00	21.21	22.36
	$(L/R_T)_e$	32.0	37.5	44.8	56.1	60.9	65.2	69.7
	$(SA/R_T^2)_e$	1633	2166	2989	4540	5250	6000	6740
6.0	$(R/R_T)_e$	11.83	13.42	15.49	18.71	20.00	21.21	22.36
	$(L/R_T)_e$	29.5	34.4	41.0	51.2	55.3	59.4	63.2
	$(SA/R_T^2)_e$	1508	1994	2741	4150	4800	5450	6190
7.0	$(R/R_T)_e$	11.83	13.42	15.49	18.71	20.00	21.21	22.36
	$(L/R_T)_e$	28.0	32.6	38.7	48.0	52.0	55.6	59.0
	$(SA/R_T^2)_e$	1435	1894	2596	3860	4460	5080	5680

$(R/R_T)_e$  — exit radius normalized to throat radius

$(L/R_T)_e$  — nozzle length (throat to exit) normalized to throat radius

$(SA/R_T^2)_e$  — total nozzle surface area normalized to the square of the throat radius

FIGURE 2 PERFORMANCE PRELIMINARY

 NTS TASK V  
 M.R. = 5.0

Alt	Pk	15K					25K				
		300	500	1000	1500	2000	300	500	1000	1500	2000
100	Pc										
	1acde	472.6	474.2	472.4	472.5	472.0	472.2	472.0	472.2	472.4	472.5
	2K.L.	5.9	4.0	7.1	1.2	5.0	0.8	4.3	2.8	1.6	1.2
	3B.L.L.	3.3	3.1	2.9	2.5	3.1	2.5	2.9	2.8	2.5	2.4
	4D.L.	3.6	3.6	3.6	3.6	3.6	3.6	3.6	3.6	3.6	3.6
	5F.P.L.	4.2	4.2	4.2	4.2	4.2	4.2	4.2	4.2	4.2	4.2
160	1acde	474.8	475.0	475.2	475.3	474.8	475.4	474.8	475.0	475.2	475.3
	2K.L.	6.0	4.1	2.2	1.4	5.2	0.8	4.5	2.9	1.2	0.7
	3B.L.L.	4.0	3.8	3.6	3.4	3.7	3.0	3.6	3.4	3.0	2.9
	4D.L.	3.2	3.2	3.2	3.2	3.2	3.2	3.2	3.2	3.2	3.2
	5F.P.L.	4.7	4.8	4.8	4.8	4.7	4.8	4.7	4.8	4.8	4.8
	1sp del	450.9	459.1	461.4	462.5	458.0	463.6	460.7	462.3	463.0	463.8
240	1acde	477.7	472.9	478.1	478.2	477.9	478.3	477.7	477.9	478.1	478.3
	2K.L.	6.2	4.2	2.3	1.5	5.5	0.9	4.8	3.1	1.8	0.8
	3B.L.L.	4.8	4.6	4.3	4.1	4.5	3.7	4.3	4.1	3.8	3.5
	4D.L.	2.8	2.8	2.8	2.8	2.8	2.8	2.8	2.8	2.8	2.8
	5F.P.L.	4.8	4.8	4.8	4.8	4.8	4.8	4.8	4.8	4.8	4.8
	1sp del	459.1	461.5	463.9	465.0	460.1	466.1	463.1	464.9	465.6	466.4
350	1acde	481.1	481.2	481.4	481.5	481.1	481.6	481.1	481.2	481.4	481.6
	2K.L.	6.5	4.3	2.4	1.6	5.8	0.9	5.3	3.4	1.3	0.9
	3B.L.L.	5.9	5.7	5.4	5.0	5.6	4.7	5.4	4.9	4.7	4.5
	4D.L.	2.4	2.4	2.4	2.4	2.4	2.4	2.4	2.4	2.4	2.4
	5F.P.L.	4.8	4.8	4.8	4.8	4.8	4.8	4.8	4.8	4.8	4.8
	1sp del	461.5	464.0	466.4	467.2	462.5	469.0	465.7	467.6	468.4	469.2
400	1acde	482.1	482.2	482.4	482.5	482.1	482.6	482.1	482.2	482.4	482.6
	2K.L.	6.8	4.4	2.5	1.6	5.9	1.0	5.4	3.5	2.0	0.9
	3B.L.L.	6.3	6.1	5.2	5.4	6.0	4.8	5.7	5.3	5.0	4.8
	4D.L.	2.3	2.3	2.3	2.3	2.3	2.3	2.3	2.3	2.3	2.3
	5F.P.L.	4.8	4.8	4.8	4.8	4.8	4.8	4.8	4.8	4.8	4.8
	1sp del	462.1	464.6	467.1	468.0	463.5	469.7	466.3	468.2	469.1	470.1
450	1acde	483.3	483.4	483.6	483.7	483.3	483.8	483.3	483.4	483.6	483.8
	2K.L.	6.6	4.4	2.5	1.2	6.0	1.1	5.5	3.6	2.1	1.5
	3B.L.L.	6.7	6.4	6.1	5.2	6.3	5.1	5.6	5.1	5.4	5.1
	4D.L.	2.2	2.2	2.2	2.2	2.2	2.2	2.2	2.2	2.2	2.2
	5F.P.L.	4.8	4.8	4.8	4.8	4.8	4.8	4.8	4.8	4.8	4.8
	1sp del	463.0	465.6	468.0	469.3	464.0	470.5	467.2	469.1	470.1	471.0
500	1acde	483.9	484.0	484.2	484.3	483.9	484.4	483.9	484.0	484.2	484.4
	2K.L.	6.7	4.5	2.6	1.7	6.0	1.1	5.5	3.7	2.1	1.5
	3B.L.L.	7.0	6.8	6.3	6.0	6.7	5.7	6.3	6.0	5.6	5.4
	4D.L.	2.1	2.1	2.1	2.1	2.1	2.1	2.1	2.1	2.1	2.1
	5F.P.L.	4.8	4.8	4.8	4.8	4.8	4.8	4.8	4.8	4.8	4.8
	1sp del	463.3	465.8	468.4	469.7	464.3	470.0	467.4	469.6	470.5	471.4

FIGURE 3 PERFORMANCE PRELIMINARY

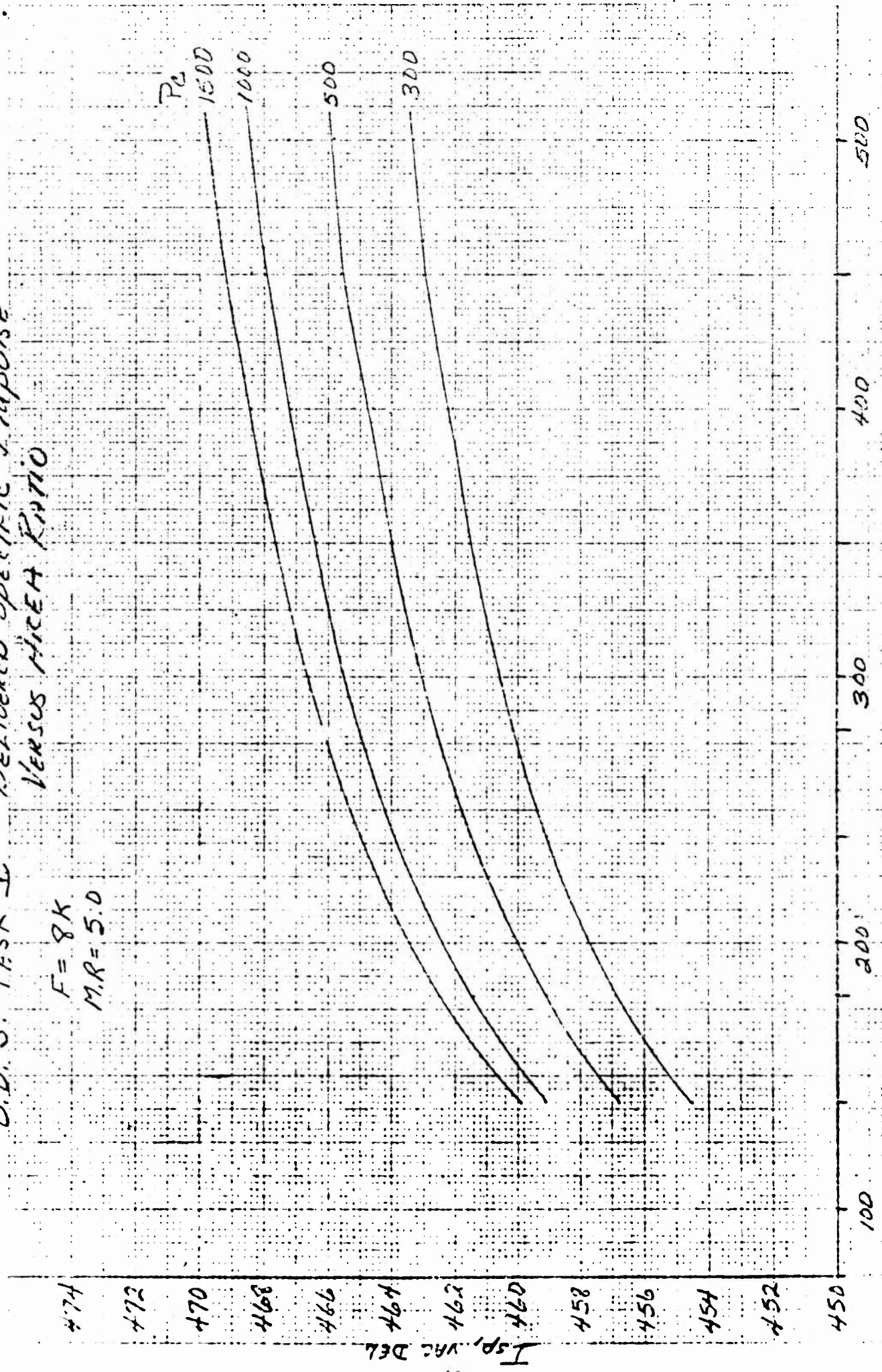
INC TASK V  
W.R. = 7.0

Alt	Type	15K				25K				35K				45K				55K			
		300	500	1000	1500	2000	2500	3000	3500	4000	4500	5000	5500	6000	6500	7000	7500	8000	8500	9000	9500
300	Isdc	466.3	467.4	468.3	468.8	469.3	469.8	470.4	471.2	472.0	472.6	473.2	473.8	474.4	475.0	475.6	476.2	476.8	477.4	478.0	478.6
	Isdc	17.2	17.3	17.4	17.5	17.6	17.7	17.8	17.9	18.0	18.1	18.2	18.3	18.4	18.5	18.6	18.7	18.8	18.9	19.0	19.1
	Isdc	4.1	4.1	4.1	4.1	4.1	4.1	4.1	4.1	4.1	4.1	4.1	4.1	4.1	4.1	4.1	4.1	4.1	4.1	4.1	4.1
	Isdc	5.5	5.6	5.7	5.7	5.7	5.7	5.7	5.7	5.7	5.7	5.7	5.7	5.7	5.7	5.7	5.7	5.7	5.7	5.7	5.7
	Isdc	4.7	4.7	4.7	4.7	4.7	4.7	4.7	4.7	4.7	4.7	4.7	4.7	4.7	4.7	4.7	4.7	4.7	4.7	4.7	4.7
	Isdc	435.7	440.8	445.9	448.5	451.6	454.1	456.6	459.1	461.6	464.1	466.6	469.1	471.6	474.1	476.6	479.1	481.6	484.1	486.6	489.1
350	Isdc	470.4	471.2	472.0	472.6	473.2	473.8	474.4	475.0	475.6	476.2	476.8	477.4	478.0	478.6	479.2	479.8	480.4	481.0	481.6	482.2
	Isdc	17.2	17.3	17.4	17.5	17.6	17.7	17.8	17.9	18.0	18.1	18.2	18.3	18.4	18.5	18.6	18.7	18.8	18.9	19.0	19.1
	Isdc	4.1	4.1	4.1	4.1	4.1	4.1	4.1	4.1	4.1	4.1	4.1	4.1	4.1	4.1	4.1	4.1	4.1	4.1	4.1	4.1
	Isdc	5.5	5.6	5.7	5.7	5.7	5.7	5.7	5.7	5.7	5.7	5.7	5.7	5.7	5.7	5.7	5.7	5.7	5.7	5.7	5.7
	Isdc	4.7	4.7	4.7	4.7	4.7	4.7	4.7	4.7	4.7	4.7	4.7	4.7	4.7	4.7	4.7	4.7	4.7	4.7	4.7	4.7
	Isdc	438.4	443.2	448.8	451.6	454.1	456.6	459.1	461.6	464.1	466.6	469.1	471.6	474.1	476.6	479.1	481.6	484.1	486.6	489.1	491.6
400	Isdc	474.4	475.5	476.0	476.5	477.1	477.6	478.2	478.7	479.3	479.8	480.4	480.9	481.5	482.0	482.6	483.1	483.7	484.2	484.8	485.3
	Isdc	18.1	18.2	18.3	18.4	18.5	18.6	18.7	18.8	18.9	19.0	19.1	19.2	19.3	19.4	19.5	19.6	19.7	19.8	19.9	20.0
	Isdc	4.1	4.1	4.1	4.1	4.1	4.1	4.1	4.1	4.1	4.1	4.1	4.1	4.1	4.1	4.1	4.1	4.1	4.1	4.1	4.1
	Isdc	5.5	5.6	5.7	5.7	5.7	5.7	5.7	5.7	5.7	5.7	5.7	5.7	5.7	5.7	5.7	5.7	5.7	5.7	5.7	5.7
	Isdc	4.7	4.7	4.7	4.7	4.7	4.7	4.7	4.7	4.7	4.7	4.7	4.7	4.7	4.7	4.7	4.7	4.7	4.7	4.7	4.7
	Isdc	440.8	445.9	451.6	454.1	456.6	459.1	461.6	464.1	466.6	469.1	471.6	474.1	476.6	479.1	481.6	484.1	486.6	489.1	491.6	494.1
450	Isdc	479.3	480.0	480.8	481.2	481.7	482.2	482.7	483.2	483.7	484.2	484.7	485.2	485.7	486.2	486.7	487.2	487.7	488.2	488.7	489.2
	Isdc	19.4	19.5	19.6	19.7	19.8	19.9	20.0	20.1	20.2	20.3	20.4	20.5	20.6	20.7	20.8	20.9	21.0	21.1	21.2	21.3
	Isdc	4.1	4.1	4.1	4.1	4.1	4.1	4.1	4.1	4.1	4.1	4.1	4.1	4.1	4.1	4.1	4.1	4.1	4.1	4.1	4.1
	Isdc	5.5	5.6	5.7	5.7	5.7	5.7	5.7	5.7	5.7	5.7	5.7	5.7	5.7	5.7	5.7	5.7	5.7	5.7	5.7	5.7
	Isdc	4.7	4.7	4.7	4.7	4.7	4.7	4.7	4.7	4.7	4.7	4.7	4.7	4.7	4.7	4.7	4.7	4.7	4.7	4.7	4.7
	Isdc	443.4	448.7	454.9	457.9	460.4	462.9	465.4	467.9	470.4	472.9	475.4	477.9	480.4	482.9	485.4	487.9	490.4	492.9	495.4	497.9
500	Isdc	482.2	482.8	483.6	484.0	484.4	484.8	485.2	485.6	486.0	486.4	486.8	487.2	487.6	488.0	488.4	488.8	489.2	489.6	490.0	490.4
	Isdc	20.4	20.5	20.6	20.7	20.8	20.9	21.0	21.1	21.2	21.3	21.4	21.5	21.6	21.7	21.8	21.9	22.0	22.1	22.2	22.3
	Isdc	4.1	4.1	4.1	4.1	4.1	4.1	4.1	4.1	4.1	4.1	4.1	4.1	4.1	4.1	4.1	4.1	4.1	4.1	4.1	4.1
	Isdc	5.5	5.6	5.7	5.7	5.7	5.7	5.7	5.7	5.7	5.7	5.7	5.7	5.7	5.7	5.7	5.7	5.7	5.7	5.7	5.7
	Isdc	4.7	4.7	4.7	4.7	4.7	4.7	4.7	4.7	4.7	4.7	4.7	4.7	4.7	4.7	4.7	4.7	4.7	4.7	4.7	4.7
	Isdc	446.6	451.9	457.9	460.4	462.9	465.4	467.9	470.4	472.9	475.4	477.9	480.4	482.9	485.4	487.9	490.4	492.9	495.4	497.9	500.4

Figure 4

D.D. S. TASK II DELIVERED SPECIFIC IMPULSE  
VERSUS AREA RATIO

$F = 8K$   
 $M.R. = 5.0$



Exit Area Ratio

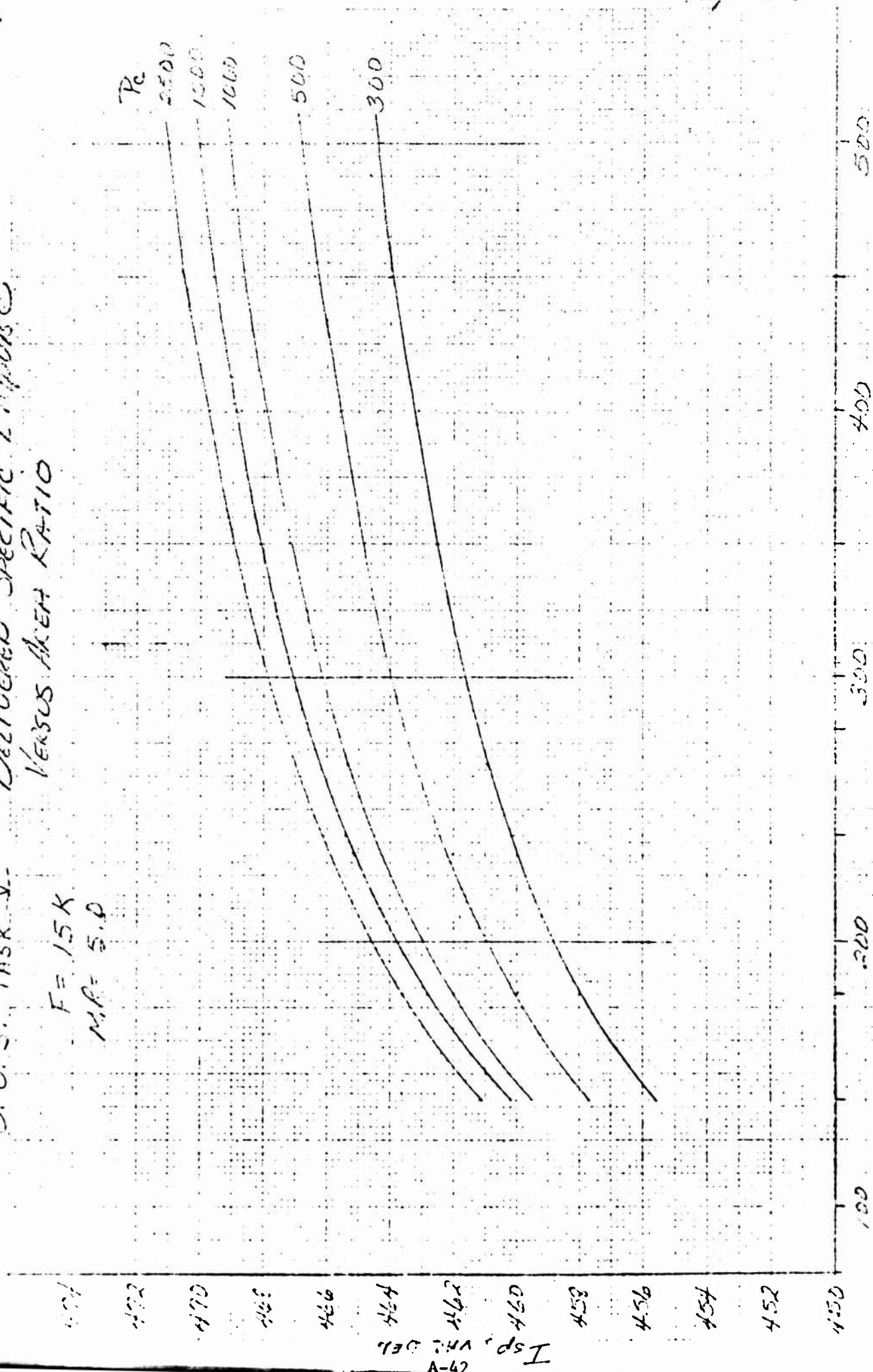
$I_{sp, vac Del}$

Figure 5

D. O. S. TASK V. DELIVERED SPECIFIC IMPULSE  
VERSUS AREA RATIO

$F = 15 K$

$M.P. = 5.0$



EXIT AREA RATIO

$I_{sp, \text{VH, DEL}}$   
A-42

C.O.S. TRUCK V

DELIVERED SPECIFIC TORQUE

VERSUS AREA RATIO

$F = 25K$

$M.R. = 5.0$

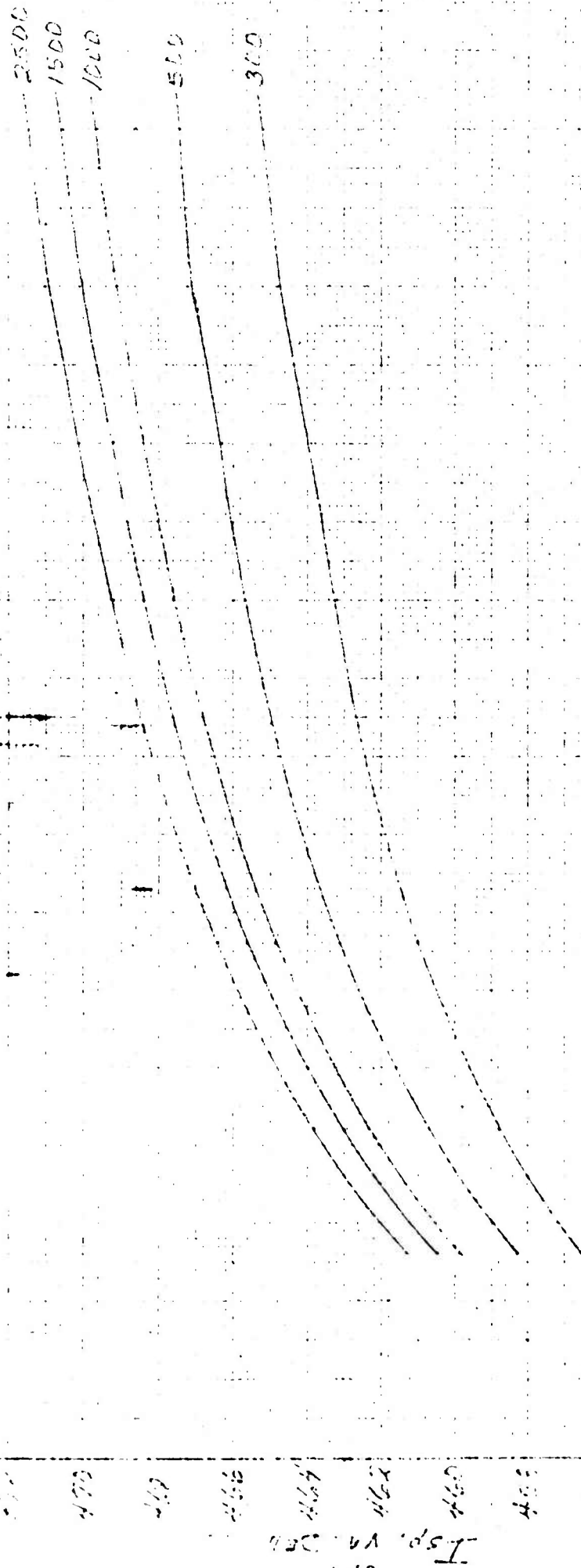
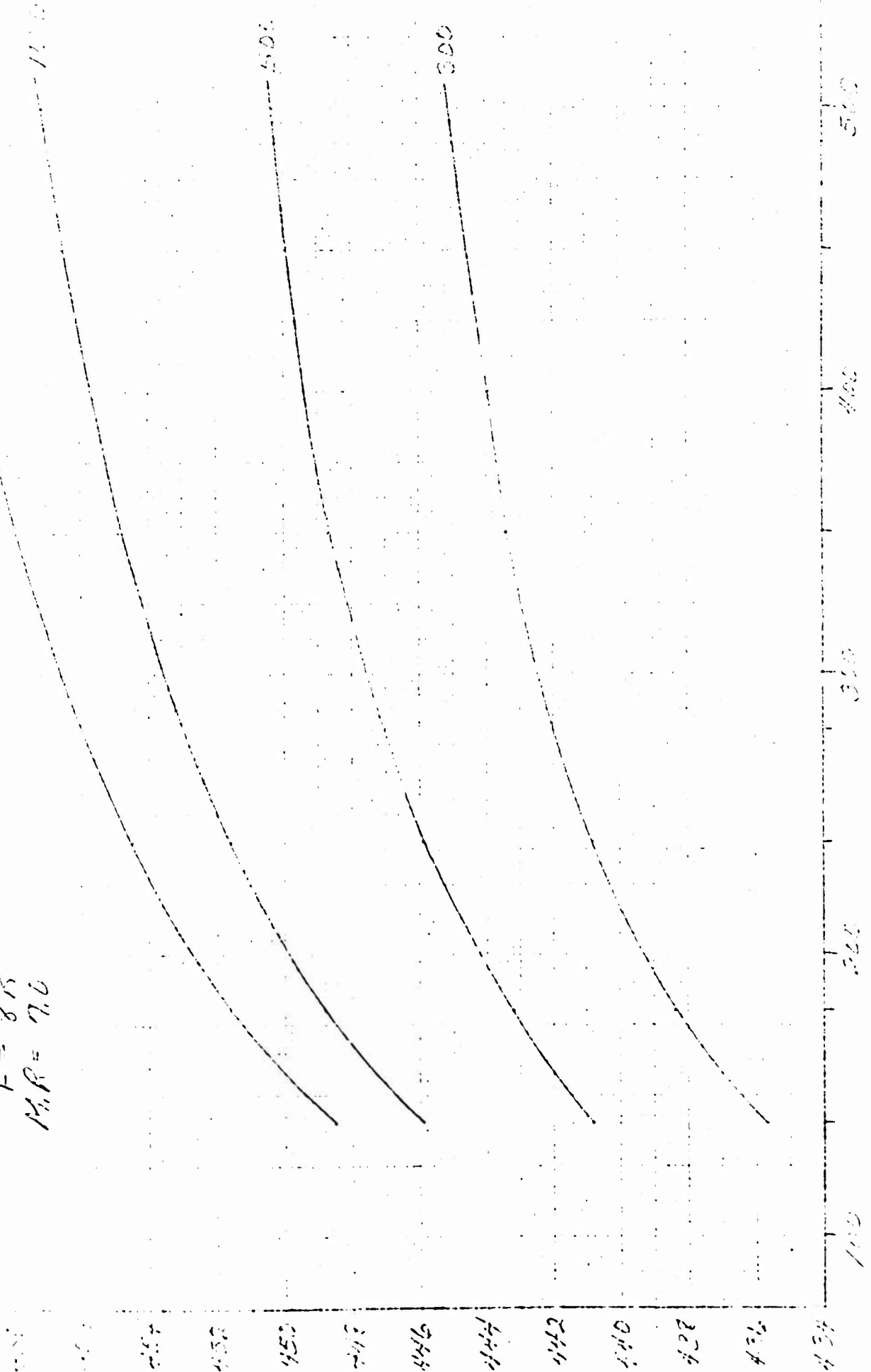


Fig. 10

EXIT AREA RATIO

O.D.S. Task IV Denivered Specific Table  
Versus Area Ratio

$F = 8K$   
 $M_R = 7.0$



Exit Area Ratio



D.O.S. Task V. *Dynamic Specific  
Input-Output Ratio*

$F = 15K$   
 $M.K = 3.0$

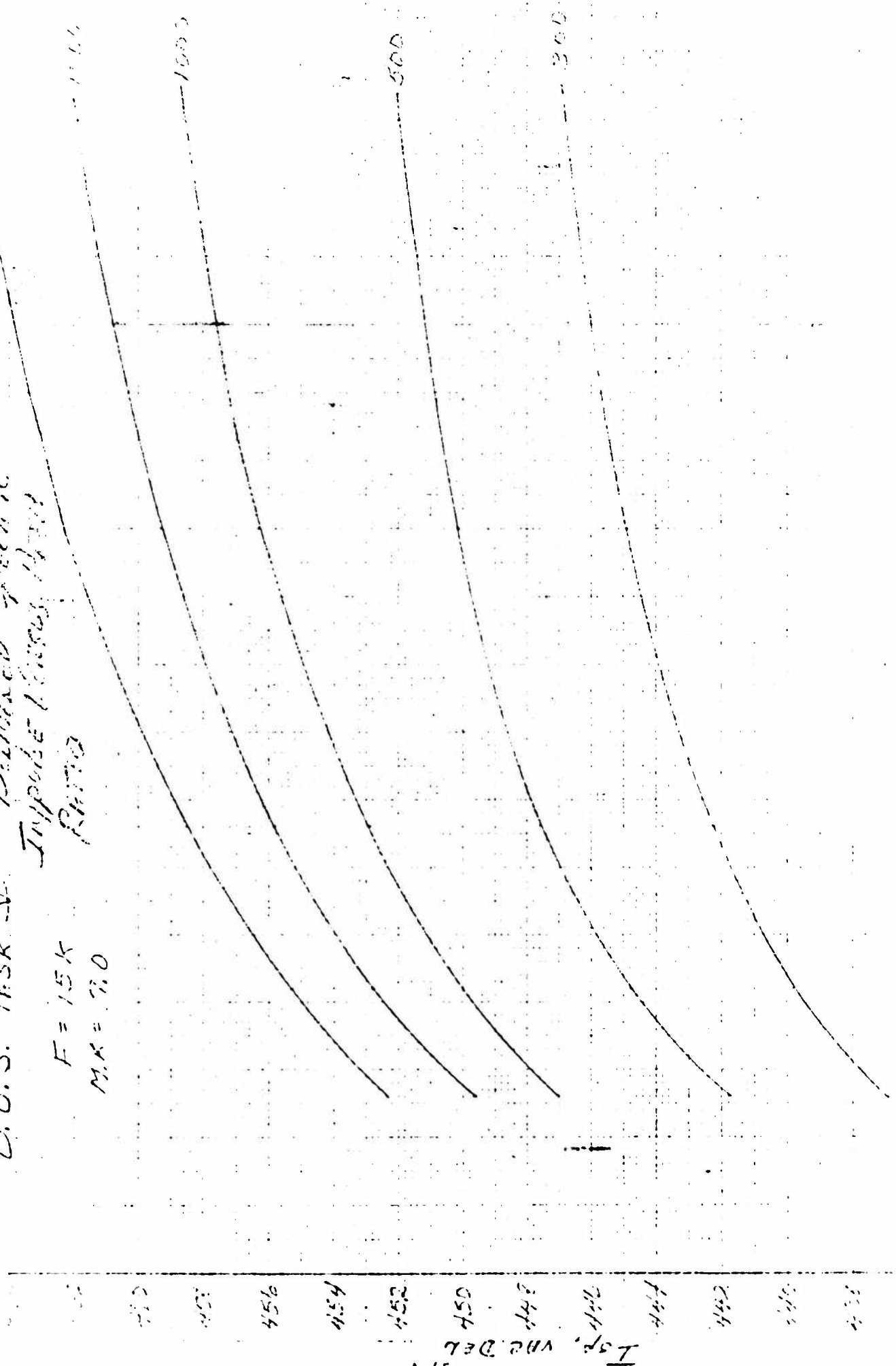


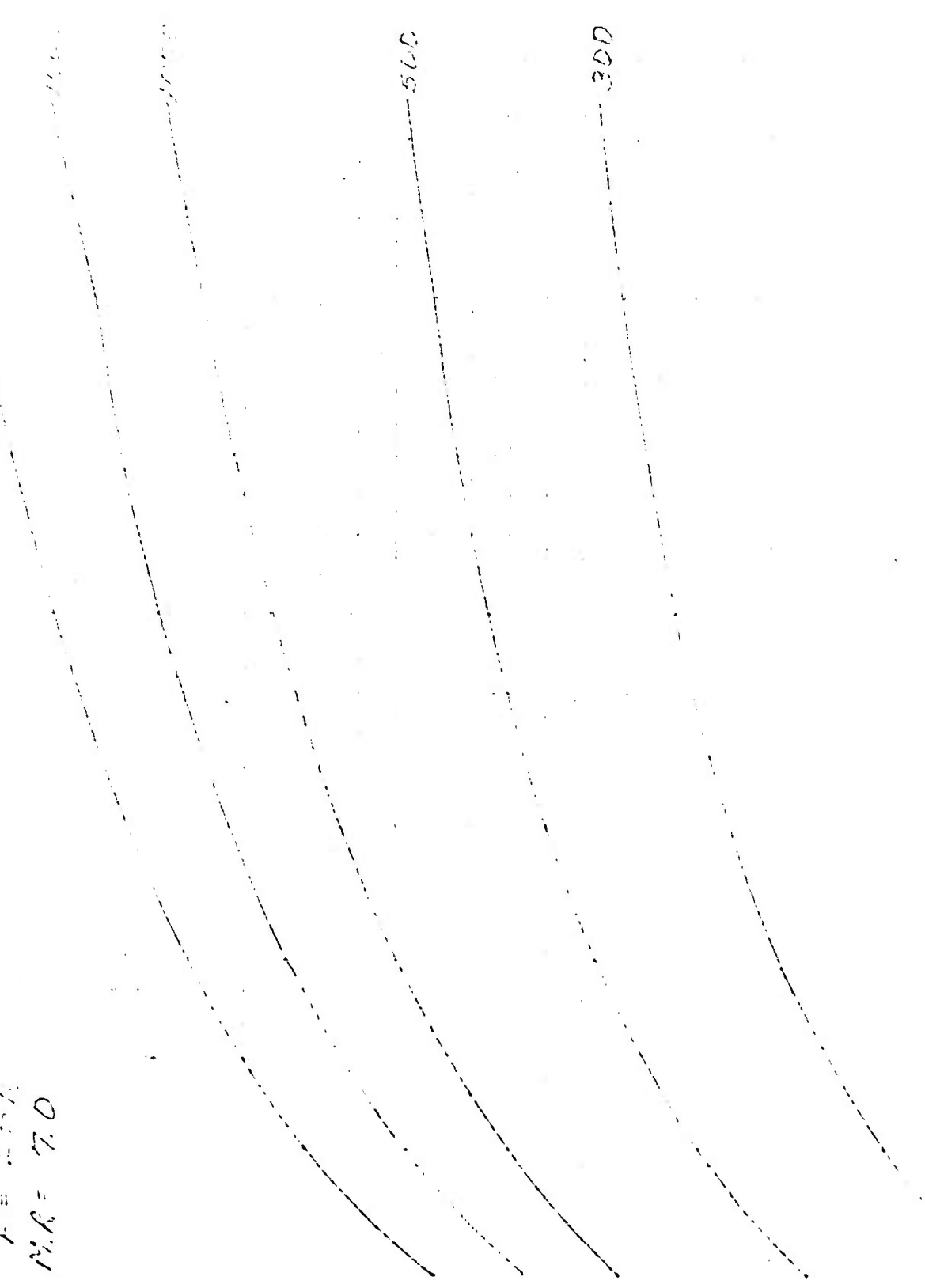
Figure 18



Figure 1

Radius of Gyration  $I_g = 100$   
 Moment of Inertia  $I = 1000$

N.O.S. Test V  
 $F = 2.5k$   
 $M.R. = 7.0$



440 445 450 455 460 465 470 475 480 485 490 495 500 505 510 515 520 525 530 535 540 545 550 555 560 565 570 575 580 585 590 595 600

## INTERIM JANNAF METHODS TCA PERFORMANCE PREDICTION

The OOS performance analyses have been revised in accordance with the performance methodology outlined for the Space Shuttle Main Engine Proposal. The new methodology caused a small change in the one-dimensional equilibrium performance theoretical baseline for OOS performance predictions. The major change involved in the performance revision was the effect of new  $H_2O_2$  system reaction rate constants on the kinetic loss calculation. Figure enclosed lists the four dissociation recombination reactions and four binary exchange reactions, along with their respective rate constants, which were considered in the kinetic loss calculations. Shown are the rates used in previous calculations and those recommended for use on the SSME Proposal. Argon is the "third body" for the dissociation recombination reactions shown in the figure enclosed. This figure is a tabulation of the third body efficiencies relative to Argon for all other species considered. It can be seen that a major change in the updated kinetic loss calculation was the determination of the effect a particular third body has on a given dissociation recombination reaction rate.

## RESULTS AND DISCUSSION

The slight increase in the one-dimensional equilibrium performance baseline for the OOS studies resulted from changes in propellant enthalpies and oxidizer composition. See Reference (b) for an exact breakdown on propellant properties. Theoretical performance was increased from 0.2 to 0.3 lbf-sec/lbm at all mixture ratios.

The effect of the new kinetic reaction rates was to reduce the kinetics loss from 30 to 60 percent of the initial calculation, depending on the mixture ratio, chamber pressure, and thrust level. The reduced kinetics losses resulted in increased delivered vacuum performance at all combinations of thrust and chamber pressure. The effect of performance of the new kinetic

loss calculation was greatest at mixture ratio seven. An example case is shown below to explain the performance gain versus mixture ratio trend caused by revising the kinetics loss.

Thrust = 25,000 lbf       $P_c = 1500$  psia      Area Ratio = 450

<u>Mixture Ratio</u>	<u><math>\Delta KL</math> (old) (lbf-sec/lbm)</u>	<u><math>\Delta KL</math> (new) (lbf-sec/lbm)</u>	<u>Change</u>
5	1.5	0.7	-0.8
6	3.0	1.5	-1.5
7	6.4	3.1	-3.3

After revision of theoretical performance and kinetics losses for all cases, new values of delivered vacuum impulse were calculated. The technique used was similar to that described in Reference (a) for the original analyses. Enclosure (3) through (12) are plots of revised specific impulse versus area ratio for all combinations of mixture, ratio, thrust level, and chamber pressure.

Enclosure (1)

REFERENCE REACTION SET FOR O<sub>2</sub>/H<sub>2</sub> SYSTEM

<u>Reaction</u>	<u>Rate</u>	
	<u>Old</u>	<u>New</u>
$H + OH + Ar \rightarrow H_2O + Ar$	$1.0 \times 10^{19} T^{-1.0}$	$7.5 \times 10^{23} T^{-2.6}$
$H + H + Ar \rightarrow H_2 + Ar$	$7.5 \times 10^{18} T^{-1.0}$	$2.0 \times 10^{18} T^{-0.966}$
$O + O + Ar \rightarrow O_2 + Ar$	$1.9 \times 10^{16} T^{-0.5}$	$1.2 \times 10^{17} T^{-1.0}$
$H + O + Ar \rightarrow OH + AR$	$2.0 \times 10^{18} T^{-1.0}$	$4.0 \times 10^{18} T^{-1.0}$
$H_2 + OH \rightarrow H_2O + H$	$6.0 \times 10^{11} \exp [-5.0/RT]$	$2.19 \times 10^{13} \exp [-5.15/RT]$
$OH + OH \rightarrow H_2O + O$	$1.0666 \times 10^{13} \exp [-0.96671/RT]$	$5.75 \times 10^{12} \exp [-0.78/RT]$
$H + OH \rightarrow H_2 + O$	$1.4 \times 10^{12} \exp [-5.19/RT]$	$7.33 \times 10^{12} \exp [-7.3/RT]$
$OH + O \rightarrow O_2 + H$	$3.2 \times 10^{11} T^{-0.47}$	$1.3 \times 10^{13}$

UNITS:

Recombination Rate

cm<sup>6</sup>/mole<sup>2</sup>-sec

Binary Exchange Rate

cm<sup>3</sup>/mole -sec

Temp, T

°K

RT

Kcal/mole

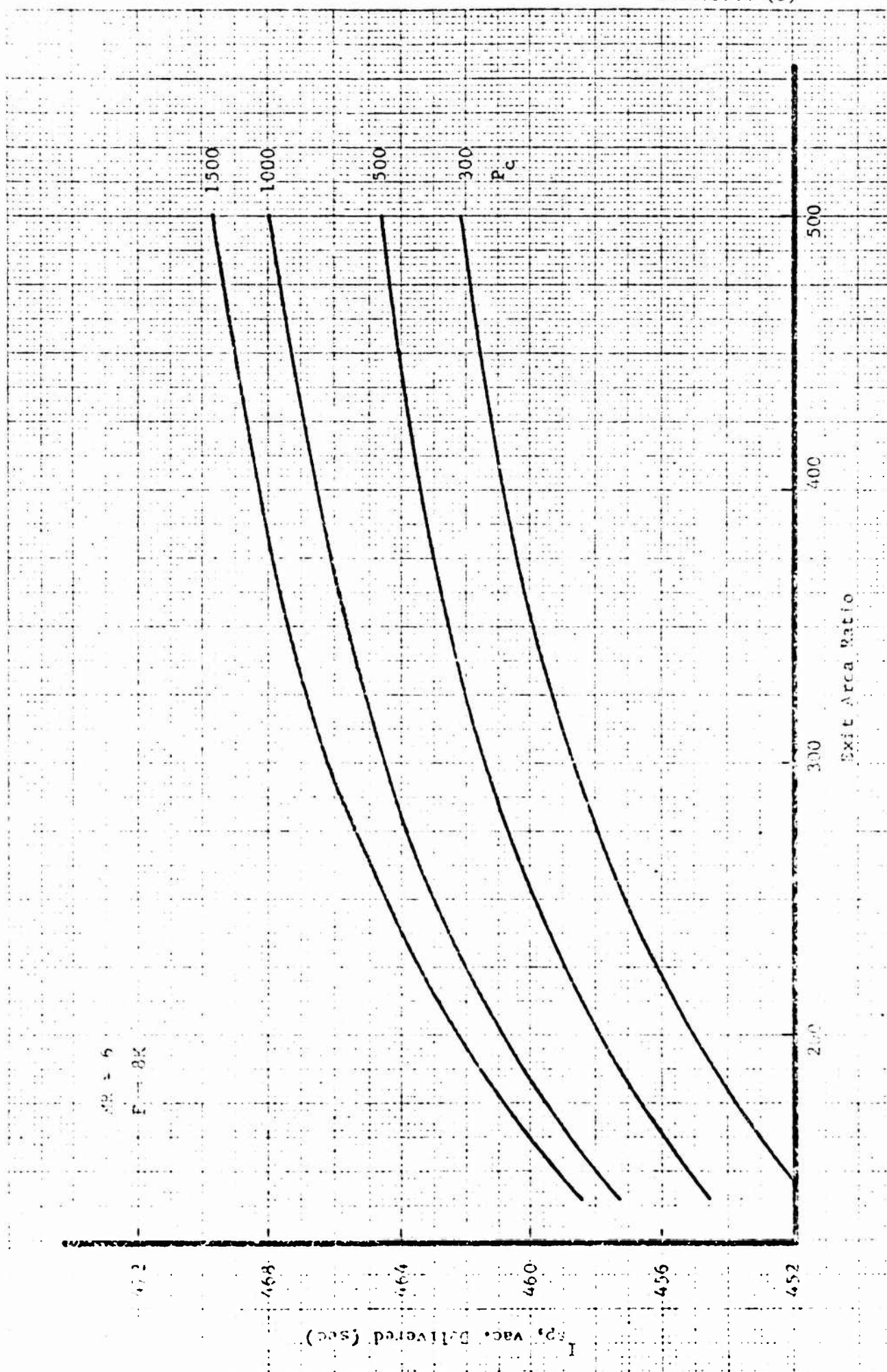
# RF COMBINATION RATE EXPRESSIONS AND THIRD BODY EFFICIENCIES IN THE H-O SYSTEM\*

Recombination System and Base Rate Expression

Third Bodies and Efficiencies	H + OH + Ar		H + H + Ar		O + O + Ar		H + O + Ar	
	Old	New	Old	New	Old	New	Old	New
	$7.5 \times 10^{23} T_K^{-2.6}$		$2.0 \times 10^{18} T_K^{-0.966}$		$1.2 \times 10^{17} T_K^{-1}$		$4 \times 10^{18} T_K^{-1}$	
H <sub>2</sub>	1.0	5	1.0	0.5	1.0	5	1.0	5
H <sub>2</sub> O	1.0	20	1.0	6	1.0	5	1.0	5
O <sub>2</sub>	1.0	5	1.0	0.5	1.0	4.5	1.0	5
N <sub>2</sub>	1.0	4	1.0	0.5	1.0	4	1.0	4
H	1.0	12.5	1.0	9.0	1.0	12.5	1.0	12.5
O	1.0	12.5	1.0	9.0	1.0	12.5	1.0	12.5
OH	1.0	12.5	1.0	9.0	1.0	12.5	1.0	12.5

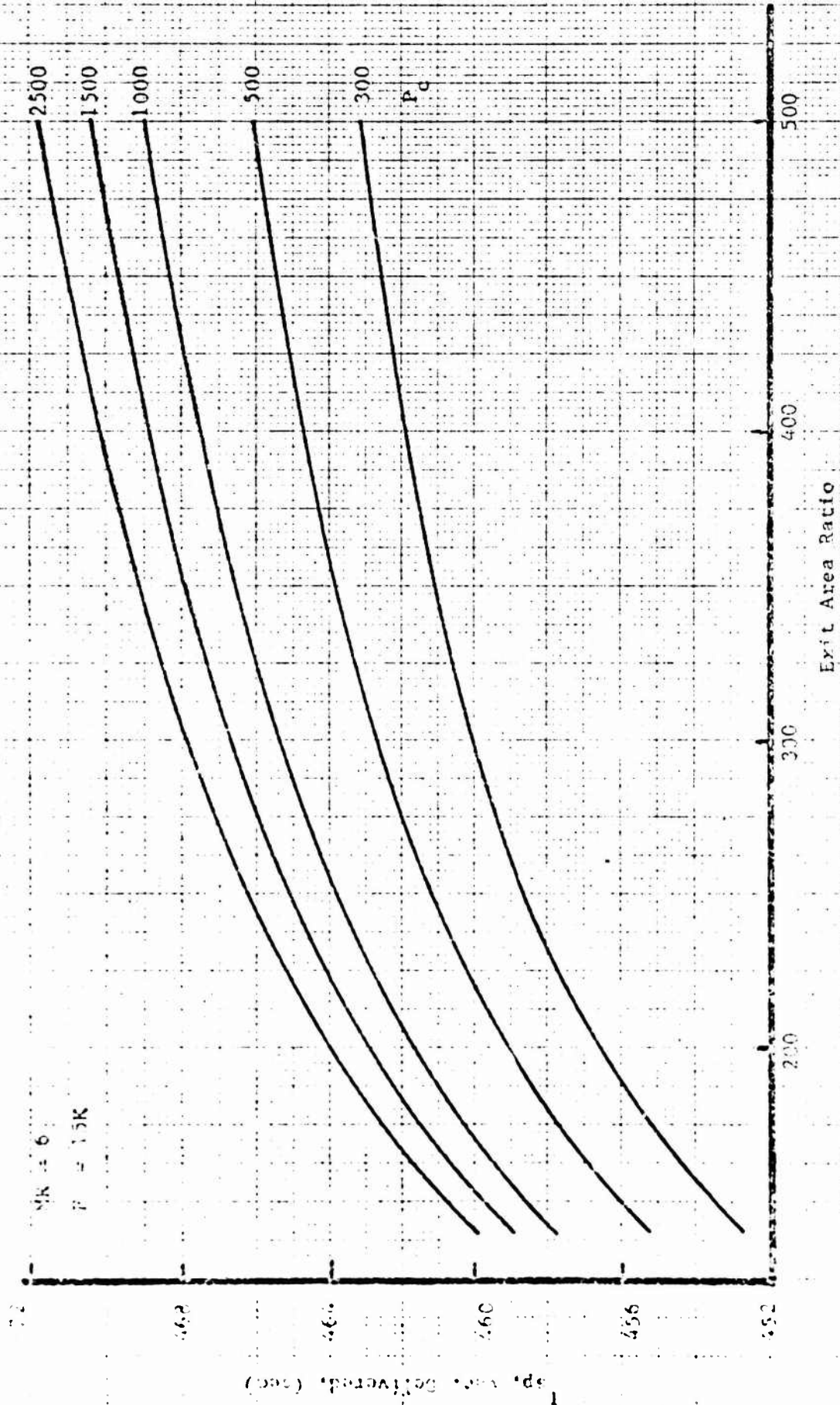
Units: cm<sup>6</sup>/mole<sup>2</sup>-sec

Enclosure (2)



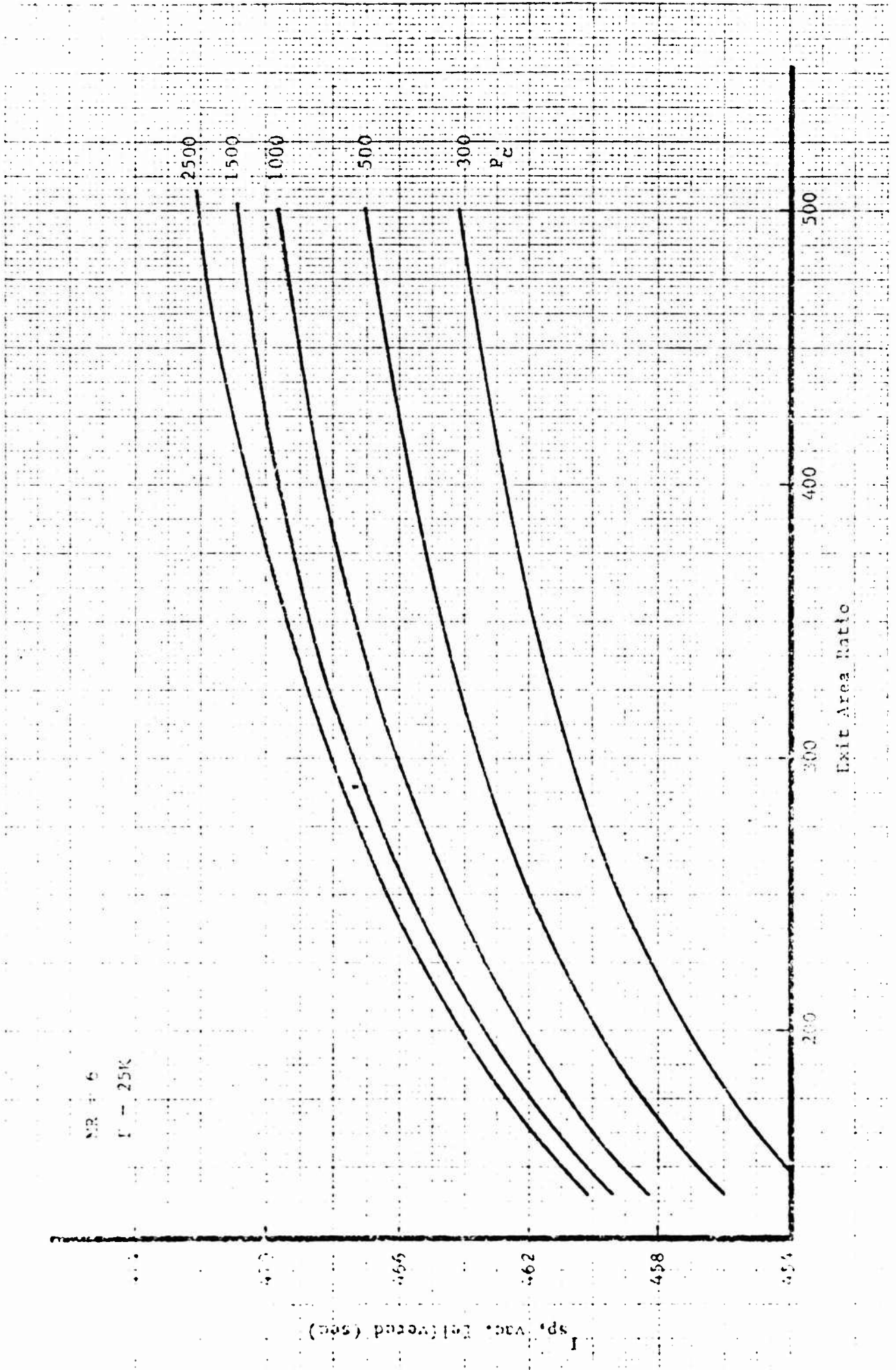
EUGENE DIEZGEN CO.  
MADE IN U.S.A.

NO. 347-100 DIEZGEN GRAPH PAPER  
100% RECYCLED PAPER



Revised Performance, Mixture Ratio = 6,  
Thrust = 15K lbf



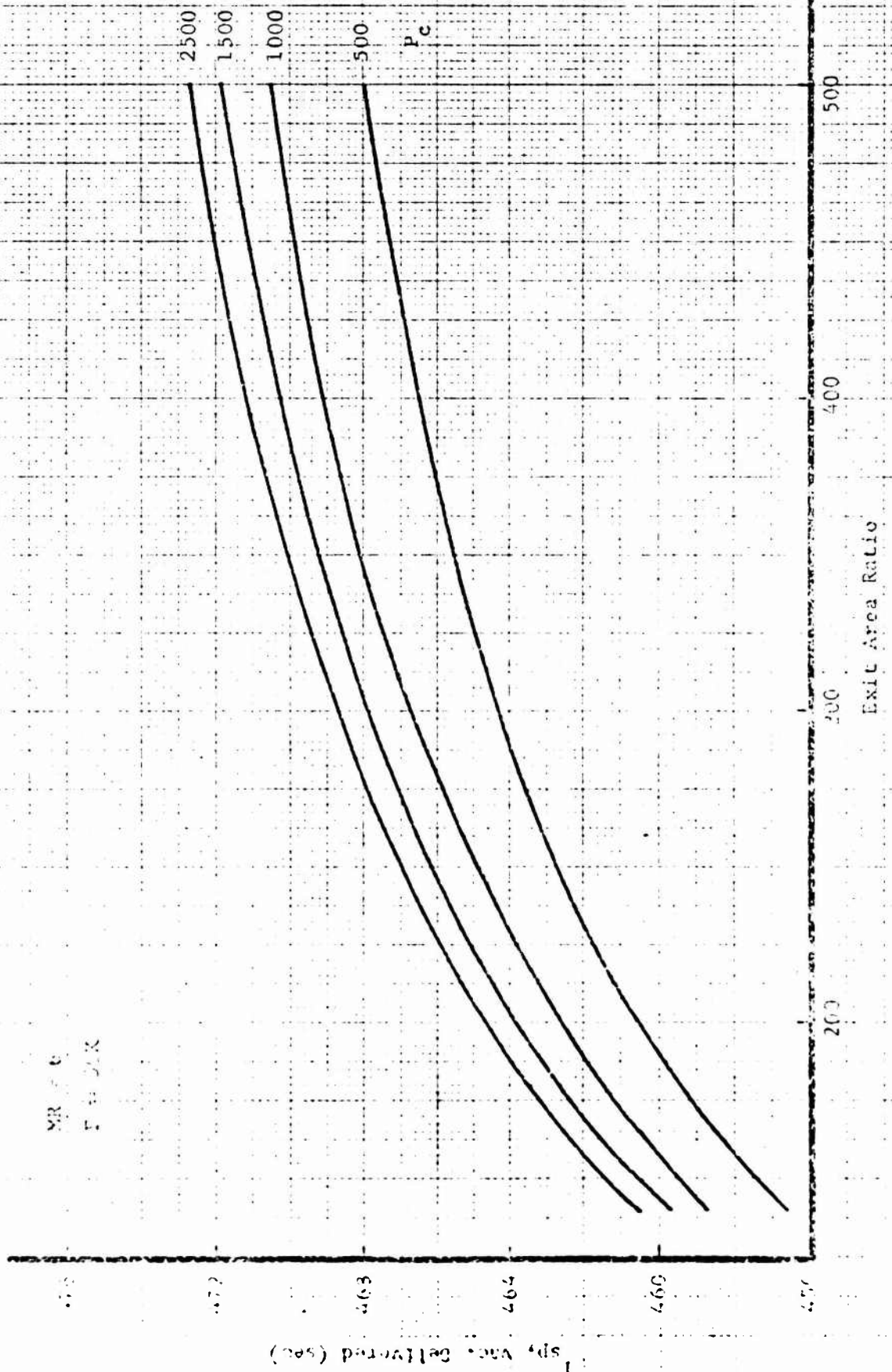


Revised Performance, Mixture Ratio = 6,  
Thrust = 25K lbf

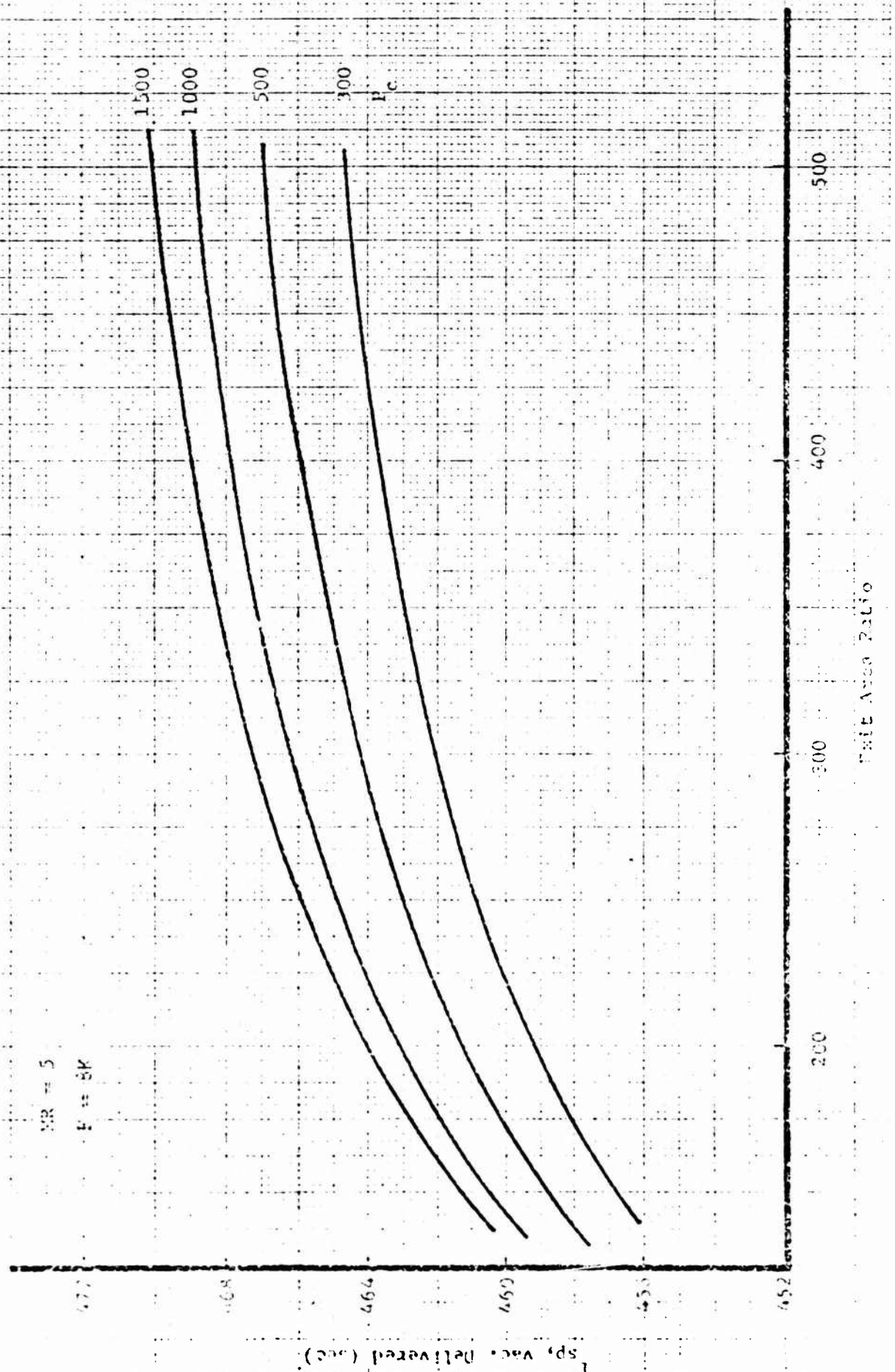


PURVIS DIETZEN CO.  
WILMINGTON, DE.

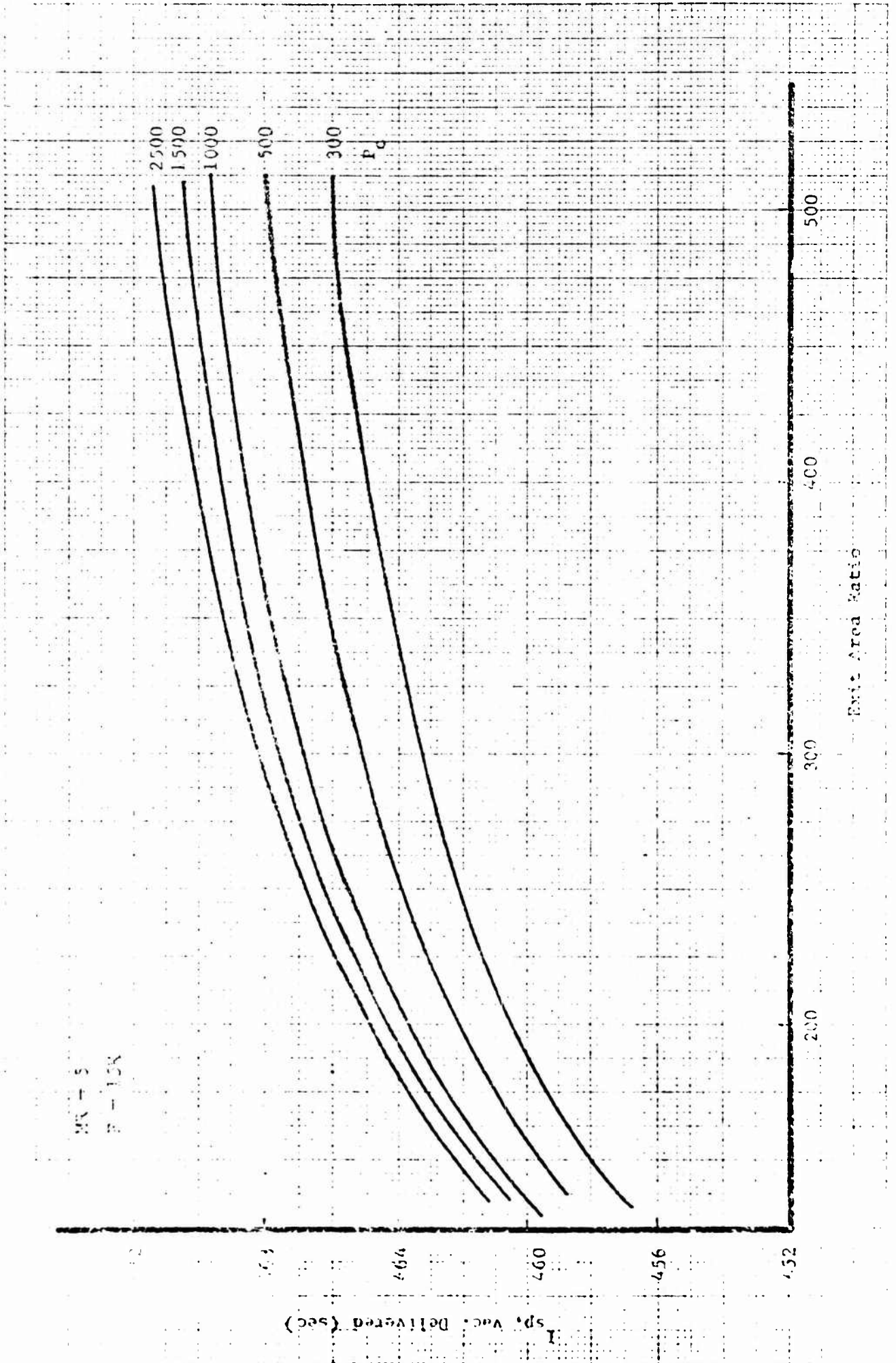
REVISION 1, 10/10/60, CRASH DATA  
REVISION 2, 10/10/60, CRASH DATA



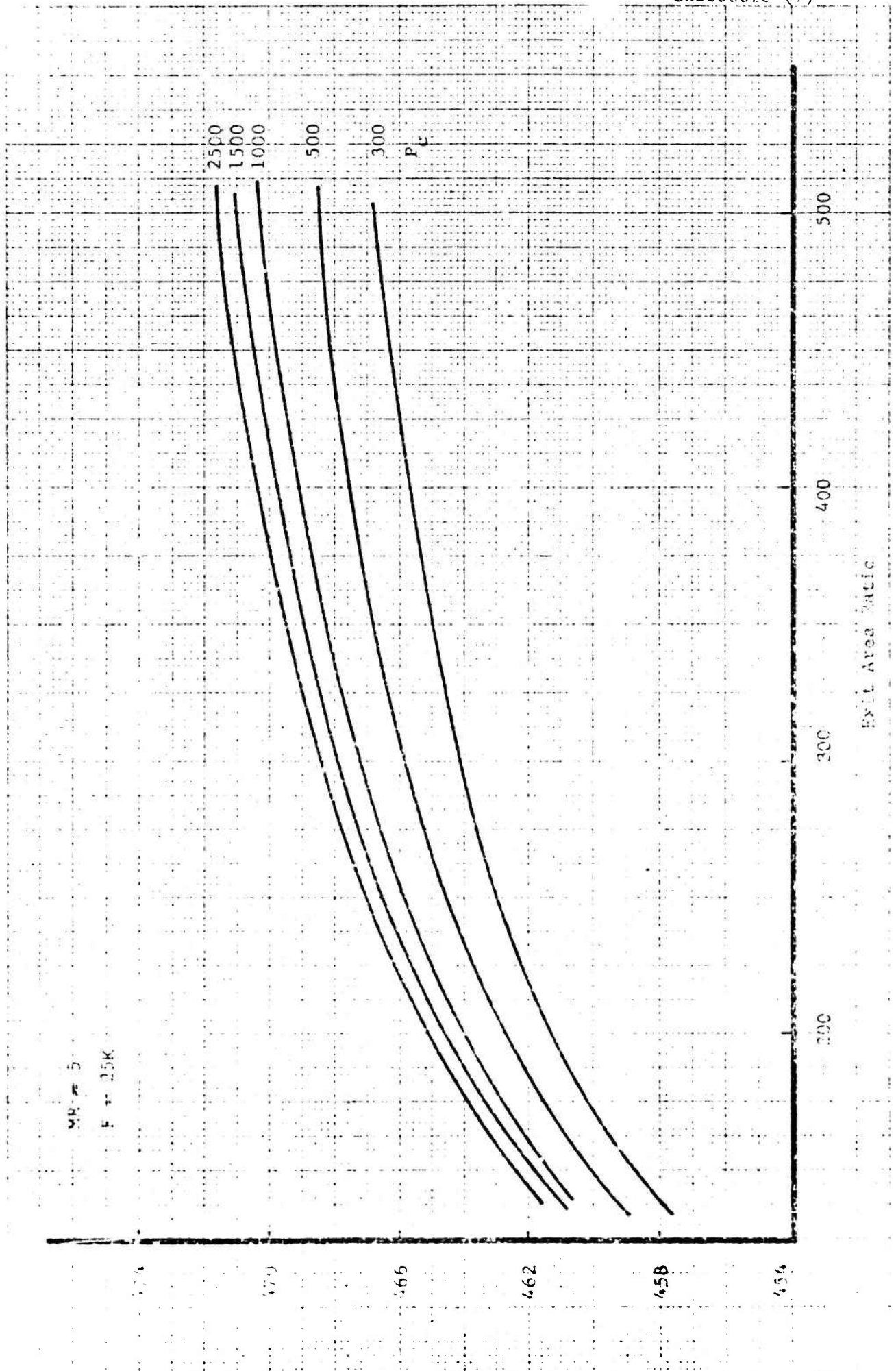
Revised Performance, Mixture Ratio = 6,  
Thrust = 50K lbf



Revised Performance, Mixture Ratio = 5,  
Thrust = 8K lbf



Revised Performance, Mixture Ratio = 5,  
 Thrust = 15K lbf

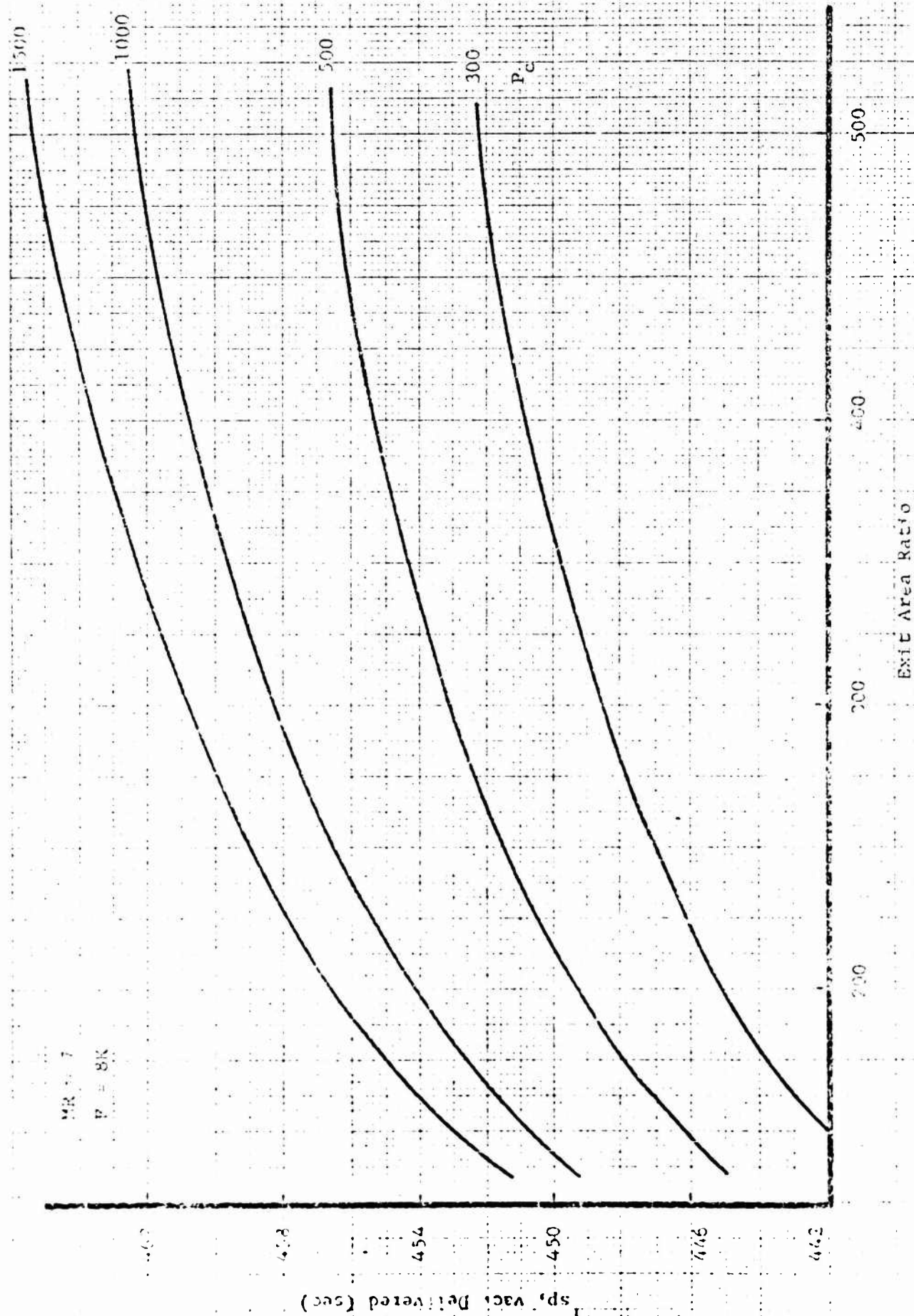


Revised Performance, Mixture Ratio = 5,  
Thrust = 25K lbf

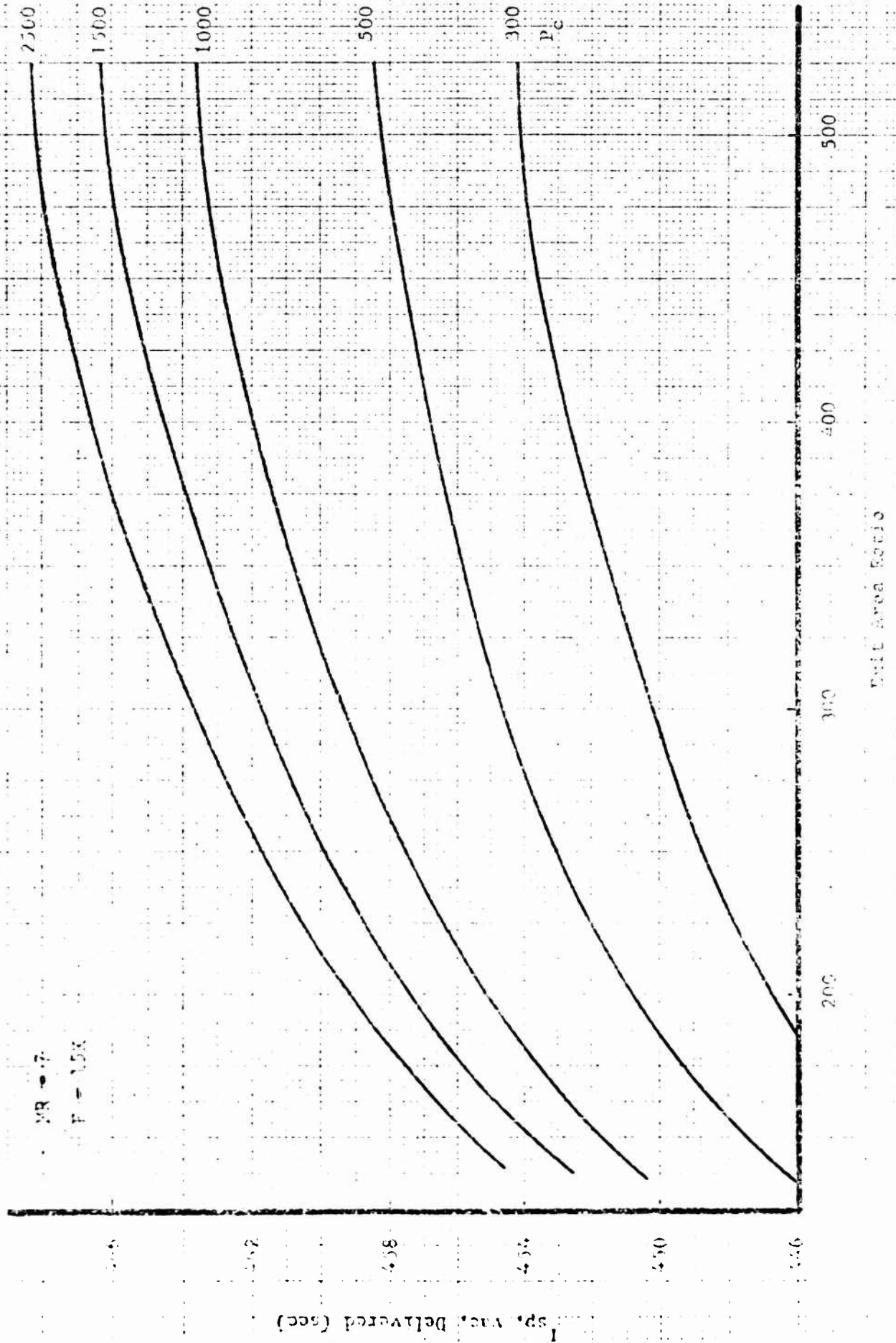


FUGRO DIERZEN CO.  
MASSACHUSETTS

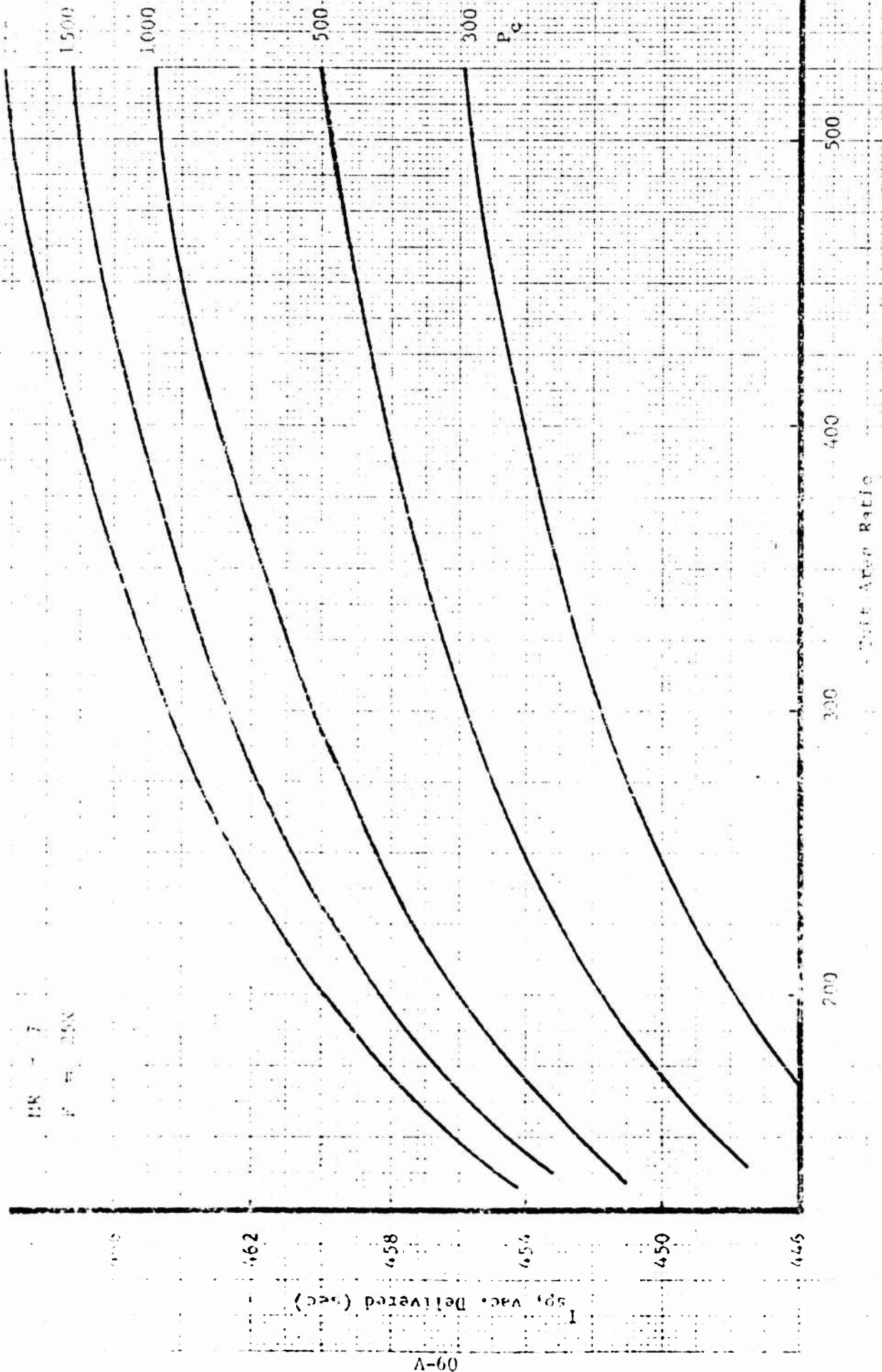
NO. 100-1000, DISTRICT ENGINEER, MAINE



Revised Performance, Mixture Ratio = 7,  
Thrust = 8K lbf



Revised Performance, Mixture Ratio = 7,  
Thrust = 15K lbf



Revised Performance, Mixture Ratio = 7,  
Thrust = 25K lbf

**Appendix B**

**HEAT TRANSFER ANALYSIS**



Enclosed is the final report summarizing the heat transfer analytical support given to Task IV and Task V of the OOS program. This effort involved an extensive parametric study with engine thrust, chamber pressure, mixture ratio, and engine cycles. A radiation-cooled nozzle extension, a tube-bundle nozzle extension, and a copper nozzle were the components investigated in the study. This report covers analyses conducted from March 9, 1971 through May 7, 1971.

28 May 1971

TCER 9641:0116

OOS TASK IV AND TASK V  
HEAT TRANSFER ANALYSIS

FINAL REPORT

28 May 1971

By

A. C. Kobayashi

Approved by:

F. H. Miller, Supervisor  
Thermodynamics  
Engine Components Department

A E R O J E T   L I Q U I D   R O C K E T   C O M P A N Y  
Engine Components Department                      Sacramento, California

## TABLE OF CONTENTS

	<u>Page</u>
I INTRODUCTION	1
II RADIATION-COOLED NOZZLE EXTENSION	1
A. Introduction and Assumption	1
B. Results and Conclusions	2
III TUBE BUNDLE NOZZLE EXTENSION	2
A. Tube-Bundle Coolant Outlet Study	3
1. Analytical Approach	3
2. Results	3
B. Tube-Bundle Coolant Inlet Study	4
1. Analytical Approach	4
2. Results	5
C. Tube-Bundle Coolant Bulk Temperature Rise and Pressure Drops	5
IV COPPER NOZZLE	6
A. Copper Nozzles, $8 = \text{in.}$ Chamber, $MR = 6.0$	6
1. Analytical Approach	6
a. Nozzle Geometry	6
b. Gas-Side	6
c. Coolant-Side	7
d. Parametric Study at $MR = 6.0$	8
(1) 8K Thrust	8
(2) 14.15K Thrust	9
(3) 25K Thrust	9
e. The Effect of Chamber Length as Pressure Drop and Temperature Rise	9

Table of Contents (cont.)

	<u>Page</u>
f. Mixture Ratio Parameter Study	10
V CONCLUDING REMARKS	10

## LIST OF FIGURES

<u>Figure No.</u>		<u>Page</u>
1	Radiation View Factor Through Nozzle Exit	
2	Radiation-Cooled Nozzle Extension Wall Temperatures	
3	Tube-Bundle to Copper Nozzle Transition Area Ratio Study Coolant Outlet	
4	Tube-Bundle Coolant Inlet Parameter Study	
5	Copper Nozzle Geometry	
6	Copper Nozzle Coolant Inlet Parameters @ MR = 6.0	
7	8K Thrust - Effects of Mach No. on Thermal Parameters	
8	8K Thrust - Effects of $P_c$ on Thermal Parameters	
9,10	14.15K Thrust - Effects of Mach No. on Thermal Parameters	
11	14.15K Thrust - Effects of $P_c$ on Thermal Parameters	
12,13	25K Thrust - Effects of Mach No. on Thermal Parameters	
14	25K Thrust - Effects of $P_c$ on Thermal Parameters	
15	Pressure Drop Per Inch of Chamber Length	
16	Coolant Bulk Temperature Rise Per Inch of Chamber Length	
17	Correction for Mixture Ratio Applied to Values at MR = 6.0	

## NOMENCLATURE

$A$	=	flow area
$C_p$	=	heat capacity
$d$	=	diameter
$h$	=	heat transfer coefficient
$k$	=	thermal conductivity
$Nu$	=	Nusselts Number, $hd/k$
$Pr$	=	Prandtl number, $C_p \mu / k$
$T$	=	Temperature
$\dot{W}_T$	=	total propellant flow
$\rho$	=	density
$\mu$	=	viscosity
$\nu$	=	kinematic viscosity

### Subscript

$b$	=	bulk
$f$	=	film
$w$	=	wall

## I INTRODUCTION

The Orbit-to-Orbit Shuttle (OOS) contract is a throttleable,  $\text{LO}_2/\text{LH}_2$  engine study program involving a "rubber" engine with varying thrust ( $F$ ), varying chamber pressures ( $P_c$ ), a  $F/P_c$  range of 10 to 40, and varying combustion mixture ratios (MR). Engine cycle variation is another important variable, i.e., staged-combustion cycle, bleed cycle, expander cycle, and gas-generator cycle. These variables were investigated to determine the effects upon the heat transfer parameters of the engine.

Task IV and Task V heat transfer studies can be divided into three major categories, (1) radiation-cooled nozzle extension, (2) tube-bundle nozzle extension, and (3) copper nozzle thrust chamber. The purpose of this report is to summarize and document the heat transfer analysis in support of these tasks.

## II RADIATION-COOLED NOZZLE EXTENSION

### A. INTRODUCTION AND ASSUMPTIONS

A parametric study was conducted to determine the radiation-cooled nozzle extension wall temperatures for thrust to chamber pressure ratio ( $F/P_c$ ) varying from 10 to 50. Wall temperatures were calculated for area ratios from 60 to 500 with no film cooling.

The  $\text{LO}_2/\text{LH}_2$  combustion gas transport properties for a mixture ratio (MR) of 6.0 were used for  $P_c = 500, 1000, 1500, \text{ and } 2500$  psia for a 25K thrust engine or for  $F/P_c$  of 10 to 50. The wall material was assumed to have an emissivity of 0.85 both on the interior and exterior surfaces.

The exterior surface was assumed to radiate to space with a view factor of 1.0 while the interior surface was assumed to radiate out the nozzle exit at the 500:1 area ratio; the corresponding calculated interior view factor is shown in Figure (1). The 500:1 area ratio nozzle contour used for this study is reported in Ref. 1.

## B. RESULTS AND CONCLUSIONS

The results of this study are shown in Figure (2) where a plot of wall temperatures versus area ratio for varying  $P_c$  is shown. This figure may be used to determine the area ratio at which the radiation-cooled extension may be utilized. For example, refractory metals are limited to a maximum design temperature of approximately 2200°F which limits the design to a minimum area ratio of approximately 225:1 at  $P_c = 500$  psia or 475:1 for  $P_c = 2500$  psia. On the other hand, material such as AGCarb-101 has higher allowable design temperatures which permits the radiation-cooled extension to begin at lower area ratios, e.g., approximately 40:1 at  $P_c = 500$  psia and 190:1 at  $P_c = 2500$  psia. If gas-side film cooling were to be applied, lower wall temperature will result allowing designs to lower area ratios.

The wall temperature curves in Figure (2), therefore, allows the selection of the transition area ratio (without film cooling) at which radiation-cooled nozzle extension may begin for most material design temperatures.

## III TUBE-BUNDLE NOZZLE EXTENSION

The tube-bundle nozzle extension parameter study was again a preliminary study to determine the following three items: (1) the coolant outlet



area ratio, i.e., the copper-nozzle to tube-bundle transition point, (2) the coolant inlet area ratio, and (3) the coolant bulk temperature rise and pressure drop through the tube-bundle. The following paragraphs discuss the assumption and the results of these three items.

#### A. TUBE-BUNDLE COOLANT OUTLET STUDY

The purpose of this parametric study was to generate results which can be used as a guide in selecting the copper-nozzle to tube-bundle transition area ratio; the design parameter would be the gas-side wall temperature of the tube.

##### 1. Analytical Approach

The hot-gas-side parameters covered a range of  $F/P_c$  of 16.7 to 83.3, i.e.,  $P_c = 300, 500, 1000, 1500$  psia at the 25K thrust levels all at  $MR = 6.0$ . A coolant outlet temperature ( $250^\circ R$ ) and pressure (2200 psia) were estimated based upon previous calculations conducted for the OOS proposal. The parametric study involved a point study at five area ratios (6, 8, 10, 14 and 20), and for varying coolant outlet velocities achieved by varying the number of 0.015-in. wall, 0.250-in. dia. tubes. The results of this study is shown in Figure (3).

##### 2. Results

The gas-side tube wall temperatures (TWG) versus coolant outlet velocity for various area ratios are shown in Figure (3) with  $P_c$  cross-plots. As anticipated, the lower area ratios require higher coolant velocities and lower  $P_c$  to maintain constant wall temperatures. For example, for a  $1500^\circ F$  wall temperature, a coolant velocity of approximately 35 ft/sec is required

for an area ratio of 20:1 ( $P_c = 350$  psia), but a velocity of 85 ft/sec is required at 6:1 ( $P_c = 500$  psia). This figure may be used as a guide in selecting the transition area ratio between the tube bundle and the copper nozzle, for a constant  $P_c$  or constant  $T_{wg}$ . Increasing coolant velocities results in increasing pressure drop, therefore, it is desirable to minimize outlet velocities.

## B. TUBE-BUNDLE COOLANT INLET STUDY

This study was very similar to the previous tube-bundle coolant outlet parametric study. The purpose here was to determine the coolant inlet area ratio since cooling with cold hydrogen (50 to 60°R) is more difficult than heated hydrogen (150 - 250°R) primarily due to the difference in transport properties.

### 1. Analytical Approach

The same hot gas-side parameters as the coolant outlet studies were used. The coolant-side inlet bulk temperatures and pressures were varied with  $P_c$  as follows:

$P_c$ psia	300	500	1000	1500	2500
$T_{IN}$ , °R	54	68	85	100	140
$P_{IN}$ , psia	700	1180	2300	3500	5900

The coolant inlet temperatures increase with increasing inlet pressure due to the energy input by the pump, assuming a pump efficiency of 50 percent. The analytical procedure was to make a point study of varying area ratios and coolant velocities using the above coolant inlet parameters.

## 2. Results

Figure (4) is a summary of the tube-bundle coolant inlet study showing the gas-side tube wall temperatures versus coolant velocity for varying area ratios. Those curves may be used as a guide to select the coolant inlet area ratio for the tube bundle.

### C. TUBE-BUNDLE COOLANT BULK TEMPERATURE RISE AND PRESSURE DROPS

A preliminary tube-bundle nozzle extension parameter study was conducted to determine the coolant bulk temperature rise and pressure drop; these results are preliminary because the design of this component is not yet finalized. The primary purpose of this analysis was to obtain coolant bulk temperatures and pressures to be used as an inlet parameter for the subsequent copper nozzle study. The tube bundle consisted of a two-pass system with an exit area ratio of 225:1.

A  $F/P_c$  range of 10 to 50 was investigated and the following is a summary of the analysis.

$F/P_c$	10	16.7	25	50
MR	6.0	6.0	6.0	6.0
$T_{IN}, ^\circ R$	140	100	85	68
$P_{IN}, \text{psia}$	5900	3500	2300	1180
Inlet & Exit $A_c/A_t$	6.5	5.5	6.0	6.5
$\Delta T$	89	132	169	254
$\Delta P$	77	71	68	60

IV COPPER NOZZLE

The parametric study of the copper nozzle section was the major task of this OOS heat transfer analysis. Every parameter that would affect the various engine cycles was included in this extensive effort. The following is a detailed discussion of the analytical approach and the results.

Initially the study was conducted at  $MR = 6.0$  for an 8-in. chamber length, i.e., distance from injector face to throat. An additional study was subsequently made to determine, (1) the effect of increased chamber length on coolant pressure drop and temperature rise and (2) the effect of mixture ratio ( $MR = 5.0$  and  $7.0$ ).

A. COPPER NOZZLE, 8-IN. CHAMBER,  $MR = 6.0$ 1. Analytical Approach

## a. Nozzle Geometry

Three Zirconium-copper nozzle contours were assumed to obtain three chamber pressures ( $P_c$ ) at each of three thrust levels analyzed ( $F = 8, 14.15$  and  $25K$ ). The contours and coolant channel widths versus axial distance were held constant at each thrust level as shown in Figure (5); the number of channels were varied for each contour to maintain the channel width shown. However, the channel heights were varied with each thrust and  $P_c$  variations to achieve throat Mach numbers of approximately 0.5; a typical channel height profile is also shown in Enclosure (5).

## b. Gas-Side

The gas-side heat transfer coefficient used was

a modified form of the simplified Bartz (Ref. 2) correlation as follows:

$$*h_g = 0.026 \frac{1}{d^{0.2}} \left[ \frac{C_p \mu}{Pr} \right]^{0.2} \left[ \frac{W_T}{A} \right]^{0.8}$$

A nomenclature description is included at the conclusion of this report.

In the expansion region of the nozzle the gas-side coefficient included a two-dimensional axisymmetric flow correction.

### c. Coolant-Side

The following Hess and Kunz (Ref. 3) heat transfer correlation was used for the  $LH_2$  coolant.

$$*Nu_f = 0.0208 \left[ \frac{\rho_f v_b d}{\mu_f} \right]^{0.8} Pr_f^{0.4} (1 + 0.01457 \mathcal{X}_w / \mathcal{X}_b)$$

The constant of the coefficient (0.208) in the above correlation was reduced to 0.0177 for the straight tube section; 0.0208 was used in the throat region only, to account for increased cooling due to the throat curvature.

For each thrust and  $P_c$ , three coolant inlet total pressure to  $P_c$  ratios ( $P_{in}/P_c$ ) were investigated. These were  $P_{in}/P_c = 2.5$ , 2.1 and 1.8 representing approximately the following engine cycles respectively, the expander cycle, the staged-combustion cycle, and the bleed cycle. Each  $P_{in}/P_c$  ratio required different copper nozzle coolant inlet temperature and pressures, and these inlet parameters all included the  $\Delta T$  and  $\Delta P$  of the tube bundle. The coolant inlet parameters for the copper nozzle at  $MR = 6.0$  are given in Figure (6).

\* See Nomenclature at beginning of report.

## d. Parametric Study at MR = 6.0

At each of the three thrust levels, (F = 8K, 14.15K, and 25K) three  $P_c$  levels were studied for each of the three  $P_{in}/P_c$  ratios. At each  $P_c$ , channel height was varied uniformly along the nozzle to achieve three throat Mach numbers around 0.5. Thermal-cycle life,  $\Delta T_w$ , and gas-side wall temperatures ( $T_{wg}$ ) at the throat with coolant pressure drop ( $\Delta P$ ) and temperature rise ( $\Delta T$ ) are the primary parameters of interests. The results of these studies and the interrelationships of these parameters are discussed in the following paragraphs.

## (1) 8K Thrust

The effect of coolant velocity or throat Mach number on  $\Delta T_w$ ,  $T_{wg}$ , and  $\Delta P$  for varying  $P_{in}/P_c$  ratios at  $P_c = 275, 485, \text{ and } 850 \text{ psia}$  are shown in Figure (7). The  $\Delta T_w$  and  $T_{wg}$  are quite insensitive to Mach numbers, between 0.36 and 0.54. The coolant pressure drops are affected especially at the higher  $P_c$  levels. For example, at  $P_{in}/P_c$  ratio of 2.1, the  $\Delta P$  at Mach no. of 0.5 is predicted to be approximately 800 psi while at 0.4 it is 500 psi.

A cross plot of Figure (7) is shown in Figure (8) where the effects of  $P_c$  (300 to 1200 psia) are shown for the same parameters. All parameters increase with increasing  $P_c$ . These curves indicate that for a constant  $P_c$  and a constant Mach number,  $\Delta T_w$  increased with decreasing  $P_{in}/P_c$  ratio while at the same time the  $\Delta P$  decreases with decreasing  $P_{in}/P_c$  ratio. For  $P_{in}/P_c$  ratio of 2.1 and Mach no. of 0.5, the  $\Delta T_w$  increase from 500 to 900 as  $P_c$  increases from 275 to 1100 psia. For the same condition the  $\Delta P$  increases from 250 to 1175 psi.

## (2) 14.15K Thrust

The  $\Delta T_w$  and  $T_{wg}$  vs. Mach number are shown in Figure (9) while  $\Delta P$  vs Mach number is shown in Figure (10). A cross plot of  $\Delta T_w$ ,  $T_{wg}$ ,  $T_B$  out and  $\Delta P$  vs  $P_c$  (500 to 1500 psia) are shown in Figure (11). All parameters are higher than at the 8K level. For example, at  $P_{in}/P_c$  ratio of 2.1 and Mach number of 0.5,  $\Delta T_w$  increases from 575 to 950 as  $P_c$  increases from 450 to 1600 psia. Pressure drop increases substantially from 400 to 1400 over the same  $P_c$  range.

## (3) 25K Thrust

The effects of Mach number are shown in Figures (12) and (13) for the 25K thrust studies. The cross-plot, shown in Figure (14) covers a  $P_c$  range of 850 to 2600 psia. At this thrust and  $P_c$  levels the thermal parameters are affected quite substantially. For example, the  $\Delta T_w$  at Mach number of 0.5 at  $P_{in}/P_c$  ratio of 2.1, increases from 650 to 1050 as  $P_c$  increases from 850 to 2500 psia. The  $\Delta P$  at these same conditions increases from 800 to 2500 psi. However, the  $\Delta P$  is greatly affected by the Mach number, e.g., the  $\Delta P$  at Mach number of 0.4 is 1500 psi at  $P_c = 2500$  psia.

e. The Effect of Chamber Length on Pressure Drop and Temperature Rise

All the previous results were based upon a chamber length of 8 in. (injector face to throat). It may be desirable to increase the chamber length, the cylindrical section, to increase the coolant bulk temperature rise, however, a corresponding increase in  $\Delta P$  would occur. In this study, the coolant channel height is assumed constant.



Figure (15) represents the effect of chamber length upon coolant pressure drop per inch of chamber length ( $\Delta P/\text{in.}$ ). Pressure drop is apparently independent of thrust but is affected by  $P_c$ , throat Mach number, and engine cycle, i.e.,  $P_c/(P_{in}/P_c)$  ratios of 2.5, 2.1, and 1.8. Enclosure (16) is a curve of  $\Delta T$  per inch ( $\Delta T/\text{in.}$ ) of chamber length for varying  $P_c$  for the three thrust levels, 8K, 14.15K and 25K, all for  $MR = 6.0$ . At the 25K thrust level the  $\Delta T/\text{in.}$  increases from approximately  $10^\circ\text{F}/\text{in.}$  at  $P_c = 500$  psia to  $20^\circ\text{F}/\text{in.}$  at  $P_c = 2500$  psia. These results indicate that the  $\Delta T/\text{in.}$  is just a function of thrust and chamber pressure because the Mach number is assumed constant.

#### f. Mixture Ratio Parameter Study

Since all the previous studies were conducted for  $MR = 6.0$ , Task V was to determine the effects on these studies at  $MR$  of 5.0 and 7.0. Figure (17) presents the  $MR$  effects at a constant Mach number in terms of percent change of  $\Delta T_w$ ,  $T_{wg}$ ,  $\Delta P/\text{in.}$ ,  $\Delta T/\text{in.}$ , and  $\Delta P$  versus  $MR$  and these results may be applied for the three thrust levels investigated.

The  $\Delta T_w$  increases approximately 3 percent at  $MR = 5.0$  and decreases 5 percent at  $MR = 7.0$ . The coolant pressure drop and the coolant pressure drop per inch of chamber length,  $\Delta P/\text{in.}$ , had the same trend. However the gas-side wall temperature and the coolant bulk temperature rise per inch of chamber length both decreased at  $MR = 5.0$  and 7.0. These changes are primarily due to the changes in coolant flow which affect the coolant bulk temperatures and velocities.

#### V CONCLUDING REMARKS

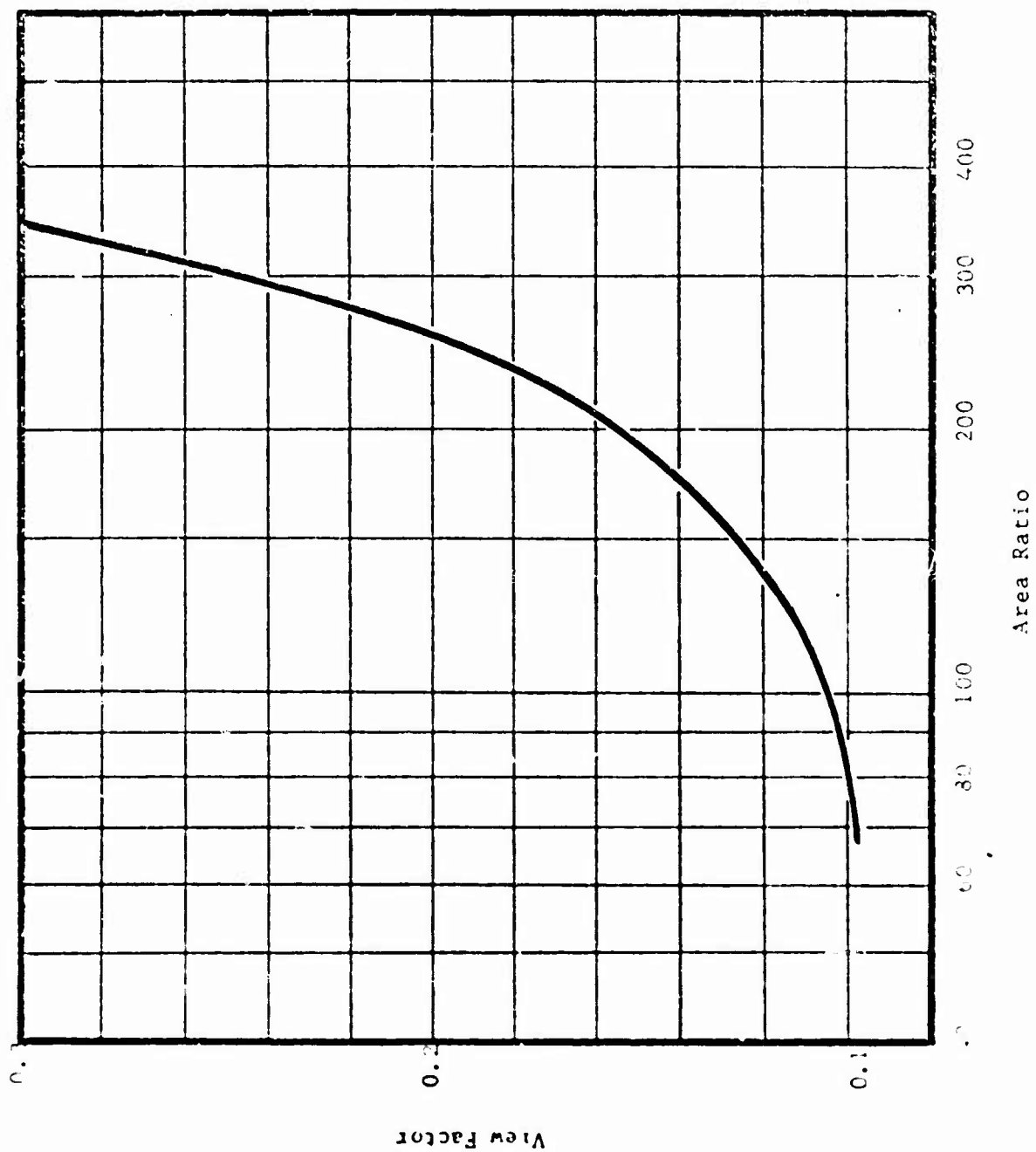
These eleven Figures (7 thru 17) may be used as a guide to the OOS

engine design study. All the necessary thermal parameters involved in such a study may be obtained from these curves. It must be remembered that these are used only as a guide since no final nozzle coolant channel configuration was ever selected. A more detailed design study will be conducted in the following Task I of the OOS study program.

REFERENCES

- (1) Memorandum 9642:1010, J. W. Salmon to W. P. Luscher, Subj: "OOS Preliminary Nozzle Contour Data", dtd. 22 March 1971
- (2) Bartz, D. R., "A Simple Equation for Rapid Estimation of Rocket Nozzle Convective Heat Transfer Coefficients", Jet Propulsion, January 1959, p. 59
- (3) Hess, H. L., and Kunz, H. R., "A Study of Forced Convection Heat Transfer to Supercritical Hydrogen", ASME Journal of Heat Transfer, Feb. 1965, p. 41

LOS RADIATION-COOLED SKIRT  
RADIATION VIEW FACTOR  
THROUGH NOZZLE EXIT



# OOS RADIATION NOZZLE EXTENSION

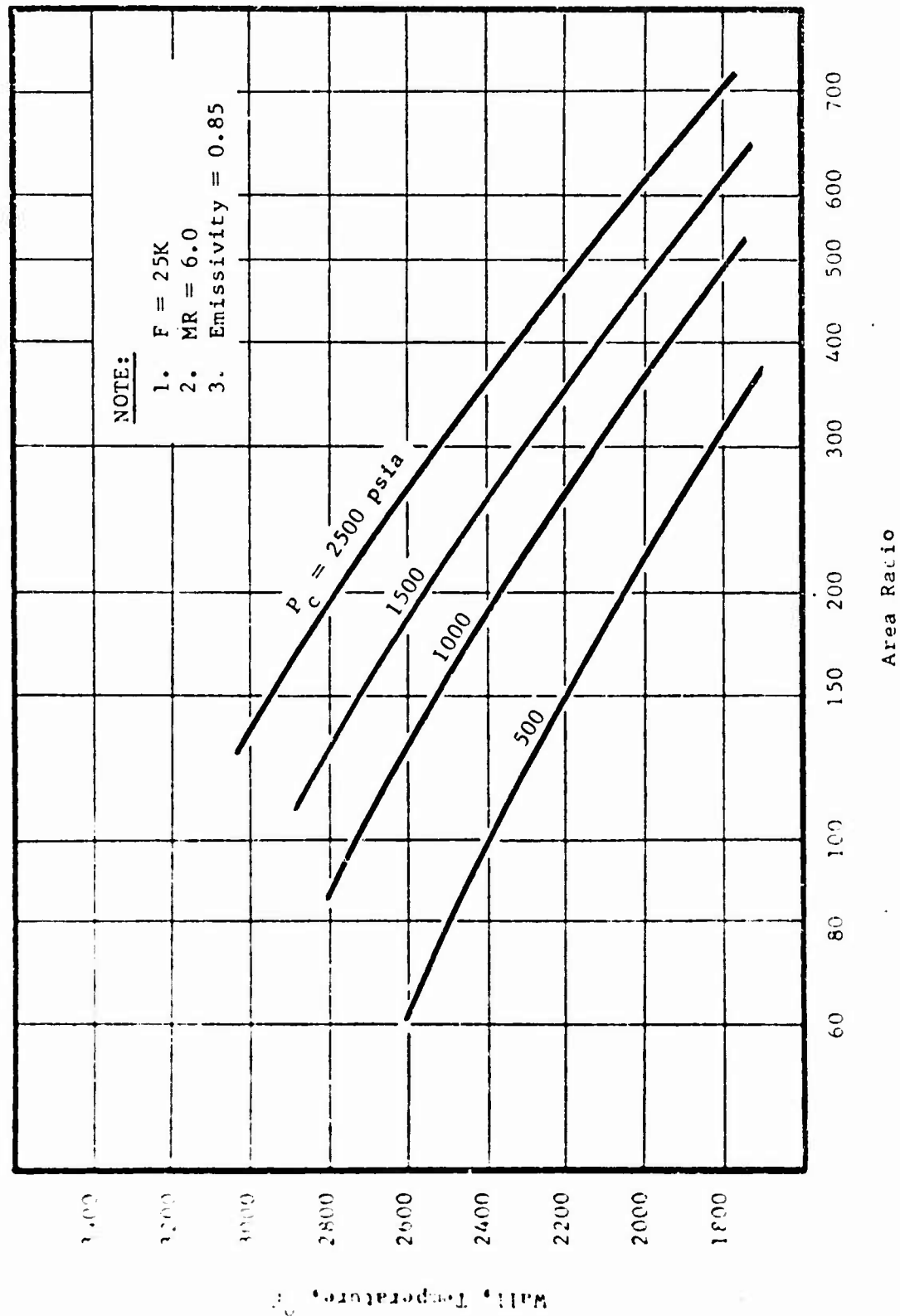
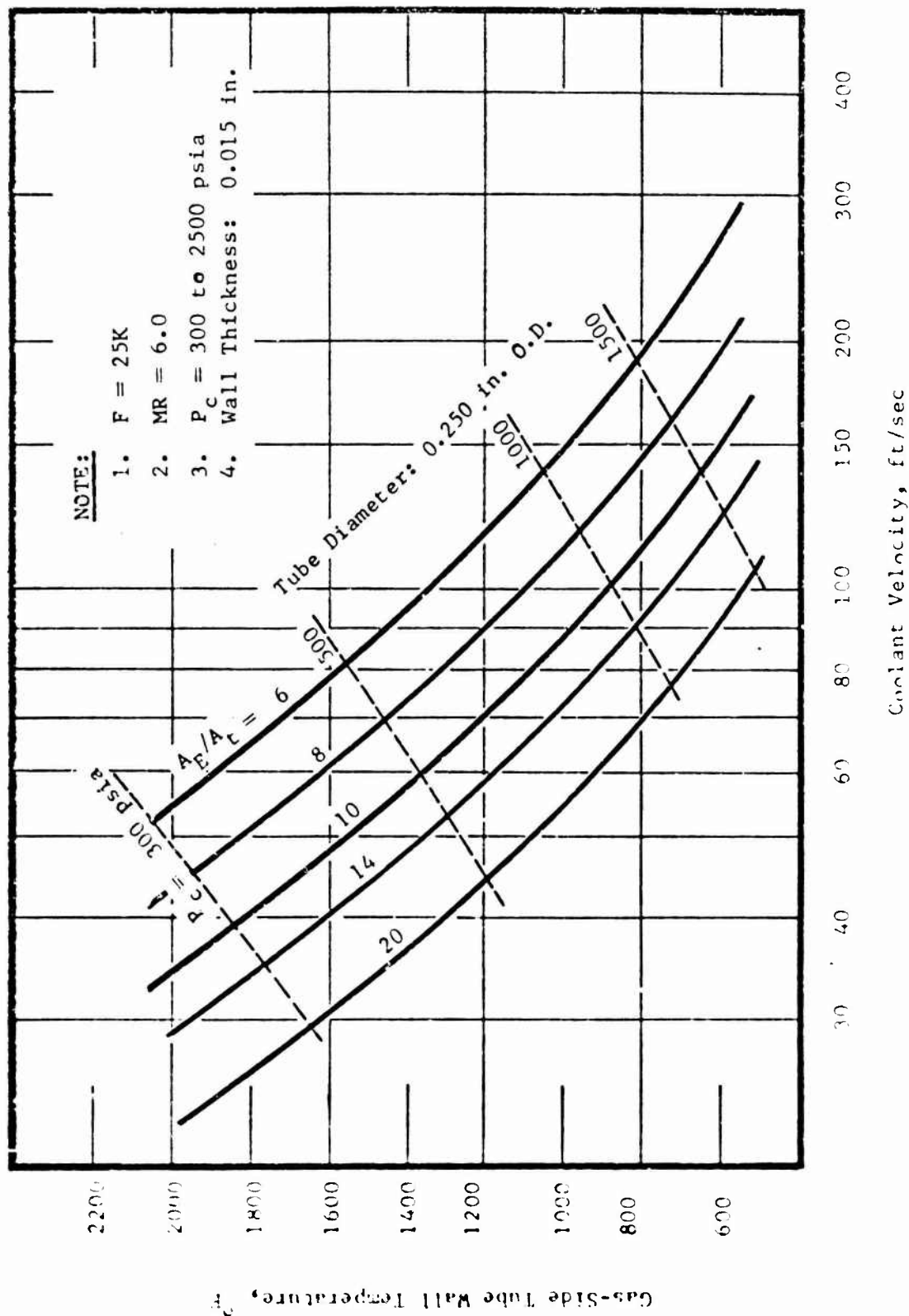


Figure 2

# COS TUBE BUNDLE TO COPPER NOZZLE

## TRANSITION AREA RATIO STUDY

### COOLANT OUTLET



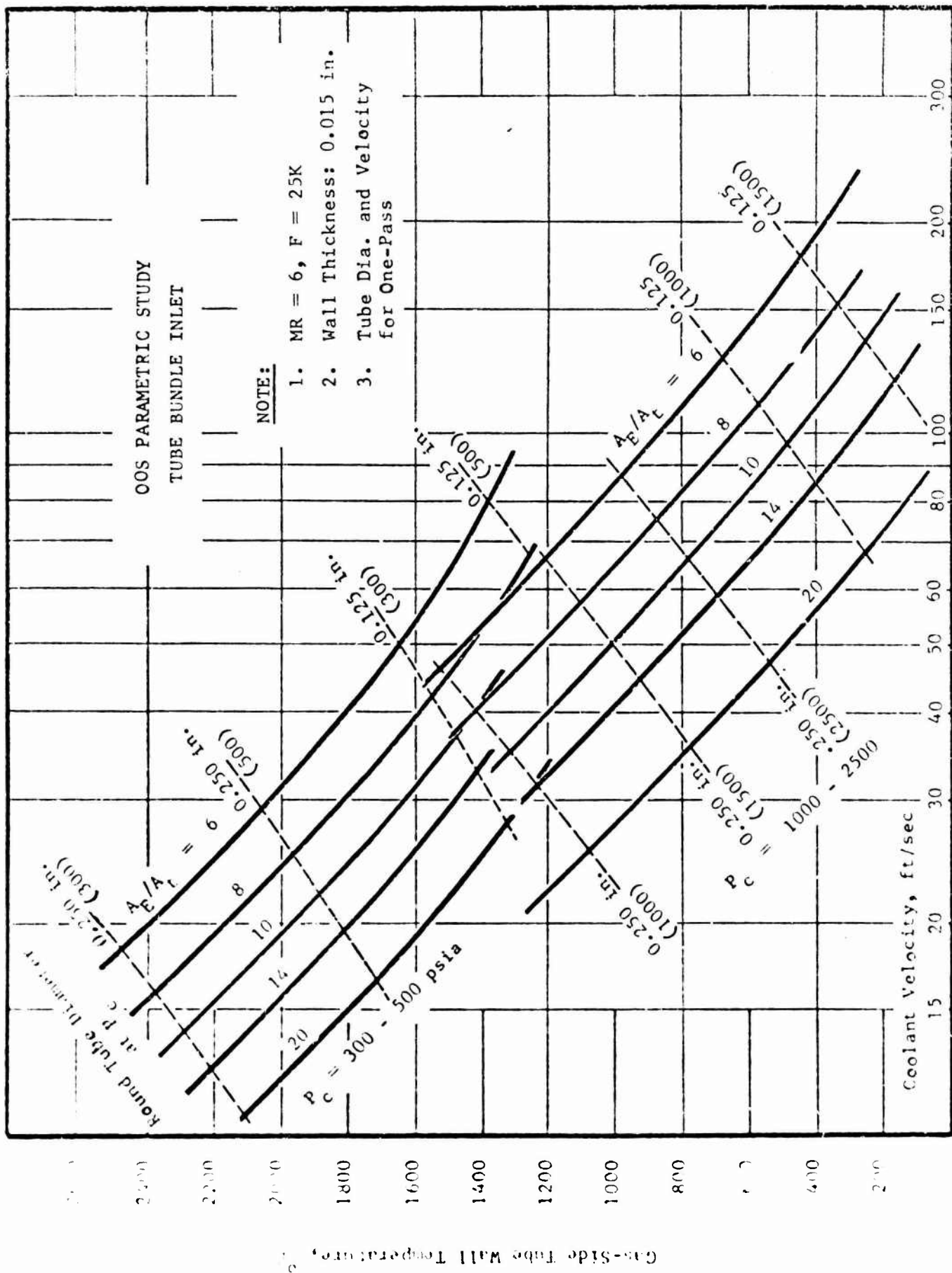
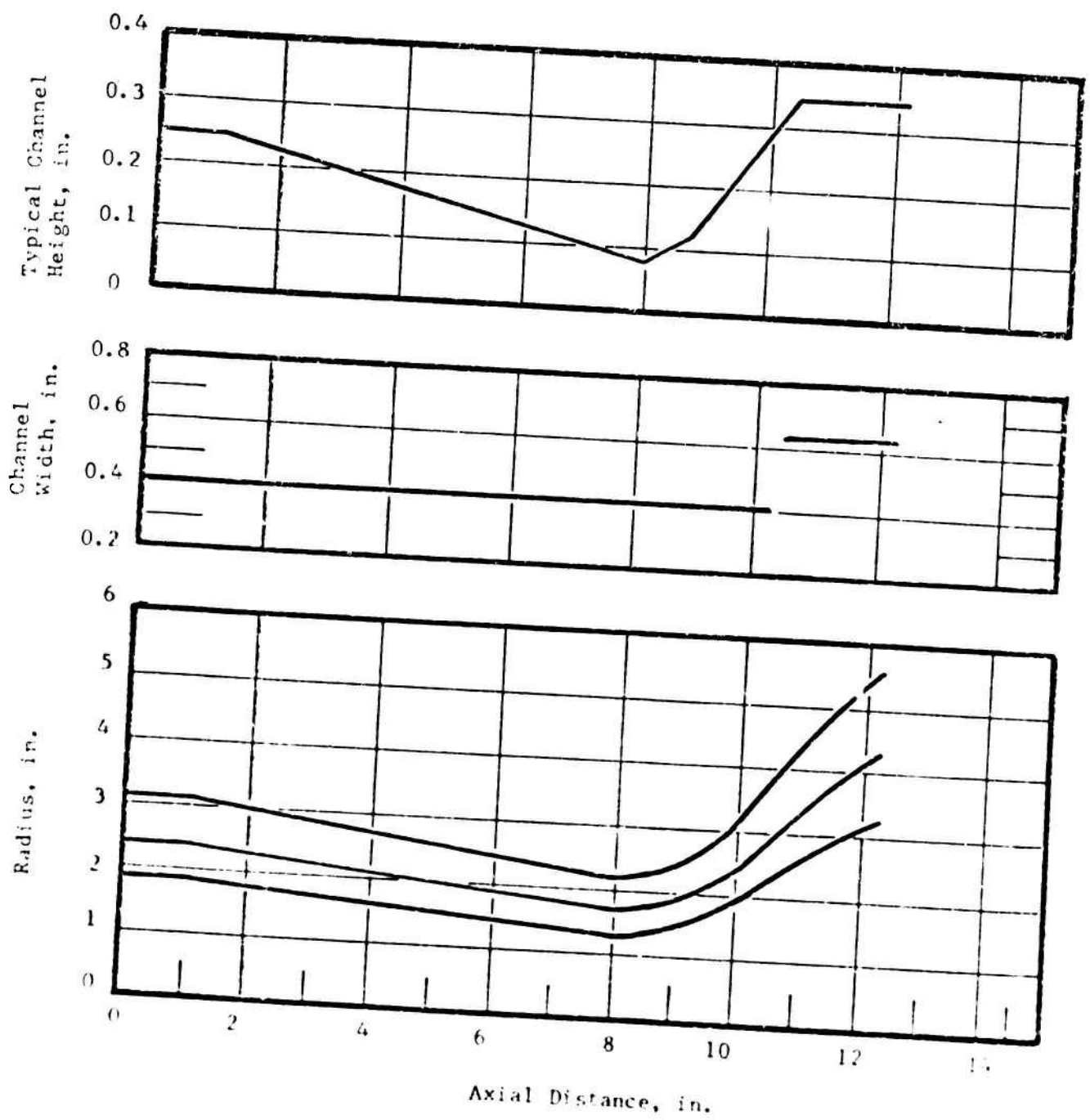


Figure 1



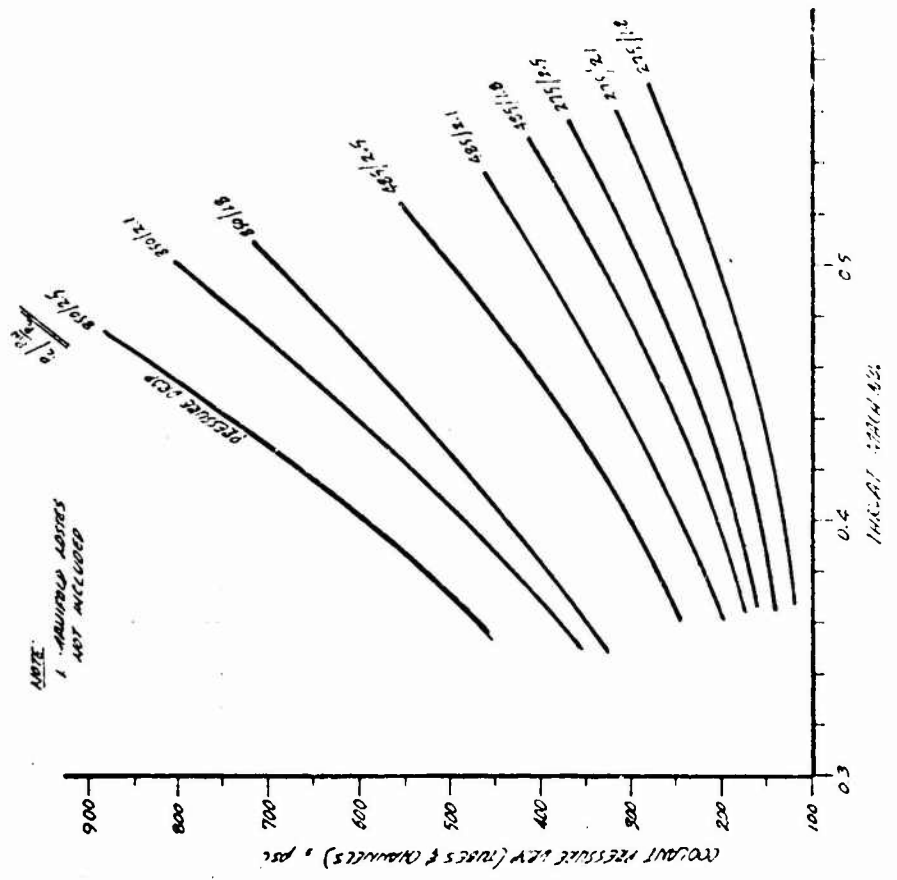
# OOS PARAMETER STUDY COPPER NOZZLE GEOMETRY



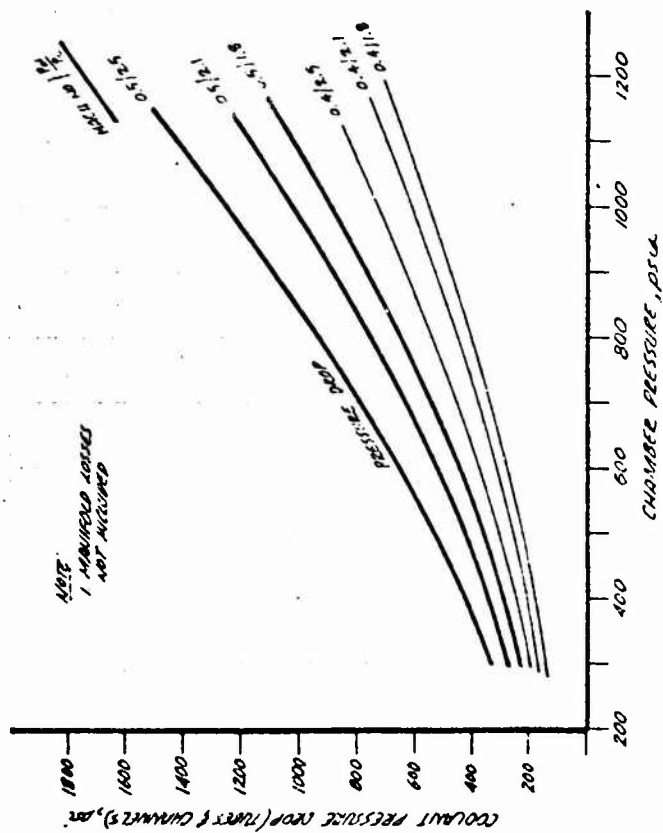
OOS PARAMETER STUDY  
COPPER NOZZLE COOLANT  
LH<sub>2</sub> INLET PARAMETERS  
MR = 6.0

$P_{IN}/P_C$	Chamber Press.	THRUST, LB					
		8000		14,150		25,000	
		$T_{IN}$	$P_{IN}$	$T_{IN}$	$P_{IN}$	$T_{IN}$	$P_{IN}$
2.5	275	229 <sup>°R</sup>	658 psia	220 <sup>°R</sup>	617 psia	210	522 psia
	485	234	1190	224	1159	216	1088
	850	242	2108	233	2085	225	2031
	1500	263	3737	255	3720	247	3679
	2650	290	6615	282	6602	275	6572
2.1	275	223	548	214	507	204	412
	485	226	996	216	965	208	894
	850	235	1768	226	1745	218	1691
	1500	248	3137	240	3120	232	3079
	2650	275	5555	267	5542	260	5512
1.8	275	218	465	209	424	799	329
	485	221	850	211	820	203	748
	850	227	1513	218	1490	210	1436
	1500	227	1513	218	1490	210	1436
	2650	268	4760	260	4747	253	4717

005 PARAMETER STUDY  
 5000 lb ME=60  
 8-in. CHANNEL

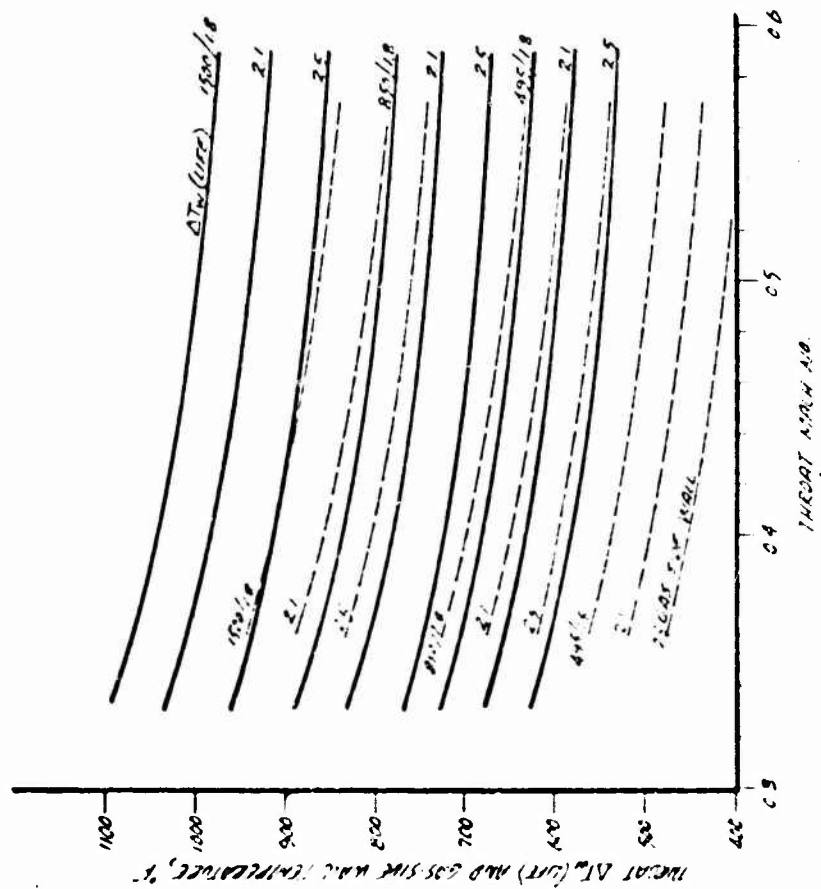


8-in CHAMBER

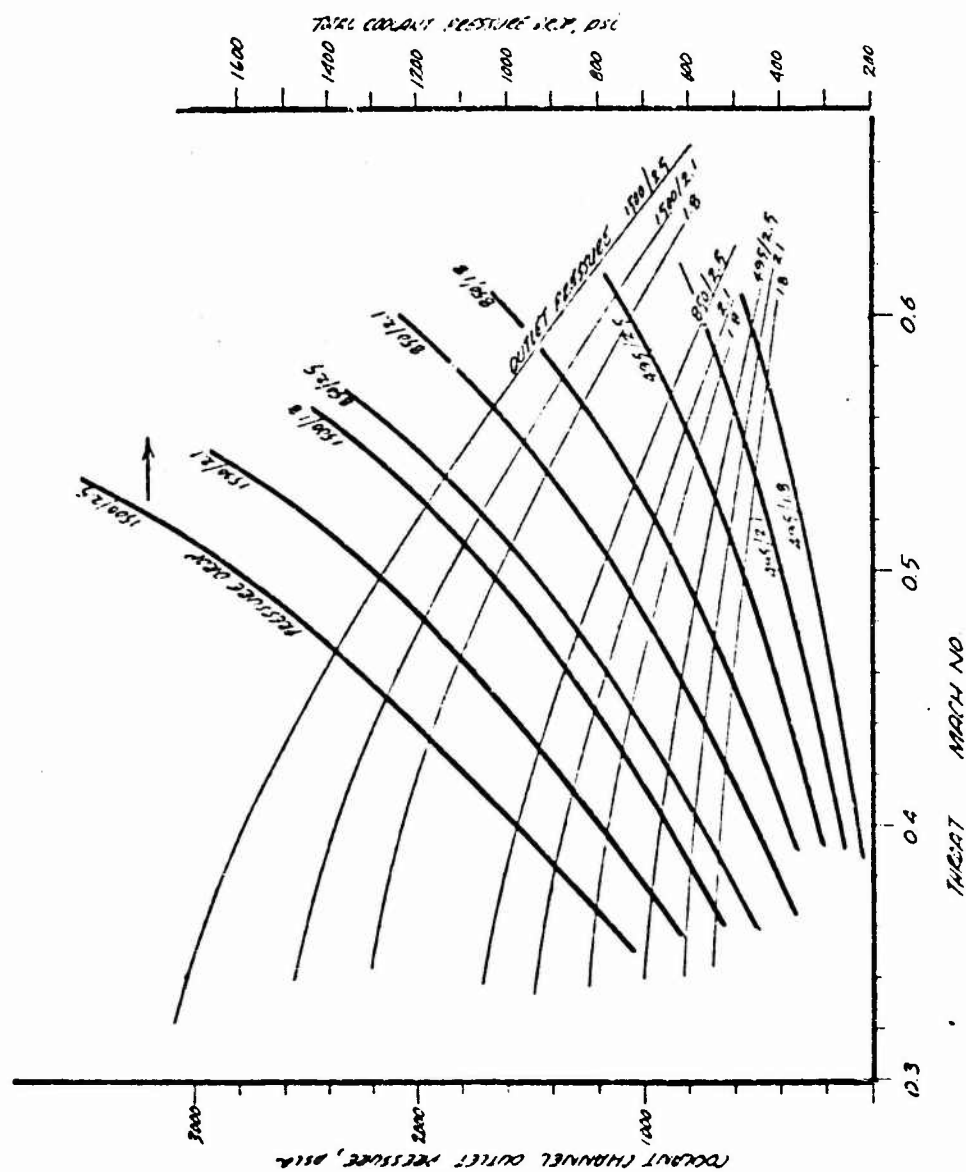


B-26

005 PARAMETRIC STUDY  
 F=14,150 lb MR=6.0

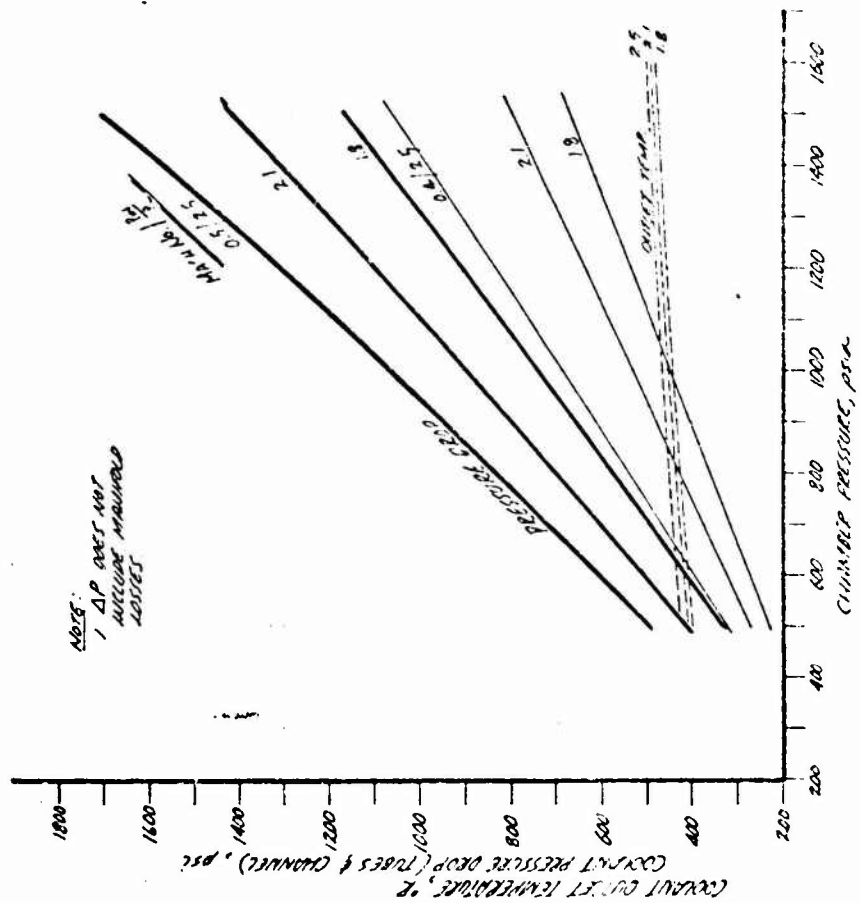
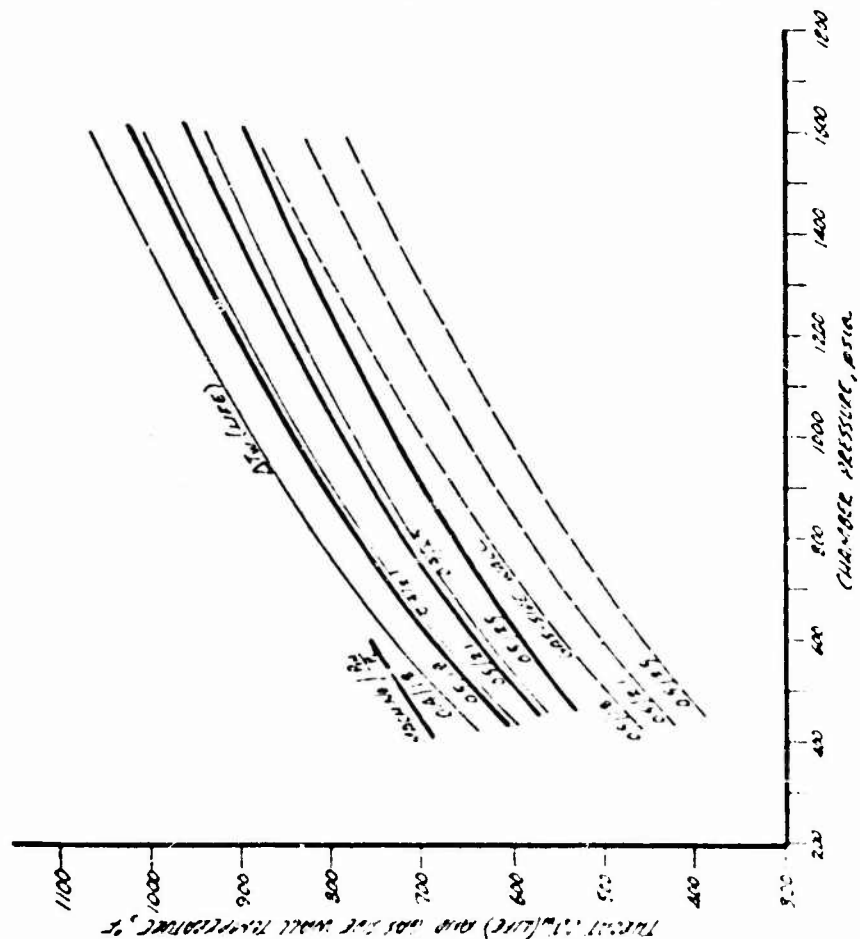


Q-in Chapter



11-22-14

005 PARAMETER STUDY  
 F=14,150 lb. MR=60  
 8-in. CHANNEL



NOTE:  
 1. AP NOT MET  
 INCREASE MAINTAINED  
 TESTS



DO5 PACQUETTE STUDY  
 PLANT  $\Delta T_w$  (LINE) F GAS-SIDE WALL TEMPERATURE  
 F=25,000 lb ME=6.0

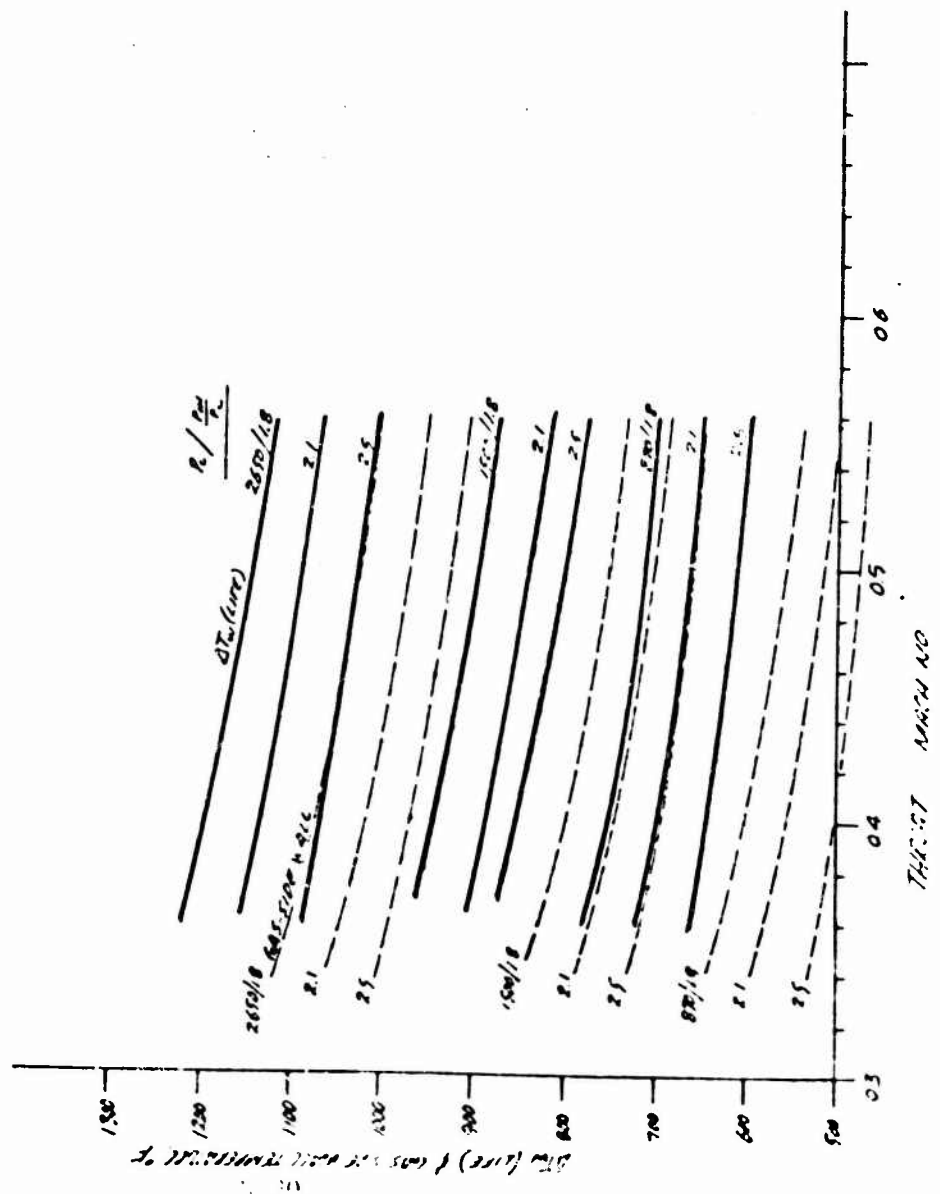
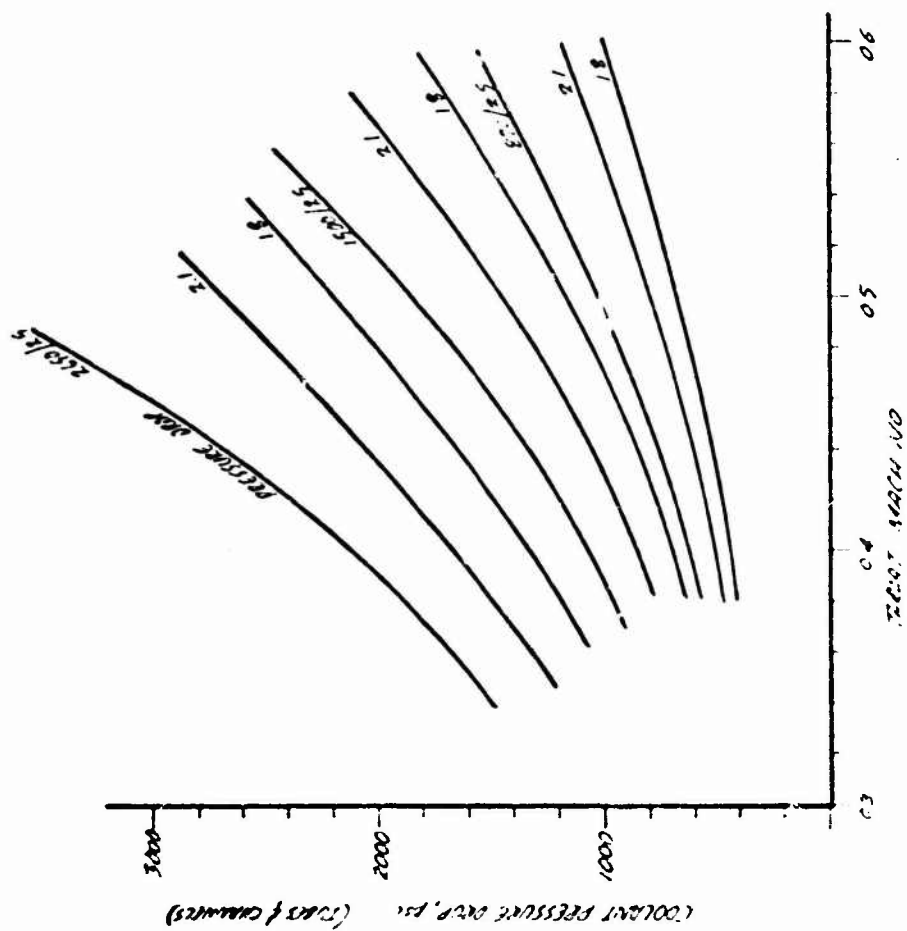


Figure 12



005 PARAMETER STUDY  
CONSTANT PRESSURE RISE VS TURBINE NO  
P=25.000/4 K2=5.0  
B=10 C=0.0002

# 005 PARAMETER STUDY

F-25,000 lb MR=6.0

8-in CHANNEL

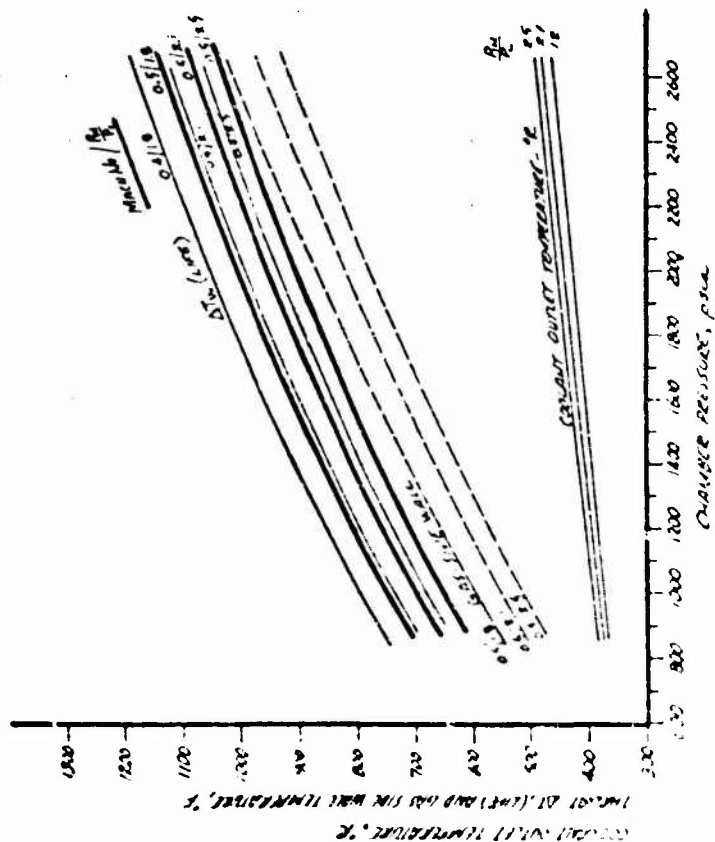
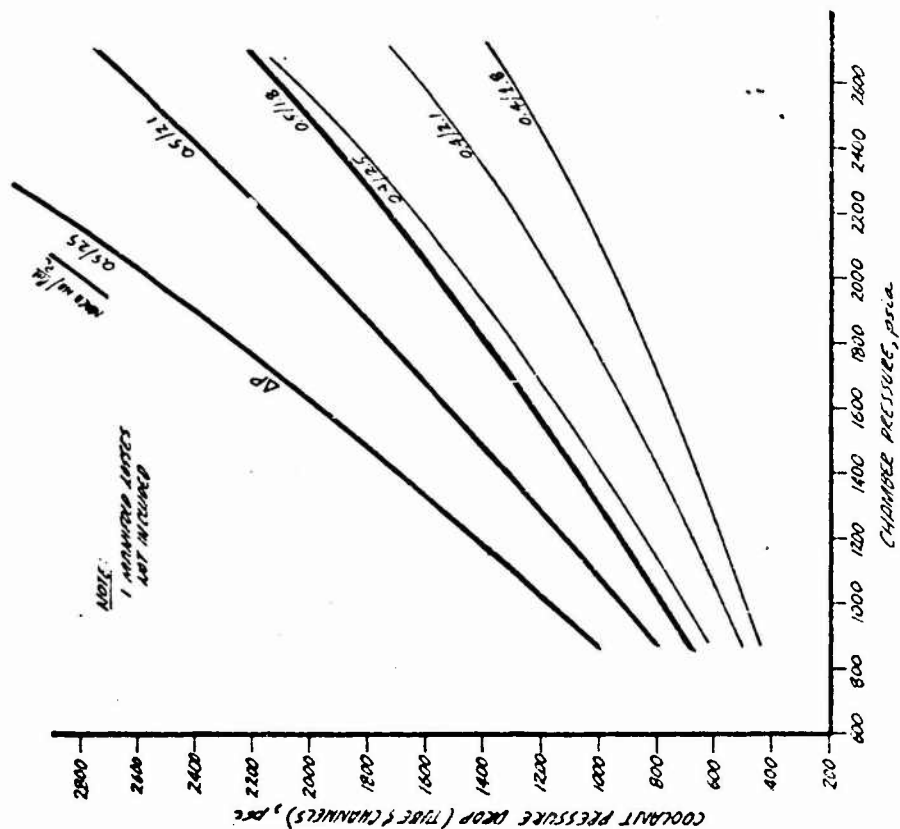
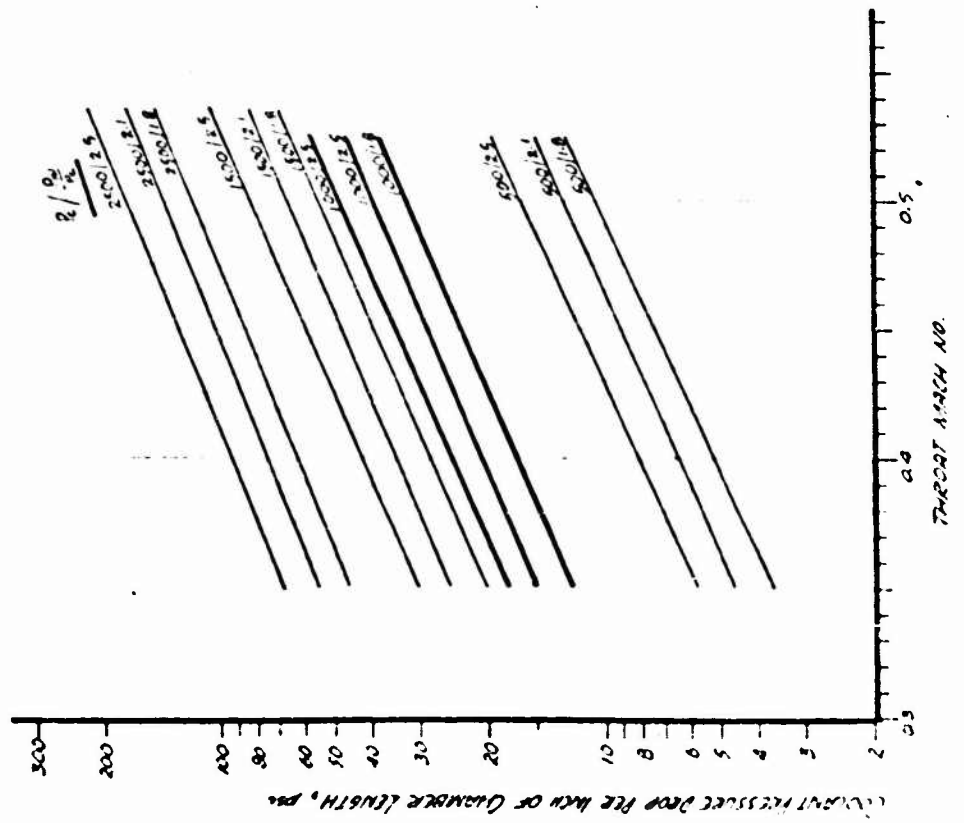
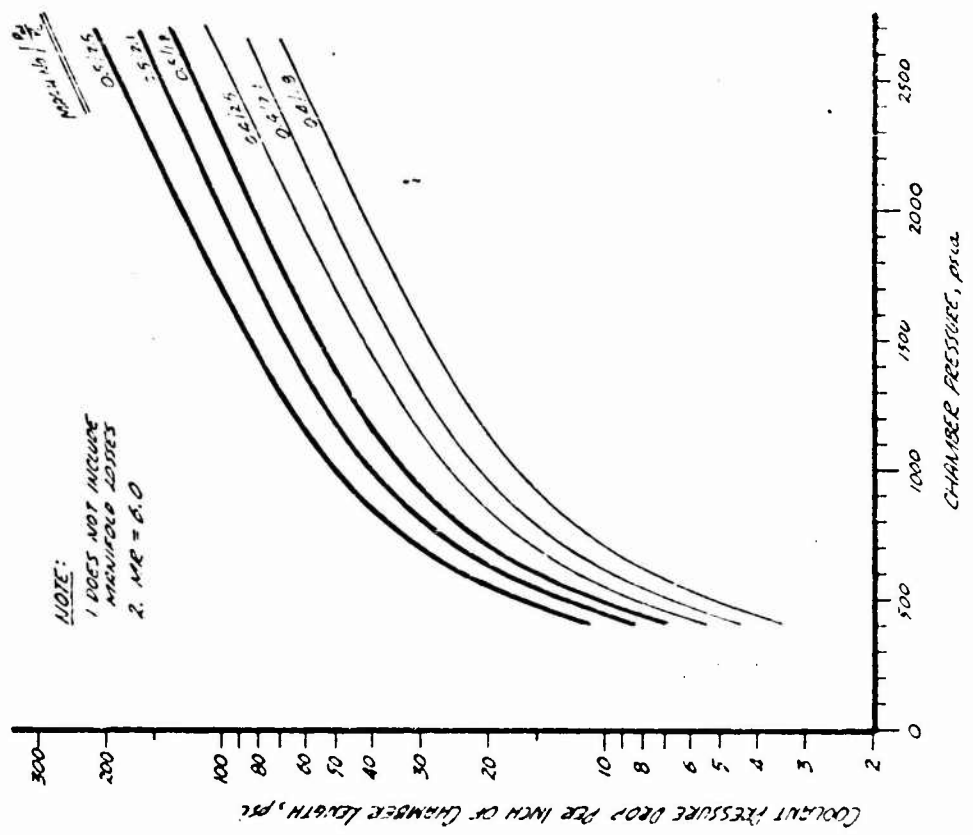


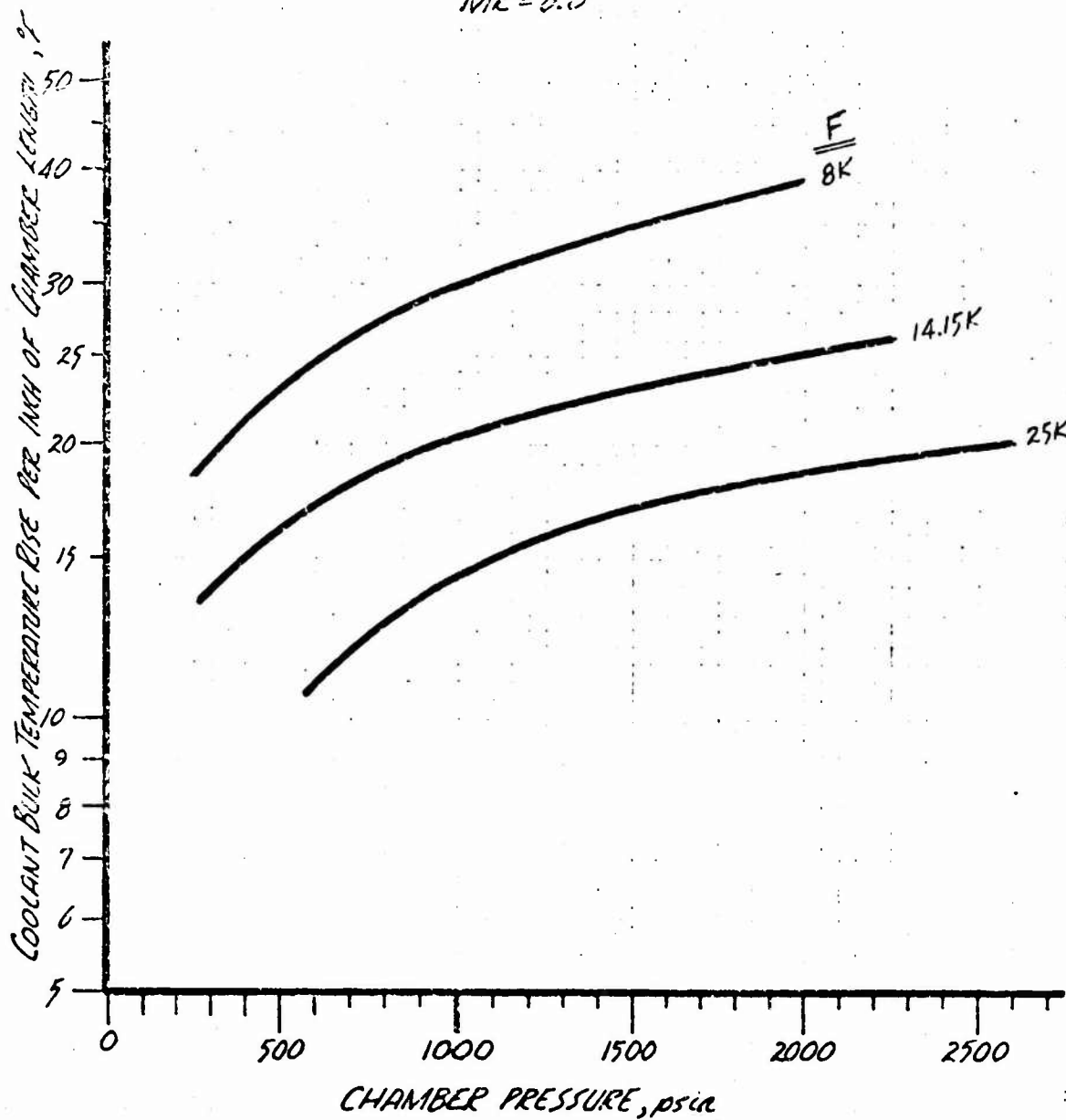
Figure 14

OOS PARAMETER STUDY  
PRESSURE DROP PER INCH OF CHAMBER LENGTH  
ADDITIVE TO THE 8-IN. CHAMBER



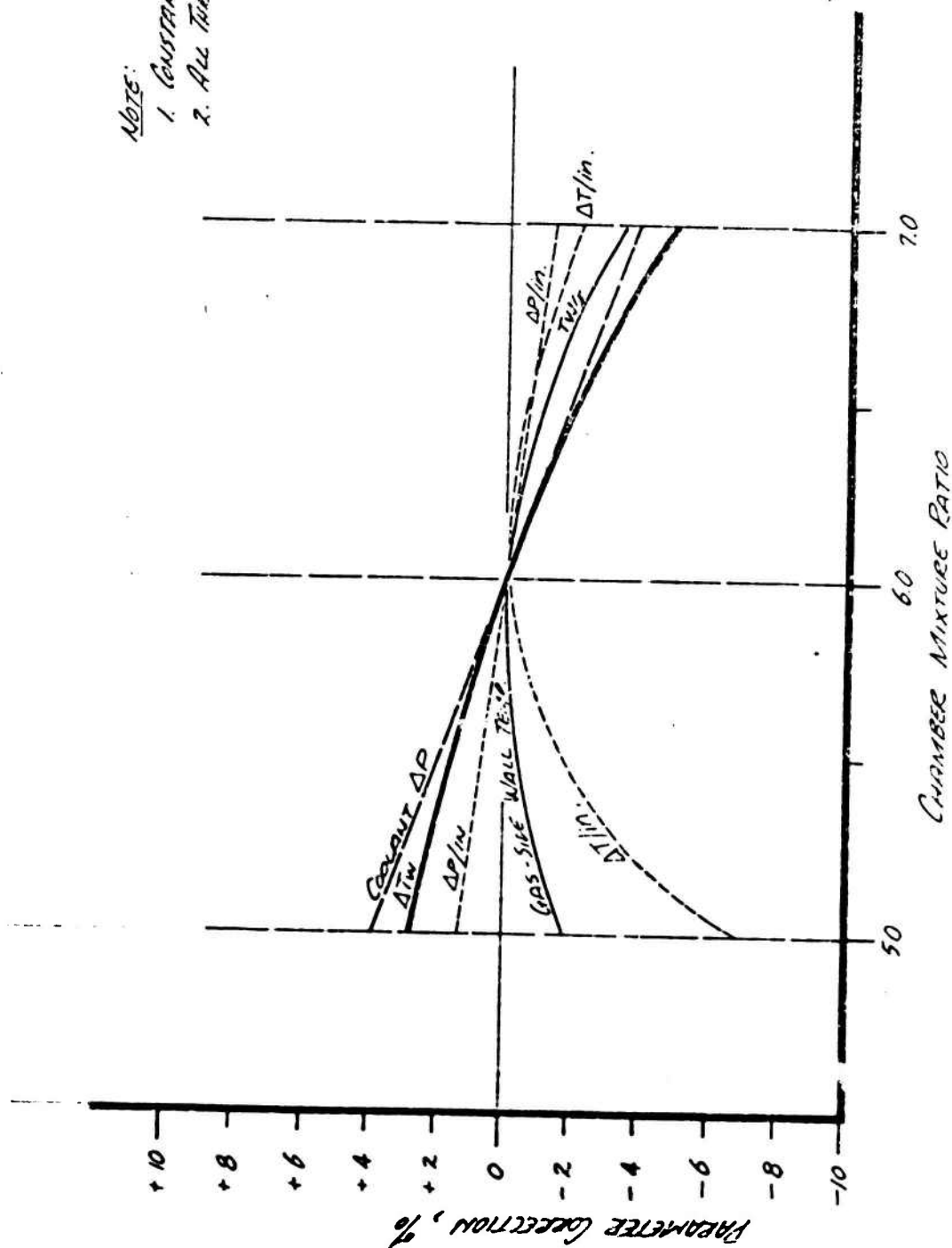
0.05 PARAMETER STUDY  
COOLANT BULK TEMPERATURE RISE PER INCH OF  
CHAMBER LENGTH - ADDITIVE TO THE 8-IN. CHAMBER

MR=6.0



OOS PARAMETER STUDY  
CORRECTION FOR MIXTURE RATIO  
APPLIED TO VALUES AT M2=6.0

Note:  
 1. Constant Mach No.  
 2. All Thrust Levels



MEMORANDUM

To: D. W. Culver 10 September 1971  
ACK:sm:9641:0652


From: A. C. Kobayashi

Subject: Orbit-to-Orbit Shuttle (OOS) Task I and Task III;  
Heat Transfer Final Report .

Copies to: S. Adair, D. David, W. P. Luscher, C. McCargar, R. W. Michel,  
F. H. Miller, V. H. Ransom, J. W. Salmon, R. C. Schindler,  
L. K. Severud, C. E. Teague, 9641 File

Enclosure: (1) OOS Task I and Task III Heat Transfer Analysis  
Final Report

A final report summarizing the heat transfer analysis in support of Task I and III of the OOS program is enclosed with this memorandum. The primary analytical support was given to (1) the preburner (2) the main injector vane, (3) the nozzle extension, and (4) the copper nozzle. This report includes the analytical support given to Task I and III from May 10, 1971 through August 27, 1971.

  
A. C. Kobayashi  
Thermodynamics  
Analysis Section

Approved by:

F. H. Miller, Supervisor  
Thermodynamics  
Analysis Section

8 September 1971

TCER 9641:024

OOS TASK I AND III  
HEAT TRANSFER ANALYSIS

FINAL REPORT

8 September 1971

by

A. C. Kobayashi

Approved by:

*F. H. Miller*

F. H. Miller, Supervisor  
Thermodynamics  
Engine Components Department

A E R O J E T   L I Q U I D   R O C K E T   C O M P A N Y

Engine Components Department

Sacramento, California



## TABLE OF CONTENTS

	<u>Page</u>
I INTRODUCTION	1
II MISCELLANEOUS ANALYTICAL SUPPORT	1
A. 50K Thrust Parameter Study	1
B. Thermal Radiation to Vehicle Base	2
C. Preburner to Turbine Manifold Interface	3
III PREBURNER	3
A. Introduction	3
B. Results	5
IV MAIN INJECTOR VANE	6
A. Introduction	6
B. Results	6
V NOZZLE EXTENSION	7
VI COPPER NOZZLE	8
A. Introduction	8
B. Throttling 10:1	9
C. Coolant Bypass	10
D. Off-Engine Mixture Ratio	10
E. Engine Mixture Ratio of 5.0 and 7.0	11
F. Boundary Layer Mixture Ratio	12

FIGURES

1. 50K Thrust - Effect of Throat Mach No. on Thermal Parameters
2. 50K Thrust - Effect of  $P_c$  on Thermal Parameters
3. Radiation Heat Transfer to Vehicle Base
4. Preburner to Turbine Manifold Flange Temperature Profile
5. Preburner Wall Temperatures - 1/8 in. OD Tubes
6. Preburner Coolant Bulk Temperature - 1/8-in. OD Tubes
7. Preburner-Effect of Reducing  $LO_2$  Flow Area
8. Preburner- Nominal Design Wall Temperatures
9. Preburner - Nominal Design Coolant Bulk Temperature
10. Preburner - Nominal Design Density Variations
11. Main Injector Vane - Nominal Design Density Variations
12. Copper Nozzle Channel Geometry
13. Thrust Chamber -  $LH_2$  Coolant  $\Delta P$  and  $\Delta T$  Versus Inlet Pressure
14. Copper Nozzle - Effects of Coolant Bypassing
15. Copper Nozzle - Effect of Off Engine MR = 5.5 and 6.5
16. Copper Nozzle - Effect of Engine MR = 5.0 and 7.0
17. Copper Nozzle - Life Cycle,  $\Delta P$ ,  $\Delta T_{Bulk}$  vs. MR = 5.0, 6.0, 7.0
18. Copper Nozzle - Boundary Layer MR Study Thermal Parameters
19. Copper Nozzle - Life Cycle,  $\Delta P$ ,  $\Delta T_{Bulk}$  vs. Boundary Layer MR

## I INTRODUCTION

This is the final report summarizing all the heat transfer analysis conducted in support of the Task I and Task II of the Orbit-to-Orbit Shuttle (OOS) engine study contract. This report is written in the order the analytical work was conducted and no attempt to differentiate the analytical work into Tasks will be made. The analytical results in this report have all been previously forwarded to and discussed with the OOS project engineers and the emphasis of this report will, therefore, be on the analytical approach and the presentation of the analytical results with a minimum of discussion of these results.

This report discusses the following major topics in the order listed: (1) miscellaneous analytical support, (2) preburner chamber, (3) main injector vanes, (4) nozzle extension, and (5) copper nozzle.

## II MISCELLANEOUS ANALYTICAL SUPPORT

This section of the report includes heat transfer analysis that does not fall under the other four categories previously mentioned; however, it does not imply that these results are of less importance. Included in the discussion is, (1) a 50K-thrust engine parameter study, (2) an analysis of thermal radiation to the vehicle base, and (3) a preburner to turbine-manifold flange interface study.

### A. 50K Thrust Parameter Study

A parameter study similar to that presented in Task IV (Ref. 1) was conducted for the 50,000 lb thrust level. The analytical approach and

## II Miscellaneous Analytical Support (cont.)

assumptions were identical to that discussed in Ref. 1. The results are shown in Figures 1 and 2. Throat  $\Delta T_w$  ( $T_{wg} - T_{back}$ ), throat gas-side wall temperature ( $T_{wg}$ ), and coolant pressure drop for varying throat Mach number is shown in Figure 1. The effect of chamber pressure ( $P_c$ ) on these thermal parameters are shown in Figure 2. These results were used as an extension of the Task IV data package and was completed on 15 June 1971.

## B. Thermal Radiation to Vehicle Base

In considering a radiation-cooled nozzle extension as a design candidate, there was some concern as to the heat transfer rate from this nozzle extension to the vehicle base. An analysis was conducted to determine this heat transfer rate. The following assumptions were made for the analysis:

## Vehicle:

Base Radius	900 in.
Axial Position	20 in. above throat

## Engine:

Thrust	25,000 lb
Chamber Pressure	1800 psia
Mixture Ratio ( $LO_2/LH_2$ )	6.0
Skirt Emissivity	0.85

Contours for both the 270:1 and 450:1 area ratio nozzles were investigated. The CONFAC II (Ref. 2) computer program was used to calculate the view factors

## II Miscellaneous Analytical Support (cont.)

from the nozzle extension's exterior surface to the vehicle base. Utilizing the radiation-cooled nozzle extension temperatures reported in Ref. 1, the total heat transfer rate to the vehicle base was calculated and plotted in Figure 3. This figure represents the total heat transfer rate to the vehicle base versus area ratio, i.e., the longer the radiation-cooled section the greater the total heat load. For example, if the 450:1 nozzle extension were to extend from area ratio of 50:1 to the nozzle exit, the maximum heat transfer would occur, i.e., 14 Btu/sec. Area ratios less than 50:1 were not considered since radiation-cooled extensions begin at much larger area ratios. The heat transfer rates shown were forwarded to the project engineer on 21 May 1971.

### C. Preburner to Turbine Manifold

A two-dimensional steady-state analysis of the preburner to turbine manifold flange interface was conducted to provide the Stress Department with a temperature profile. Both interfacing parts were made of steel with no thermal contact resistance assumed. The hot gas-side temperature was assumed to be 1400°F with a stagnant-gas boundary along the turbine manifold wall. The results of the analysis is shown in Figure 4. The preburner remained cold (-260°F) while the turbine manifold temperature averaged approximately 500°F. This analysis was complete on 30 July 1971.

## III PREBURNER

### A. Introduction

Heat transfer analysis of the preburner was conducted to design

## III Preburner (cont.)

an oxidizer ( $\text{LO}_2$ ) cooled cylindrical chamber. There were two primary design criteria, (1) to minimize the wall temperatures, and (2) to preheat the oxidizer to insure gas-phase outlet condition under all operating conditions.

The following assumptions were made for the 25K thrust engine preburner study:

## Hot-Gas Side

Chamber Diameter (I.D.)	3.0 in.
Mixture Ratio ( $\text{LO}_2/\text{LH}_2$ )	0.87
Temperature	1900 °R
Flowrate	14.36 lb/sec

## Coolant Side

Coolant	$\text{LO}_2$
Flowrate	6.7 lb/sec
Inlet Pressure	3252 psia
Inlet Temperature	209 °R

## Tubes

Material	347 Stainless
Wall Thickness	0.015 in.

Other thrust levels (15K, 10K, 7.5K and 5K) were also investigated. The analysis was conducted utilizing the heat exchanger program which includes two-phase flow heat transfer (Ref. 3).

## III Preburner (cont.)

## B. Results

Preliminary analytical results indicated that 79 tubes, 1/8-in. O.D. was the right number of tubes and tube size to satisfy the design criteria. The predicted wall temperatures and coolant bulk temperatures versus preburner lengths for varying thrust levels are shown in Figures 5 and 6, respectively. The preburner length required to insure  $O_2$  gas outlet conditions at the 5K thrust level was too long i.e., approximately 16 in. or more. A decision was then made to keep the same number of tubes but to utilize a U-tube design to reduce the coolant flow area.

The effect of reducing the coolant flow area (in 25 percent increments) on the coolant bulk temperature is shown in Figure 7. As expected this figure indicated that 25 percent of the 1/8-in. O.D. tube flow area predicted the minimum length required (6.0 in.) at 5K for  $O_2$  gas conditions. This flow area U-tube configuration was selected as the nominal preburner design. The predicted wall temperatures and coolant bulk temperatures are shown in Figures 8 and 9 for varying thrust.

The effect of this nominal design on the  $O_2$  density for varying length at varying thrust levels is shown in Figure 10. This figure clearly illustrates the length required (6.0 in. or more) to maintain  $O_2$  outlet conditions away from the two-phase region, i.e., under the two-phase dome, for varying thrust conditions.

IV MAIN INJECTOR VANE

## A. Introduction

The main injector vanes are cooled by  $\text{LO}_2$  which is injected at the vane tips which combusts with the fuel rich turbine exhaust gases in the main combustion chamber. Analysis of the vanes were conducted to determine the wall temperatures and the  $\text{LO}_2$  bulk temperature. Like the preburner the  $\text{LO}_2$  coolant is to be injected in the gas phase for optimum engine performance and combustion stability at all thrust levels. One important variable is, therefore, the vane length.

The following are the hot gas side assumptions used in the analysis of the 25K thrust engine vanes.

## Hot Gas Side

Flow Area	7.3 in <sup>2</sup>
Mixture Ratio ( $\text{LO}_2/\text{LH}_2$ )	0.87
Temperature	1856 °R
Flowrate	14.56 lb/sec

The vanes are made of OHFC copper with coolant channels somewhat elliptical and the walls approximately 0.050-in. thick. All analysis was conducted with the heat exchanger computer program.

## B. Results

Analysis was conducted at varying engine thrust levels for a mixture ratio of 6.0 and the following tabulation is a summary of the predicted heat transfer parameters.



MAIN INJECTOR VANE  
HEAT TRANSFER SUMMARY

Thrust, lb.	25K	15K	10K	7.5K	5K
LO <sub>2</sub> Flowrate, lb/sec	39.3	23.9	16.3	12.4	8.4
LO <sub>2</sub> Inlet Pressure, psia	2392	1344	877	675	426
LO <sub>2</sub> Inlet Temperature, °R	209	191	183	180	176
*Gas-Side Wall Temperature, °R	1550	1240	1100	1000	910
*Coolant-Side Wall Temperature, °R	1480	1209	1080	985	900
*Coolant Bulk Temperature, °R	422	322	296	304	282
*Coolant Pressure, psia	2260	1300	858	645	420

\* Approximately 2.7 in. from the LO<sub>2</sub> inlet

The effect of vane length on the density of LO<sub>2</sub> for the varying thrust levels are shown in Figure 11. This figure indicates that a copper vane approximately 3-in. long would insure a gas phase injection of the oxygen for all thrust levels.

V NOZZLE EXTENSION

The hydrogen-cooled nozzle extension consists of a tube bundle attached to the copper nozzle at 6:1 area ratio and extends to the nozzle exit at approximately 280:1 area ratio. The circular tubes are of 347 stainless steel with 0.015-in. wall thickness. The primary tube bundle design consists of a two-pass, 190 tube configuration at  $A_E/A_t = 6$ , bifurcated at  $A_E/A_t = 30$  to 380 tubes and bifurcated again at  $A_E/A_t = 125$  to 760 tubes.

## V Nozzle Extension (cont.)

Heat transfer analysis was conducted to determine the thermal parameters of this extension and the following tabulation is a summary of this analysis for the 25K thrust level.

25K THRUST ENGINE NOZZLE EXTENSION  
HEAT TRANSFER SUMMARY

<u>Coolant</u>	<u>Hydrogen</u>
Coolant Inlet Pressure, psia	4150
Coolant Inlet Temperature °R	101
Chamber Pressure, psia	1200
Chamber Mixture Ratio	6.0
Hot Gas Flowrate, lb/sec	53.6
Total Number of Tubes	190/380/760
Tube Material	347 Stainless
Tube Wall Thickness	0.015 in.
Maximum Gas-Side Wall Temperature	760 °F
Maximum Coolant Side Wall Temperature	350 °F
Maximum Coolant Velocity	900 ft/sec
Coolant Pressure Drop	100 psi
Coolant Bulk Temperature Rise	260 °F

VI COPPER NOZZLE

## A. Introduction

The copper nozzle section is the engines main combustion chamber. It has a conical convergence section, a throat diameter of 1.51 in. and extends to area ratio 6:1. The hydrogen coolant flows in one pass from the nozzle

## VI Copper Nozzle (cont.)

extension at  $A/A_t = 6:1$  up through the throat to the vaned injectors. A preliminary parametric study was conducted to determine the nominal coolant channel geometry shown in Figure 11. It consists of 121 channels with the channel width and height varied as shown. The minimum height is at the throat (0.071 in.) where the channel and land width are both 0.040 in.

An extensive study was conducted for the copper nozzle to investigate the effects of varying parameters on the nozzle gas-side wall temperature ( $T_{wg}$ ),  $\Delta T_w$  ( $T_{wg} - T_{Back}$ ), coolant pressure drop and coolant temperature rise. One of the most critical parameter is  $T_{wg}$  and  $\Delta T_w$  which determines the fatigue cycle life. The copper nozzle was analyzed under these following variables; (1) throttling 10:1, (2) coolant bypass, (3) 5.5 and 6.5 mixture ratio, (4) 5.0 and 7.0 mixture ratio, and (5) boundary-layer control. The following paragraphs discusses the effect of these variables on the copper nozzle design for a thrust-chamber design that extends to an area ratio of 280:1.

## B. Throttling 10:1

Analysis of throttling the engine down to the 10:1 thrust level indicated that the critical thermal parameters such as the gas-side wall temperature and  $\Delta T_w$  both decreased at throttled conditions. These studies concluded that the copper nozzle designed for a 25K thrust engine will operate at the lower thrust levels without heat transfer problems.

## VI Copper Nozzle (cont.)

Coolant pressure drop is an important parameter which affects the engine balance and is particularly sensitive at the throttled conditions. A parameter study was conducted to show the effects of varying coolant inlet pressures on the coolant pressure drop at 25K, 5K and 2.5K thrust levels. The resulting coolant pressure drop ( $\Delta P$ ) and temperature rise ( $T_B$ ) is shown in Figure 13; these  $\Delta P$  and  $\Delta T_B$  values include the nozzle extension. This figure is to be used to conduct engine balance studies.

## C. Coolant Bypass

A study was made to determine if an increase in fatigue life cycle could be gained by taking portions of the coolant flow and bypassing the copper nozzle without changing the coolant channel geometry. The results of this study is shown in Figure 14.

The throat  $T_{wg}$  and  $\Delta T_w$  with coolant  $\Delta T_B$  and  $\Delta P$  are shown as a function of percent of nominal (7.55 lb/sec) coolant flow bypassed. The parameters governing fatigue life cycle ( $T_{wg}$  and  $\Delta T_w$ ) increases with increased bypass flow. Smaller coolant channels may be designed to satisfy the  $T_{wg}$  and  $\Delta T_w$  requirements but would result in increased  $\Delta P$  due to reduced hydraulic diameters. The conclusion of this study is that for a fixed nozzle design, bypassing the coolant flow does not increase life cycle.

## D. Off-Engine Mixture Ratio

It was necessary to determine the effects of off-engine mixture ratio (MR) conditions for the nominal copper nozzle design from the heat

## VI Copper Nozzle (cont.)

transfer standpoint. Off engine MR is defined as nominal design MR  $(6.0) \pm 0.5$  or at MR = 5.5 and 6.5. This study was conducted at the 25K thrust level,  $P_c = 1800$  psia, and with a fixed coolant channel geometry. The effect of the MR is shown in Figure 15. The gas-side wall temperature, ( $T_{wg}$ ),  $\Delta T_w$ , coolant bulk temperature rise and pressure drop are shown versus mixture ratio. The  $T_{wg}$  and  $\Delta T_w$  both increase (approximately 10 to 30°F) at the off MR conditions while the coolant temperature rise and pressure drop both decrease slightly.

## E. Engine Mixture Ratio of 5.0 and 7.0

Another question to be answered was to determine what happens to the thermal parameters at an engine mixture ratio of 5.0 and 7.0. This study involves the copper nozzle with the channel geometry as a variable and was made at the 25K thrust level with  $P_c = 1800$  psia. The coolant channel was uniformly varied at each MR and the resulting thermal parameters is shown in Figure 16. This figure includes  $T_{wg}$ ,  $\Delta T_w$  and coolant pressure drop ( $\Delta P$ ) versus Mach number for MR = 5.0, 6.0 and 7.0. As anticipated the  $T_{wg}$  and  $\Delta T_w$  decreases with increasing throat Mach no. while at the same time the  $\Delta P$  increases. However at any constant Mach no. the  $T_{wg}$  and  $\Delta T_w$  both increases at MR = 5.0 and 7.0 as compared to MR = 6.0.

The effect of these thermal parameters on fatigue life cycle ( $N_T$ ) is shown in Figure 17 where  $N_T$  is plotted versus MR for varying Mach no. Also shown are the coolant bulk temperature rise and pressure drop. These curves indicate that  $N_T$  decreases at MR = 5.0 and 7.0 relative to MR = 6.0.

## VI Copper Nozzle (cont.)

## F. Boundary-Layer Mixture Ratio

This study was conducted to determine what the reduction in boundary-layer mixture ratio would have on the copper nozzle design. This boundary-layer control is sometimes referred to as barrier MR control and the purpose is to reduce the MR adjacent to the wall to reduce the heat transfer to the nozzle. The hot gas and coolant flow rate was assumed equal to that at  $MR = 6.0$ . Only the hot gas side temperature and heat transfer coefficients were varied with MR. Again the trade-off with nozzle coolant geometry was studied. The thermal parameters are shown in Figure 18 versus throat Mach no. for varying boundary-layer MR (from  $MR = 6.0$  to  $2.0$ ).

The  $T_{wg}$  and  $\Delta T_w$  decreased with increasing Mach no., however, at a constant Mach no. these values were at a maximum at boundary-layer  $MR = 5.0$ . A cross-plot is shown in Figure 19 where the  $T_{wg}$  and  $\Delta T_w$  were converted to fatigue life cycle ( $N_T$ ).

Figure 19 clearly shows the advantage of increased  $N_T$  at the lower boundary layer MR. The coolant bulk temperature rise and pressure drop is relatively unchanged from an engine  $MR = 6.0$  without boundary-layer control.

TCER 9641:024

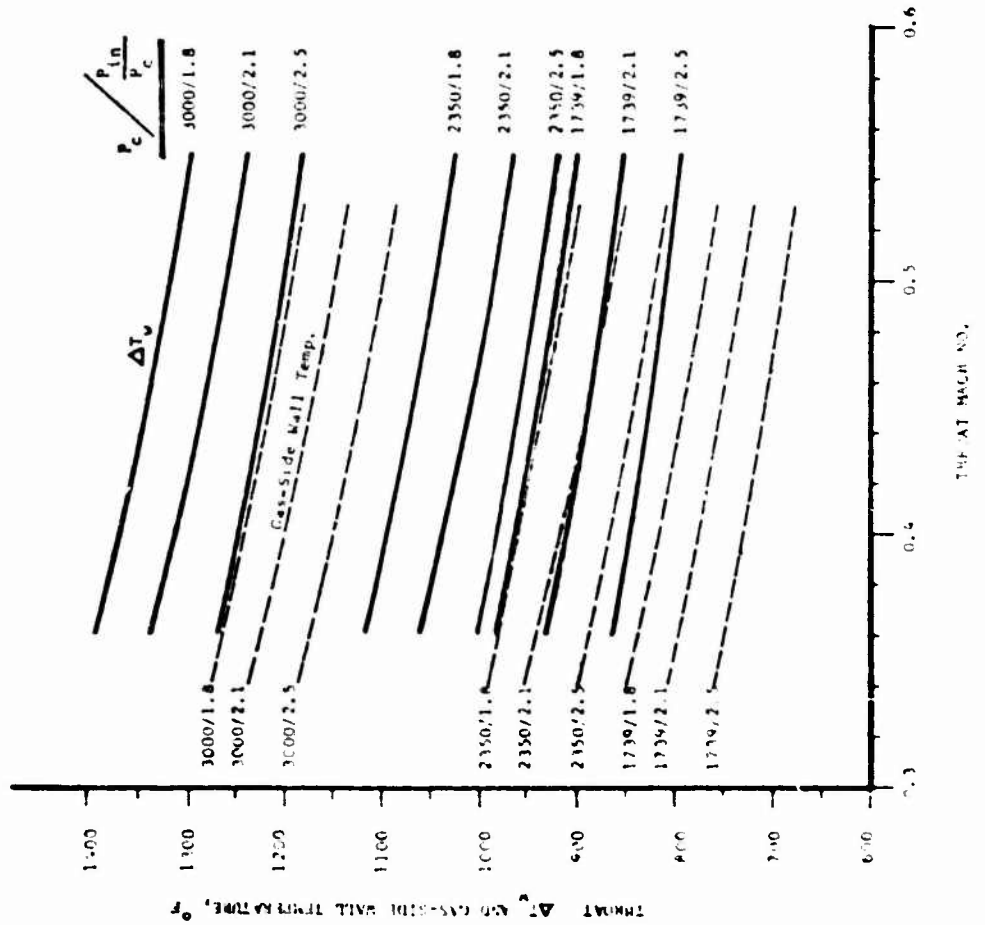
REFERENCES

1. A. C. Kobayashi, OOS Task IV and Task V Heat Transfer Analysis - Final Report, ALRC Engine Components Dept. TCER 9641:0116, 28 May 1971
2. K. A. Toups, A General Computer Program for The Determination of Radiant-Interchange Configuration and Form Factors - Confac II, NAA Space and Inf. Sys. Div., SID 65-1043-2, October 1965
3. Memorandum 9641:0644, J. W. Daily to Distribution, Subj: "HEXSIP, HEXSIP/V2, and HEXSIP/V3 Heat Exchanger Program Update", dtd. 24 June 1971

# 008 PARAMETER STUDY

$P = 50,000$  lb.  $MR = 6.0$

8-in. Chamber



NOTE:  
1. Manifold Losses  
Not Included

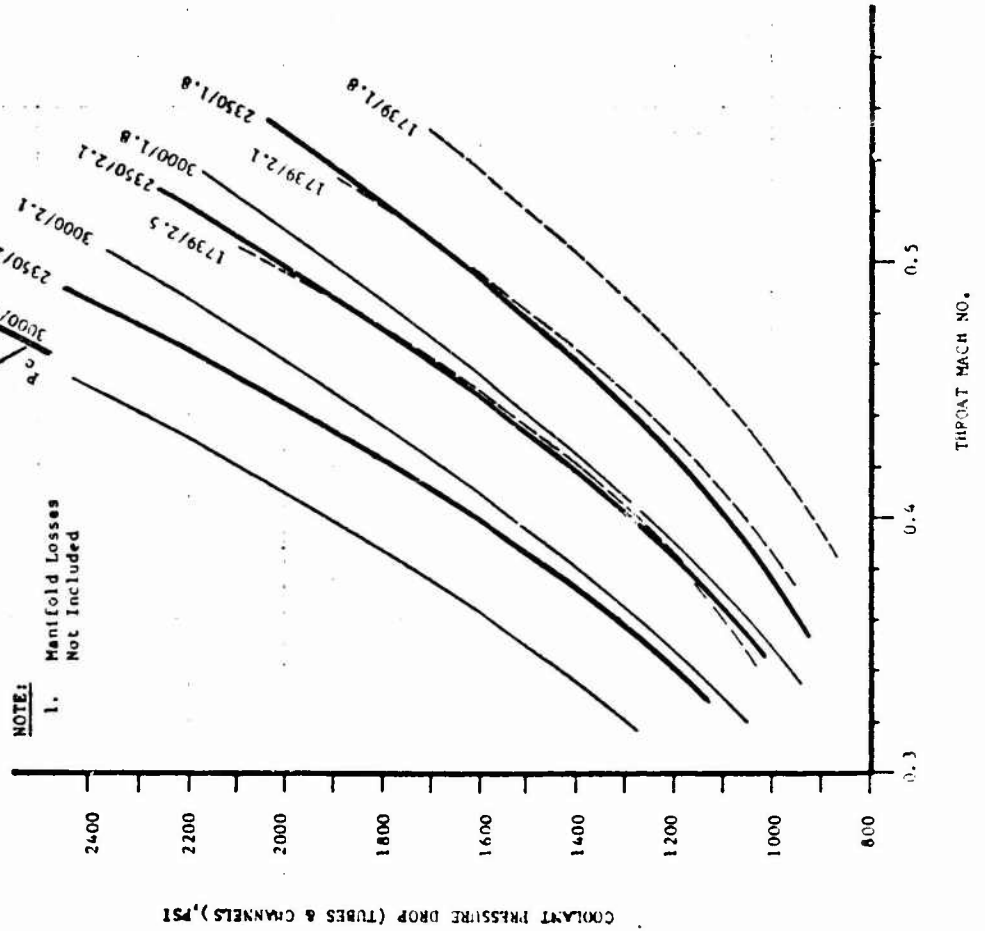


Figure 1



00S PARAMETER STUDY  
 $P = 50,000 \text{ lb. in.}^2$   
 $\delta = 6.0$   
 8-in. Chamber

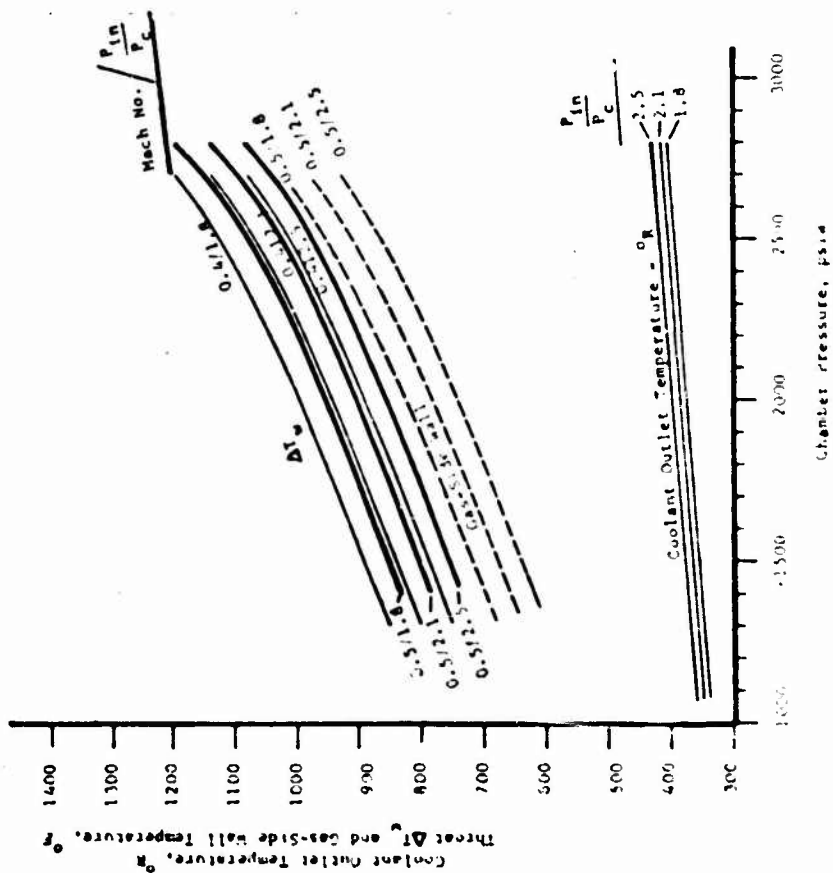
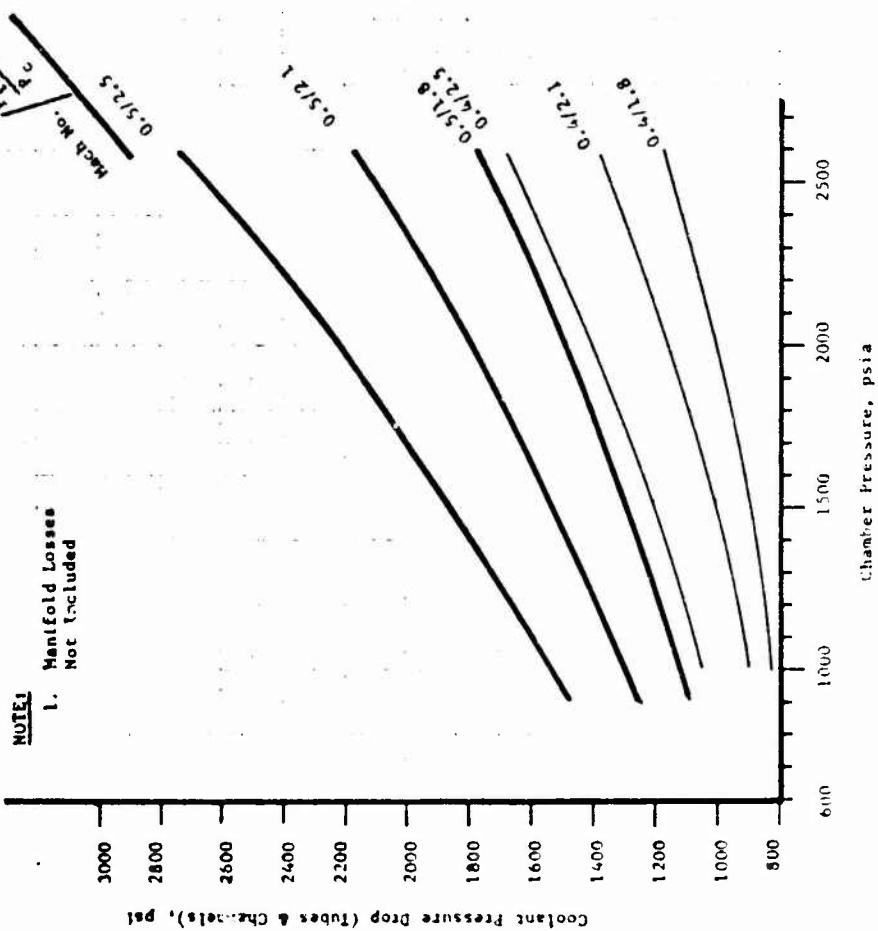
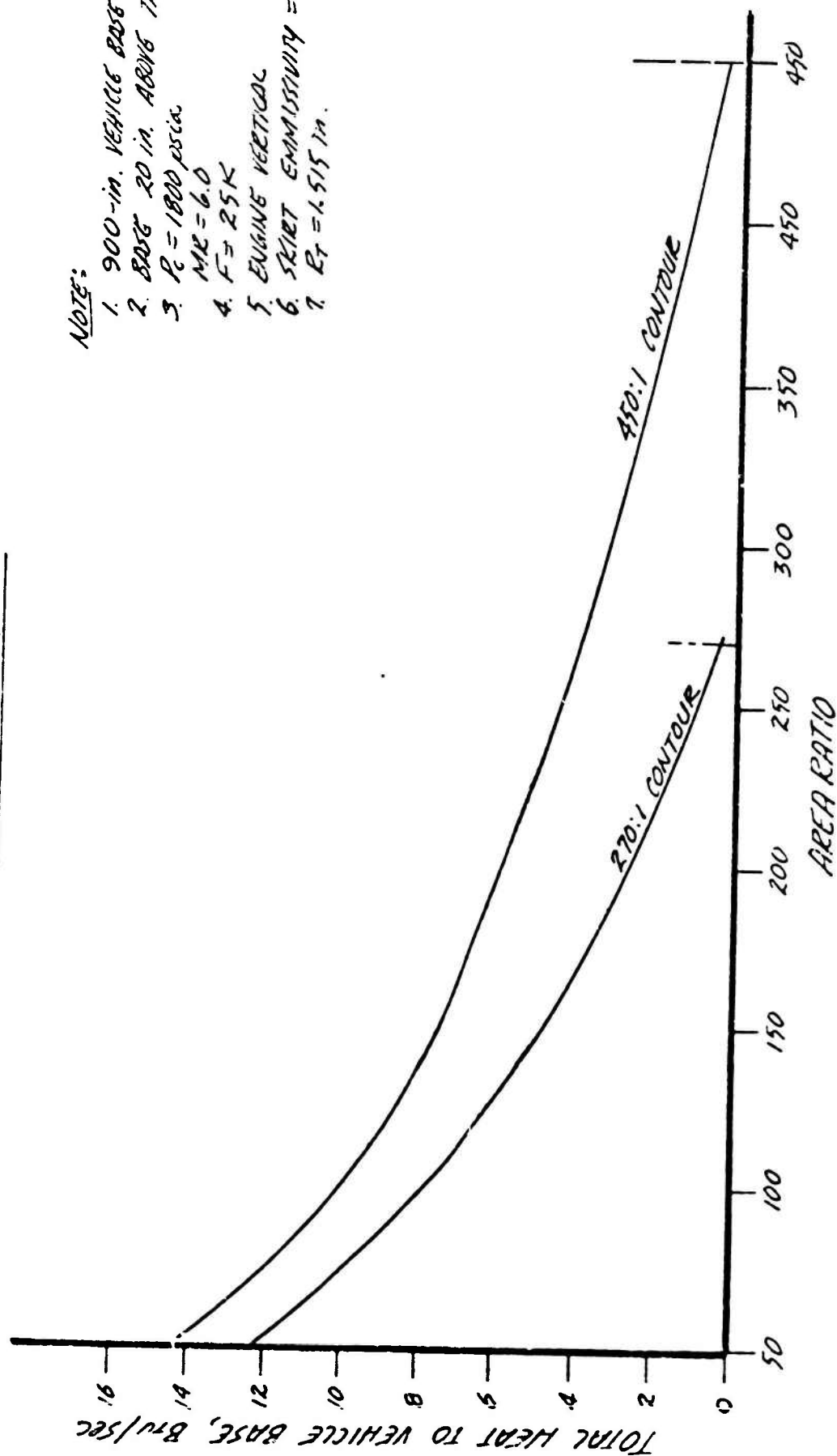


Figure 2

Q05 ENGINE  
RADIATION TO VEHICLE BASE  
FROM RADIATION-COOLED  
NOZZLE EXTENSION

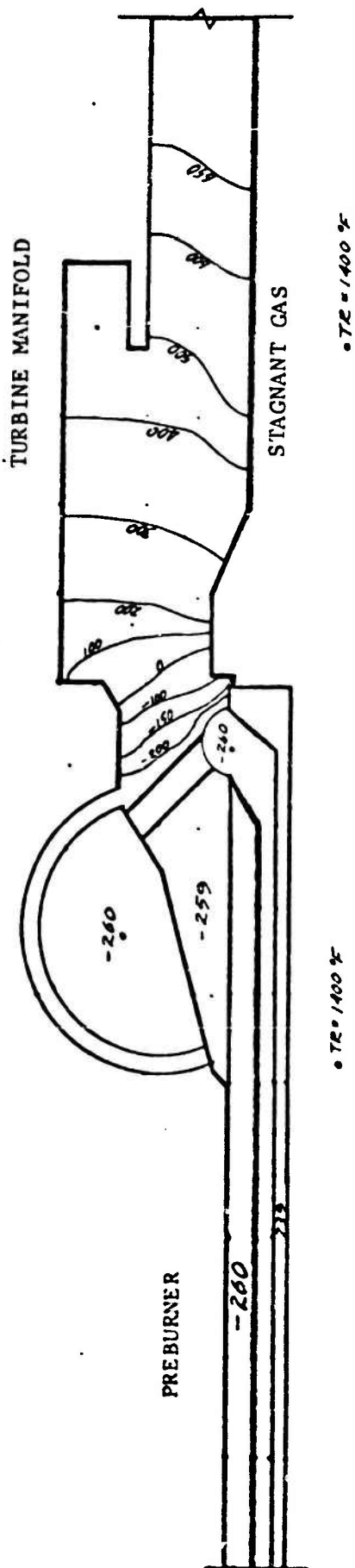
- NOTE:
1. 900-in. VEHICLE BASE RADIUS
  2. BASE 20 in. ABOVE THREAT
  3.  $P_c = 1800$  psia  
 $M_R = 6.0$
  4.  $F = 25K$
  5. ENGINE VERTICAL
  6. SILET EMISSIVITY  $= 0.85$
  7.  $E_T = 1.515$  in.



00S PREBURNER TO TURBINE MANIFOLD JOINT  
TEMPERATURE DISTRIBUTION  
STEADY-STATE CONDITIONS

NOTE:

1. All Temp. in °F



OOS PREBURNER STUDY  
TUBE WALL TEMPERATURES FOR  
1/8 IN. O.D. TUBES

NOTE:

1.      Gas-Side
- - - - - Coolant-Side
2. 3/4 Stainless Tubes
3. 0.015 in. Wall Thickness
4. No Film Cooling

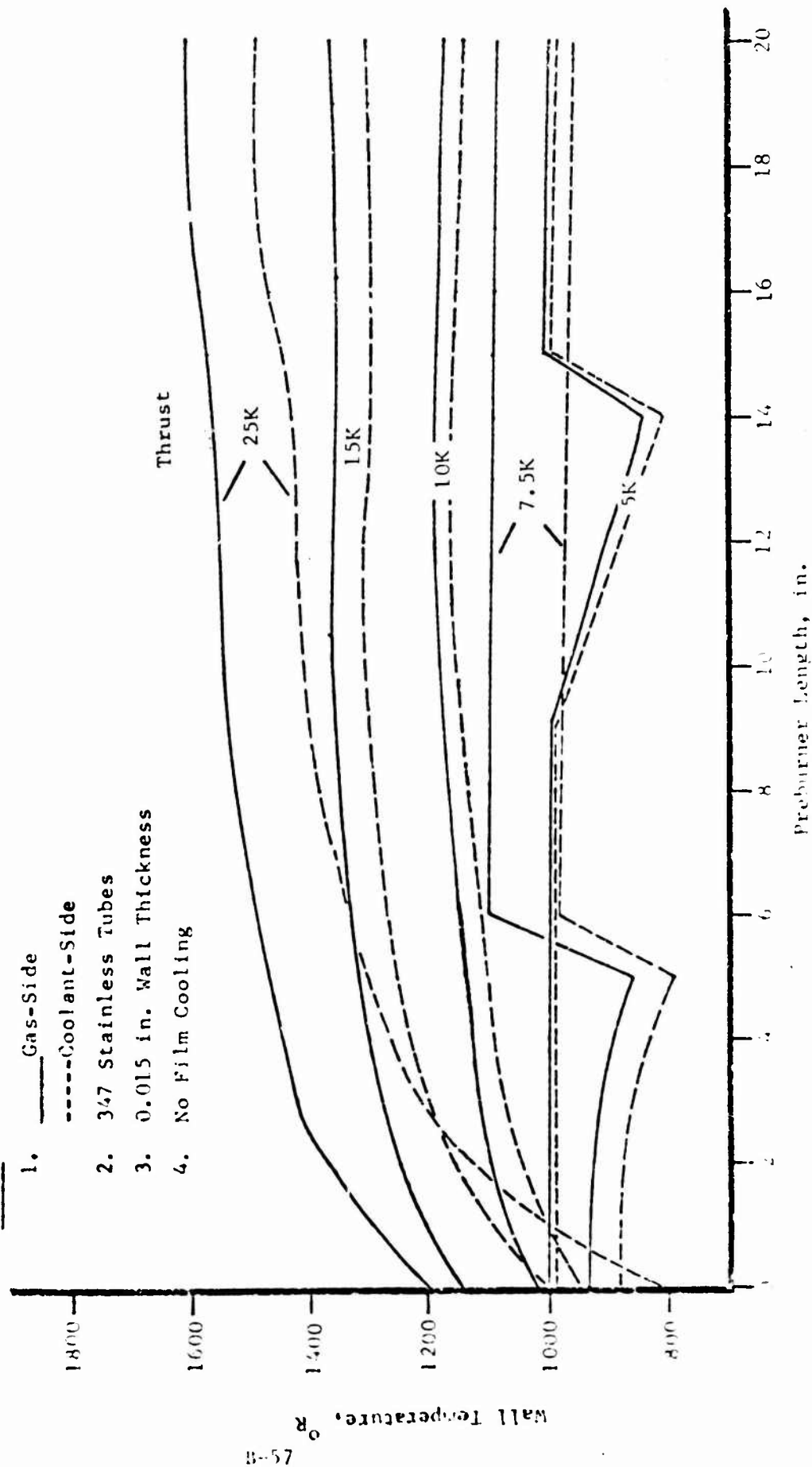
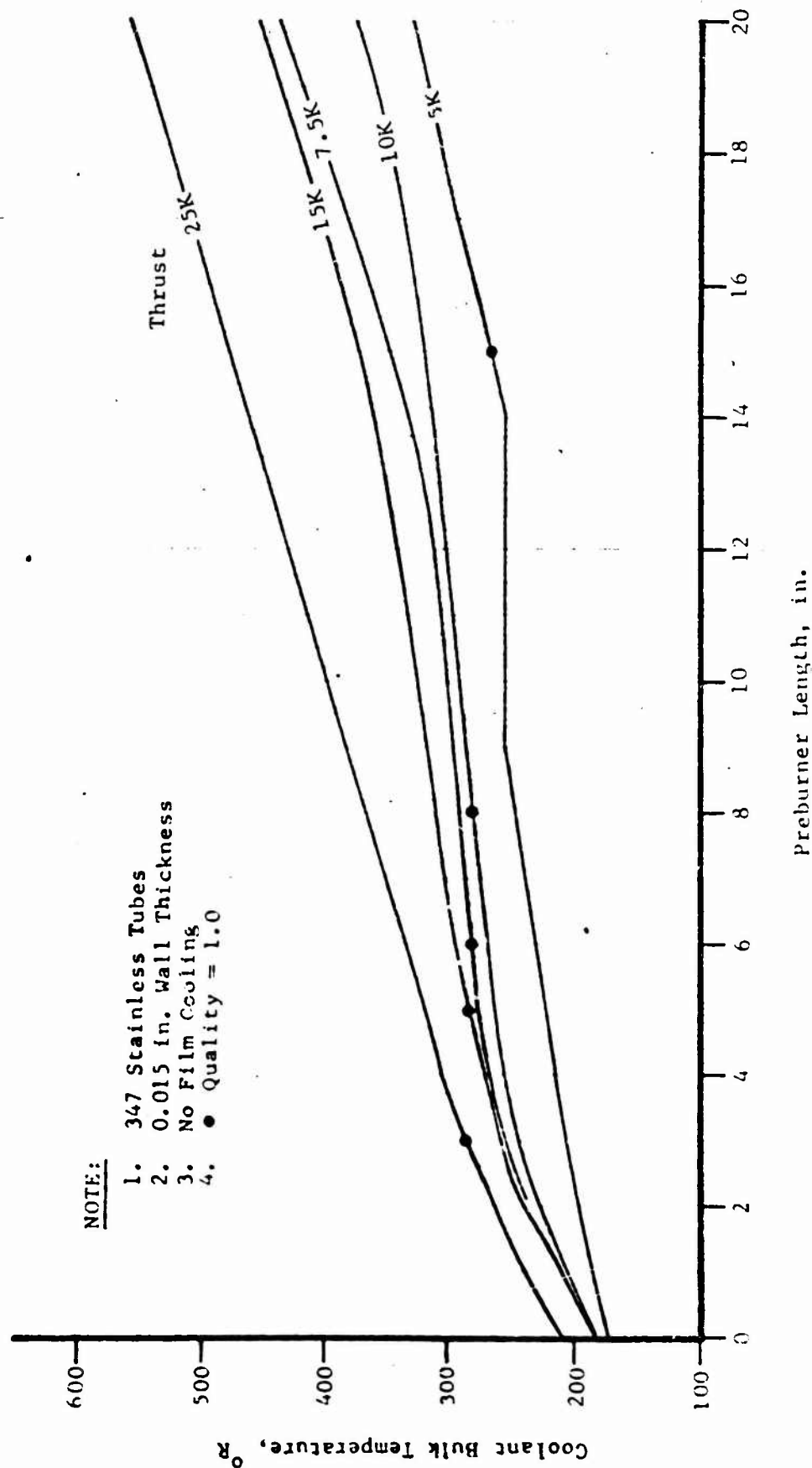
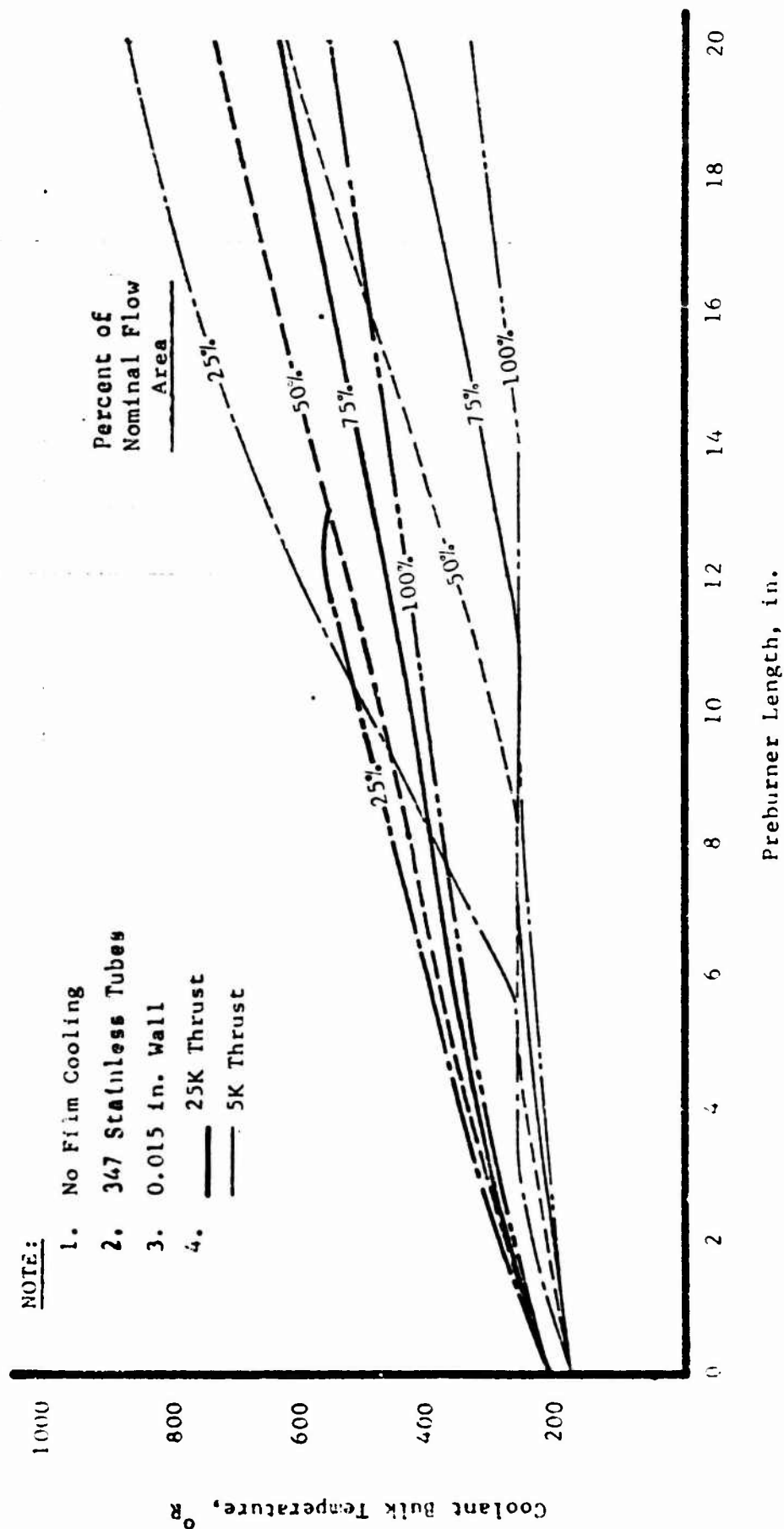


Figure 5

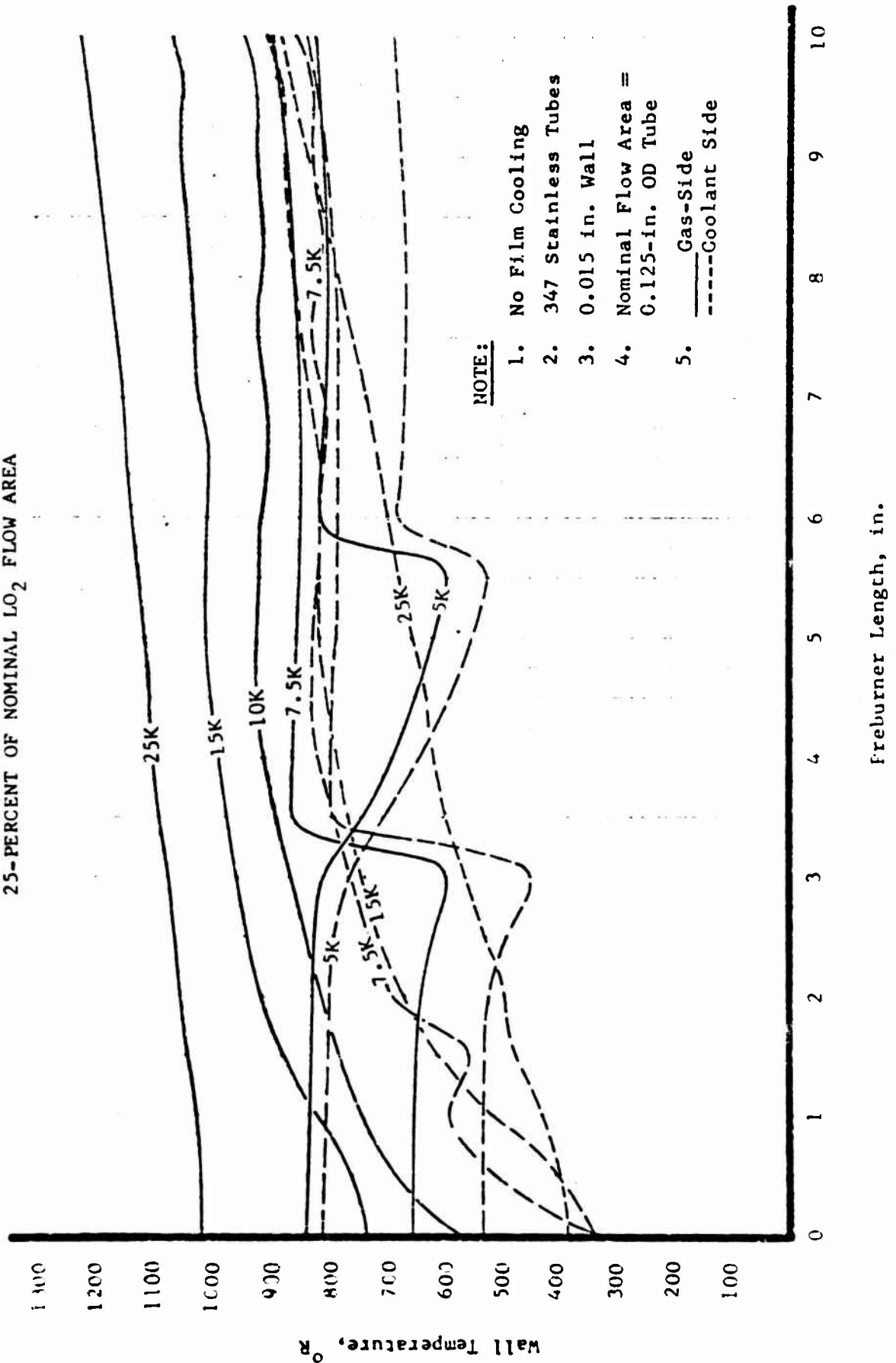
OOS PREBURNER STUDY  
 $\text{LO}_2$  COOLANT BULK TEMPERATURE RISE  
 FOR 1/8 in. O.D. TUBE CHAMBER



# OOS PREBURNER STUDY EFFECT OF REDUCING $\text{LO}_2$ FLOW AREA



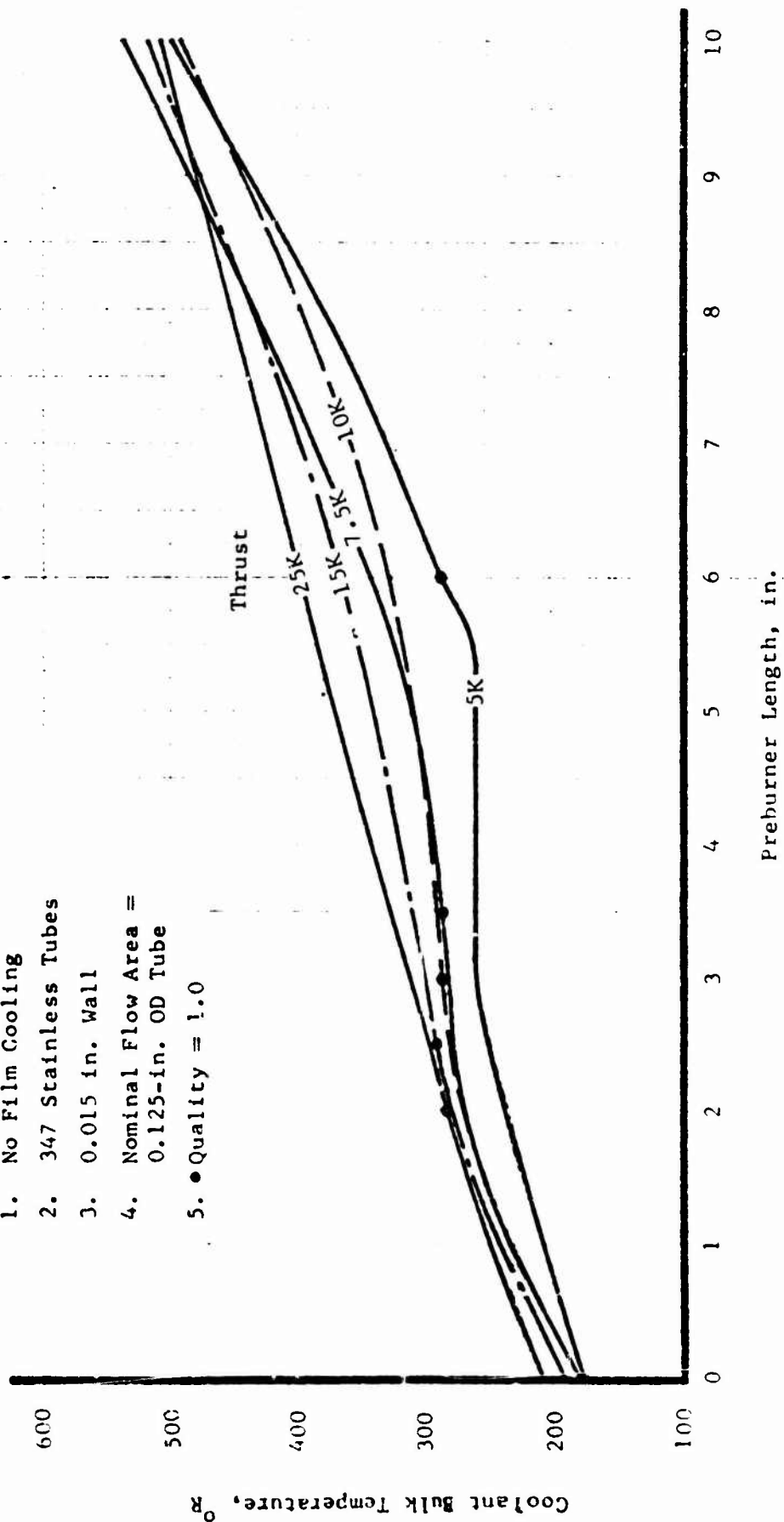
OOS PREBURNER STUDY  
TUBE WALL TEMPERATURES FOR  
25-PERCENT OF NOMINAL  $\text{LO}_2$  FLOW AREA



OOS PREBURNER STUDY  
 $\text{LO}_2$  BULK TEMPERATURE RISE FOR  
 25-PERCENT OF NOMINAL  $\text{LO}_2$  FLOW AREA

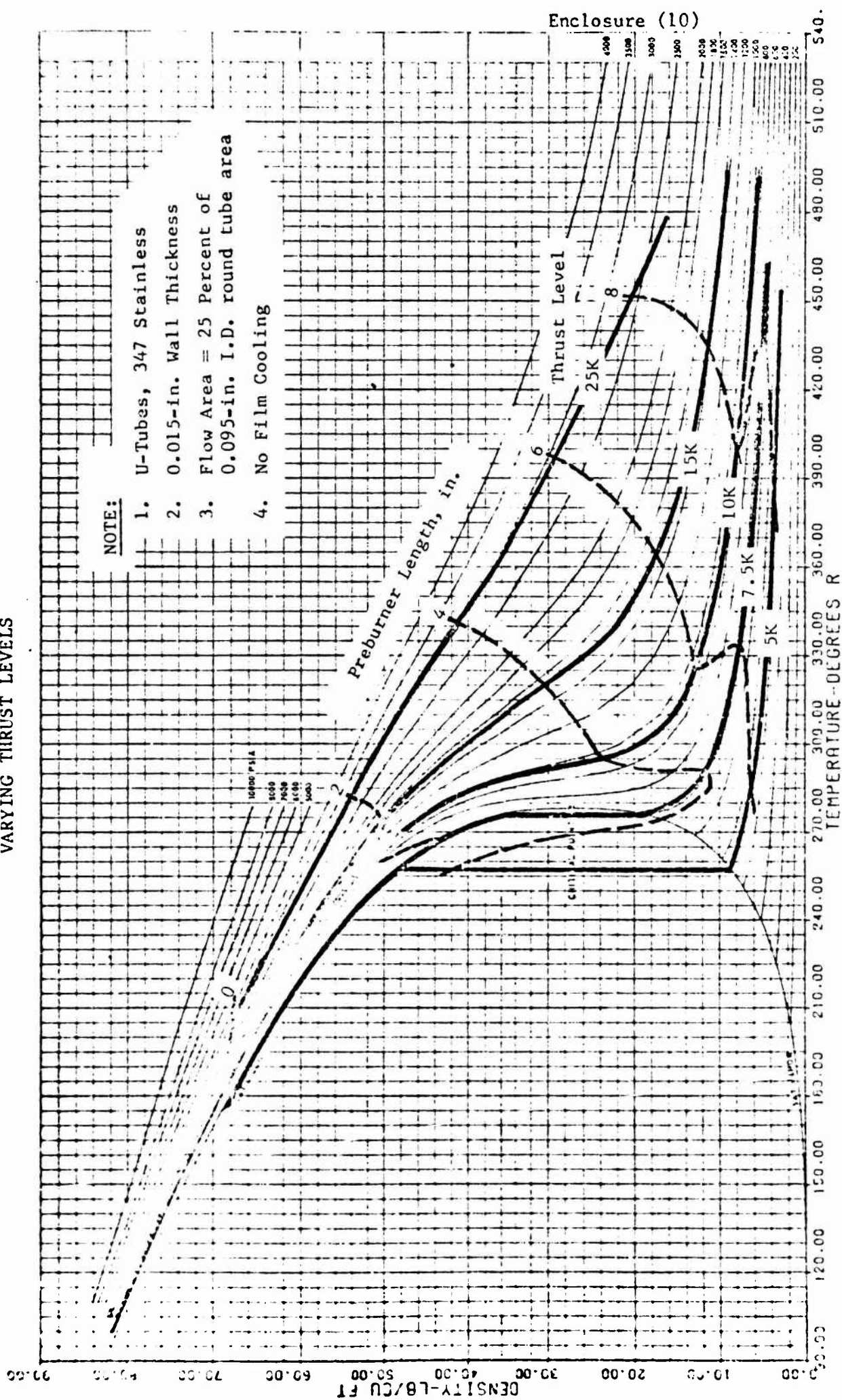
NOTE:

1. No Film Cooling
2. 347 Stainless Tubes
3. 0.015 in. Wall
4. Nominal Flow Area =  
0.125-in. OD Tube
5. • Quality = 1.0





# 00S PREBURNER STUDY EFFECT OF PREBURNER LENGTH AT VARYING THRUST LEVELS



DENSITY OF OXYGEN

OOS VANES STUDY  
EFFECT OF VANE LENGTH AT  
VARYING THRUST LEVELS

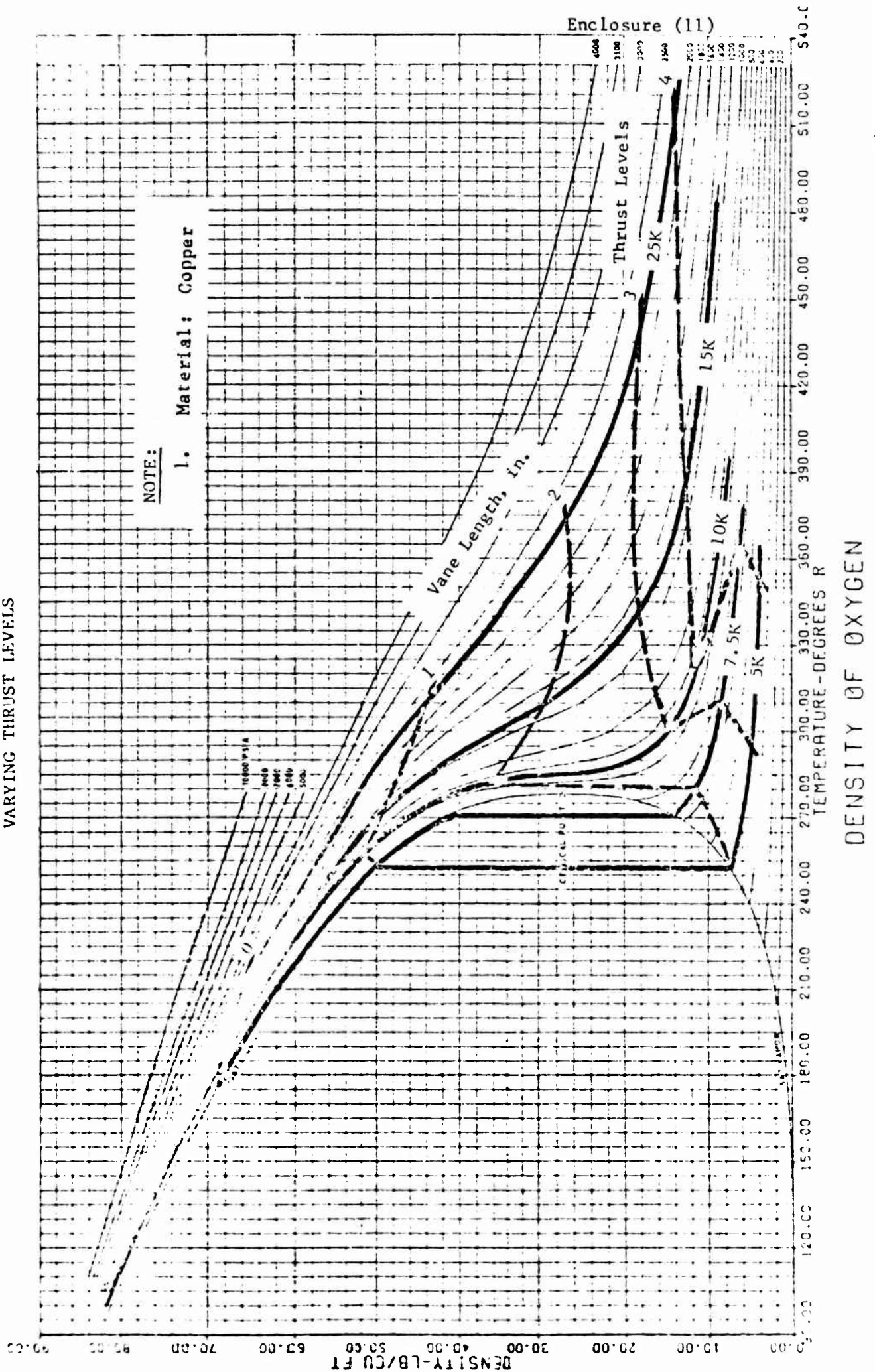
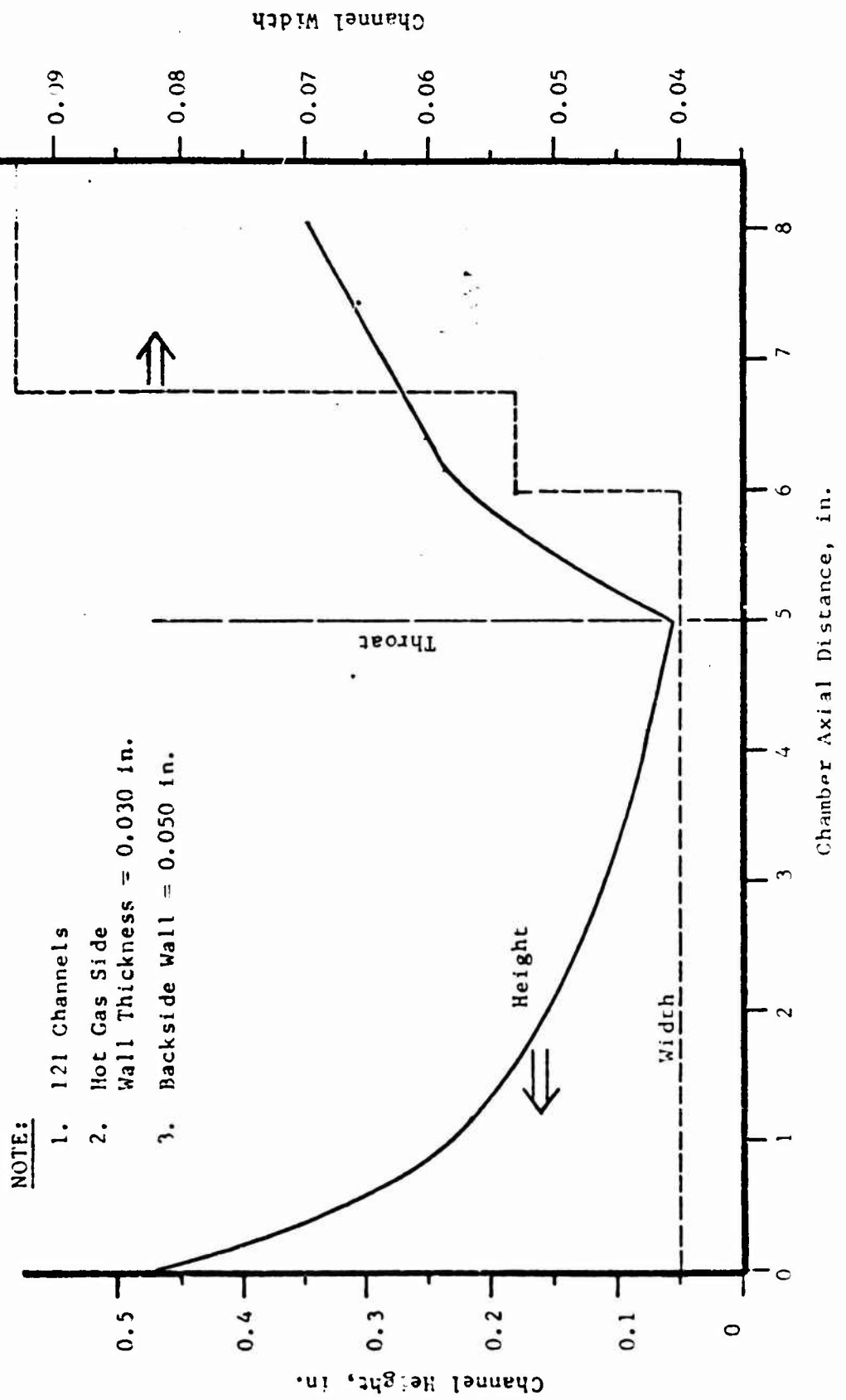


Figure 11

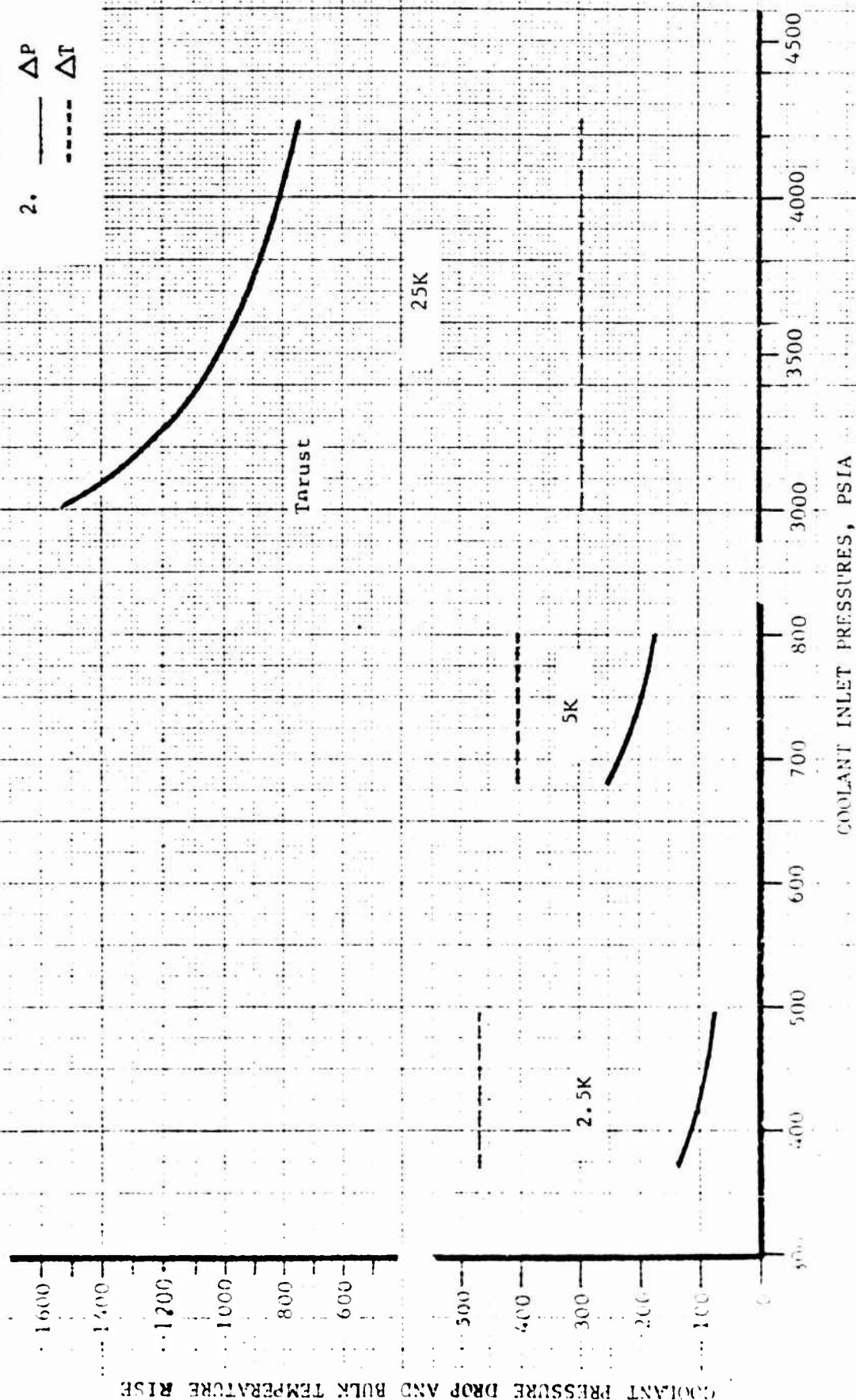
OOS COPPER CHAMBER  
COOLANT CHANNEL GEOMETRY



OOS TURBINE CHAMBER  
 $\text{Ln}_2$  COOLANT PRESSURE DROP AND  
 BULK TEMPERATURE RISE FOR VARY INLET PRESSURES

NOTE:

1. Manifold Losses  
Not Included
2.  $\Delta P$  ———  
 $\Delta T$  - - - -

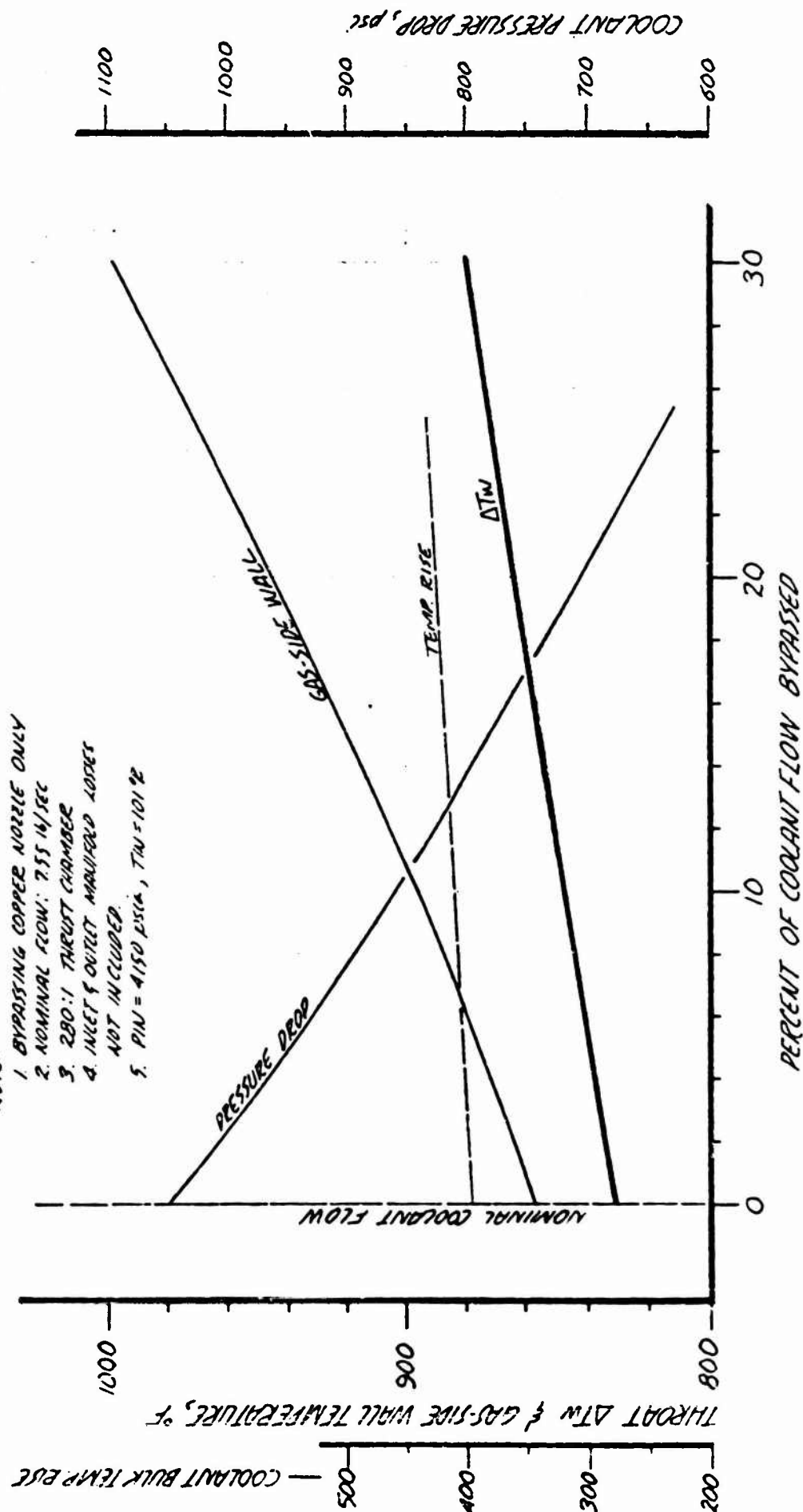




# 00S COPPER NOZZLE EFFECT OF BYPASSING COOLANT FLOW $F = 25\text{ K}$ $P_c = 1800\text{ psia}$

NOTE:

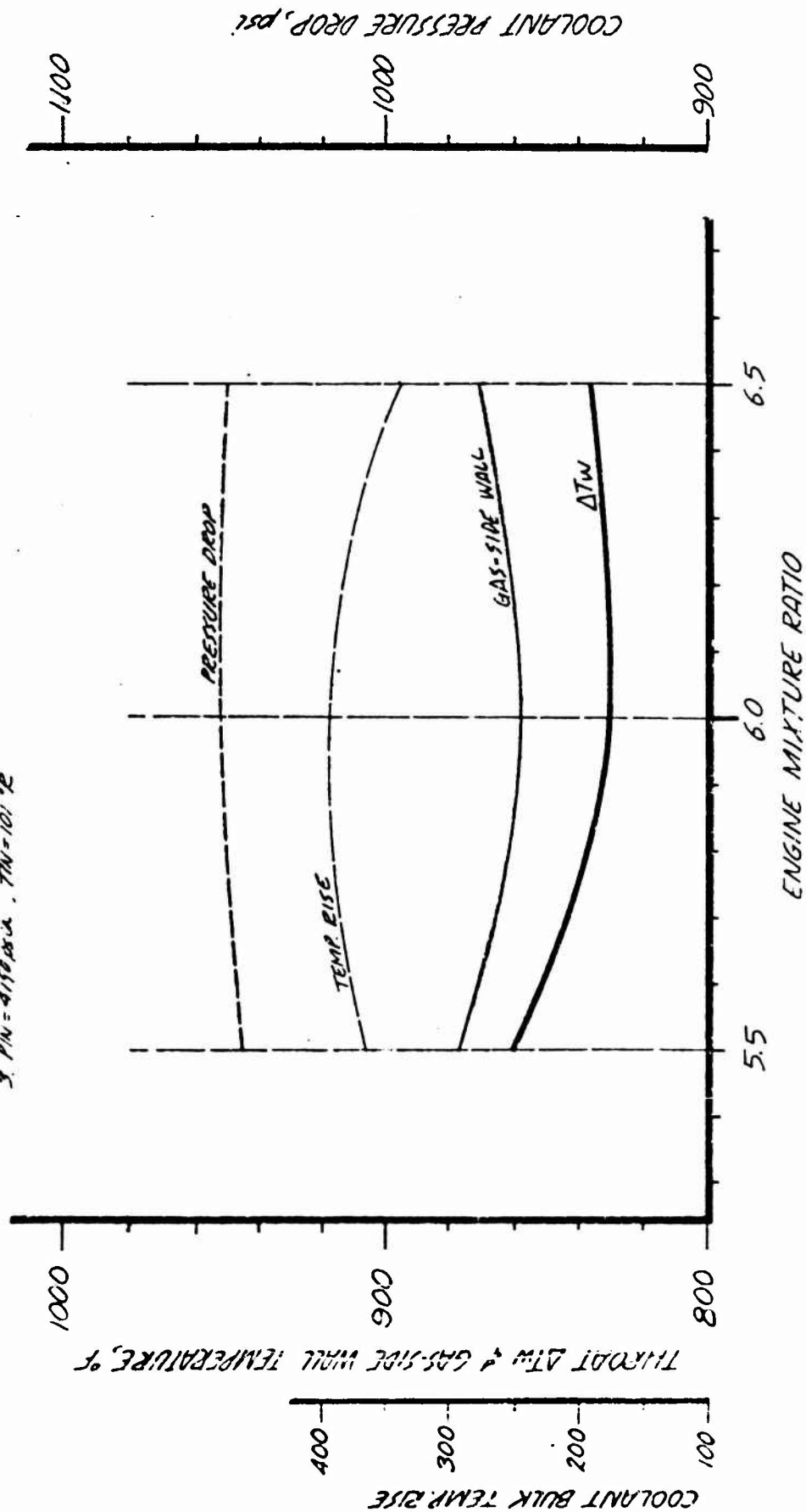
1. BYPASSING COPPER NOZZLE ONLY
2. NOMINAL FLOW:  $7.55\text{ in}^3/\text{SEC}$
3.  $280:1$  THRUST CHAMBER
4. INLET & OUTLET MANIFOLD LOSSES NOT INCLUDED
5.  $P_{IN} = 4150\text{ psia}$ ,  $T_{IN} = 101^\circ\text{R}$



005 COPPER NOZZLE  
EFFECT OF ENGINE MIXTURE RATIO  
FIXED COOLANT CHANNEL GEOMETRY  
F=25K PC=1800 psia

NOTE:

1. 280:1 THRUST CHAMBER
2. MANIFOLD LOSSES NOT INCLUDED
3.  $P/M = 4150 \text{ psia}$ ,  $T/M = 101^\circ \text{R}$



005 COPPER NOZZLE  
ENGINE MIXTURE RATIO STUDY  
F=25K PC=1800 psia

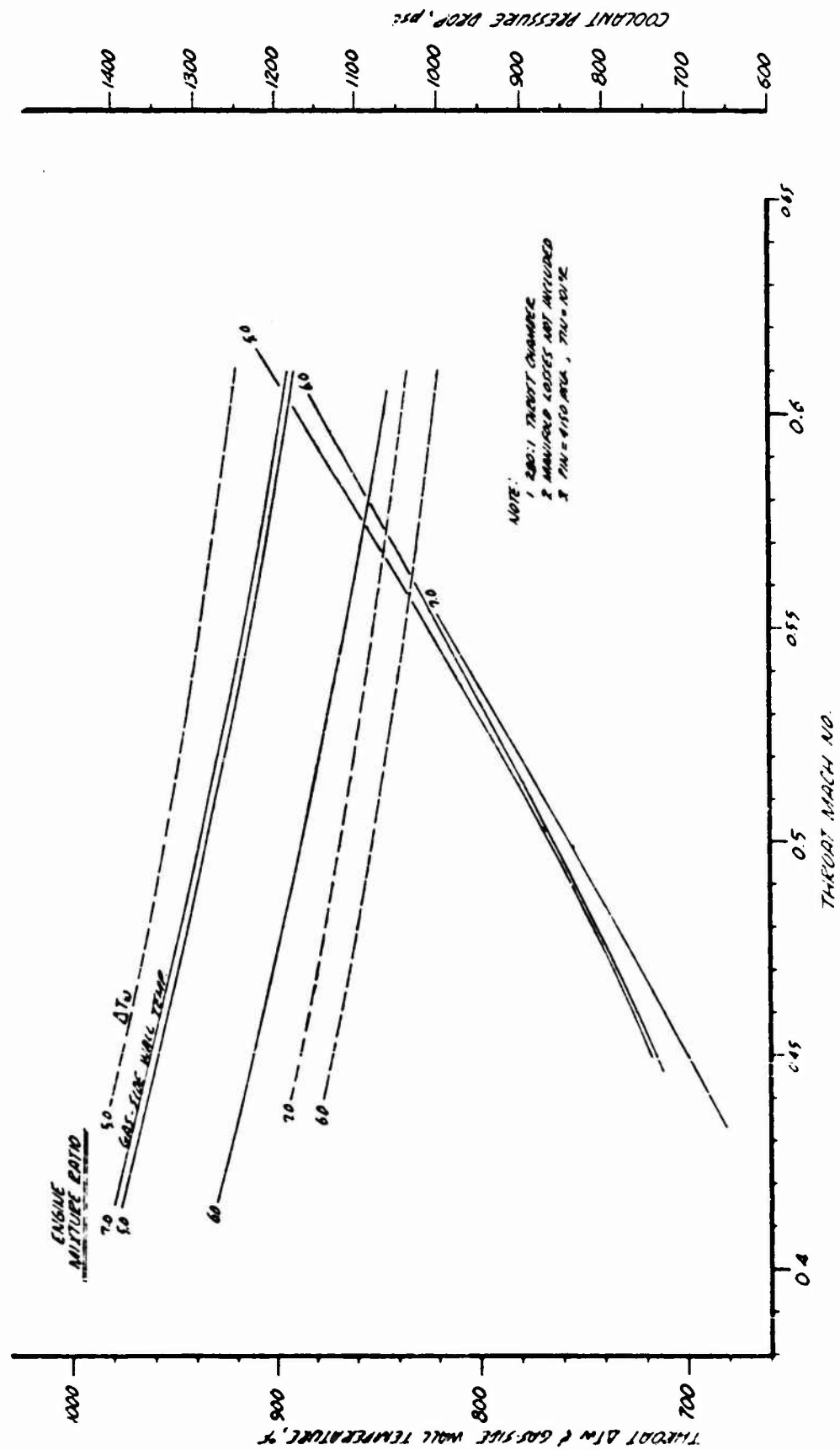
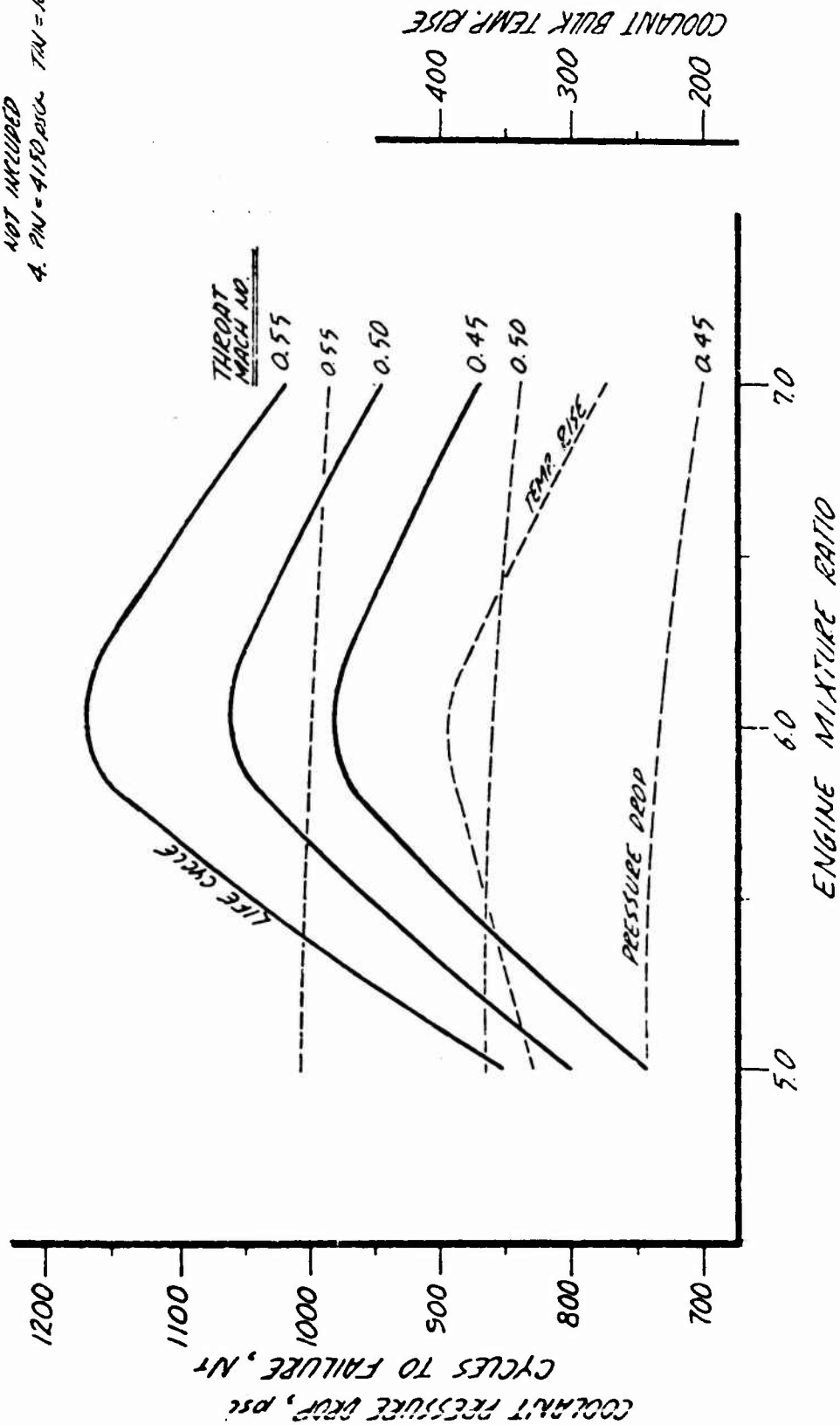


Figure 16

# 005 COPPER NOZZLE COOLANT BULK TEMPERATURE RISE AND PRESSURE DROP VERSUS ENGINE MIXTURE RATIO

## NOTES:

1. THRUST CHAMBER: 280:1
2.  $F = 25 \text{ K}$ ,  $P_C = 1800 \text{ psia}$
3. INLET & OUTLET MANIFOLD LOSSES  
NOT INCLUDED
4.  $P_{IN} = 4150 \text{ psia}$ ,  $T_{IN} = 101^\circ \text{C}$





005 COPPER NOZZLE  
BOUNDARY-LAYER MIXTURE RATIO STUDY  
CORE MR=60 F=25K PC=1800 PSI

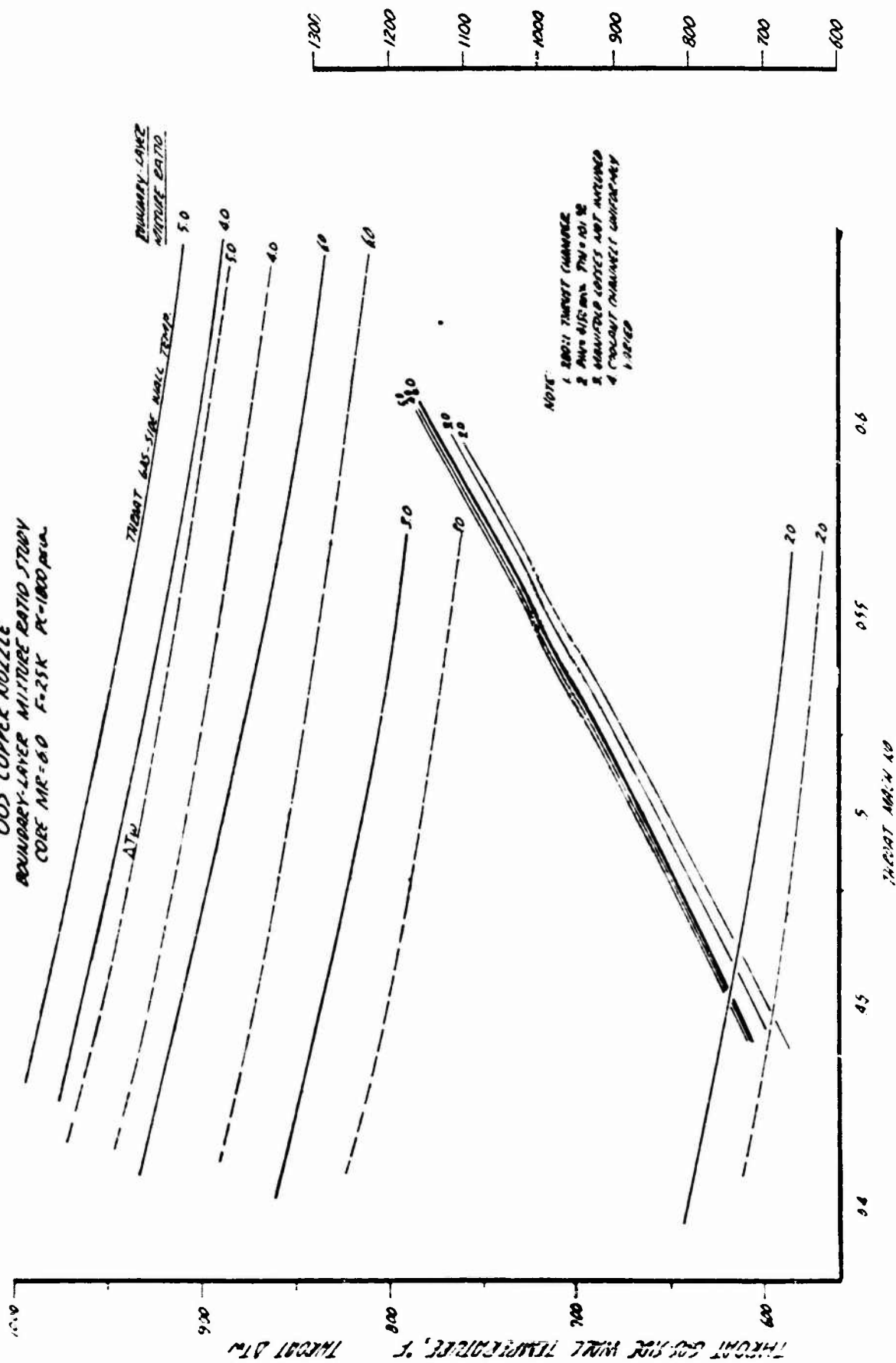


Figure 18

OOS COPPER NOZZLE  
BOUNDARY-LAYER MIXTURE RATIO  
VERSUS LIFE CYCLE AND COOLANT PRESSURE DROP

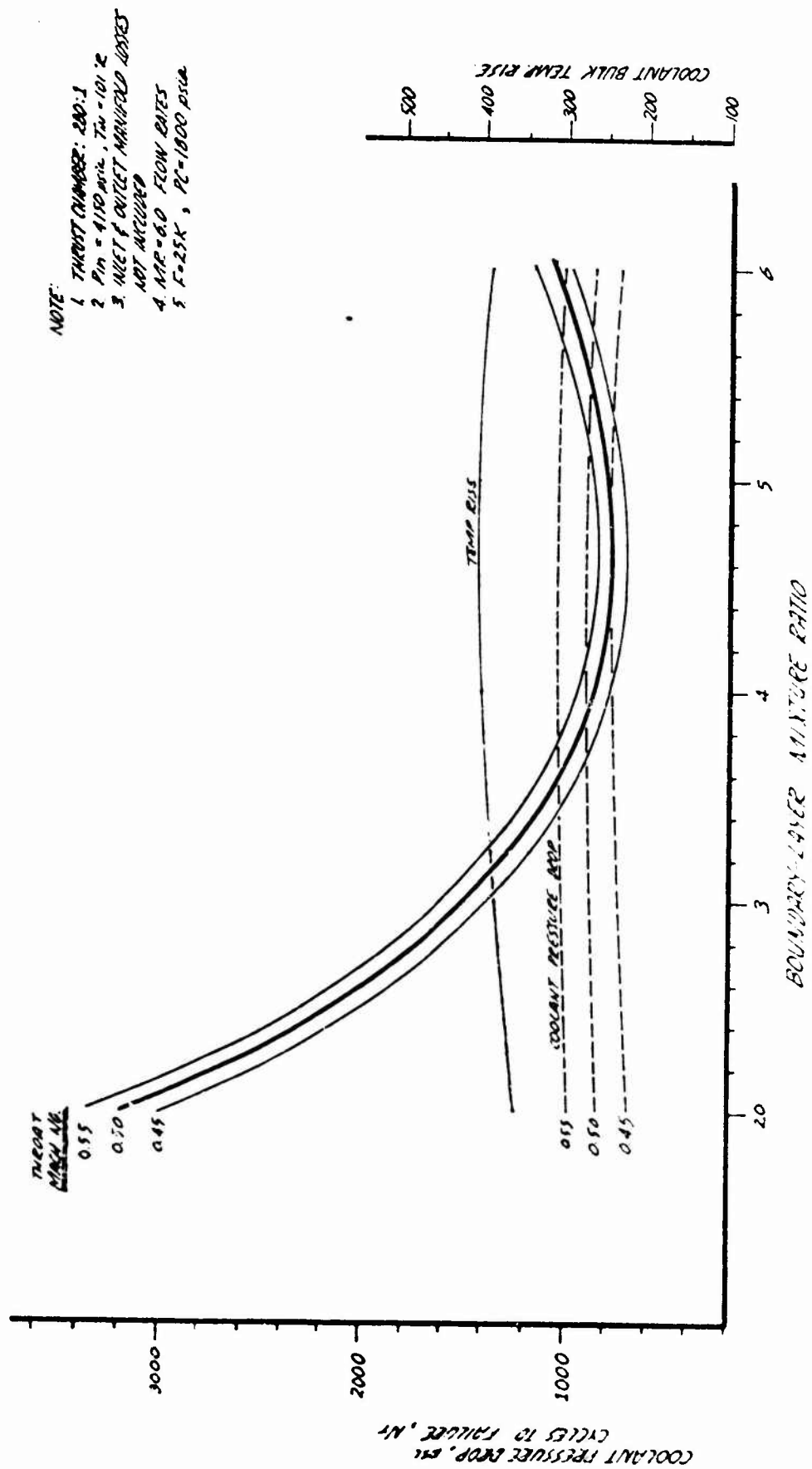
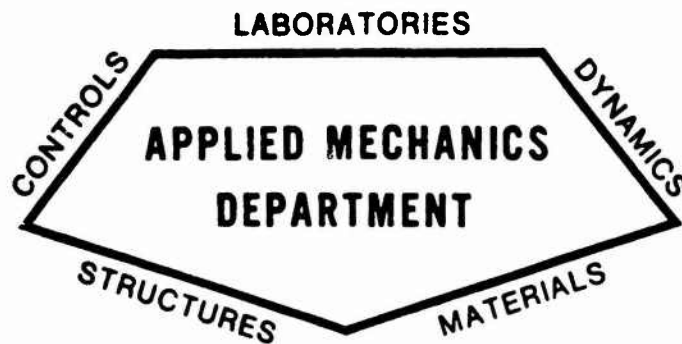


Figure 19

**Appendix C**

**STRUCTURAL ANALYSIS**

STRUCTURAL ANALYSIS OF COMBUSTION COMPONENTS  
FOR OOS 25K ENGINE



## STRUCTURAL ENGINEERING SECTION

REPORT NO. SA-00S-CC-03

STRUCTURAL ANALYSIS OF COMBUSTION  
COMPONENTS FOR OOS 25<sup>K</sup> ENGINE

PREPARED BY:

G. H. Skopp  
Engineering Specialist  
Structural Engineering Section

APPROVED BY:

R. D. Entz, Supervisor  
Advanced Design  
Structural Engineering Section  
Engineering

DATE 23 July 1971



AEROJET LIQUID ROCKET COMPANY

SACRAMENTO, CALIFORNIA

## TABLE OF CONTENTS

	<u>Page</u>
I. Introduction	1
II. Summary of Results	1
III. Discussion of Results	6
IV. Conclusion and Recommendations	10
V. Analysis	11
A. Design Criteria	11
B. Loads and Environment	12
C. Material Properties	13
D. Design Strength Factors	21
E. Method of Analysis	22
VI. Calculations	25
A. Preburner Assembly	25
B. Regen Tube Bundle	37
C. Pressure Jacket	53
D. Combustion Chamber	57
E. Outer Thrust Support Cone	67
F. Injector/Combustion Chamber Bolted Joint	71
G. Injector Vanes	75
VII. References	79

## LIST OF FIGURES

<u>Figure</u>	<u>Title</u>	<u>Page</u>
1	Mechanical Properties of ARMCO 22-13-5 Sheet and Bar	14
2	ARMCO 22-13-5 LCF Data	16
3	Mechanical Properties of Zirconium Copper	17
4	Zirconium Copper LCF Life	18
5	Mechanical Properties of Boron Deoxidized Copper	19
6	BD-CU Low Cycle Fatigue Life @ 1000°F	20
7	Preburner Chamber Configuration	25
8	OOS Preburner Study Tube Wall Temperatures for 25% of Nominal LO <sub>2</sub> Flow Area	26
9	OOS Preburner Study LO <sub>2</sub> Bulk Temperature Rise for 25% of Nominal LO <sub>2</sub> Flow Area	27

### LIST OF FIGURES (cont.)

<u>Figure</u>	<u>Title</u>	<u>Page</u>
10	OOS Preburner Study Tube Wall, $T_{wg}$ , and $LO_2$ Bulk Temperature, $T_B$ , Gradients at $25^K$ lb Thrust	32
11	Preburner Low Cycle Fatigue Life at $25^K$ lb Thrust	33
12	Regen Nozzle Tube Bundle Geometry	37
13	OOS Regen Nozzle Tubes Temperature Profiles @ $25^K$	38
14	OOS Regen Nozzle Tubes LCF Life Predictions	43
15	Main Combustion Chamber Assembly	53
16	Chamber Channel Parameters	57
17	Isothermal Data for Copper Nozzle @ $\epsilon = 2:1$ (fwd of throat) Steady State Solution	58
18	Isothermal Data for Copper Nozzle @ Throat Steady State Solution	59
19	Isothermal Data for Copper Nozzle @ $\epsilon = 6:1$ (aft of throat) Steady State Solution	60
20	Zirconium Copper OOS Chamber LCF Requirements	65
21	OOS TCA Life Requirements	66
22	Injector/Chamber Bolted Joint Configuration	71
23	Injector Vane Geometry	75

### LIST OF TABLES

<u>Table</u>	<u>Title</u>	<u>Page</u>
I	Summary of Margins of Safety	3
II	Low Cycle Fatigue Life Predictions	5
III	Copper Chamber Geometry and Design Loads	61
IV	Copper Chamber Induced Stresses	62
V	Margins of Safety in Copper Chamber	63
VI	Low Cycle Fatigue in Copper Chamber	64

## I. INTRODUCTION

This report presents the structural analysis of the combustion components for the Orbit-Orbit Shuttle Baseline Configuration per ALRC assembly drawing No. 1161568. The components under consideration were the Preburner Assembly, Regen Nozzle Tube Bundle, Combustion Chamber Assembly and Main Injector Vanes.

In addition to material strength considerations, emphasis was given to service life predictions since thermal cycle and total lifetime requirements were relatively severe, particularly in relation to space shuttle requirements. The combustion components will be subjected to high temperatures during operation while supporting structures will remain at temperatures close to cryogenic hydrogen and/or cryogenic oxygen. Repetitive strain induces mechanical loads which in turn could cause buckling and/or low cycle fatigue. Thus, consideration must be given to temperature distribution, operating environment, physical and mechanical properties of the materials, geometry and loading conditions.

A description of each component and the pertinent design data are given in the section dealing with that component as well as in Section V of this report, which also provides a brief description of the assumptions and methods applied. Section II summarizes the results of the analyses while Section III presents a more comprehensive discussion of the results. Section VI contains the calculations performed for each component.

## II. SUMMARY OF RESULTS

Tables I and II provide a summary of results of the structural analyses of the combustion components of the OOS engine. Table I presents the material strength evaluation while Table II shows the low cycle fatigue life predictions.

The minimum margin of safety of 0.00 (yield) occurred at the crown of the preburner tubes and in the combustion chamber channel at expansion ratio 6:1. A safety factor of 1.20 was applied to the pressure loading in each case. The induced stresses in the preburner tubes are a result of hoop membrane plus discontinuity bending whereas the induced stress in the



combustion chamber channel is primarily bending. Consideration was given to the increased loading capability of the material in the inelastic region when loaded by bending moments.

Table II summarizes the LCF predictions at maximum thrust and nominal mixture ratio of 6.0. The baseline combustion components require no replacement over the entire 1500 cycle/50 hours service life, except for the main combustion chamber which must be replaced at each overhaul (300 cycles) in order to attain a safety factor of 4.0 on thermal cycles. Total operating lifetime in the 10 to 50 hour range has little effect on cyclic life for the combustion components, with the exception of the injector vane which is subjected to some thermal creep damage, but is still capable of meeting the life requirements.

TABLE I

## SUMMARY OF MARGINS OF SAFETY

Component	Critical Loading Environment	Material	Maximum Induced Stress, psi	Type of Stress	Allowable Stress, psi	Margin of Safety	Ref. Page No.
A.-Preburner Assy 1.-Tubes	Proof Pressure= 3900 psi (yield) Temperature, T <sub>wg</sub> = 765°F	Armco 22-13-5 Stainless Steel Tube	13,795 + 40,600	Hoop Tension + Discontinuity Bending	46,000 + 57,500	0.00 (yield)	30
	Proof Pressure= 3360 psi (yield) Temperature, T = 45°F	Armco 22-13-5 Stainless Steel Tube	63,500	Hoop Tensile Stress	65,500	0.03 (yield)	35
	Proof Pressure= 3900 psi (yield) Temperature, T = R.T.	Armco 22-13-5 Stainless Steel Sheet	35,000	Meridional Tension Stress	75,000	1.14 (yield)	36
B.-Regen Nozzle Tubes ø c = 30:1	Proof Pressure= 5100 psi (yield) Temperature, T <sub>wg</sub> = 550°F	Armco 22-13-5 Stainless Steel Tube	Radius Thickness (R/t)=9.15	Hoop Tensile Stress	(R/t) <sub>cr</sub> = 9.42	0.03 (yield)	40
C.-Corbustion Chamber Assy 1.-Pressure Jacket	Proof Pressure= 2040 psi (yield) Temperature, T = R.T.	Armco 22-13-5 Stainless Steel Wire	53,000	Hoop Tensile Stress	55,000	0.04 (yield)	54
	Proof Pressure= 4500 psi (yield) Temperature, T = R.T.	Armco 22-13-5 Stainless Steel Sheet	57,600	Meridional Tension Stress	75,000	0.30 (yield)	55

TABLE I (CONT.)

Component	Critical Loading Environment	Material	Maximum Induced Stress, psi	Type of Stress	Allowable Stress, psi	Margin of Safety	Ref. Page No.
3.-Chamber-Channel at Fuel Coolant Inlet, $\epsilon=6:1$	Pressure Diff., $\Delta P = 4430$ psi (yield). Temp., $T_{wg} = 209^\circ F$	Zirconium Copper	10,700	Bending	10,700	0.00 (yield)	63
4.-Outer Shell Thrust Support Cone	Combination of Thrust and gim-baling angular acceleration of 40 rad/sec <sup>2</sup> @ Temp.=R.T.	Armco 22-13-5 Stainless Steel Sheet	-34,780	Meridional Compressive Stress	73,000	1.16 (yield)	69
5.-Injector/Chamber Flange	Combination of Thrust and gim-baling angular acceleration of 40 rad/sec <sup>2</sup> @ Temp.=R.T.	Armco 22-13-5 Stainless Steel Bar	12,850	Bending	46,000	2.58 (yield)	74
6.--(24) $\frac{1}{4}$ 28-UNF Bolts	Combination of Thrust and gim-baling angular acceleration of 40 rad/sec <sup>2</sup> @ Temp.=R.T.	Alloy Steel-Rockwell Hardness C38	5,525 lb	Tension	6,910 lb	0.25 (ult)	73
D.-Injector Vanes	Differential Pressure $\Delta P = 480$ psi (yield) Temperature, $T_{wg} = 400^\circ F$	Boron Deoxidized Copper (OFHC)	6,000	Bending	6,860	0.14 (yield)	76

TABLE II

## LOW CYCLE FATIGUE LIFE PREDICTIONS

Component	Location	Material	Gas-Side Wall Temperature, $T_{wg}$ , °F	Maximum Thermal Gradient $\Delta T$ , °F	Induced Strain, %	Number of Cycles to Failure
A.-Preburner Assy Tubes	Crown of Tube at Oxidizer Coolant Outlet	Armco 22-13-5 Stainless Steel Tube	765.0	720.0	0.99	8,800
B.-Regen Nozzle Tubes	Crown of Tube at Fuel Coolant Inlet, $\epsilon = 6:1$	Armco 22-13-5 Stainless Steel Tube	664.0	1024.0	1.00	10,200
C.-Combustion Chamber	Gas-Side Wall of Channel at Fuel Coolant Exit (Injector Face)	Zirconium Copper	838.0	857.0	1.63	1,220
D.-Injector Vane	Vane Trailing Edge	Boron Deoxidized Copper (OFHC)	1,000.0	600.0	0.65	12,000 (no hold time) 7,000 (50 hours total time duration)

### III. DISCUSSION OF RESULTS

The design conditions considered in the study were direct stresses from pressure and mechanical loading, thermal stresses induced by either internal or external restraints, fatigue life, and creep-rupture or creep damage effects on buckling and fatigue life. The life requirements of 300-1500 cycles, combined with a factor of safety of four, put the OOS engine into the intermediate fatigue life range. Both ultimate strength and ductility of the materials contribute significantly in this range, with little advantage from either a very ductile low-strength material or a high strength non-ductile material. This means that the fatigue life is influenced mostly by the OOS engine design (thermal gradients) and performance, and cannot be greatly increased by material selection.

Several simplifying assumptions have been used repeatedly in the study. Thermal strains are estimated by use of the expression

( $\Delta\epsilon_t = k\alpha\Delta T$ ), where

$\Delta\epsilon_t$  = total strain range, in./in.

$\alpha$  = coefficient of thermal expansion, in./in./°F

$\Delta T$  = temperature difference between hot structure and colder restraining structure, °F

$k$  = geometric constant determined for each component, using results of SSEM or OOS computer solutions for baseline.

For the regions where detailed thermal analyses of the structure were not available, propellant bulk temperatures were conservatively assumed as the restraint temperature.

A safety factor of four was used as a goal for the OOS combustion components life in order to be consistent with the Space Shuttle Main Engine, and materials were selected so as to be insensitive to total duration (creep damage) in all components except the main injector vanes which was selected for ease of fabrication with multiple braze cycles, while still meeting the life requirements based upon a linear cumulative damage analysis.

#### A. PREBURNER ASSEMBLY

The preburner assembly consists of a series of 1/8" O.D., Armco 22-13-5 "U" tubes with strips of Armco 22-13-5 wire welded into the tubes to give the desired oxidizer flow area. The tubes are then welded together to form a 3.0 inch diameter chamber. A discontinuity analysis was performed which indicated that the critical region occurred at the crown due to internal pressure and discontinuity bending stresses. The minimum margin of safety of 0.00 (yield) was calculated considering a bending modulus of yield equal to 1.25 times the allowable tensile yield strength, and an applied safety factor of 1.20. The bending modulus accounts for the nonlinear stress distribution in the inelastic range due to bending. Thermal buckling and thermal creep were not significant considerations since the thermal gradients were not severe. The preburner has a minimum predicted fatigue life of 8800 thermal cycles at maximum thrust and nominal mixture ratio of 6.0. The critical location is the hot crown at the outlet end of the chamber assembly. The desired number of cycles to be attained is 6,000 which includes a safety factor of 4.0 (see Figure 11).

The total duration of 50 hours is not significant since the maximum temperature (765°F) is below the Armco 22-13-5 creep threshold.

A weld efficiency of 85% was considered in order to evaluate the preburner chamber thickness, which resulted in a margin of safety of 0.03 (yield) for basic hoop stress.

#### B. REGEN NOZZLE TUBES

The regen nozzle tube bundle consists of 190 tubes between expansion ratio,  $\epsilon$ , 6:1 and 30:1, after which the number of tubes is increased to 380 up to expansion ratio,  $\epsilon$ , 125:1. The tubes are fabricated from Armco 22-13-5 and are a minimum of 0.015 in. thick while the outer diameter varies from 0.128 in. @  $\epsilon = 6:1$  to 0.275 in. prior to bifurcation at  $\epsilon = 30:1$  and 0.1375 in. to 0.280 in. @  $\epsilon = 125:1$ . The critical location for the tubes, for material strength considerations occurs at expansion ratio 30:1 prior to bifurcation where a margin of safety of 0.03 (yield) was calculated. Thermal

buckling and thermal creep were negligible considerations at the relatively low thermal gradients.

The minimum predicted fatigue life is 10,200 cycles at maximum thrust and nominal mixture ratio of 6.0. The critical region is the hot tube crown at the 6:1 area ratio coolant inlet where the maximum thermal gradient occurs. Predicted fatigue life is shown in Figure 14. Total time duration is not significant since the maximum temperature (707°F) is below the creep threshold for Armco 22-13-5.

Using equations derived from references 11 and 12, the number and geometry of the tube bundle support rings were determined. Rings will be placed at expansion ratios 15:1, 30:1, and 80:1. The required minimum thickness for the rings is 0.021 in. for a ring width of 1.0 in. and was based primarily on the hoop strength requirement rather than the column buckling effect.

#### C. CHAMBER ASSEMBLY

The pressure jacket is a single layer of Armco 22-13-5 stainless steel wire wrapped around the zirconium copper combustion chamber. Using a standard Washburn & Moen wire gauge #12, a margin of safety of 0.04 (yield) was calculated considering basic hoop stress at the most critical location at the oxidizer coolant outlet. For ease of fabrication, the wire diameter of 0.105 in. will be constant despite the reduced loading downstream of the critical location. The additional thermally induced load imposed on the wire wrapped jacket by the combustion chamber was neglected because the effect is expected to be small. As compensation, the additional material strengths at the anticipated colder temperatures was not considered; rather, the room temperature material properties were used in the analysis. Since the wire temperatures and thermal gradients were low, low cycle fatigue predictions will be very high.

The zirconium copper has 120 channels of variable width and height and extends from expansion ratio,  $\epsilon = 2:1$ , forward of the throat, to  $\epsilon = 6:1$ , aft of the throat. Based upon material strength considerations, the critical location occurs at expansion ratio 6:1 where the minimum margin of safety of 0.00 (yield) was calculated for the channel width in bending. The calculation considered an idealization referred to as the plastic hinge which assumes that the elastic moment distribution for a beam fixed at both ends holds until the moment at the ends equal maximum moment, after which the ends "rotate" freely with no further change of end moment. The loading can then be increased until the moment at the center of the beam also equals the maximum moment which will correspond to a pinned end beam (Reference 15). The chamber has a predicted LCF life of 1220 cycles at the coolant exit for maximum thrust and nominal mixture ratio of 6.0. Higher (6.5) mixture ratios are more severe, lower MR is less damaging. Reduced throttle settings are also less damaging since gas-side wall temperatures, ( $T_{wg}$ ) will be lower. The 1220 cycles to failure indicates that for a required safety factor of 40 minimum, the chamber must be replaced every 300 cycles or overhaul period. The total time duration of 10 hours will be of little significance since no zirconium copper creep damage was noted in ALRC fatigue test data up to 1000°F (Reference 4). Figures 20 and 21 were prepared, based upon both ALRC and NAR test data and assumptions stated, in order to relate LCF predictions with induced thermal gradients.

The outer shell thrust support cone transmits the thrust and inertial loading from the regen nozzle tubes to the injector/chamber flange, by-passing the chamber. The cone was analyzed for maximum thrust, and inertial loading due to a failsafe angular acceleration of 40 rad/sec<sup>2</sup>. \*

The meridional strength requirements at the minimum radius is the governing criteria rather than buckling, and results in a margin of safety of 1.16 (yield). This is over and above the safety factor of 1.20 on thrust and 1.10 on inertial loading. The outer shell will be relatively cool and LCF life predictions will be high.

\*An ALRC requirement based upon failure of the actuator during gimbaling at maximum velocity, and the nozzle contacting a stop, coming to rest within 0.10 sec.



The injector/chamber bolted joint was analyzed for the meridional loading induced by the pressure expulsion force at the joint and inertial force due to  $40 \text{ rad/sec}^2$  angular acceleration. (24) 1/4-28 UNF bolts were used resulting in a margin of safety of 0.25 (ult) for bolts of 190,000 psi allowable ultimate strength.

#### D. INJECTOR VANE

The oxidizer flow channels in the Boron Deoxidized (OFHC) copper injector vanes were analyzed as flat plates and/or beams, fixed at both ends, subjected to a uniformly distributed load. The critical location occurred at the forward end of the injector where liquid oxidizer enters and the unsupported span length is maximum. A margin of safety of 0.14 (yield) was calculated when considering a bending modulus of yield of 1.25 times the tensile yield allowable strength and an applied factor of safety of 1.20 to the differential pressure of 400 psi.

The predicted fatigue life is 12,000 cycles without creep damage, which will reduce to 7,000 cycles at 50 hours total duration by use of the linear cumulative damage theory. Critical location is the outer vane platelet where strains are induced by the axial thermal gradient.

#### IV. CONCLUSIONS AND RECOMMENDATIONS

A. The combustion components of the OOS engine as reviewed in this report appear structurally adequate to withstand the anticipated temperatures and pressures during operating without failure although some local permanent deformation is expected.

B. All components with the exception of the main combustion chamber appear to have an adequate low cycle fatigue life to meet the no replacement requirements of 1500 cycles, and attain a minimum safety factor of 4.0 on engine life. The main combustion chamber must be replaced at each overhaul or 300 cycles in order to attain a minimum safety factor of 4.0.

C. It is recommended that a test program be performed to verify the material thermal fatigue/creep properties for both the Armco 22-13-5 and copper used in the analysis since present test data is so limited as to preclude using statistical methods to establish a design criteria.

D. It is further recommended that additional structural analyses be performed on those components not considered in this report, such as the AGCarb skirt, igniter, etc.

## V. ANALYSIS

### A. DESIGN CRITERIA

#### 1. Structural Requirements

Components should possess sufficient strength, rigidity, and other necessary physical characteristics required to survive the critical loading conditions that exist within the envelope of mission requirements.

##### a. Deflection Criteria

Each component shall not deflect or otherwise deform during exposure to the design environment such that the tactical performance of the component, or any assembly of which the component is a part, is degraded below specification limits.

##### b. Yield Criteria

Deformation indicating permanent set under design yield load environment shall be avoided. Tensile yield stress shall be that stress which provides 0.2 percent permanent strain, and strains in excess of this value will be considered permanent set. Local yielding is permitted provided it is limited and not detrimental to proper engine operation.

c. Ultimate Criteria

The structure is required to withstand design ultimate load environment without rupture, collapse or other catastrophic failure.

2. Factor of Safety

The factor of safety is an arbitrary factor meant to account for uncertainties and slight variations from item to item in material properties, fabrication quality and loading distributions. The following factors of safety shall be used in the analysis when applicable:

<u>Condition</u>	<u>Factor of Safety</u>
Minimum Yield	1.10
Minimum Ultimate	1.40
Limit Pressure	1.00 x MEOP (Maximum Expected Operating Pressure)
Proof Pressure	1.20 x Limit Pressure
Burst Pressure	1.50 x Limit Pressure
Low Cycle Fatigue	4.0 (on number of engine firings)
Thermal Creep	1.50 on critical (R/t) buckling parameter

B. LOADS AND PARAMETERS (Reference 1)

1. Thrust (F): Baseline engine will have  $F=25,000$  lbf.
2. Chamber Pressure ( $P_C$ ): Baseline engine will have  $P_C = 1800$  psi.
3. Gimbal angular acceleration ( $\alpha$ ):  $5.0$  radians/sec<sup>2</sup>.  
For failsafe design,  $\alpha = 40$  radians/sec<sup>2</sup>. (See note on page 9).
4. Overall expansion ratio ( $\epsilon$ ): Baseline engine will have  $\epsilon = 270$ .
5. Temperature (T): Temperature profiles are noted in each component section.
6. Initial flight + 4 refurbishments: 300 thermal cycles and 10 lifetime hours.
7. Initial overhaul + 4 overhauls at end of service: 1500 thermal cycles and 50 lifetime hours.

## C. MATERIAL PROPERTIES

### 1. Armco 22-13-5 Stainless Steel (References 2 and 3)

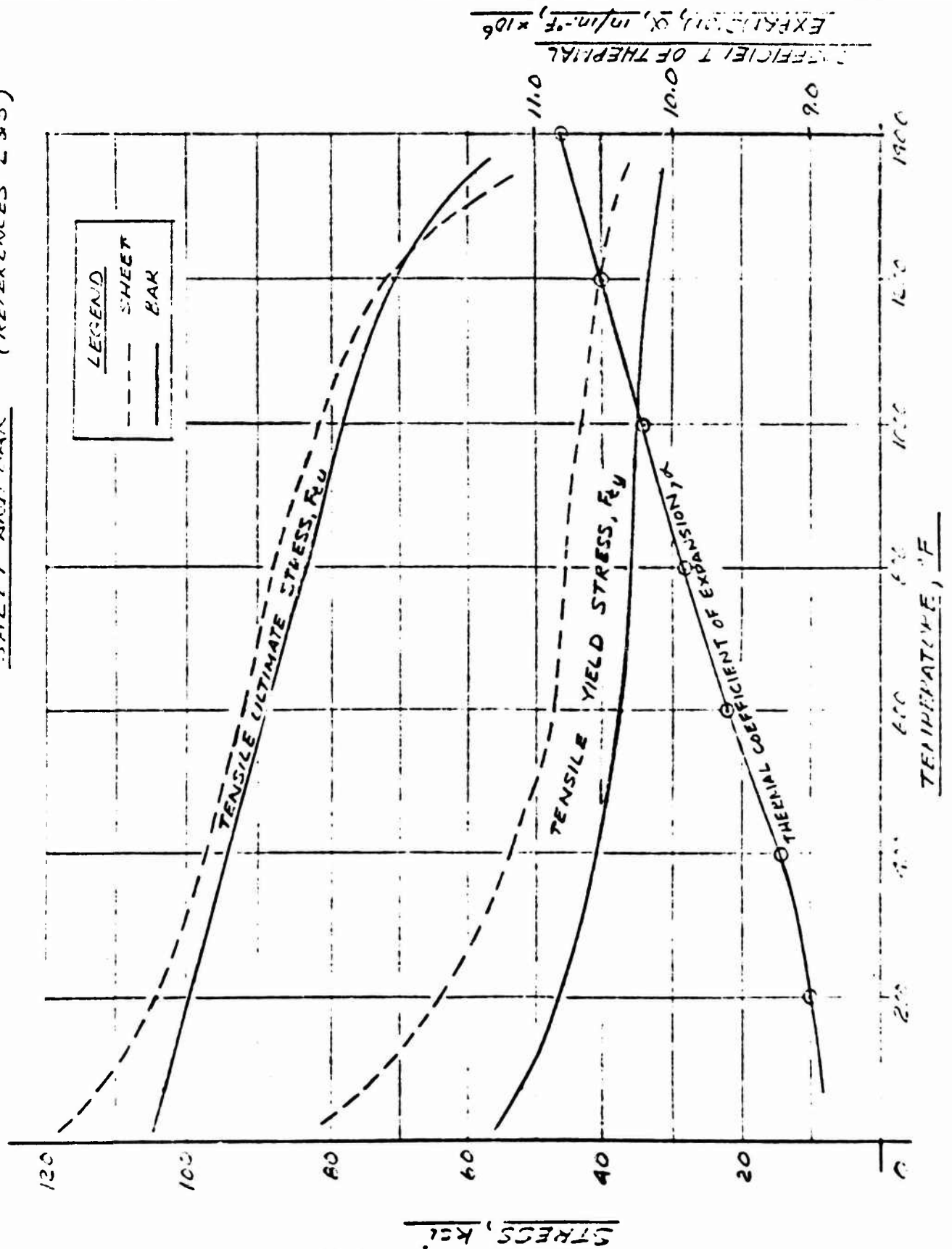
	<u>Bar</u>	<u>Sheet</u>
Modulus of Elasticity, E, @ R.T., psi	28.0x10 <sup>6</sup> (estimated)	
*Tensile Strength, F <sub>tu</sub> , @ R.T., psi	103,000	112,000 (See Figure 1)
*Yield Strength, F <sub>ty</sub> , @ R.T., psi	55,000	75,000 (See Figure 1)
Elongation, e (in 2.0 inches), %	45.0	36.5
Reduction of Area, RA, %	65.0	--
Density, ρ, lb/in. <sup>3</sup>	0.285	
Coefficient of Thermal Expansion, α, in./in.-°F	(See Figure 1)	
Cyclic Life	(See Figure 2)	

### 2. Zirconium Copper (References 4 and 5)

Modulus of Elasticity, E, @ R.T., psi	17.0x10 <sup>6</sup> (See Figure 3)	
Tensile Strength, F <sub>tu</sub> , @ R.T., psi	27,100	(See Figure 3)
Yield Strength, F <sub>ty</sub> , @ R.T., psi	10,700	(See Figure 3)
Elongation, e (in 1.0 inch), %	38.0	
Reduction of Area, RA, %	69.0	
Density, ρ, lb/in. <sup>3</sup>	0.323	
Coefficient of Thermal Expansion, α, in./in.-°F	(See Figure 3)	
Cyclic Life	(See Figure 4)	

\*The yield and ultimate strength allowables used for Armco 22-13-5 annealed bar and tubing were adjusted to 80% of typical tensile yield and 85% of typical tensile ultimate strengths in accordance with recommendations from the ALRC Materials Engineering Section.

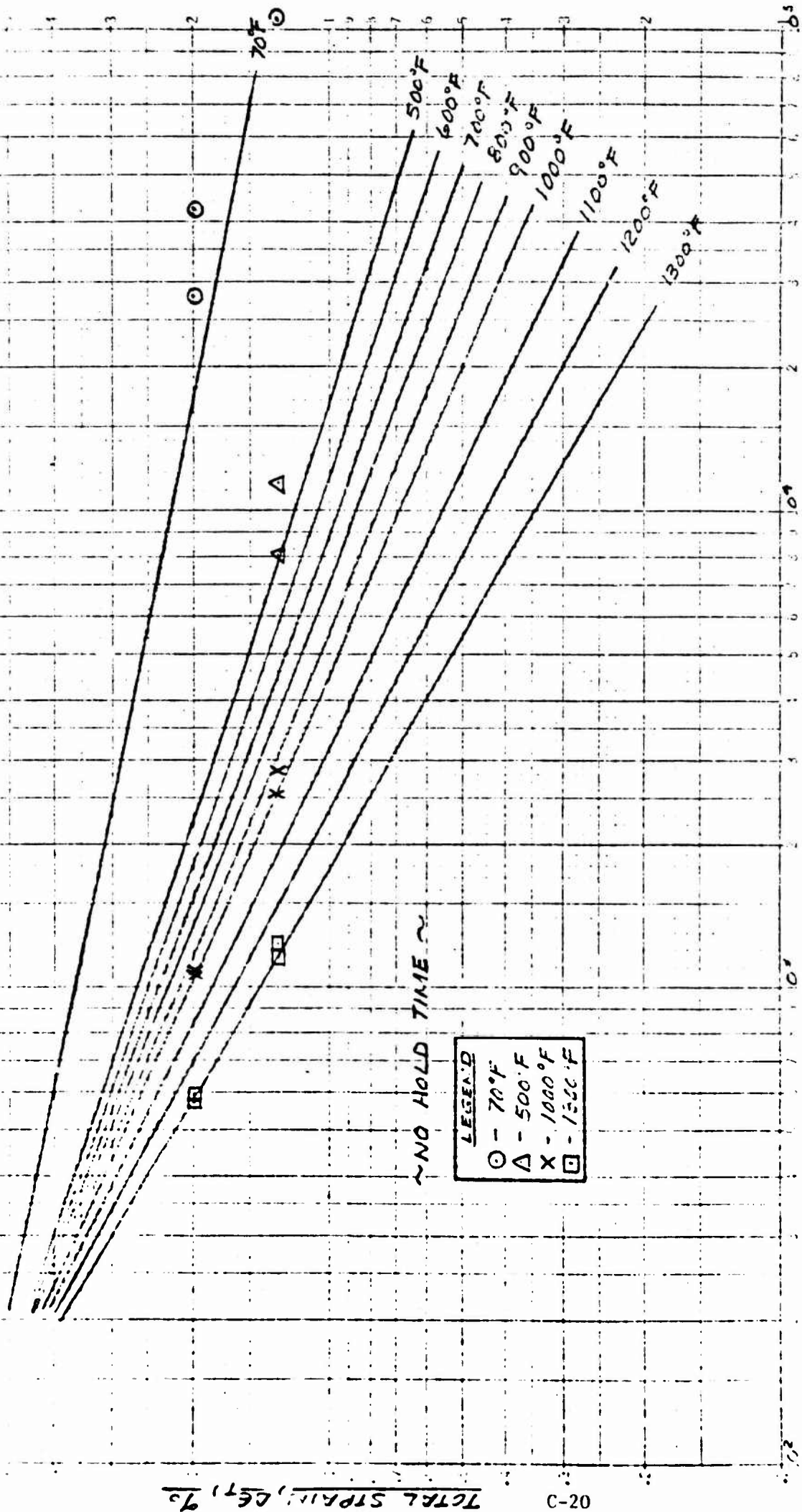
FIGURE 1 - MECHANICAL PROPERTIES OF ARNICO 22-13-5  
SHEET AND BAR (REFERENCES 2 & 3)



	<u>Bar</u>	<u>Sheet</u>
3. <u>Boron Deoxidized Copper</u> (References 4 and 5)		
Modulus of Elasticity, E, @ R.T., psi	17.0x10 <sup>6</sup>	(See Figure 5)
Tensile Strength, F <sub>tu</sub> , @ R.T., psi	27,500	(See Figure 5)
Yield Strength, F <sub>ty</sub> , @ R.T., psi	5,600	(See Figure 5)
Density, e, lb/in. <sup>3</sup>	0.323	
Coefficient of Thermal Expansion, α, in./in.-°F		(See Figure 5)
Cyclic Life		(See Figure 6)
4. <u>AGCarb-101</u> (Reference 6)		<u>Conical Specimens</u>
Modulus of Elasticity, E, @ R.T., psi		2.5x10 <sup>6</sup>
Tensile Strength, F <sub>tu</sub> , @ R.T., psi		3,200
Compressive Strength, F <sub>cu</sub> , @ R.T., psi		5,000
Density, ρ, lb/in. <sup>3</sup>		0.054
Coefficient of Thermal Expansion, α, in./in.-°F		1.85x10 <sup>-6</sup>
5. <u>1/4-28 UNF Bolts</u> (Reference 7)		
Tensile Strength, F <sub>tu</sub> , psi	190,000	
Yield Strength, F <sub>ty</sub> , psi	170,000	
Ultimate Tensile Load, lb	6,910	
Yield Tensile Load, lb	6,180 (calculated)	

FIGURE 2 - ARMCO E2-13-5 LCF DATA

(REFERENCE 4)



CYCLES TO FAILURE,  $N_F$

TOTAL STRAIN,  $\epsilon_T$ , %



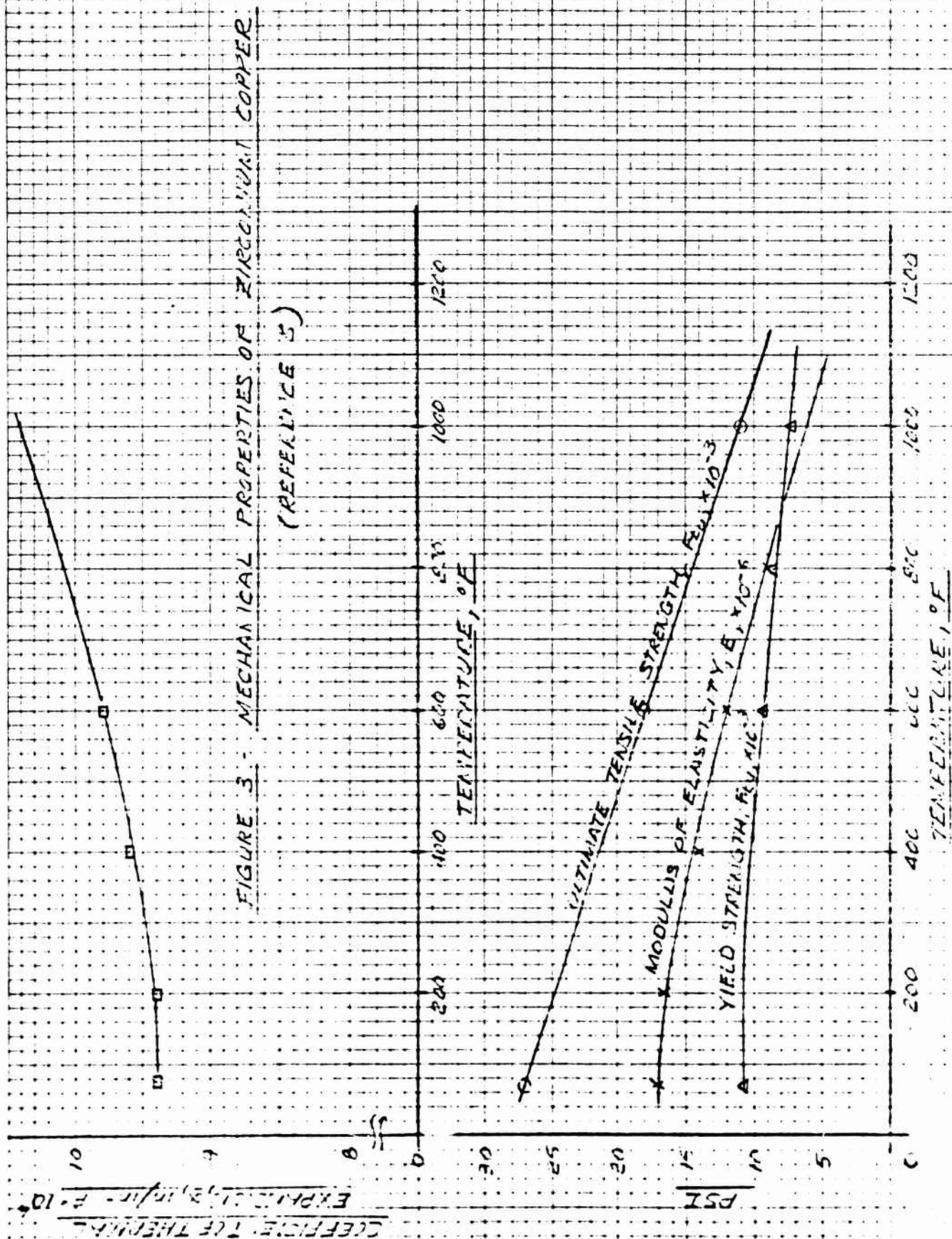
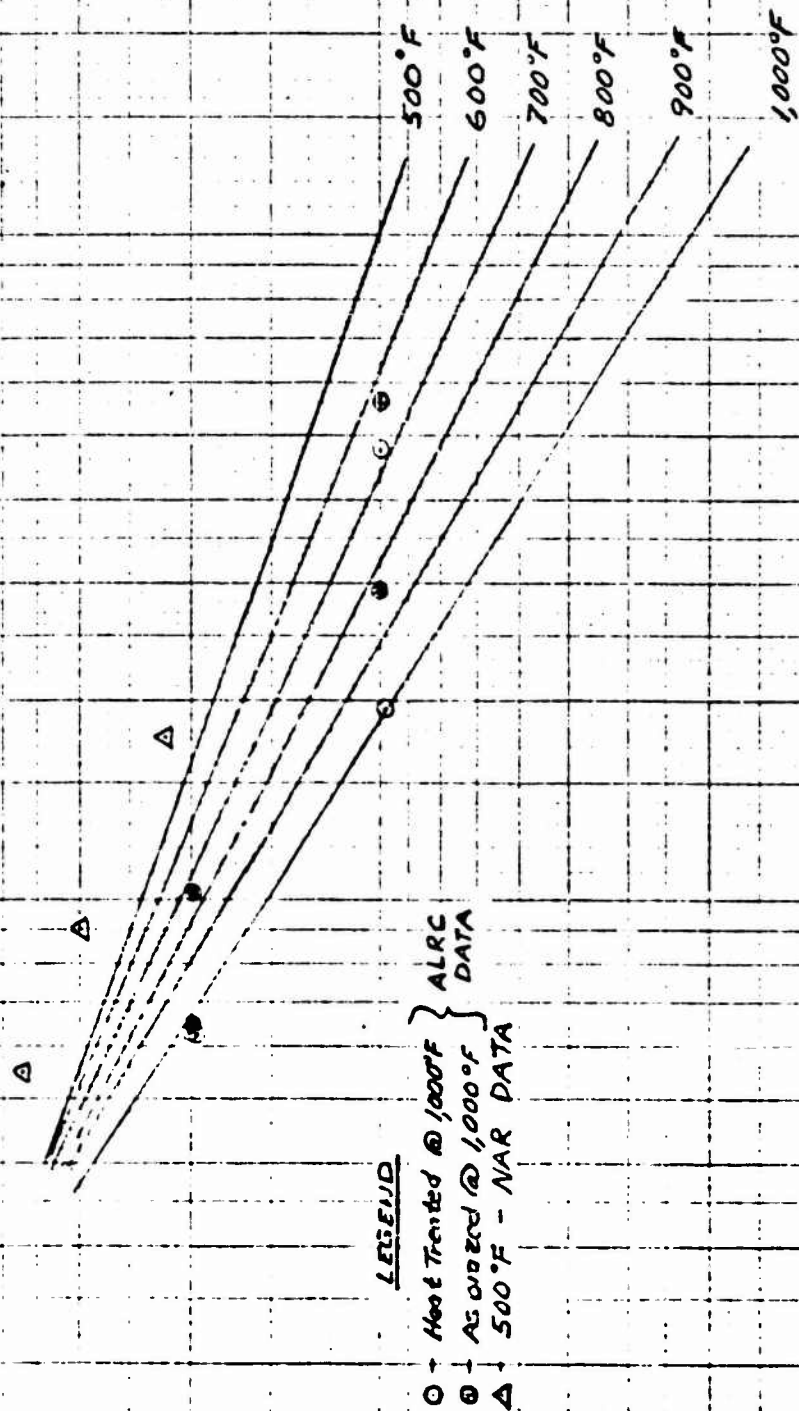




FIGURE 4 - ZIRCONIUM COPPER LCF LIFE - REFERENCE 4

(NO HOLD TIME)



CYCLES TO FAILURE,  $N_f$

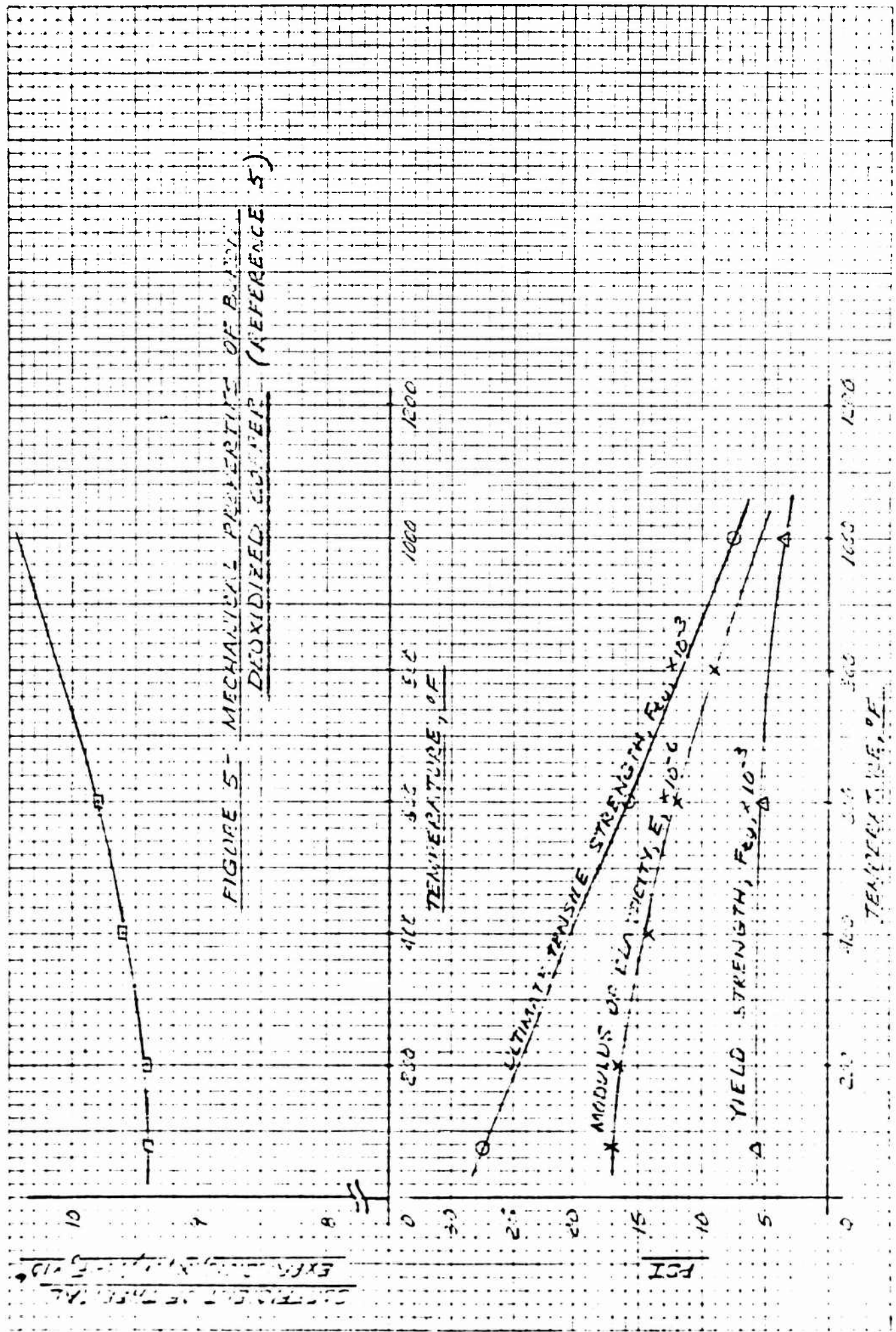
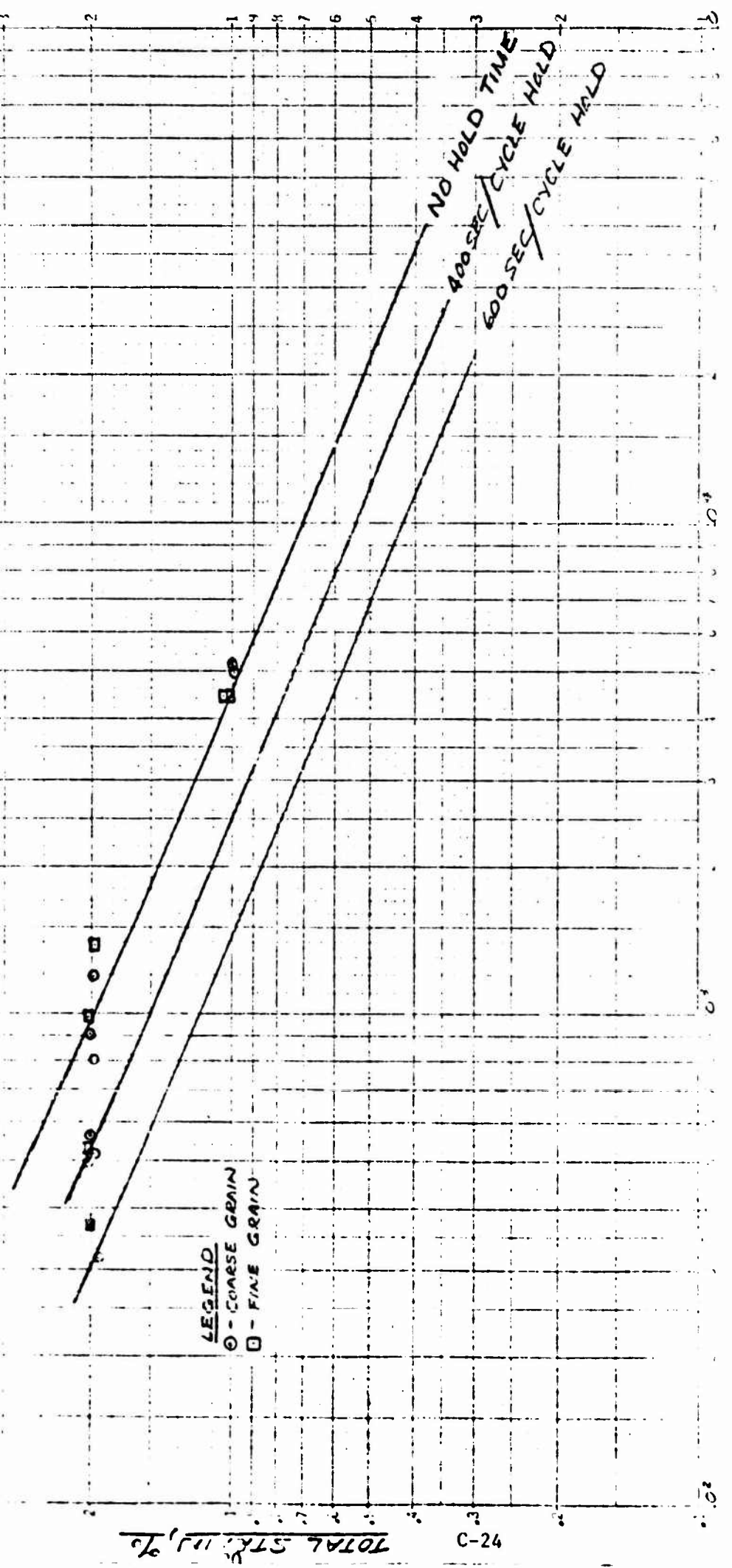


FIGURE 6 - BD-CU LOW CYCLE FATIGUE LIFE @ 1000°F  
(REFERENCE 4)



NUMBER OF CYCLES TO FAILURE

#### D. DESIGN STRENGTH FACTORS

##### 1. Bending Modulus of Yield and/or of Rupture

In general, it is assumed that whenever bending and membrane stress occur about any one axis, the stresses are additive algebraically and the interaction curve is a straight line. That is, failure is assumed to occur when some critical stress,  $F_{ty}$  or  $F_{tu}$ , is reached, or  $R_A + R_B = 1$  where:

$$R_A = \frac{\text{Membrane Design Stress}}{\text{Allowable Membrane Stress}}$$

$$R_B = \frac{\text{Bending Design Stress}}{\text{Allowable Membrane Stress}}$$

This assumption is highly conservative when bending stresses extend into the plastic range. The interaction of bending plus membrane stress lies above the straight line assumption provided that bending causes the predominant stress. In other words, the apparent allowable stress for plastic bending is much larger than the membrane allowable. The magnitude of apparent bending allowable stress depends on shape and material properties of the cross section in bending. Under these conditions, a Bending Modulus of Yield or of Rupture may be applied to the membrane allowable stress to determine the bending stress allowable.

A Bending Modulus of Rupture equal to 1.50 x allowable ultimate stress or a Bending Modulus of Yield of 1.25 x allowable yield stress was considered where appropriate in order to calculate margins of safety. These factors were determined in accordance with Reference (8). Therefore, the expression for  $R_b$  becomes:

$$R_b = \frac{\text{Bending Design Stress}}{\text{Bending Modulus of Rupture Ultimate}}$$

or

$$R_b = \frac{\text{Bending Design Stress}}{\text{Bending Modulus of Yield Yield}}$$

## 2. Welded and Brazed Joint Strength Factor

Welding efficiencies equal to 95% for electron beam welds and 85% for fusion welded joints will be considered for both the weld metal and the adjacent parent metal. For materials heat treated after welding, the allowable strength for the parent metal in the heat treated condition may be used but the weld-metal allowables will still be based upon the efficiencies assumed above (see Reference 9). The strength of brazed joints must be determined experimentally for the type of joint under consideration, i.e., braze material, clearance, material to be joined, etc. For preliminary design purposes 80% of tensile ultimate may be considered for copper/copper brazed joint.

### E. METHOD OF ANALYSIS

It was assumed that all firings would occur at altitude, i.e., no start transient asymmetric loads would occur and that vacuum conditions only would apply. The critical parameters considered were thrust ( $F$ ), chamber pressure ( $P_c$ ), and gimbal angular acceleration ( $\alpha$ ). The effects of the thermal environment were considered for low cycle fatigue life and thermal buckling, but secondary stresses due to temperature were neglected. Formulas and relationships from Reference (10) and similar handbooks, and results of previous analyses (References 11, 12, and 13) were utilized wherever applicable.

The following is a list of the critical structural load parameters considered for each of the components.

#### 1. Preburner Assembly

- a. Radius/thickness, ( $R/t$ ), dependent upon internal pressure and mean wall temperature for tubes and welded chamber assembly.
- b. Upper bound of ( $R/t$ ) limited by thermal buckling and/or thermal creep criteria.
- c. Maximum tube crown temperature-fatigue life limited.

2. Regen Tube Bundle

- a. (R/t) dependent upon internal pressure and mean wall temperature
- b. Upper bound of (R/t) limited by thermal buckling and/or thermal creep criteria
- c. Maximum tube crown temperature-fatigue life limited

3. Regen Tube Bundle Support Ring:Size and Spacing (Dependent Parameters)

- a. Nozzle internal pressures and tube temperatures
- b. Thrust level and gimbaling accelerations - column buckling effect

4. Zirconium Copper Liner

- a. Temperature differential from gas side-to-backside jacket - maximum temperature fatigue life limited
- b. Effect of channel width/land ratio, channel width bending and shear

5. Pressure Jacket

- a. Chamber pressure - biggest effect
- b. Jacket temperature

6. Outer Shell (Thrust Cone)

- a. Gimbal angular accelerations and nozzle inertia
- b. Axial thrust, combined with (a)
- c. May be limited by strength or buckling - (R/t) critical

7. Injector Flange

- a. Chamber Pressure
  - b. Gimbal accelerations and nozzle inertia
  - c. Axial thrust level
- } worst combination



### Life Prediction Methods

In order to avoid costly non-linear computer analyses of the combustion components operating in the plastic range, some simplifying assumptions were used. Thermal strains were estimated by use of the expression,  $\epsilon_T = k\alpha\Delta T$

Where:  $\epsilon_T$  = total strain range, in./in.  
 $\alpha$  = coefficient of thermal expansion, in./in.-°F  
 $\Delta T$  = temperature difference between hot surface ( $T_{wg}$ ) and colder restraining structure, °F  
 $k$  = geometric constant determined for each component based upon results of computer solutions for similar structures.

For the regions where detailed thermal profiles of the structure were not available, propellant bulk temperatures were conservatively used as the restraint temperature.

Figures 2, 4, and 6 show plots of fatigue life versus total strain for the three basic OOS materials. The boron deoxidized copper curves show a reduction in fatigue life due to compressive hold periods. To assess the creep damage effects, a cumulative damage theory (Reference 14) was applied per the following expression:

$$\sum \frac{N}{N_f} + \sum \frac{t}{t_R} = 1$$

where:  $N$  = number of thermal cycles applied  
 $N_f$  = number of thermal cycles to failure with no creep damage  
 $t$  = total duration applied, hours  
 $t_R$  = total time to rupture, hours



# VI. CALCULATIONS

## A. PREBURNER ASSEMBLY

### DESIGN DATA

MATERIAL — APMCO 22-13-5 Stainless Steel Sheet/Tube  
Ultimate Strength,  $F_{tu}$  = 112,000 psi  
Yield Strength,  $F_{ty}$  = 75,000 psi } @ Room Temperature  
Coefficient of Thermal Expansion,  $\alpha$  =  $9.85 \times 10^{-6}$  in/in-°F (1-200°F)

### LOADS

Thermal Gradients — See Figures 8 & 9  
Pressure

- 1) Tube Pressure = 3250 psi
  - 2) Chamber Pressure = 2500 psi
- } Limit Load (MEOP)

### CONFIGURATION

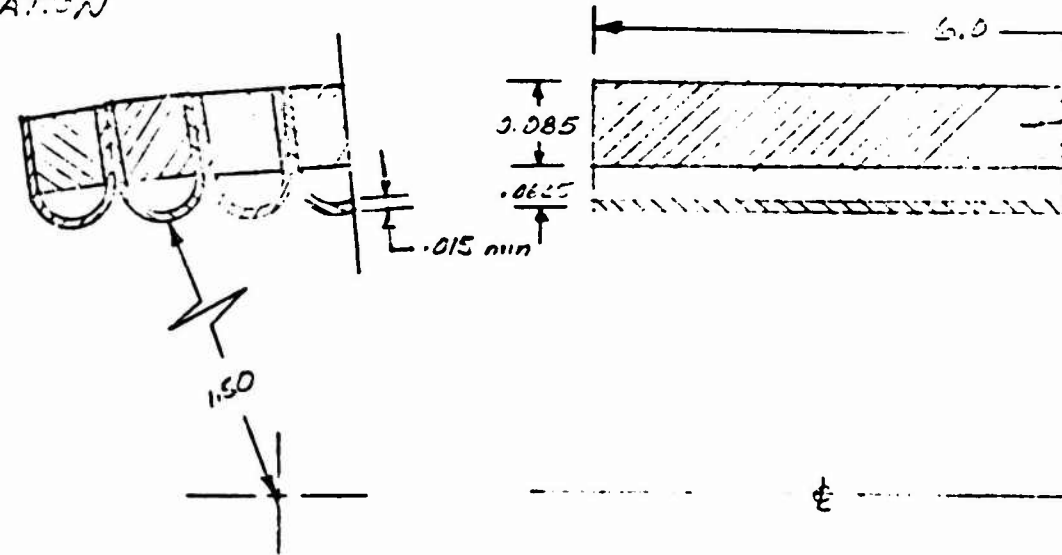


FIGURE 7 PREBURNER CHAMBER CONFIGURATION



FIG. 8 - OOS PREBURNER STUDY  
TUBE WALL TEMPERATURES FOR  
25-PERCENT OF NOMINAL  $LO_2$  FLOW AREA

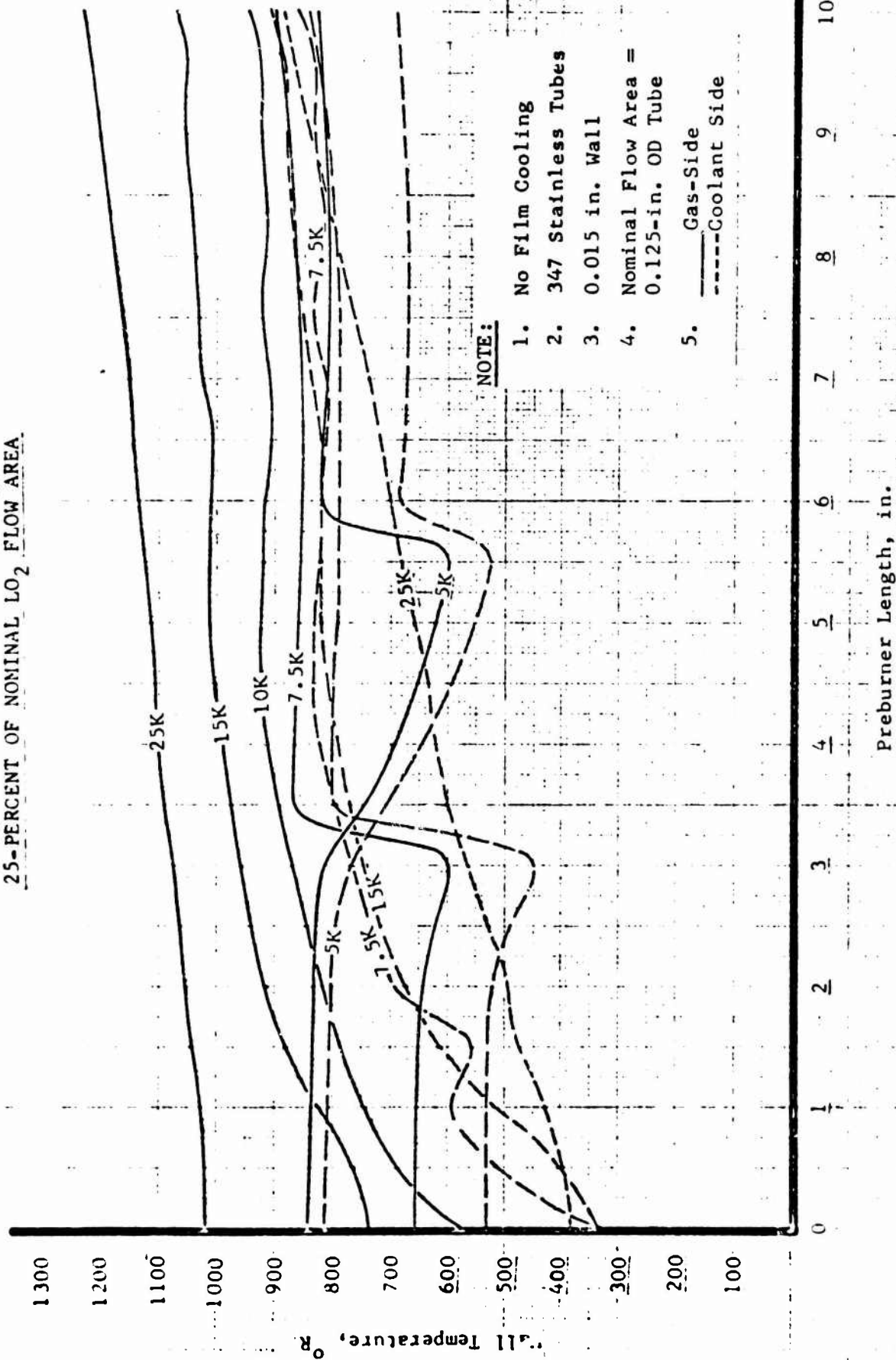
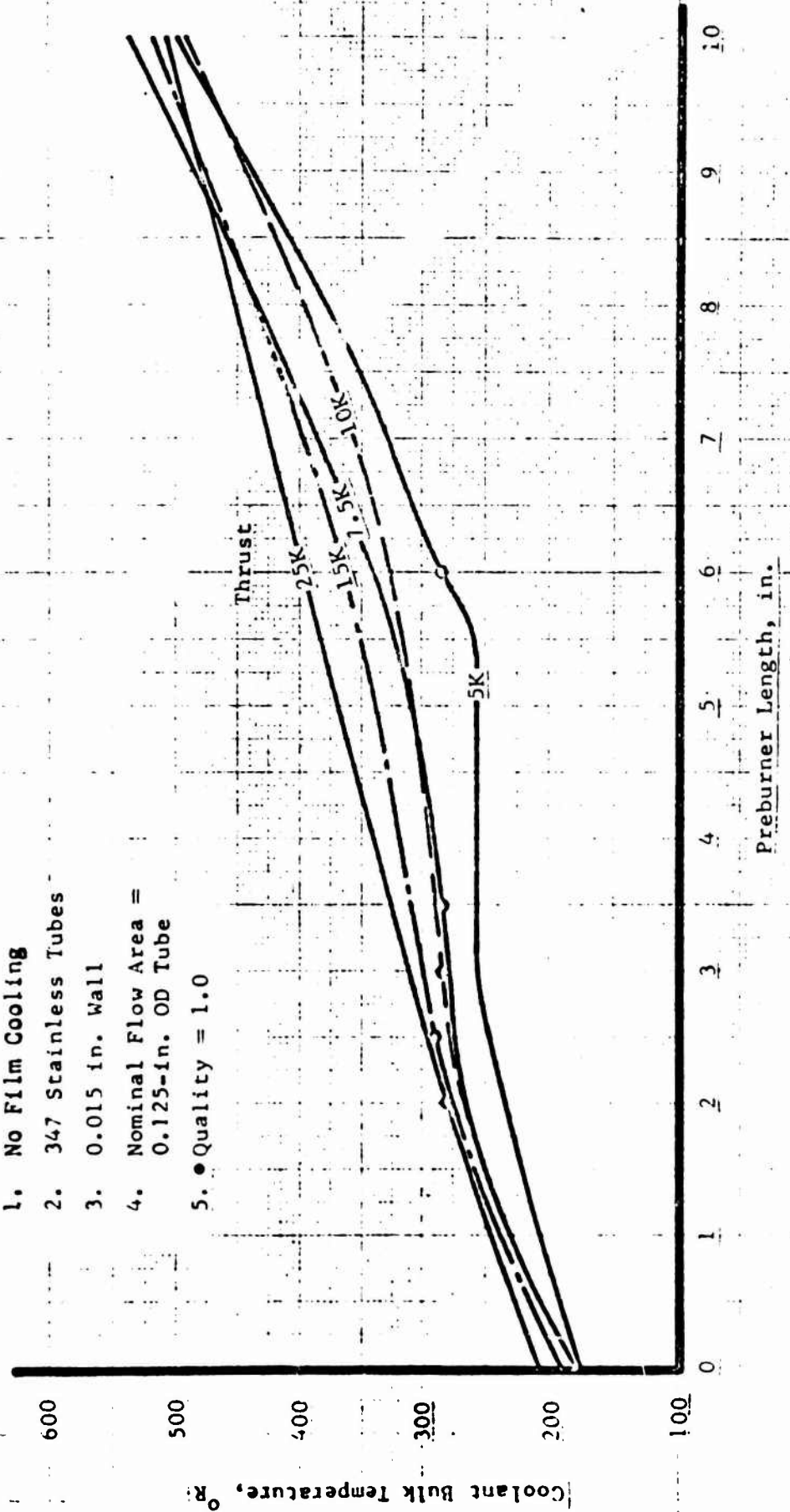


FIG. 9-008 PREBURNER STUDY  
 LO<sub>2</sub> BULK TEMPERATURE RISE FOR  
 25-PERCENT OF NOMINAL LO<sub>2</sub> FLOW AREA

NOTE:

1. No Film Cooling
2. 347 Stainless Tubes
3. 0.015 in. Wall
4. Nominal Flow Area =  
0.125-in. OD Tube
5. • Quality = 1.0





REPORT NO.

SA-035-CC-03

PAGE 25 OF 51

SUBJECT

DATE

7/12/71

WORK ORDER

1811-03-103

BY

GHS

CHK. BY

DATE

# 1- TUBE ANALYSIS

Assume: Fixity @ Junction of tube and wire  
Neglect External Pressure

## a. Discontinuity Analysis

Let: Radial deflection due to pressure =  $\frac{0.85 PR^2}{Et}$  ... Ref. 10, Case 1, Pg. 26B

Determine Force, W, which would induce an equivalent deflection.  
... Reference 16, Case 3:

$$\Delta R = \frac{0.85 PR^2}{Et} = \frac{0.0744 WR^3}{EI}$$

$$W = \frac{0.85 F I}{0.0744 R t}$$

$$\text{but: } I = \frac{t^3}{12}$$

$$\therefore W = 11.4 \frac{P t^2}{R 12}, \text{ lbs/in.}$$

## Proof Criteria

$$W = 0.95 \frac{P t^2}{R}$$

where:  $P = 3250 (1.20) = 3900 \text{ psi (yield)}$   
 $t = 0.015 \text{ in.}$   
 $R = 0.055 \text{ in.}$

$$W = 15.20 \text{ lb/in. (yield)}$$

Reference 16, Case:

Max Moment,  $M = 0.3183 VJR$

$$M = 0.3183 (15.20) (0.055) = 0.266 \text{ in-lb/in. (yield)}$$

$$\text{Bending Stress, } \sigma'_y = \frac{M}{I/c} = \frac{6M}{t^2}$$

where:  $I/c = \frac{t^2}{6}$ , for a 1.0" wide rectangular section  
 $t = \text{thickness, in.}$

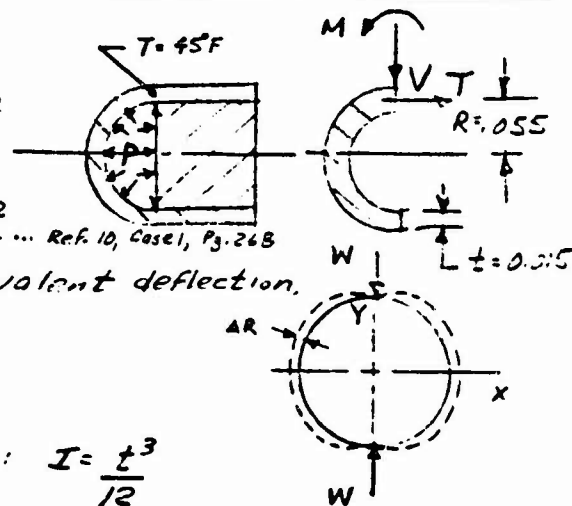
$$\sigma'_{by} = \frac{6 (0.266)}{(0.015)^2}$$

$$\sigma'_{by} = 71,600 \text{ psi (yield)}$$

Assume: Bending Modulus of Yield =  $1.25 F_{ty}$  ... Reference 8

$F_{ty @ 45^\circ F} = 77,000 \text{ psi}$  ... see Figure 1

$$M.S. = \frac{1.25 (77,000)}{71,600} - 1 = \underline{\underline{0.35 \text{ (yield)}}}$$





SUBJECT

DATE

7/12/71

WORK ORDER

1811-15-120

BY

GAS

CHK. BY

DATE

Ultimate Criteria

(From previous page)

$$W = 0.95 \frac{P t^2}{R}$$

$$\text{where: } P = 3250(1.50) = 4875 \text{ psi (ult)} \\ t = 0.015 \text{ in.} \\ R = 0.055 \text{ in.}$$

$$W = 19.0 \text{ lb/in (ult)}$$

Reference 16, Case 3:

$$\text{Max. Moment, } M = 0.2163 WR$$

$$M = 0.2163(19.0)(0.055) = 0.333 \text{ in-lb/in (ult)}$$

$$\text{Bending Stress, } \sigma_{bu} = \frac{6 M}{t^2}$$

$$\sigma_{bu} = \frac{6(0.333)}{(0.015)^2}$$

$$\sigma_{bu} = 89,000 \text{ psi (ult)}$$

Assume: Bending Modulus of Rupture = 1.50  $F_{tu}$  ... Reference 8

$$F_{tu @ 45^\circ F} = 113,000 \text{ psi} \quad \dots \text{ Figure 1}$$

$$M.S. = \frac{1.50(113,000)}{89,000} - 1 = \underline{0.97 \text{ (ult)}}$$



7/12/71

1811-SS-103

BY

GHS

CHK. BY

b. At Crown

Reference 16, Case 3:

$$\begin{aligned} \text{Mom, } M &= 0.1817 WR = 0.1817 (15.20) (0.055) \\ &= 0.152 \text{ in-lb/in.} \end{aligned}$$

$$\begin{aligned} \text{Normal Force, } T &= -0.500 W = -0.500 (15.20) \\ &= -7.60 \text{ lb/in.} \end{aligned}$$

Applied Stress,  $\bar{\sigma}_y$ 

$$\begin{aligned} \bar{\sigma}_y &= \frac{PR}{t} - \frac{T}{t} \pm \frac{6M}{t^2} \\ &= \frac{3900(.055)}{.015} - \frac{7.60}{.015} \pm \frac{6(.152)}{(.015)^2} \\ &= 14,300 - 505 \pm 40,600 \\ &= 13,795 \pm 40,600 \end{aligned}$$

Allowable Strength,  $\bar{\sigma}_{ty}$ 

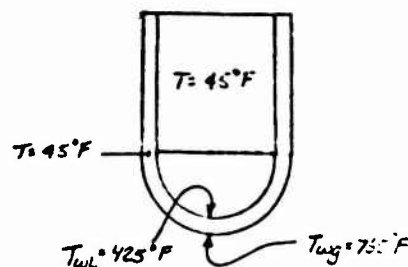
$$\bar{\sigma}_{ty @ 745^\circ\text{F}} = 46,000 \text{ psi} \quad \dots \text{ Figure 1}$$

$$R_H = \frac{13,795}{46,000} = 0.30$$

$$R_B = \frac{40,600}{1.25(46,000)} = \frac{0.70}{1.00}$$

$$M.S. = \frac{1}{1.00} - 1 = \underline{\underline{0.00}} \text{ (yield)}$$

(Note: From previous calculation, proof or yield criteria governs.)





SUBJECT

DATE

7/12/71

WORK ORDER

1811-00-15

BY

GHS

CHK. BY

DATE

c.- THERMAL BUCKLING AT CROWN

$$\left(\frac{R}{t}\right)_{\max} = \frac{0.24}{\alpha \Delta T} \dots \text{Ref. 17}$$

where: R = Outside Radius = 0.0625 in.

t = Thickness = 0.015 in.

$\alpha$  = Thermal Coefficient of

expansion =  $7.8 \times 10^{-6} \text{ in/in}^{\circ}\text{F}$

$\Delta T = (T_{wg} - T_B) = 720^{\circ}\text{F}$

$T_{wg}$  = Gas Side Wall Temp. =  $765^{\circ}\text{F}$

$T_B$  = Coolant Bulk Temp. =  $45^{\circ}\text{F}$

$$\left(\frac{R}{t}\right)_{\max} = 34.0$$

$$\frac{R}{t} = \frac{0.0625}{0.015} = 4.17$$

$$M.S. = \frac{34.0}{4.17} - 1 = \underline{\underline{7.15}}$$

d.- THERMAL CREEP

Assume a Safety factor of 1.5 for  $(R/t)_{\max}$  in order to account for thermal Creep.

$$\therefore \left(\frac{R}{t}\right)_{cr.} = \frac{34.0}{1.5} = 22.7$$

$$M.S. = \frac{22.7}{4.17} - 1 = \underline{\underline{4.44}}$$

e.- LOW CYCLE FATIGUE LIFE

Let: total strain,  $\epsilon_T = 1.4 \alpha \Delta T$

where:  $\alpha = 9.8 \times 10^{-6} \text{ in/in}^{\circ}\text{F}$   
(see Figure 1)

$$\epsilon_T = 1.4 (9.8) 10^{-6} (720) \times 100$$

$$\epsilon_T = 0.986 \%$$

From Figure 2,  $1.4 = 5600$  cycles to failure > 6,000 cycles

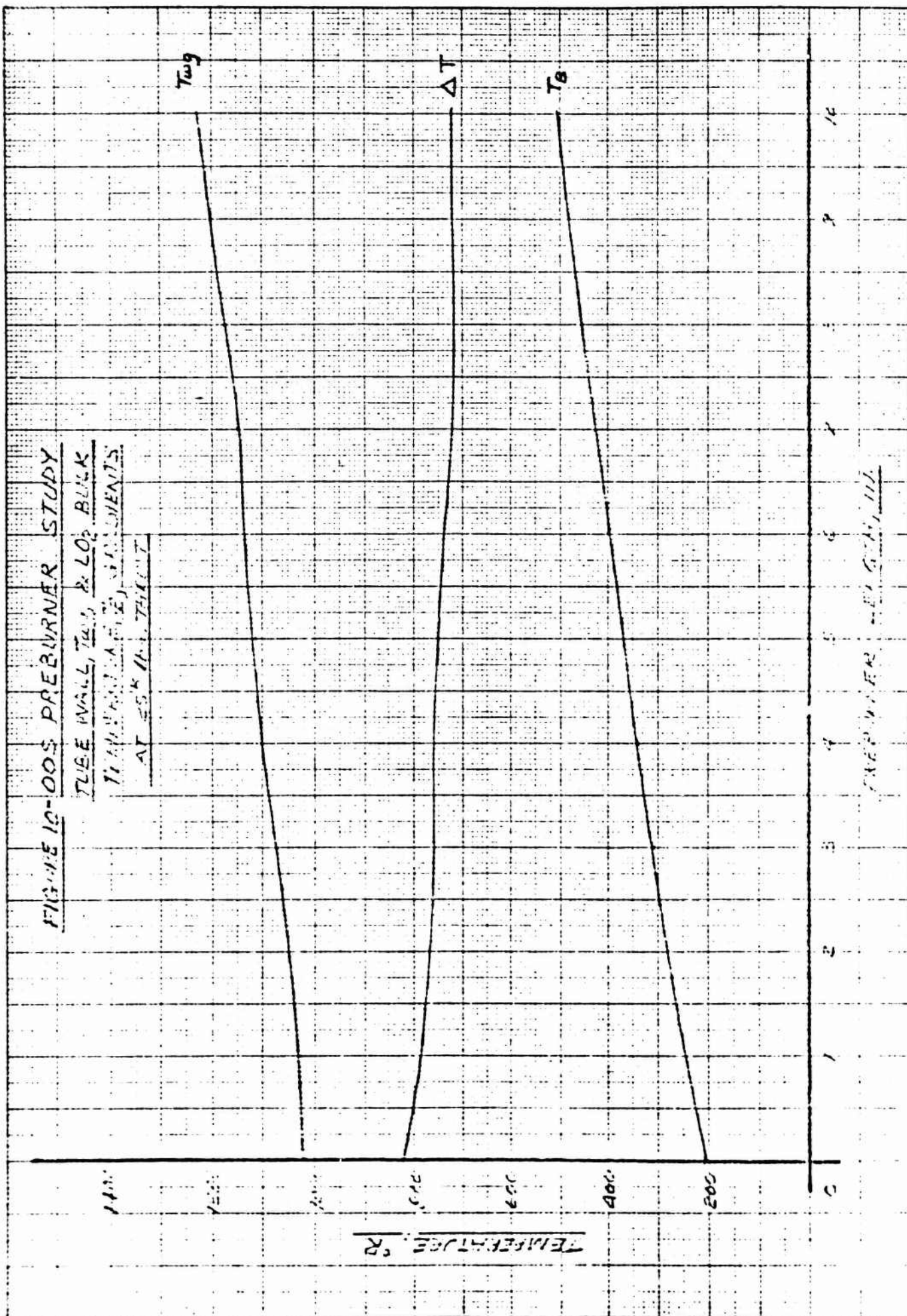
see Figure 11 for LCF Life vs Preburner Length.

FIGURE 10-005 PREBURNER STUDY

TUBE WALL,  $T_{wg}$ , & LOG BULK

TEMPERATURES, °R

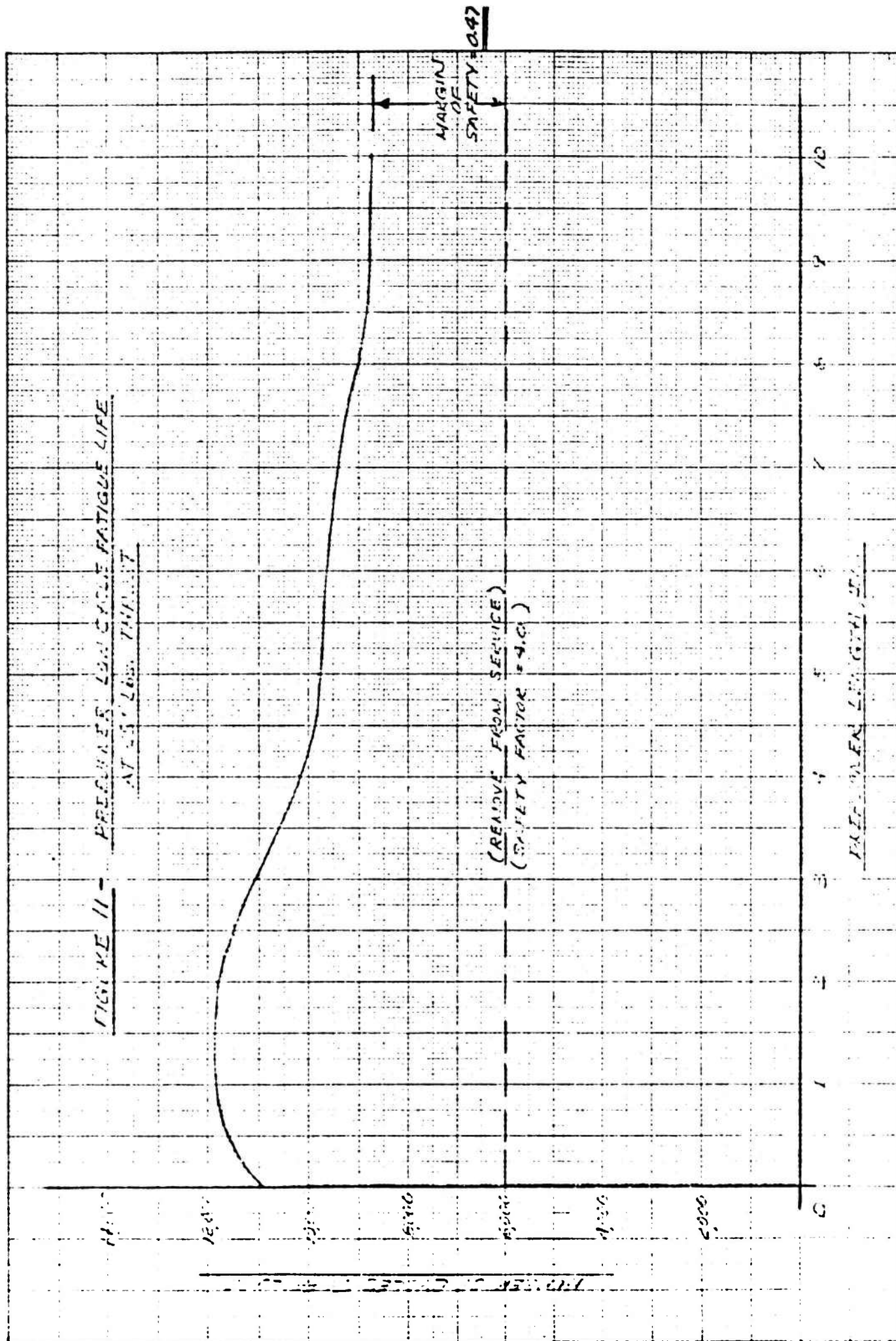
AT 25% IN. THICK



PREBURNER - FIG. 10-005



FIGURE 11 - FREQUENCY LOG CYCLE FATIGUE LIFE  
AT 25,000 THUNDER







SUBJECT

DATE

7/12/71

WORK ORDER

1811-25-123

BY

GHS

CHK. BY

DATE

F. Welded Joint between Tube And WireMax Force,  $F = PA$ where:  $P = 1.5(3250) = 4875 \text{ psi/lt.}$   
 $A = \text{Area, in}^2$ 

$$F = 4875(.095)(1.0) = 463 \text{ lbs/in (ult.)}$$

$$\text{Shear Area, } A_s = 2(0.085)(1.0) = 0.16 \text{ in}^2/\text{in.}$$

$$\text{Shear Stress, } F_{su} = \frac{463}{0.160} = 2,900 \text{ psi}$$

Assume: Weld Efficiency = 85%

Shear Ultimate Allowable = .50  $F_{tu}$  (Assumed)

$$\therefore F_{su} = (0.85)(0.50)(113,000) = 48,000 \text{ psi} \quad \dots \text{ Figure 1}$$

@ 45°F

$$M.S. = \frac{48,000}{2,900} - 1 = \underline{\underline{\text{Large (ult.)}}}$$



SUBJECT		DATE 7/12/71
		WORK ORDER 1811-03-123
BY GHS	CHK. BY	DATE

2. CHAMBER ANALYSISBASIC HOOP STRENGTHYIELD CRITERIA

$$\tau_{hy} = 1.20 \frac{PR}{t} \quad \dots \text{Ref. 10, Case 1, Pg. 268} \quad \text{where: } P = 2800 \text{ psi}$$

$$R = 1.6050 \text{ in.}$$

$$t = 0.085 \text{ in.}$$

1.20 = Safety Factor on Yield

$$\tau_{hy} = 63,500 \text{ psi (yield)}$$

Assume: 85% Weld efficiency ... Reference 9

$$T_w = 45^\circ F$$

$$\therefore F_{ty} = 0.85 (77,000) = 65,500 \text{ psi} \quad \dots \text{See Figure 1}$$

$$M.S. = \frac{65,500}{63,500} - 1 = \underline{\underline{0.03}} \text{ (yield)}$$

ULTIMATE CRITERIA

$$\text{let: } p = 1.50 (2400) = 4200 \text{ psi (ult)}$$

$$\tau_{hu} = 79,500 \text{ psi (ult)}$$

$$F_{tu} = 0.85 (113,000) = 96,000 \text{ psi} \quad \dots \text{See Figure 1}$$

$$M.S. = \frac{96,000}{79,500} - 1 = \underline{\underline{0.20}} \text{ (ult)}$$



SUBJECT

DATE

7/13/71

WORK ORDER

1811-06-103

BY

GHS

CHK. BY

DATE

3.- OXIDIZER TORUS (assume uniform configuration) <sub>t</sub>

Reference 10, Pg. 274, Case 20

YIELD CRITERIA

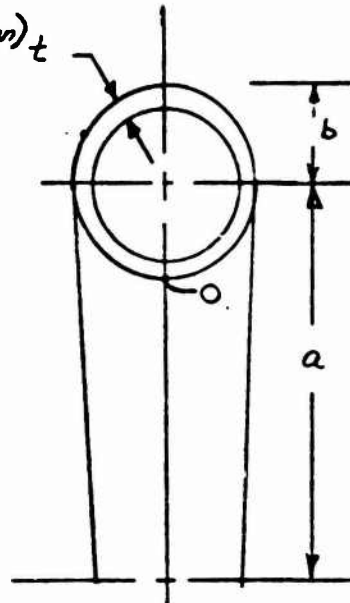
$$\text{Max Stress, } \bar{\sigma} = \frac{pb}{t} \left( \frac{2a-b}{2a-2b} \right) @ 0$$

$$\text{where: } p = 3255 (1.20) = 3900 \text{ psi (yield)}$$

$$b = 0.325 \text{ in.}$$

$$a = 1.900 \text{ in.}$$

$$t = 0.040 \text{ in.}$$



$$\sigma_y = 35,000 \text{ psi (yield)}$$

$$F_{ty @ RT} = 75,000 \text{ psi} \dots \text{See Figure 1}$$

$$M.S. = \frac{75,000}{35,000} - 1 = \underline{\underline{1.14}} \text{ (yld)}$$

ULTIMATE CRITERIA

$$\text{let: } p = 1.50 (3255) = 4890 \text{ psi (ult)}$$

$$\sigma_u = 43,750 \text{ psi (ult)}$$

$$F_{tu @ RT} = 112,000 \text{ psi}$$

$$M.S. = \frac{112,000}{43,750} - 1 = \underline{\underline{1.56}} \text{ (ult)}$$



SUBJECT

DATE

7/24/77

WORK ORDER

1811-JS-03

BY

GHSkopp

CHK. BY

DATE

B.- REGEN NOZZLE TUBE BUNDLEDESIGN DATA

MATERIAL ~ ARMCO 22-13-5 Stainless Steel Sheet/Tube

Ultimate Strength,  $F_{tu}$  = 112,000 psi } @ Room TemperatureYield Strength,  $F_{ty}$  = 75,000 psi }Coefficient of Thermal Expansion,  $\alpha$  =  $9.75 \times 10^{-6}$  in/in-°F (0-710°F)LOADS

Thermal Gradients - See Figure 13

Pressure

- 1) Tube Pressure = 4250 psi } LIMIT LOAD  
2) Plenum Pressure = 1800 psi } (MEOP)

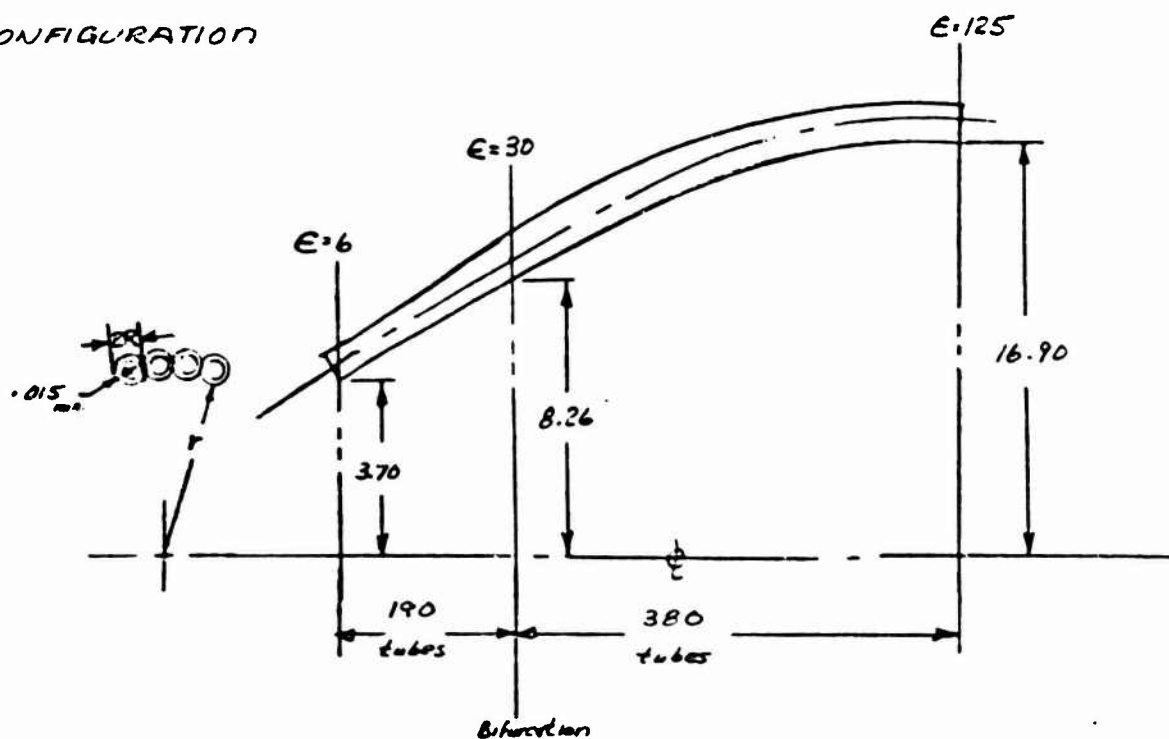
CONFIGURATION

FIGURE 12- REGEN NOZZLE TUBE BUNDLE GEOMETRY





SUBJECT

DATE

7/14/71

WORK ORDER

1811-25-102

BY

GHS

CHK. BY

DATE

# 1.- REGENTURE ANALYSIS

@ expansion ratio,  $\epsilon = 6.0$

MR = 6.0

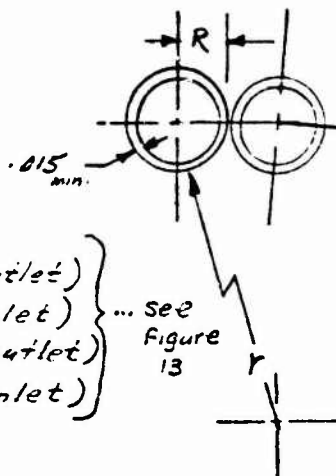
Thrust = 25,000 lbs

Plenum Pressure = 1500 psi

Number of Tubes = 190

Temperature - wall gas side;  $T_{wg} = \begin{cases} 707^\circ\text{F (outlet)} \\ 664^\circ\text{F (inlet)} \end{cases}$

Coolant Bulk Temperature,  $T_b = \begin{cases} -190^\circ\text{F (outlet)} \\ -360^\circ\text{F (inlet)} \end{cases}$



## Proof Pressure Criteria

See Reference 12, Figure 12, Page 34

$$\left. \begin{aligned} \textcircled{a} \quad P_c' &= \frac{4250}{2.5} = 1700 \text{ psi} \\ T_{wg} &= 707^\circ\text{F} \end{aligned} \right\} (R/t)_{\max} = 9.03$$

$$R_{\max} = \frac{1.250}{n} \left( \frac{\epsilon F}{P_c} \right)^{1/2} \quad \dots \text{Reference 11, Pg. 4}$$

where:  $\epsilon = 6.0$

$F = 25,000 \text{ lbs}$

$P_c = 1500 \text{ psi}$

$n = 190 \text{ tubes}$

$$R_{\max} = 0.0615 \text{ in.}$$

$$t_{\min} = 0.015 \text{ in.}$$

$$R/t = 4.10$$

$$M.S. = \frac{9.03}{4.10} - 1 = \underline{\underline{1.20 \text{ (margin)}}}$$

Check Thermal Creep & Buckling ~ see Reference 12, Figure 12, Pg. 34

Assume Safety Factor of 1.50 on thermal buckling

$$(R/t)_{cr} = \frac{24.0}{1.50} = 19.30 \text{ (outlet) } \left\{ \begin{aligned} T_{wg} &= 707^\circ\text{F} \\ T_b &= -190^\circ\text{F} \end{aligned} \right.$$

$$M.S. = \frac{19.30}{4.10} - 1 = \underline{\underline{3.71}}$$

$$(R/t)_{cr} = \frac{24.0}{1.50} = 16.0 \text{ (inlet) } \left\{ \begin{aligned} T_{wg} &= 664^\circ\text{F} \\ T_b &= -360^\circ\text{F} \end{aligned} \right.$$

$$M.S. = \frac{16.00}{4.10} - 1 = \underline{\underline{2.90}}$$



@ expansion ratio,  $E = 30$

$$T_{wg} = \begin{cases} 550^\circ\text{F (Inlet)} \\ 500^\circ\text{F (outlet)} \end{cases}$$

$$T_e = \begin{cases} -320^\circ\text{F (Inlet)} \\ -213^\circ\text{F (outlet)} \end{cases}$$

See Figure 13

See Reference 12, Figure 12, Pg. 34

$$\left. \begin{aligned} P_c' &= 1700 \text{ psi} \\ T_{wg} &= 550^\circ\text{F} \end{aligned} \right\} (R/t)_{\max} = 9.42$$

$$R_{\max} = \frac{1.280}{n} \left( \frac{E F}{P_c} \right)^{1/2} \dots \text{Reference 11, Pg. 4}$$

where:  $E = 30$

$F = 25,000 \text{ lbs}$

$P_c = 1800 \text{ psi}$

$n = 190 \text{ tubes}$

$$R_{\max} = 0.1375 \text{ in.}$$

$$t_{\min} = 0.015$$

$$R/t = 9.15$$

$$M.S. = \frac{9.42}{9.15} - 1 = \underline{\underline{0.03}} \text{ (y/d)}$$

Design Information

$P_c = 1800 \text{ psi}$

$R_{\max} = 0.1375 \text{ in.}$

$$R/t = 9.15$$

$$M.S. = \frac{9.42}{9.15} - 1 = \underline{\underline{1.05}} \text{ (y/d)}$$

Check Thermal Stress Buckling - See Reference 12, Figure 12, Pg. 34

$$(P/t)_{\max} = 19.20 \text{ (inlet)} \left\{ \begin{aligned} T_{wg} &= 550^\circ\text{F} \\ T_e &= -320^\circ\text{F} \end{aligned} \right\} \text{ See Figure 13}$$

$$M.S. = \frac{19.20}{9.15} - 1 = \underline{\underline{1.11}}$$



AEROJET-GENERAL CORPORATION  
SACRAMENTO • CALIFORNIA

REPORT NO  
SA-005-CC-03

PAGE 4/1 OF 2/1

DATE  
7/15/71

WORK ORDER  
1811-25-13

BY  
GHS

CHK. BY

DATE

@ expansion ratio,  $E = 125$

$$\left. \begin{array}{l} T_{wg} = 5^{\circ}F \\ T_B = -267^{\circ}F \end{array} \right\} \text{ see Figure 13}$$

see Reference 12, Figure 12, Pg. 34

$$\left. \begin{array}{l} @ P_c' = .1700 \text{ psi} \\ T_{wg} = 5^{\circ}F \end{array} \right\} (R/t)_{max} = 16.25$$

$$R_{max} = \frac{1.280}{n} \left( \frac{E F}{P_c} \right)^{1/2} \quad \dots \text{ Reference 11, Pg. 4}$$

where:  $E = 125$

$F = 25,000 \text{ lbs}$

$P_c = 1800 \text{ psi}$

$n = 380 \text{ tubes}$

$$R_{max} = 0.140 \text{ in.}$$

$$t_{min} = 0.015 \text{ in.}$$

$$R/t = 9.37$$

$$M.S. = \frac{16.25}{9.37} - 1 = \underline{\underline{0.73}} \text{ (yield)}$$

(Thermal creep or buckling are negligible)





SUBJECT

DATE

7/15/71

WORK ORDER

1811-06-103

BY

GHS

CHK. BY

DATE

LOW CYCLE FATIGUE

$$\epsilon_T = K \alpha \Delta T$$

where:  $K = 1.00$  (function of constraint)

$$\Delta T = T_{wg} - T_b$$

 $T_{wg}$  = Wall Gas-Side Temp, °F $T_b$  = Coolant Bulk Temp, °F $\alpha$  = Thermal coefficient of expansion, in/in-°F@ Expansion ratio,  $\epsilon = 6.0$ 

$$T_{wg} = 664^\circ\text{F}$$

$$T_b = -360^\circ\text{F}$$

Inlet Conditions — see Figure 13

$$\alpha = 9.68 \times 10^{-6} \text{ in/in-}^\circ\text{F} \text{ (0-664}^\circ\text{F)} \text{ — see Figure 1}$$

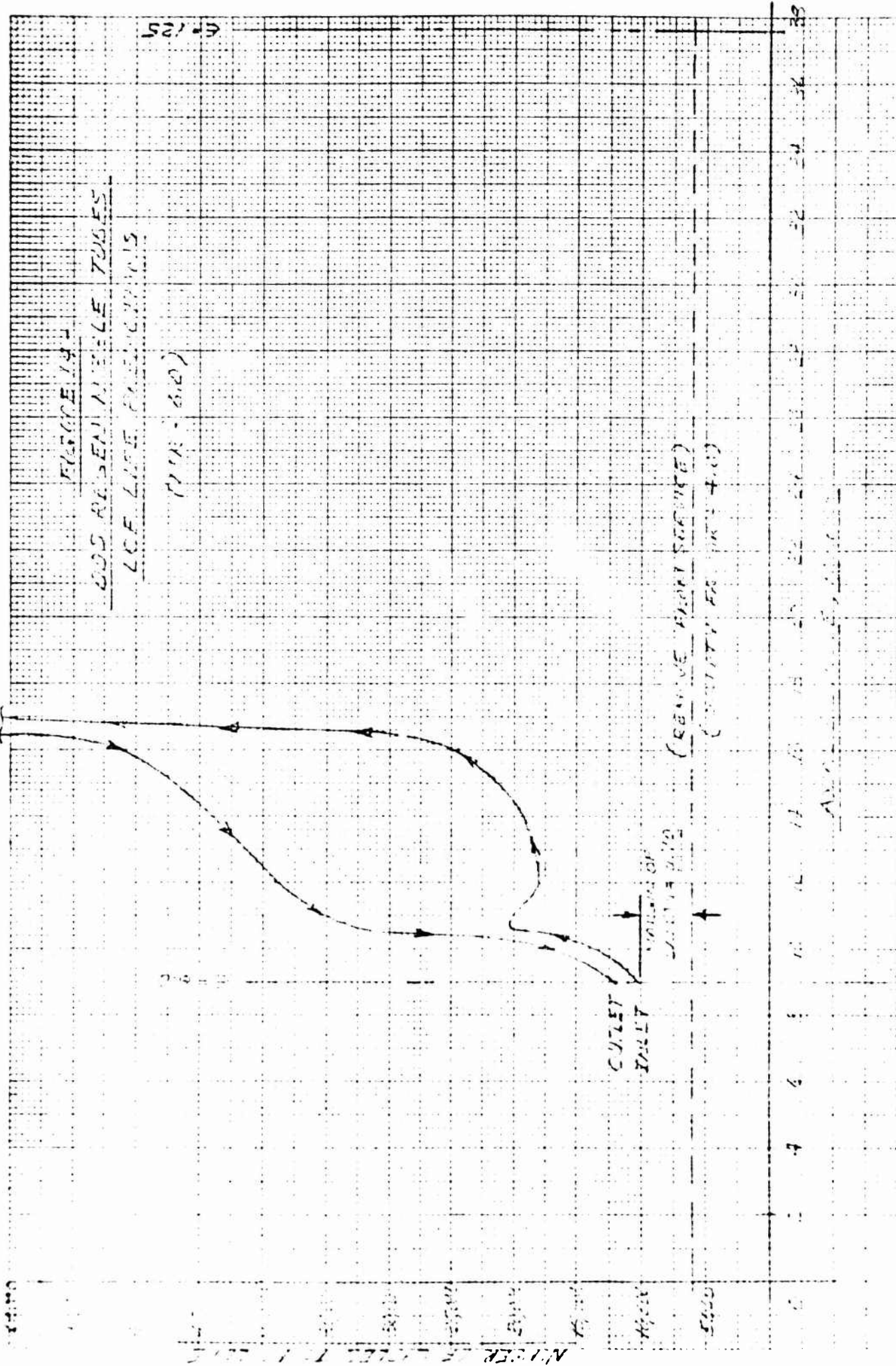
$$\epsilon_T = 0.995\%$$

see Figure 2

$N_f = 10,200$  cycles to failure, no hold time. Hold time for ARMCO 22-13-5 Stainless Steels at temperatures below  $T_{wg} = 1,000^\circ\text{F}$  result in negligible degradation (Ref. 12)

Figure 14 is a plot of predicted LCF Life for regon nozzle tubes. Critical location occurs at inlet, ( $\epsilon = 6.0$ )

$$M.S. = \frac{10,200}{6,000} - 1 = \underline{\underline{0.70}}$$

[illegible]



SUBJECT

DATE

7/15/74

WORK ORDER

1811-06-103

BY

GHS

CHK. BY

DATE

2.- RESECTION TUBE SECTION RING SIZE & SPACINGPressure Loading

$$L = 0.603 \left( \frac{F_{ty}}{np} \right)^{1/2} \left( \frac{EF}{P_c} \right)^{1/4}$$

... Reference 11, Pg. 4

where: L = Ring Spacing, in.

E = Expansion Ratio

F = Motor Thrust = 25,000 lbs

P<sub>c</sub> = Plenum Pressure = 1800 psi

n = No. of Tubes

F<sub>ty</sub> = Yield Strength, psi

p = chamber pressure = p, psi

$$L = 1.162 \left( \frac{F_{ty}}{np} \right)^{1/2} E^{1/4}$$

Assume: E = 6.0

n = 190

p = 1.20(1800)(0.025) = 54.0 psi (yield) @ E = 6.0

F<sub>ty</sub> = 46,000 psi @ T = 700°F ... Figure 1

$$\therefore L = 3.86 \text{ in.}$$

$$Z, \text{ Axial Length} = L \cos \phi$$

where:  $\phi \approx 37^\circ$ 

$$Z = 3.03 \text{ in.}$$

$$E = \underline{13.0}$$

Assume: E = 13.0

n = 190 tubes

p = 1.2(1800)(0.00675) = 14.6 psi (yield) @ E = 13.0

F<sub>ty</sub> = 48,000 psi @ T = 550°F

$$\therefore L = 9.68 \text{ in.}$$

$$Z = 9.68 \cos 34^\circ = 7.95 \text{ in.}$$

$$E = 49.0$$

let: E = 30.0 (3 bifurcation)

n = 300

p = 1.2(1800)(0.0030) = 6.5 psi (yield) @ E = 30.0

F<sub>ty</sub> = 48,000 psi @ T = 550°F

$$L = 13.70$$

$$Z = 13.70 \cos 25.5^\circ = 12.35 \text{ in.}$$

$$E = \underline{97.0}$$



Assume:  $E = 87.0$   
 $n = 350$  tubes  
 $p = 1.25(1800)(.0008) = 1.7$  psi (yield) @  $E = 87.0$   
 $F_{ty} = 75,000$  psi @  $75^\circ F$   
 $L = 38.2$  in.  
 $Z = 38.2 \cos 20^\circ = 35.8$  in.  
 $E \geq 125.0$

∴ Maximum of Three rings required, and possibly two may be sufficient, since this analysis is very conservative. Next check Tube Length for Thrust, angular acceleration loading and buckling criteria

BUCKLING CRITERIA

$$L_{cr} = \frac{6100}{n} \left( \frac{E F / P_c}{[4.53 M + (E F / P_c)^{1/2} T_e]} \right)^{1/2}$$

... Reference 11, Pg. 4

let:  $n = 190$  tubes  
 $E = 6.0$   
 $F = 25,000$  lbs  
 $P_c = 1800$  psi  
 $\phi = 37^\circ$

$$L_{cr} = \frac{2000}{(4.53 M + 9.12 T_e)^{1/2}}$$

where:  $M$  = Moment due to angular acceleration, in-lbs  
 $T_e$  = Thrust @  $E$ , lbs

$$T_e = P_1 A_1 (1 + \gamma M_1^2) - P_2 A_2 (1 + \gamma M_2^2) \quad \dots \text{Reference 18}$$

where:  $A_1 = \text{Area } \phi = 6.0, = 40.84 \text{ in}^2$   
 $P_1 = \text{Pressure } \phi = 6.0, = 54.0 \text{ psi (yield)}$   
 $M_1 = M_2 = \text{No. } \phi = 6.0, = 2.915$   
 $A_2 = \text{Area } \phi = 2.10, = 19.44 \text{ in}^2$   
 $P_2 = \text{Pressure } \phi = 2.10, = 2.71 \text{ psi (yield)}$   
 $M_2 = M_1 = \text{No. } \phi = 2.10, = 2.915$   
 $\gamma = \text{Ratio of specific heats} = 1.20$

$$T_e = -4,967.6 \text{ lbs (yield)} - \text{compressive}$$



DATE  
7/24/71

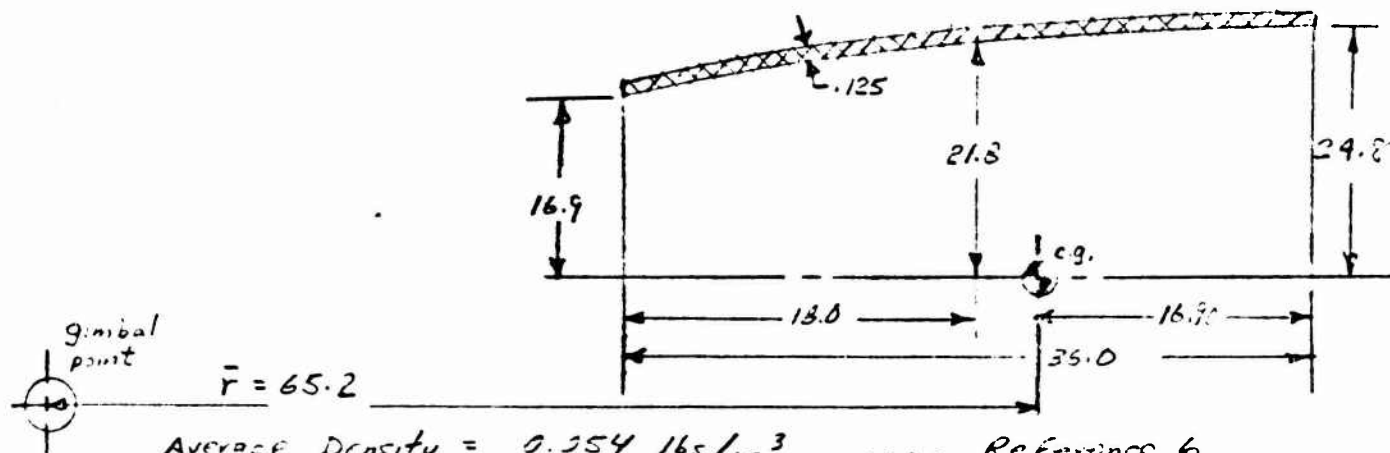
WORK ORDER  
1811-06-103

BY  
GHS

CHK. BY

DATE

DETERMINE INERTIAL LOADING OF AG CARB NOZZLE



Average Density =  $0.254 \text{ lbs/in}^3$  ... Reference 6

Weight = 32.90 lbs

Mass,  $m = \frac{32.90}{386.4} = 0.085 \frac{\text{lbs-sec}^2}{\text{in.}}$

Moment of Inertia,  $I_0 = 28.0 \text{ in-lb-sec}^2$

Inertial Force,  $F = m \bar{r} \alpha = 0.085(65.2) \alpha = 5.53 \alpha$ , lbs.

where:  $\alpha$  = angular acceleration,  
 $\text{rad/sec}^2$

Inertial Moment,  $I_1$ ,  $I_1 = I_0 \alpha + F(\bar{r} - x_0)$  ... Reference 19

$$M_1 = 28.0 \alpha + 5.53 \alpha (65.2 - 18.0)$$

where:  $x_0$  = distance from gimbal point  
to  $\text{cg.} = 18.0 \text{ in.}$

$$M_1 = 285 \alpha$$

Apply Safety Factor for external loading

$$M_1 = 1.1(285) \alpha = 313.5 \alpha$$



SUBJECT

DATE

7/16/71

WORK ORDER

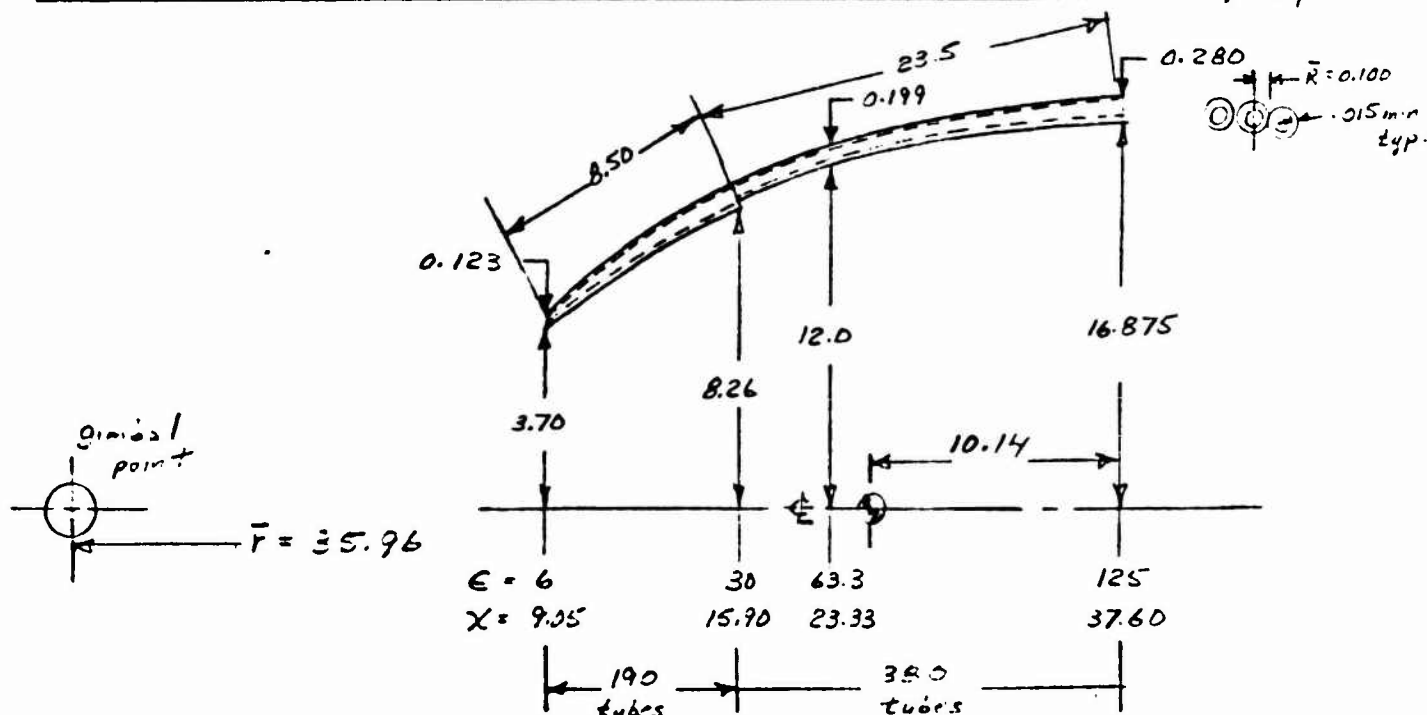
1811-25-125

BY

GHS

CHK. BY

DATE

DETERMINE EQUIVALENT DENSITY FOR REGEN TUBE BUNDLE,  $\rho_{eq}$ 

Wt of Tube Bundle = Volume  $\times$  Density = Prismoid Volume  $\times$  Equivalent Density  
 Ref. 20:  $2\pi \bar{R} t (\eta_0 L_0 + \eta_2 L_2) \rho = V \times \rho_{eq}$

$$\rho_{eq} = \frac{2\pi \bar{R} t \rho (\eta_0 L_0 + \eta_2 L_2)}{V} = \frac{22.3}{V}$$

where:  $\bar{R}$  = Mean Tube Radius = 35.96 in  
 $t$  = Tube Thickness = 0.015 in  
 $\rho$  = Density = 0.25 lb/in<sup>3</sup>  
 $\eta_0$  = 190 tubes  
 $\eta_2$  = 380 tubes  
 $L_0$  = Tube Length = 8.50 in  
 $L_2$  = Tube Length = 23.5 in  
 $V$  = Prismoid Volume, in<sup>3</sup>

Ref. 20:

$$V = \frac{\pi H}{6} \left[ (R_o^2 + 4R_i^2 + r_o^2) - (R_i^2 + 4R_o^2 + r_i^2) \right] = 444.22 \text{ in}^3$$

where:  $H$  = Axial Length = 32.50 in  
 $R_o$  = Outer Max Radius = 17.5 in  
 $H_o$  = Outer Radius at top of tube  
 $r_o$  = Outer Min Radius = 17.5 in  
 $R_i$  = Inner Max Radius = 16.5 in  
 $H_i$  = Inner Radius at top of tube  
 $r_i$  = Inner Min Radius = 16.5 in



SUBJECT

DATE  
7/13/71WORK ORDER  
1811-05-103

BY

GHS

CHK BY

DATE

$$\therefore \rho_{eq} = \frac{28.23}{444.22} = 0.064 \text{ lb/in}^3$$

INERTIAL LOADING

$$\text{Weight} = 28.42 \text{ lbs}$$

$$\text{Mass, } m = \frac{28.42}{386.4} = 0.074 \frac{\text{lb-sec}^2}{\text{in.}}$$

$$\text{Moment of Inertia, } I_0 = 11.3 \text{ in-lb-sec}^2$$

$$\text{Inertial Force, } F = m\ddot{r}\alpha = 0.074(35.96)\alpha = 2.6\alpha, \text{ lbs}$$

$$\text{Inertial Moment, } M_2 = I_0\alpha + F(\bar{r} - x_1) \quad \dots \text{Reference 19}$$

$$M_2 = 11.3\alpha + 2.6\alpha(35.96 - 18.60)$$

$$M_2 = 56.4\alpha, \text{ in-lbs}$$

Apply Safety Factor for external loading

$$M_2 = 1.1(56.4)\alpha = 62.0\alpha, \text{ in-lbs.}$$



SUBJECT

DATE

7/24/71

WORK ORDER

1841-03-123

BY

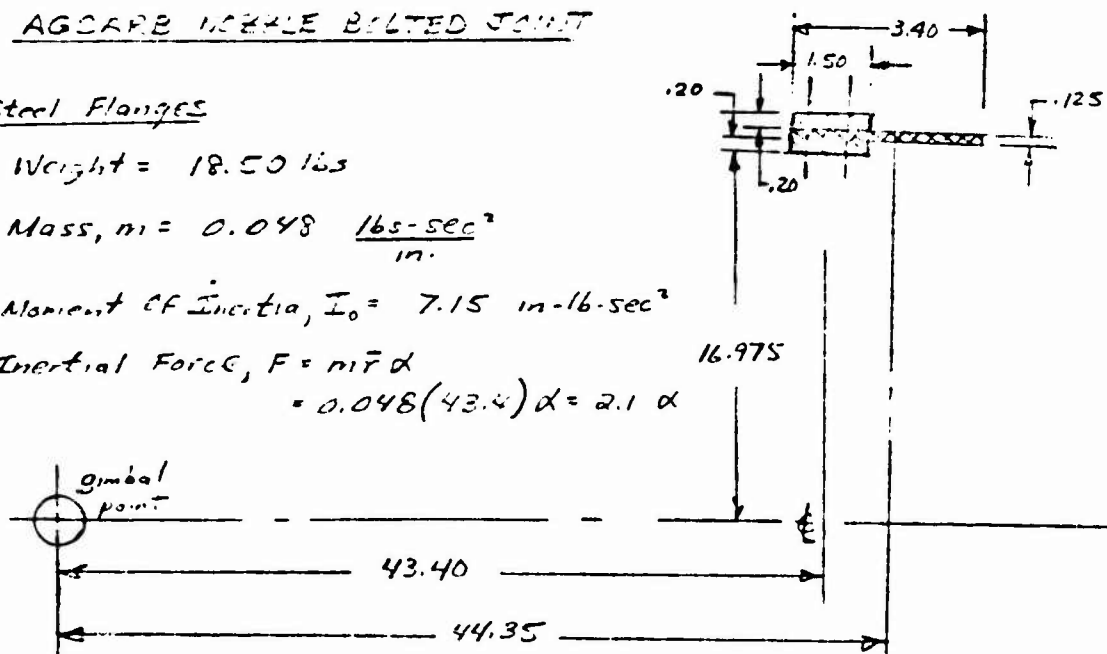
GHS

CHK BY

DATE

AGCARE NOZZLE BELTED JOINTSteel Flanges

Weight = 18.50 lbs

Mass,  $m = 0.048 \frac{\text{lbs-sec}^2}{\text{in.}}$ Moment of Inertia,  $I_0 = 7.15 \text{ in-lb-sec}^2$ Inertial Force,  $F = m\bar{r}\alpha$   
 $= 0.048(43.4)\alpha = 2.1\alpha$ 

Inertial Moment,  $M_3 = I_0\alpha + F(\bar{r}-x) \quad \dots \text{Reference 19}$   
 $= 7.15\alpha + 2.1(43.4 - 18.6)\alpha$   
 $= 57.15\alpha \times 1.1 = 63.0\alpha, \text{ in-lbs}$   
 ← Safety Factor

AGCARE

Weight = 2.42 lbs

Mass,  $m = 0.0064 \frac{\text{lbs-sec}^2}{\text{in.}}$ Moment of Inertia,  $I_0 = 0.965 \text{ in-lb-sec}^2$ Inertial Force,  $F = m\bar{r}\alpha$   
 $= 0.0064(44.35)\alpha = 0.284\alpha, \text{ lbs.}$ 

Inertial Moment,  $M_4 = I_0\alpha + F(\bar{r}-x) \quad \dots \text{Reference 19}$   
 $= 0.965\alpha + 0.284\alpha(44.35 - 18.60)$   
 $= 8.265\alpha \times 1.1 = 9.1\alpha, \text{ in-lbs}$   
 ← Safety Factor





SUBJECT

DATE

7/26/71

WORK ORDER

1811-55-123

BY

GHS

CHK. BY

DATE

SUMMATION OF MOMENTS @  $\epsilon = 6.0$ 

$$M = \sum_{n=1}^4 M_n = (313.5 + 62.0 + 63.0 + 9.1) \alpha$$

$$M = 447.5 \alpha, \text{ in-lbs}$$

$$\text{let: } \alpha = 5 \text{ rad/sec}^2$$

$$\therefore M = 2,238.0 \text{ in-lbs}$$

$$L_{cr} = \frac{2380}{(4.53 \times 2,238 + 9.12 \times 4,967.6)^{1/2}} \quad \dots \text{ See Pg. 45}$$

$$L_{cr} = 10.1 \text{ inches} > 3.86 \text{ inches} \quad \dots \text{ see pg. 44}$$

$\therefore$  Pressure Loading Governs Unsupported Tube Length

$$\text{let: } \alpha = 40 \text{ rad/sec}^2 \text{ max.}$$

$$M = 17,904.0 \text{ in-lbs}$$

$$L_{cr} = 6.70 \text{ inches} > 3.86 \text{ inches} \quad \dots \text{ see pg. 44}$$

$\therefore$  Pressure Loading will always govern tube length  
at expansion ratio,  $\epsilon = 6.0$

Repeat Problem (7)  $\epsilon = 30$ 

$$M_1 = [28.0 \alpha + 5.53 \alpha (65.2 - 25.3)] 1.1 = 278.0 \alpha$$

$$M_2 = [11.3 \alpha + 2.60 \alpha (35.96 - 25.30)] 1.1 = 42.9 \alpha$$

$$M_3 = [7.15 \alpha + 2.10 \alpha (43.40 - 25.30)] 1.1 = 49.7 \alpha$$

$$M_4 = [0.955 \alpha + 0.284 \alpha (44.35 - 25.30)] 1.1 = \frac{7.0 \alpha}{377.6 \alpha, \text{ in-lbs}}$$

$$T_c = P_2 A_c (1 + 8' h_c^2) - P_e A_e (1 + 8' h_e^2) \quad \dots \text{ Reference 1B}$$

$$\text{where: } P_2 = 6.5 \text{ psi (yield) } @ \epsilon = 30$$

$$A_2 = 214.90 \text{ in}^2 @ \epsilon = 30$$

$$M_2 = 4.04$$

(see pg. 45 for other values)

$$T_c = 34,252.8 - 30,954.2 = -2,201.4 \text{ lbs (yield)} - \text{compressive}$$



REPORT NO SA-005-CC-13	PAGE 51 OF 91
DATE 7/21/71	
WORK ORDER 1811-25-103	
BY GHS	CHK. BY
DATE	

$$L_{cr} = \frac{6100}{n} \frac{(EF/P_c)(\cos \phi)^{1/2}}{[4.53M + (EF/P_c)^{1/2}T_0]^{1/2}} \quad \dots \text{Reference 11, Pg. 4}$$

where:  $n = 380$  tubes

$E = 30.0$

$F = 25,000$  lbs

$P_c = 1,800$  psi

$\phi = 25.5^\circ$

$$L_{cr} = \frac{6340}{(4.53M + 20.4T_0)^{1/2}}$$

let:  $\alpha = 5 \text{ rad/sec}^2$ ,  $M = 1,886 \text{ in-lbs (yield)}$

$\therefore L_{cr} = 27.5 \text{ in.} > 13.70 \text{ inches} \quad \dots \text{See Page 44}$

let:  $\alpha = 40 \text{ rad/sec}^2$ ,  $M = 15,100 \text{ in-lbs (yield)}$

$\therefore L_{cr} = 18.85 \text{ in.} > 13.70 \text{ inches} \quad \dots \text{see Page 44}$

$\therefore$  Pressure Load governs support ring spacing rather than buckling criteria.



SUBJECT

DATE

7/26/71

WORK ORDER

1811-05-123

BY

GHS

CHK BY

DATE

DETERMINE SUPPORT RING THICKNESS

$$t = \frac{pLnR}{\pi b F_t \cos \phi} \quad \dots \text{Reference 11, Pg. 33}$$

Substitute expressions for L & R from pages 44 & 39, respectively

$$\therefore t = \frac{1.77}{b \cos \phi} \epsilon^{3/4} \left( \frac{p}{F_{ty} n} \right)^{1/2}$$

let:  $\epsilon = 6$

$p = 54.0 \text{ psi (yield)}$

$n = 190 \text{ tubes}$

$F_{ty} = 46,000 \text{ psi @ } 700^\circ\text{F}$

$\phi = 37^\circ$

$$t = \frac{0.021}{b} \text{ in. or } 0.021 \text{ @ } b = 1.0 \text{ inch.}$$

where:  $b = \text{ring width, in.}$

let:  $\epsilon = 30$

$p = 6.5 \text{ psi (yield)}$

$n = 380 \text{ tubes}$

$F_{ty} = 48,000 \text{ psi @ } 55^\circ\text{F}$

$\phi = 25.5^\circ$

$$t = \frac{0.015}{b} \text{ in. or } 0.015 \text{ @ } b = 1.0 \text{ inch.}$$

where:  $b = \text{ring width, in.}$



SUBJECT

DATE

7/26/71

WORK ORDER

1811-05-103

BY

GHS

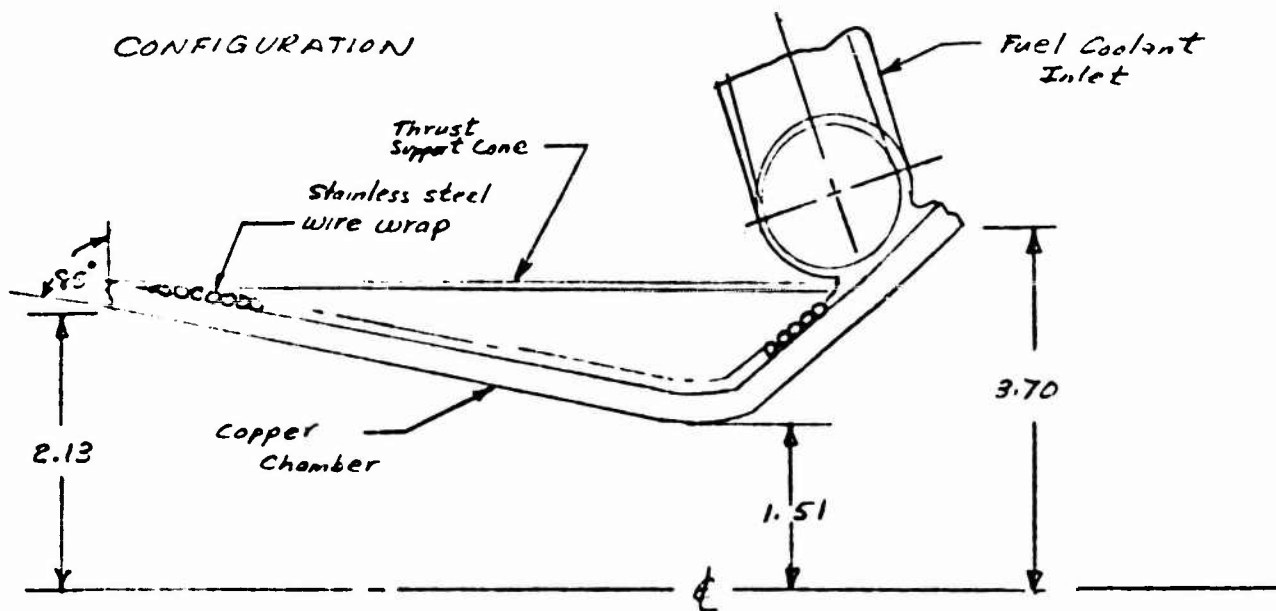
CHK. BY

DATE

C. PRESSURE JACKETDESIGN DATA

MATERIAL - ARMCO 22-13-5 Stainless Steel Bar/Wire

Ultimate Strength,  $F_{tu} = 103,000 \text{ psi}$   
 Yield Strength,  $F_{ty} = 55,000 \text{ psi}$  } @ R.T.

LOADSThermal ~  $-19^{\circ}\text{F}$  to  $-120^{\circ}\text{F}$ Plenum Pressure =  $1800 \text{ psi}$  ~ (MEOP)CONFIGURATIONFIGURE 15 - MAIN COMBUSTION CHAMBER ASSEMBLY



SUBJECT

DATE

7/26/71

WORK ORDER

1811-23-103

BY

GHS

CHK. BY

DATE

1.- PRESSURE JACKET

Single layer of wire wrapped around Zirconium Copper Chamber. Critical Location occurs at Coolant exit (Injector Face).

YIELD CRITERIA

$$\text{wire diameter, } d = \frac{1.275 p r}{F_{ty} \sin \phi}$$

... Reference 11, Pg. 47

$$\text{where: } p = 1700 (1.20) = 2040 \text{ psi (ult)}$$

$$r = 2.13 \text{ in.}$$

$$F_{ty} = 55,000 \text{ psi @ R.T. - Ref. 2}$$

$$\phi = 85^\circ$$

$$d = 0.101 \text{ in.}$$

ULTIMATE CRITERIA

$$\text{let: } p = 1700 (1.50) = 2550 \text{ psi (ult)}$$

$$F_{tu} = 95,000 \text{ psi @ R.T.}$$

$$d_{min} = 0.073 \text{ in} < 0.101$$

Reference 21, Pg. 19:

$$\therefore \text{Min wire diameter} = 0.105 \sim \text{Washburn \#2}$$

Moen Wire Gauge #1012

$$M.S. = \frac{0.105}{0.101} - 1 = \underline{\underline{0.04}} \text{ (yield)}$$

$$M.S. = \frac{0.105}{0.073} - 1 = \underline{\underline{0.44}} \text{ (ult)}$$



SUBJECT

DATE

7/25/71

WORK ORDER

1811-25-103

BY

GHS

CHK. BY

DATE

2. FUEL COOLANT TORUS

Reference 10, Pg. 274, Case 20

YIELD CRITERIA

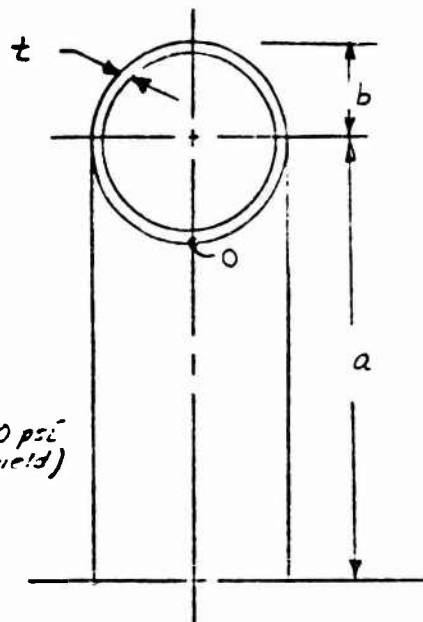
$$\text{Max Stress, } T = \frac{p \cdot b}{t} \left( \frac{2a-b}{2a-2b} \right) @ 0$$

$$\text{where: } p = 3750 (1.20) = 4500 \text{ psi (yield)}$$

$$b = 0.875 \text{ in.}$$

$$a = 5.30 \text{ in.}$$

$$t = 0.075 \text{ in.}$$



$$\sigma_y = 57,600 \text{ psi (yield)}$$

$$F_{ty @ R.T.} = 75,000 \text{ psi} \dots \text{Figure 1}$$

$$M.S. = \frac{75,000}{57,600} - 1 = \underline{\underline{0.30 \text{ (yield)}}}$$

ULTIMATE CRITERIA

$$\text{let: } p = 1.50 (3750) = 5625 \text{ psi (ult)}$$

$$\sigma_u = 72,000 \text{ psi (ult)}$$

$$F_{tu @ R.T.} = 112,000 \text{ psi} \dots \text{Figure 1}$$

$$M.S. = \frac{112,000}{72,000} - 1 = \underline{\underline{0.55 \text{ (ult)}}}$$



SUBJECT

DATE

7/25/71

WORK ORDER

1811-08-103

BY

GHS

CHK. BY

DATE

DETERMINE INERTIAL LOADING OF FUEL COOLANT TORUS

$$\text{WEIGHT, } W = 2\pi R t (2\pi r) \rho = 4\pi^2 R r t \rho \quad \dots \text{Reference 20}$$

$$\text{where: } R = 0.875 \text{ in.}$$

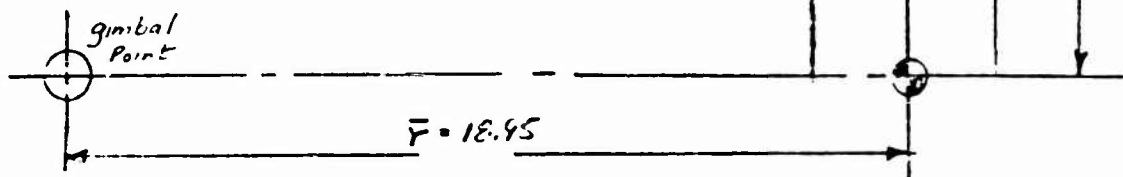
$$t = 0.075 \text{ in.}$$

$$r = 5.30 \text{ in.}$$

$$\rho = 0.265 \text{ lb/in}^3$$

$$W = 3.93 \text{ lbs}$$

$$\text{Mass, } m = \frac{3.93}{386.4} = 0.010 \frac{\text{lbs} \cdot \text{sec}^2}{\text{in.}}$$



Reference 22:

$$\text{Moment of Inertia, } I_0 = m \left( \frac{r^2}{2} + \frac{5R^2}{8} \right) = 0.15 \text{ in} \cdot \text{lbs} \cdot \text{sec}^2$$

$$\text{Inertial Force, } F = m \bar{r} \alpha = 0.010 (18.75) \alpha = 0.19 \alpha, \text{ lbs}$$

$$\text{Inertial Moment, } M_s = I_0 \alpha + F(\bar{r} - x) \quad \dots \text{Reference 19}$$

$$M_s = 0.15 \alpha + 0.19 (18.75 - x) \alpha$$

let:  $x = 6.15 \text{ in.}$  from gimbal point  
to min. radius of Thrust cone

$$M_s = 2.58 \alpha, \text{ in} \cdot \text{lbs.}$$



SUBJECT

DATE

7/26/71

WORK ORDER

1811-66-103

BY

GHS

CHK. BY

DATE

D.- COPPER COMBUSTION CHAMBERDESIGN DATA

MATERIAL ~ Zirconium Copper

Ultimate Strength,  $F_{tu} = 27,100 \text{ psi}$  } @ R.T.Yield Strength,  $F_{ty} = 10,700 \text{ psi}$  }Coefficient of Thermal Expansion,  $\alpha = 10 \times 10^{-6} \text{ in/in-}^\circ\text{F}$  (0-800°F)LOADS

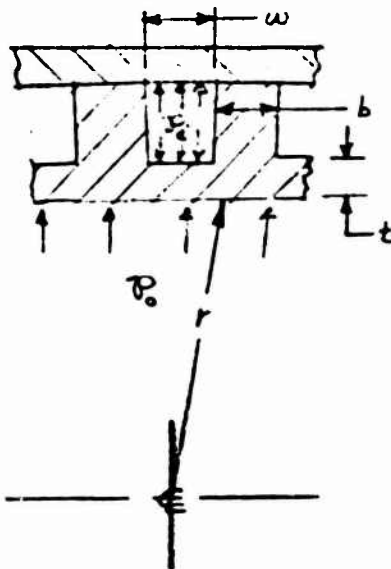
Thermal Gradients - see Figures 17, 18 &amp; 19

Pressure

1) Channel Pressure

@ inlet,  $P = 3,736.0 \text{ psi}$ @ exit,  $P = 2,682.0 \text{ psi}$ LIMIT LOAD  
(MEOP)

2-) Plenum Pressure = 1800 psi

CONFIGURATION - see Table IIIFIGURE 16- CHAMBER CHANNELPARAMETERS



SUBJECT

DATE

WORK ORDER

DATE

BY

GHS

CHK. BY

Ref: COMPUTER RUN 7/15/77  
INPUT BY KOBEN, J. - 2

NOTE: NO SCALE

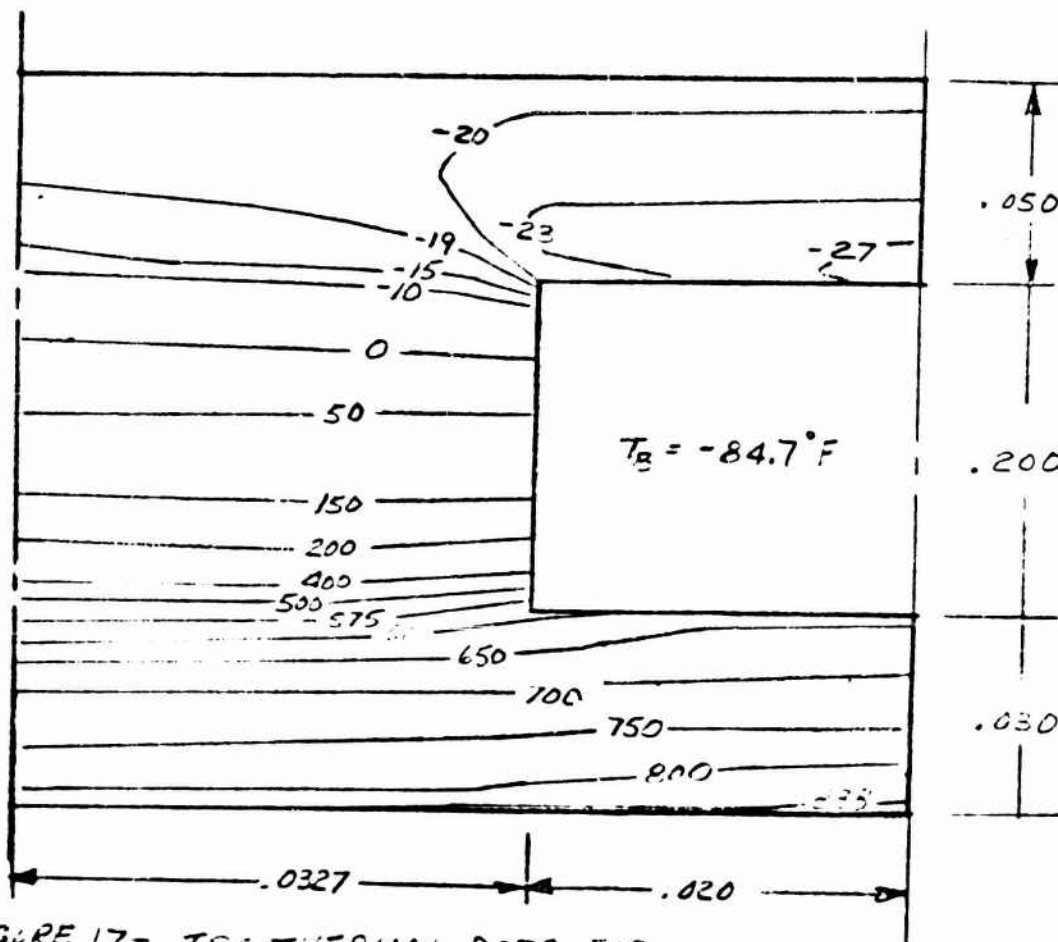


FIGURE 17- ISO-THERMAL DATA FOR  
COPPER NOZZLE  $G_0/E = 2:1$  (Rad. & Thrust)  
STEADY STATE SOLUTION

Coolant Pressure = 2600 psi } MEOP  
Chamber Pressure = 1700 psi }  
Thrust = 25,000 lbs  
MR = 6.0

SUBJECT

DATE

WORK ORDER

BY

GHS

CHK. BY

DATE

REF: COMPUTER P. 463 7/17  
INPUT BY KENYASHI

NOTE: NO SCALE

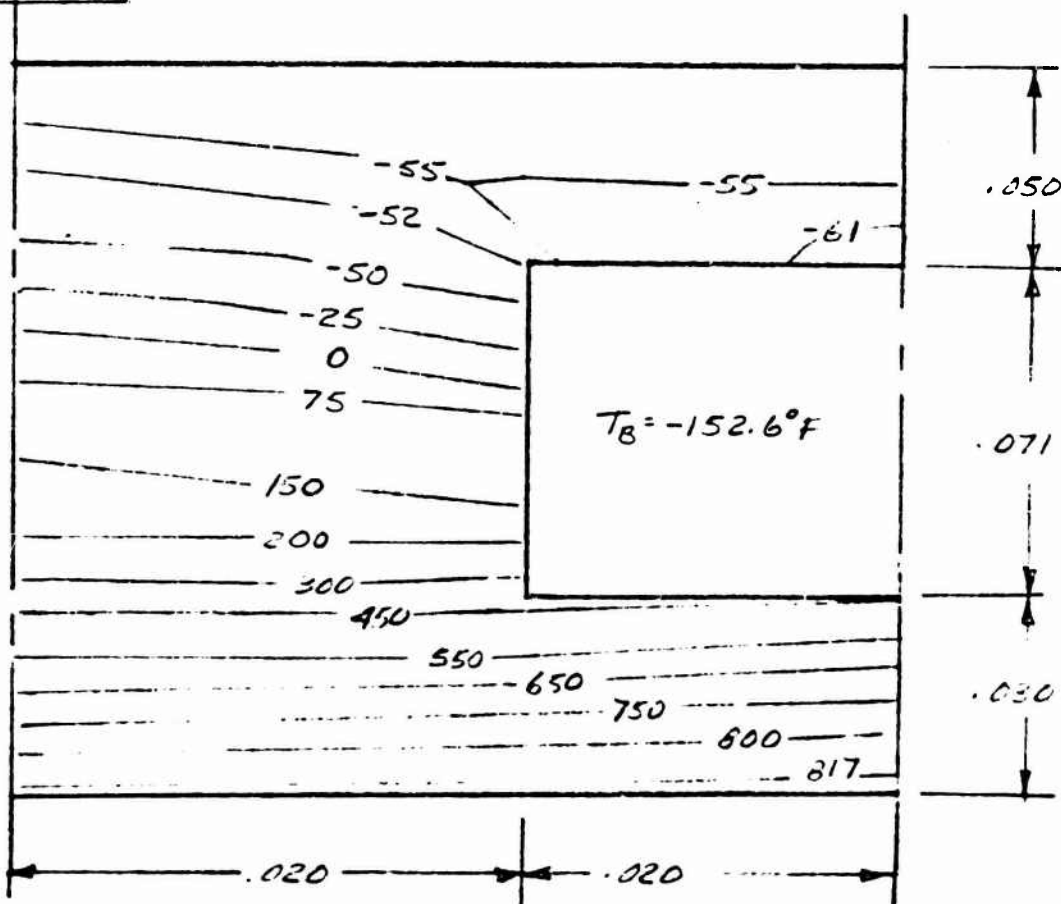


FIGURE 15- ISOTHERMAL DATA FOR  
COPPER NOZZLE @ THROAT  
STEADY STATE SOLUTION

Coolant Pressure = 2658 psi  
Chamber Pressure = 1016 psi } MEOP  
Thrust = 25,000 lbs  
M.R. = 6.0



DATE	5/21/77
WORK ORDER	1811-85-28
DATE	

BY	GHS
----	-----

CHK. BY	
---------	--

Ref.: Computer Run dtd. 7/10  
Input by Katsyash

NOTE: NO SCALE

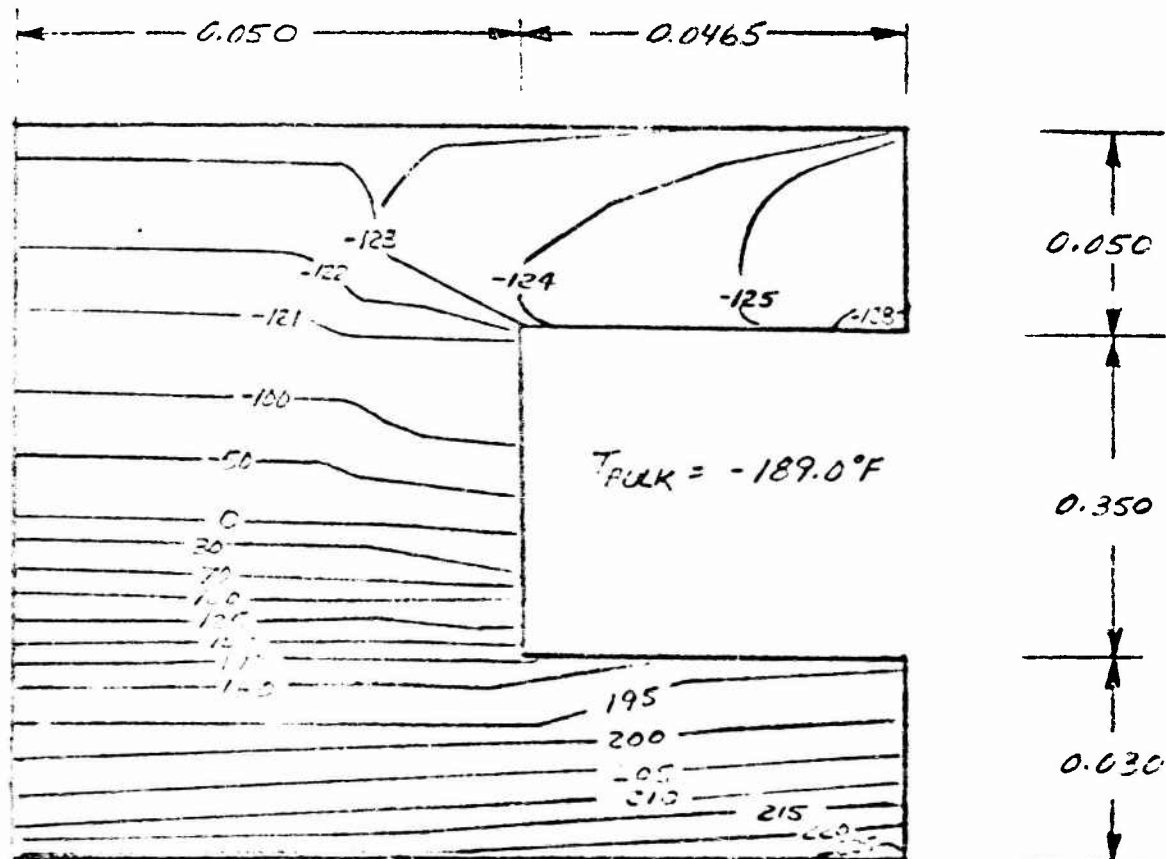


FIGURE 19- ISO THERMAL DATA FOR

COPPER NOZZLE @ E=6:1 (AFT OF THROAT)

STEADY STATE SOLUTION

Coolant Pressure = 3736 psi } MEOP  
 Chamber Pressure = 45 psi }  
 Thrust = 25,000 lbf  
 M.R. = 6.0



SUBJECT

DATE

7/26/71

WORK ORDER

1811-65-103

BY

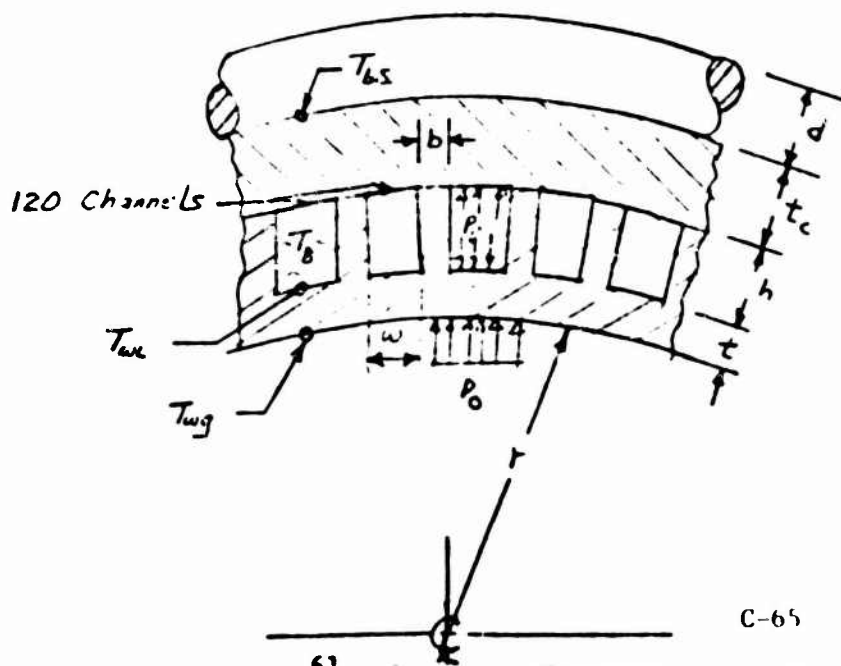
GHS

CHK. BY

DATE

TABLE III - COPPER CHAMBER  
GEOMETRY AND DESIGN LOADS

	COOLANT INLET (E=6.0)	THROAT	COOLANT EXIT (INJECTOR FACE)
Channel width, $w$ , in.	0.093	0.040	0.040
Wall Thickness, $b$ , in.	0.100	0.040	0.065
channel thickness, $t$ , in.	0.030	0.030	0.030
channel height, $h$ , in.	0.350	0.071	0.200
cover thickness, $t_c$ , in.	0.050	0.050	0.050
wire wrap dia., $d$ , in.	0.105	0.105	0.105
Gas Side Wall Temp, $T_{wg}$ , °F	225.0	817.0	838.0
Back Side Wall temp, $T_{bs}$ , °F	-123.0	-55.0	-19.0
$\Delta T = T_{wg} - T_{bs}$ , °F	348.0	872.0	857.0
Coolant Bulk Temp, $T_b$ , °F	-187.0	-153.0	-85.0
Liquid-Side Wall Temp, $T_{wl}$ , °F	173.0	446.0	624.0
Chamber Pressure, $P_c$ , psi	45.0	1016.0	1700.0
Coolant Pressure, $P_i$ , psi	3735.0	2858.0	2682.0
Inner Radius, $r$ , in.	3.70	1.51	2.13





SUBJECT

DATE

7/26/71

WORK ORDER

1811-06-103

BY

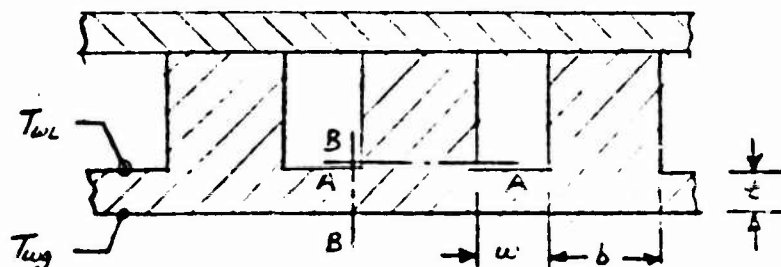
GHS

CHK. BY

DATE

### TABLE II- COPPER CHAMBER INDUCED STRESSES

LOCATION	$P_0, \text{psi}$	$P_i, \text{psi}$	$\Delta P, \text{psi}$	$w, \text{in}$	$b, \text{in}$	$t, \text{in}$	$T_{wL}, ^\circ\text{F}$	$T_{wL}, ^\circ\text{F}$	$T_{wL}, ^\circ\text{F}$	$\gamma_{BE}^{(1)}$	$\sigma_y^{(2)}$	$\sigma_{RA}^{(3)}$
COOLANT INLET (E=6.0)	45	3736	3691	.093	.100	.030	225	193	209	5730	8400	2345
THROAT	1016	2858	1842	.040	.040	.030	517	446	637	1225	320	326
COOLANT EXIT (INJECTOR FACE)	1700	2662	982	.040	.065	.030	838	624	731	655	437	-1045



$$(1) \quad \gamma_{BE} = \frac{\Delta P w}{2t} \quad (\text{AVERAGE SHEAR STRESS ACROSS SECTION B-B})$$

$$(2) \quad \sigma_y = \frac{\Delta P}{4} \left( \frac{w}{t} \right)^2 \quad (\text{BENDING STRESS REQUIRED @ FULL PLASTIC HINGE})$$

$$(3) \quad \sigma_{RA} = \Delta P \left( \frac{w}{b} \right) - P_0 \quad (\text{AVERAGE RADIAL STRESS IN WALL})$$



SUBJECT

DATE

7/24/71

WORK ORDER

1811-06-103

BY

GHS

CHK BY

DATE

TABLE II - MARGINS OF SAFETY IN COPPER CHAMBER

A. SHEAR - MARGINS IN COPPER CHAMBER

LOCATION	$T_{avg}, ^\circ F$	Minimum* SHEAR ALLOWABLE, psi	SHEAR @ MEOP, psi	SHEAR @ PRISF, psi	SHEAR @ BURST, psi	ULTIMATE MARGIN OF SAFETY
COOLANT INLET (E=6.0)	209	12,300	5,730	6,880	8,600	0.43
THROAT	637	8,800	1,225	1,470	1,240	3.77
COOLANT EXIT (INJECTOR FACE)	731	8,200	655	786	995	7.53

$$* F_{su} \approx \frac{1}{2} F_{tu} \quad (\text{Assumed})$$

B. BENDING STRESS - MARGINS IN COPPER CHAMBER

LOCATION	YIELD STRENGTH, psi	ULTIMATE STRENGTH, psi	STRESS @ PROOF, psi	STRESS @ BURST, psi	YIELD MARGIN OF SAFETY	ULTIMATE MARGIN OF SAFETY
COOLANT INLET (E=6.0)	10,700	24,500	10,700	13,350	0.00	0.93
THROAT	9,000	17,500	995	1,230	8.13	LARGE
COOLANT EXIT (INJECTOR FACE)	8,500	16,200	525	655	LARGE	LARGE

C. WALL RADIAL STRESS - MARGINS IN COPPER CHAMBER

LOCATION	YIELD STRENGTH, psi	ULTIMATE STRENGTH, psi	STRESS @ PROOF, psi	STRESS @ BURST, psi	YIELD MARGIN OF SAFETY	ULTIMATE MARGIN OF SAFETY
COOLANT INLET (E=6.0)	10,700	24,500	4,060	5,100	1.65	3.80
THROAT	9,000	17,500	995	1,240	8.05	LARGE
COOLANT EXIT (INJECTOR FACE)	-8,500	-16,200	-1,315	-1,640	5.46	LARGE



SUBJECT

DATE

7/26/71

WORK ORDER

1811-25-113

BY

GHS

CHK. BY

DATE

TABLE VI- LOW CYCLE FATIGUE LIFE IN COPPER CHAMBER

LOCATION	$T_{wg},$ °F	$T_{bs},$ °F	$\Delta T,$ °F	K	$\alpha,$ in/in-°F	$\Delta \epsilon_T^*$ %	$N_F,$ cycles To Failure
COOLANT INLET ( $E=6.0$ )	225.0	-123.0	348.0	1.9	$7.59 \times 10^{-6}$	0.63	6200
THROAT	817.0	-55.0	872.0	1.9	$10.0 \times 10^{-6}$	1.66	1240
COOLANT EXIT (INJECTOR FACE)	828.0	-19.0	847.0	1.9	$10.0 \times 10^{-6}$	1.63	1220

$$* \Delta \epsilon_T = K \alpha \Delta T$$

where:  $\Delta \epsilon_T$  = Total Strain, in/in

$K$  = Constant (function of constraint)

$\alpha$  = Coefficient of Thermal expansion, in/in-°F

$\Delta T = (T_{wg} - T_{bs})$

$T_{wg}$  = Wall Gas-Side Temperature, °F

$T_{bs}$  = Back Side Wall Temperature, °F

FIGURE 20 - ZIRCONIUM COPPER

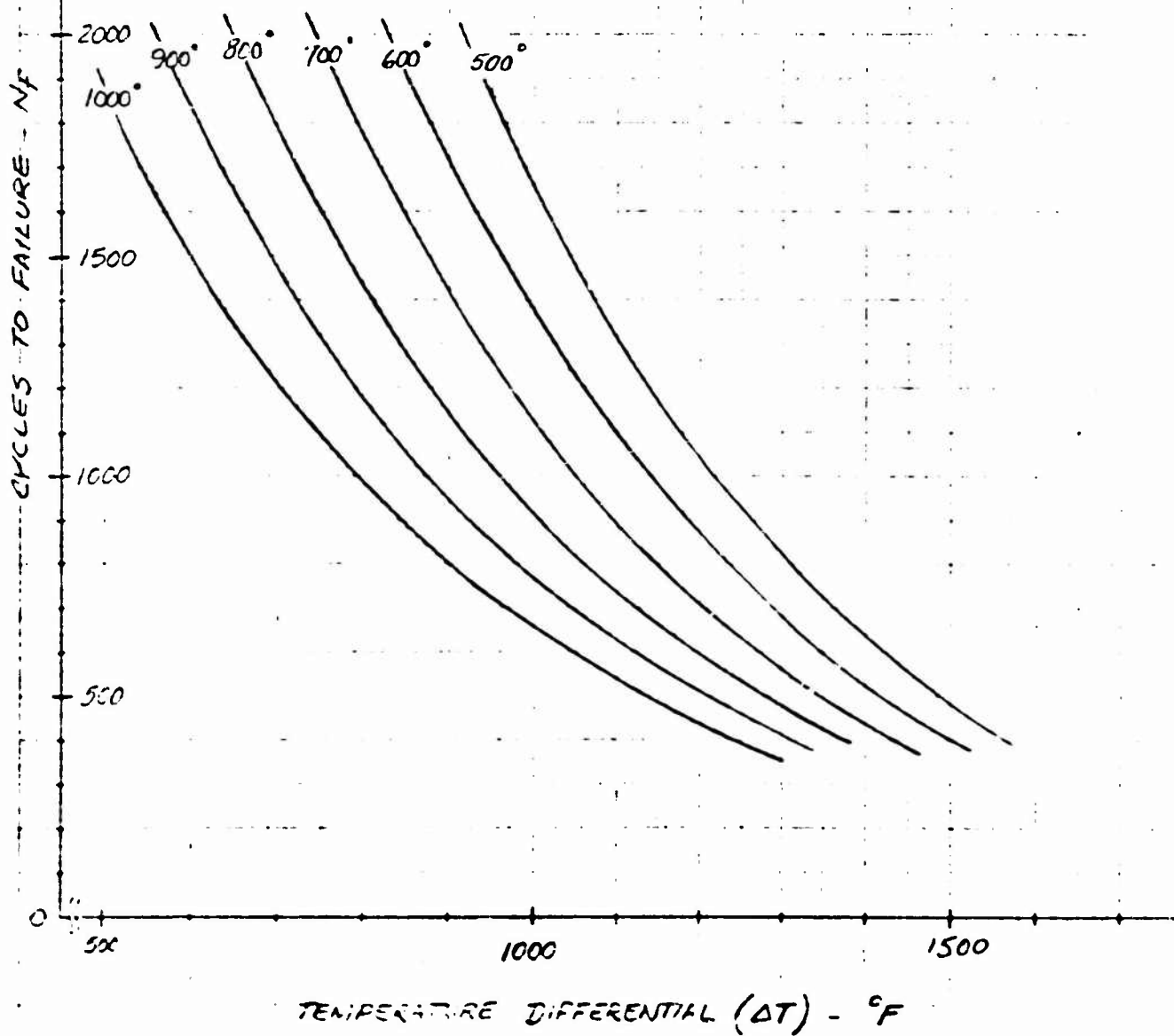
CDS CHAMBER LCF REQMENTS

(NO HOLD TIME DATA)

NOTE: ASSUMPTION MADE THAT:

$$\Delta E_t = (2\alpha \Delta T)$$

$$\Delta T = (T_{WG} - T_{BULK})$$

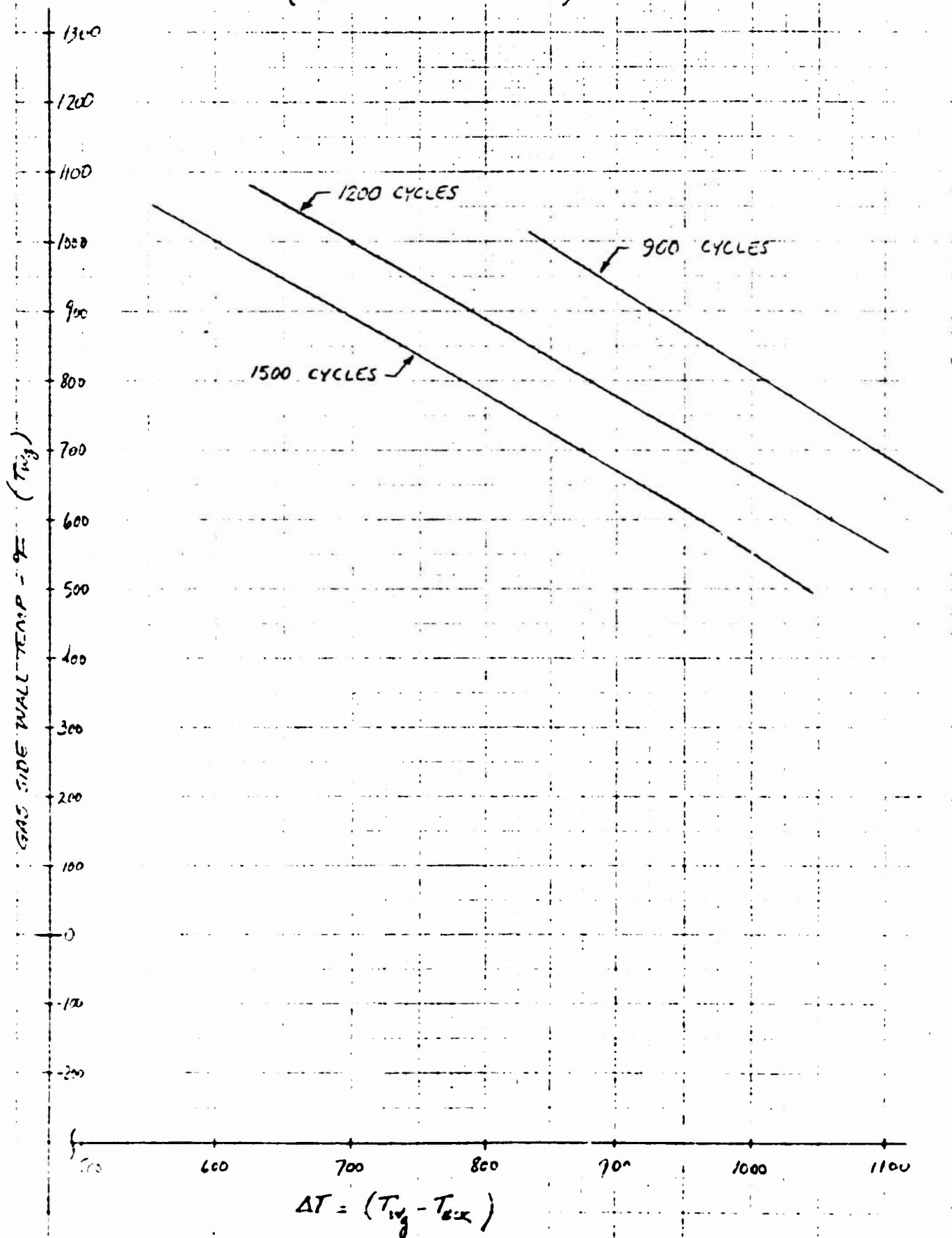


7-1-71

ADK - GNS



FIGURE 21 -  
00S TCA LIFE REQUIREMENTS  
 (NO HOLD TIME DATA)



7-1-71  
 ABE-GMS



SUBJECT

DATE

7/26/71

WORK ORDER

1811-5-123

BY

GHS

CHK BY

DATE

E.- THRUST SUPPORT CONEDESIGN DATA

MATERIAL - ARLICO 22-13-5 STAINLESS STEEL SHEET

Ultimate Tensile Strength,  $F_{tu} = 112,000 \text{ psi}$   
 Yield Strength,  $F_{ty} = 75,000 \text{ psi}$  } @ R.T.

## LOADS

THRUST,  $T_e = P_t A_t (1 + \gamma M_t^2) - P_e A_e (1 + \gamma M_e^2)$   
 Inertial Moment,  $M = \sum [I_{oi} \alpha + m_i \bar{r}_i \alpha (\bar{r}_i - x_i)]$  } Ref. 11,  
 Eq. 52

CONFIGURATION ~ See Pages 53 &amp; 68



SUBJECT

DATE

7/26/71

WORK ORDER

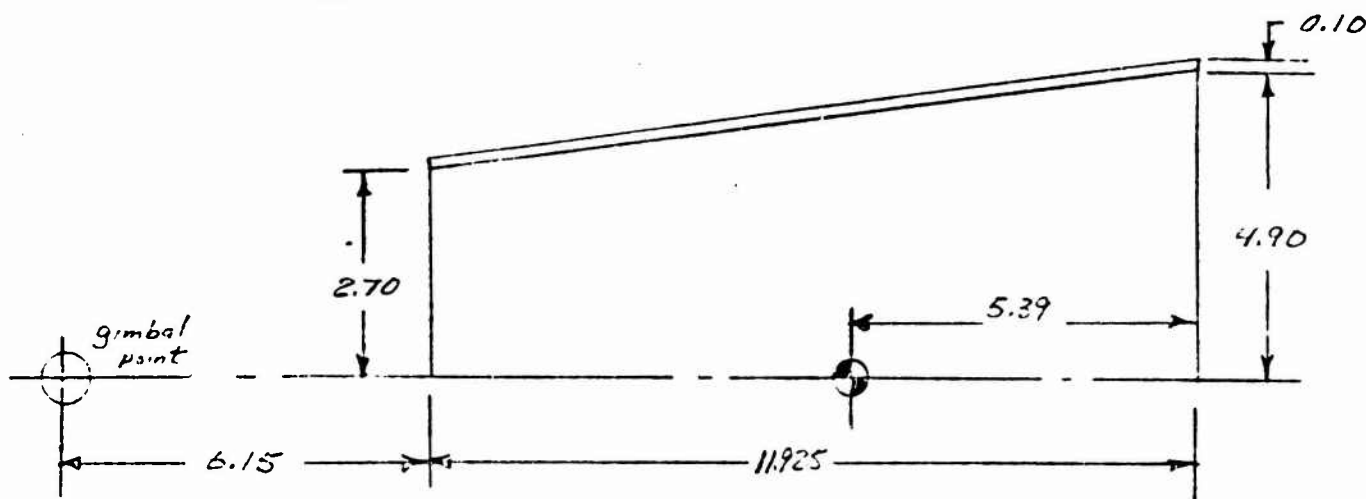
1811-66-103

BY

GHS

CHK. BY

DATE

DETERMINE INERTIAL LOADING OF THRUST CONEWeight,  $W = 6.21 \text{ lbs}$ 

$$\text{Mass, } m = \frac{6.21}{386.4} = 0.021 \frac{\text{lbs-sec}^2}{\text{in.}}$$

Moment of Inertia,  $I_0 = 5.381 \text{ in-lbs-sec}^2$ Inertial Force,  $F = m\ddot{r}\alpha = 0.021(12.585)\alpha = 0.266\alpha \text{ lbs.}$ Inertial Moment,  $M_g = I_0\alpha + F(\bar{r}-x) \dots \text{Reference 19}$   
where:  $x = 6.15 \text{ in.}$ 

$$= 0.381\alpha + 0.266\alpha(12.585 - 6.15)$$

$$= 2.12\alpha \text{ , in-lbs}$$

Sum Moments @ Minimum Radius

$M_1 = 38.0\alpha + 5.53\alpha(35.2 - 6.15) =$	$354.5\alpha$	- ASSEMBLY FRAME
$M_2 = 11.3\alpha + 2.40\alpha(35.96 - 6.15) =$	$38.7\alpha$	- REPAIR TUBES
$M_3 = 7.15\alpha + 3.10\alpha(43.40 - 6.15) =$	$95.5\alpha$	- STEEL FLANGE
$M_4 = 0.965\alpha + 0.284\alpha(44.35 - 6.15) =$	$11.8\alpha$	- ASSEMBLY EXTENSION
$M_5 = 0.15\alpha + 0.19\alpha(18.95 - 6.15) =$	$2.7\alpha$	- FUEL TUBES
$M_6 = 0.381\alpha + 0.266\alpha(12.585 - 6.15) =$	$2.1\alpha$	- THRUST CONE
$\Sigma M_i = 545.5\alpha$		



SUBJECT

DATE

7/25/71

WORK ORDER

1811-66-103

BY

GHS

CHK. BY

DATE

DETERMINE THRUST LOADING

(assume thrust from throat to exit is reacted through thrust support cone)

$$T_c = P_t A_t (1 + \gamma M_t^2) - P_e A_e (1 + \gamma M_e^2) \quad \dots \text{Reference 18}$$

$$\text{where: } P_t = (1.2)(1800)(.5645) = 1220 \text{ psi (gms)}$$

$$A_t = 7.17 \text{ in}^2$$

$$M_t = 1.0$$

$$\gamma = 1.20$$

(see Pg. 45 for other values)

$$T_c = 19,244.3 - 30,954.2 = -11,709.9 \text{ lbs (yield)}$$

MERIDIONAL LOADYIELD CRITERIA

$$N_f = \pm \frac{1.1 M'}{\pi r^2} - \frac{T_c}{2\pi r}$$

$$\text{where: } M = 545.5 \alpha, \text{ in-lbs}$$

$$T_c = -11,709.9, \text{ lbs (yield)}$$

$$r = 2.70 \text{ in.}$$

$$N_f = \pm 26.2 \alpha - 591.0$$

$$\text{let: } \alpha = 5 \text{ rad/sec}^2$$

$$N_{f_{\max}} = -823.0 \text{ lb/in.}$$

$$\text{Meridional Stress, } \tau_{ny} = \frac{N_{f_{\max}}}{t} = \frac{-823.0}{0.050}$$

$$\tau_{ny} = -16,440 \text{ psi (yield)}$$

$$F_{cy} = F_{ty} = 75,000 \text{ psi} \quad \dots \text{Figure 1}$$

$$M.S. = \frac{75,000}{16,440} - 1 = \underline{\underline{3.56}} \text{ (yield)}$$

$$\text{let } \alpha = 40 \text{ rad/sec}^2$$

$$N_{f_{\max}} = -1739.0 \text{ lb/in.}$$

$$\tau_{ny} = 34,760 \text{ psi (yield)}$$

$$M.S. = \frac{75,000}{34,760} - 1 = \underline{\underline{1.16}} \text{ (yield)}$$



DATE

7/26/71

WORK ORDER

1811-00-103

SUBJECT

BY

GHS

CHK. BY

DATE

ULTIMATE CRITERIA

$$N\phi = \frac{1.4621 - T_c}{\pi r^2} \left( \frac{1.50}{1.20} \right)$$

$$N\phi = 33.3 \alpha - 865$$

$$\text{let: } \alpha = 5 \text{ rad/sec}^2$$

$$N\phi_{\max} = -1031.5 \text{ lb/in. (ult)}^{\pm}$$

$$T_{\max} = 20,630 \text{ psi (ult)}^{\pm}$$

$$F_{cu} = F_{tu} = 112,000 \text{ psi} \quad \dots \text{ Figure 1}$$

Q.R.T.

$$M.S. = \frac{112,000}{20,630} - 1 = \underline{\underline{4.43}} \text{ (ult)}^{\pm}$$

$$\text{let: } \alpha = 40 \text{ rad/sec}^2$$

$$N\phi_{\max} = 2197.0 \text{ lb/in. (ult)}^{\pm}$$

$$T_{\max} = 43,940 \text{ psi}$$

$$M.S. = \frac{112,000}{43,940} - 1 = \underline{\underline{1.54}} \text{ (ult)}^{\pm}$$

BUCKLING CRITERIA (assume cone may be treated as a cylinder)

$$\sigma_{cr} = 0.3 \frac{E t}{r} \quad \dots \text{ Ref. 10, Pg. 313} \quad \text{where: } E = 28.0 \times 10^6 \text{ psi}$$

$$t = 0.050 \text{ in.}$$

$$r = 2.70 \text{ in.}$$

$$\sigma_{cr} = 155,700 \text{ psi} > 112,000 \text{ psi}$$

$\therefore$  Compressive stress governs design



SUBJECT

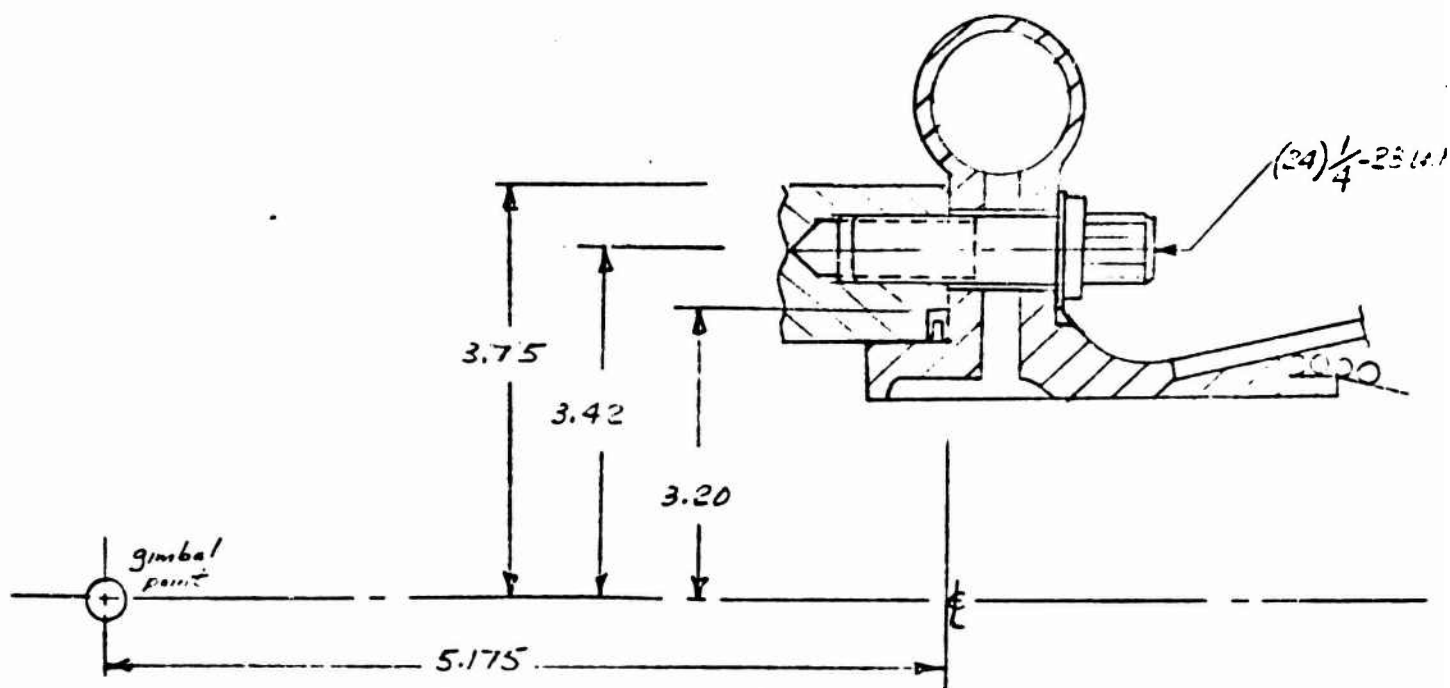
DATE  
7/26/71WORK ORDER  
1811-53-103

BY

GHS

CHK BY

DATE

F. - INJECTOR/CHAMBER BOLTED JOINTFIGURE 22- BOLTED JOINT CONFIGURATIONSUM MOMENTS AT JOINT INTERFACE

$$\begin{aligned}
 M_1 &= 28.0\alpha + 5.53\alpha(65.2 - 5.175) = 360.0\alpha - \text{AGCANE NOZZLE} \\
 M_2 &= 11.3\alpha + 2.60\alpha(35.96 - 5.175) = 91.2\alpha - \text{REGEN TUBES} \\
 M_3 &= 7.15\alpha + 2.10\alpha(43.40 - 5.175) = 87.5\alpha - \text{STEEL PLATES} \\
 M_4 &= 0.965\alpha + 0.234\alpha(44.35 - 5.175) = 12.1\alpha - \text{AGCANE EXTENSION} \\
 M_5 &= 0.15\alpha + 0.19\alpha(12.25 - 5.175) = 2.8\alpha - \text{FUEL TUBES} \\
 M_6 &= 0.381\alpha + 0.206\alpha(13.325 - 5.175) = 2.4\alpha - \text{THRUST SONE} \\
 M_7 &= 0.131\alpha + 0.288\alpha(18.055 - 5.175) = 3.8\alpha - \text{CHAMBER SET OF THRUST} \\
 M_8 &= 0.153\alpha + 0.225\alpha(11.240 - 5.175) = 1.5\alpha - \text{CHAMBER FUEL SETBACK}
 \end{aligned}$$

$$\Sigma M = 561.3\alpha$$

THRUST LOADING

$$T_e = P_s A_s (1 + \gamma M_s^2) - P_e A_e (1 + \gamma M_e^2) \quad \dots \text{Reference 18}$$

$$\text{where: } P_s = 1.26(1800)(3.981) = 2140 \text{ psi (psf)}$$

$$A_s = 32.3 \text{ in}^2$$

$$M_s = 0.131$$

$$\gamma = 1.20$$

(see pg. 95 for other values)

$$T_e = 70,545.2 - 30,954.2 = 39,591.0 \text{ lbs (yield)} - \text{Tensile}$$



SUBJECT

DATE

7/25/71

WORK ORDER

1811-66-103

BY

GHS

CHK. BY

DATE

YIELD CRITERIAMeridional Load

$$N_{\phi} = \frac{1.1 M}{\pi r^2} + \frac{T_e}{2\pi r}$$

$$\text{let: } M = 561.3 \text{ in-lbs}$$

$$\alpha = 5 \text{ rad/sec}^2$$

$$T_e = 39,591.0 \text{ lbs (yield)}$$

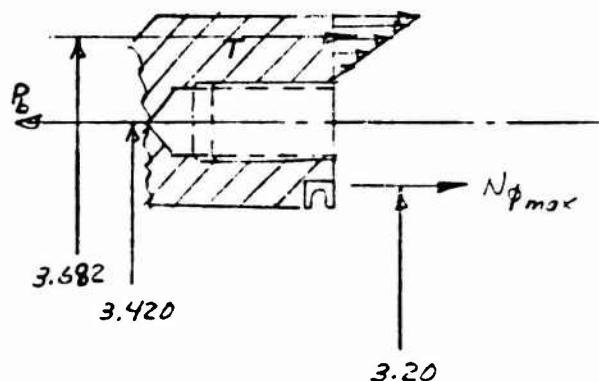
$$r = 3.20 \text{ in.}$$

$$N_{\phi_{\text{mer}}} = 96.0 + 1977 = 2,073 \text{ lb/in (yield)}$$

Additional Load due to "prying" of Flanges

$$T = \frac{2,073(3.42 - 3.20)}{(3.682 - 3.420)} \times \frac{3.20}{3.42}$$

$$T = 1,630 \text{ lb/in (yield)}$$



$$P_{b_y, \text{Total Bolt Load}} = 2,073 + 1,630 = 3,703 \text{ lb/in. (yield)}$$

$$\text{Bolt Spacing, } z = \frac{2\pi r}{n}$$

$$\text{where: } r = 3.42 \text{ in.}$$

$$n = 24 \text{ bolts}$$

$$z = 0.895 \text{ in/bolt}$$

$$P_{b_y, \text{Total Bolt Load}} = 3,703(0.895) = 3,320 \text{ lb (yield)}$$

Assume: Unbrako Series 1960 Bolts ... Reference 7

$$F_{tu} = 190,000 \text{ psi}$$

$$F_{ty} = 170,000 \text{ psi}$$

$$P_{bu} = 6,910 \text{ lbs}$$

$$P_{by} = 6,200 \text{ lbs}$$

$$\text{M.S.} = \frac{6200}{3,320} - 1 = \underline{\underline{0.87}} \text{ (yield)}$$

$$\text{let: } \alpha = 40 \text{ rad/sec}^2$$

$$N_{\phi_{\text{mer}}} = 2745 \text{ lb/in (yield)}$$

$$P_{b_y} = 4,400 \text{ lb (yield)}$$

$$\text{M.S.} = \frac{6200}{4,400} - 1 = \underline{\underline{0.41}} \text{ (yield)}$$



SUBJECT

DATE

7/23/71

WORK ORDER

1811-06-103

BY

GHS

CHK. BY

DATE

ULTIMATE CRITERIAMeridional Load

$$N\phi = \frac{1.4 M}{\pi r^2} + \frac{T_e}{\pi r} \left( \frac{1.50}{1.20} \right)$$

$$N\phi_{max} = 122.5 + 2470.0 = 2592.5 \text{ lb/in. (ult)}$$

$$P_{bu} = 4150 \text{ lb (ult)}$$

$$M.S. = \frac{6910}{4150} - 1 = \underline{\underline{0.66}} \text{ (ult)}$$

$$\text{let: } \dot{\phi} = 40 \text{ rad/sec}^2$$

$$N\phi_{max} = 3450 \text{ lb/in (ult)}$$

$$P_{bu} = 5525 \text{ lb (ult)}$$

$$M.S. = \frac{6910}{5525} - 1 = \underline{\underline{0.25}} \text{ (ult)}$$



REPORT NO.  
SA-005-CC-03

PAGE 74 OF 21

SUBJECT

DATE  
7/26/71WORK ORDER  
1811-06-113

BY

GHS

CHK. BY

DATE

CHECK FLANGEMoment about bolt circle Radius,  $M_b$ 

$$M_b = 2,073 (3.420 - 3.20) \left( \frac{3.20}{3.42} \right) \\ = 427.0 \text{ in-lbs/in. (yield)}$$

$$K = \frac{0.895 - 2(.139)}{0.895} = 0.690$$

$$\text{Bending Stress, } T_{by} = \frac{6 M_b}{k t^2}$$

where:  $M_b = 427.0 \text{ in-lbs/in.}$   
 $k = 0.690$   
 $t = 0.55 \text{ in.}$

$$T_{by} = 12,300 \text{ psi (yield)}$$

Normal Load due to Coolant Flow

$$N = 1.2 \text{ PA}$$

where:  $P = \text{Fuel coolant outlet pressure}$   
 $= 2332 \text{ psi}$

$$A = \text{Coolant Flow area in Flange} \\ = \frac{\pi (.250)^2}{4} = 0.0493 \text{ in}^2$$

$$N = 159.0 \text{ lbs (yield)}$$

$$\text{Flange resistance area, } A_f = (0.895 - .278) 0.55 - 0.0493 = 0.290 \text{ in}^2$$

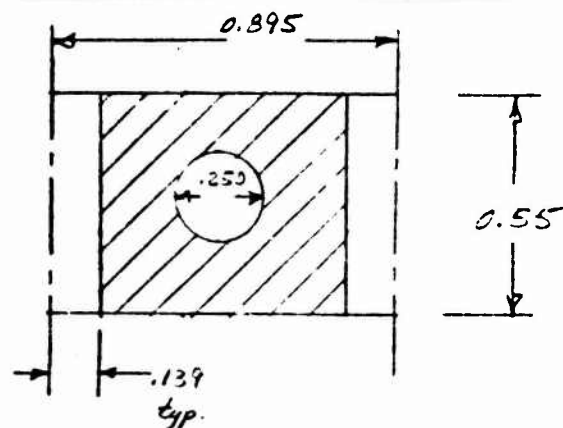
$$\text{Normal Stress} = \frac{159.0}{0.29} = 550 \text{ psi}$$

$$\text{Total Stress} = 12,300 + 550 = 12,850 \text{ psi}$$

$$F_{ty} = 46,000 \text{ psi} \dots \text{Figure 1}$$

$$\text{M.S.} = \frac{46,000}{12,850} - 1 = \underline{\underline{2.56}} \text{ (yield)}$$

(NOTE: Yield Criteria Governs)





SUBJECT

DATE

7/1/71

WORK ORDER

181-06-103

BY

GHSkapp

CHK. BY

DATE

G.- COPPER INJECTOR VANE

DESIGN DATA

MAT'L: OFHC COPPER

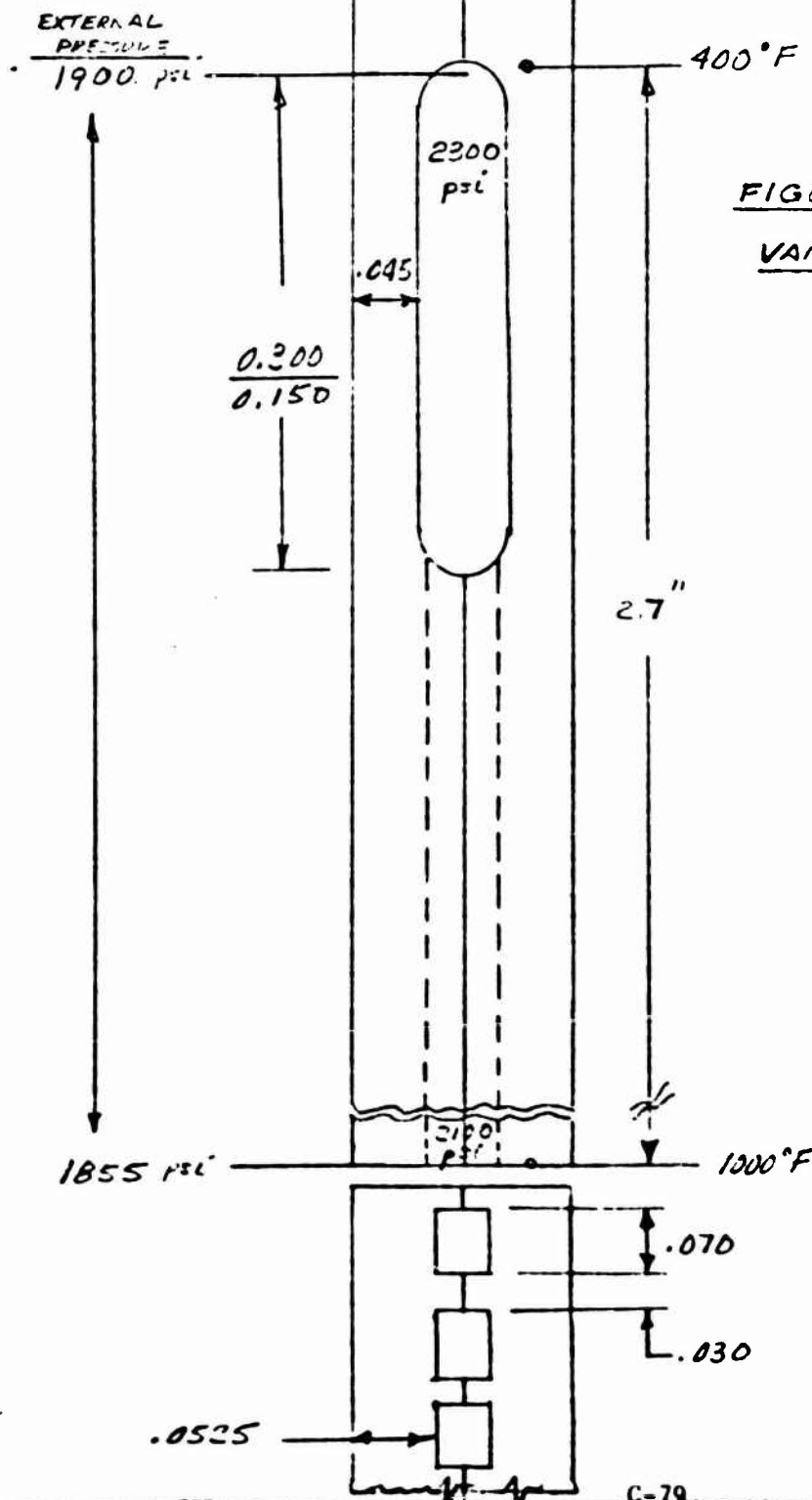


FIGURE 23- INJECTOR  
VANE GEOMETRY



SUBJECT

DATE

7/23/71

WORK ORDER

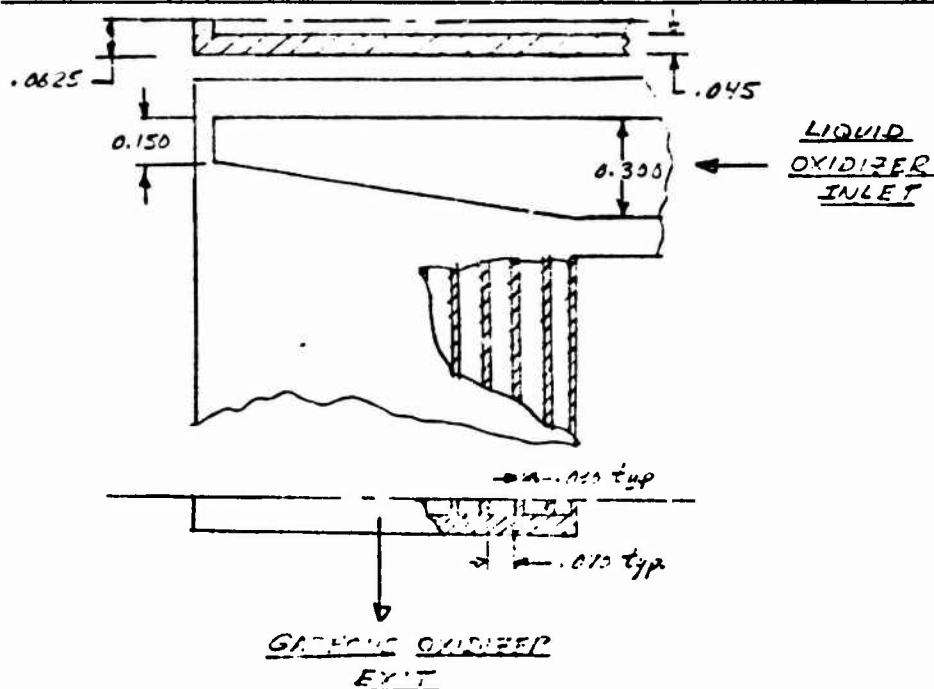
1811-06-103

BY

GHS

CHK. BY

DATE



ASSUME: TAPERED INLET MAY BE TREATED AS A FLAT PLATE  
SEE REFERENCE 10, CASE 41, PGS. 205, 217 & 218

$$\text{Max Stress} = \frac{\beta u b^2}{t^2}$$

let:  $\beta = 0.50$  @  $q/b \rightarrow \infty$   
 $w = 1.25(2350 - 125) = 430 \text{ psi (yield)}$   
 $b = 0.225 \text{ in. (equiv. rectangular sect.)}$   
 $t = 0.045 \text{ in.}$

$$= 6,500 \text{ psi (yield)}$$

$$F_{ty} = 5,500 \text{ psi} \dots \text{See Figure 5}$$

$$\text{Bending Modulus of Yield} = 1.25 F_{ty} = 6,860 \text{ psi}$$

$$M.S. = \frac{6,860}{6,000} - 1 = \underline{\underline{0.14 \text{ (yield)}}}$$

#### Ultimate Criteria

$$\text{Max Stress} = 6,000 \left( \frac{1.50}{1.25} \right) = 7,500 \text{ psi (ult)}$$

$$F_{tu} = 20,000 \text{ psi} \dots \text{See Figure 5}$$

$$\text{Bending Modulus of Rupture} = 1.50 F_{tu} = 30,000 \text{ psi}$$

$$M.S. = \frac{30,000}{7,500} - 1 = \underline{\underline{3.00 \text{ (ult)}}}$$





SUBJECT

DATE

7/26/71

WORK ORDER

1811-06-103

BY

GHS

CHK. BY

DATE

LOW CYCLE FATIGUE LIFE

$$\Delta E_T = K \alpha \Delta T$$

where:  $K = 2.5$  - constant (function of constraint)

$$\alpha = 13.2 \times 10^{-6} \text{ in/in-}^\circ\text{F}$$

$$\Delta T = T_{\text{avg}} - T_{\text{B.S.}} = 150^\circ\text{F}$$

$$T_{\text{avg}} = 1000^\circ\text{F}$$

$$T_{\text{B.S.}} = 850^\circ\text{F}$$

$$\Delta E_T = 0.38\%$$

$$N_f = 40,000 \text{ cycles} \sim \text{no hold time creep effects}$$

Assume: 50 HOURS total hold time

$$* N_f' = 23,200 \text{ cycles}$$

CONSIDER AXIAL THERMAL GRADIENT

$$\text{let: } K = 1.05$$

$$\Delta T = (1000 - 400) = 600^\circ\text{F}$$

$$\Delta E_T = 0.645\%$$

$$N_f = 12,000 \text{ cycles} \sim \text{no hold time creep effects}$$

$$* N_f' = 7,000 \text{ cycles @ 50 hours total time duration}$$

$$* N_f' = N_f \left( 1 - \frac{t}{t_R} \right)$$

... Ref. 14

where:  $t = 50 \text{ hours}$

$t_R = 120 \text{ hours @ } 1000^\circ\text{F} \dots \text{Ref. 13}$

## VII. REFERENCES

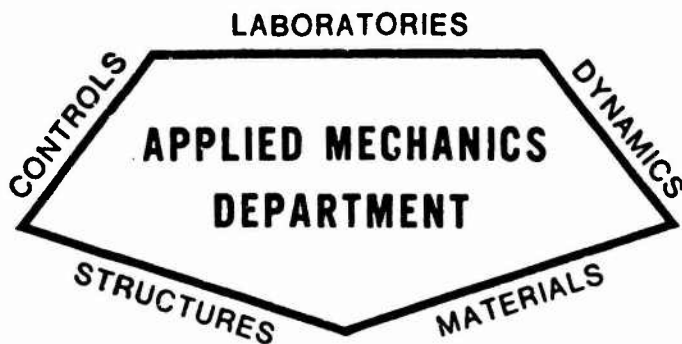
1. Exhibit "A", Technical Requirements, Contract FO4611-71-C-0040 AFRPL (LKDS), 5 February 1971.
2. Product Data, "ARMCO 22-13-5 Stainless Steel Bar and Wire," ARMCO Steel Corporation, Advanced Materials Division, Baltimore, Maryland.
3. Developmental Alloy Data Bulletin, "ARMCO 22-13-5 Stainless Steel Sheet and Strip," ARMCO Steel Corporation, Advanced Materials Division, Baltimore, Maryland.
4. "Space Shuttle Main Engine Definition Study Phase B Data," AJ 550 Materials Technology Programs, DRDSE-278, Part B, NASA Contract No. NAS8-26188, Aerojet Liquid Rocket Company, Sacramento, California 95813, 21 April 1971.
5. Janser, G. R., "Material Design Property Data Sheets," ME-70-164, Aerojet Liquid Rocket Company, Sacramento, California 95813, 1 September 1970.
6. Davis, H. O., Kotfila, R. J., Schleicher, W. J., "The Fabrication and Properties of the Fibrous Graphite Composite, AGCarb-101," Tech. Report No. ME-69-242, Aerojet Liquid Rocket Company, Sacramento, California 95813, December 1969.
7. Unbrako Socket Screws 1960 Series, Standard Pressed Steel Co., Jenkintown, Pennsylvania, 19046, 1967.
8. Niles, A. S., Newell, J. S., "Airplane Structures," Vol. 1, 4th ed., John Wiley and Sons, New York, N. Y., 1954.
9. "Metallic Materials and Elements for Aerospace Vehicle Structures," MIL-HDBK-5A, Change Notice 4, Superintendent of Documents, U.S. Government Printing Office, Washington, D.C., 5 January 1970.

10. Roark, R. J., "Formulas for Stress & Strain, 3rd ed., McGraw-Hill Book Co., Inc., New York, N. Y., 1954.
11. Skopp, G. H., "Orbit-Orbit Shuttle Parametric Studies," Report No. SA-OOS-CC-01, Aerojet Liquid Rocket Co., Sacramento, California, 7 May 1971.
12. Skopp, G. H., "Structural Design Studies and 25<sup>k</sup> Engine Evaluation for OOS Combustion Components," Report No. SA-OOS-CC-02, Aerojet Liquid Rocket Co., Sacramento, California, June 24, 1971.
13. Entz, R. D., "Task III-Parametric Studies of OOS Combustion Components," Report No. SA-OOS-CC-04, Aerojet Liquid Rocket Co., Sacramento, Calif., 23 July 1971.
14. Manson, S. S., and Halford, G. R., "A Method of Estimating High-Temperature Low-Cycle Fatigue Behavior of Materials," presented at International Conference on Thermal and High-Strain Fatigue Institute of Metals, London, 1967.
15. Shanley, F. R., "Strength of Materials," McGraw-Hill Book Co., Inc., New York, N. Y., 1957.
16. Bornsheuer, "German Ring Report," Peenemunde Army Proving Grounds, Karlshagen, Germany, June 1944.
17. Avery, L. R., Cavayanis, G. S., Michky, G. L., "Thermal-Fatigue Tests of Restrained Combustor-Cooling Tubes," Experimental Mechanics, 7 (6), June 1967, Pg. 256-264.
18. Westphal, W. R., "Computation of Ejection Force on the Movable Portion of a Nozzle," Aerojet-General Corporation, Sacramento, California, 14 July 1959.

19. McLean, W. G., Nelson, E. W., "Engineering Mechanics,"  
Schaum Publishing Co., New York, N. Y., 1952.
20. Dull, R. W., and Dull, R., "Mathematics for Engineers,"  
3rd edition, McGraw-Hill Book Co., Inc., New York, N. Y., 1951.
21. "Handbook of Mechanical Spring Design," Associated Spring  
Corporation, Bristol, Connecticut, 06010, 1964.
22. Oberg, E., and Jones, F. D., "Machinery's Handbook," The  
Industrial Press, New York 13, New York, 1953.



OOS TRUBOMACHINERY PARAMETRIC STRENGTH  
AND LIFE CYCLES ANALYSIS, TURBINE ROTORS  
AND IMPELLERS



## STRUCTURAL ENGINEERING SECTION

REPORT NO. SA-OOS-TM-01

OOS TURBOMACHINERY PARAMETRIC STRENGTH  
AND LIFE CYCLES ANALYSIS, TURBINE ROTORS  
AND IMPELLERS

PREPARED BY:

*LW Bartholf*

L. W. Bartholf  
Engineering Specialist  
Structural Engineering Section

APPROVED BY:

*LK Severud*

L. K. Severud, Manager  
Structural Engineering Section  
Engineering

DATE 18 May 1971



AEROJET LIQUID ROCKET COMPANY

SACRAMENTO, CALIFORNIA

## TABLE OF CONTENTS

	<u>Page</u>
I. Introduction	1
II. Discussion	1
III. Conclusions	2
. Analysis	
A. Turbine Blades	3
B. Turbine Wheels	7
C. Impellers	10
1. Strength	
2. Life	

## I. INTRODUCTION

The purpose of this report is to show how various parameters effect the stresses, material requirements and life capabilities of rotating machinery turbine rotors and impellers. The curves presented are intended as a preliminary guide to choosing materials and operating speeds. They would not serve as a structural analysis of point design operating conditions since too many other considerations which could not be included in this report enter into the final design structural evaluation.

## II. DISCUSSION

The curves presented for turbine blades assumes the material is steel, the blades taper with a linear area variation and include a factor of safety of 1.4 on the material ultimate strength. For preliminary design these assumptions are adequate to describe a blade geometry. However, considerations of blade tilt stresses, gas bending stresses, vibratory stresses and thermal stresses are needed to make final structural evaluations. If the blades are subjected to long periods of operation at high temperature the material ultimate strength should be interpreted as the stress to rupture or stress to adverse creep deformation whichever is the controlling criteria.

The curves for turbine wheels are fitted to past analyses of optimized steel turbine wheels as the data points indicate. The allowable mean blade speed should be taken as the minimum of that determined for burst and that for gross yielding. The burst factor used in the burst speed calculations varies from wheel to wheel and between materials. Generally it will fall within the range shown of .6 to .8 and with proper design and material selection could even be expected to exceed .8. The design factors of 1.2 on burst and 1.17 on gross yielding are those recommended for use as the turbine wheel structural design criteria.

The impeller stress vs tip speed curves are also fitted to past analyses of optimized shrouded titanium impellers. The same general comments made for turbine wheels about burst and gross yielding speeds are applicable to the impeller curves. Note that curves are presented to include aluminum and steel which are also candidate materials, in addition to titanium, for many impeller applications. Another significant impeller design consideration which lends itself to graphic interpretation and is presented in this report is the fracture mechanics concepts of critical flaw size and flaw growth to critical size. The critical flaw size is a function of material toughness, applied stress and flaw shape. For this report the most severe flaw shape parameter was assumed eliminating this variable from the curves. Comprehensive material fracture toughness and flaw growth data are not readily available. However, the available data and the curves presented do indicate the trends and the significance of flaws in determining the life cycle limitations of pump impellers.

### III. CONCLUSIONS

Parametric data regarding tip speed limitations and approximate life cycle capabilities have been presented for the OOS turbine wheels and pump impellers applications. These data accordingly should prove useful in carrying out the parametric system analyses. Additional in-depth analyses will be required to ascertain accurate structural characteristics of the selected design configuration.



## OOS PARAMETRIC STUDY

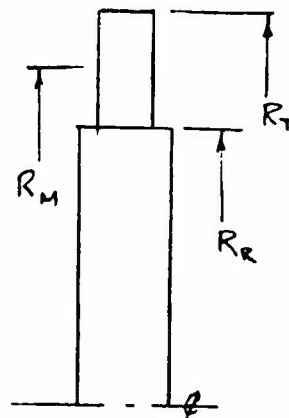
BY L.W. BARTHOLF

CHK. BY

III ANALYSISA. TURBINE BLADE STRESS:

THE CENTRIFUGAL STRESS AT THE BLADE ROOT IS GIVEN BY:

$$\sigma_{CF} = \frac{\rho \omega^2}{g A_R} \int_{R_R}^{R_T} A r dr$$

WHERE:  $\rho$  = METAL DENSITY (LB/IN<sup>3</sup>)  
 $g$  = ACCELERATION OF GRAVITY (IN/SEC<sup>2</sup>)

$$\omega = \frac{12 V_M}{R_M}$$

 $V_M$  = MEAN BLADE SPEED (FT/SEC) $R_M$  = MEAN BLADE RADIUS (IN) $A$  = AREA OF CROSS SECTIONFOR A CONSTANT CROSS-SECTION BLADE:

$$\sigma_{CF} = \frac{\rho \omega^2 A_R}{g A_R} \int_{R_R}^{R_T} r dr = \frac{\rho \omega^2}{12g} (R_T^2 - R_R^2) = \frac{\rho}{g} \omega^2 \left( \frac{R_T + R_R}{2} \right) (R_T - R_R)$$

$$\text{SINCE: } \omega^2 = \frac{144 V_M^2}{R_M^2}$$

$$R_M = (R_T + R_R)/2$$

$$h = (R_T - R_R) = \text{BLADE HEIGHT}$$

$$\sigma_{CF} = \frac{\rho}{g} \left( \frac{144 V_M^2}{R_M^2} \right) (R_M)(h)$$

$$\boxed{\sigma_{CF} = .001 V \cdot N \cdot h}$$

$$\sigma_{CF} = \frac{\rho}{g} \left( \frac{144 V_M^2 h}{R_M} \right)$$



REPORT NO.	PAGE 4 OF 22
DATE	4/28/71
WORK ORDER	1811-06-101
DATE	

# OOS PARAMETRIC STUDY

BY L.W. BARTHOLF	CHK BY
---------------------	--------

## TURBINE BLADE STRESS:

FOR TAPERED BLADES WITH LINEAR AREA VARIATION THE CENTRIFUGAL STRESS IS GIVEN BY:

$$\sigma_{CF} = \frac{\rho}{g} \left( \frac{144 v^2 h}{R_m} \right) \phi$$

where:  $\phi$  IS A FUNCTION OF THE TIP TO ROOT AREA RATIO.

SHORT TIME

SINCE THE ALLOWABLE STRESS  $\sigma_{CF, allow}$  IS USUALLY EQUAL TO THE MATERIAL ULTIMATE STRENGTH ( $F_{tu}$ ) DIVIDED BY THE APPROPRIATE SAFETY FACTOR (F.S.) I WILL DEVELOPE A FAMILY OF CURVES FOR THE ALLOWABLE TIP SPEED VS MATERIAL ULTIMATE STRENGTH.

FOR A F.S. = 1.4 ON ULTIMATE WHICH IS A TYPICAL SAFETY FACTOR FOR FLIGHT WEIGHT DESIGN THE FOLLOWING RELATIONS EXIST:

$$\sigma_{CF, allow} = \frac{F_{tu}}{1.4}$$

$$\therefore \frac{F_{tu}}{1.4} = \frac{144 \rho v^2 \left( \frac{h}{R_m} \right) (\phi)}{g}$$

## FOR STEEL MATERIAL

$$F_{tu, req'd} = .15 v^2 \left( \frac{h}{R_m} \right) (\phi)$$

FOR  $R_T/R_R < 1.5$  THE FOLLOWING APPROXIMATION HOLDS FOR PRELIMINARY DESIGN:

$A_T/A_R$	$\phi$
1.0	1.0
.5	.75
.2	.6
0	.5

LIMIT



SUBJECT

OOS PARAMETRIC STUDY

DATE

4/28/71

WORK ORDER

1811-06-101

BY

L.W. BARTHOLF

CHK. BY

DATE

TURBINE BLADE CENTRIFUGAL STRESS:

MEAN BLADE SPEED (V) FT/SEC	$V^2$ (FT <sup>2</sup> /SEC <sup>2</sup> )	$h/R_M$	$\phi=1$ $F_{tu reqd}$ (KSI)	$\phi=.5$ $F_{tu reqd}$ (KSI)
500	.25 (10) <sup>6</sup>	.1	3.8	1.9
1000	1.0 (10) <sup>6</sup>	.1	15.0	7.5
1500	2.25 (10) <sup>6</sup>	.1	33.8	16.9
2000	4.0 (10) <sup>6</sup>	.1	60.0	30.0
2500	6.25 (10) <sup>6</sup>	.1	94.0	47.0

MEAN BLADE SPEED (V) (FT/SEC)	$h/R_M$	$\phi=1$ $F_{tu reqd}$ (KSI)	$\phi=.5$ $F_{tu reqd}$ (KSI)
500	.3	11.5	5.7
1000	.3	45.0	22.5
1500	.3	103.0	51.5
2000	.3	180.0	90.0
2500	.3	282.0	146.0





AEROJET-GENERAL CORPORATION  
SACRAMENTO • CALIFORNIA

REPORT NO.

PAGE 6 OF 22

AGCS 0800-11

SUBJECT

OOS PARAMETRIC STUDY

DATE  
4/28/71

WORK ORDER  
1811-06-101

BY

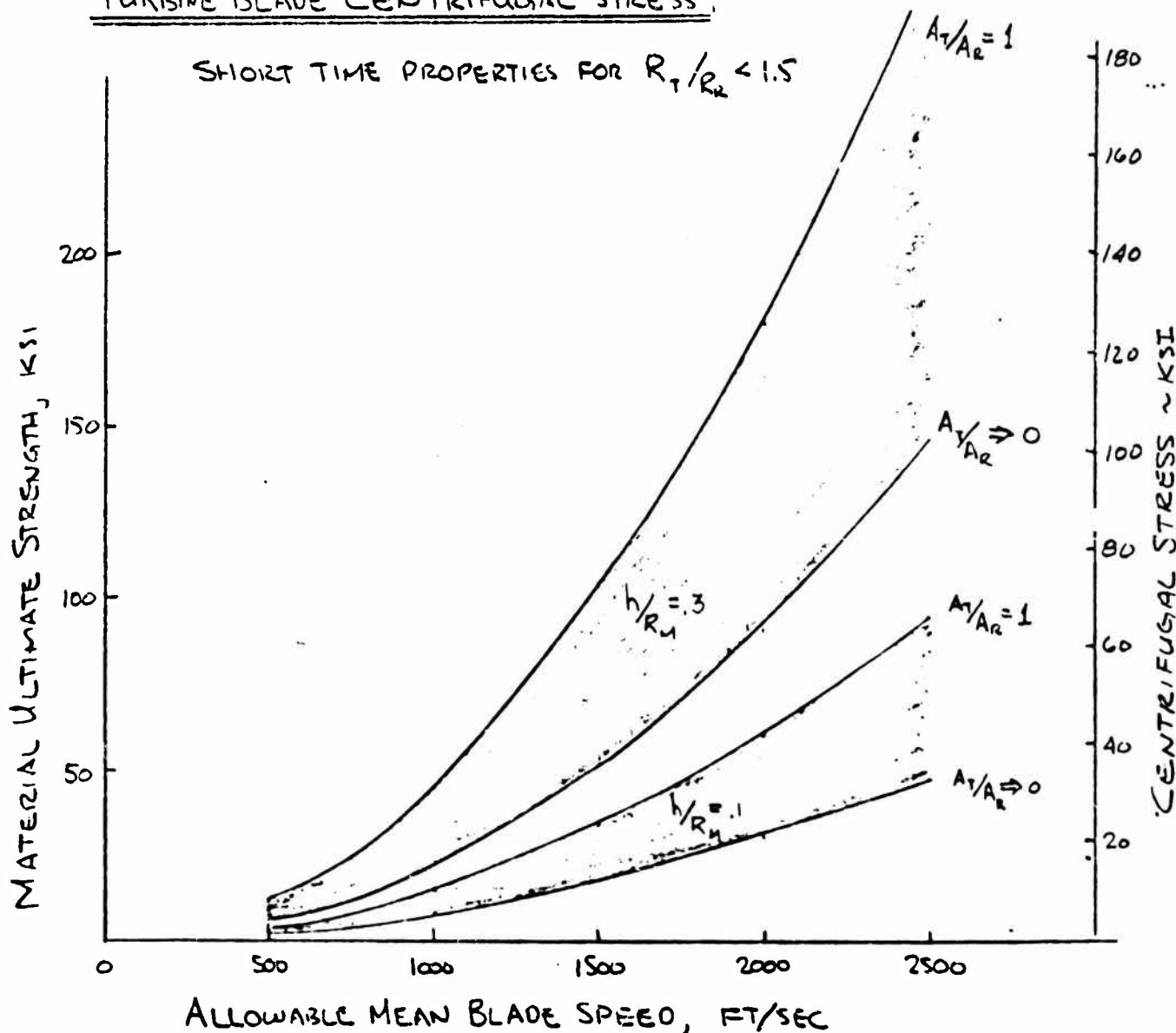
L.W. BARTHOLF

CHK. BY

DATE

### TURBINE BLADE CENTRIFUGAL STRESS

SHORT TIME PROPERTIES FOR  $R_T/R_R < 1.5$





SUBJECT

OOS PARAMETRIC STUDY

DATE

4/26/71

WORK ORDER

1811-06-101

BY

L.W. BARTHOLF

CHK. BY

DATE

### B. TURBINE WHEEL PARAMETRIC ANALYSIS

BASED ON PAST ANALYSES OF STEEL TURBINE WHEELS WITH FIR TREE BLADE ATTACHMENTS THE FOLLOWING GENERAL DATA WAS YIELDED:

SSME: MEAN BLADE SPEED = 1550 FT/SEC

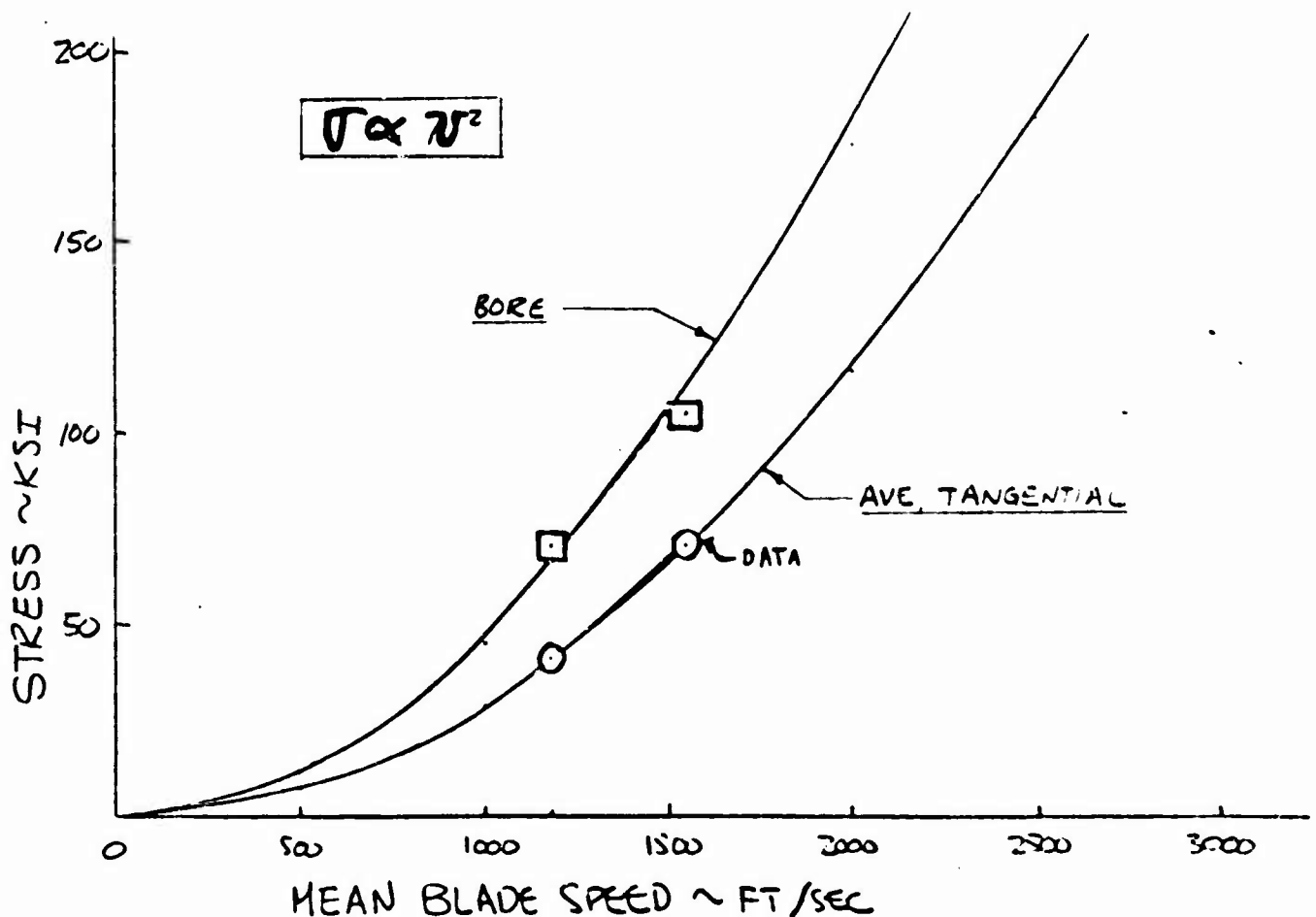
AVERAGE TANGENTIAL STRESS = 70 KSI

BORE STRESS = 105 KSI

TITAN: MEAN BLADE SPEED = 1180 FT/SEC

AVE. TANGENTIAL STRESS = 41 KSI

BORE STRESS = 70 KSI





SUBJECT

## OOS PARAMETRIC STUDY

DATE

4/26/71

WORK ORDER

1911-06-101

BY

L.W. BARTHOLF

CHK. BY

DATE

BURST SPEED CALCULATIONS:

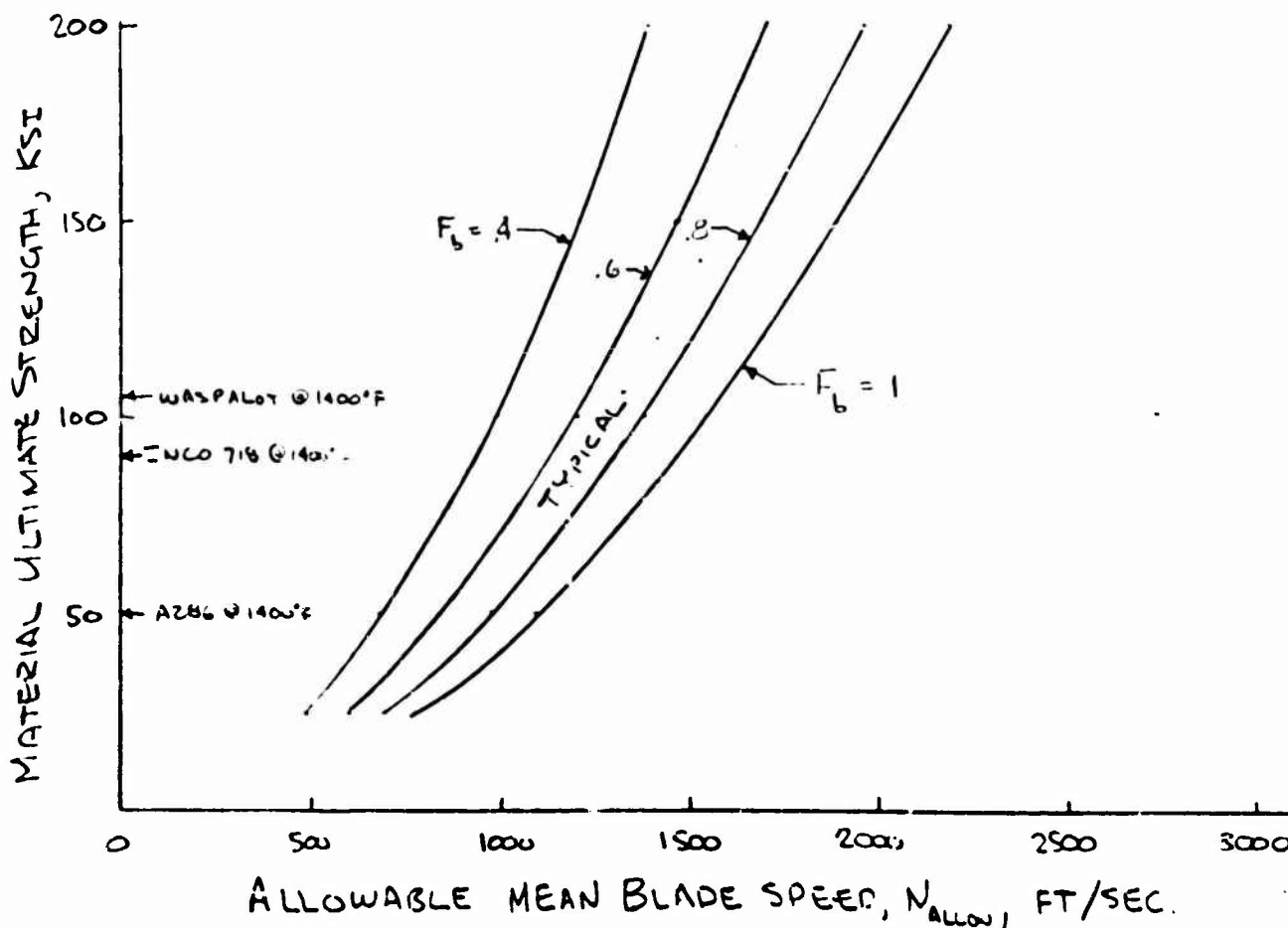
$$N_{\text{BURST}} = N \sqrt{\frac{F_b \cdot F_{tu}}{\bar{\sigma}_{AT}}} ; N_{\text{ALLOW}} = \frac{N_{\text{BURST}}}{1.2}$$

$N$  = SPEED FOR WHICH  $\bar{\sigma}_{AT}$  IS COMPUTED

$\bar{\sigma}_{AT}$  = AVERAGE TANGENTIAL STRESS

$F_{tu}$  = ULTIMATE TENSILE STRENGTH OF MATERIAL

$F_b$  = BURST FACTOR WHICH EXPRESSES FRACTION OF  $F_{tu}$  OBTAINED AT BURST SPEED. IT IS DEPENDENT ON RATIO OF MAX. TANGENTIAL STRESS TO  $\bar{\sigma}_{AT}$ , MATERIAL DUCTILITY, AND PERHAPS THE LOCAL MAX. STRESS STATE RELATED TO FRACTURE TOUGHNESS.





DATE  
4/27/71

WORK ORDER  
1311-06-101

# OOS PARAMETRIC STUDY

BY

L.W. BARTHOLF

CHK. BY

DATE

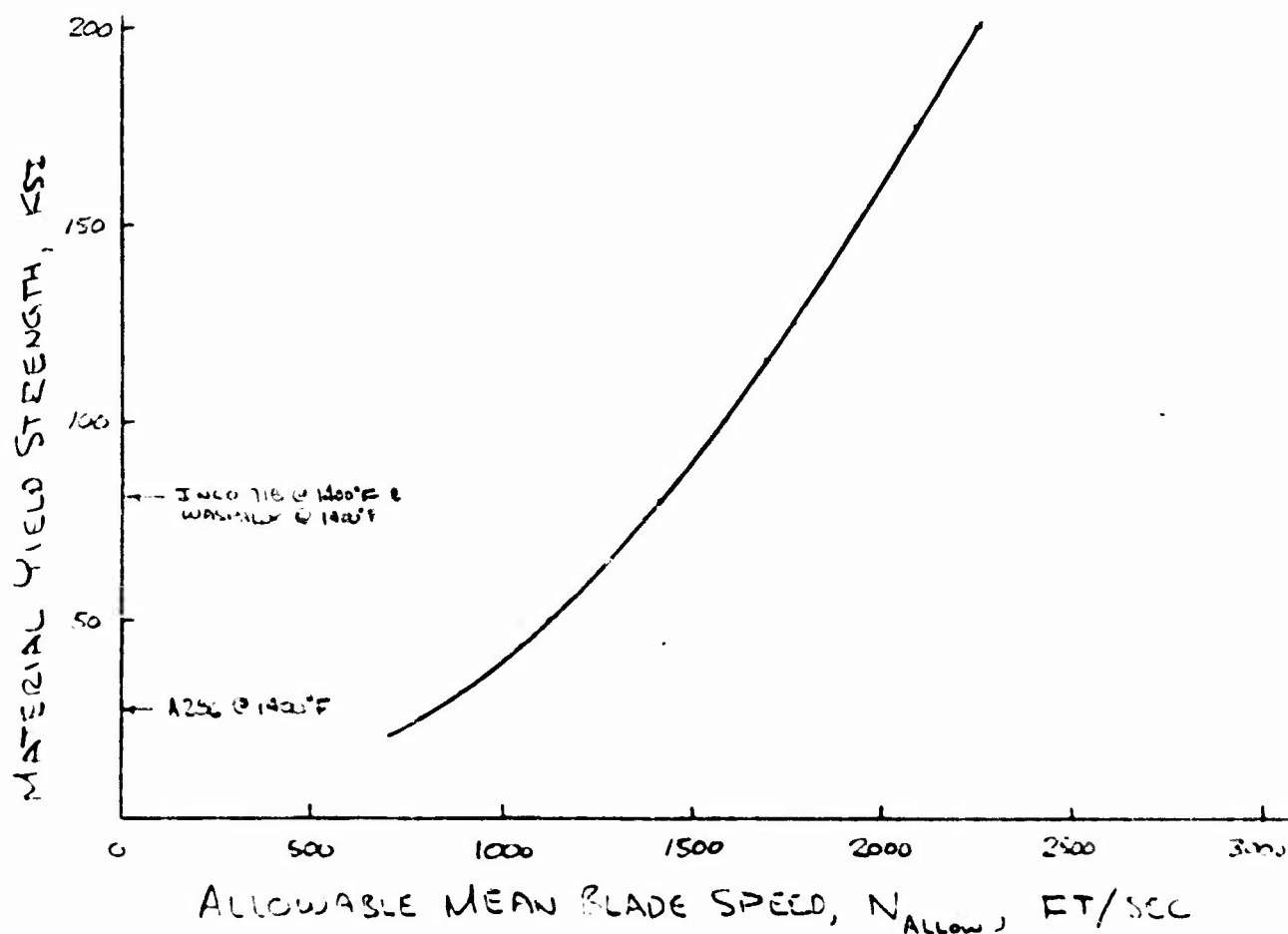
## GROSS YIELD SPEED CALCULATIONS

$$N_{\text{GROSS YIELD}} = N \sqrt{\frac{F_{ty}}{\tau_{AT}}} ; N_{\text{ALLOW}} = \frac{N_{GY}}{1.17}$$

$N$  = SPEED FOR WHICH  $\tau_{AT}$  IS COMPUTED

$\tau_{AT}$  = AVERAGE TANGENTIAL STRESS

$F_{ty}$  = YIELD TENSILE STRENGTH OF MATERIAL





4/22/71

1811-06-101

## OOS PARAMETRIC STUDY

BY

L.W. BARTHOLF

CHK. BY

C. IMPELLER PARAMETRIC ANALYSIS:

PAST ANALYSES ON SHROUDED TITANIUM IMPELLERS FROM THE SSME AND NERVA PROGRAMS YIELDED THE FOLLOWING GENERAL DATA:

SSME: TIP SPEED = 2055 FT/SEC  
AVERAGE TANGENTIAL STRESS = 55 KSI  
BORE STRESS = 94 KSI

NERVA: TIP SPEED = 1500 FT/SEC  
AUE. TANGENTIAL STRESS = 30 KSI  
BORE STRESS = 50 KSI

THE ABOVE DATA POINTS, ALONG WITH THE RELATION THAT STRESS IS PROPORTION TO SQUARE OF THE SPEED, WAS USED TO GENERATE THE CURVES BELOW. TO ACCOUNT FOR MATERIAL VARIATION THE STRESS WAS VARIED WITH THE DENSITY SO THAT:

$$\text{ALUMINUM: } \sigma_{AL} \approx \frac{.10}{.15} \sigma_{TITAN} = .67 \sigma_{TITAN}$$

$$\text{STEEL: } \sigma_{STEEL} \approx \frac{.30}{.15} \sigma_{TITAN} = 2.0 \sigma_{TITAN}$$



AEROJET-GENERAL CORPORATION  
SACRAMENTO • CALIFORNIA

REPORT NO.

PAGE 11 OF 22

AGC-100-11

SUBJECT

COS PARAMETRIC STUDY

DATE

4/22/71

WORK ORDER

1911-06-101

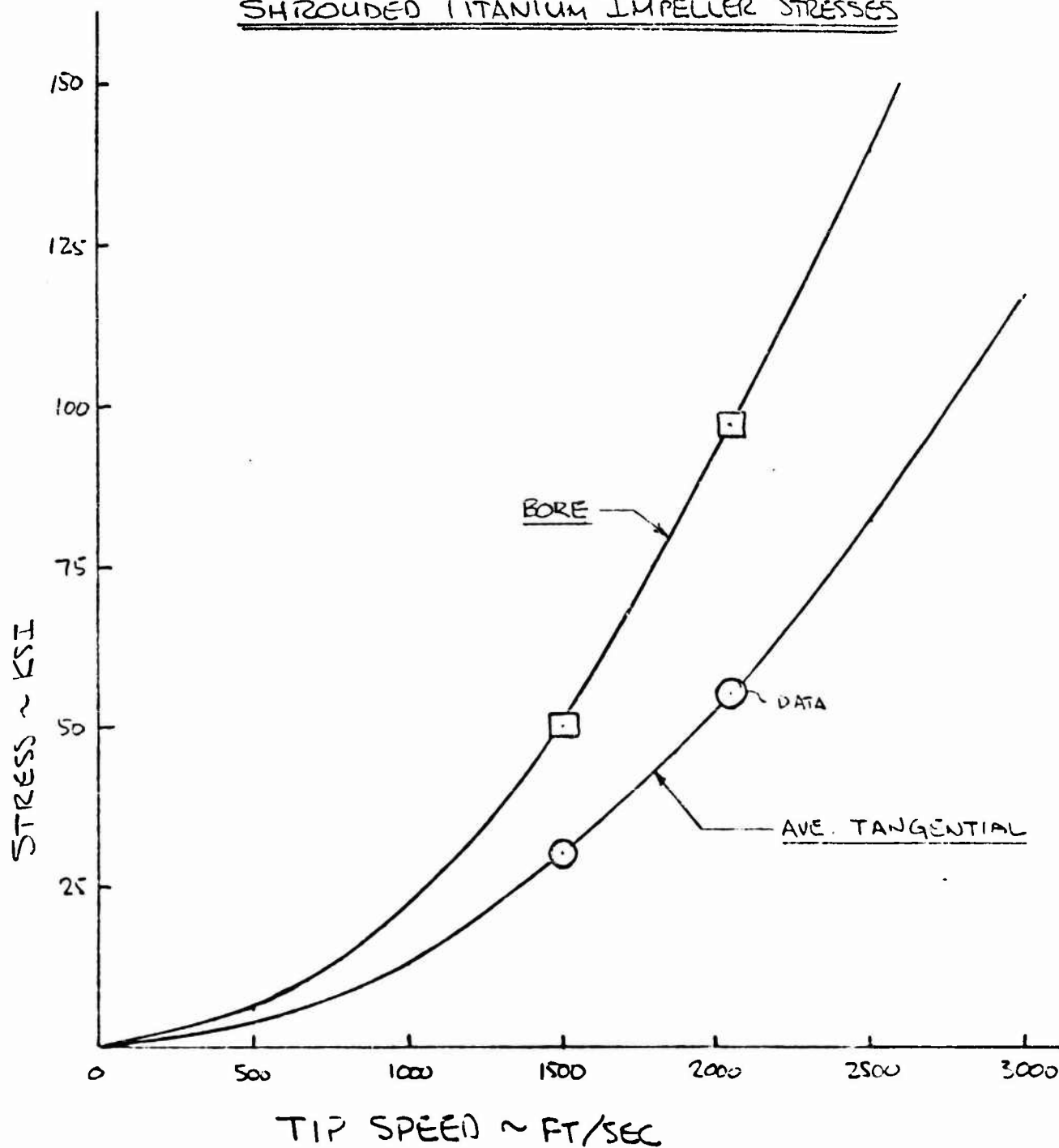
BY

L.W. BARTHOLF

CHK BY

DATE

SHROUDED TITANIUM IMPELLER STRESSES





DATE  
4/22/71

WORK ORDER  
1811-06-103

DATE

# OOS PARAMETRIC STUDY

BY

L.W. BARTHOLF

CHK. BY

## BURST SPEED CALCULATION:

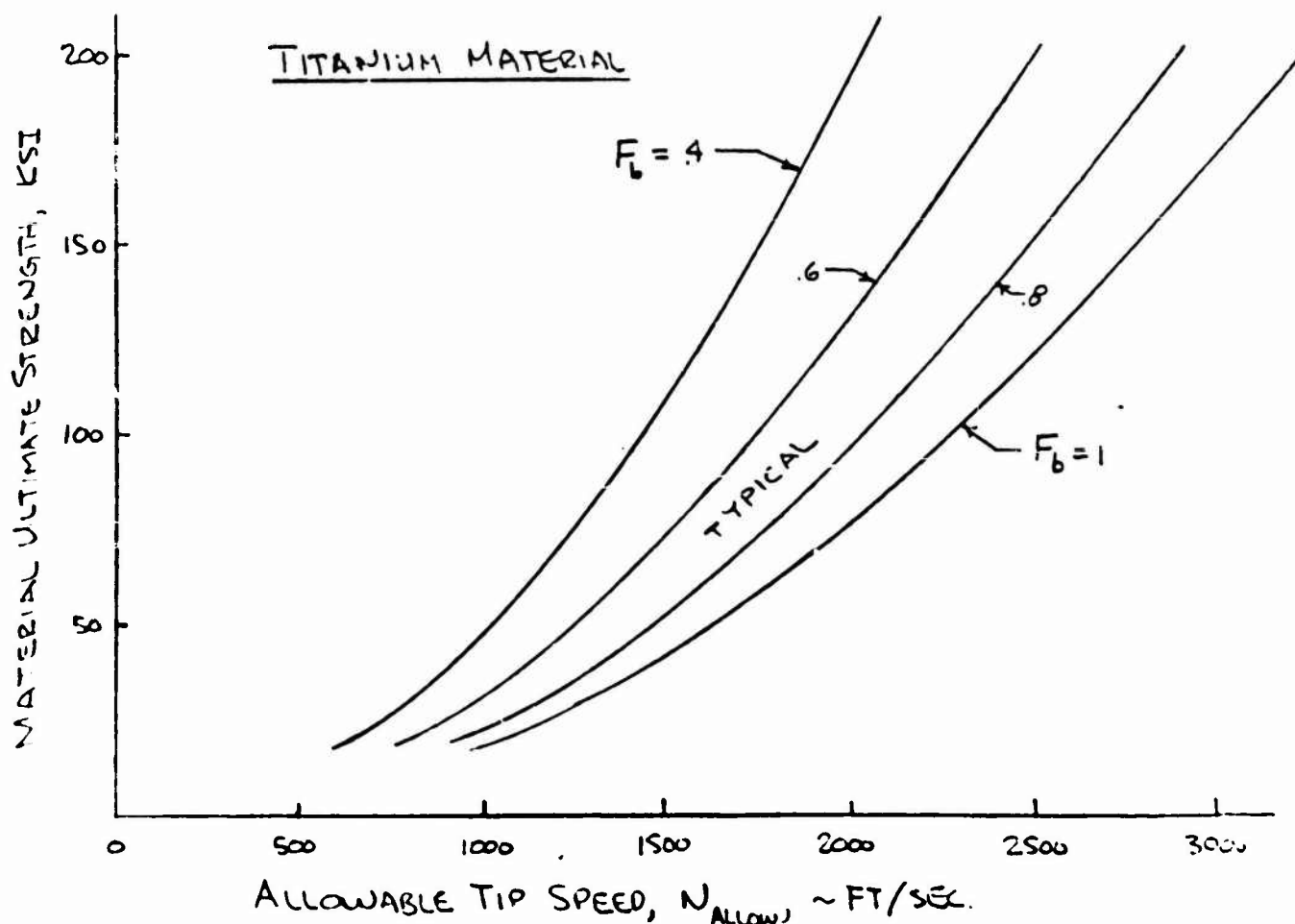
$$N_{BURST} = N \sqrt{\frac{F_b \cdot F_{tu}}{\bar{\sigma}_{AT}}} \quad ; \quad N_{ALLOW} = \frac{N_{BURST}}{1.2}$$

$N$  = SPEED FOR WHICH  $\bar{\sigma}_{AT}$  IS COMPUTED

$\bar{\sigma}_{AT}$  = AVERAGE TANGENTIAL STRESS

$F_{tu}$  = ULTIMATE TENSILE STRENGTH OF MATERIAL

$F_b$  = BURST FACTOR WHICH EXPRESSES FRACTION OF  $F_{tu}$  OBTAINED AT BURST SPEED. IT IS DEPENDENT ON RATIO OF MAX. TANGENTIAL STRESS TO  $\bar{\sigma}_{AT}$ , MATERIAL DUCTILITY, AND PERHAPS THE LOCAL MAX. STRESS STATE RELATED TO FRACTURE TOUGHNESS.





AEROJET-GENERAL CORPORATION  
SACRAMENTO • CALIFORNIA

REPORT NO.

PAGE 13 OF 22

DATE

4/22/71

WORK ORDER

1811-D6-103

BY

L.W. BARTHOLOMEW

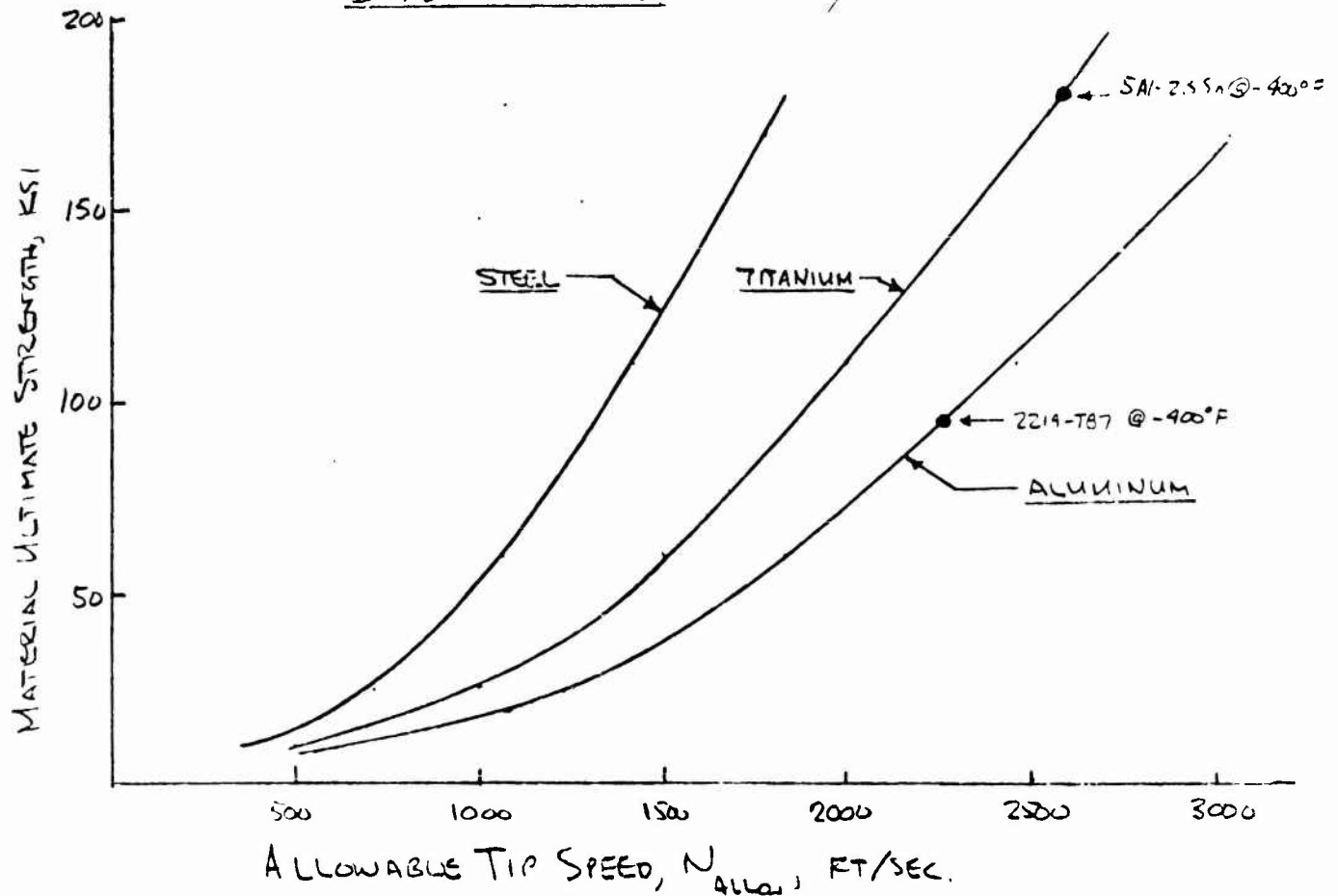
CHK BY

DATE

INW 718 @ -400°F

## IMPELLER MATERIAL VS ALLOWABLE TIP SPEED

BURST FACTOR = .7





DATE  
4/22/71WORK ORDER  
1811-06-103

BY

L.W. BARTHOLF

CHK BY

DATE

## OOS PARAMETRIC STUDY

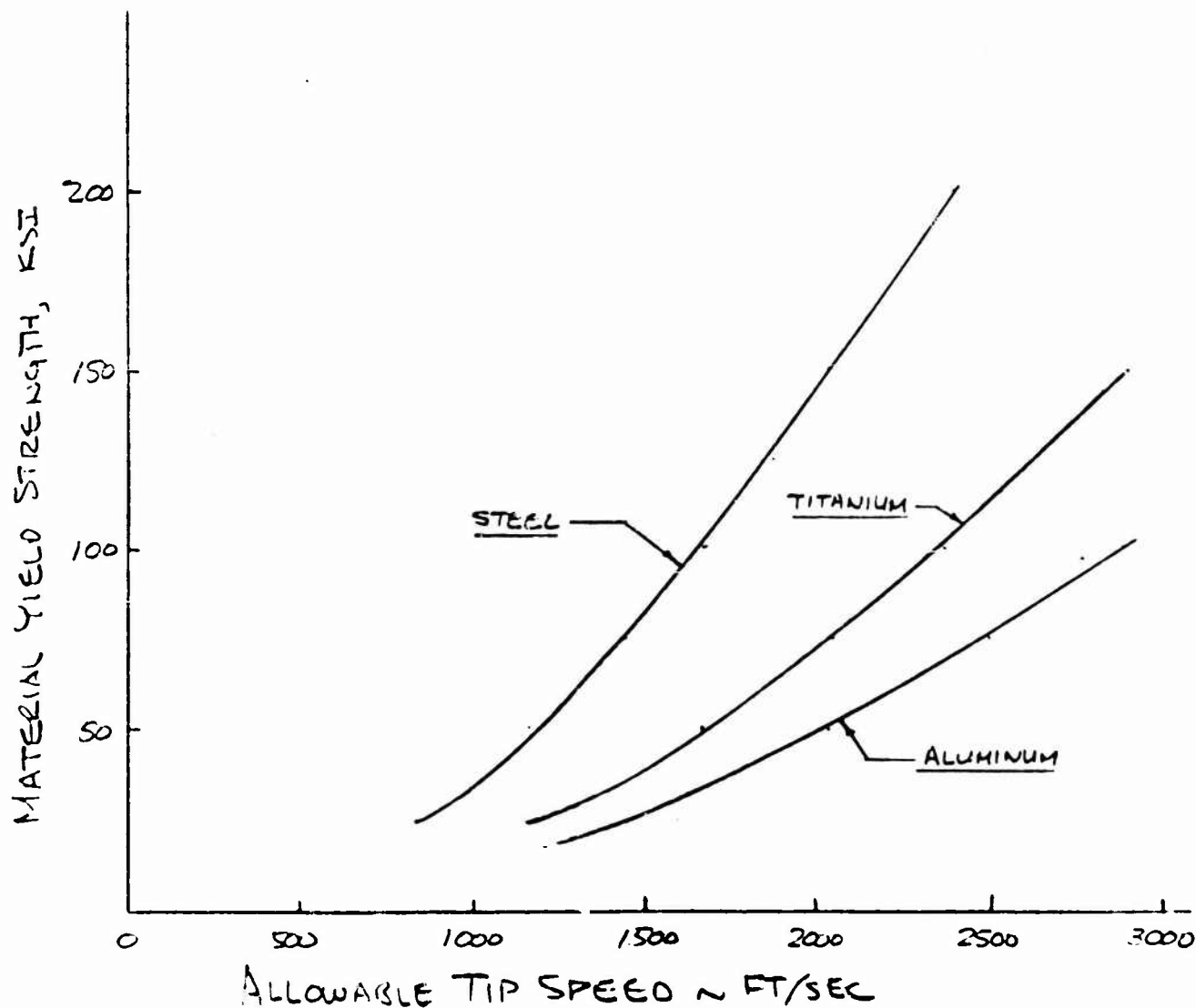
GROSS YIELD SPEED CALCULATIONS:

$$N_{\text{GROSS YIELD}} = N \sqrt{\frac{F_{ty}}{\tau_{AT}}} \quad ; \quad N_{\text{ALLOW}} = \frac{N_{GY}}{1.17}$$

$N$  = SPEED FOR WHICH  $\tau_{AT}$  IS COMPUTED

$\tau_{AT}$  = AVERAGE TANGENTIAL STRESS

$F_{ty}$  = YIELD STRENGTH OF MATERIAL





OOS PARAMETRIC STUDY

4/22/71

1811-06-103

L.W. BARTHOLF

CRITICAL FLAW SIZE @ -420°F

$$a_{cr} = 0.21 \left( \frac{K_{IC}}{\sigma} \right)^2$$

Where:  $K_{IC}$  = CRITICAL STRESS INTENSITY

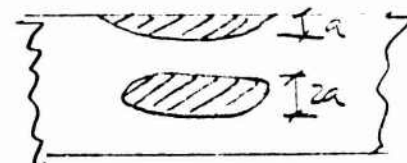
$\sigma$  = APPLIED PEAK STRESS

$a_{cr}$  = CRITICAL FLAW SIZE

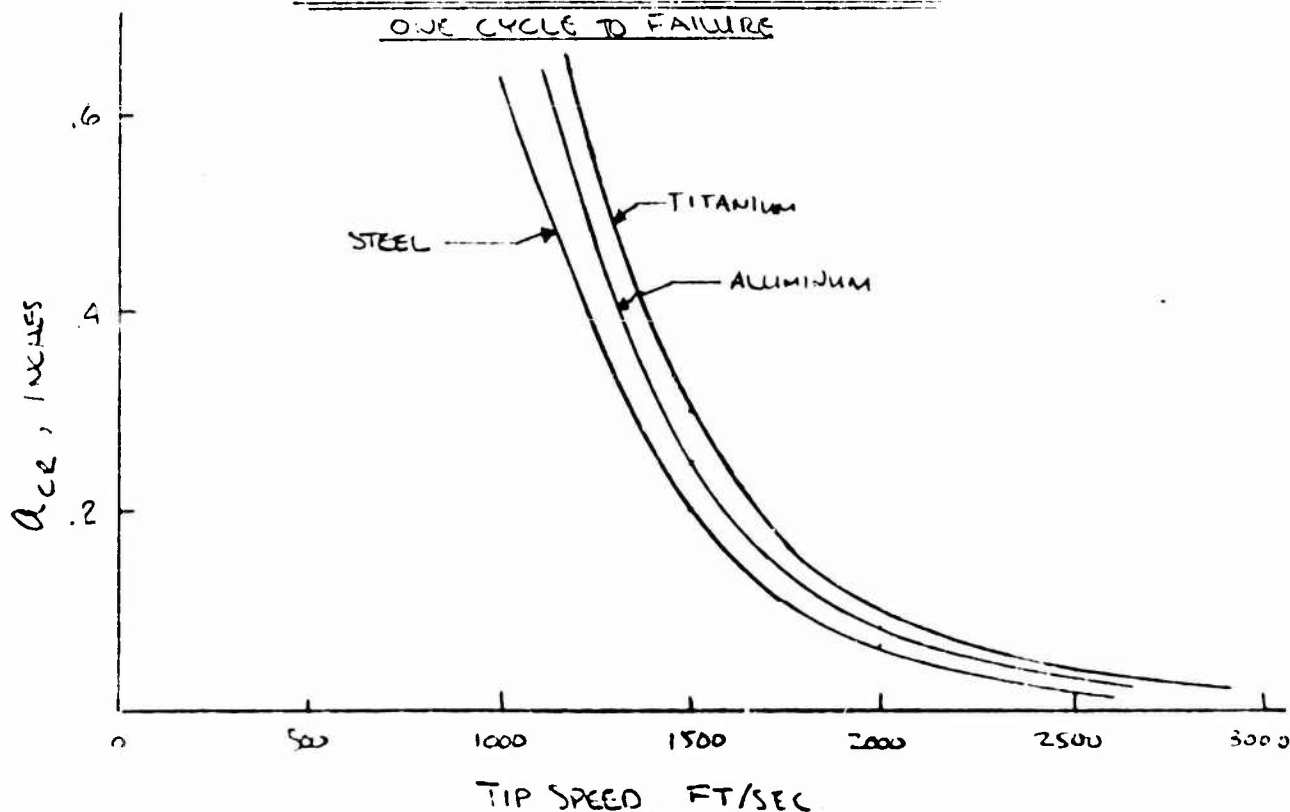
$K_{IC} = 60 \text{ KSI} \sqrt{\text{INCH}}$  @ -420°F  
FOR SA1-2.13A TITANIUM

$K_{IC} = 97 \text{ KSI} \sqrt{\text{INCH}}$  @ -420°F  
FOR INCOVEL 718

$K_{IC} = 37 \text{ KSI} \sqrt{\text{INCH}}$  @ -420°F  
FOR 2219-T97



CRITICAL FLAW SIZE VS TIP SPEED  
ONE CYCLE TO FAILURE





# OOS PARAMETRIC STUDY

DATE

4/23/71

WORK ORDER

1811-06-103

BY

L.W. BARTHOLF

CHK. BY

DATE

## ALLOWABLE INITIAL FLAW SIZE FOR 1200 CYCLES

$$a_i = 0.21 \left( \frac{K_{II}}{\sigma_{PEAK}} \right)^2$$

@ -420°F

$$\left\{ \begin{array}{l} K_{II} = 20 \text{ KSI} \sqrt{\text{IN}} \text{ TITANIUM (SAI-252)} \\ K_{II} = .5(97) = 49 \text{ KSI} \sqrt{\text{IN}} \text{ INCO 718} \\ K_{II} = .7(37) = 26 \text{ KSI} \sqrt{\text{IN}} \text{ 2219-T97 AL} \end{array} \right.$$

TITANIUM			STEEL			ALUMINUM		
N (FT/SEC)	$\sigma_p$ (KSI)	$a_i$ (IN)	N FT/SEC	$\sigma_p$ (KSI)	$a_i$ (IN)	N (FT/SEC)	$\sigma_p$ (KSI)	$a_i$ (IN)
500	12	.58	500	24	.84	500	8	2.2
1000	28	.11	1000	56	.15	1000	19	.40
1500	50	.034	1500	100	.048	1500	34	.12
2000	87	.011	2000	174	.016	2000	58	.042
2500	140	.004	2500	280	.006	2500	94	.016
3000	200	.002	3000	400	.003	3000	135	.008



DATE

SUBJECT

# OOS PARAMETRIC STUDY

DATE

4/23/71

WORK ORDER

1811-06-103

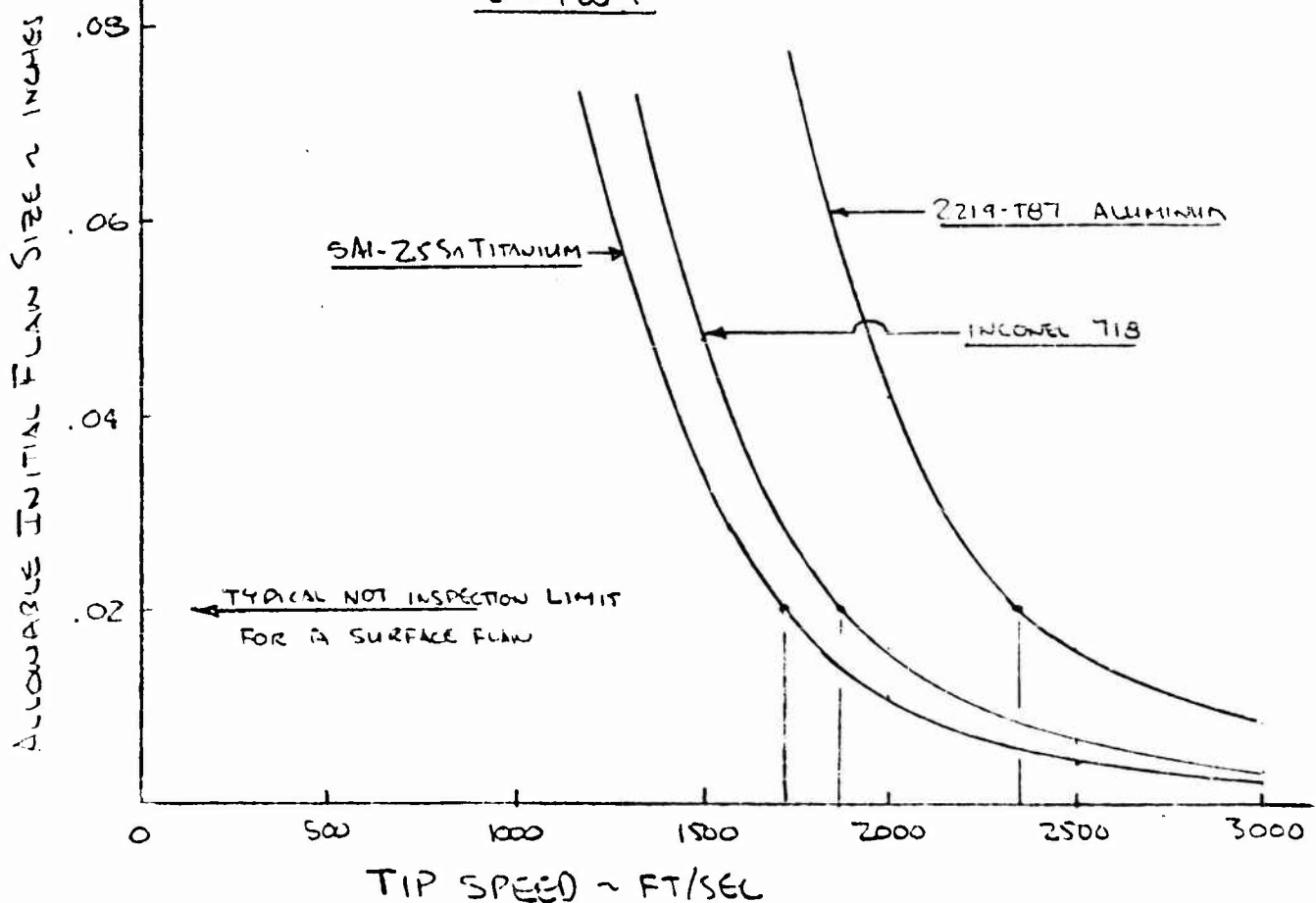
BY

L.W. BARTHOLF

CHK. BY

DATE

## ALLOWABLE FLAW SIZE VS TIP SPEED FOR FAILURE IN 1200 CYCLES @ -420°F





AEROJET-GENERAL CORPORATION  
SACRAMENTO • CALIFORNIA

REPORT NO

PAGE 18 OF 22

DATE

5/10/71

WORK ORDER

1811-06-103

DATE

# OOS PARAMETRIC STUDY

BY

L.W. BARTHOLOMEW

CHK BY

## FLAW SIZE VS CYCLES TO FAILURE ESTIMATION:

$$\text{GIVEN: } K_{II} = \sqrt{\sigma_{\text{PEAK}} \frac{\sqrt{a_i}}{Q_I}}$$

FOR INCONEL 718 @ -300°F (LIQUID OXYGEN),  $K_{IC} = 97 \text{ KSI} \sqrt{\text{IN}}$

INITIAL FLAW SIZE $a_i$ (INCHES)	$\sqrt{\frac{a_i}{Q_I}}$	TIP SPEED (FT/SEC)	PEAK STRESS $\sigma_p$ (KSI)	$K_{II}$ KSI $\sqrt{\text{IN}}$	$K_{II}/K_{IC}$	CYCLES TO FAILURE
.005	.154	1000	56	8.6	.09	~ 3000
.01	.218	↑	↑	12.2	.13	~ 2500
.02	.308	↑	↑	17.3	.18	~ 2300
.04	.435	↑	↑	24.4	.25	2000
.06	.535	↓	↓	30.0	.31	1900
.08	.615	1000	56	34.5	.36	1600
.005		1500	100	15.4	.16	2400
.01		↑	↑	21.8	.23	2100
.02		↑	↑	30.8	.32	1700
.04		↑	↑	43.5	.45	1300
.06		↓	↓	53.5	.55	900
.08		1500	100	61.5	.64	700
.005		2000	174	26.8	.28	1900
.01		↑	↑	38.0	.39	1500
.02		↑	↑	53.5	.55	900
.04		↑	↑	75.7	.78	350
.06		↓	↓	93.0	.96	40
.08		2000	174	107	.71	< 1
.005		2500	280	43	.44	1250
.01		↑	↑	61	.63	700
.02		↑	↑	86	.88	150
.04		↓	↓	122	> 1	< 1
.06		2500	280	150	> 1	< 1



AEROJET-GENERAL CORPORATION  
SACRAMENTO • CALIFORNIA

4000-0600-11

SUBJECT

OOS PARAMETRIC STUDY

REPORT NO

PAGE 19 OF 22

DATE

5/10/71

WORK ORDER

1811-06-103

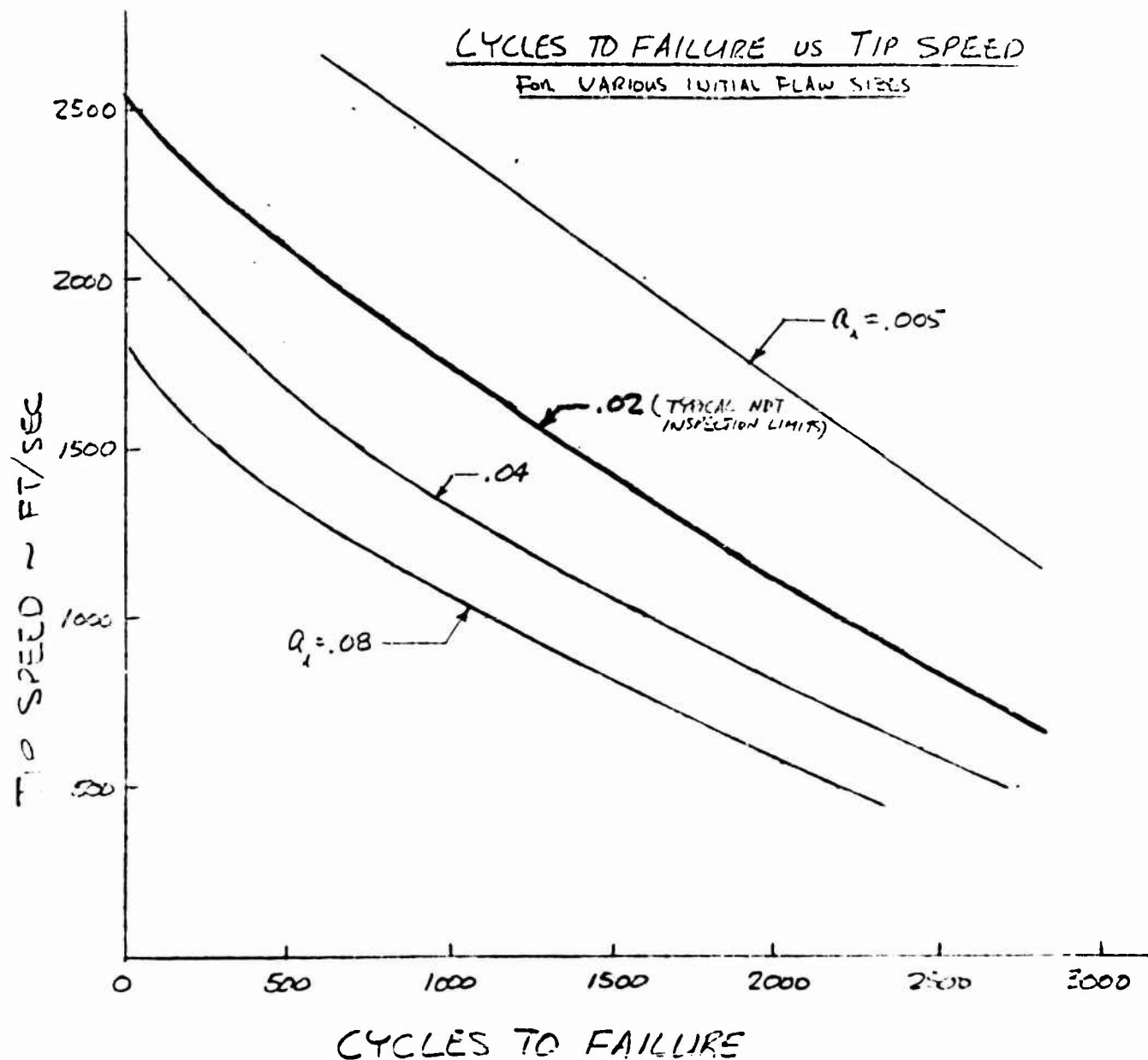
BY

L.W. BARTHOLF

CHK BY

DATE

TITANIUM SA1-25Sn IN LIQUID HYDROGEN ( $K_{IC} = 60 \text{ KSI} \sqrt{\text{IN}}$ )





AEROJET-GENERAL CORPORATION  
SACRAMENTO • CALIFORNIA

REPORT NO

PAGE 20 OF 22

DATE  
5/10/71

WORK ORDER  
1811-06-103

DATE

# OOS PARAMETRIC STUDY

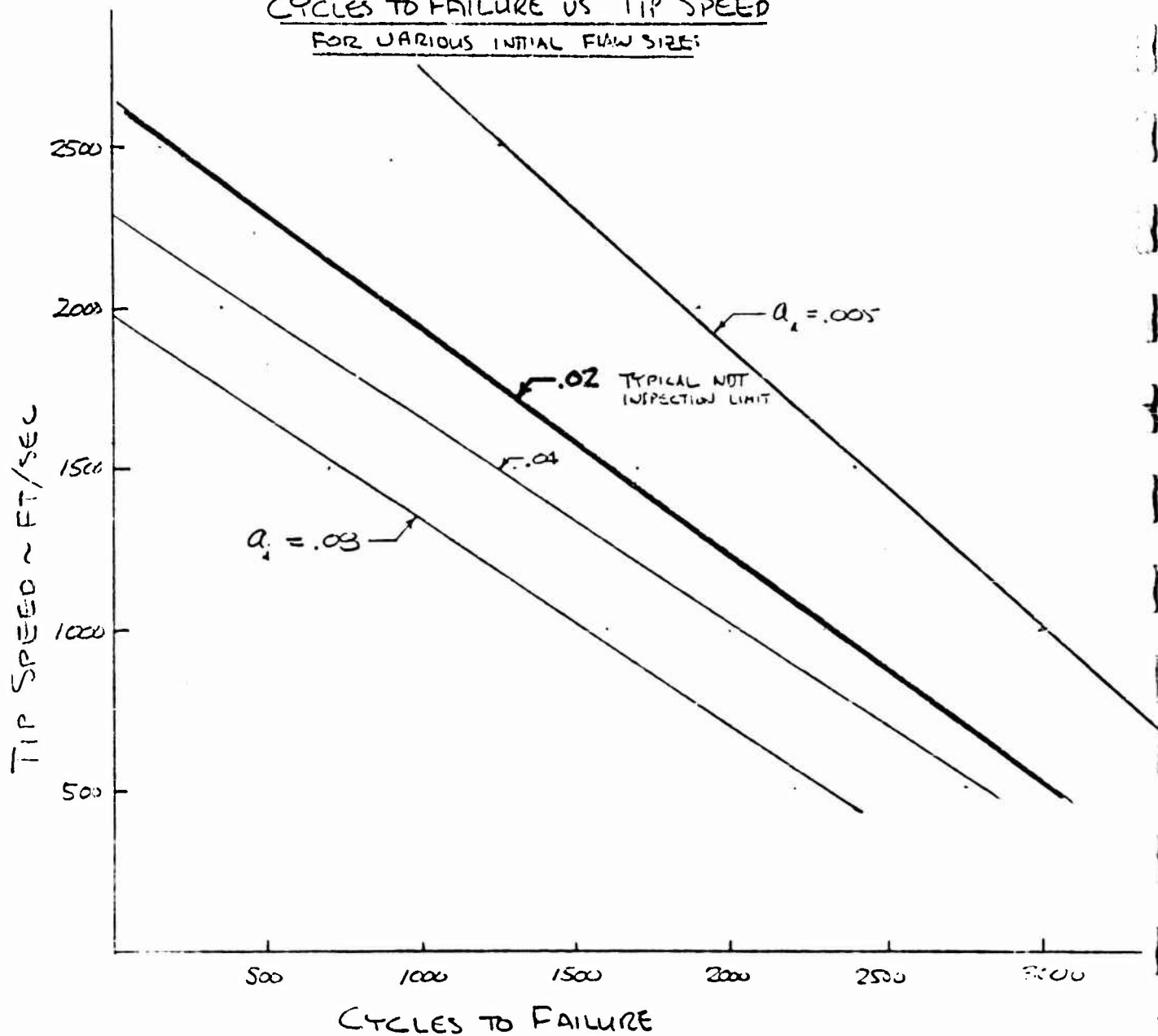
BY

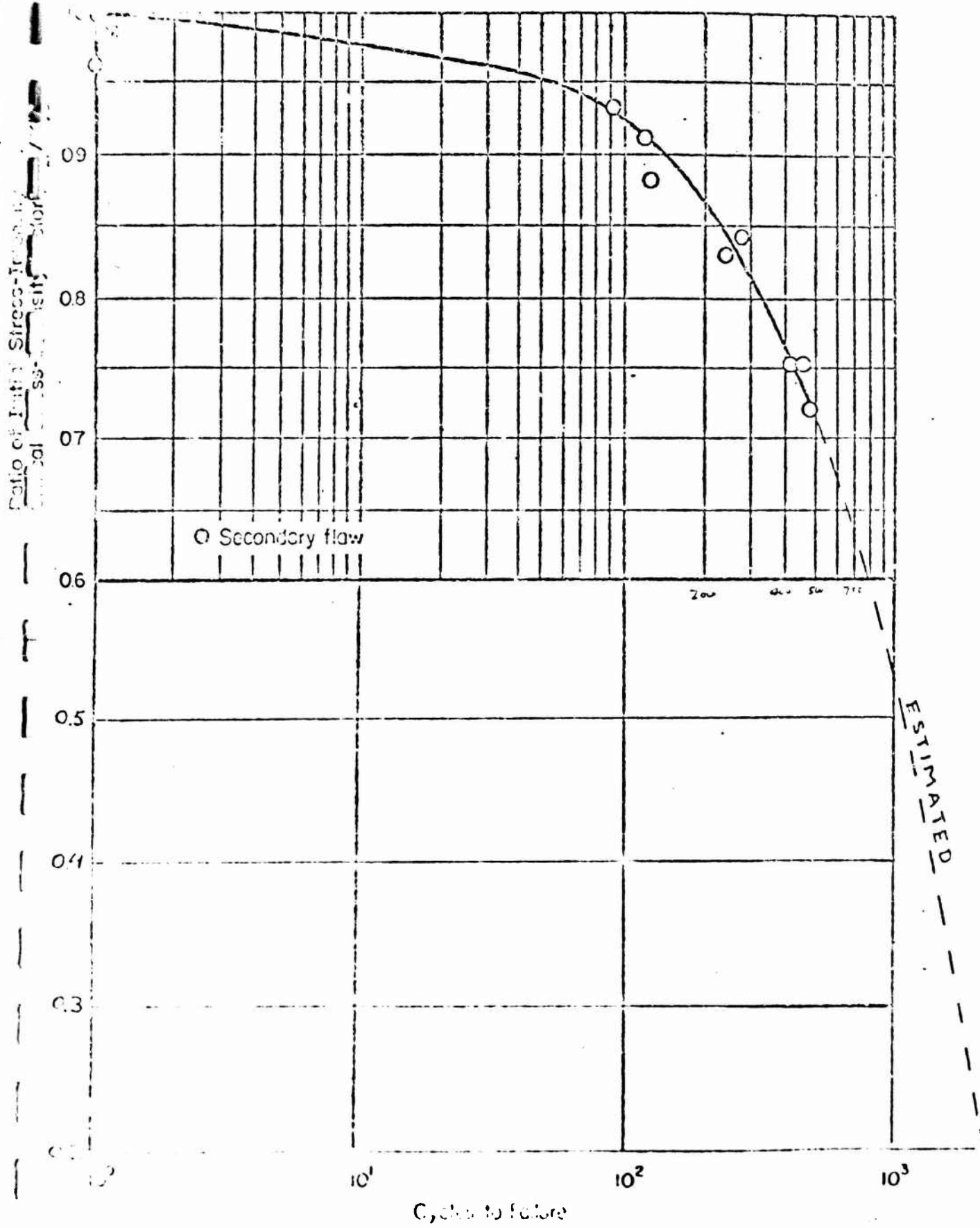
L.W. BARTHA

CHK BY

## INCONEL 718 IN LIQUID OXYGEN ( $K_{IC} = 97 \text{ KSI} \sqrt{\text{IN}}$ )

### CYCLES TO FAILURE VS TIP SPEED FOR VARIOUS INITIAL FLAW SIZES



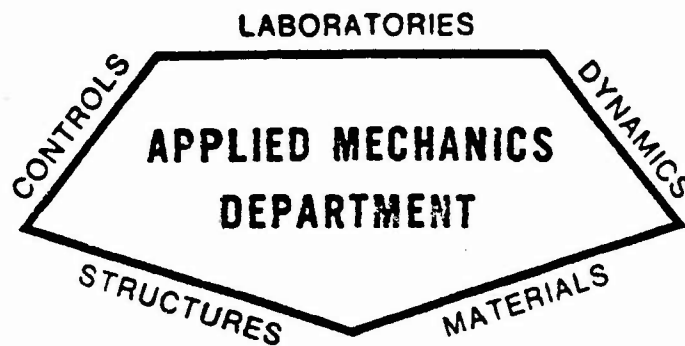


INCONEL 718 SHEET MATERIAL FATIGUE RESULTS  
IN LIQUID OXYGEN  $K_{IC} = 97 \text{ KSI } \sqrt{\text{IN}}$  (SEE )





STRUCTURAL DESIGN STUDIES AND 25K ENGINE  
EVALUATION FOR OOS COMBUSTION COMPONENTS



## STRUCTURAL ENGINEERING SECTION

REPORT NO. SA-OOS-CC-02

STRUCTURAL DESIGN STUDIES AND 25<sup>K</sup>  
ENGINE EVALUATION FOR  
OOS COMBUSTION COMPONENTS

PREPARED BY:

G. H. Skopp  
Engineering Specialist  
Structural Engineering Section

APPROVED BY: \_\_\_\_\_ DATE 24 June 1971

R. D. Ellis, Supervisor  
Advanced Test  
Structural Engineering Section  
Engineering



AEROJET LIQUID ROCKET COMPANY

SACRAMENTO, CALIFORNIA

## TABLE OF CONTENTS

	<u>Page</u>
I. Introduction	1
II. Summary of Results	2
III. General Discussion	2
A. Critical Ratio of Radius to Thickness $(R/t)_{cr}$	2
B. Low Cycle Fatigue	4
IV. Conclusion	5
V. Design Criteria	5
A. Loads	5
B. Factors of Safety	5
C. Material Properties	6
VI. Analysis	6
A. Main Injector Vane	6
1. Description	6
2. Discussion	7
3. Sample Calculations	9
B. Regen Tube Bundle	12
1. Description	12
2. Discussion	12
3. Sample Calculations	15
C. Preburner Tubes	17
1. Discussion	17
2. Sample Calculations	18
VII. References	37

## LIST OF FIGURES

<u>Figure</u>	<u>Title</u>	<u>Page</u>
1	Design Criteria	23
2	Material Properties of ARNCO 22-13-5 Sheet	24
3	ARNCO 22-13-5 Low Cycle Fatigue Sheet	25
4	ARNCO 22-13-5 S-N Data (1.3% Strain)	26
5	ARNCO 22-13-5 S-N Data (2.0% Strain)	27
6	Material Properties of ARNCO 22-13-5	28
7	Material Properties of ARNCO 22-13-5 (1.3x10 <sup>-4</sup> RTU-in./in. <sup>2</sup> -sec-°F)	29
8	Material Properties of ARNCO 22-13-5 (3.3x10 <sup>-4</sup> RTU-in./in. <sup>2</sup> -sec-°F)	30
9	Material Properties of ARNCO 22-13-5 (5.0x10 <sup>-4</sup> RTU-in./in. <sup>2</sup> -sec-°F)	31

LIST OF FIGURES (CONT.)

<u>Figure</u>	<u>Title</u>	<u>Page</u>
10	Injector Vane LCF Life ( $K=3 \times 10^{-4}$ BTU-in./in. <sup>2</sup> -sec-°F)	32
11	Regen Tube Thermal Profile	33
12	Regen Tube Parameters	34
13	Regen Tube LCF Life Costing	35
14	ARMCO 22-13-5 LCF Life @ Various Hold Times	36

## I. INTRODUCTION

The purpose of this report is to present the results of the parametric study performed for the OOS injector vane outer plate, the nozzle regen tube bundle and the preburner chamber. The latter structures will be fabricated from tubes in order to provide regenerative cooling by flowing cryogenic hydrogen. The injector vane outer plate is constructed to approximate a series of tubes. The crowns of these tubes are subjected to high temperatures during operation while the tube supporting structure remains at temperatures close to the cryogenic hydrogen (cryogenic oxygen in the case of the preburner tubes and injector vane plate). Because of the constraint of the supporting structure, repetitive thermal strain induces mechanical loads at the tube crowns which in turn may cause buckling and/or low-cycle thermal fatigue. In order to analyze these combustion components, consideration must be given to temperature distribution, operating environment, physical and mechanical properties of the materials, geometry and loading conditions. The intent of the work performed and reported herein is to provide preliminary design information which will aid the designer to make decisions concerning geometry, loading and material selection, but does not negate the necessity for a comprehensive review in the judgement of the structural analyst.

The combustion components analyzed were all idealized as circular tubes with different degrees of constraints dependent upon their configuration. A description of each component is presented in the section dealing with that component.

Section III contains a brief description of the assumptions and methods of derivation of the design curves, while in the component sections, application of the curves is described, illustrated with sample calculations.

## II. SUMMARY OF RESULTS

This report presents data applicable for preliminary design of tubes for regenerative cooled combustion components and similar structures for the OOS rocket engine. The data are presented in curve form to facilitate usage and may be used to aid the designer to make decisions concerning geometry, loading and material selection. The curves were prepared based upon pressure loading criteria, thermal buckling and low cycle fatigue characteristics of ARMCO 22-13-5 stainless steel.

## III. GENERAL DISCUSSION

### A. CRITICAL RATIO OF RADIUS TO THICKNESS $(R/t)_{cr}$

The nozzle tube bundle was analyzed for pressure loading, thermal buckling and low cycle fatigue. A plot of tube radius to thickness,  $(R/t)_{max}$  vs wall gas-side temperature,  $T_{wg}$ , is presented in Figure 12. To evaluate pressure loading, basic hoop stress was considered for both proof pressure and burst pressure using the following relationships: Reference (6), pg. 268.

#### Yield Criteria

$$(R/t) = \frac{F_{ty}}{1.20 P} \quad \dots(1)$$

where:  $R$  = Tube-mean radius, in.

$t$  = Thickness, in.

$p$  = Maximum Expected Operating Pressure, psi

$F_{ty}$  = Tensile Yield Strength, psi

Safety Factor = 1.20

#### Ultimate Criteria

$$(R/t) = \frac{F_{tu}}{1.50 P} \quad \dots(2)$$

where:  $F_{tu}$  = Ultimate Tensile Strength, psi

Safety Factor = 1.50

For ARMCO 22-13-5 stainless steel, the yield criteria governed the ultimate criteria. A relationship of tube pressure equal to 1000 psi was assumed and based upon yield strengths, curves

were plotted for chamber pressures of 2500, 1800, 1000 and 500 psi. The safety factors used were similar to the Space Shuttle Main Engine design criteria.

Figure 12 may also be used where tube pressure is not 2-1/2 times the chamber pressure (such as in the preburner) by dividing the tube design pressure by 2-1/2 and entering Figure 12 with this "pseudo" chamber pressure.

Figures 7 and 8 have similar data plotted for the injector vane plate. In these figures maximum radius to contain pressure is plotted versus minimum thickness as a function of wall gas-side temperatures. On the basis of a specified thermal conductivity and heat flux, the thermal gradient across the wall was calculated and a yield strength for the vane plate was determined.

To evaluate thermal buckling the following expression was used:  
References (3) and (4)

#### Thermal Buckling

$$(R/t) = \frac{0.24}{\alpha(\Delta T)(F)(S.F.)} \quad \dots(3) \quad \text{where:}$$

$\alpha$  = Coefficient of Thermal expansion, in./in.-°F  
 $\Delta T = T_{wg} - T_B$   
 $T_{wg}$  = Wall gas-side temperature, °F  
 $T_B$  = Coolant bulk temperature, °F  
 $F$  = Degree of restraint = 1 (full restraint)  
 $S.F.$  = Safety Factor = 1.0

Coolant bulk temperatures of -360°F and 0°F were considered and values of (R/t) were calculated and also plotted in Figure 12. A survey of the literature indicated that the above expression was satisfactory for minimizing the buckling problem at the tube crown. However, thermal creep effects which are difficult to analytically evaluate were neglected. Consequently, a safety factor of 1.5 to 2.0 is suggested in expression (3) above (dependent upon operating environment). Thermal buckling results from Figure 12 should be modified accordingly. The resultant minimum (R/t) from the above discussion is  $(R/t)_{cr}$ .



## B. LOW CYCLE FATIGUE

Low cycle fatigue test data for ARMCO 22-13-5 up to temperatures of 1300°F including hold times of 600 seconds were reported in Reference (2). The data were plotted and presented in Figures 3, 4, and 5.

The following assumptions were made:

1. For the range shown in Figure 3, the relationships were linear on the log-log scale.
2. Linear interpolation was assumed for temperatures between those reported, and
3. In order to evaluate hold times, Figures 4 and 5 were prepared, assuming that 75% of the damage occurs within the first six to ten hours.

For the nozzle regen tube bundle, axial strains were calculated using the following expression: Reference (9)

$$\epsilon = K\alpha\Delta T \quad \dots(4) \quad \text{where:} \quad \begin{aligned} \epsilon &= \text{Total strain, in./in.} \\ K &= 0.80 \text{ (function of constraint)} \\ \alpha &= \text{Coefficient of thermal expansion, in./in.-}^\circ\text{F} \\ \Delta T &= T_{wg} - T_B \\ T_{wg} &= \text{Wall gas-side temperature, } ^\circ\text{F} \\ T_B &= \text{Coolant bulk temperature, } ^\circ\text{F} \end{aligned}$$

For an assumed  $T_B$ , the strains due to bulk temperatures of -360°F, and 0°F, were calculated and the number of cycles to failure were determined from Figure 3. Results were plotted in Figure 13 versus wall gas-side temperatures,  $T_{wg}$ .

Figure 14 also shows number of cycles to failure plotted against total strains for hold times of 1, 10, and 100 hours at 1000°F and 1100°F. The effect of hold times appears negligible below these temperatures. Figure 14 has wider application since it may be used where induced strains do not conform to the above expression, i.e., constraints may be more rigid,  $K > 0.80$ . Figure 14 is plotted using the data in Figures 4 and 5.

For the injector vane plate, a K of 1.35 was used in the above expression to determine axial strains at different wall gas-side temperatures. Corresponding LCF life was determined and plotted in Figures 9 and 10 versus the thermal gradient between the wall gas-side temperature and the restraining structure or oxidizer bulk temperature. For a specified thermal conductivity and heat flux the plate thickness may be related to the wall thermal gradient. This information is also included in Figures 9 and 10, while the sample problem on page 8 illustrates the usage of these curves.

#### IV. CONCLUSION

Curves are presented which will aid the designer to predict thermal low cycle fatigue life as well as to determine preliminary design configurations. However, the data presented do not obviate the necessity of performing a more comprehensive analysis in the judgement of the structural analyst, nor preclude the necessity of obtaining additional test data to substantiate designs. The curves presented are most valuable qualitatively to establish trends, and an understanding of the problem rather than presenting quantitative solutions.

#### V. DESIGN CRITERIA

##### A. LOADS

1. Chamber pressure = 1800 psi @ 25K thrust - Figure 1.
2. Temperature profiles as noted in component sections.

##### B. FACTORS OF SAFETY

##### 1. Strength Factors

- 1.20 vs minimum yield
- 1.50 vs minimum ultimate

##### 2. Tube Buckling

- 1.5 on critical (R/t) buckling parameter

### 3. Fatigue

4.00 on lower bound of ALRC task data.

#### C. MATERIAL PROPERTIES

The tubes and injector plates will be fabricated from ARMCO 22-13-5 sheet stock because of its excellent low cycle fatigue characteristics as well as its high strength at high temperatures. Figure 2 shows mechanical properties varying with temperatures. The ultimate tensile strength plotted is 85% of the typical values reported by the ARMCO Steel Corporation (Reference 1) while the tensile yield strength is 80%. This is in conformance with recommendations from the ALRC Materials Engineering Section for design allowable strengths.

Figure 3 shows the low cycle fatigue life characteristics at various test temperatures and includes data for hold times of 600 seconds per cycle in both tension and compression at 1300°F, as reported in Reference 2. Figures 4 and 5 further illustrate the effects of hold times at different temperatures for compressive strains of 1.3% and 2.0% respectively. Figure 5 also includes a curve of 2% tensile strain at 1300°F and it is apparent that this condition imposes the most severe LCF life degradation reported. The test data indicate that the effect of hold time up to 1000°F is negligible and that LCF life is reduced with increased total induced strain. It is also anticipated that most of the damage due to hold times will occur early, within the first 6 hours.

## VI. ANALYSIS

### A. MAIN INJECTOR VANE

#### 1. Description

Main injector vane consists of six platelets, two each of the vanes shown in Figure 6, which illustrates half of a vane assembly. Liquid enters the vane, plate (a) and is directed by the channels to the orifice of plate (b), and then down through the grooves of plate (c). Plate (c)

is subjected to the maximum thermal gradient having liquid oxidizer on one side, and the hot products of combustion on the other. The oxidizer undergoes a phase change of from 100% gas at full thrust, to a minimum of 70% quality at minimum thrust. The gaseous oxidizer flows through the lower orifice of plate (b) back to the nozzle configuration of plate (a) and is injected into the main stream of the hot gas flow entering the thrust chamber.

Plate (c) will be etched to achieve the desired groove configuration, and electro polished on the hot gas side to remove excess metal. The final configuration will approximate a series of half tubes which will have flexibility and thus minimize the induced plastic strains due to the high thermal gradients, and improve low cycle fatigue life.

## 2. Discussion

Plate (c), Figure 6, was assumed to be a series of cylindrical half tubes. The pressure holding capability was evaluated on the basis of hoop strength. A 1.20 and 1.50 factor of safety was applied to proof pressure and burst pressure respectively. The plate was also evaluated for thermal buckling using an empirical expression from References 3 and 4. The critical condition resulted from the application of proof pressure.

Assuming a heat flux of  $6 \text{ BTU/in.}^2\text{-sec}$ , per recommendation of the heat transfer section and a thermal conductivity of  $2 \times 10^{-4} \text{ BTU-in./in.}^2\text{-sec-}^\circ\text{F}$ , curves were plotted, Figure 7, showing the maximum radius to hold pressure for a specified wall thickness as a function of the wall gas side temperature. Figure 8 is a similar plot for thermal conductivity of  $3 \times 10^{-4} \text{ BTU-in./in.}^2\text{-sec-}^\circ\text{F}$ . The thermal conductivity of chromium nickel stainless steels will vary from  $2 \times 10^{-4}$  to  $3 \times 10^{-4} \text{ BTU-in./in.}^2\text{-sec-}^\circ\text{F}$  between  $100^\circ\text{F}$  and  $1000^\circ\text{F}$  respectively. As an example of the usage of the curves, see Figure 8, assume a wall thickness of 0.040 inch and find the corresponding maximum radius of 0.74 inch at  $800^\circ\text{F}$  wall gas side temperature.

Figures 9 and 10 relate low cycle fatigue life with thermal gradients between the wall gas-side and the oxidizer bulk temperature as a function of wall gas side temperature for thermal conductivities of  $2 \times 10^{-4}$  and  $3 \times 10^{-4} \text{ BTU-in./in.}^2\text{-sec-}^\circ\text{F}$  respectively. The following example will illustrate the usage of these curves.

### Design Data

$T_B$ , bulk temperature of liquid oxygen =  $200^\circ\text{R}$  ( $-260^\circ\text{F}$ )

$T_{WL}$ , liquid side wall temperature =  $250^\circ\text{R}$  ( $-210^\circ\text{F}$ )

$t$ , wall thickness = 0.050 inch

$k$ , thermal conductivity =  $3 \times 10^{-4}$  BTU-in./in.<sup>2</sup>-sec- $^\circ\text{F}$

From Figure 10, a wall thickness of 0.050 inch corresponds to a wall thermal gradient,  $\Delta T$ , of  $1000^\circ\text{F}$ .

$$\begin{aligned} T_{wg}, \text{ gas side wall temperature} &= T_{WL} + \Delta T \\ &= -210 + 1000 = 790^\circ\text{F} \end{aligned}$$

@ $\Delta T = T_{wg} - T_B$	}	<u>From Figure 10</u> $N_f = 3,700$ cycles
$\Delta T = 790 - (-260)$		
$\Delta T = 1050^\circ\text{F}$		
and $T_{wg} = 790^\circ\text{F}$		

Assume: Number of life cycles are inadequate. A minimum of 6,000 cycles is desired. Try  $t = 0.040$  inch.

From Figure 10, the wall thermal gradient =  $800^\circ\text{F}$

$$T_{wg} = -210 + 800 = 590^\circ\text{F}$$

@ $\Delta T = 590 - (-260)$	}	<u>From Figure 10</u> $N_f = 10,600$ cycles
$\Delta T = 850^\circ\text{F}$		
and $T_{wg} = 590^\circ\text{F}$		

@ $t = 0.040$ inch	}	<u>From Figure 8</u> $R_{\max} = 0.92$ inch
and $T_{wg} = 590^\circ\text{F}$		



SUBJECT

3- SAMPLE CALCULATIONS

DATE

5/20/71

WORK ORDER

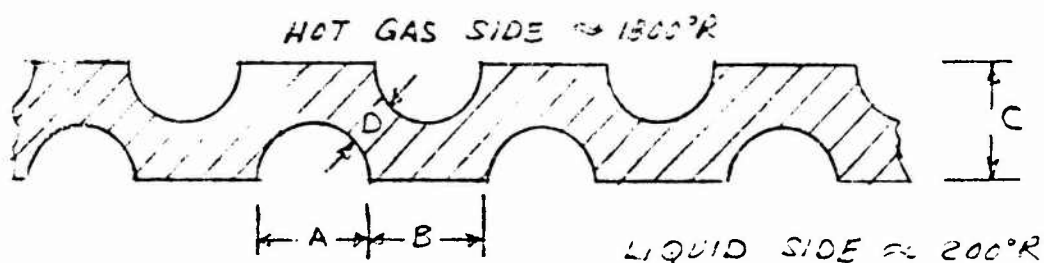
1811-05-001

BY

GHSkopp

CHK. BY

DATE

MAIN INJECTOR VANEOuter Plate ~ photo etched designDENSE LSTA

$$T_{hg} = 1400^{\circ}R$$

$$T_{wl} = 200^{\circ}R$$

$$P_{max} = 2500 \text{ psi}$$

MATERIAL = ALUMINUM 2024-T3 Sheet

$$F_{tu} = 109,000 \text{ psi}$$

$$F_{ty} = 75,000 \text{ psi}$$

$$E = 29,000,000 \text{ psi}$$

$$\alpha = 13.0 \times 10^{-6} / \text{in}^{\circ}F \text{ (70}^{\circ}\text{--}1000^{\circ}F)$$

② R.T.



SUBJECT

DATE

5/20/71

WORK ORDER

121-25-001

BY

GHS

CHK. BY

DATE

1-1) PRESSURE AND TEMPERATURE

Assume: Cylindrical Configuration to evaluate pressure holding capability of outer plate



$$\text{ hoop stress, } \sigma_h = \frac{PR}{t}$$

... Reference (6), Pg. 268

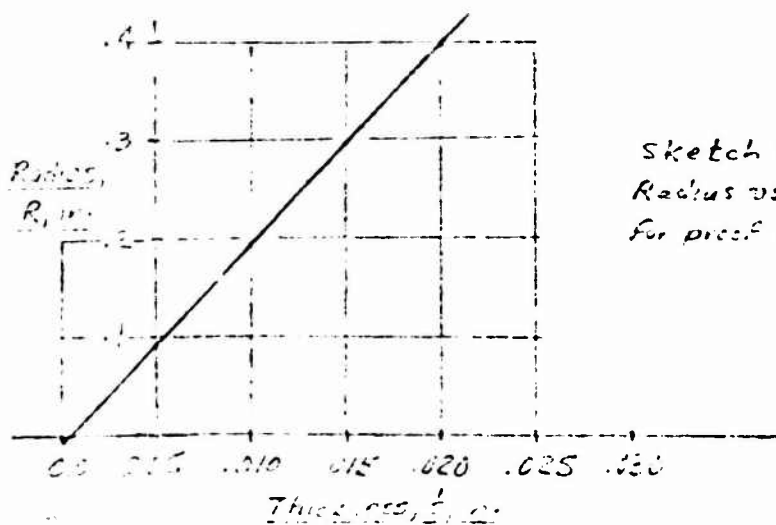
(a) Yield Criteria

$$R/t = \frac{\sigma_h}{P} = \frac{F_{ty}}{1.2 P}$$

$$(a) \text{ mean Temp} = \frac{1425 + 200}{2} = 800^\circ R = 340^\circ F, F_{ty} = 56,000 \text{ psi} - \text{Fig. 2}$$

$$\therefore R/t = \frac{56,000}{1.2 (2350)} = 19.85$$

$$R = 19.85 t$$



Sketch (a)  
Radius vs Thickness  
for proof pressure condition

(b) Ultimate Criteria

$$R/t = \frac{F_{tu}}{1.5 P} = \frac{91,000}{1.5 (2350)} = 27.2 > 19.85$$

(c) Flaking Criteria (Reference 3)

$$R/t = \frac{0.4}{\alpha \Delta T} = \frac{0.4}{75000^\circ (1000 - 100)} = 21.9 > 19.85$$

Yield Criteria Controls



DATE  
5/20/71

WORK ORDER  
1811-05-001

BY  
GHS

CHK. BY

DATE

## 2.- LOW CYCLE FATIGUE

let:  $\phi = 6870 \text{ in/in}^2 \cdot \text{sec}$  ... (assumed per recommendation of Heat Transfer section)

$K = 3 \times 10^{-4} \text{ BTU/sec-in}^2 \cdot ^\circ\text{F/in}$  ... see Reference 5, Pg. 2.5.1.1 @ 1000°F

$\phi = \frac{K \Delta T}{\Delta x}$  ... Heat Transfer Expression for conduction through a wall

$$\frac{\Delta x}{\Delta T} = \frac{K}{\phi} = \frac{3 \times 10^{-4}}{6} = \underline{\underline{5 \times 10^{-5} \text{ in/}^\circ\text{F}}}$$

(1) For LCF LIFE = 6,000 cycles @ 900°F,  $\Delta E_f = 1.00\%$   
(see Figure 3)

$$\Delta E_f = K \alpha \Delta T$$

where:  $K = 1.35$  (assumed)  
 $\alpha = 10.05 \times 10^{-6} \text{ in/in}^2 \cdot ^\circ\text{F}$   
@  $T_{avg} = 900^\circ\text{F}$  - Fig. 2

$$\therefore \Delta T = \frac{0.010}{1.35(10.05)10^{-6}} = 740^\circ\text{F}$$

(2) For LCF LIFE = 3,600 cycles @ 900°F,  $\Delta E_f = 1.25\%$   
(see Figure 3)

$$\Delta T = \frac{0.0125}{1.35(10.05)10^{-6}} = 925^\circ\text{F}$$

(3) For LCF LIFE = 1,200 cycles @ 1100°F,  $\Delta E_f = 1.70\%$   
(see Figure 3)

$$\Delta T = \frac{0.0170}{1.35(10.30)10^{-6}} = 1230^\circ\text{F}$$



## 8. REGEN TUBE BUNDLE

### 1. Description

The regen tube bundle under consideration in this report extends from expansion ratio 6 to expansion ratio 145 with a bifurcation occurring at expansion ratio 30. This is a two pass system with 160 tubes prior to bifurcation and 320 tubes afterwards. Each tube has a constant minimum thickness of 0.015 inch, but the radius varies with position from 0.073 inch minimum to 0.179 inch maximum. The expression to determine the radius is as reported in Reference (7):

$$\text{Radius, } R = \frac{1.28}{n} \left( \frac{\epsilon F}{P_c} \right)^{1/2}$$

where:  $\epsilon$  = expansion ratio

$n$  = number of tubes = 160

$P_c$  = chamber pressure = 1800 psi

$F$  = motor thrust = 25,000 lb

The tubes will be fabricated from ARMCO 22-13-5 stainless steel. Mechanical properties and thermal low cycle fatigue data are presented in Figures 2, 3, 4 and 5.

### 2. Discussion

Figure 11 presents the regen tube thermal profile for various chamber pressures. Maximum thermal gradient occurs at 500 psi which makes this condition low cycle fatigue critical as compared to the 2500 psi condition, which would be strength critical. The tubes were evaluated for their pressure carrying capability on the basis of induced hoop stress for a design pressure of 2-1/2 times the chamber pressure, and including a 1.20 factor of safety for yield. Resultant maximum radius/thickness ratios,  $(R/t)$ , are plotted in Figure 12 versus gas side wall temperature,  $T_{wg}$ , as a function of chamber pressures. In addition, thermal buckling was considered, using the following expression from Reference 3.

$$(R/t)_{cr} = \frac{0.24}{\alpha \Delta T}$$

Where:  $\alpha$  = coefficient of thermal expansion, in./in.-°F

$\Delta T$  = thermal gradient, °F

It is apparent that at 500 psi chamber pressure thermal buckling is critical at gas side wall temperatures greater than 350°F. However, at pressures greater than 1,000 psi, thermal buckling is no longer a structural consideration, although thermal creep may be at temperatures greater than 1000°F.

Figure 13 presents low cycle fatigue life versus gas side wall temperature for the limits of -360°F and 0°F liquid bulk temperatures,  $T_B$ . The following example will illustrate usage of Figures 12 and 13:

### Example

#### Design Data

Motor thrust = 25,000 lb

Chamber pressure = 1800 psi maximum

Number of tubes =  $\begin{cases} 160 & \text{from } \epsilon = 6 \text{ to } \epsilon = 30 \\ 320 & \text{from } \epsilon = 30 \text{ to } \epsilon = 145 \end{cases}$

Minimum tube thickness = 0.015 inch

Liquid bulk temperature = -360°F

From Figure 11, @  $\epsilon = 20$   
 $P_c = 500 \text{ psi}$  }  $T_{wg} = 870^\circ\text{F}$

From Figure 12, @  $T_{wg} = 870^\circ\text{F}$   
 $T_B = -360^\circ\text{F}$  }  $(R/t) = 19.5$

To evaluate thermal creep, let safety factor = 1.5

$$\therefore (R/t)_{cr} = \frac{19.5}{1.5} = 13.0$$

$$\text{Radius, } R = \frac{1.28}{n} \left( \frac{\epsilon F}{P_c} \right)^{1/2} = 0.133 \text{ inch, where: } \begin{aligned} n &= 160 \text{ tubes} \\ \epsilon &= 30 \\ F &= 25,000 \text{ lb} \\ P_c &= 1800 \text{ psi} \end{aligned}$$

$$R/t = \frac{.133}{.015} = 8.90$$

$$M.S. = \frac{13.0}{8.90} - 1 = 0.46$$

Again

$$\left. \begin{array}{l} \text{From Figure 11, @ } \epsilon = 20 \\ P_c = 1800 \text{ psi} \end{array} \right\} T_{wg} = 200^\circ\text{F}$$

$$\left. \begin{array}{l} \text{From Figure 12, @ } T_{wg} = 200^\circ\text{F} \\ P_c = 1800 \text{ psi} \end{array} \right\} (R/t)_{cr} = 12.0$$

$$\text{M.S.} = \frac{12.0}{8.9} - 1 = 0.35 \text{ (yield)}$$

$$\left. \begin{array}{l} \text{From Figure 13, @ } T_{wg} = 870^\circ\text{F} \\ T_B = -360^\circ\text{F} \end{array} \right\} N_f = 6,200 \text{ cycles}$$



SUBJECT

## 3.- REGEN TUBE ANALYSIS

## SAMPLE CALCULATIONS

BY

GHSKOPP

CHK. BY

DATE

5/25/71

WORK ORDER

1811-05-001

DATE

## BASELINE DESIGN

$$E = 6$$

$$t = 0.015 \text{ in.}$$

$$P_c = 1800 \text{ psi} \quad (\text{Tube Pressure} = 2.5 P_c)$$

$$F = 25,000 \text{ lbs}$$

$$R_{max} = \frac{1.280 (E F / P_c)^{1/2}}{n} \dots \text{REF. (7)}$$

$$= 4.75 E^{1/2} / n$$

$$\text{let: } n = 160 \text{ tubes}$$

$$\therefore R_{max} = 0.073 \text{ in.}$$

$$(R/t) = \frac{0.073}{0.015} = 4.86$$

$$\textcircled{1} E = 6, P_c = 1800 \text{ psi}, T_{wg} \approx 260^\circ\text{F} \quad - \text{FIGURE 11 (PETROL PATH)}$$

$$(R/t)_{cr} = 11.0 > 4.86 \quad - \text{FIGURE 12}$$

$$M.S. = \frac{11.5}{4.86} - 1 = \underline{\underline{1.26}} \quad (\text{good})$$

$$\textcircled{2} E = 30$$

$$n = 160 \text{ tubes}$$

$$R = 0.143 \text{ in.}$$

$$(R/t) = 10.9$$

$$\text{FIGURE 11} - T_{wg} \approx 170^\circ\text{F} \quad (\text{@ } E = 30, P_c = 1800 \text{ psi \& PETROL PATH})$$

$$\text{FIGURE 12} - (R/t)_{cr} = 12.3 \quad (\text{@ } T_{wg} = 150^\circ\text{F})$$

$$M.S. = \frac{12.3}{12.3} - 1 = \underline{\underline{0.13}} \quad (\text{good})$$

$$\textcircled{3} E = 145$$

$$n = 320 \text{ tubes}$$

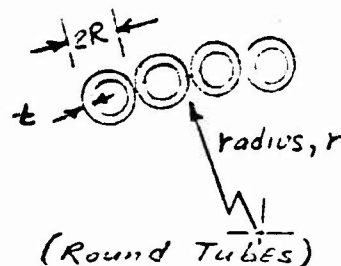
$$R = 0.173$$

$$(R/t) = \frac{0.173}{0.015} = 11.9$$

$$\text{FIGURE 11} - T_{wg} \approx 4^\circ\text{F}$$

$$\text{FIGURE 12} - (R/t)_{cr} = 13.5$$

$$M.S. = \frac{13.5}{13.5} - 1 = \underline{\underline{0.13}} \quad (\text{good})$$



$$E = \left( \frac{r}{r_{throat}} \right)^2$$



$$T_{wg}, \text{ALLOY TEMPERATURE} = 875^{\circ}\text{F}$$

$$T_{wg}, \text{LIQUID SIDE TEMP} = 795^{\circ}\text{F}$$

$$T_{mean} = 235^{\circ}\text{F}$$

$$F_{ty} = 44,000 \text{ psi} \dots \text{Figure 2}$$

$$\sigma_H = \frac{PR}{t}$$

$$\text{@ } E = 6, R/t = 4.86 \dots (\text{see previous page})$$

$$\sigma_H = (2.5)(500)(1.2)(4.86) = 7300 \text{ psi}$$

$$M.S. = \frac{44,000}{7,300} - 1 = \underline{\underline{5.02}} \text{ (yield)}$$

$$\text{@ } E = 125, T_{wg} = 510^{\circ}\text{F}, R/t = 11.9 (\text{see previous page})$$

$$T_{mean} = 502^{\circ}\text{F}, F_{ty} = 50,000 \text{ psi} \dots \text{Figure 2}$$

$$\sigma_H = (2.5)(500)(1.2)(11.9) = 17,900 \text{ psi}$$

$$M.S. = \frac{50,000}{17,900} - 1 = \underline{\underline{1.79}} \text{ (yield)}$$

### LCF LIFE

$$LE_T = 0.5 \alpha LE_T \dots \text{Reference (9), Figure 3}$$

$$\text{At } T_B = -265^{\circ}\text{F}$$

$$T_{wg} = 875^{\circ}\text{F} \quad \text{@ } E = 23.2 \quad P_c = 500 \text{ psi}$$

$$\alpha = 10^{-5} \text{ in/in-}^{\circ}\text{F} \dots \text{Figure 2}$$

$$LE_T = (0.8)(10^{-5})(875 - [-365]) = 0.47\%$$

$$N_f = 3,000 \text{ cycles} - \text{LCF CURVES Figure 3}$$

### (ALTERNATE PROCEDURE)

$$\text{FROM FIGURE 13- @ } T_B = -360^{\circ}\text{F}$$

$$T_{wg} = 875^{\circ}\text{F}$$

$$N_f = 6,000 \text{ cycles}$$

NOTE: IN THE LACK OF PRESENT DATA, LONG-TERM TESTS (UP TO 10,000 CYCLES) DO NOT HAVE AN APPROPRIATE EFFECT AT THIS TEMPERATURE AND STRAIN (SEE FIGURE 4)

## C. PREBURNER TUBES

### 1. Discussion

It was proposed that the preburner chamber would be fabricated from ARMCO 22-13-5 1/8 inch tubes with an external wire wrap. The design of the tubes for internal pressure and low cycle fatigue was evaluated using the method and curves developed in this report. The calculations and results are shown in Paragraph 2, Sample Calculations.

Figure 12 was developed for an internal tube pressure of 2.5 times the chamber pressure. For those cases where this relationship does not exist, a "pseudo" chamber pressure may be calculated in order to use the curves. For example, the preburner tube pressure is 3255 psi. When divided by 2.5, the result is 1300 psi which is less than 1800 psi chamber pressure at full thrust. However, using 1300 psi and the proper gas-side wall temperature, Figure 12 may be entered and a critical  $(R/t)_{cr}$  established. For the preburner tubes the  $(R/t)_{cr} = 11.4$  with a resultant margin of safety of 1.75 (yield).

Figure 14 is a plot of strain versus number of cycles to failure at 1000 and 1100°F for hold times ranging from 1 to 100 hours. When this curve is applied to the preburner tube design conditions, the LCF life prediction is 4500 cycles for 10 hours hold time. 6,000 cycles is desired.

An attempt was made to determine the effects of wire wrapping the preburner tubes. It soon became apparent that with the proposed wire thickness to resist the longitudinal as well as hoop load, the wrapping could not be readily accomplished without incurring some damage to the tubes. Consequently because of the low LCF prediction and fabrication problems, the preburner is being further evaluated.



2.- SAMPLE CALCULATIONS

BY

GHS

CHK. BY

PREBURNER TUBES

DESIGN DATA

100% Max THRUST

30% THRUST

Pressure, Chamber 2800 psi

705 psi

Tube Pressure 3255 psi

815 psi

Tube THICKNESS, in. = 0.015

Tube Diameter, in. = 0.125

Chamber Diameter, in. = 3.000

MATL. : ARMCO 22-13-5

SAFETY FACTOR = 1.20 (yield)

$T_{wg}$ , Gas Side Wall Temperature = 1475°R

$T_b$ , Liquid Bulk Temperature = 324°R

$\phi$ , Heat Flux = 4 BTU/IN.<sup>2</sup>-SEC

$K$ , Thermal Conductivity,  $3 \times 10^{-4}$  BTU-IN./IN.<sup>2</sup>-SEC-°F

} Data from  
Heat Transfer Section



SUBJECT

DATE

6/24/71

WORK ORDER

1811-56-103

BY

GHS

CHK BY

DATE

(a) YIELD CRITERION

Assume Full Tube Pressure acts on Tubes. Neglect chamber pressure.

$$q, \text{ Heat Flux} = 4 = \frac{k \Delta T}{\Delta x}$$

$$\Delta T = \frac{4(\Delta x)}{k} = \frac{4(.015)}{3 \times 10^{-4}} = 200^\circ \text{F}$$

$$T_{wg} = 1475^\circ \text{R} = 1015^\circ \text{F}$$

$$T_m = 1015 - \frac{200}{2} = 915^\circ \text{F}$$

NOTE: Figure 12 is based upon a tube pressure equal to  $2\frac{1}{2}$  times the chamber pressure. Determine a "pseud." chamber pressure by dividing Tube pressure by  $2\frac{1}{2}$ .

$$p'_c = \frac{3255}{2.5} = 1300 \text{ psi}$$

$$\left. \begin{array}{l} \text{From Figure 12 @ } T_{wg} = 915^\circ \text{F} \\ p'_c = 1300 \text{ psi} \end{array} \right\} (R/t)_{cr} = 11.4$$

$$R/t = \frac{0.0625}{0.0156} = 4.15$$

$$M.S. = \frac{11.4}{4.15} - 1 = \underline{\underline{1.75}} \text{ (yield)}$$

From Figure 12, it is apparent that yield criterion governs.





AEROJET-GENERAL CORPORATION  
SACRAMENTO CALIFORNIA

REPORT NO.

SA-005-CC-02

PAGE 20 OF 27

DATE

6/24/71

WORK ORDER

1811-06-103

BY

GHS

CHK. BY

DATE

(b) LOW CYCLE FATIGUE

$$\Delta \epsilon_T = 0.8 \alpha \Delta T$$

$$= 0.8 (10.20) 10^{-6} (1151.0)$$

$$\Delta \epsilon_T = 0.940 \%$$

where:  $\alpha = 10.20 \times 10^{-6} \text{ in./in.-}^\circ\text{F}$   
(see Figure 2)

$$\Delta T = (T_{wg} - T_B) = 1151^\circ\text{F}$$

$$T_{wg} = 1475 - 460 = 1015^\circ\text{F}$$

$$T_B = 324 - 460 = -136^\circ\text{F}$$

From Figure 14: @ 0.94% Strain  
and 1000°F

$N_f = 4800$  cycles For 1 hour total hold time in Compression

$N_f = 4500$  cycles For 10 hours total hold time in Compression

Alt. method

Figure 13 @  $T_{wg} = 1015^\circ\text{F}$   
 $T_B = -136.0^\circ\text{F}$

$N_f = 4800$  cycles (600 sec. Hold Time per cycle)



SUBJECT

DATE

6/11/71

WORK ORDER

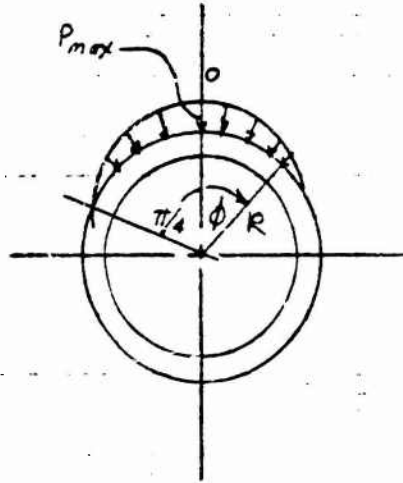
1811-05-001

BY

GHSKOPP

CHK. BY

DATE

(C) EXTERNAL LOADING  
DUE TO WIRE WRAPDetermine:  $P_{max}$ 

see: Reference (8),

$$P = P_{max} \cos 2\phi$$

$$R_i = 0.0475 \text{ in.}$$

$$\text{let: } R_o = 0.0525 \text{ in.}$$

$$t = 0.015 \text{ in.}$$

$$I = \frac{\pi}{4} (R_o^4 - R_i^4) = 8.3 \times 10^{-10} \text{ in}^4$$

$$\bar{R} = 0.0550 \text{ in.}$$

$$\frac{F}{2} = \int_0^{\pi/4} P_{max} \cos 2\phi \cos \phi R d\phi$$

$$\begin{aligned} \frac{F}{2} &= P_{max} R \int_0^{\pi/4} 2 \cos^3 \phi d\phi - \cos \phi d\phi \\ &= P_{max} R \left[ 2 \cdot \frac{1}{3} \sin \phi (\cos^2 \phi + 2) \right]_0^{\pi/4} - \left[ \sin \phi \right]_0^{\pi/4} \\ &= P_{max} R \left[ \left( 2 \cdot \frac{1}{3} \cdot \frac{\sqrt{2}}{2} \left( \frac{2}{4} + 2 \right) - 0 \right) - \left( \frac{\sqrt{2}}{2} - 0 \right) \right] \end{aligned}$$

$$\frac{F}{2} = P_{max} R \frac{\sqrt{2}}{3}$$

$$P_{max} = \frac{3F}{2\sqrt{2}R}$$

$$M = K_m P_{max} R^2 = K_m \frac{3}{2\sqrt{2}} \frac{F}{R} R^2 = 1.06 K_m F R$$

$$Q = K_Q P_{max} R = 1.06 K_Q F$$

$$H = K_H P_{max} R = 1.06 K_H F$$

$$\phi = 0$$

$$K_m = -0.11392$$

$$K_Q = 0.17557$$

$$M = -1.06(-0.11392) F (-0.015) = -0.00665 F \text{ in-in.}$$

$$N = 1.06(0.17557) F = 0.1861 F \text{ in.}$$

$$\tau = \frac{N}{A} \pm \frac{M/C}{I}$$

$$\text{where: } A = \pi(R_o^2 - R_i^2) = 8.3 \times 10^{-4} \text{ in}^2$$

$$C = 0.0525 \text{ in.}$$



AEROJET-GENERAL CORPORATION  
SACRAMENTO • CALIFORNIA

AGCS FORM 1

REPORT NO.

SA-005-CC-02

PAGE 52 OF 57

SUBJECT

DATE

6/24/71

WORK ORDER

1811-56-143

BY

GHS

CHK. BY

DATE

$$\sigma = \frac{.3660 F}{3.058 \times 10^{-3}} + \frac{.00663 F (.0625)}{8.3 \times 10^{-6}}$$

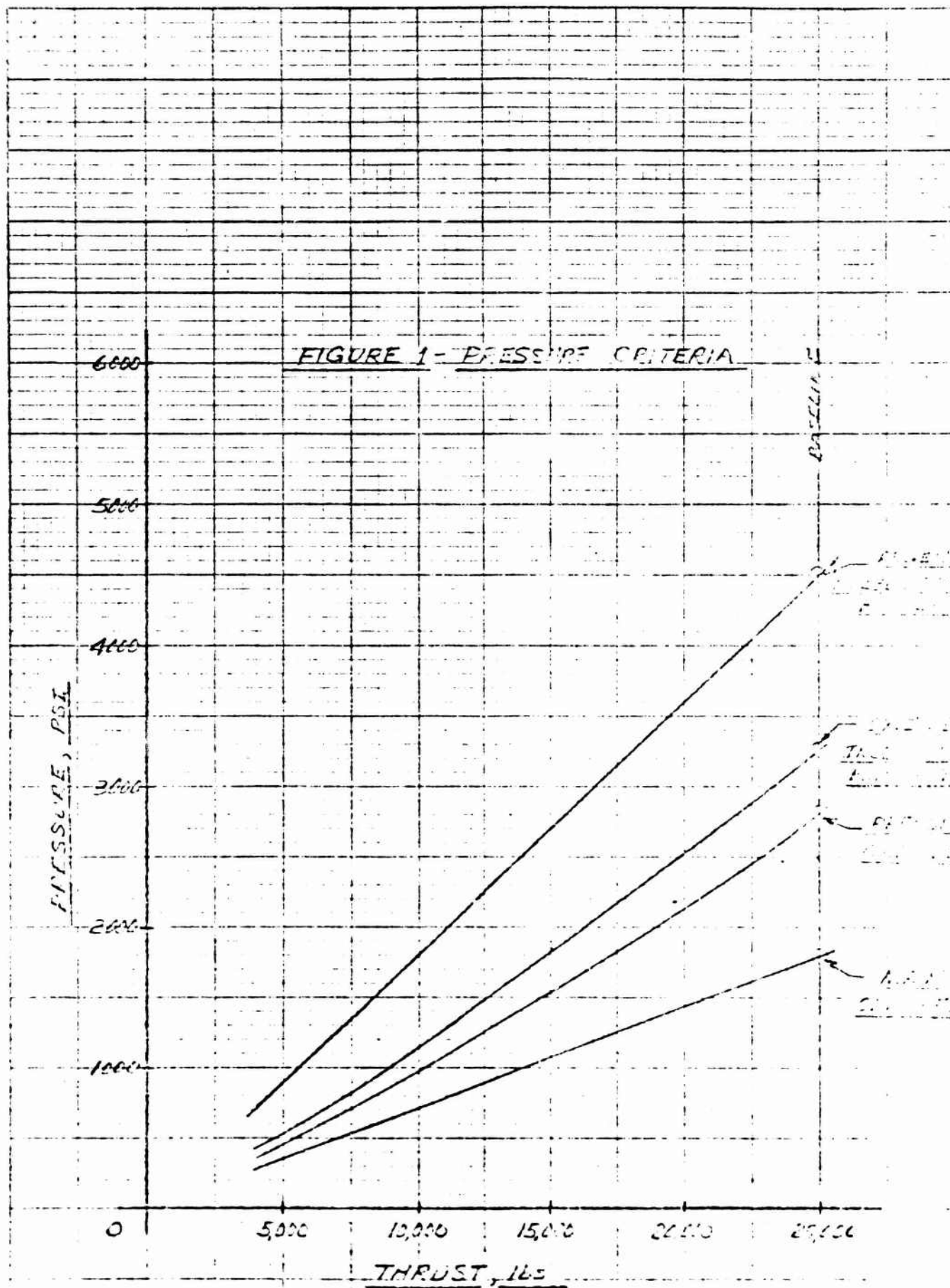
$$\sigma = 119.2 F \pm 50 F$$

$$\sigma_{max} = 169.2 F$$

$$95\% F_{ty} = 44,000 \text{ psi} \quad \dots \text{ Figure 2}$$

$$\therefore F = \frac{44,000}{169.2} = 260 \text{ lbs.}$$

$$P_{max} = \frac{3(260)}{2\sqrt{2}} = 4,425 \text{ lb/in.}$$





4008 0800-11

SUBJECT

DATE  
5/20/71

WORK ORDER  
1811-05-001

BY

GHS

CHK. BY

DATE

FIGURE 2 - MECHANICAL PROPERTIES OF ARMCO 22-13-5  
SHEET (REFERENCE)

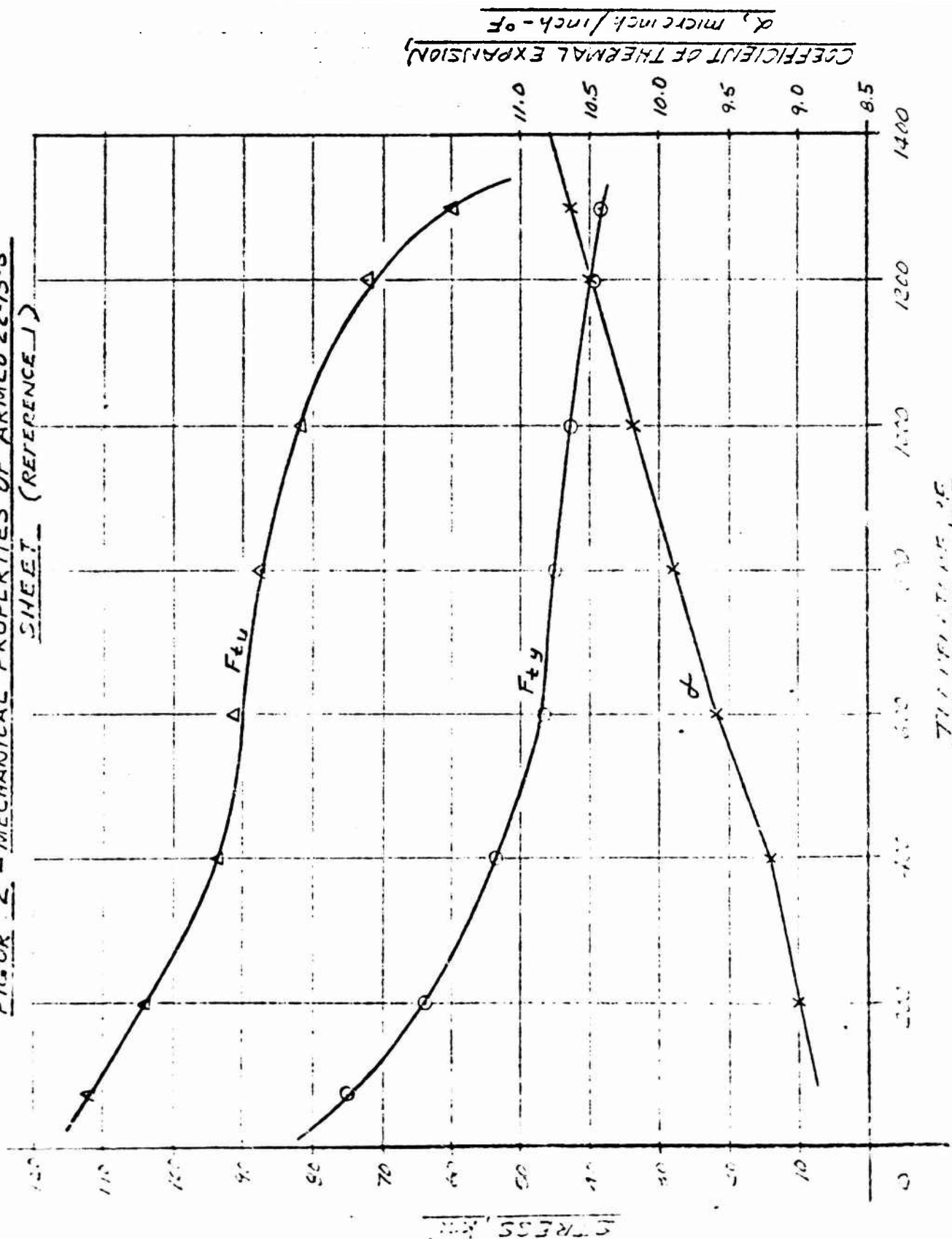


FIGURE 3 - ARMCO-22-13-5 LOW CYCLE FATIGUE  
LIFE (REFERENCE 2)

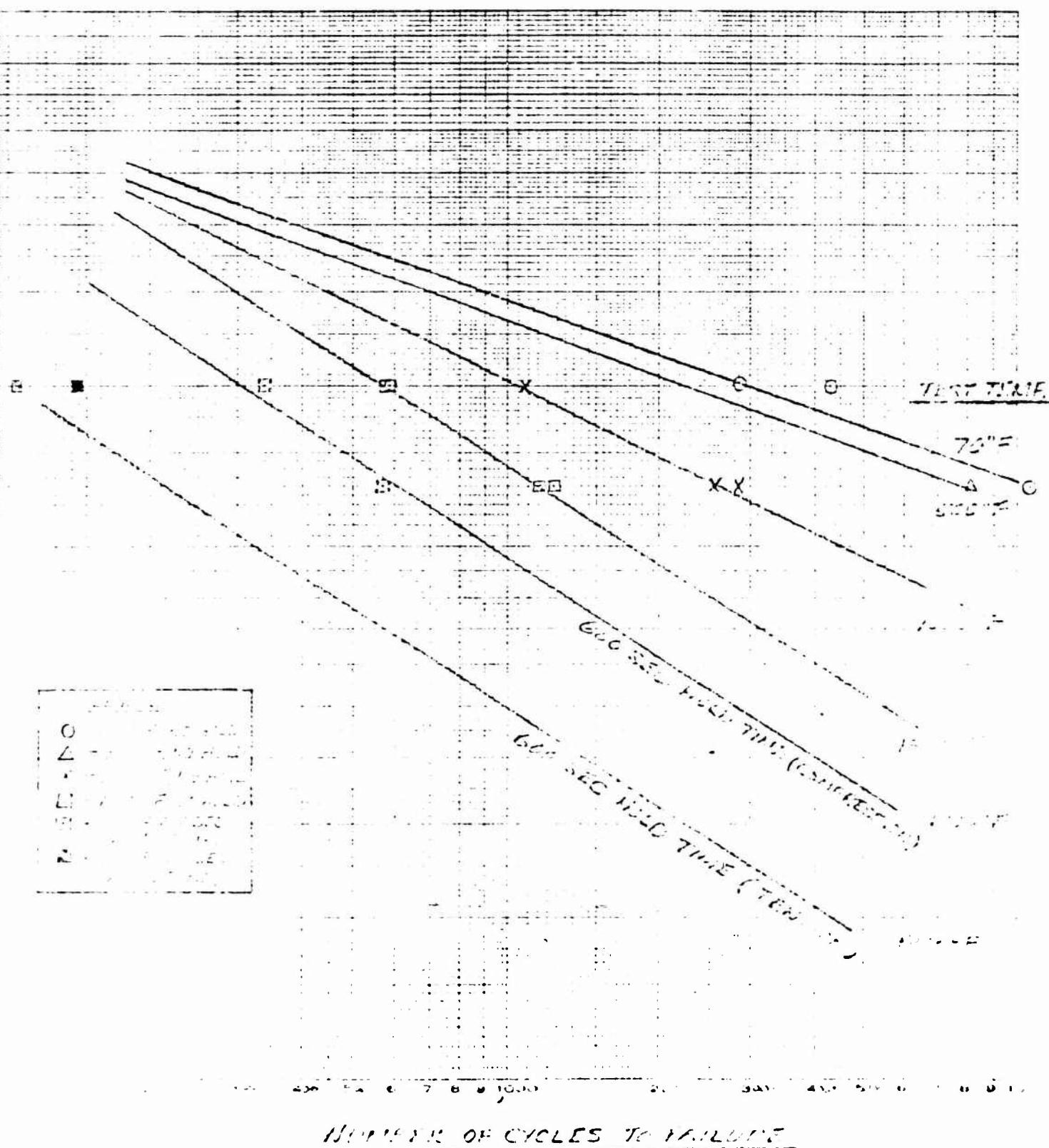


FIGURE 4 - APMCO 22-13-5 LCF DATA (1.3% STRAIN)

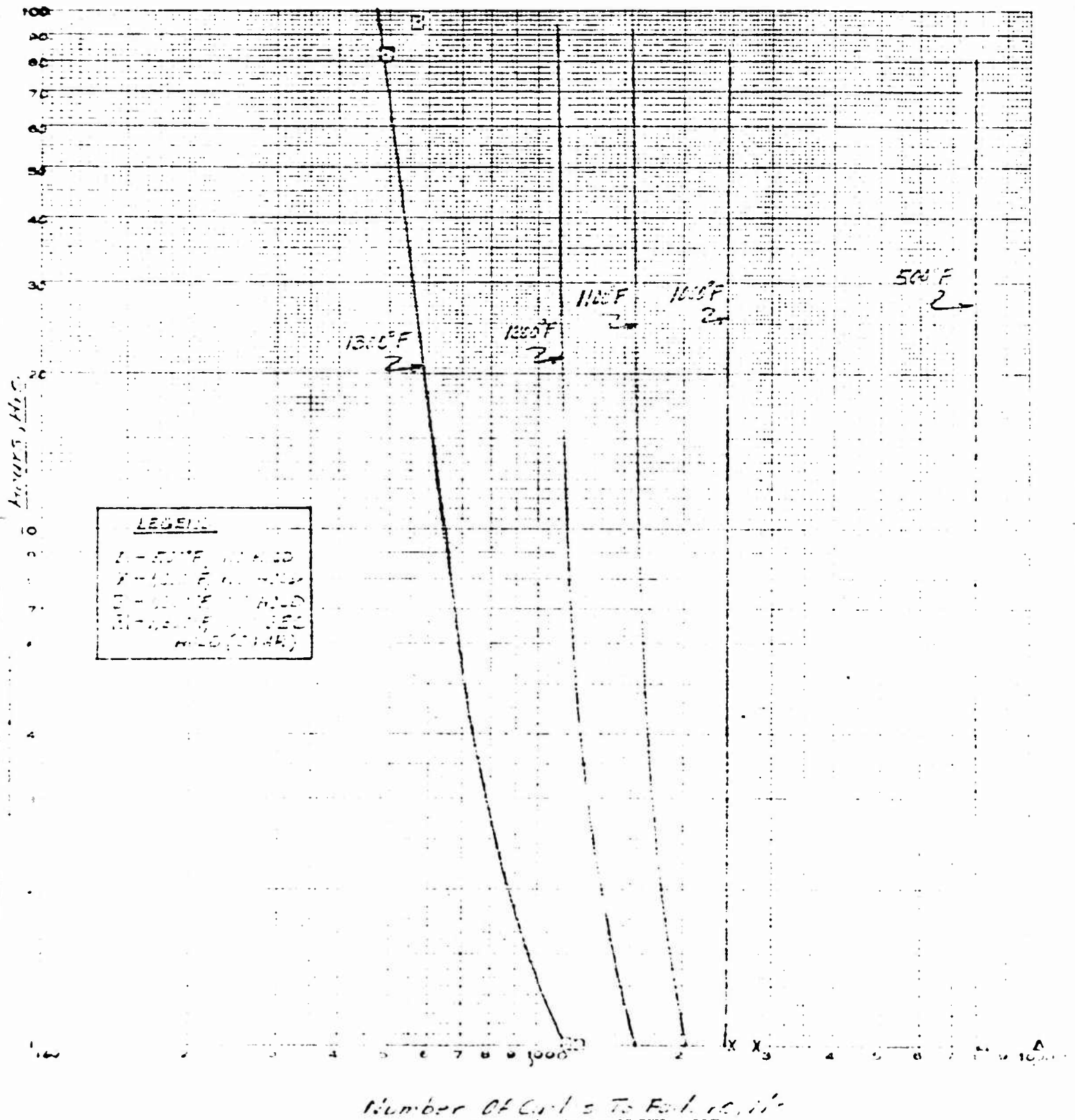
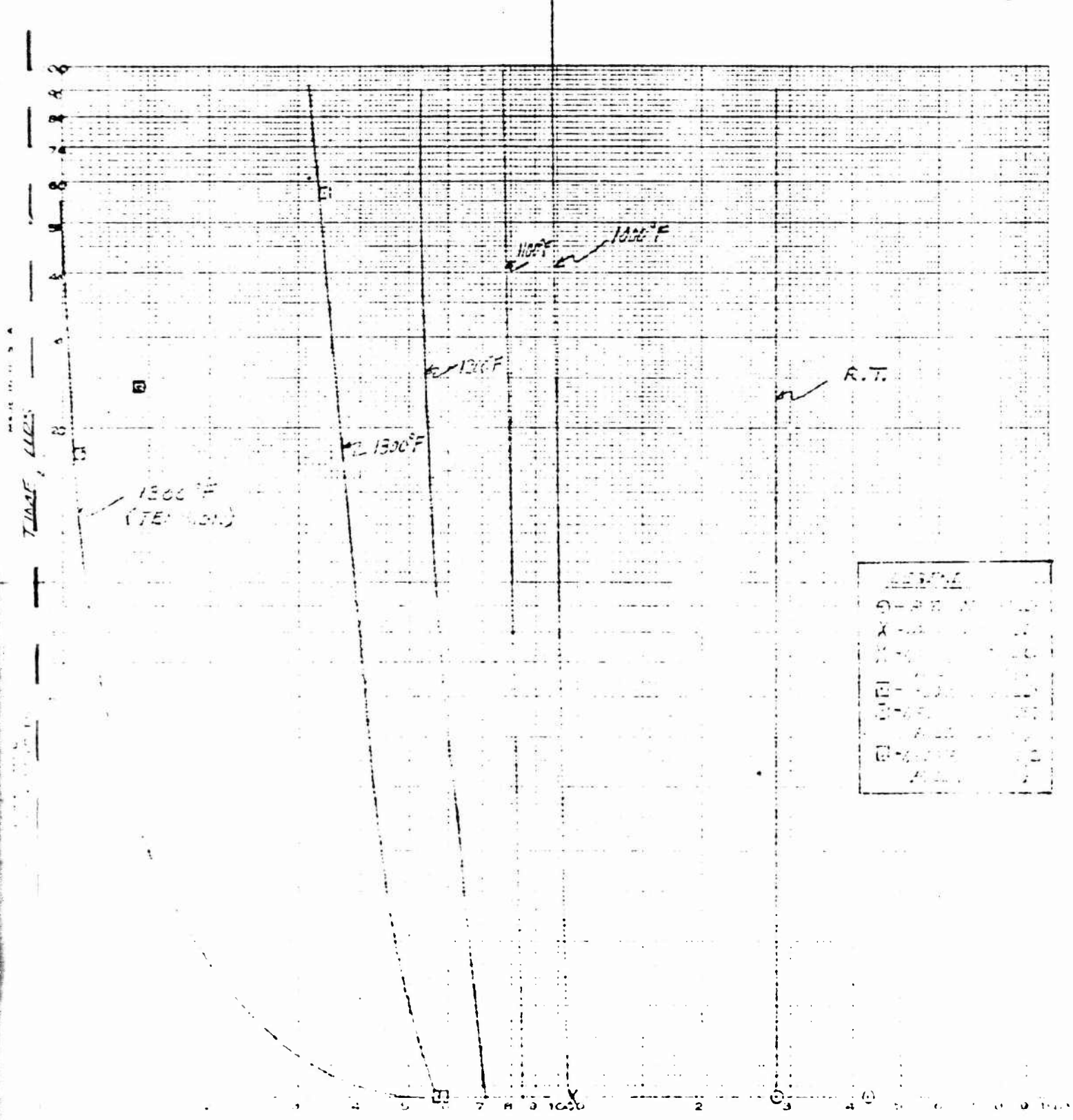




FIGURE 5 - ARMCO 22-13-5 LCF DATA (2.0% STRAIN)

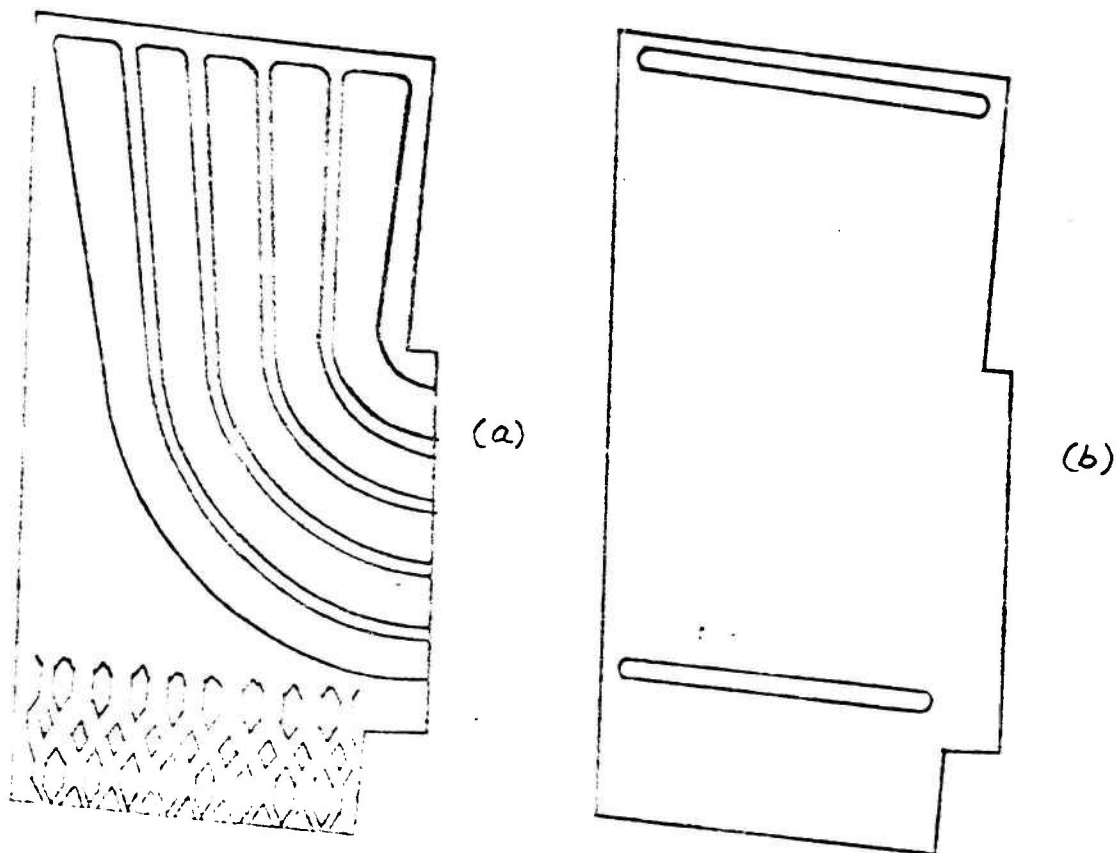


Number of Cycles to Failure,  $N_f$

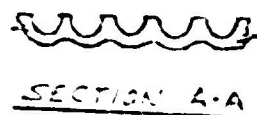
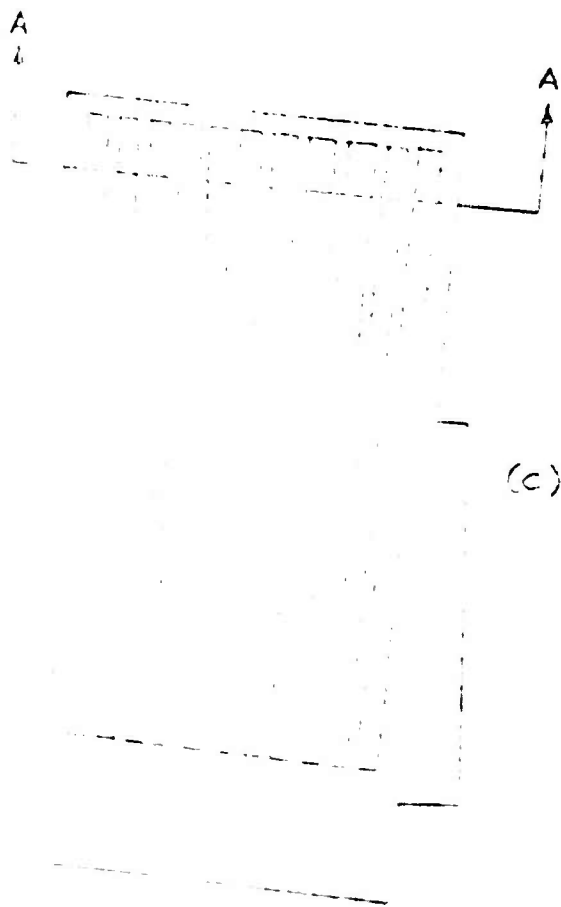
Curves are based on 2.0% Strain in Compression Unless Otherwise Indicated



FIGURE 6      MAIN INJECTOR HALF VANE



~ NOT TO SCALE ~



NOTE:

TOTAL VANE ASSEMBLY CONSISTS  
OF TWO EACH OF ABOVE PLATTERS.



TEMPERATURE PROFILE FOR VARIOUS PERCENTAGES

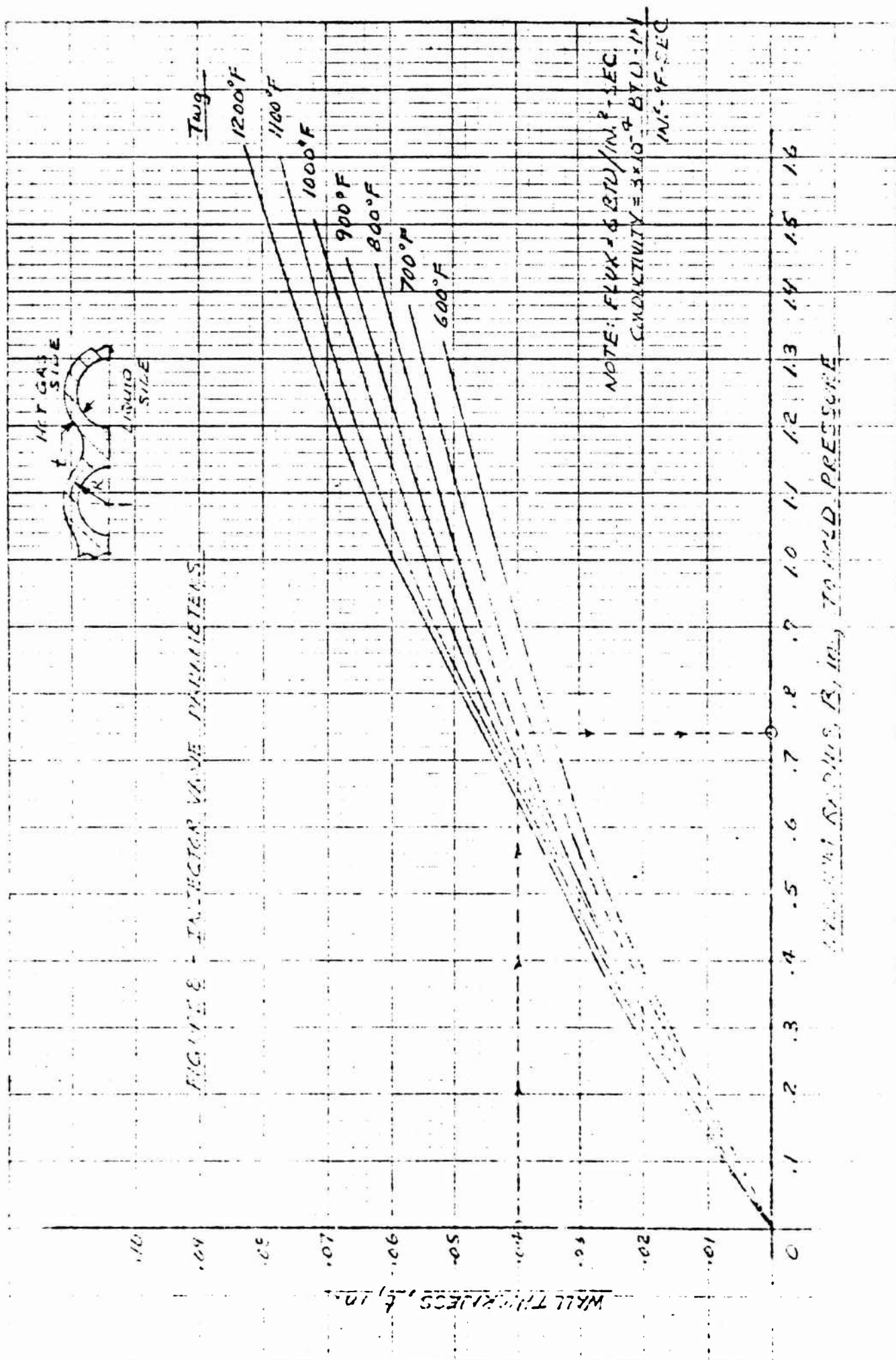
0.00  
0.01  
0.02  
0.03  
0.04  
0.05  
0.06  
0.07  
0.08  
0.09  
0.10

Temp  
1200°F  
1100°F  
1000°F  
900°F  
800°F  
700°F  
600°F

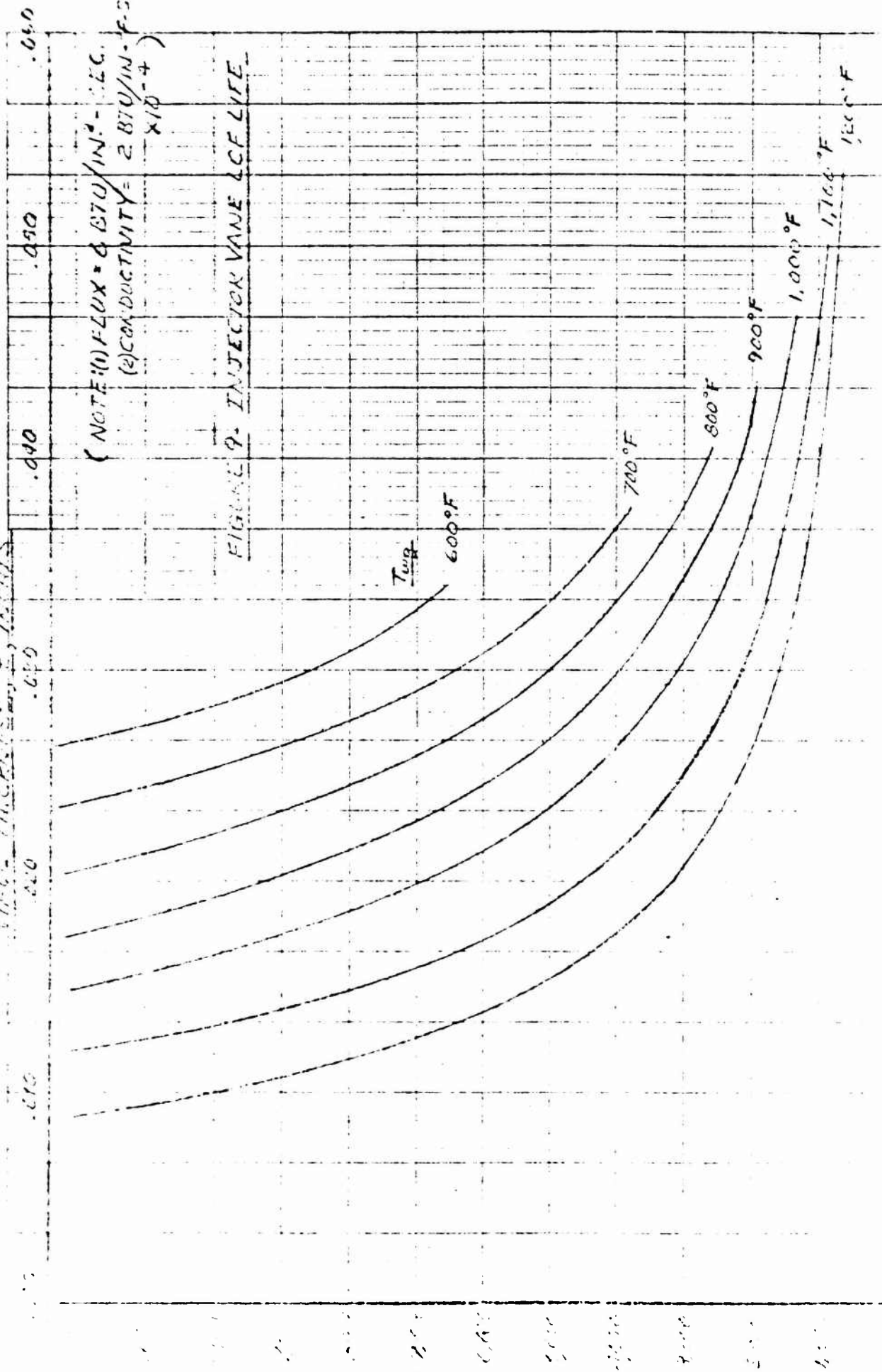
NOTE: FLUX = 8 BTU/IN<sup>2</sup> SEC.  
CONDUCTIVITY =  $2 \times 10^{-9}$  BTU-IN  
/IN<sup>2</sup>°F-SEC

15

TEMPERATURE PROFILE FOR VARIOUS PERCENTAGES

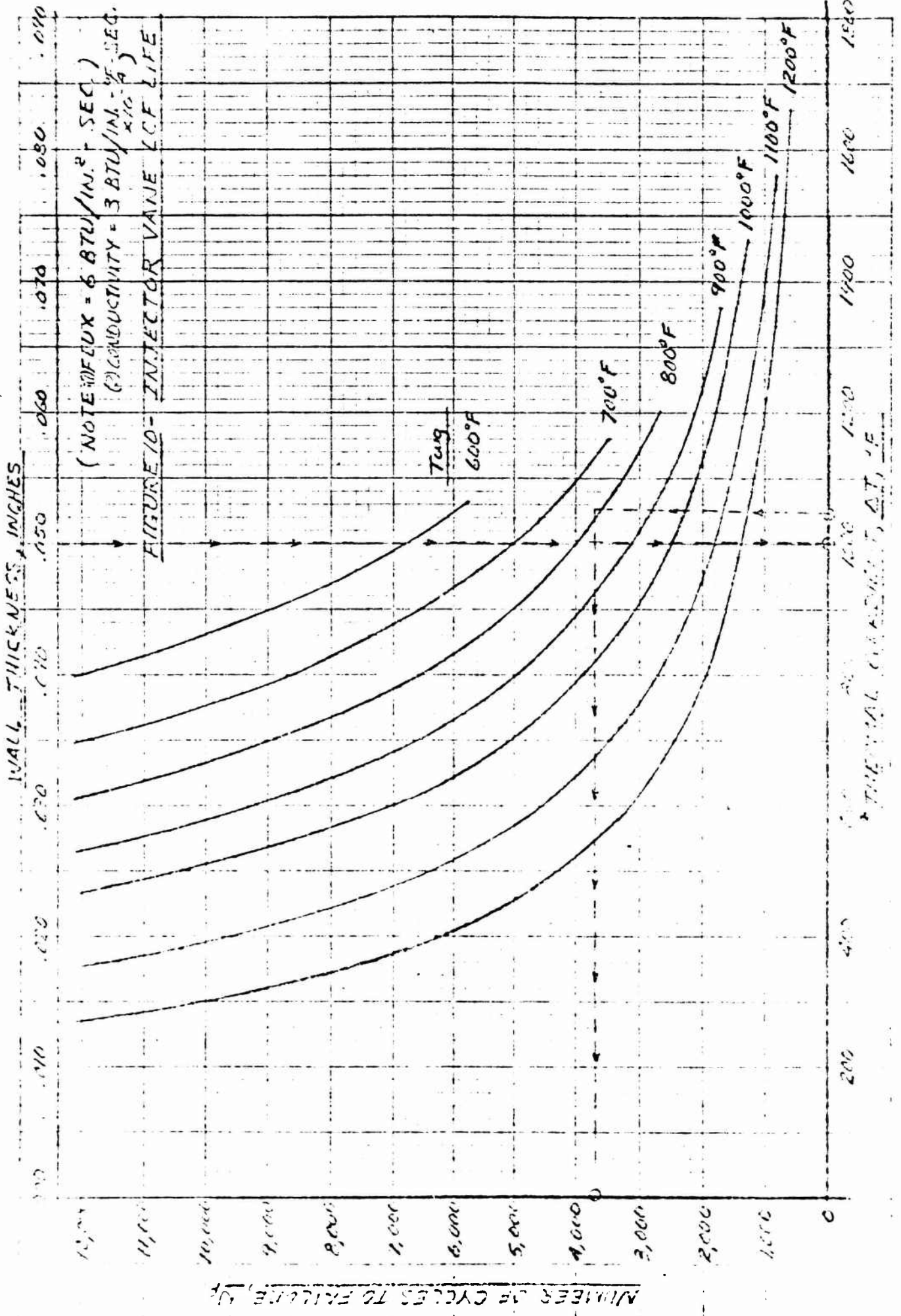


WALL THICKNESS, INCHES

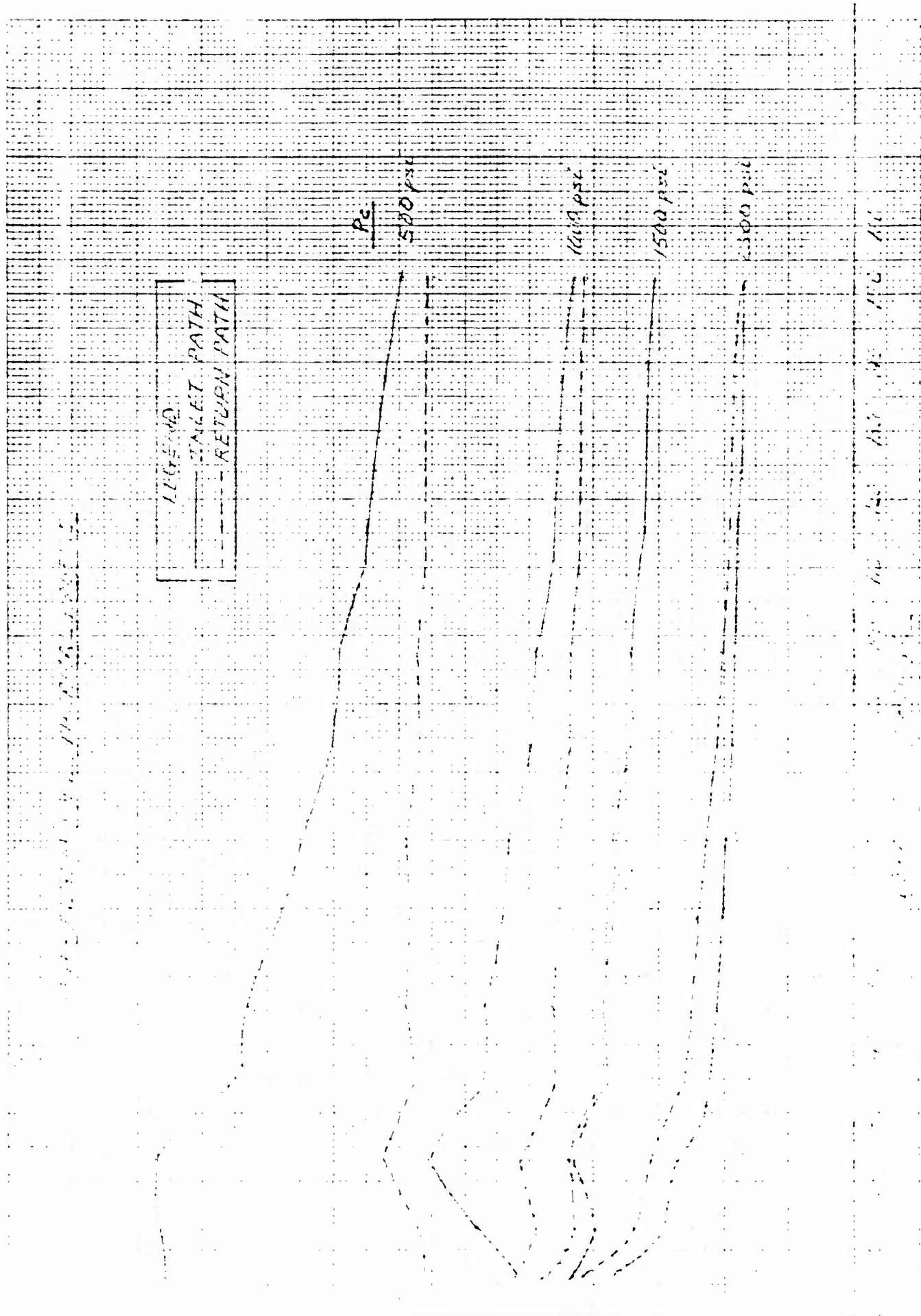


(NOTE: (1) FLUX = 0.870/IN.<sup>2</sup> - SEC.  
(2) CONDUCTIVITY = 2.870/IN.-F.-IN.  
X 10<sup>-4</sup>)

FIGURE 9. INJECTOR VANE LCF LIFE









AEROJET-GENERAL CORPORATION  
SACRAMENTO • CALIFORNIA

REPORT NO

SA-005-CC-33

PAGE 34 OF 37

DATE

5/14/71

WORK ORDER

1811-06101

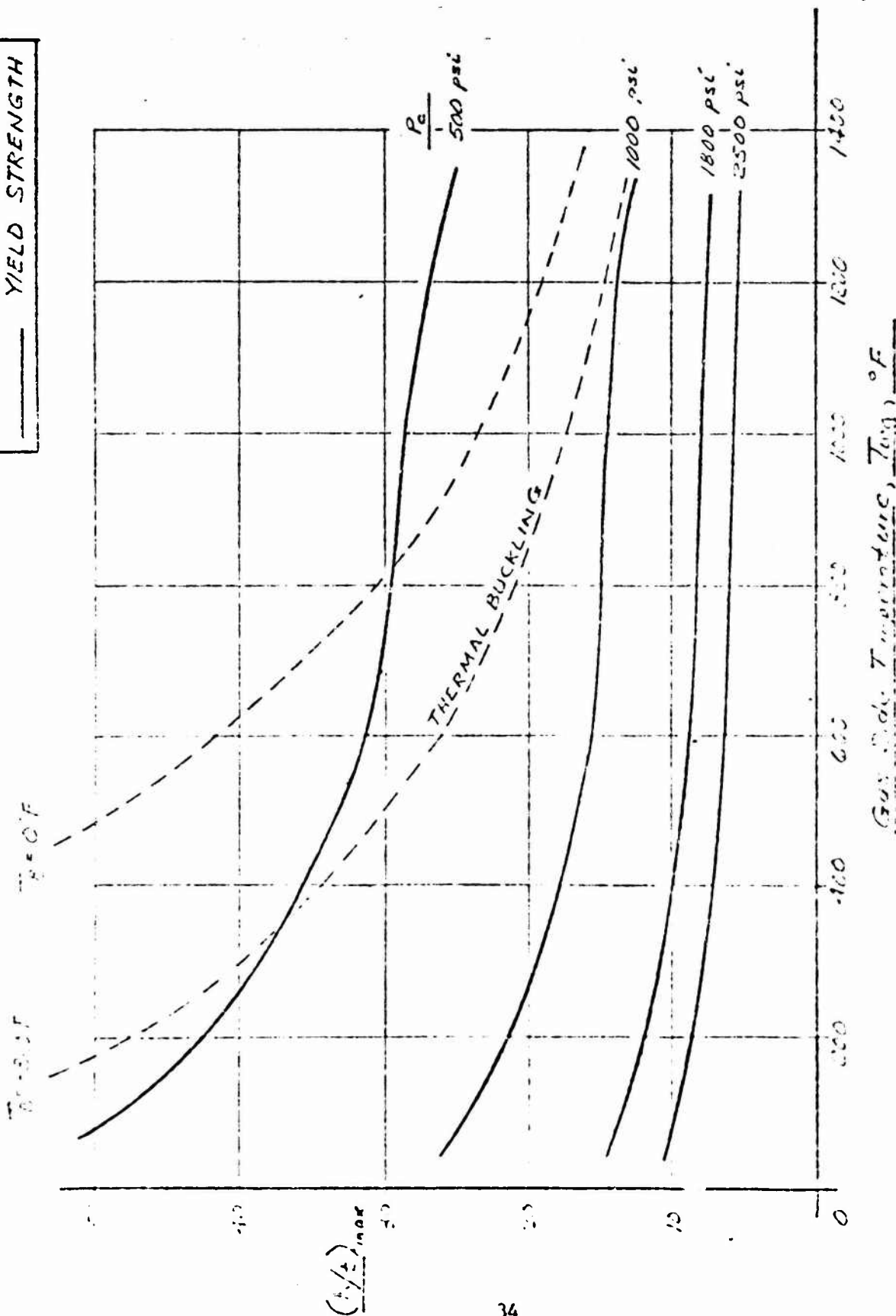
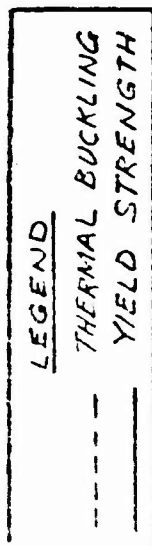
FIGURE 12 REGEN. TUBE PARAMETERS

BY

GHS

CHK. BY

DATE



(NOTE: TOTAL PRESSURE = 2500 psi)

FIGURE 13 - REGENERATOR LCF LIFE VS  $T_{avg}$

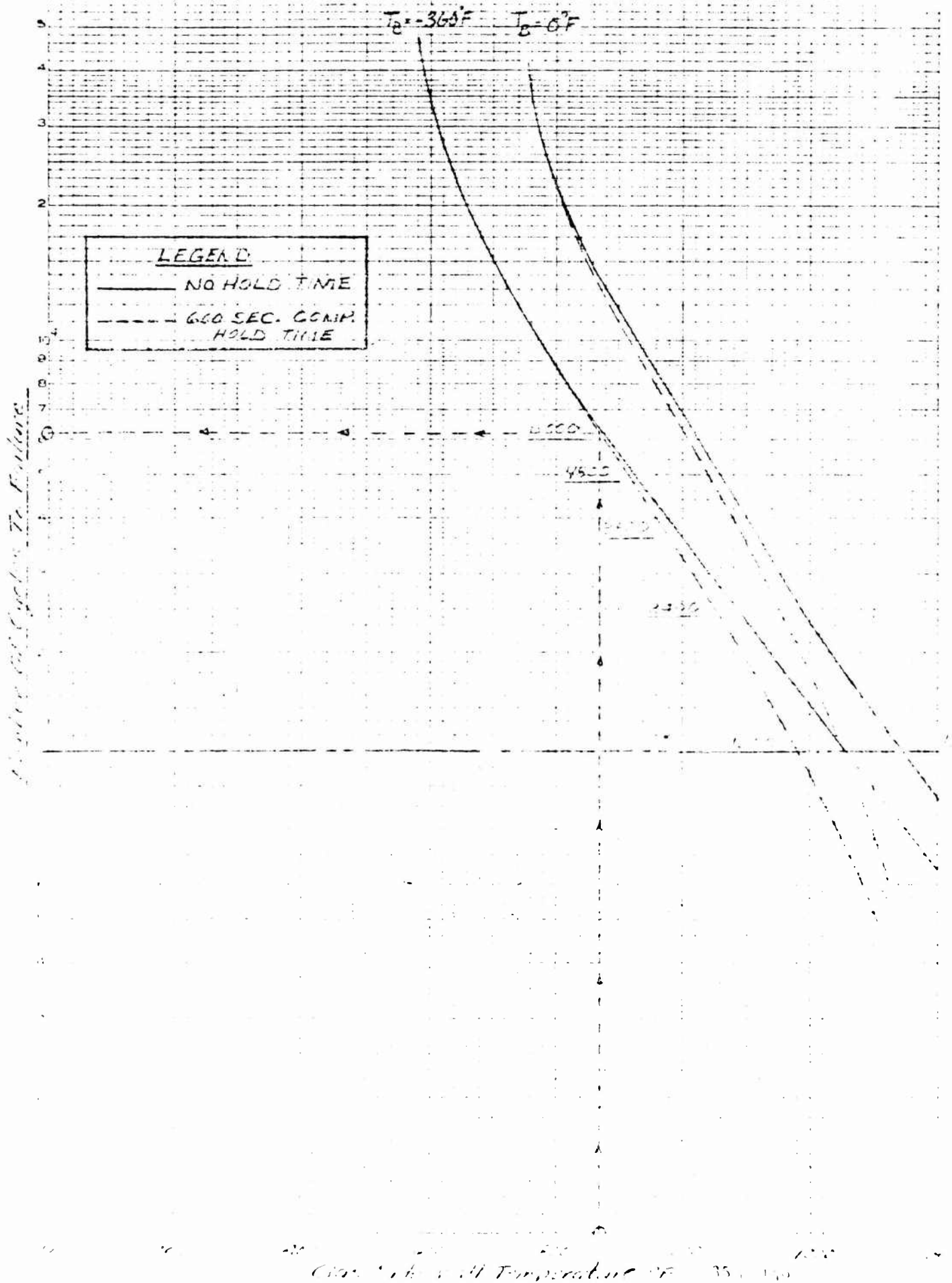
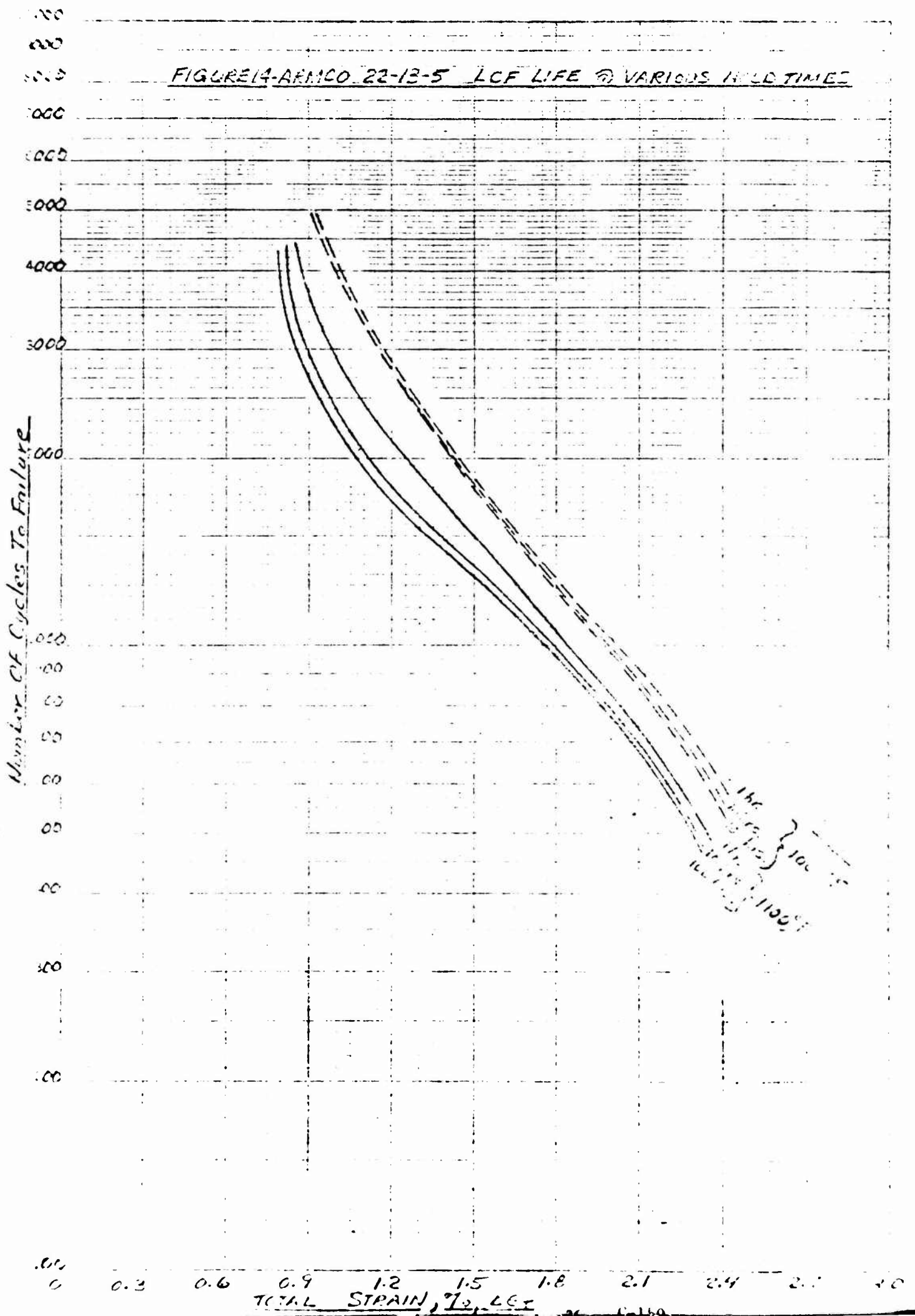




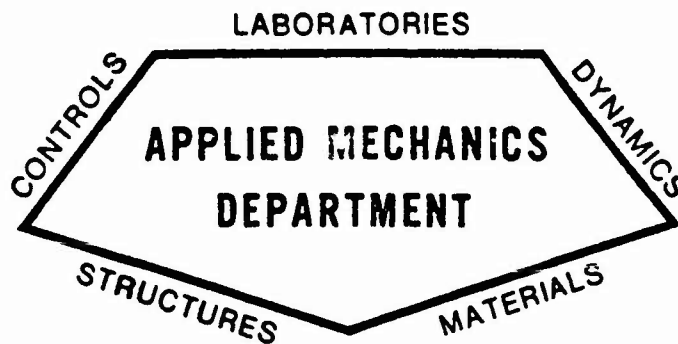
FIGURE 14-ARMCO 22-13-5 LCF LIFE @ VARIOUS HOLD TIMES



## VII. REFERENCES

1. "ARMCO 22-13-5 Stainless Steel Sheet and Strip," Developmental Alloy Data Bulletin, Armco Steel Corporation, Advanced Materials Division, Department LA-6270, P. O. Box 1697, Baltimore, Maryland 21203.
2. "AJ550 Materials Technology Programs," DRDSE-278, Part B, NASA Contract No. NAS 8-26188, Aerojet Liquid Rocket Company, Sacramento, California 95813, March 1971.
3. Avery, L. R., Carayanis, G. S., Michky, G. L., "Thermal-Fatigue Tests of Restrained Combustor-Cooling Tubes," Experimental Mechanics, 7 (6), June 1967, Pg. 256-264.
4. Neudecker, J. W., King, C. R., "Thermal-Fatigue Tests of Rocket-Nozzle Coolant Tubes," Society for Experimental Stress Analysis, 21 Bridge Square, Westport, Connecticut, October 1969.
5. "Metallic Materials and Elements for Aerospace Vehicle Structures," Change Notice 4, Superintendent of Documents, U.S. Government Printing Office, Washington, D. C., 20402, January 5, 1970.
6. Roark, R. J., "Formulas for Stress and Strain," 3rd ed., McGraw-Hill Book Co., Inc., New York, N. Y., 1954.
7. Skopp, G. H., "Orbit-Orbit Shuttle Parametric Studies, SA-OOS-CC-01, Aerojet Liquid Rocket Company, Sacramento, Calif., May 7, 1971.
8. Bornscheuer, "German Ring Report," Peenewunde Army Proving Grounds, Karlshagen, Germany, June 1944.
9. Severud, L. K., "A Survey of Structural Engineering Analysis and Test Practices in the Design of Liquid Rocket Engines," Report No. SM-5, Aerojet Liquid Rocket Company, Sacramento, Calif., June 1970.

OOS TPA CRITICAL SPEED ANALYSES



## STRUCTURAL ENGINEERING SECTION

REPORT NO. SA-OOS-TM-1

OOS FTPA CRITICAL  
SPEED ANALYSES

PREPARED BY:

*L. W. Bartholf*

L. W. Bartholf  
Engineering Specialist  
Structural Engineering Section

APPROVED BY:

*L. K. Severud*

L. K. Severud, Manager  
Structural Engineering Section  
Engineering

DATE July 1971



AEROJET LIQUID ROCKET COMPANY

SACRAMENTO, CALIFORNIA

## TABLE OF CONTENTS

	<u>Page</u>
I. Introduction	1
II. Method of Analysis	1
III. Summary of Results	1
IV. Conclusions	2
V. Analysis	2
A. Design Criteria	2
B. Operating Speeds	3
C. Detailed Results	4
Appendix I	12

## LIST OF FIGURES

<u>Figure</u>	<u>Title</u>	<u>Page</u>
1	Critical Speed vs Bearing Spring Constants	4
2	Turbine End Bearing Whirl Loads	5
3	Pump End Bearing Whirl Loads	6
4	OOS Fuel Turbopump Concept with Full Flow Turbine Driven Inducer	9
5	OOS FTPA Mode Shapes	10
6	OOS FTPA Critical Speed Stiffness and Lumped Mass Model	11

## LIST OF TABLES

<u>Table</u>	<u>Title</u>	<u>Page</u>
I	Rotor Dynamic Analysis Parameters	7

## I. INTRODUCTION

The following report contains the critical speed analyses which have been performed for the OOS Fuel Turbopump assembly as shown on Figure 4. The design investigated incorporates 25 mm angular contact bearings at the pump end and 20 mm angular contact bearings for the turbine end.

Parametric studies were initially performed for the rotor shaft to demonstrate feasibility. These analyses are included in the report as Appendix I. Following the parametric studies, a more detailed analysis was performed for the turbopump design selected. The results of these analyses are presented in the main body of the report.

## II. METHOD OF ANALYSIS

The enclosed analysis was accomplished using a computer program which predicts bearing loads, shaft deflections and critical speeds. It is based on a lumped parameter method of analysis for determining forced lateral vibrations of a beam having variable section properties. As output, the program computes the amplitudes of shears, moments, slopes and deflection attributable to harmonic forcing functions and in addition determines the rotary inertia and gyroscopic effects for rotating shafts.

## III. SUMMARY OF RESULTS

The results of the rotor-only parametric analysis are shown in Figure 1 where the first three rotor critical speeds are plotted versus effective radial stiffness at the bearing supports. These results indicate that with an effective radial stiffness of about  $0.03 \times 10^6$  lb/in. at each bearing the operating requirements can be met as follows:

For $K_{eff} = .06 \times 10^6$ lb/in. per bearing set	
$N_{1R} = 16000$ rpm	} shaft rigid critical speeds
$N_{2R} = 24000$ rpm	
$N_{3B} = 92000$ rpm	shaft bending critical speed

$N_{1R}$  and  $N_{2R}$  are rotor natural frequencies that are controlled mainly by effective stiffness (K) at the bearings, whereas  $N_{3B}$  is controlled principally by shaft bending stiffness (EI).

As seen from Figures 2 and 3 the proposed operating speed range for the FTPA results in fairly low bearing reactions due to whirl loads for both bearing sets. These loads are approximately:

<u>Operating Condition</u>	<u>Total Reaction/Brg. Set (lb)</u>	
	<u>Turbine End</u>	<u>Pump End</u>
MPL	24	35
NPL	20	10

The appendix contains earlier parametric studies which were performed during the preliminary design phase of this study. It contains curves of radial stiffness versus shaft speed for proposed turbopumps having two and three stages and having various inducer designs. These data formed the background for the final investigations.

#### IV. CONCLUSION

1. Shaft critical speed requirements can be met by the turbopump configuration analyzed.

#### V. ANALYSIS

##### A. DESIGN CRITERIA

1. All rotor critical speeds shall be 15% removed from any operating speed.
2. No natural frequencies of the turbopump assembly shall exist within the normal operating speed range of 32000 rpm (MPL) and 80000 rpm (NPL).

B. OPERATING SPEEDS

Minimum Power Level, MPL	= 32000 rpm
Normal Power Level, NPL	= 80000 rpm





# 005 CRITICAL SPEED ANALYSIS

DATE  
7/12/71

WORK ORDER

BY

L.W. BARTHOLF

CHK. BY

DATE

## C. DETAILED RESULTS

005 FTPA (SELECTED CONFIGURATION)

- LATERAL VIBRATION  
- FORWARD CIRCULAR WHIRL

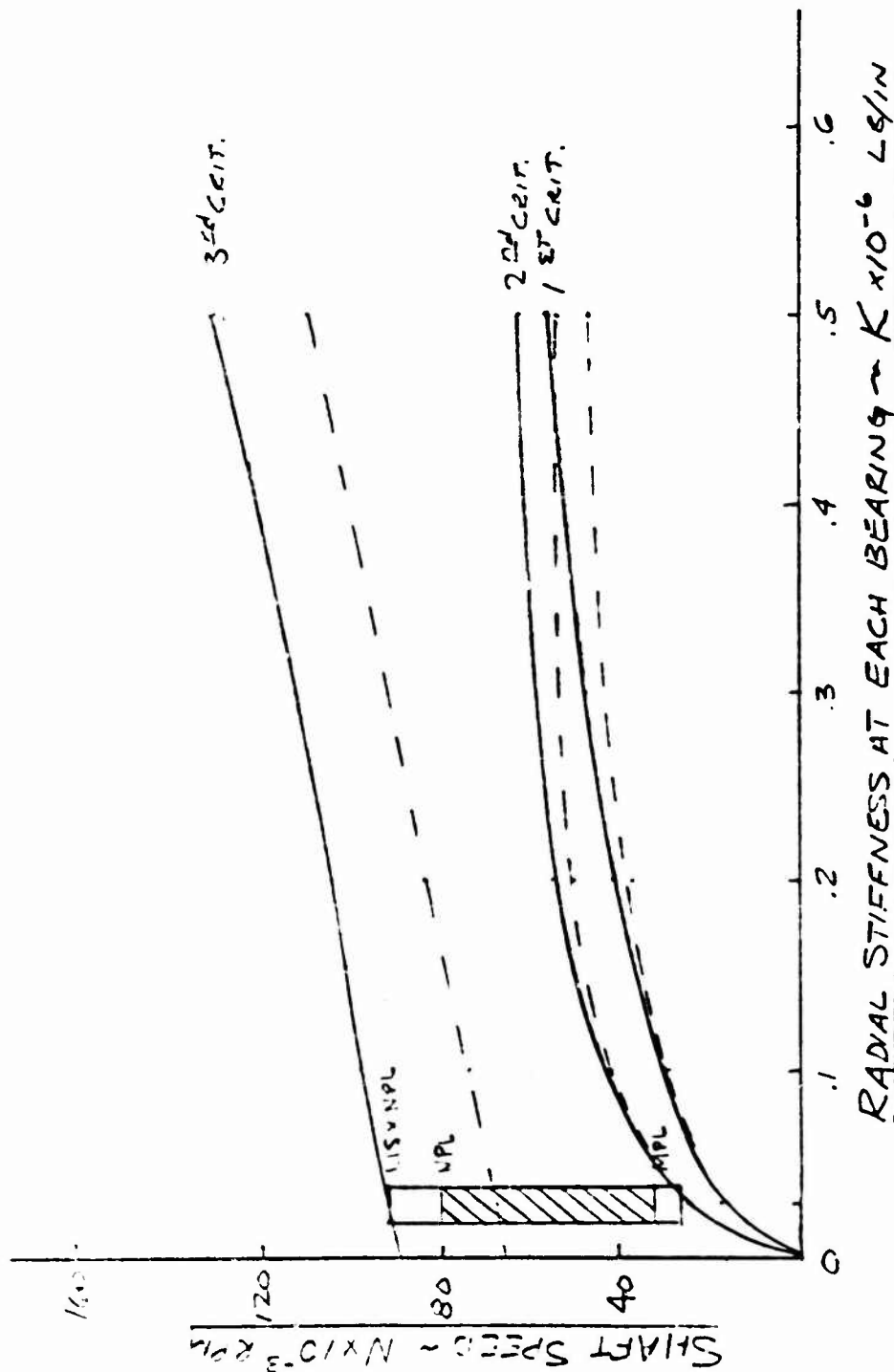


FIG. 1

CRITICAL SPEED VS. BEARING SPRING CONSTANTS



ALC-1000011

SUBJECT

005 CRITICAL SPEED ANALYSIS

DATE  
7/13/71

WORK ORDER

BY

L W BARTHOLO

CHK BY

DATE

TURBINE END BEARING WHIRL LOADS

1 MIL DIAMETRAL CLEARANCE AT BEARING SET CENTERS

CONICAL WHIRL

$K = .03(10)^6 \text{ LB/IN/BEARING} = .06(10)^6 \text{ LB/IN/SET}$

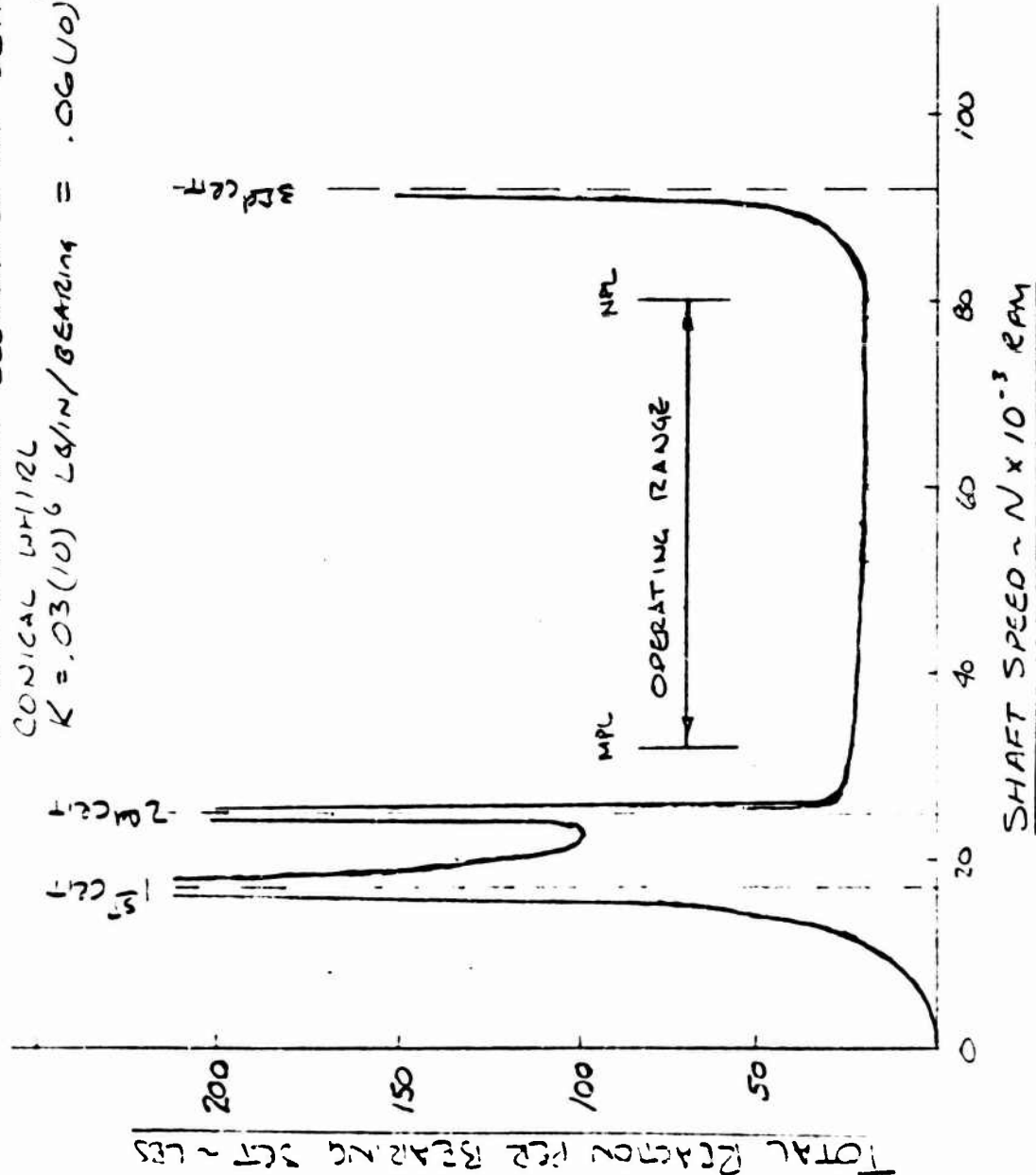


FIGURE 2



AEROJET-GENERAL CORPORATION  
SACRAMENTO • CALIFORNIA

REPORT NO.

PAGE 1 OF 1

DATE

7/12/61

WORK ORDER

DATE

# ODS CRITICAL SPEED ANALYSIS

BY

L.W. BAETHOLF

CHK BY

## PUMP END BEARING WHIRL LOADS

1 MIL DIAMETRAL CLEARANCE AT BEARING SET CENTERS

CONICAL WHIRL

$K = .03(10)^6 \text{ LB/IN/BEARING} = .06(10)^6 \text{ LB/IN/SET}$

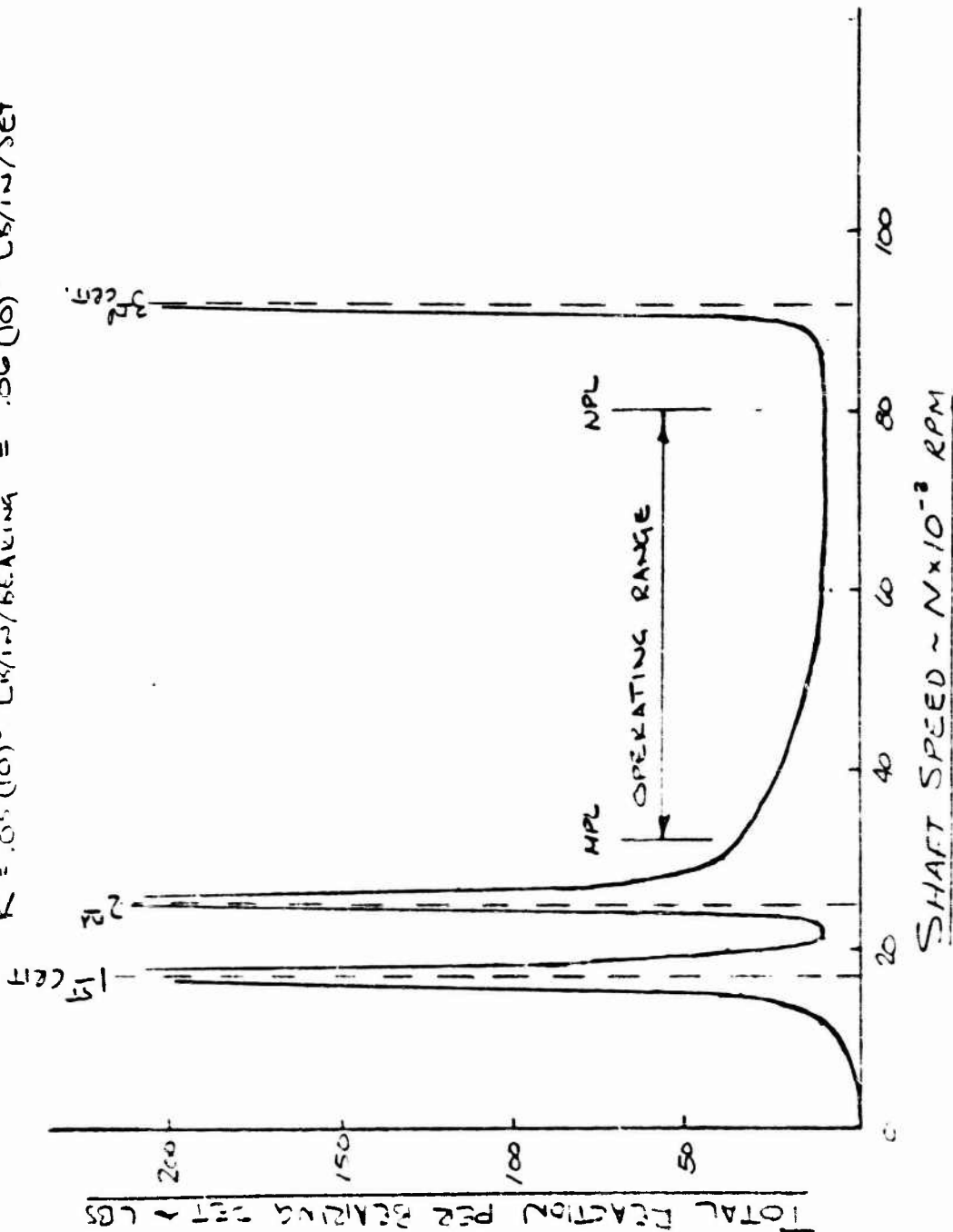


FIGURE 3



DRAWN BY: J. J. J.

SUBJECT:

## OOS CRITICAL SPEED ANALYSIS

DATE

7/12/71

WORK ORDER

BY

L.W. BARTHOLF

CHK BY

DATE

OOS FTPA CRITICAL SPEED MODEL, TABLE I

$$E_{STL} = 25 (10)^6, \quad E_{TAN} = 16 (10)^6$$

STA	L (IN)	EI	W (LBS)	$J_{EFF}$	K	C	G	$P_1$	$P_2$	$P_3$
701	.25	17 (10) <sup>6</sup>	1.0	.002	0	1	11 (10) <sup>6</sup>	2.6 (10) <sup>6</sup>	0	0
702	.33	17 (10) <sup>6</sup>	0	0	↑	↑	↑	0	↑	↑
703	.33	17 (10) <sup>6</sup>	1.0	.002	↑	↑	↑	22 (10) <sup>6</sup>	↑	↑
704	.65	17 (10) <sup>6</sup>	.7	0	↓	↑	↑	0	↑	↑
705	.25	5 (10) <sup>6</sup>	.1	0	0	↑	↑	↑	↑	↑
706	.33	1 (10) <sup>6</sup>	.1	0	K	↑	↑	↑	↑	↑
707	.33	1 (10) <sup>6</sup>	.1	0	K	↑	↑	↑	↑	↑
708	.33	1 (10) <sup>6</sup>	.1	0	K	↑	↑	↑	↑	↑
709	.25	1 (10) <sup>6</sup>	.1	0	0	↑	↓	↑	↑	↑
710	.12	2 (10) <sup>6</sup>	0	0	↑	↑	11 (10) <sup>6</sup>	↓	↑	↑
711	.36	5 (10) <sup>6</sup>	0	0	↑	↑	6 (10) <sup>6</sup>	0	↑	↑
712	.40	14 (10) <sup>6</sup>	1.3	.003	↑	↑	↑	.6 (10) <sup>6</sup>	↑	↑
713	.37	14 (10) <sup>6</sup>	0	0	↑	↑	↑	0	↑	↑
714	.50	7 (10) <sup>6</sup>	.15	0	↑	↑	↑	0	↑	↑
715	.49	7 (10) <sup>6</sup>	0	0	↑	↑	↑	0	↑	↑
716	.30	14 (10) <sup>6</sup>	1.0	.002	↑	↑	↑	-.5 (10) <sup>6</sup>	↑	↑
717	.30	14 (10) <sup>6</sup>	0	0	↓	↑	↓	0	↑	↑
718	.30	7 (10) <sup>6</sup>	0	0	↓	↑	6 (10) <sup>6</sup>	↑	↑	↑
719	.13	3 (10) <sup>6</sup>	.1	0	0	↑	11 (10) <sup>6</sup>	↑	↑	↑
720	.33	.8 (10) <sup>6</sup>	.1	0	K	↑	↑	↑	↑	↑
721	.30	.3 (10) <sup>6</sup>	.1	0	K	↑	↑	↑	↑	↑
722	.31	.3 (10) <sup>6</sup>	.1	0	K	↑	↑	↑	↑	↑
723	.29	.5 (10) <sup>6</sup>	.1	0	0	↑	11 (10) <sup>6</sup>	↑	↑	↑
724	.29	.3 (10) <sup>6</sup>	0	0	↑	↑	6 (10) <sup>6</sup>	↑	↑	↑
725	.11	1 (10) <sup>6</sup>	0	0	↑	↑	↑	0	↑	↑
726	.36	5 (10) <sup>6</sup>	1.0	.002	↑	↑	↑	-.2 (10) <sup>6</sup>	↑	↑
727	.43	5 (10) <sup>6</sup>	0	0	↑	↑	↑	0	↑	↑
728	.52	6 (10) <sup>6</sup>	.1	0	↓	↑	↑	0	↑	↑
729	.50	6 (10) <sup>6</sup>	.1	0	↓	↑	↑	0	↑	↑
730	.50	6 (10) <sup>6</sup>	.1	0	0	1	6 (10) <sup>6</sup>	0	0	0

$$J_{EFF} \approx \frac{W L^3}{4 E I}$$



L.W. BARTHOLOF

# CSD CRITICAL SPEED ANALYSIS

## ESTIMATE OF WHIRL FORCING FUNCTION

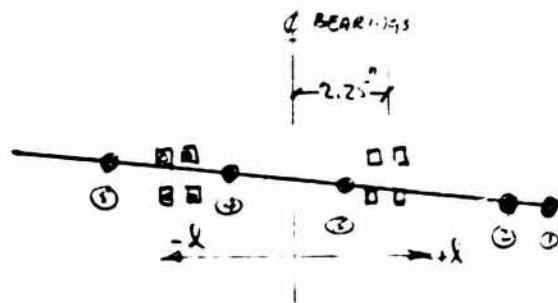
ASSUME CONICAL WHIRL WITH 1 MIL DIAMETRAL CLEARANCE AT THE CENTER OF THE BEARING SET:

$$P_1 = \frac{W}{g} y$$

$$y = A \times l$$

$$.0005 = A \times 2.25$$

$$A = .000222 = 222(10)^{-6}$$



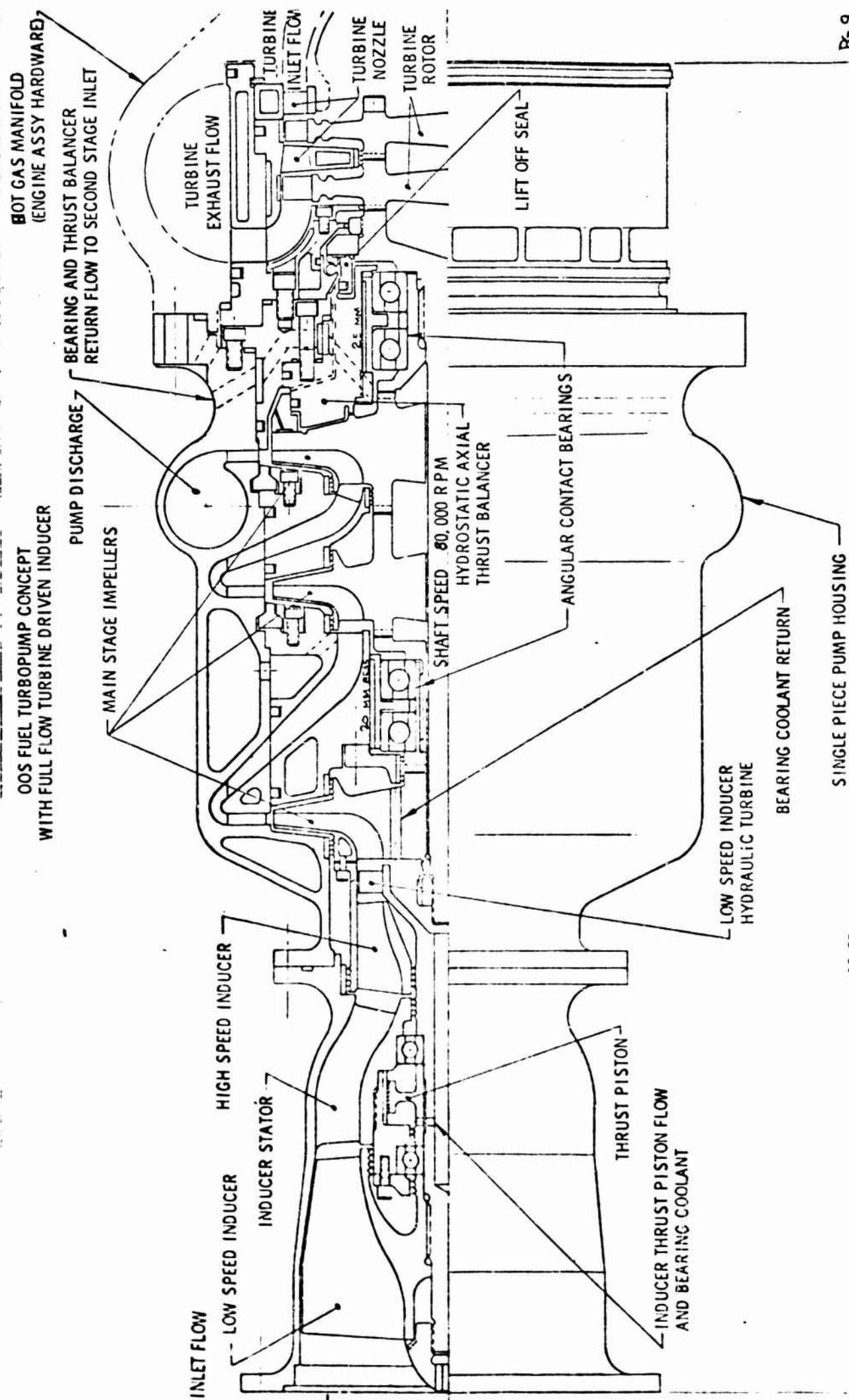
$$P_0 = \left( \frac{1}{386} \right) 222(10)^{-6} (4.5) = 2.6(10)^{-6}$$

$$P_{\odot} = \left( \frac{1}{386} \right) 222(10)^{-6} (3.8) = 2.2(10)^{-6}$$

$$P_{\ominus} = \left( \frac{1.3}{386} \right) 222(10)^{-6} (.8) = .6(10)^{-6}$$

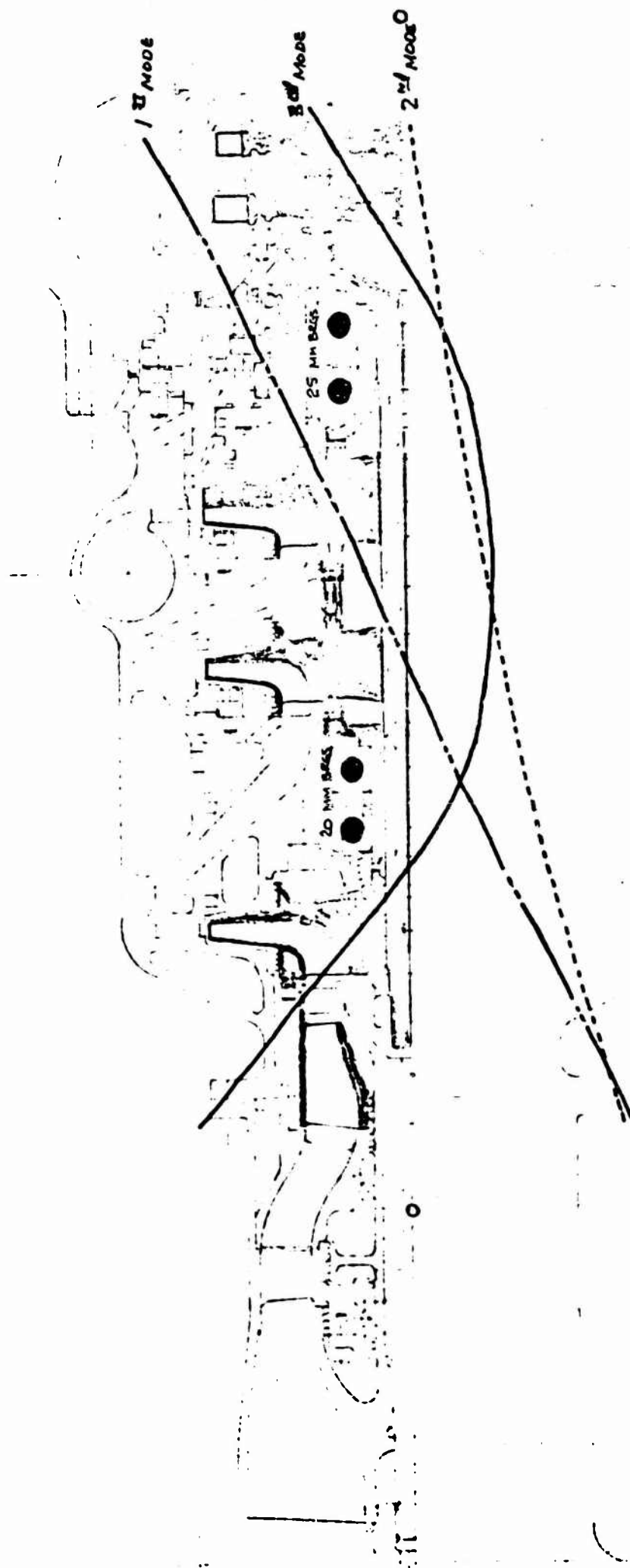
$$P_{\oplus} = \left( \frac{1.0}{386} \right) 222(10)^{-6} (-.9) = -.5(10)^{-6}$$

$$P_{\ominus} = \left( \frac{1.0}{386} \right) 222(10)^{-6} (-3.4) = -2.1(10)^{-6}$$



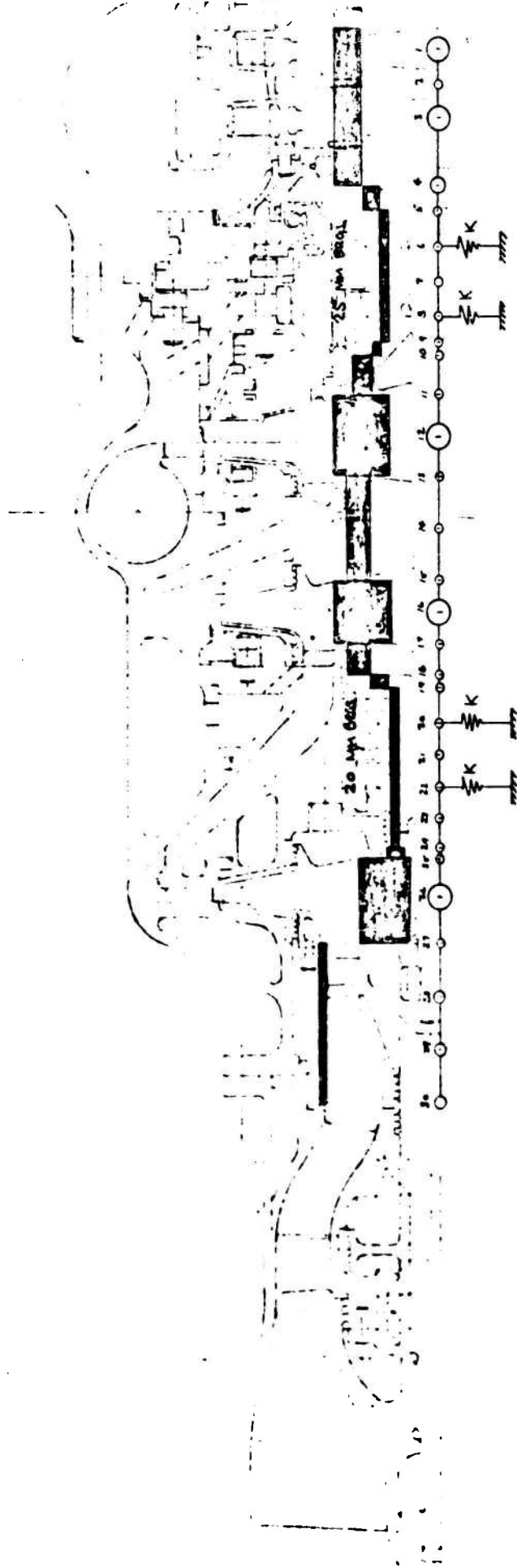
OOS FTPA  
7/8/1

OOS FTPA MODE SHAPES  
K = .03 (10)<sup>6</sup> LB/IN/BEARING



OOS FTPA  
7/8/71

# OOS FTPA CRITICAL SPEED STIFFNESS AND LUMPED MASS MODEL





**APPENDIX I**  
**PARAMETRIC STUDIES**



AEROJET-GENERAL CORPORATION  
SACRAMENTO • CALIFORNIA

REPORT NO

PAGE 1.1 OF

DATE  
6/2/71

WORK ORDER  
1911-01-101

# OOS CRITICAL SPEED

BY

L.W. BARTHOLOP

CHK BY

DATE

## OOS FTPA

### 3 STAGE WITH SHROUDED OVERLAPPING INDUCER

-- LATERAL VIBRATION  
-- FORWARD CIRCULAR WHIEL

3<sup>rd</sup> CRIT.

2<sup>nd</sup> CRIT  
1<sup>st</sup> CRIT

115XNR

NPL

1.0

SHAFT SPEED  $\sim N \times 10^3$  RPM

RADIAL STIFFNESS AT EACH BEARING  $\sim K \times 10^{-6}$  LB/IN



AEROJET-GENERAL CORPORATION  
SACRAMENTO • CALIFORNIA

REPORT NO.

PAGE 1, 2 or

DATE 6/2/71

WORK ORDER 1911-05-101

# OOS CRITICAL SPEED

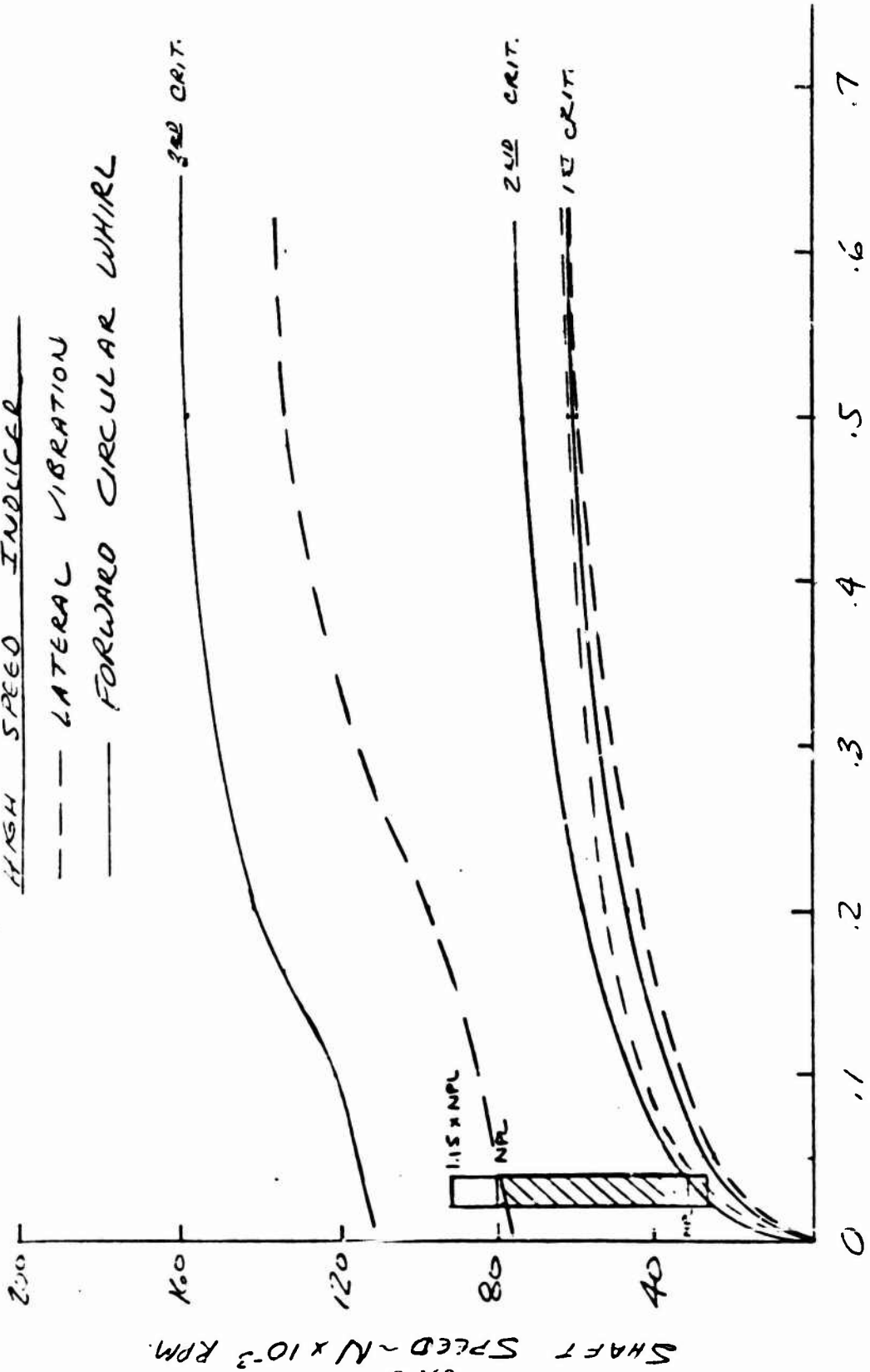
CHK BY

DATE

OOS FTPA

3 STAGE WITH CONVENTIONAL  
HIGH SPEED INDUCER

--- LATERAL VIBRATION  
--- FORWARD CIRCULAR WHIRL



RADIAL STIFFNESS AT EACH BEARING ~ K x 10<sup>-6</sup> LB/IN.



AEROJET-GENERAL CORPORATION  
SACRAMENTO • CALIFORNIA

REPORT NO.

PAGE 1.3 OF

AGC 100-11

SUBJECT

OOS CRITICAL SPEED

DATE

6/2/71

WORK ORDER

181-05-101

BY

G. ALDRICH

CHK. BY

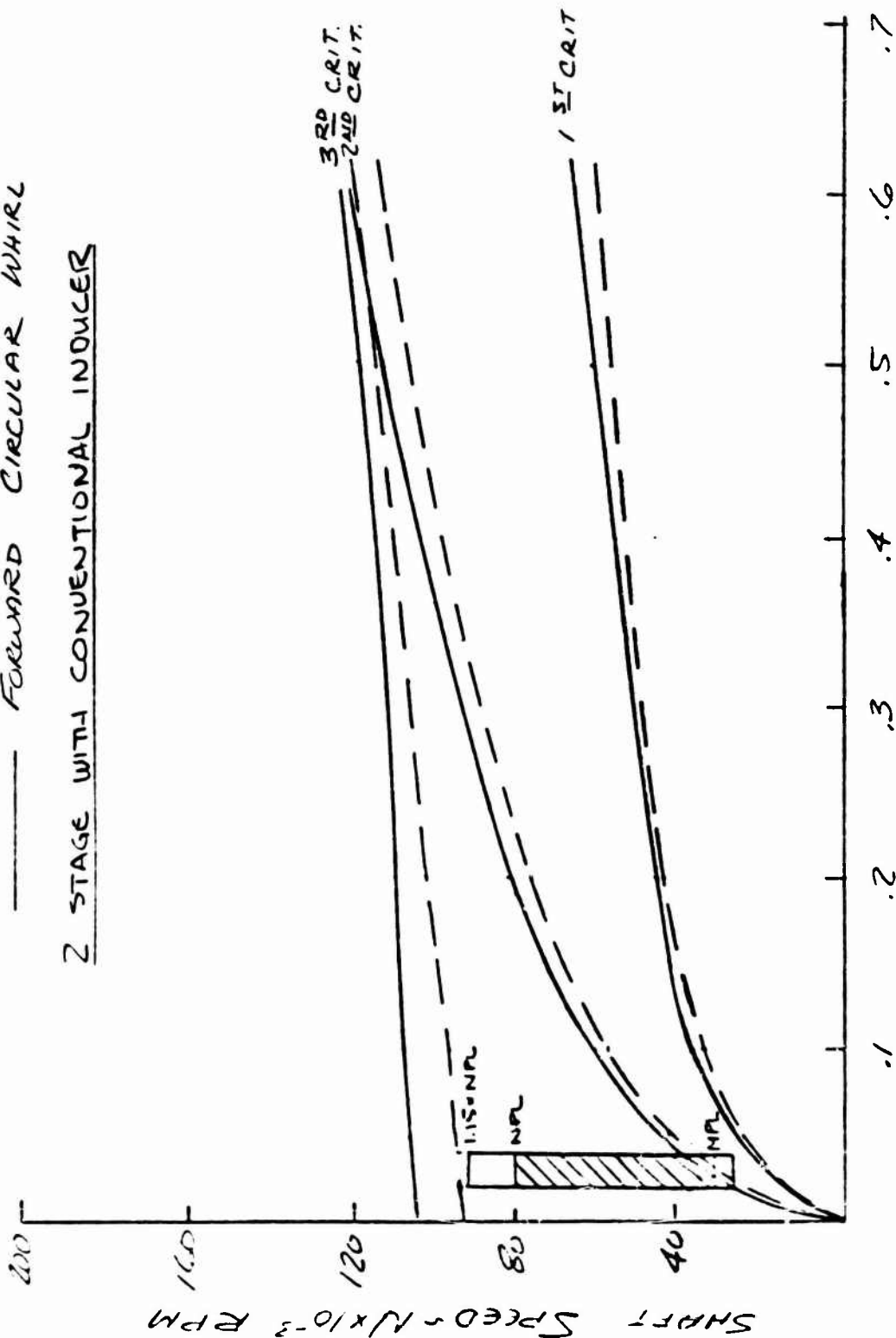
DATE

OOS FTPA

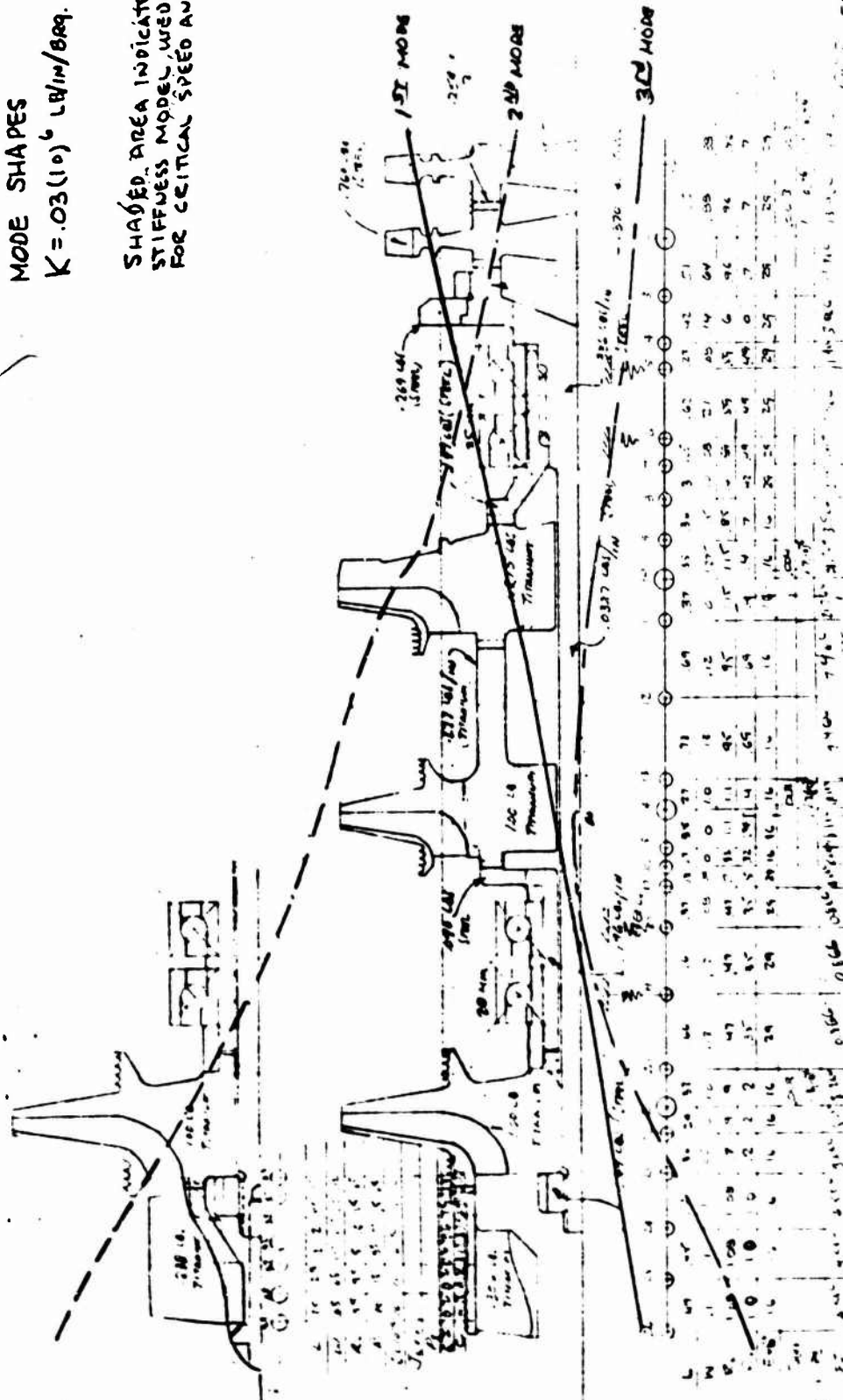
--- LATERAL VIBRATION

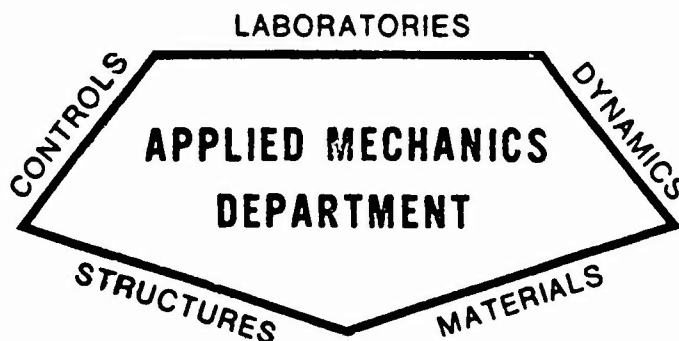
--- FORWARD CIRCULAR WHIRL

2 STAGE WITH CONVENTIONAL INDUCER



SHADED AREA INDICATES  
STIFFNESS MODEL USED  
FOR CRITICAL SPEED ANALYSIS





## STRUCTURAL ENGINEERING SECTION

REPORT NO. SA-OOS-TM-2

OOS OTPA CRITICAL  
SPEED ANALYSES

PREPARED BY:

*LW Bartholf*

L. W. Bartholf  
Engineering Specialist  
Structural Engineering Section

APPROVED BY:

*LK Severud*

L. K. Severud, Manager  
Structural Engineering Section  
Engineering

DATE July 1971



AEROJET LIQUID ROCKET COMPANY

SACRAMENTO, CALIFORNIA

## TABLE OF CONTENTS

	<u>Page</u>
I. Introduction	1
II. Method of Analysis	1
III. Summary of Results	1
IV. Conclusions	2
V. Analysis	2
A. Design Criteria	2
B. Operating Speeds	2
C. Detailed Results	3
Appendix I	11

## LIST OF FIGURES

<u>Figure</u>	<u>Title</u>	<u>Page</u>
1	Critical Speed vs Bearing Spring Constants	3
2	Turbine End Bearing Whirl Loads	4
3	Pump End Bearing Whirl Loads	5
4	OOS Oxidizer Turbopump Concept with Full Flow Turbine Driven Inducer	8
5	OOS OTPA Mode Shapes	9
6	OOS OTPA Critical Speed Stiffness and Mass Model	10

## LIST OF TABLES

<u>Table</u>	<u>Title</u>	<u>Page</u>
I	Rotor Dynamic Analysis Parameters	6

## I. INTRODUCTION

The following report contains the critical speed analyses which have been performed for the OOS Oxidizer Turbopump assembly as shown on Figure 4. The design investigated incorporates 30 mm angular contact bearings at the pump end and 20 mm angular contact bearings for the turbine end.

Parametric studies were initially performed for the rotor shaft to demonstrate feasibility. These analyses are included in the report as Appendix I. Following the parametric studies, a more detailed analysis was performed for the turbopump design selected. The results of these analyses are presented in the main body of the report.

## II. METHOD OF ANALYSIS

The enclosed analysis was accomplished using a computer program which considers bearing loads, shaft deflections and critical speeds. It is based on a lumped parameter method of analysis for determining forced lateral vibrations of a beam having variable section properties. As output, the program computes the amplitudes of shears, moments, slopes and deflection attributable to harmonic forcing functions and in addition determines the rotary inertia and gyroscopic effects for rotating shafts.

## III. SUMMARY OF RESULTS

Figure 1 presents the results of the rotor only parametric analysis. In this figure the first three rotor critical speeds are plotted versus effective radial stiffness at the bearing supports. These results show that with an effective radial stiffness of about  $0.015 \times 10^6$  pounds/inch at each bearing the operating requirements can be met as follows:

First critical speed = 12,000 rpm	} SHAFT RIGID BODY CRITICALS
Second critical speed = 16,000 rpm	
Third critical speed = 64,000 rpm	} SHAFT BENDING CRITICAL



The critical speeds of 12,000 and 16,000 rpm are rotor natural frequencies that are controlled primarily by the effective stiffness (K) at the bearings, whereas the critical speed of 64,000 rpm is controlled principally by shaft bending stiffness.

Figures 2 and 3 show that the proposed operating speed range results in moderately low magnitude bearing reactions due to the whirl loads for both bearing sets. These loads are approximately:

<u>Operating Condition</u>	<u>Total Reaction/Bearing Set (lb)</u>	
	<u>Turbine End</u>	<u>Pump End</u>
MPL	5	36
NPL	8	9

The appendix contains earlier parametric studies which were performed during the preliminary design phase of this study. It contains curves of radial stiffness versus shaft speed for proposed turbopumps having two and three stages and having various inducer designs. This data formed the background for the final investigations.

#### IV. CONCLUSION

Shaft critical speed requirements can be met by the turbopump configuration investigated.

#### V. ANALYSIS

##### A. DESIGN CRITERIA

1. Rotor critical speeds shall be a minimum of 15% removed from any operating speed.
2. No natural frequencies of the turbopump assembly shall exist between the minimum power level (MPL) and the normal power level (NPL).

##### B. OPERATING SPEEDS

Minimum Power Level, MPL	20,000 rpm
Normal Power Level, NPL	50,000 rpm



AEROJET-GENERAL CORPORATION  
SACRAMENTO CALIFORNIA

AGCS-7100-11

REPORT NO.

PAGE 3 OF

SUBJECT

OOS CRITICAL SPEED ANALYSIS

DATE  
7/14/71

WORK ORDER

BY

L.W. BARTHOLF

CHK. BY

DATE

C DETAILED RESULTS

OOS OTPA (SELECTED CONFIGURATION)

--- LATERAL VIBRATION

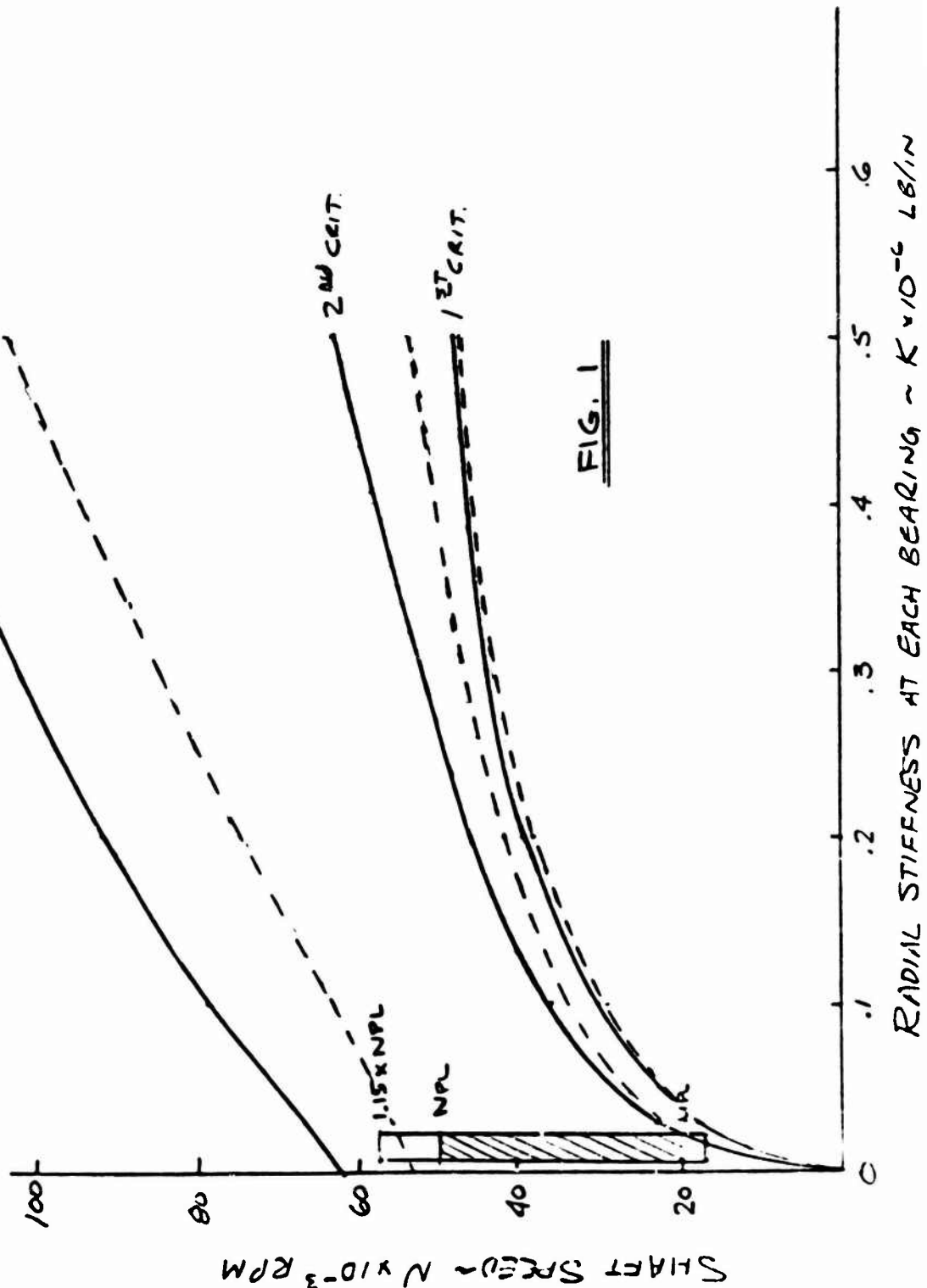
--- FORWARD CIRCULAR WHIRL

3<sup>rd</sup> CRIT.

2<sup>nd</sup> CRIT.

1<sup>st</sup> CRIT.

FIG. 1



RADIAL STIFFNESS AT EACH BEARING ~ K x 10<sup>-6</sup> LB/IN



AEROJET-GENERAL CORPORATION  
SACRAMENTO • CALIFORNIA

REPORT NO.

PAGE 11 OF

DATE

WORK ORDER

DATE

## COS CRITICAL SPEED ANALYSIS

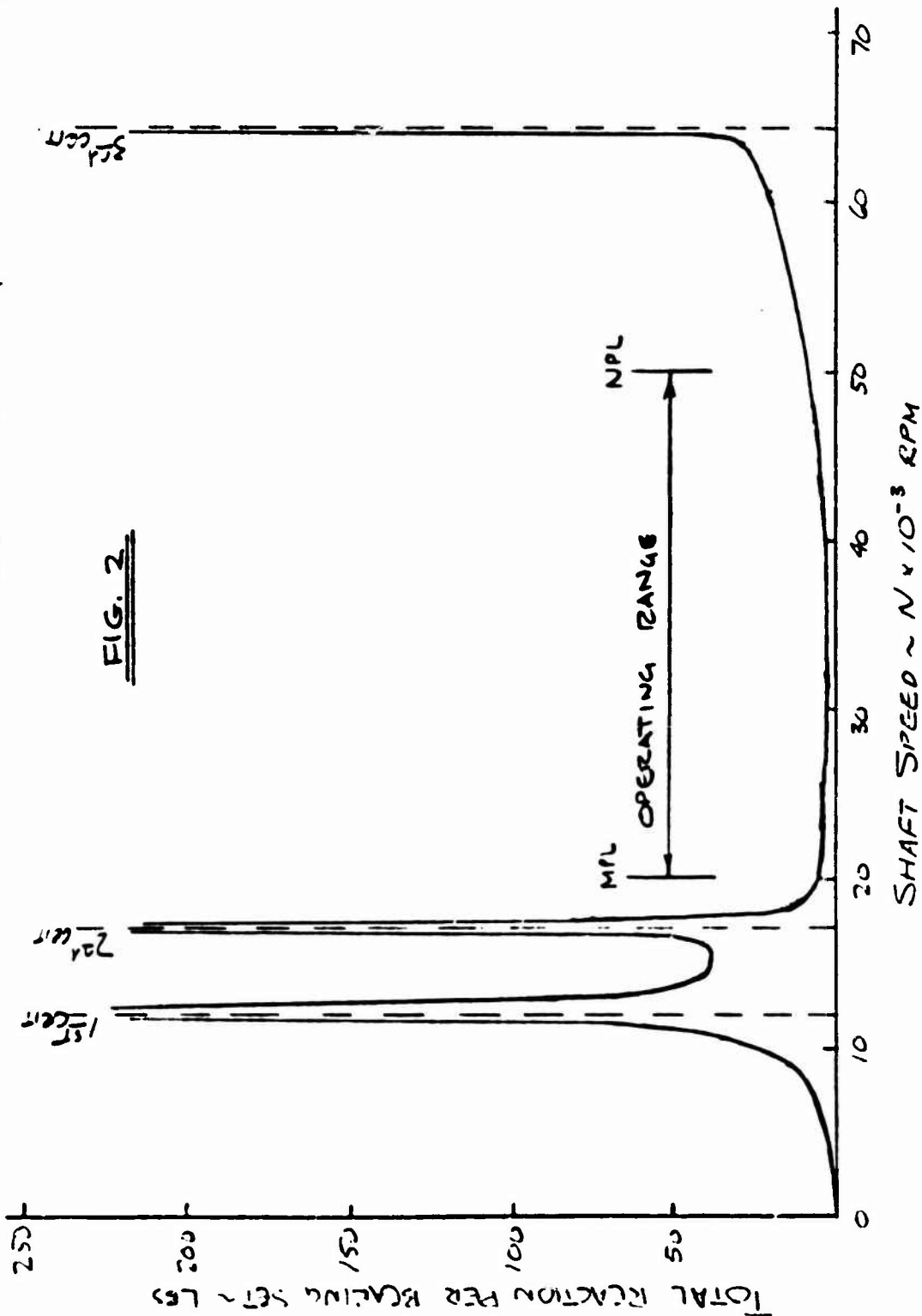
BY

L.W. BARTHOLF

CHK. BY

### TURBINE ENO BEARING WHIRL LOADS

1 MIL DIAMETRAL CLEARANCE AT BEARING SET CENTERS  
CONICAL WHIRL,  $K = 0.15(10)^6$  LB/IN/BEARING =  $.030(10)^6$  LB/IN/SET





AEROJET-GENERAL CORPORATION  
SACRAMENTO • CALIFORNIA

AGCS-OR-1011

REPORT NO

PAGE 5 OF

SUBJECT

DATE

WORK ORDER

OOS CRITICAL SPEED ANALYSIS

BY

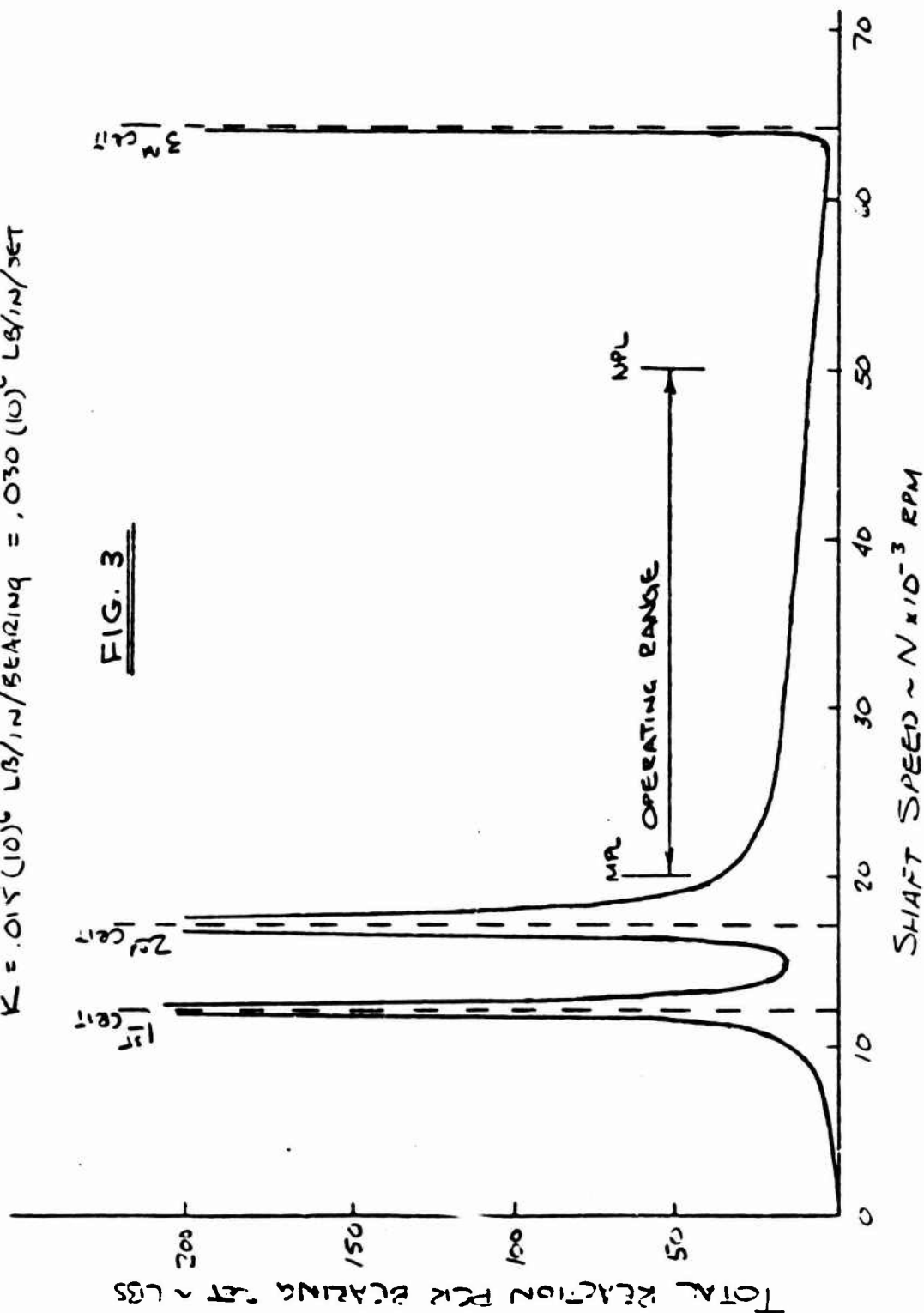
CHK BY

DATE

L.W. BARTHOLOF

### PUMP END BEARING WHIRL LOADS

1 MIL DIAMETRAL CLEARANCE AT BEARING SET CENTERS  
CONICAL WHIRL  
 $K = .015 (10)^6$  LB/IN/BEARING = .030 (10)<sup>6</sup> LB/IN/SET





AEROJET-GENERAL CORPORATION  
SACRAMENTO CALIFORNIA

AGCS-2200-11

REPORT NO.

PAGE 4 OF

SUBJECT

COS CRITICAL SPEED ANALYSIS

DATE

7/14/71

WORK ORDER

BY

L.W. BARTHOLOMEW

CHK. BY

DATE

COS OPA CRITICAL SPEED MODEL ~ TABLE I

$$E_{\text{STEEL}} = 29 (10)^6 \text{ PSI}$$

STA	L (in)	EI	W (Lb)	J <sub>EFF</sub>	K	C	G	P <sub>1</sub>	P <sub>2</sub>	P <sub>3</sub>
701	.25	18 (10) <sup>6</sup>	2	.008	0	/	11 (10) <sup>6</sup>	4.3 (10) <sup>6</sup>	0	0
702	.37	18 (10) <sup>6</sup>	.5	0	0	/	↑	0	↑	0
703	.50	18 (10) <sup>6</sup>	.5	↑	0	/	↑	0	↑	↑
704	.32	2 (10) <sup>6</sup>	.4	↑	K	/	↑	0	↑	↑
705	.35	2 (10) <sup>6</sup>	.4	↑	0	/	↑	0	↑	↑
706	.36	2 (10) <sup>6</sup>	.4	↑	K	/	↑	0	↑	↑
707	.28	2 (10) <sup>6</sup>	.4	↑	0	/	↑	0	↑	↑
708	.85	3 (10) <sup>6</sup>	.4	↑	0	/	↑	0	↑	↑
709	.93	3 (10) <sup>6</sup>	.4	↑	0	/	↑	0	↑	↑
710	.84	2 (10) <sup>6</sup>	.8	↑	0	/	↑	-1.3 (10) <sup>6</sup>	↑	↑
711	.35	2 (10) <sup>6</sup>	.1	↑	0	/	↑	0	↑	↑
712	.60	1 (10) <sup>6</sup>	.1	↑	0	/	↑	0	↑	↑
713	.22	.8 (10) <sup>6</sup>	.1	↑	K	/	↑	0	↑	↑
714	.35	.8 (10) <sup>6</sup>	.1	↑	0	/	↑	0	↑	↑
715	.33	.8 (10) <sup>6</sup>	.1	↑	K	/	↑	0	↑	↑
716	.24	.9 (10) <sup>6</sup>	.1	↑	0	/	↑	0	↑	↑
717	.76	1 (10) <sup>6</sup>	.1	↑	0	/	↑	0	↑	↑
718	.26	4 (10) <sup>6</sup>	.7	↑	0	/	↑	-1.5 (10) <sup>6</sup>	↑	↑
719	.39	4 (10) <sup>6</sup>	.1	↑	0	/	↑	0	↑	↑
720	.46	6 (10) <sup>6</sup>	.2	↑	0	/	↑	0	↑	↑
721	.47	6 (10) <sup>6</sup>	.2	↑	0	/	↑	-1.5 (10) <sup>6</sup>	↑	↑
722	.50	6 (10) <sup>6</sup>	.1	0	0	/	11 (10) <sup>6</sup>	0	0	0

$$J_{\text{EFF}} = \frac{WR^2}{4g}$$



AEROJET-GENERAL CORPORATION  
SACRAMENTO • CALIFORNIA

AGCS FORM 11

SUBJECT

REPORT NO

PAGE 7 OF

DATE

7/14/71

WORK ORDER

OOS CRITICAL SPEED ANALYSIS

BY

L.W. BARTHOLF

CHK BY

DATE

### ESTIMATE OF WHIRL FORCING FUNCTION

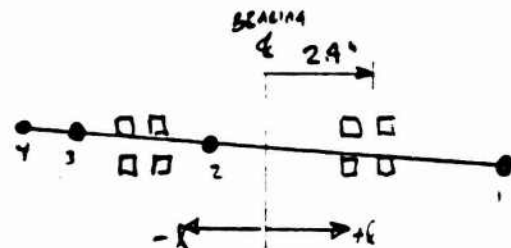
ASSUME CONICAL WHIRL WITH 1 MIL DIAMETRAL CLEARANCE AT THE CENTER OF THE BEARING SETS.

$$P_1 = \frac{W}{g} y$$

$$y = A \times l$$

$$.0005 = A \times 2.4$$

$$A = 208 (10)^{-6}$$



$$P_0 = \frac{2}{386} (208) (10)^{-6} (4) = 4.3 (10)^{-6}$$

$$P_0 = \frac{.8}{386} (208) (10)^{-6} (-8) = -.3 (10)^{-6}$$

$$P_0 = \frac{.7}{386} (208) (10)^{-6} (-4) = -.15 (10)^{-6}$$

$$P_0 = \frac{.5}{386} (208) (10)^{-6} (-5.5) = -.15 (10)^{-6}$$

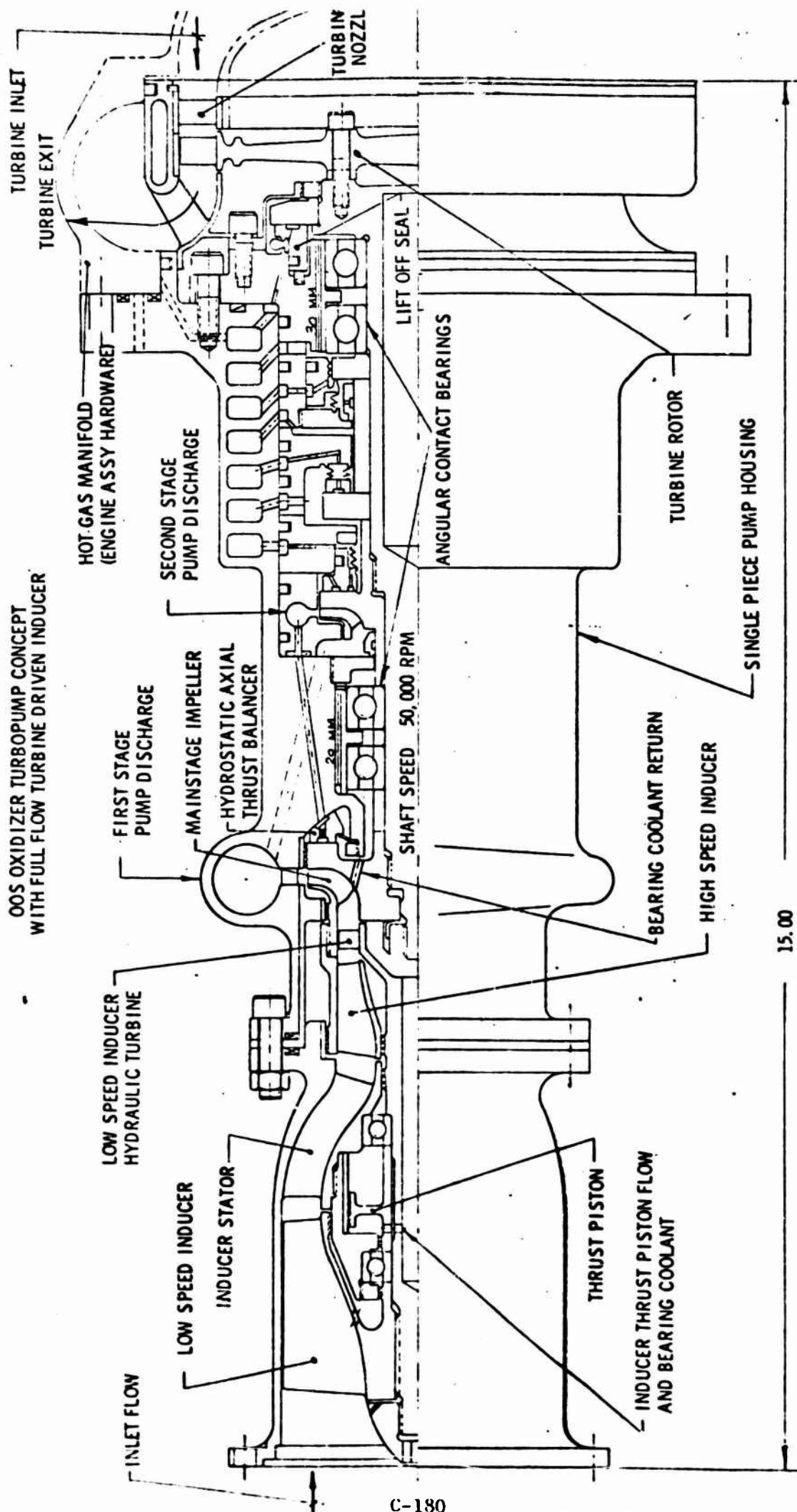
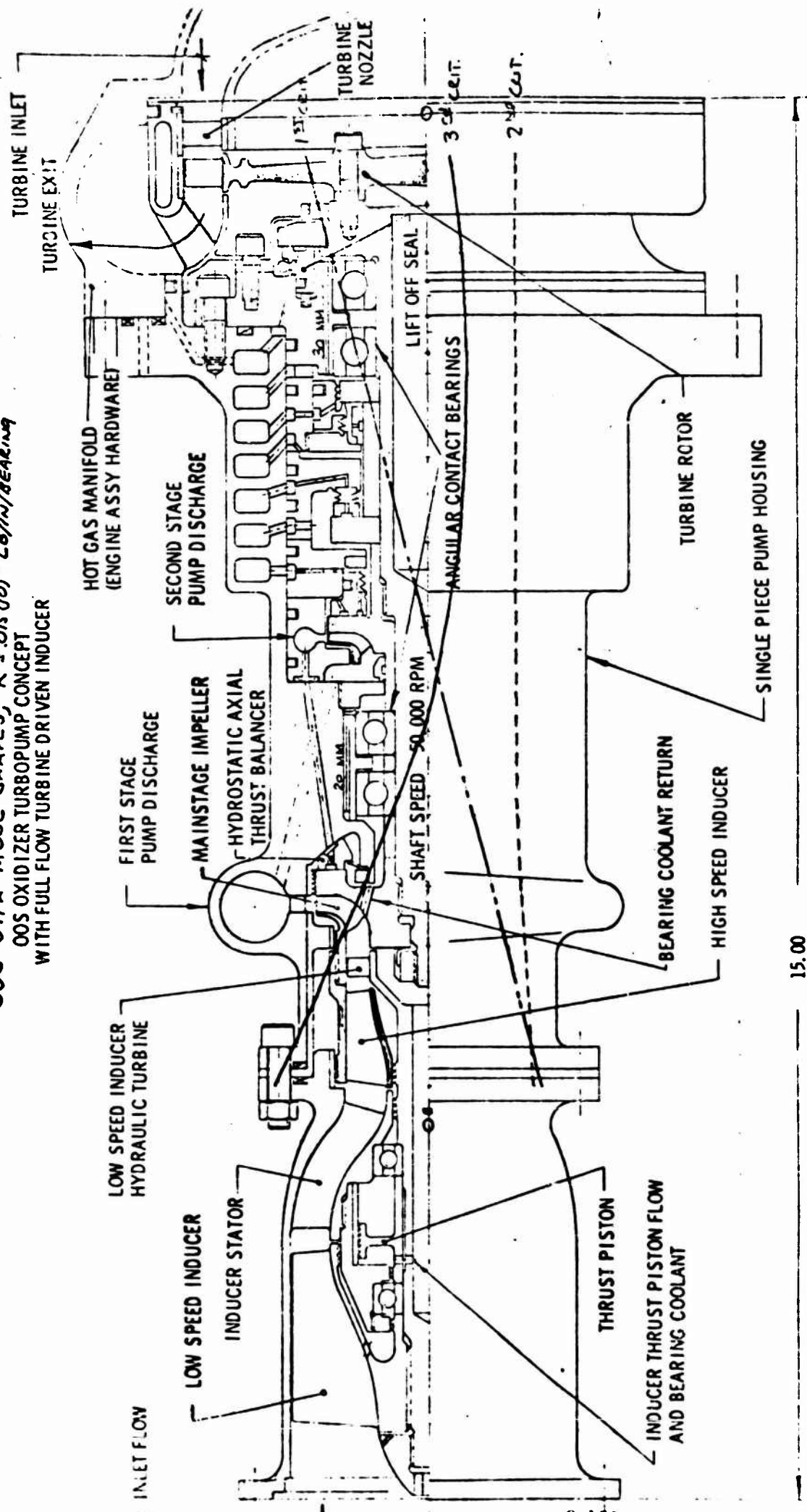


FIGURE 4

OOS OTRA MOOE SHAPES,  $K = 0.05(0.0)^6 \text{ Lb/in/bearing}$   
 OOS OXIDIZER TURBOPUMP CONCEPT  
 WITH FULL FLOW TURBINE DRIVEN INDUCER

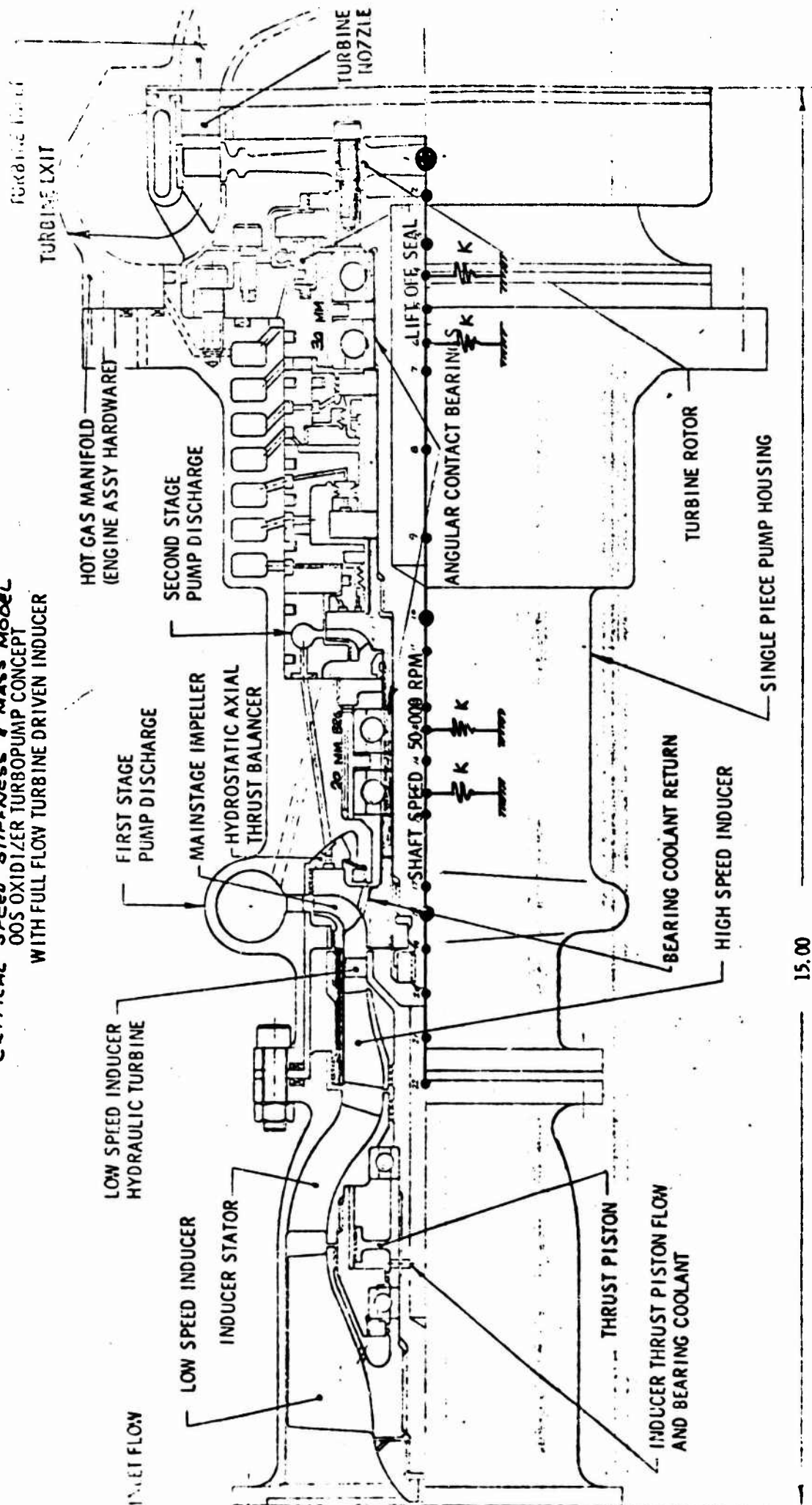


C-181

FIGURE 5



**CRITICAL SPEED STIFFNESS & MASS MODEL  
OOS OXIDIZER TURBOPUMP CONCEPT  
WITH FULL FLOW TURBINE DRIVEN INDUCER**



15.00

**APPENDIX I**  
**PARAMETRIC STUDIES**



AEROJET-GENERAL CORPORATION  
SACRAMENTO • CALIFORNIA

REPORT NO.

PAGE I.1 OF

DATE  
7/2/71

WORK ORDER

# OOS OTPA CRITICAL SPEED

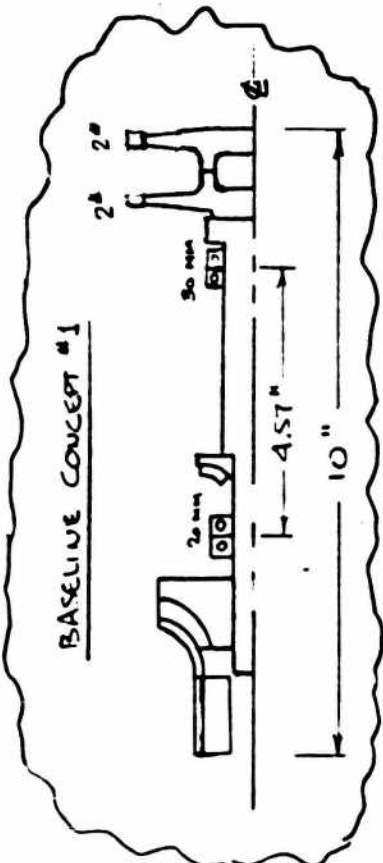
BY L W BACHOLF

CHK BY

DATE

## OOS OTPA CRITICAL SPEED SUMMARY

BASELINE CONCEPT #1



CONFIGURATION	RADIAL STIFF- NESS AT EACH BEARING (LB/IN)	LATERAL VIBRATION CRITICAL SPEED (ROTOR ONLY MODEL)		
		N <sub>1</sub>	N <sub>2</sub>	N <sub>3</sub>
1a. INCREASED BEARING SPAN 1 INCH	.3 (10) <sup>6</sup>	32000	50000	82000
1b. DECREASED TURBINE WEIGHT BY 50%		33000	51000	78000
1c. DECREASED TURBINE OVERHANG .4 INCHES		42000	50000	—
1d. (CASE A) REMOVED 2ND STAGE PUMP, WENT TO 25 MM BEA. ON PUMP END & DECREASED BEARING SPAN .8 INCHES.		36000	50000	—
1e. (CASE B) DOUBLED STIFFNESS BETWEEN TURBINE END BEARINGS AND 2ND STG. PUMP		32000	52000	—
1f. (CASE C) DOUBLED STIFFNESS BETWEEN TURBINE END BEARING AND 1ST STG. PUMP	3 (10) <sup>6</sup>	33000	50000	—
2. BASELINE CONCEPT #2 - CONVENTIONAL INDUCER	3 (10) <sup>6</sup>	34000	62000	—
		33000	50000	—

(MPL) (N )  
OPERATING RANGE = 20000 TO 50000 RPM  
WITH 15% MARGINS = 17000 TO 57500 RPM



AEROJET-GENERAL CORPORATION  
SACRAMENTO • CALIFORNIA

REPORT NO

PAGE 1.2 OF

AGCS 1000-11

SUBJECT

OOS CRITICAL SPEED

DATE

6/3/71

WORK ORDER

1911-05-101

BY

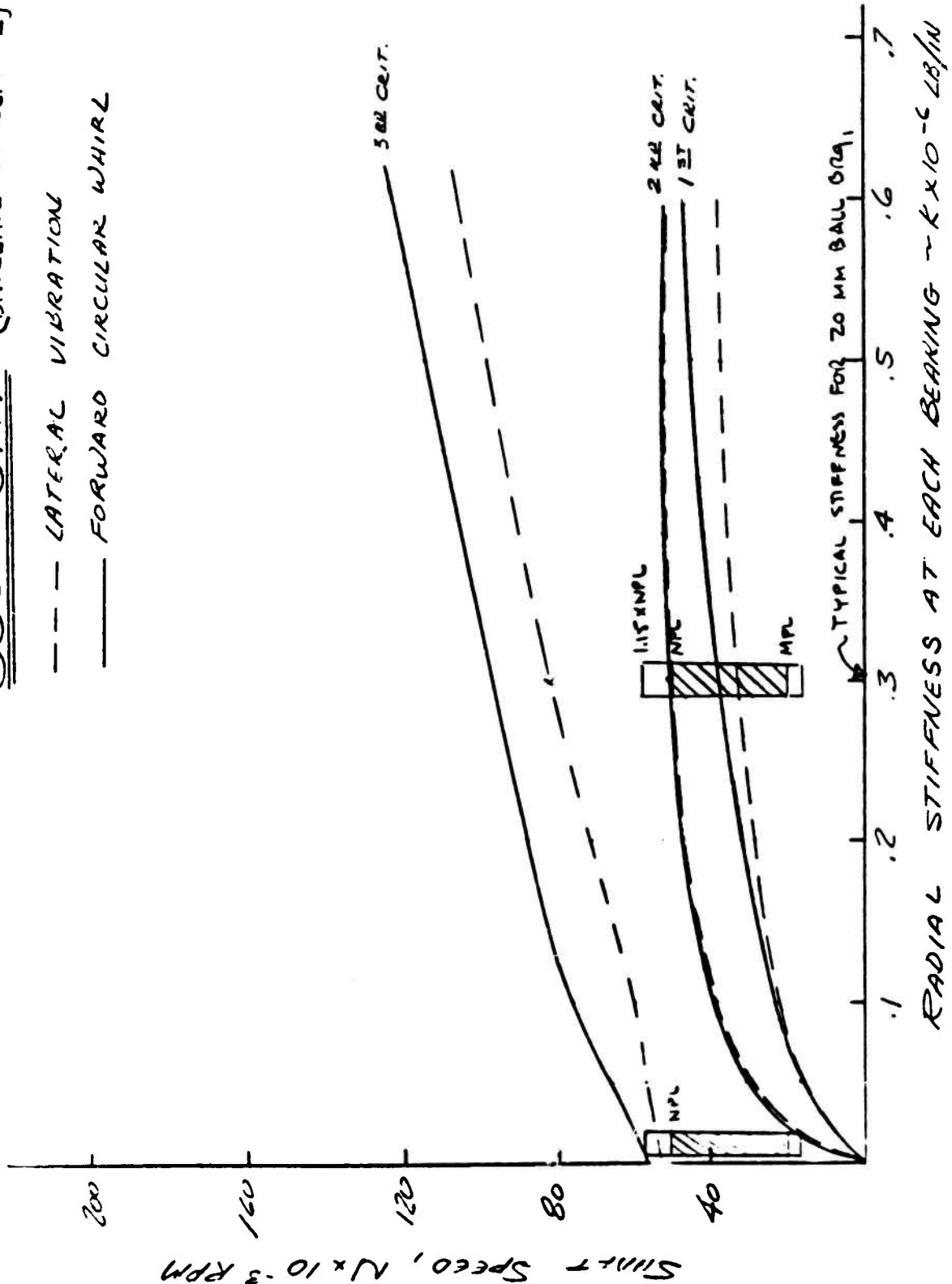
L.W. BARTHOLF

CHK BY

DATE

OOS OTPA (BASELINE CONCEPT #1)

--- LATERAL VIBRATION  
--- FORWARD CIRCULAR WHIRL





AEROJET-GENERAL CORPORATION  
SACRAMENTO • CALIFORNIA

REPORT NO.

PAGE 13 OF

DATE

WORK ORDER  
1571-55-101

DATE  
6/23/71

SUBJECT

OOS CRITICAL SPEED

BY

G. ALDRICH

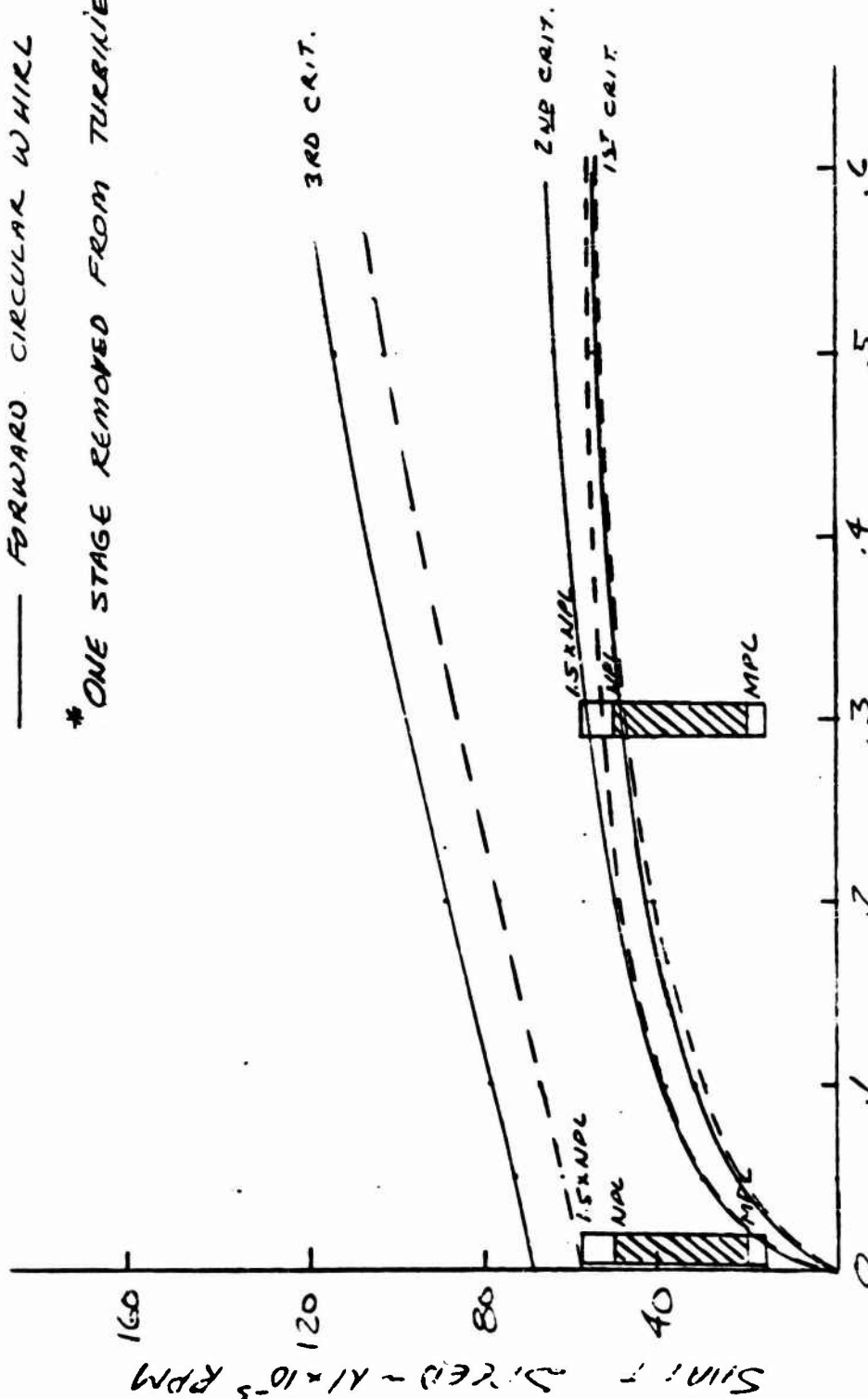
CHK. BY

OOS OTHA\* (BASELINE CONCEPT)

--- LATERAL VIBRATION

--- FORWARD CIRCULAR WHIRL

\* ONE STAGE REMOVED FROM TURBINE



RADIAL STIFFNESS AT EACH BEARING ~ K x 10^-6 LB/IN.



SUBJECT

OOS CRITICAL SPEED

DATE

6/10/71

WORK ORDER

1811-OS-101

BY

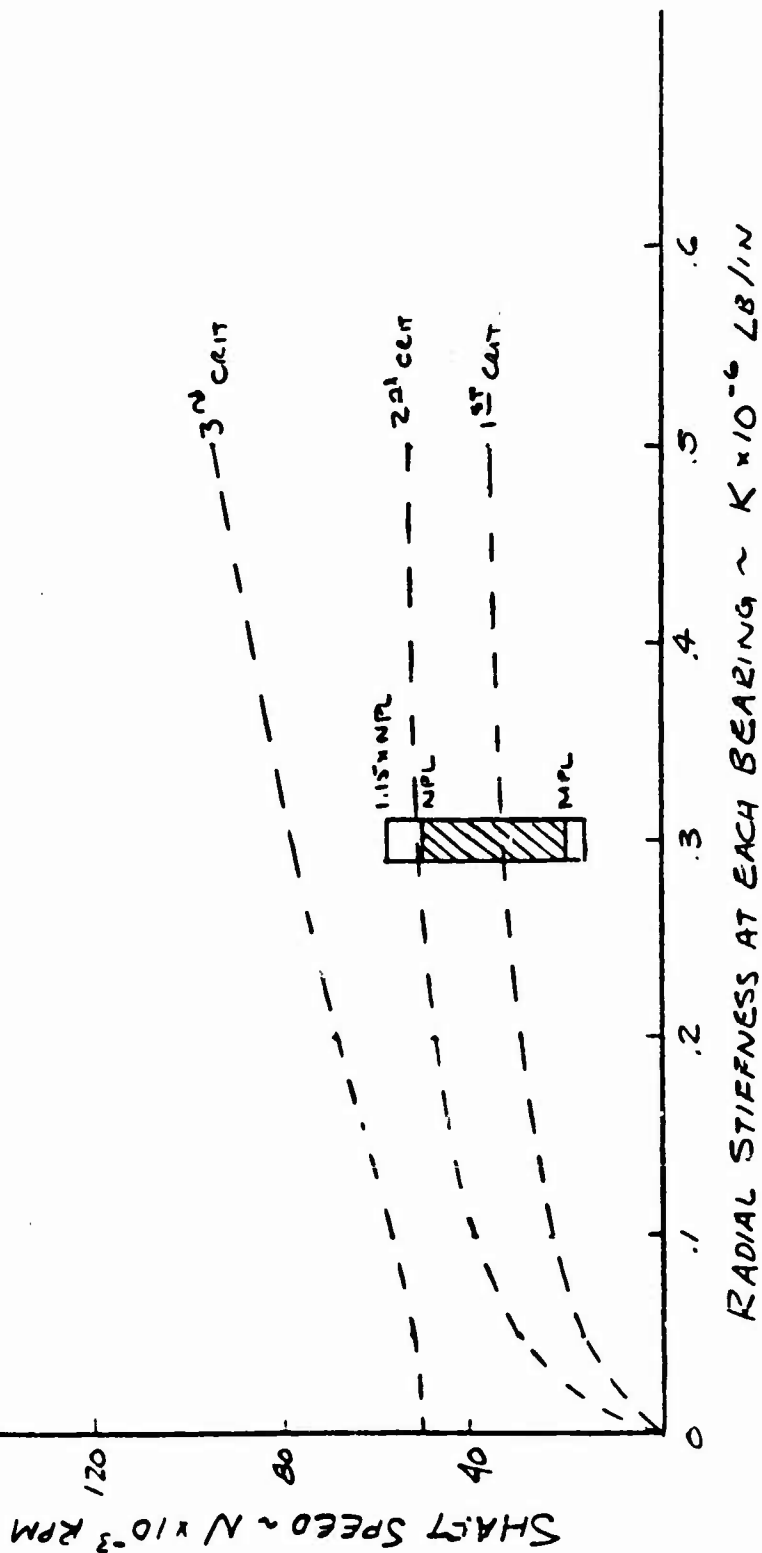
L.W. BARTHOLF

CHK BY

DATE

OOS OTPA

1a. BEARING SPAN INCREASED 1 INCH

LATERAL VIBRATION



AEROJET-GENERAL CORPORATION  
SACRAMENTO • CALIFORNIA

REPORT NO.

PAGE I.5 OF

DATE

WORK ORDER

DATE

OOS CRITICAL SPEED

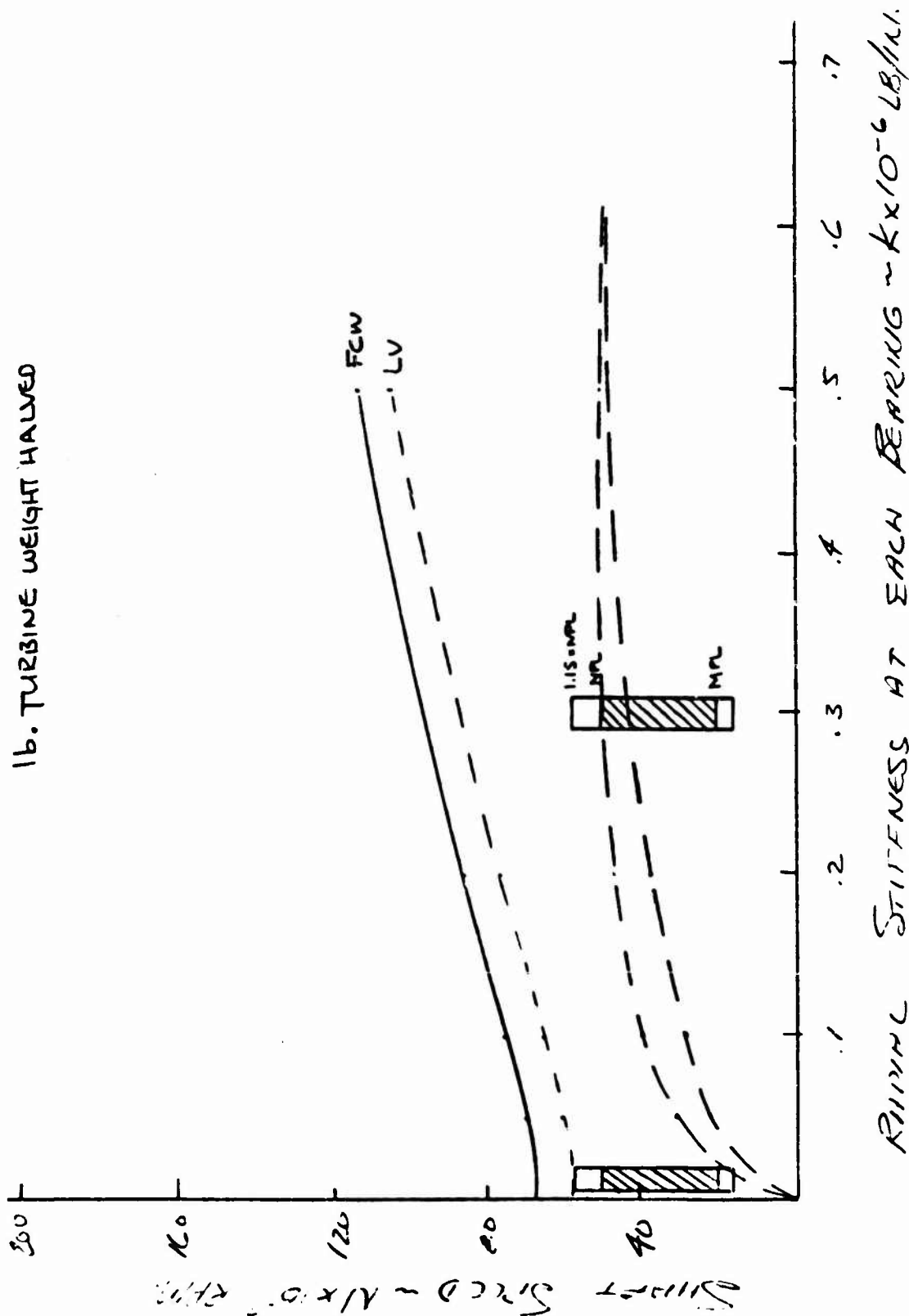
BY

C. H. DICK

CHK. BY

OOS O.T.P.A.

1b. TURBINE WEIGHT HALVED





AEROJET-GENERAL CORPORATION  
SACRAMENTO • CALIFORNIA

AGCS 7800-11

REPORT NO.

PAGE I.6 OF

SUBJECT

OOS CRITICAL SPEED.

DATE

WORK ORDER

BY

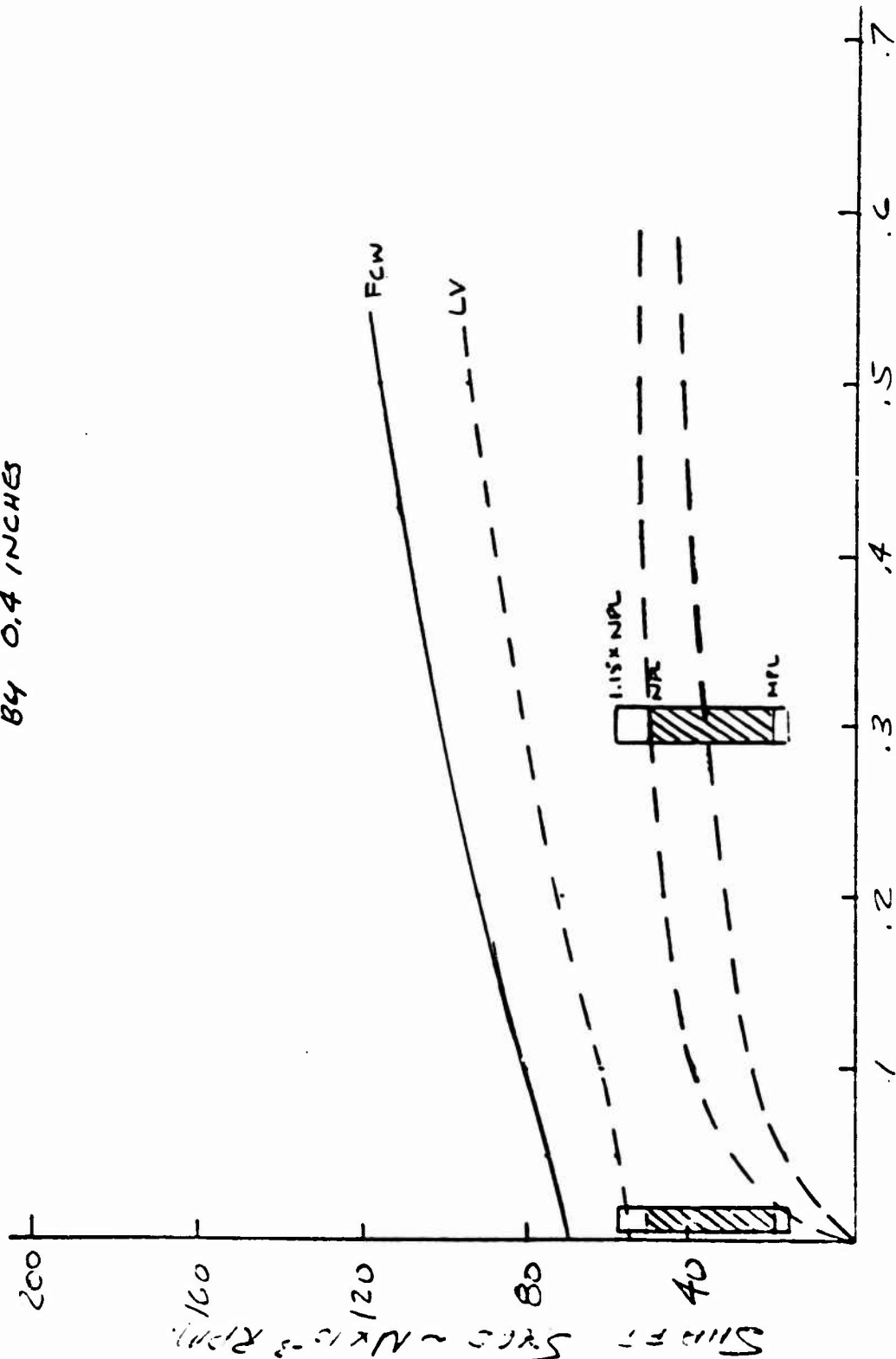
G. ALRICH

CHK BY

DATE

OOS OTPA

1c. REDUCED LENGTH OF TURBINE OVERHANG  
BY 0.4 INCHES



RADIAL STIFFNESS AT EACH BEARING  $\sim K \times 10^{-6}$  LB/IN.





AEROJET-GENERAL CORPORATION  
SACRAMENTO CALIFORNIA

REPORT NO.

AGCS-1000-11

PAGE 1.7 OF

SUBJECT

OSS CRITICAL SPEED

DATE

WORK ORDER

BY

G. HEDRICH

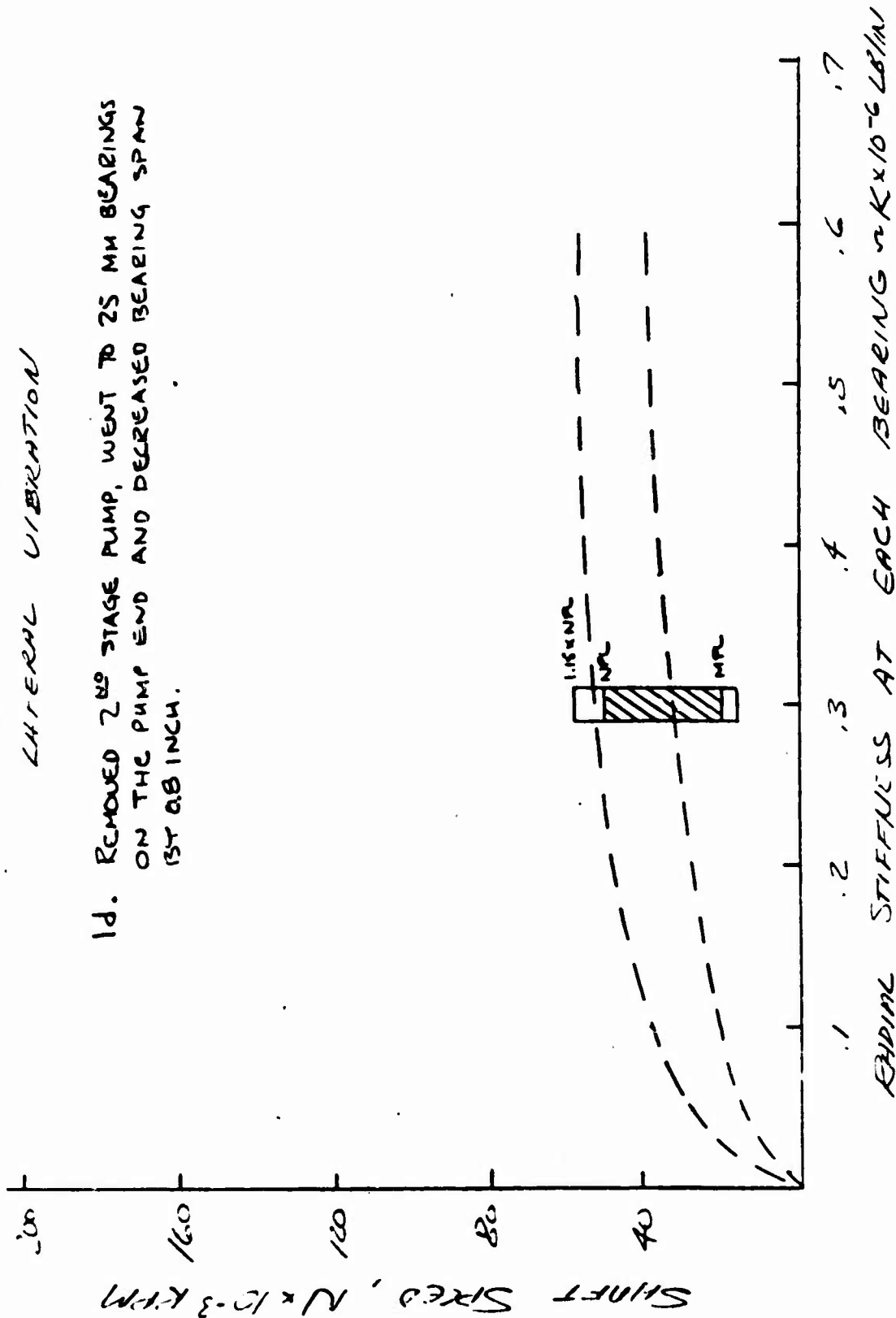
CHK. BY

DATE

OOS QTPA  
(CASE A)

LATERAL VIBRATION

1d. REMOVED 2<sup>ND</sup> STAGE PUMP, WENT TO 25 MM BEARINGS  
ON THE PUMP END AND DECREASED BEARING SPAN  
1ST 0.8 INCH.





AEROJET-GENERAL CORPORATION  
SACRAMENTO • CALIFORNIA

AGCS-0000-11

REPORT NO.

PAGE 1.4 OF

SUBJECT

OSS CRITICAL SPEED

DATE

WORK ORDER

BY

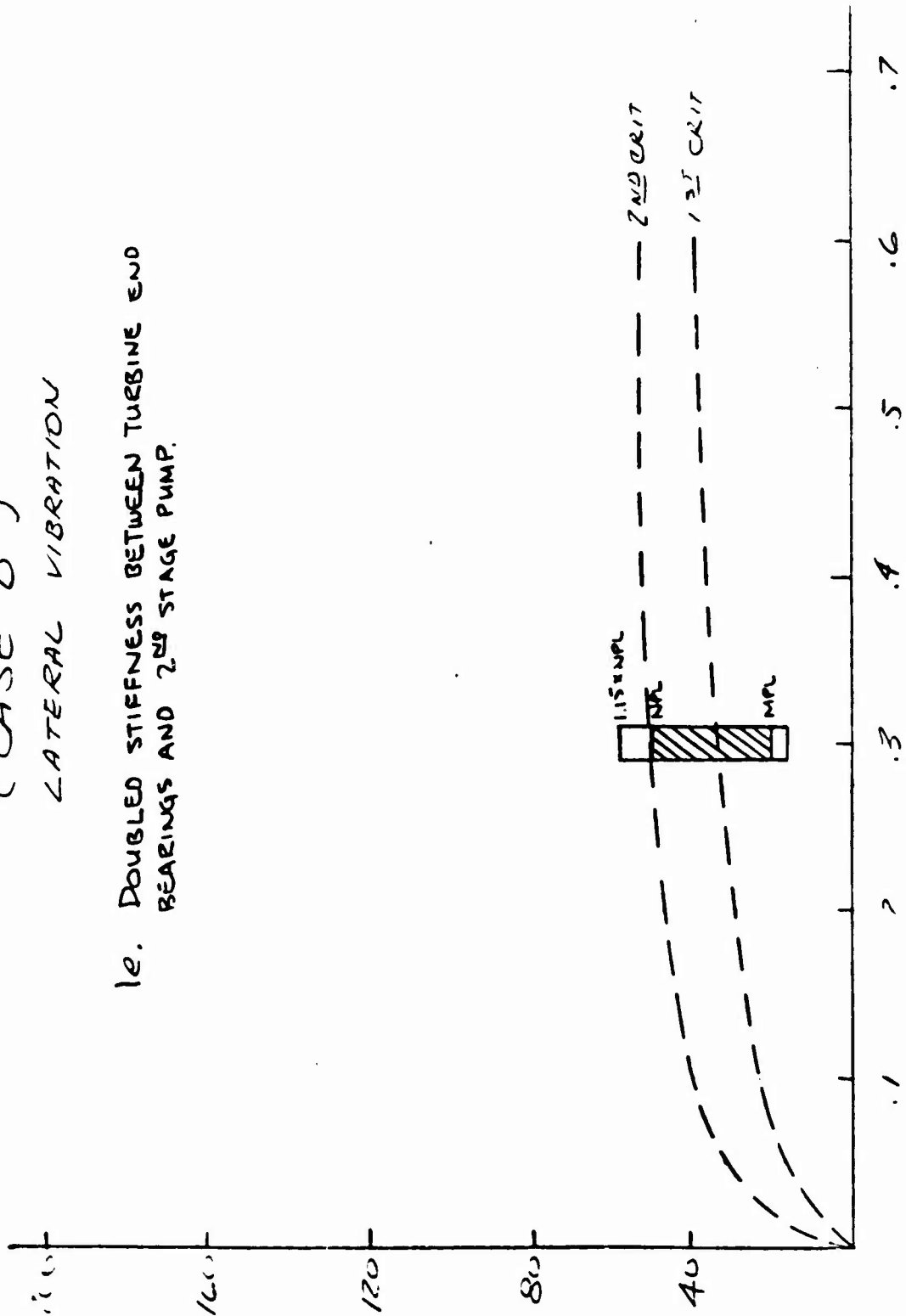
G. MILLICH

CHK BY

DATE

OOS OSPA  
(CASE B)  
LATERAL VIBRATION

1e. DOUBLED STIFFNESS BETWEEN TURBINE END  
BEARINGS AND 2ND STAGE PUMP.



AXIAL STIFFNESS AT EACH BEARING ~ KX10<sup>-6</sup> LB/IN



AEROJET-GENERAL CORPORATION  
SACRAMENTO • CALIFORNIA

REPORT NO.

PAGE 1.9 OF

DATE

WORK ORDER

DATE

ADDS 000-11

SUBJECT

005 CRITICAL SPEED

BY

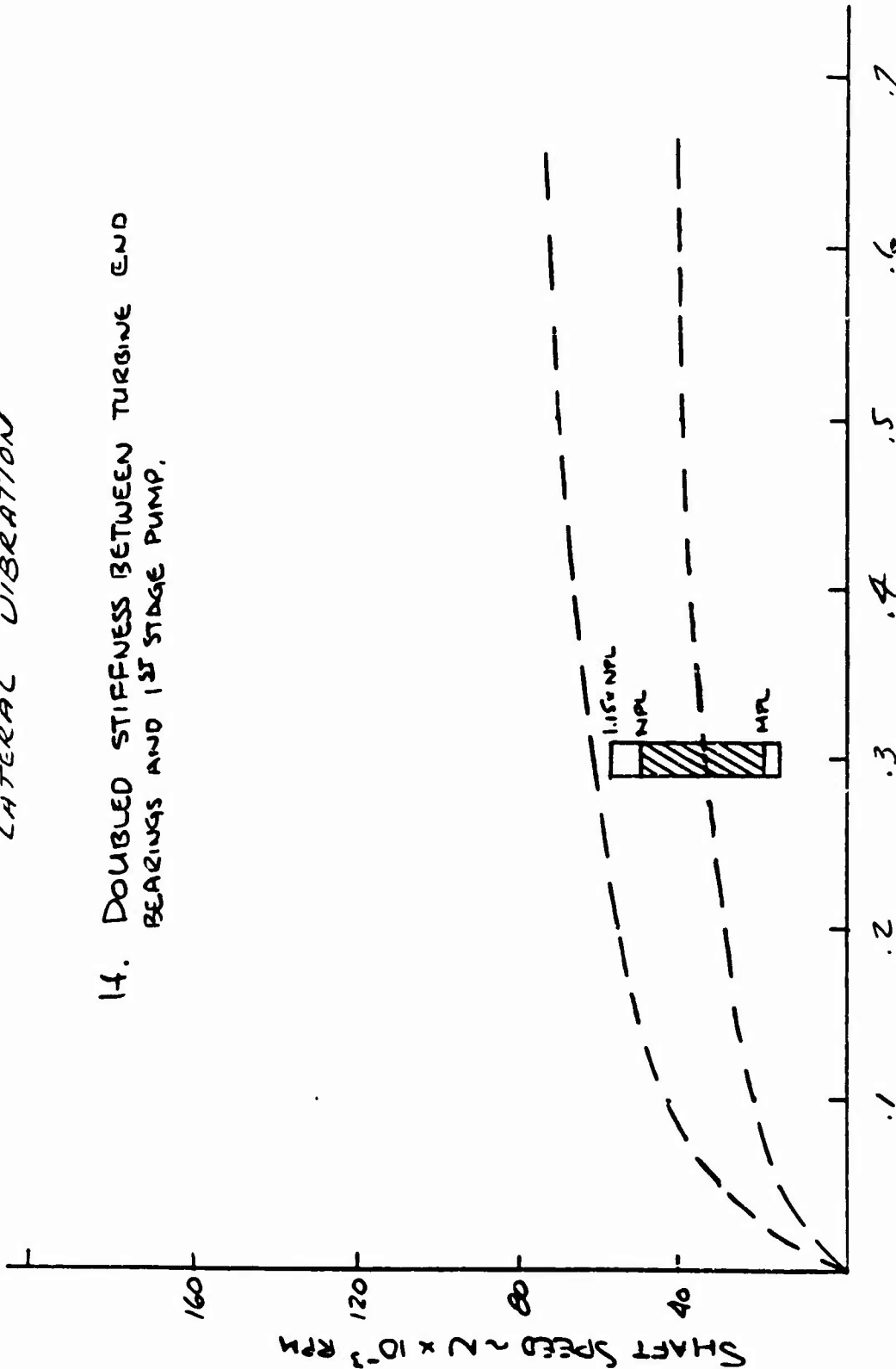
G. ALLEN

CHK BY

005 OTPA  
(CASE C)

LATERAL VIBRATION

14. DOUBLED STIFFNESS BETWEEN TURBINE END  
BEARINGS AND 1<sup>ST</sup> STAGE PUMP.



C-192



AEROJET-GENERAL CORPORATION  
SACRAMENTO • CALIFORNIA

REPORT NO

PAGE 1.10 of

PROJECT

SUBJECT

005 CRITICAL SPEED

DATE  
6/1/71

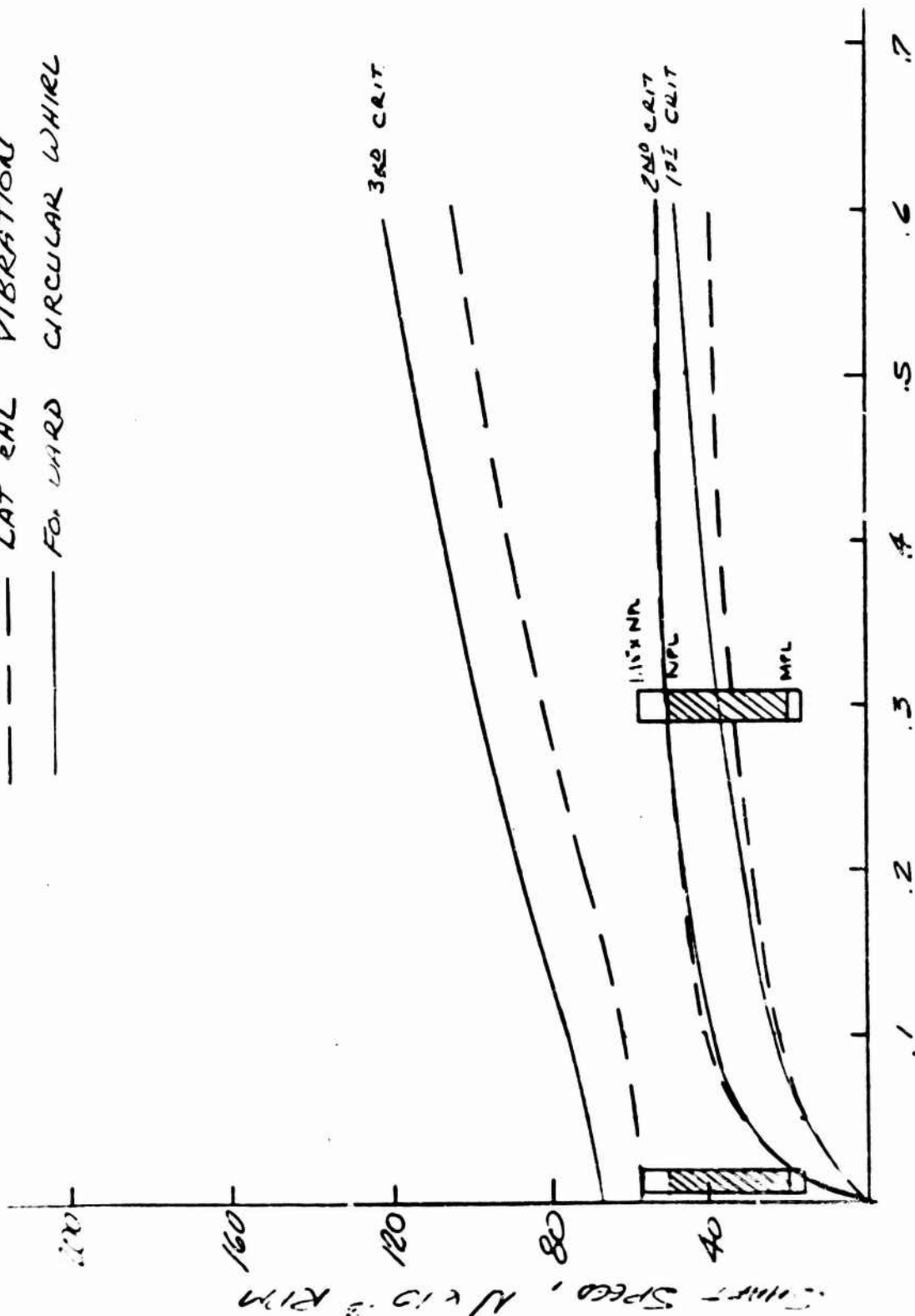
WORK ORDER  
1811-05-101

BY G. ALDRICH

CHK. BY

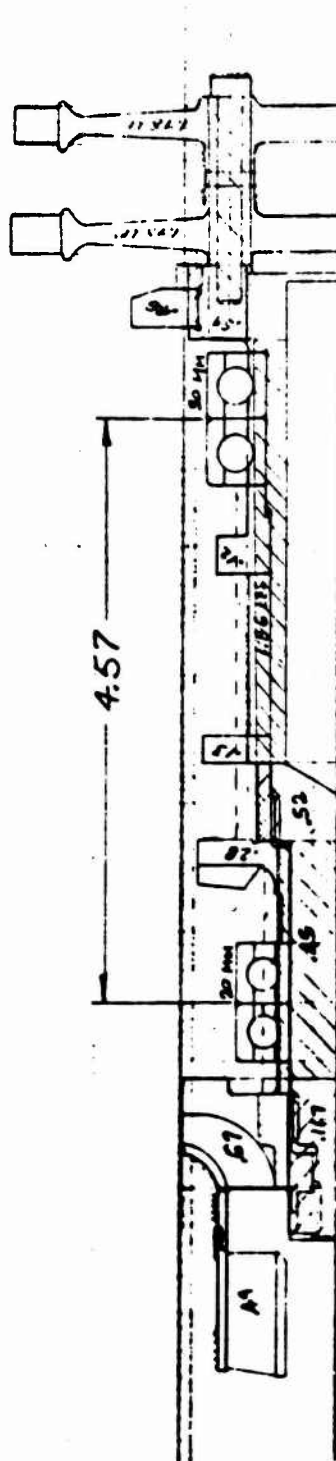
DATE

003 OTPA (CONCEPT #2)  
--- LAT EAL VIBRATION  
--- FORWARD CIRCULAR WHIRL



$N_{sum} = 50,300 \text{ R.P.M.}$

# CRITICAL SPEED STIFFNESS MODEL



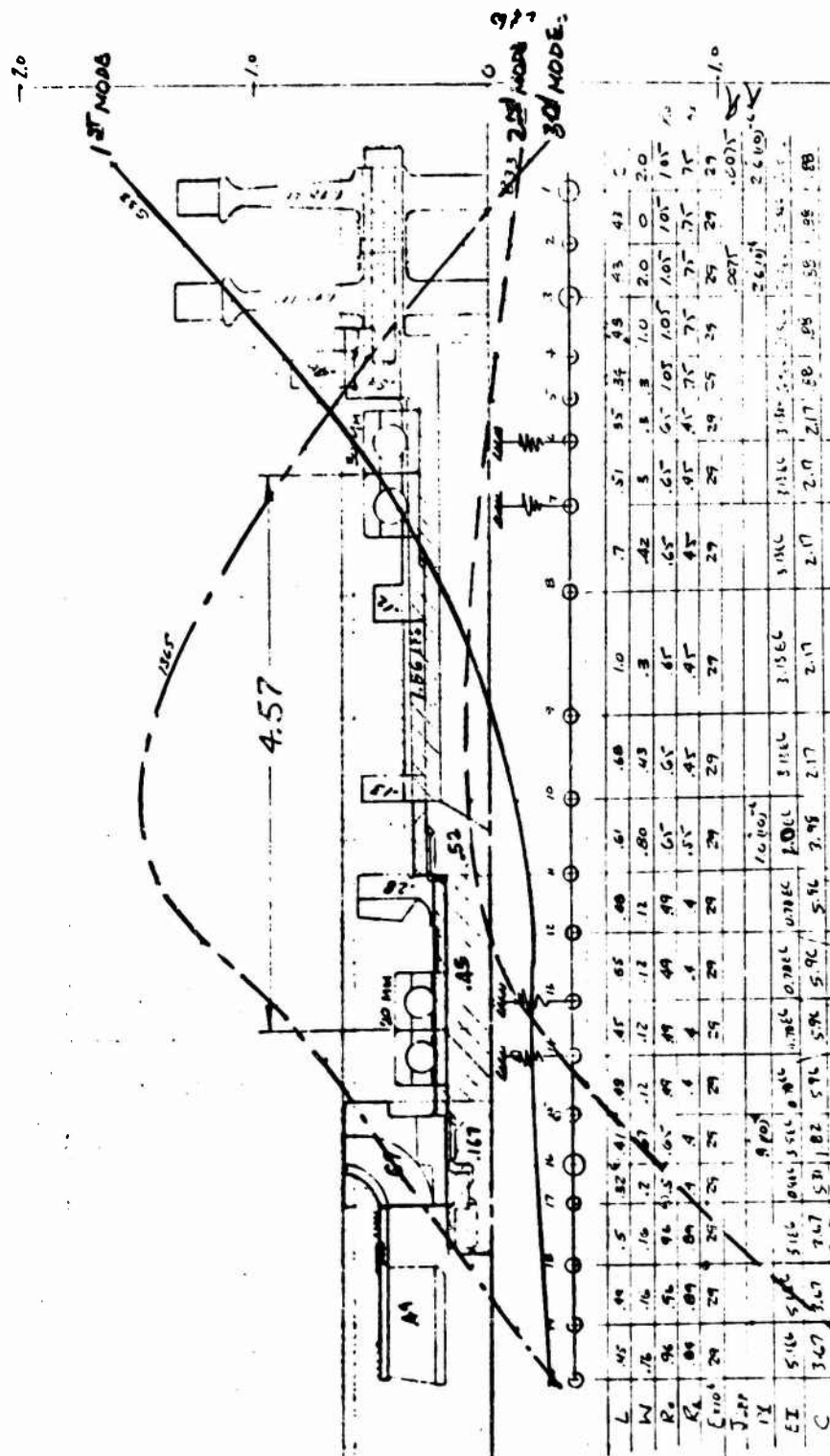
	1	2	3	4	5	6	7	8	9	10	11	12	13	14	15	16	17	18	19	20
L	.45	.49	.5	.82	.41	.48	.45	.45	.45	.45	.45	.45	.45	.45	.45	.45	.45	.45	.45	.45
W	.15	.15	.15	.2	.67	.12	.12	.12	.12	.12	.12	.12	.12	.12	.12	.12	.12	.12	.12	.12
R	.95	.95	.95	.5	.65	.95	.95	.95	.95	.95	.95	.95	.95	.95	.95	.95	.95	.95	.95	.95
K <sub>1</sub>	.04	.04	.04	.4	.4	.4	.4	.4	.4	.4	.4	.4	.4	.4	.4	.4	.4	.4	.4	.4
E <sub>100</sub>	.24	.24	.24	.24	.24	.24	.24	.24	.24	.24	.24	.24	.24	.24	.24	.24	.24	.24	.24	.24
J <sub>100</sub>																				
IX																				
ET	5.16	5.16	5.16	5.16	5.16	5.16	5.16	5.16	5.16	5.16	5.16	5.16	5.16	5.16	5.16	5.16	5.16	5.16	5.16	5.16
C	3.67	3.67	3.67	3.67	3.67	3.67	3.67	3.67	3.67	3.67	3.67	3.67	3.67	3.67	3.67	3.67	3.67	3.67	3.67	3.67

BASLINE CONCEPT NO.1  
OOS OXID PUMP  
5/27/71 G.P.

# MODE SHAPES

$$K = 3.40 \times 10^6 \text{ LB/IN/BRG.}$$

$M_{\text{sum}} = 50,000 \text{ P.M.}$

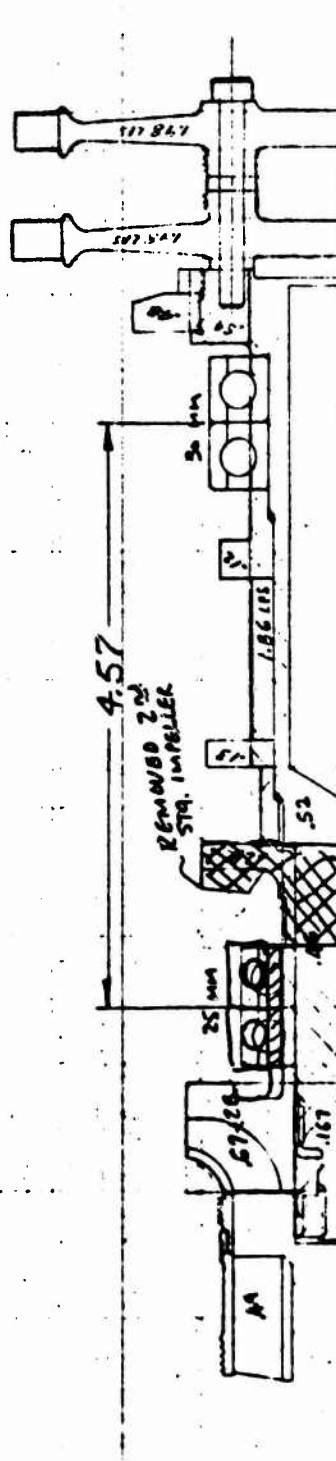


BASELINE CONCEPT NO. 1  
OOS OXID PUMP

5/2/77

CASE A (10)

## STIFFNESS MODEL CHANGES

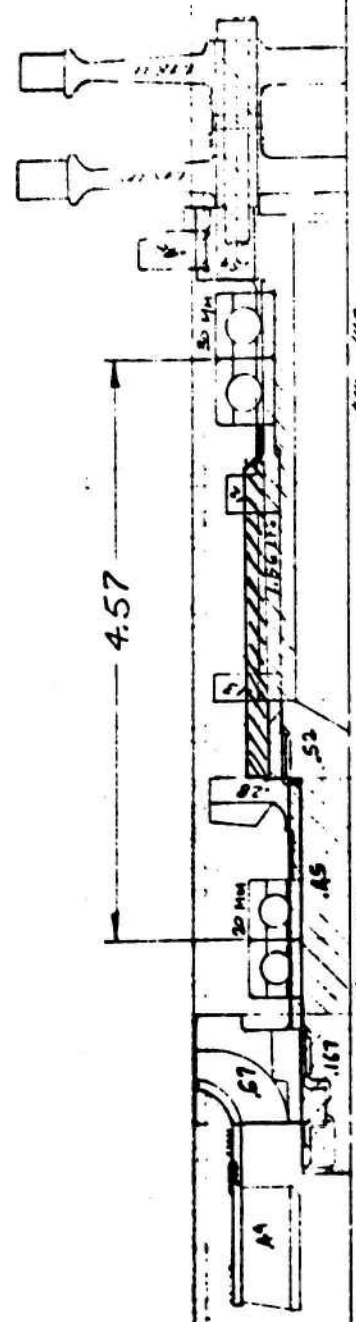


1	.45	.49	.5	.32	.41	.40	.45	.225	.61
W	.16	.16	.16	.2	.95	.14	.14	.01	.52
R	.96	.96	.96	.5	.65	.6	.6	.6	.65
R'	.89	.89	.89	.4	.4	.0	.50	.50	.55
EXD <sup>2</sup>	.29	.29	.29	.29	.29	.29	.29	.29	.29
Self									
P					.900				1.0x10 <sup>-4</sup>
E.T.	.5114	.5	.5116	.0100	.3564	.132	.1564	.1912	2.060
C <sub>0</sub>	.321	.369	.367	.54	.182	.434	.474	.414	3.98

EXHIBIT NO. 1  
005 OXID PUMP  
5/27/74 S.D.

$N_{max} = 50,300 \text{ RPM}$

**CASE B (1e)**  
**STIFFNESS MODEL CHANGES**



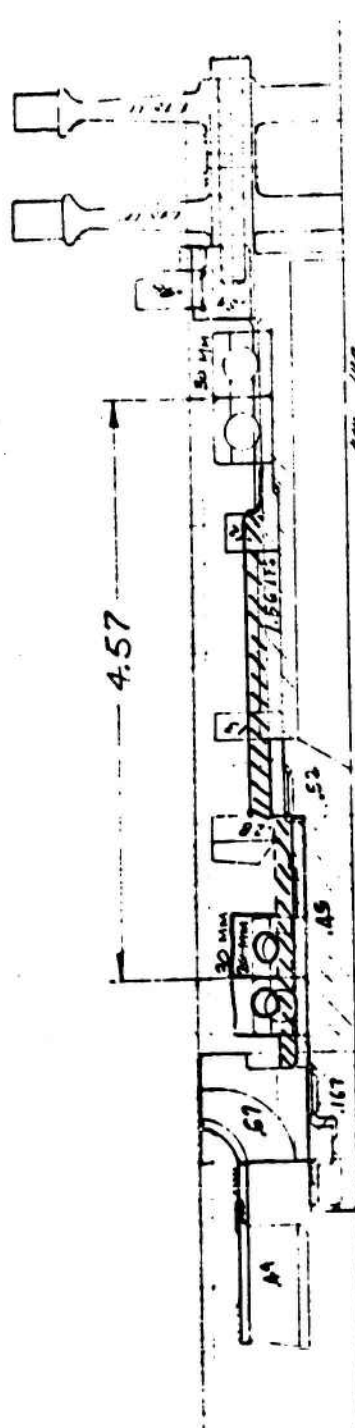
	20	18	16	14	12	10	8	6	4	3	2	1
L	.45	.44	.5	.42	.41	.40	.45	.45	.61	.68	1.0	.7
W	.15	.16	.16	.2	.17	.12	.12	.12	.12	.43	.3	.42
R <sub>1</sub>	.96	.96	.96	.5	.65	.69	.69	.65	.65	.65	.65	.65
R <sub>2</sub>	.84	.84	.84	.4	.4	.4	.4	.45	.45	.45	.45	.45
E <sub>100</sub>	29	29	29	29	29	29	29	29	29	29	29	29
J <sub>22</sub>												
IX												
EX	516	516	516	516	516	516	516	516	516	516	516	516
C	3.47	3.47	3.47	3.47	3.47	3.47	3.47	3.47	3.47	3.47	3.47	3.47

L	.61	.68	1.0	.7
W				
R <sub>1</sub>	.82	.82	.82	.82
R <sub>2</sub>	.65	.65	.65	.65
E <sub>100</sub>	29	29	29	29
J <sub>22</sub>	0	0	0	0
IX	0	0	0	0
EX	6266	6266	6266	6266
C	1.91	1.91	1.91	1.91

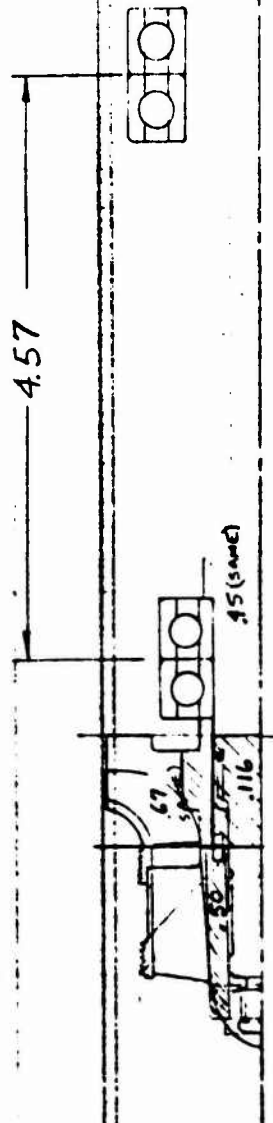
PT 105  
**00S OXID PUMP**  
5/27/70 S.P.



CASE C (14)

[illegible]

00S OXID PUMP  
5/27/77 S.F.

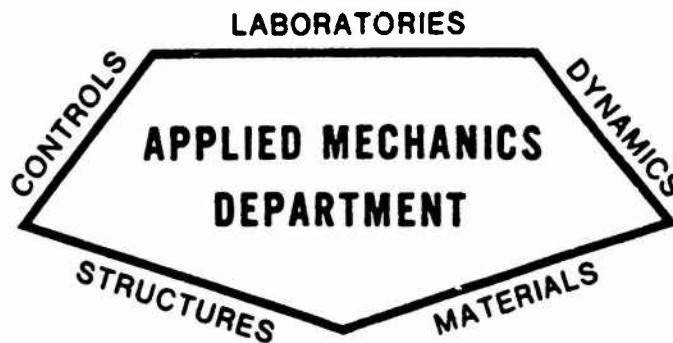


	20	19	18	17
L	45	45	45	45
W	47	47	47	47
R <sub>0</sub>	44	44	44	44
R <sub>1</sub>	27	27	27	27
C <sub>1</sub>	29	29	29	29
1615				
P <sub>1</sub>				
E <sub>1</sub>	0.7	0.7	0.7	0.7
C	34	34	34	34

BASELINE CONCEPT NO. 2  
OOS OXID PUMP



OOS TURBINE DISK PARAMETRIC STUDY - LIFE CYCLES,  
LIFETIME AND BURN DURATION



## STRUCTURAL ENGINEERING SECTION

REPORT NO. SA-OOS-TM-4

OOS TURBINE DISK PARAMETRIC  
STUDY - LIFE CYCLES, LIFETIME  
AND BURN DURATION

PREPARED BY:

L. W. Bartholf  
Engineering Specialist  
Structural Engineering Section

APPROVED BY:

L. K. Severud, Manager  
Structural Engineering Section  
Engineering

DATE 11 August 1971



AEROJET LIQUID ROCKET COMPANY

SACRAMENTO, CALIFORNIA

## TABLE OF CONTENTS

	<u>Page</u>
I. Introduction	1
II. Summary of Results	2
III. Discussion	12
IV. Conclusions	16
V. Analysis	
A. Design Criteria and Duty Cycle	17
B. Assumptions Basic to Parametric Study	22
C. Blade Root Stresses	23
D. Allowable Blade Stresses for Preliminary Design	24
E. Disk Aver. Tan. Stress Related to Mean Blade Speed	25
F. Allowable Disk Stresses for Preliminary Design	29
G. Summary of Design Sizing Criteria	30
H. Material Properties	31
I. Turbine Start Transient Effects on Blade Life	38
J. Disk Thermal Shock Strains and Cyclic Life	41
K. Disk Life Cycle Capabilities Considering Single Run Time, Number of Thermal Cycles, and Total Duration	54

## LIST OF FIGURES

<u>Figure</u>	<u>Title</u>	<u>Page</u>
1	Life Cycle Limits Related to Temperature When Only Short Duration Burns are Applied	4
2	Lifetime of Disks When Only Short Duration Burns are Applied	6
3	Turbine Disk Speed Related to Temperature and Lifetime	7
4	Lifetime of Disks When 75% of Total Life is Used in 1000 Second Duration Burns	8
5	Remaining Life Cycles When Long Duration Burns are Applied	9
6	Effect of Temperature and Number of Long Burns on Disk Short Time Cycles	10
7	Turbine Blade Start Transient Effect on Peak Thermal Strain	11
8	Response of OOS FTPA Rotor to a Step Temperature Change at the Tip (Insulated)	20
9	Response of OOS FTPA Rotor to a Convection Temperature Change (Non-Insulated)	21
10,11,12	FTPA Turbine Rotor Centrifugal Stresses	26,27,28
13,14	Waspaloy Stress to Rupture	32,33
15,16	Udimet 700 Stress to Rupture	34,35

LIST OF FIGURES (CONT.)

<u>Figure</u>	<u>Title</u>	<u>Page</u>
17	Typical Waspaloy Material Strength Data	36
18	Typical Udimet 700 Material Strength Data	37
19	Turbine Blade Start Transient Effect on Peak Thermal Strain	40
20	Biot Number and Start Transient Effect on Disk Thermal Strain	43
21	Disk Thermal Strain as a Function of Type of Heating and Turbine Inlet Temperature	49
22	Waspaloy Low Cycle Fatigue Data	50
23	Udimet 700 Low Cycle Fatigue Data	51
24	Waspaloy Disk Short Time Cycles to Failure for Various Heating Condition and $T_{II}$ 's	52
25	Udimet 700 Disk Short Time Cycles to Failure vs $T_{II}$ 's	53

## I. INTRODUCTION

The following report presents results of parametric analyses on the OOS turbine disk to determine the effect and interaction of life time, life cycles and burn duration for various turbine inlet temperatures and mean blade speeds.

The turbine disks are key components in engine design for long life and multiple starts in that they are normally exposed to severe thermal gradients due to start and shutdown transients which may precipitate fatigue failure and they are subject to high metal temperature for long duration application which could induce creep rupture failure of the disk.

This report is designed to show trends for particular design applications and should not be construed to be a structural evaluation of point designs.





SUBJECT

DATE

7/13/71

WORK ORDER

1811-05-101

## II. SUMMARY OF RESULTS

BY

L.W. BARTHOLF

CHK. BY

DATE

OOS TURBINE ROTOR - PARAMETRIC STUDY

## ASSUMPTIONS:

- NON-INSULATED ROTOR, TURBINE INLET TEMPERATURE = 1400°F
- MAXIMUM BURN DURATION = 1000 SEC.

ENGINE RUN DURATION (HRS)	TURBINE Rotor TIME AT T <sub>II</sub> (HRS)	WASPALOY			UDIMET 700		
		STRESS TO RUPTURE (KSI)	ALLOW. ATS (KSI)	* ALLOW MEAN BLADE SPEED (FT/SEC)	STRESS TO RUPTURE (KSI)	ALLOWABLE ATS (KSI)	ALLOW MEAN BLADE SPEED (FT/SEC)
2	1.5	95	59	1375	109	68	1480
10	7.5	83	52	1300	97	60	1390
20	15.0	75	47	1230	92	57	1350

- NON-INSULATED ROTOR, TURBINE INLET TEMPERATURE = 1400°F
- TOTAL ENGINE RUN DURATION = 10 HRS

MAX. BURN DURATION (SEC)	TURBINE Rotor TIME AT T <sub>II</sub> (HRS)	WASPALOY			UDIMET 700		
		STRESS TO RUPTURE (KSI)	ALLOWABLE ATS (KSI)	ALLOW MEAN BLADE SPEED (FT/SEC)	STRESS TO RUPTURE (KSI)	ALLOWABLE ATS (KSI)	ALLOW MEAN BLADE SPEED (FT/SEC)
500	5.7	85	53	1310	99	61	1400
1000	7.5	83	52	1300	97	60	1390
2000	8.5	82	51	1290	96	59	1390

$$* \text{ATS}_{\text{ALLOW}} = \frac{\sqrt{R}}{1.61}$$

$$\text{NOTE: } 1.61 = \frac{\text{SAFETY FACTOR}(1.17)^2}{\text{DESIGN FACTOR}(.35)}$$

$$* \sqrt{V}_{\text{ALLOW}} = \left( \frac{\text{ATS}}{.031} \right)^{1/2}$$



SUBJECT

DATE

7/15/71

WORK ORDER

18/1-05-101

## II. SUMMARY OF RESULTS

BY

L.W. BARTHOLF

CHK. BY

DATE

00S TURBINE ROTOR - PARAMETRIC STUDY

## ASSUMPTIONS:

- NON-INSULATED ROTOR, TURBINE INLET TEMPERATURE = VARIABLE.
- ONE 1000 SEC. BURN, FIVE 40 SEC. BURNS.

NUMBER OF THERMAL CYCLES	NUMBER OF 1000 SEC. BURNS	REQUIRED NO. OF SHORT BURNS	CALCULATED REMAINING SHORT BURNS AFTER REQUIRED 1000 SECOND BURNS.					
			WASPALLOY			UDIMET 700*		
			1400°F	1300	1200	1400	1300	1200°F
60	10	50	555	698	900	298	369	449
300	50	250	500	655	855	250	326	406
600	100	500	435	598	795	191	274	352

\* CALCULATED USING  $t/t_r = 608(10)^{-6}$  FOR WASPALLOY @ 1400°F,  $162(10)^{-6}$  @ 1300°F;  $135(10)^{-6}$  @ 1200°F AND THE FOLLOWING EQUATION\* (SEE SECTION V-K)

$$N_{rem.} = N_f \left[ 1 - \frac{N_L t}{t_r} \right] - N_L$$

$$= 310 \left[ 1 - 608(10)^{-6} N_L \right] - N_L \quad @ 1400^\circ F$$



SUBJECT

## II. SUMMARY OF RESULTS

BY

LKS

CHK. BY

THE CURVES ARE ONLY  
FOR SHORT TIME BURNS  
WHERE DURATION IS LESS  
THAN 100 SECONDS AND  
CREEP DAMAGE IS NOT  
APPLICABLE.

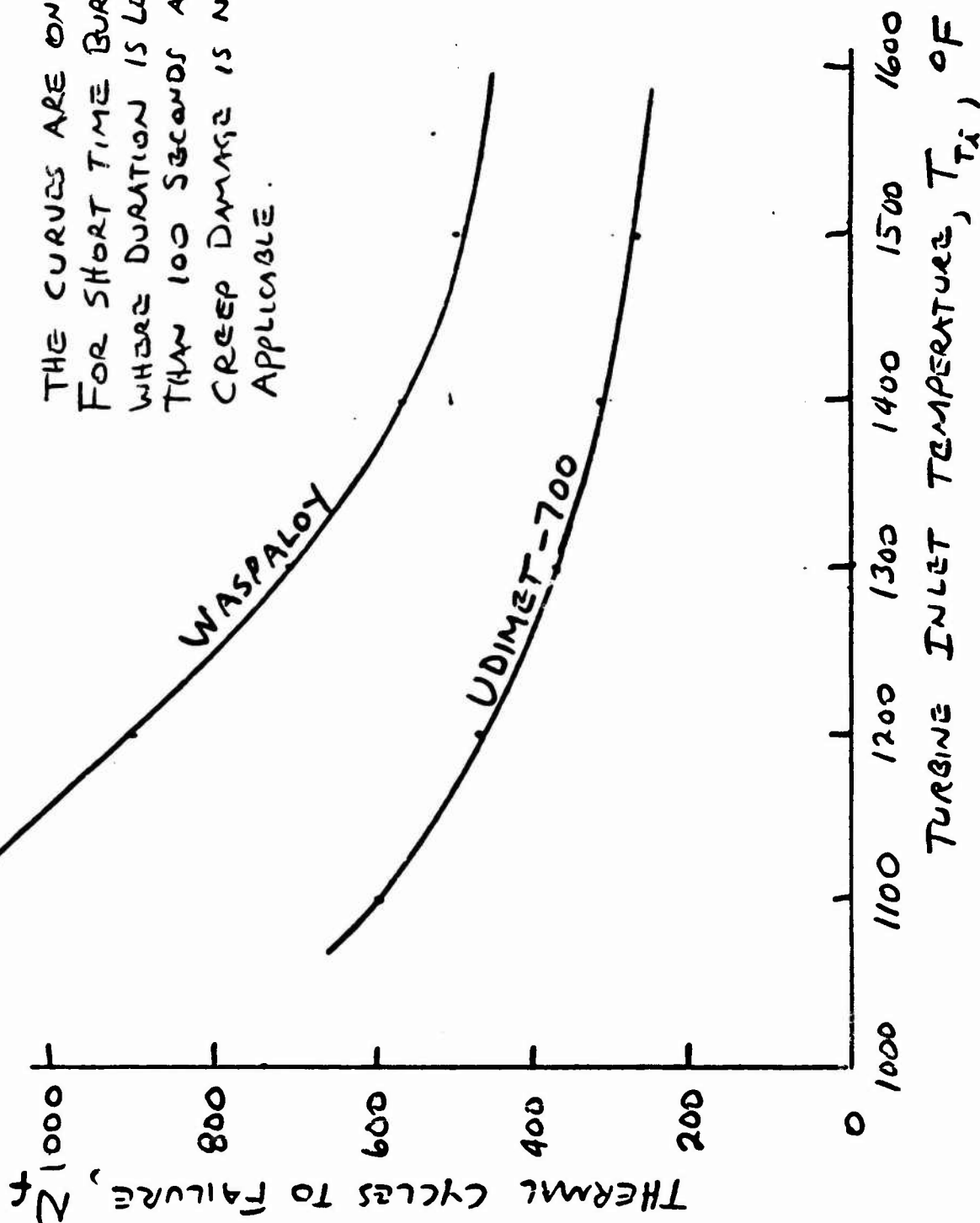


FIG. 1 - LIFECYCLE LIMITS RELATED TO TEMPERATURE WHEN ONLY SHORT DURATION BURNS ARE APPLIED.



AGCS-090011

SUBJECT

DATE

## II. SUMMARY OF RESULTS

WORK ORDER  
1811-05-101.

BY

LKS

CHK. BY

DATE

IF ALL BURNS HAVE DURATIONS LESS THAN 100 SECONDS, THEN CREEP DAMAGE PER BURN IS NEGLIGIBLE AS THE DISK AVERAGE TEMPERATURE IS LESS THAN 740°F (REF: FIG 8 ). ACCORDINLY THE DURATION THEN WOULD BE LIMITED BY THE LOW CYCLE FATIGUE LIFE CYCLES MULTIPLIED BY THE DURATION PER BURN. FOR EXAMPLE, AT A TURBINE INLET TEMPERATURE OF 1400°F A WASPALOY TURBINE DISK FATIGUE LIFE IS PREDICTED TO BE 570 CYCLES. THE TOTAL LIFETIME CAPABILITY WOULD THUS BE 570 MINUTES = 9.5 HRS FOR SHORT FIRINGS OF 60 SECONDS PER BURN. IF ALL THE BURNS WERE ONLY 10 SECONDS, THE TOTAL LIFE TIME CAPABILITY WOULD BE ONLY 95 MINUTES = 1.5 HRS. SEE THE CURVE ON THE FOLLOWING PAGE FOR THESE PARAMETERS.



SUBJECT

## II. SUMMARY OF RESULTS

BY

LKJ

CHK. BY

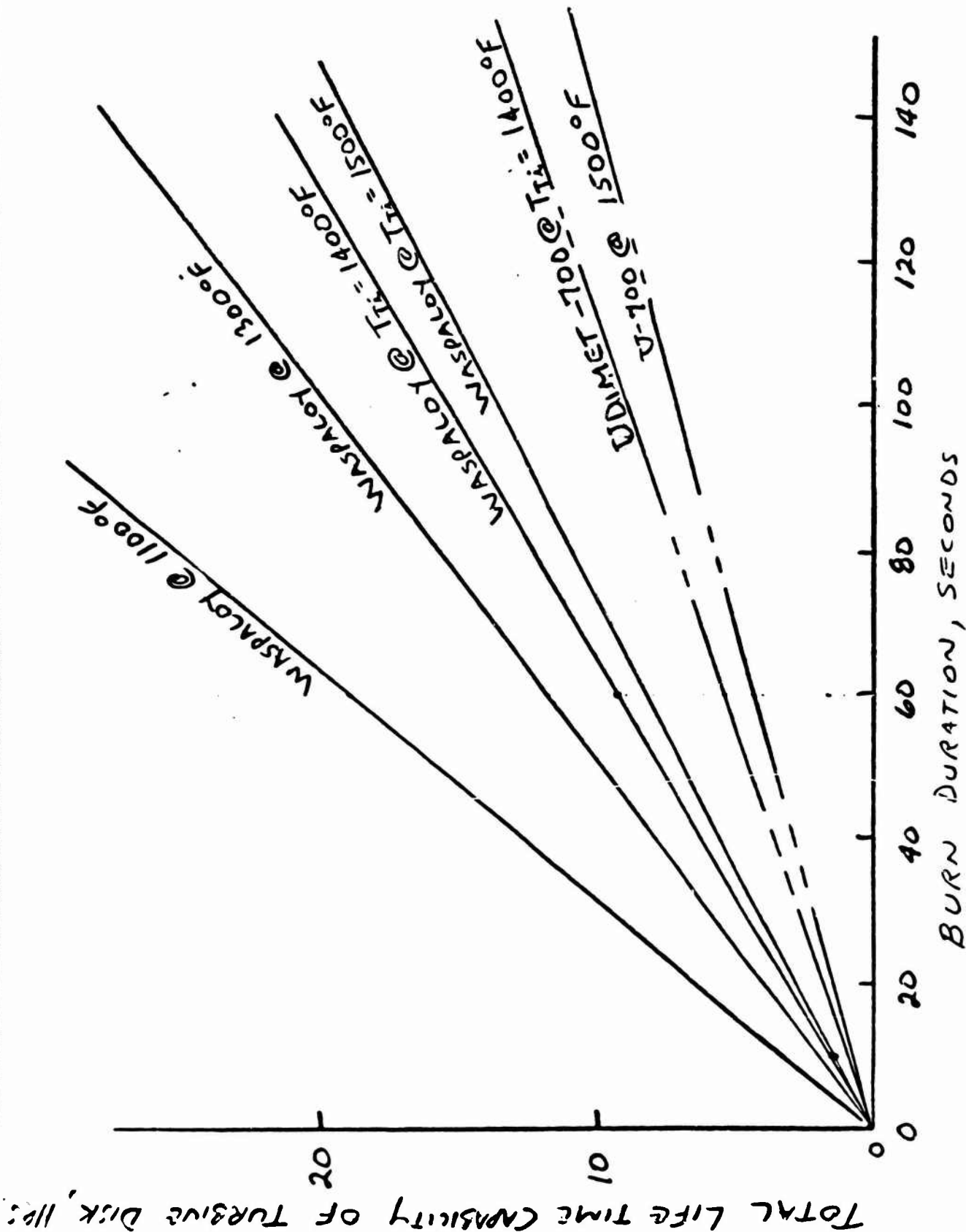


FIG. 2 - LIFETIME OF DISKS WHEN ONLY SHORT DURATION BURNS ARE APPLIED.



SUBJECT

DATE

## II. SUMMARY OF RESULTS

WORK ORDER  
1811-05-101

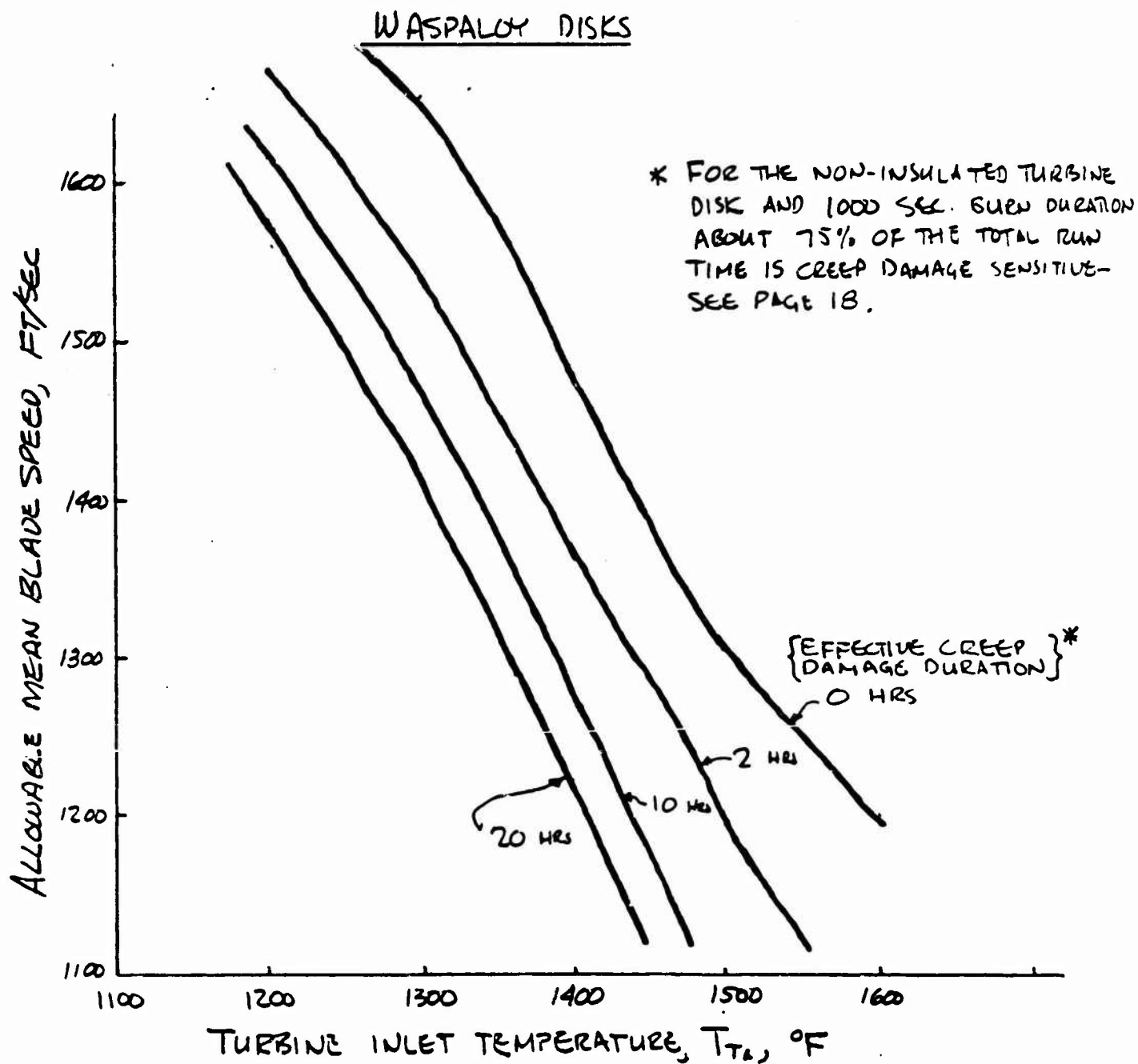
BY

LKS

CHK. BY

DATE

Fig. 3 - TURBINE WHEEL SPEED RELATED TO TEMPERATURE & LIFE TIME





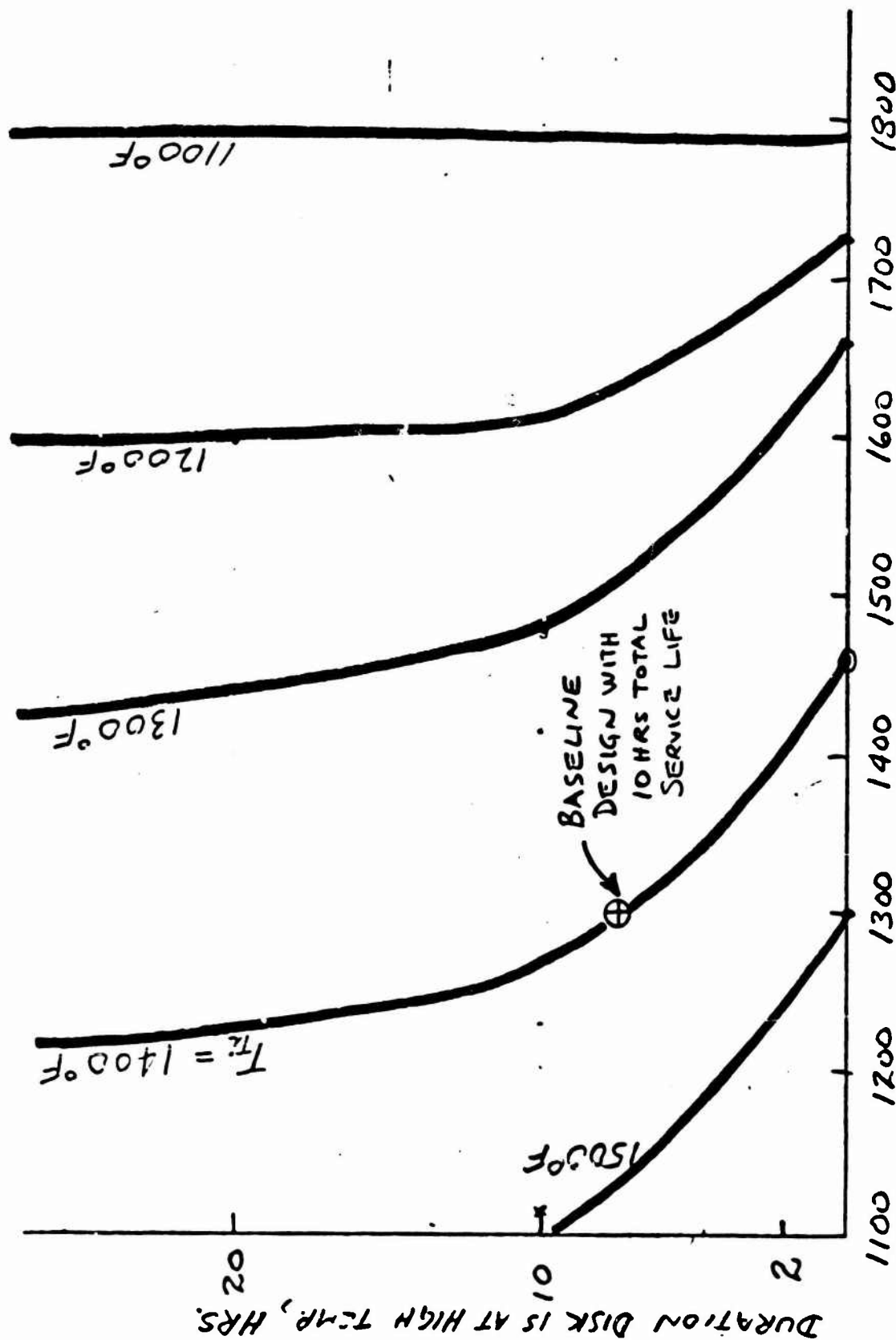
## II. SUMMARY OF RESULTS

BY

LKS

CHK. BY

WASPALCOY DISKS



ALLOWABLE MEAN BLADE SPEED BASED ON  
DISK STRENGTH, FT/SEC.

FIG. 4 - LIFETIME OF DISKS WHEN 75% OF TOTAL LIFE IS USED  
IN 1000 SECOND DURATION BURNS.



SUBJECT

OOS PARAMETRIC STUDY

DATE

7/9/71

WORK ORDER

1811-05-101

BY

G. ALDRICH

CHK BY

DATE

## II. SUMMARY OF RESULTS

TURBINE INLET TEMPERATURE = 1400°F

RIM AND SIDE HEATING (NON-INSULATED)

WASPALLOY, 1300 FT/SEC MEAN BLADE SPEED

NO SAFETY FACTORS

INCLUDED ON  $N_{SR}$

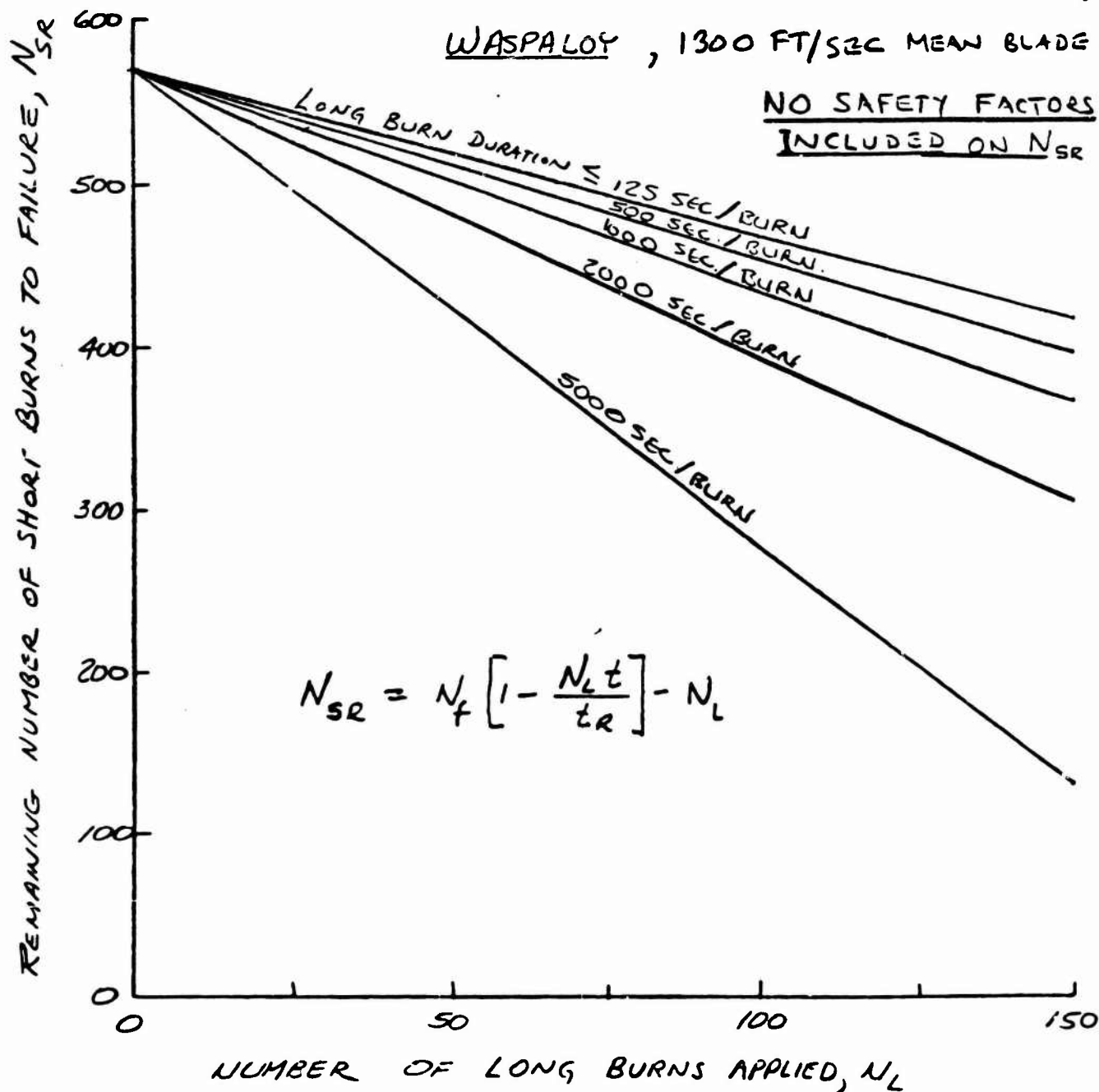


FIG. 5- REMAINING LIFE CYCLES WHEN LONG DURATION BURNS ARE APPLIED.





DATE  
7/9/71

WORK ORDER  
1811-05-101

DATE

BY

G. ALDRICH

CHK. BY

# OOS PARAMETRIC STUDY

## II. SUMMARY OF RESULTS

NO SAFETY FACTORS INCLUDED  
ON  $N_{SR}$

RIM AND SIDE HEATING TURBINE DISK LIFE CYCLES AND LIFETIME  
(WASPALLOY)

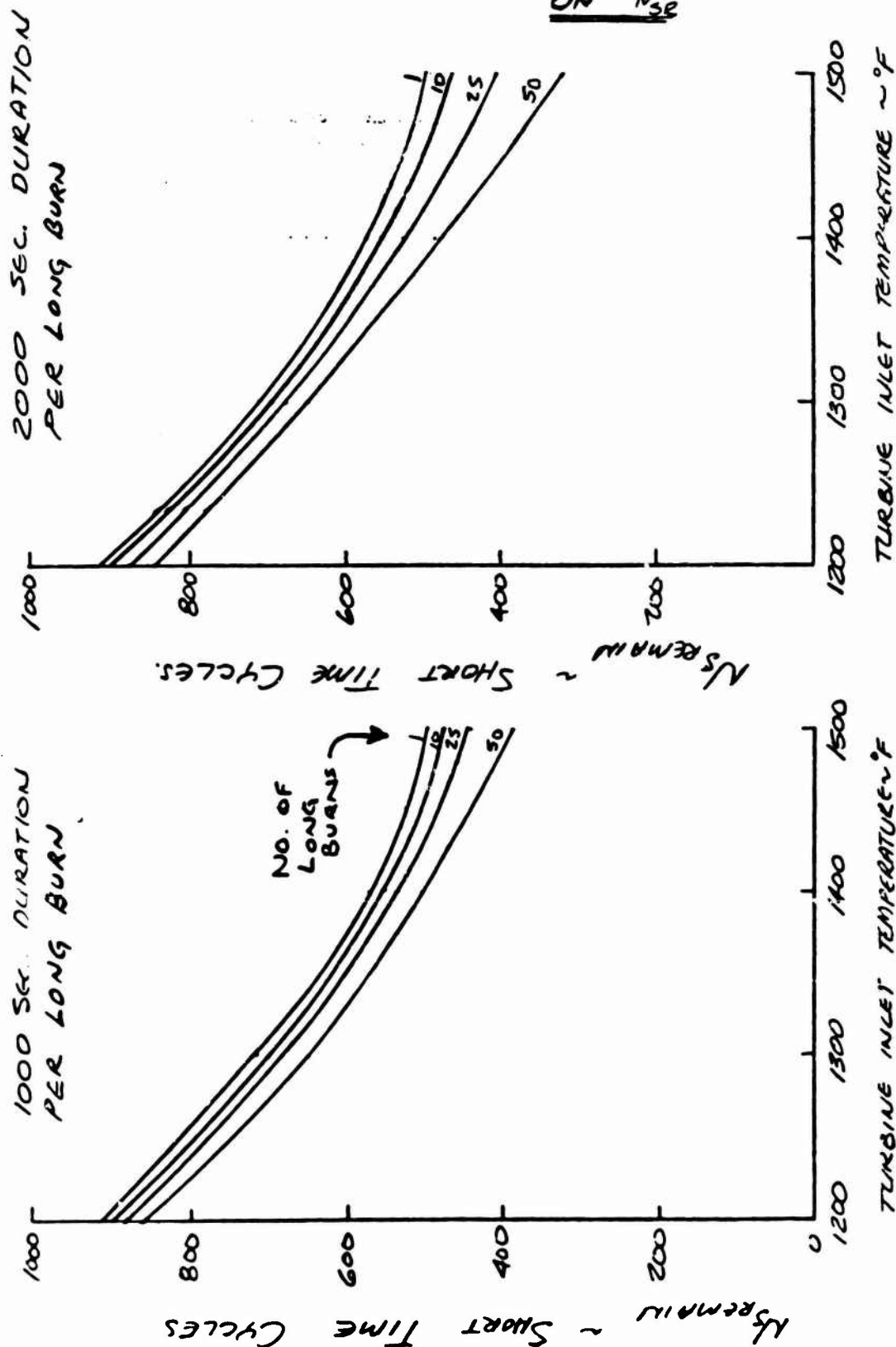
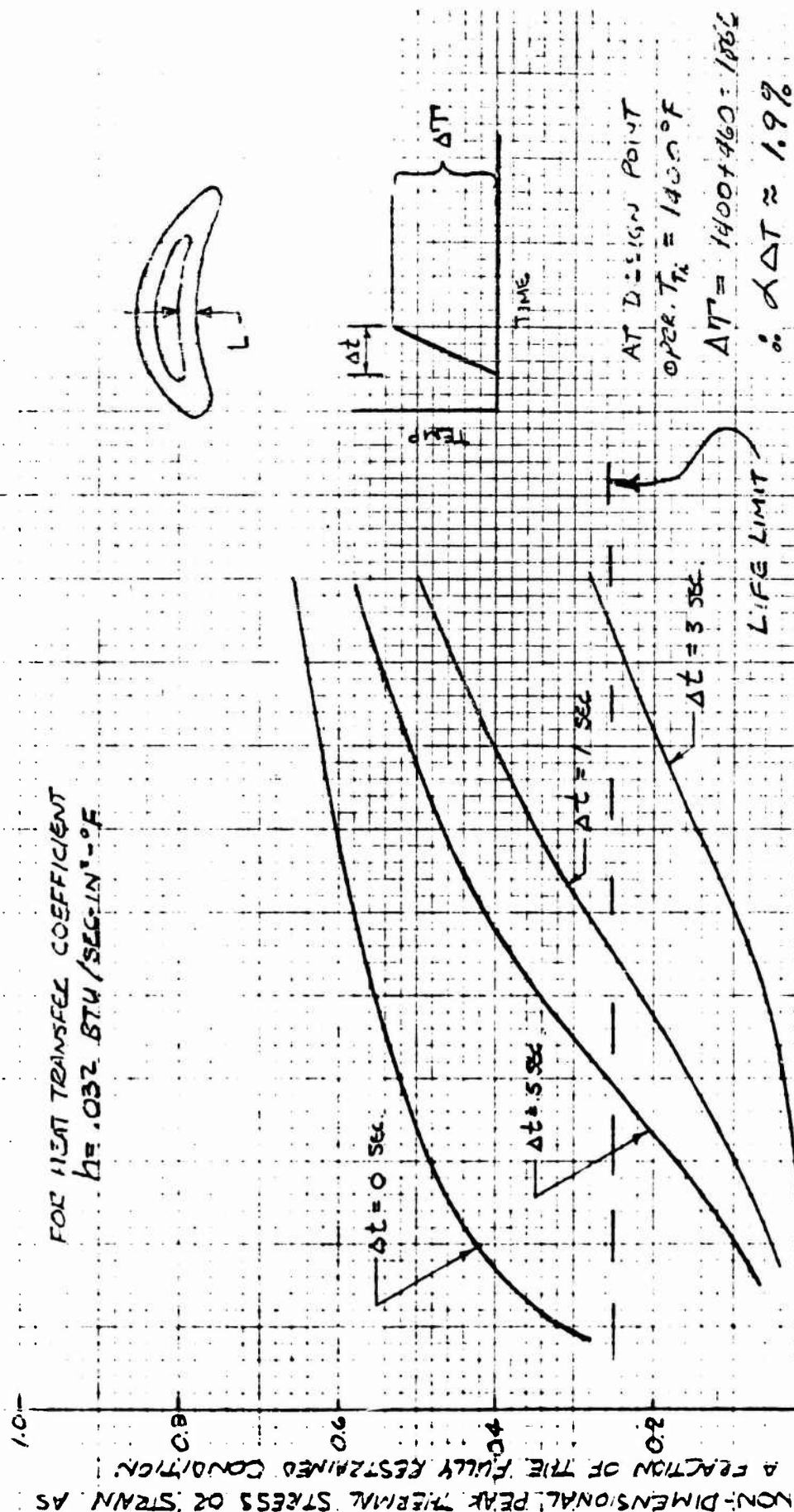


FIG. 6 - EFFECT OF TEMPERATURE AND NUMBER OF LONG BURNS  
ON DISK SHORT TIME CYCLES.

## II. SUMMARY OF RESULTS

FIG 7- TURBINE BLADE START TRANSIENT EFFECT ON PEAK THERMAL STRESS



### III. DISCUSSION

The summary of results shows some of the more significant trends which were observed in this study. Figures 1 and 2 require no elaboration. Figures 3 and 4 show the logarithmic nature of the creep damage associated with high temperatures and the sensitivity of life time to applied stress. For the design turbine inlet temperature of 1400°F Figure 4 shows large gains in mean blade speed can be made when designing between 20 and 2 hours of life-time but relatively small gains in mean blade speed result when one considers the difference between 100 and 20 hour design lives. Also notice that these differences become less noticeable when lower turbine inlet temperatures are examined.

The fact that the turbine blade start transients can be tailored to mitigate thermal shock strains by utilizing ramps of less than 3 seconds (see Figure 7) whereas the disk thermal shock strains are unaffected by ramps of this duration can be attributed mainly to the geometry of the parts. The relative massive and cold disks require a much longer start transient ramp to mitigate the thermal strains. Sections V-I and V-J go into more detail in this area.

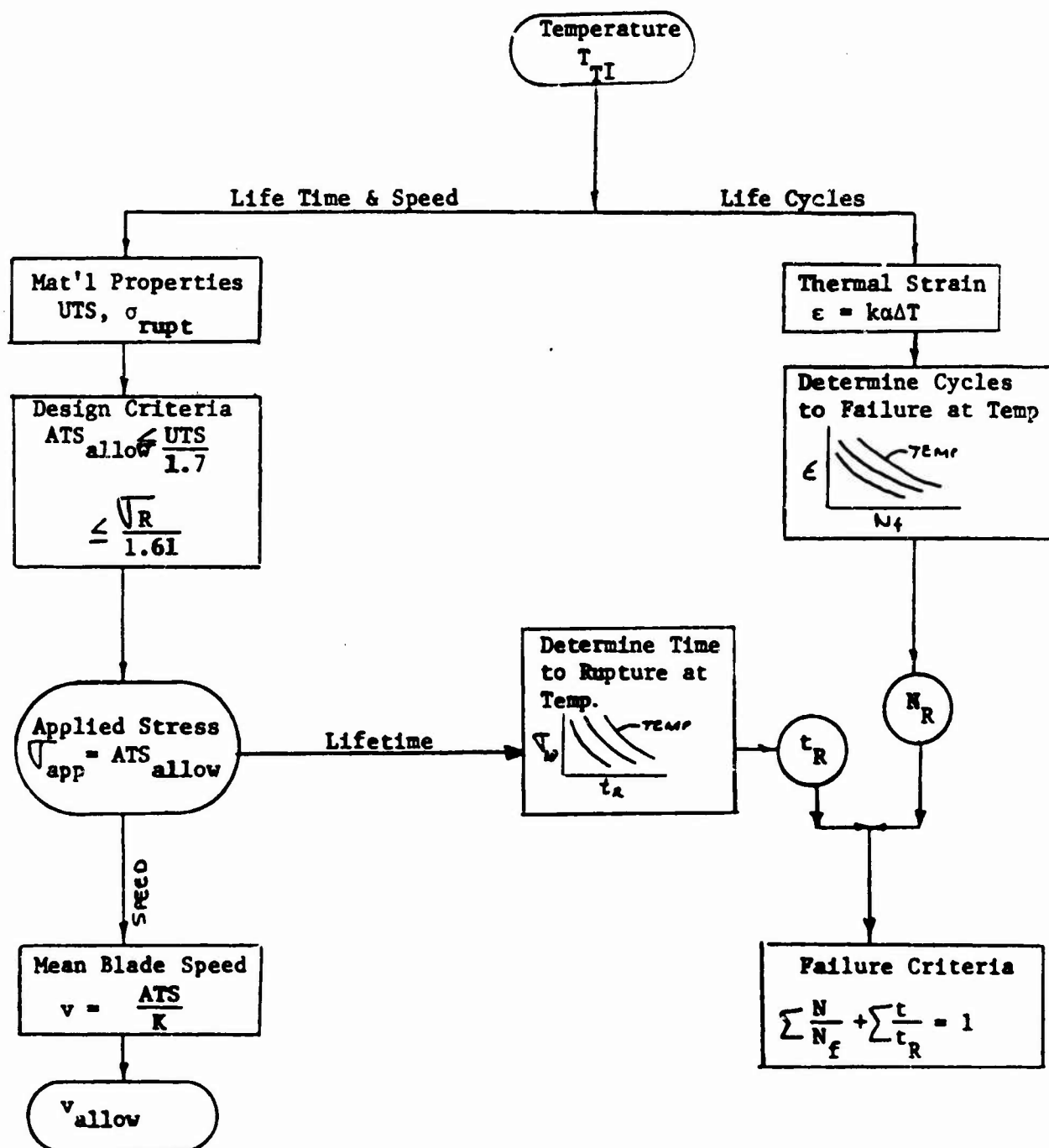
The time the rotor is at turbine inlet temperature appears several times in the summary of results and in most cases is 75% of the total engine run time. This percentage was derived in Section V-A and reflects the time which it takes the disk to heat up to temperature as seen in Figure 9. The time at temperature and the burn duration both influence the amount of creep damage or creep rupture susceptibility which forms the rational for looking at short duration firings from just a fatigue fracture aspect since run times are not long enough to cause creep damage.

The empirical relationships of disk average tangential stress to mean blade speed were derived by examining past turbine wheel analyses and compiling data from these analyses to arrive at the chosen relationship. These relationships are key factors and form the basis for determining allowable mean blade speeds in this parametric study. These equations and some assumptions basic to this study can be found in Sections V-B through V-G.

The disk thermal strains which were determined in Section V-J, also required some basic assumptions and examination of the effects of various parameters. It was this section that establishes the non-insulated turbine disk as most desirable from a life cycle approach as the thermal shock strains are estimated to be slightly less than those for an insulated disk and small changes in strain result in large changes in life cycles. The distinction between insulated and non-insulated is mainly based on the portion of the disk exposed to hot gases. On the insulated disk the rim is the only part exposed while on the non-insulated disk the rim and the majority or all of the sides could be exposed.

The interaction between fatigue damage and creep damage on disk life cycles is covered in Section V-K. The linear interaction formula was applied and a non-insulated Waspaloy disk was assumed to determine the creep damage fraction ( $t/t_R$ ) and the fatigue damage fraction ( $\frac{N}{N_f}$ ). The relationship between turbine inlet temperature and disk average tangential stress was fixed by the design allowables shown in Figure 17 for a 10 hour stress rupture life with design and safety factors of 1.61 on long time stress. The baseline design curves are shown in the summary of results, Figures 5 and 6 which shows the effects of burn duration and number of burns on short time fatigue life. This section is valuable to show trends, however, it is pointed out that life time is very sensitive to applied stress which negates the use of these curves for point design evaluation.

The following is a flow chart approach to show the basic methods used in this study to determine life cycles, lifetime and allowable mean blade speeds.



#### Procedure:

Given a turbine inlet temperature ( $T_{TI}$ ) material properties and thermal strain can be determined. ( $\Delta T = T_{TI} - T_{initial}$ ). The allowable disk average tangential stress was established in Section V.F and includes safety factors of 1.44 on short time applied stress and 1.37 on long time applied stress. For this applied stress the time to rupture ( $t_R$ ) is determined for the given  $T_{TI}$  and the allowable mean blade speed is determined from the empirical equation derived in Section V.E. The

number of short time cycles to failure ( $N_f$ ) is determined by going to the curves STRAIN vs cycles to failure and picking off the  $N_f$  associated with the estimated strain ( $\epsilon$ ) and proper temperature. To determine the combined effects of lifetime and life cycles a linear cumulative damage criteria was used where at failure the sums of the fatigue and creep damage ratios are assumed to equal one.

#### IV. CONCLUSIONS

- The disks are life cycle controlled at lower turbine inlet temperature and life time controlled at higher  $T_{TI}$ 's, for the mixes of this investigation.
- Small percentage changes in thermal shock strain result in large percentage changes in life cycles.
- Trends are readily identifiable for the various mixes of life cycles, life time and burn duration.



OOS PARAMETRIC STUDY

J. W. BARTHOLOMEW

## IV. ANALYSIS:

### A. DESIGN CRITERIA AND DUTY CYCLE

#### BASELINE DESIGN CONDITIONS:

- 10 HRS SERVICE LIFE (REUSABLE AT OVERHAUL COST = 25% - NEW)
- 300 THERMAL CYCLES
- 1000 SECOND MAXIMUM SINGLE RUN DURATION
- ASSUMED THAT THE MIX OF SHORT DURATION FIRINGS  
TO LONG DURATION IS 5:1

#### DESIGN CONDITIONS TO BE VARIED INDIVIDUALLY FOR PARAMETRIC STUDY:

- (a) SERVICE LIFE; 2 HRS, 20 HRS
- (b) THERMAL CYCLES; 60 , 600
- (c) SINGLE RUN MAX. DURATION; 500 SEC. , 2000 SEC.

#### EFFECTS OF THE ABOVE DESIGN CHANGES (a) AND (b) TO BE DETERMINED ARE THOSE ON:

- (1) TURBINE INLET TEMPERATURE
- (2) TURBINE MEAN BLADE SPEED

THE EFFECTS OF (c) ON ENGINE LIFE-CYCLE CAPABILITIES  
ARE ALSO TO BE DETERMINED.



DATE  
7/2/71WORK ORDER  
1811-05-101

## OOS PARAMETRIC STUDY

BY  
L.W. BARTHOLF

CHK. BY

DATE

A. DESIGN CRITERIA CONSIDERED

THERMAL CYCLES (BURNS)	SERVICE LIFE DUR. (HRS)	MAX. SINGLE RUN DURATION (SEC)	SHORT BURN DURATION (SEC)
60	2	500	40
300	10	1000	40
600	20	2000	40

← TASK I BASE CASE

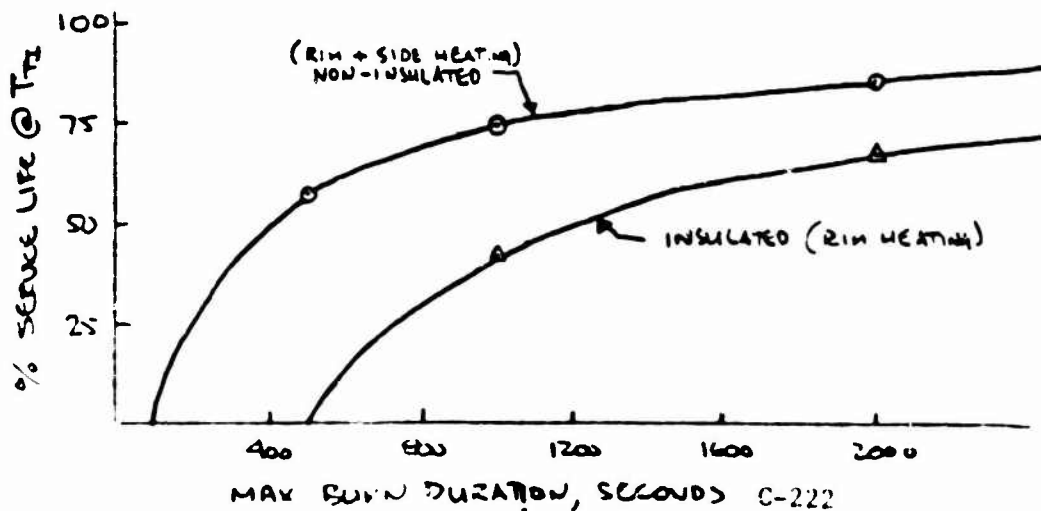
ASSUMPTION: (PER W. LUSCHER, PROGRAM ENGR MGR.)

A TYPICAL FLIGHT CONSISTS OF ONE(1) LONG DURATION BURN AND FIVE(5) SHORT DURATION BURNS.

FOR THE NON-INSULATED TURBINE DISK THE WHOLE DISK IS UP TO  $T_{Ti}$  IN ABOUT 100 SECONDS. SEE FIGURE 9. THEREFORE IN THE LONG DURATION BURNS THE DISK IS CREEP RUPTURE CONTROLLED AS SHOWN BY THE CURVE BELOW.SAMPLE CALCULATION: 1-1000 SEC. DURATION BURN } 1200 SEC. TOTAL.  
5-40 SEC. DURATION BURNS }

$$\text{NO. Flights} = \frac{36000}{1200} = 30$$

$$\text{Time @ } T_{Ti} = \frac{(1000-100)30}{3600} = 7.5 \text{ HRS} = 75\%$$





AEROJET-GENERAL CORPORATION  
SACRAMENTO • CALIFORNIA

AGCS 0800 11

REPORT NO.

PAGE 19 OF 69

SUBJECT

DATE

005 PARAMETRIC STUDY

WORK ORDER

1811-05-101

BY

LW13

CHK. BY

DATE

#### A. DESIGN CRITERIA CONT

TWO CONDITIONS OF TURBINE DISK HEATING WERE INVESTIGATED.

- (a) RIM HEATING (INSULATED DISK)
- (b) RIM & SIDE HEATING (NON-INSULATED DISK)

THE RESULTS OF THESE HEAT TRANSFER ANALYSES ARE PLOTTED ON THE FOLLOWING PAGES. NOTE THAT THE DISK WAS ASSUMED TO BE AT  $-400^{\circ}\text{F}$  INITIALLY AND THEN HIT BY THE FULL ( $T_{T1}$ ) TURBINE INLET TEMPERATURE.

THE RESULTS ARE BASED ON A FINITE ELEMENT HEAT TRANSFER COMPUTER PROGRAM. A CHECK OF THE RESULTS WAS MADE USING A LONG CYLINDER SUBJECTED TO A SUDDEN CHANGE IN ENVIRONMENT AND IS SHOWN ON THE INSULATED DISK AT 100 SECONDS.

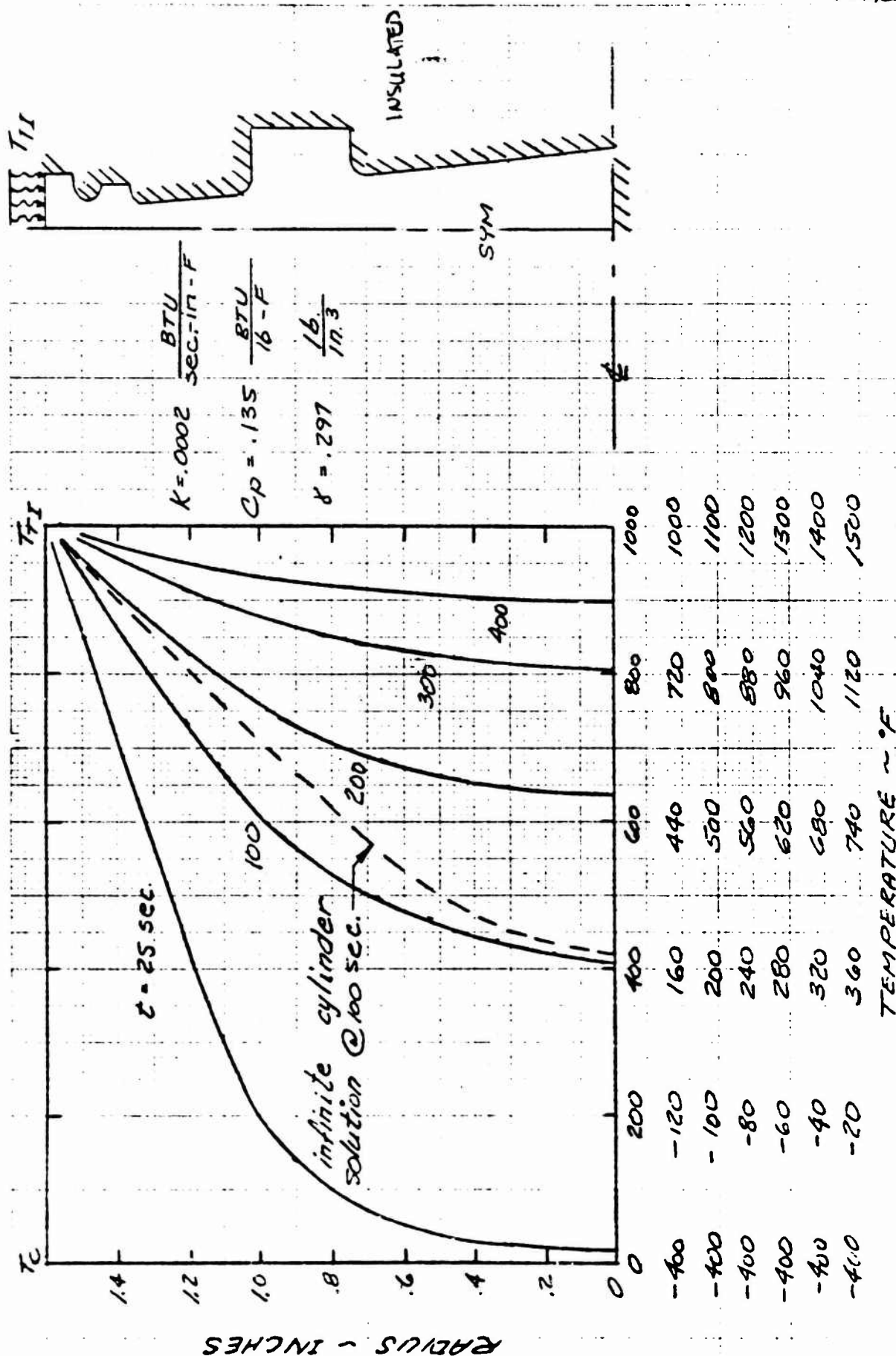


FIG. 8 - RESPONSE OF 00S 3 STAGE FTP ROTOR TO A STEP TEMPERATURE CHANGE AT THE TIP

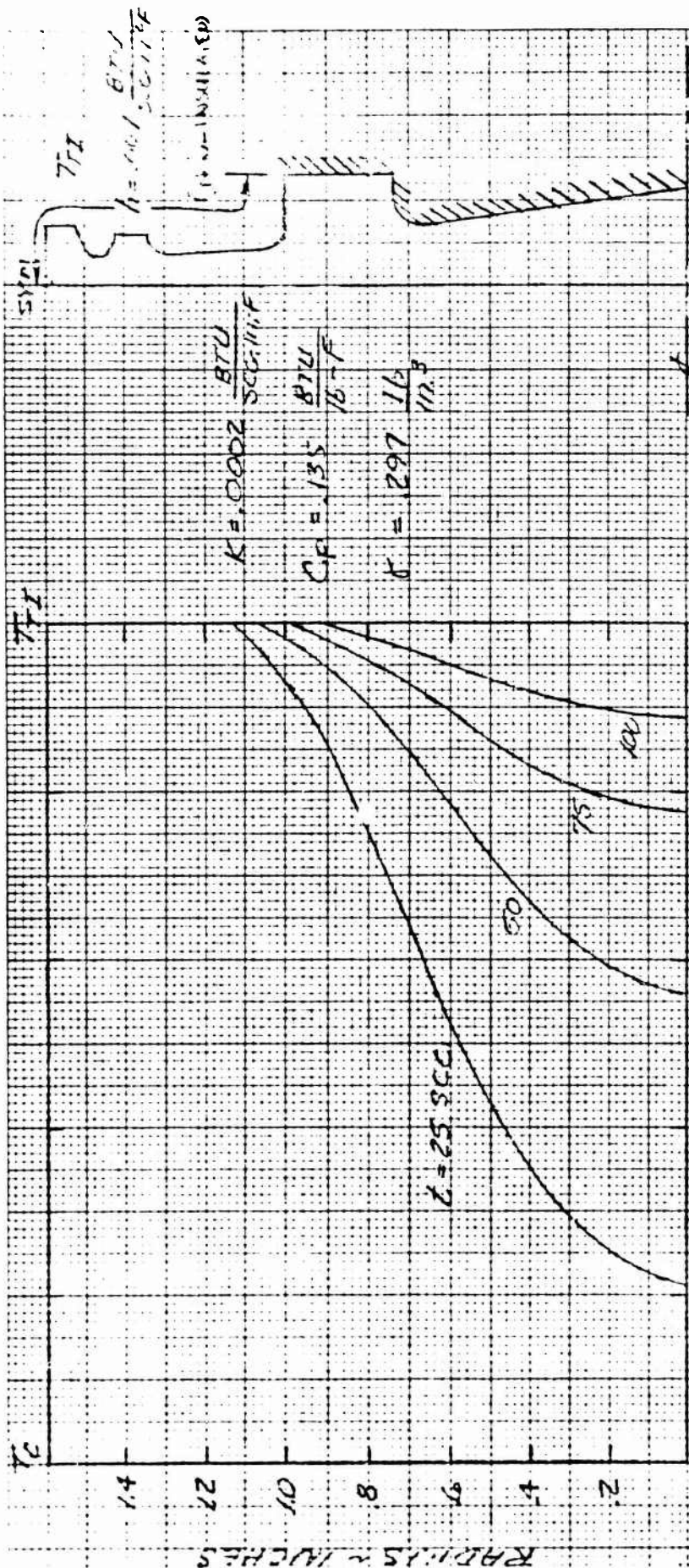


Fig. 9- REVERSE OF C.C.S. 3 STAGE FTP ROTOR TO CONVECTION AT THE TIP



FORM 000011

SUBJECT

B. ASSUMPTIONS BASIC TO PARAMETRIC STUDY

BY

LKS.

CHK. BY

## TURBINE FOR OOS APPLICATION

### ASSUMPTIONS BASIC TO PARAMETRIC STUDY

#### BLADES:

1. METAL TEMP = TURBINE INLET TEMPERATURE
2. START TRANSIENT WILL BE TAYLORED (IE, SLOW START, TEMP VS. TIME) TO LIMIT THERMAL SHOCK STRESSES AND STRAINS TO WHATEVER IS NECESSARY TO OBTAIN REQUIRED THERMAL LCF LIFE OF BLADES.
3. SERVICE LIFE WILL BE LIMITED BY CREEP RUPTURE OR DEFORMATION OF BLADES CONSIDERING BOTH BLADES AND DISK AT TURBINE INLET TEMPERATURE.
4. TIME AT LOW TEMPERATURE REGION WHERE HYDROGEN EMBRITTLEMENT DAMAGE IS MOST SEVERE IS A VERY SMALL FRACTION OF TOTAL OPERATIONAL SERVICE LIFE.

#### DISKS:

1. THERMAL SHOCK LCF FATIGUE LIFE WILL BE GOVERNED BY HOT GAS SUDDENLY APPLIED TO PRECHILLED DISK. BOTH RIM SHOCK AND SIDE WALL SHOCKS WILL BE EVALUATED.



SUBJECT

OOS PARAMETRIC STUDY

DATE

WORK ORDER

BY

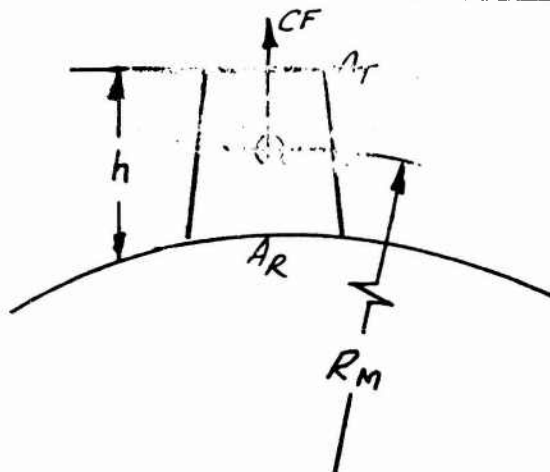
LKS

CHK BY

DATE

6/15/71

C. APPROXIMATE STRESS LEVEL AT ROOT OF TURBINE  
BUCKET - PRELIMINARY DESIGN EVALUATION



I. CENTRIFUGAL FORCE INDUCED STRESS

$$CF = MR_M \omega^2 = M v^2 / R_M \quad ; \quad v = R \omega$$

$$M = (A_R + A_T) \frac{h}{2} \frac{\delta}{g}$$

$$\text{FOR } A_R = A_T, \quad \sigma_{CF} = \frac{h \delta}{g} v \omega$$

$$\text{FOR } v \text{ UNITS} = \text{FT/SEC}, \quad \omega \text{ UNITS} = \text{RPM}$$

$$h \text{ UNITS} = \text{INCHES}$$

$$\sigma_{CF} = \left( \frac{.3}{386} \times 12 \times \frac{2\pi}{60} \right) v_{\text{FT/SEC}} \cdot \omega_{\text{RPM}} \cdot h_{\text{INCH}}$$

$$\sigma_{CF} = 0.97(10)^{-3} v_{\text{FT/SEC}} \cdot \omega_{\text{RPM}} \cdot h_{\text{INCH}}$$

(1)





SUBJECT

OOS PARAMETRIC STUDY

DATE

WORK ORDER

BY

LKS.

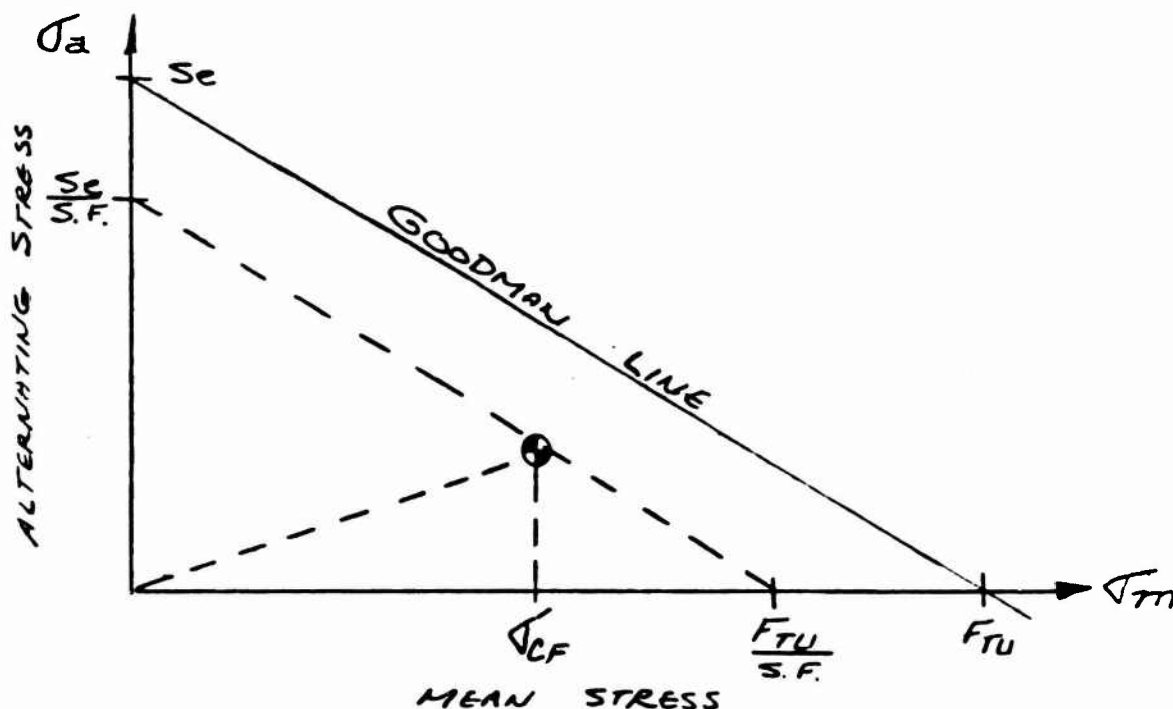
CHK BY

DATE

6/15/71

### D. ALLOWANCES FOR GAS BENDING AND VIBRATORY STRESSES.

USING THE MODIFIED GOODMAN FAILURE LINE ON A STRESS RANGE DIAGRAM AND A SAFETY FACTOR OF  $1.4 = S.F.$ , THE CENTRIFUGAL STRESS SHOULD BE KEPT BELOW ABOUT  $\frac{1}{2}$  OF  $F_{TU}$  OR  $F_{CR} =$  CREEP RUPTURE STRENGTH. THIS ALLOWS FOR A REASONABLE  $\sigma_a$  WHICH CAN ONLY BE DETERMINED IN THE DETAILED DESIGN AND DEVELOPMENT STAGE.



THUS,  $\sigma_{CF} \leq \frac{F_{TU}}{2} \text{ OR } \frac{F_{CR}}{2}$



AEROJET-GENERAL CORPORATION  
SACRAMENTO • CALIFORNIA

AGCS-0000-11

REPORT NO.

PAGE 25 OF 69

SUBJECT

OOS PARAMETRIC STUDY

DATE

WORK ORDER

BY

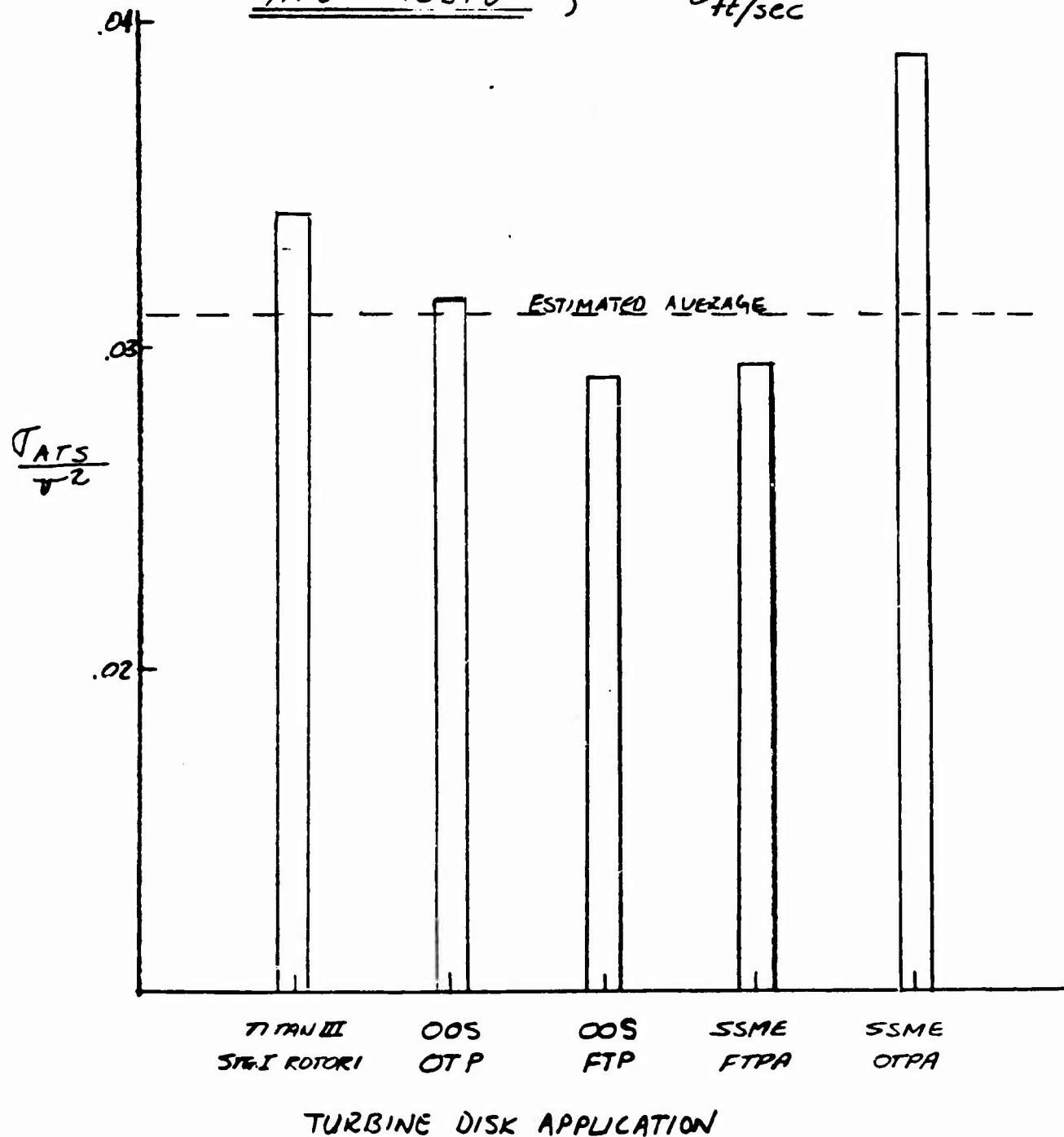
CHK. BY

DATE

6/15/71

E. RELATION OF DISK ATS TO MEAN BLADE SPEED

$ATS = .031V^2$  ;  $V$  ft/sec







AEROJET-GENERAL CORPORATION  
SACRAMENTO • CALIFORNIA

REPORT NO.

PAGE 26 OF 69

DATE

7/2/71

WORK ORDER

1811-05-101

DATE

SUBJECT

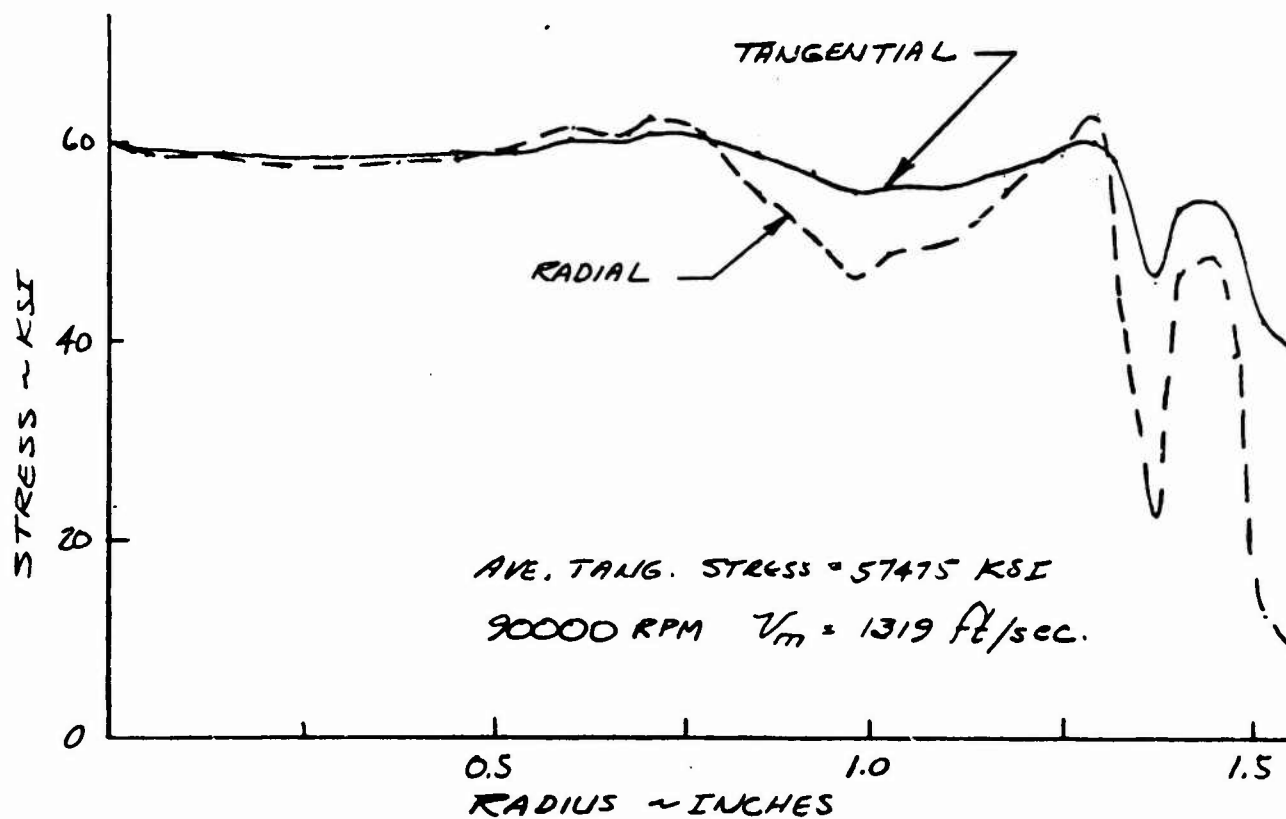
OOS PARAMETRIC STUDY

BY

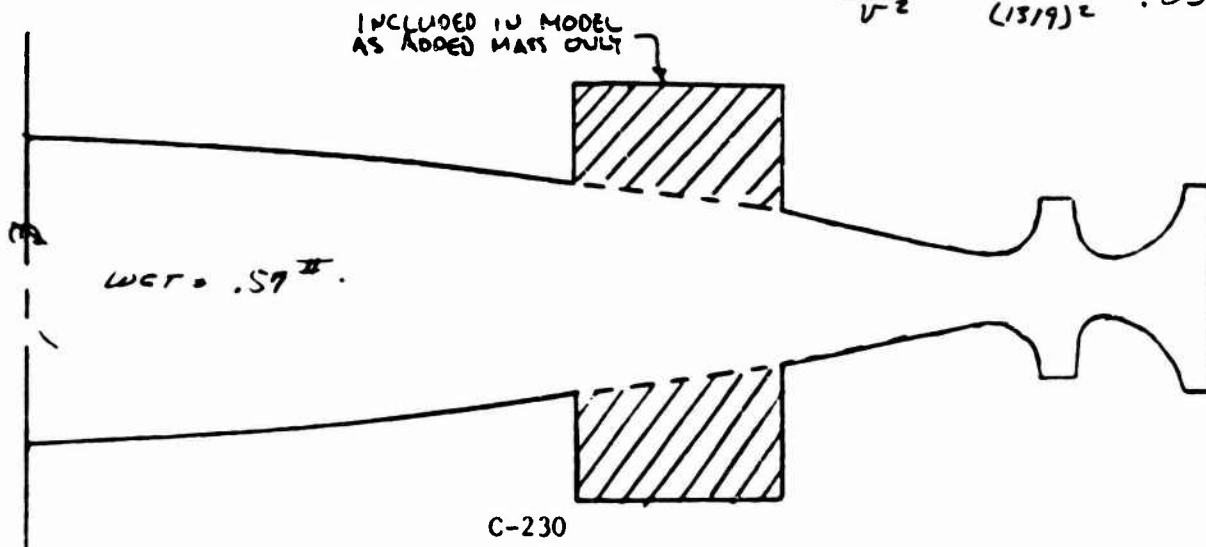
G. ALDRICH

CHK. BY

FIG. 10- FTP A TURBINE ROTOR CENTRIFUGAL STRESSES



$$\frac{ATS}{V^2} = \frac{57475}{(1319)^2} = .033$$





AEROJET-GENERAL CORPORATION  
SACRAMENTO • CALIFORNIA

REPORT NO.

PAGE 27 OF 69

AGS-000011

SUBJECT

OOS PARAMETRIC STUDY

DATE

7/6/71

WORK ORDER

1811-05-101

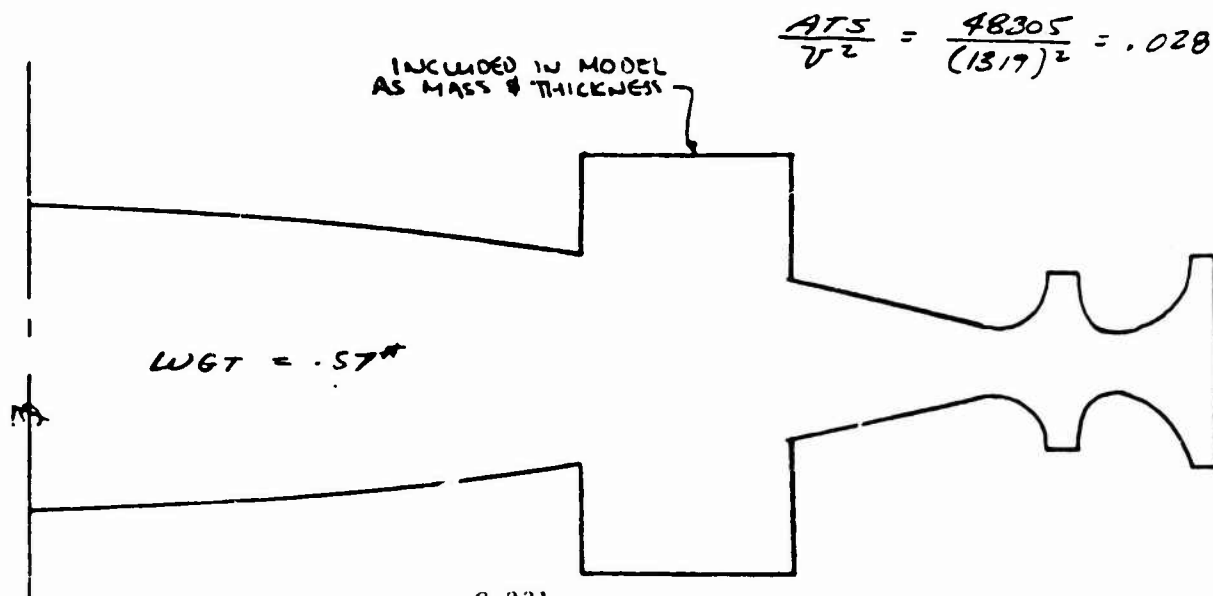
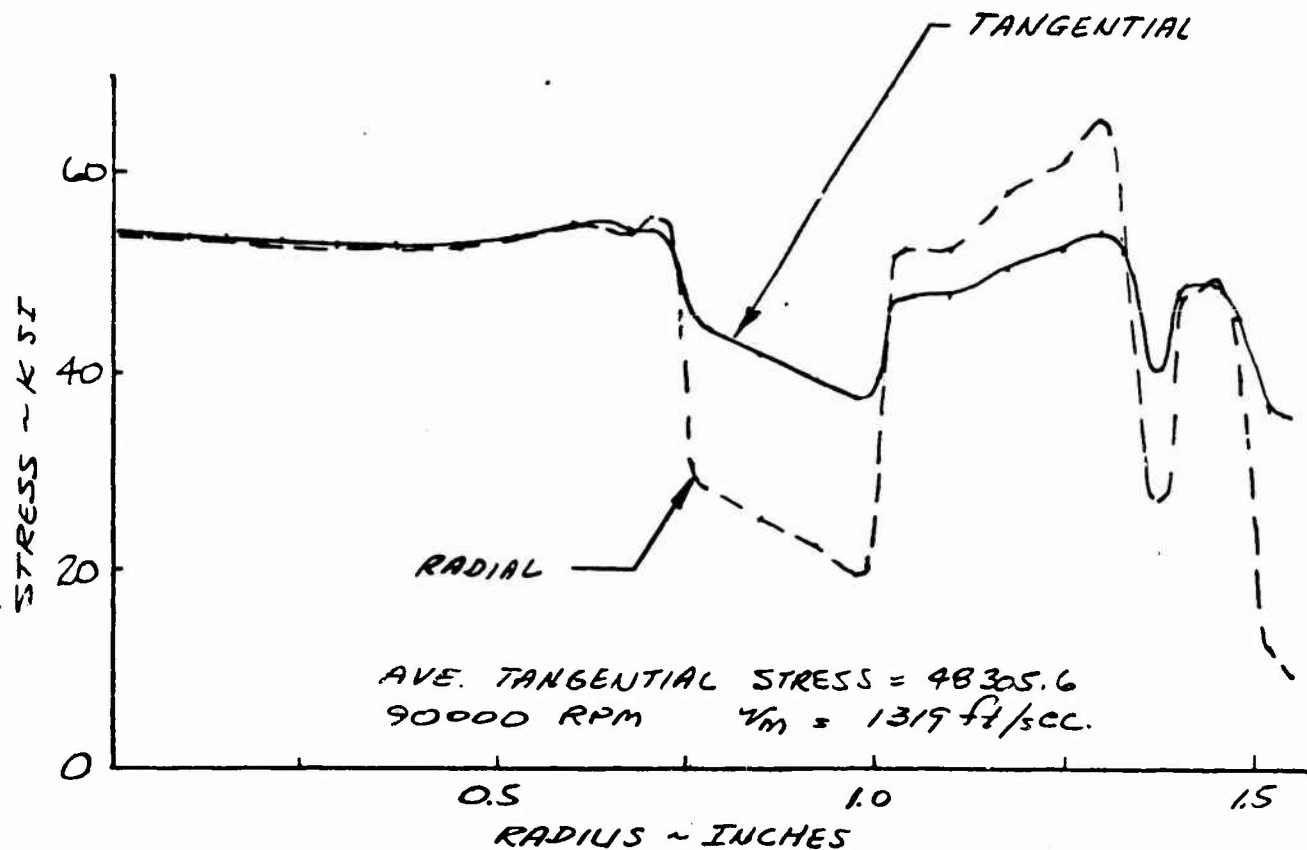
BY

G. ALORICH

CHK. BY

DATE

FIG. 11 FTPA TURBINE ROTOR CENTRIFUGAL STRESSES



$$\frac{ATS}{V^2} = \frac{48305}{(1319)^2} = .028$$

C-231



SUBJECT

OOS 3 STAGE FTPA

DATE

WORK ORDER

1811-05-101

BY

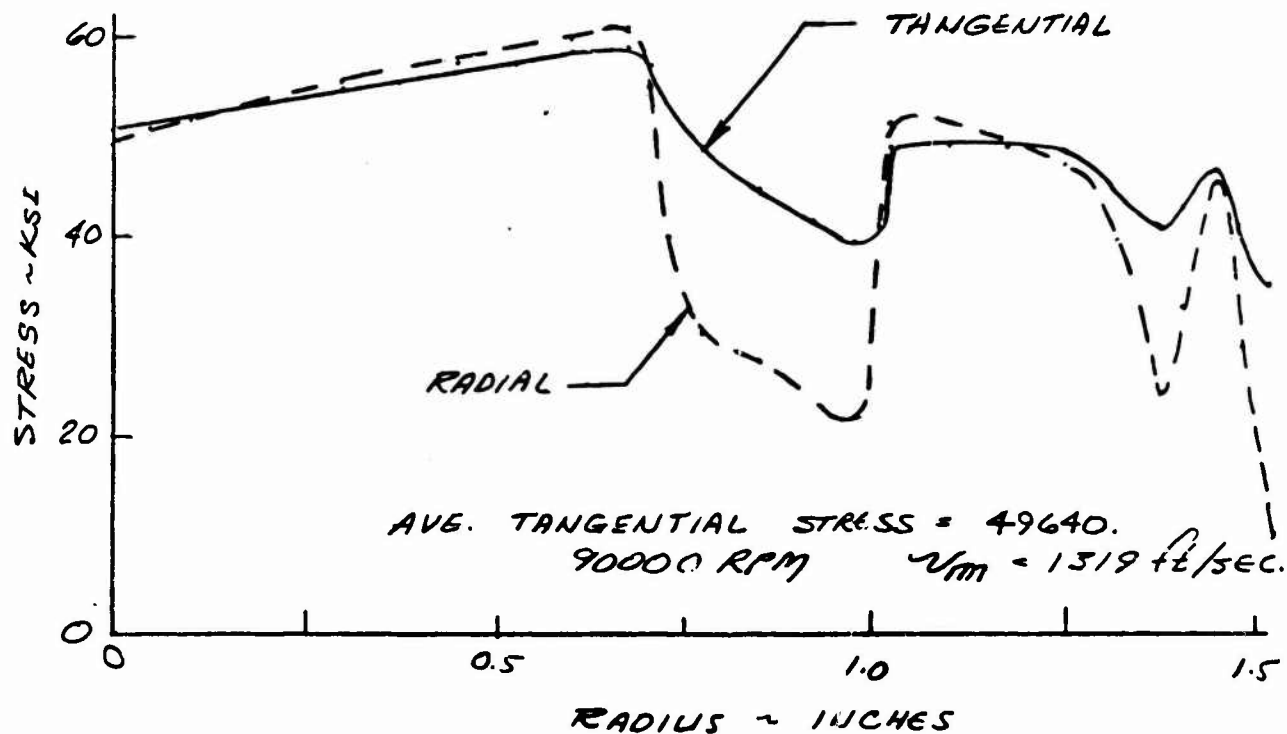
G. ALDRICH

CHK. BY

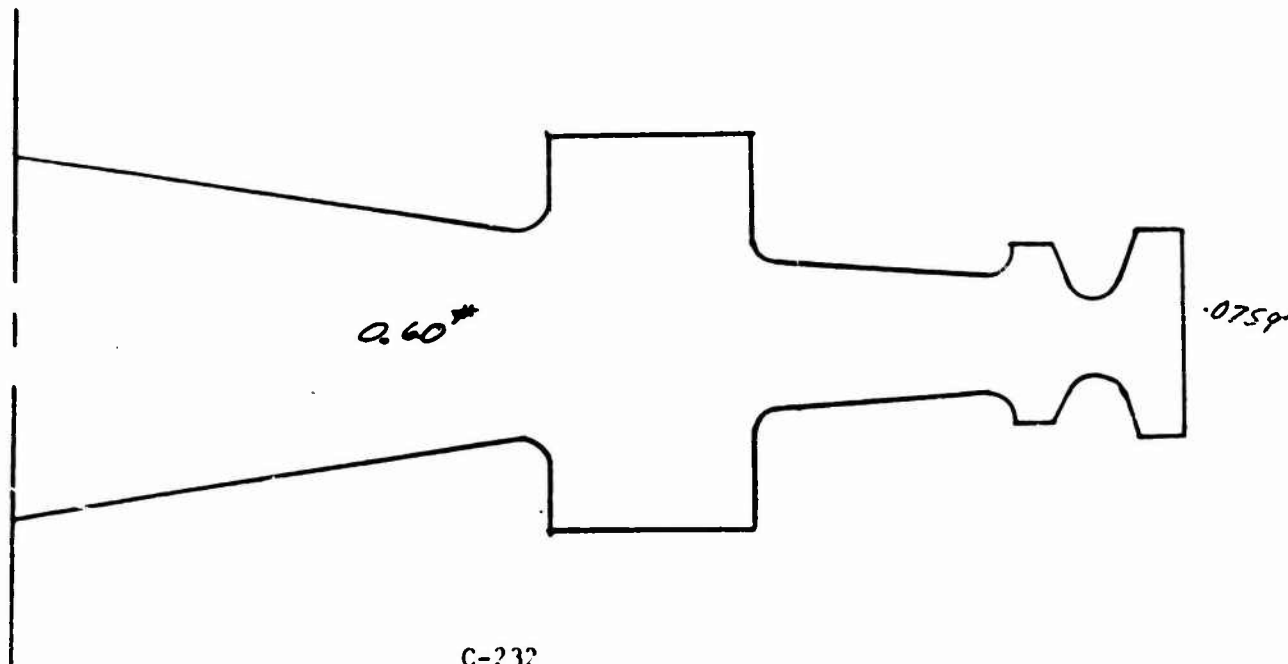
DATE

6/15/71

FIG. 12 FTPA TURBINE ROTOR CENTRIFUGAL STRESSES



$$\frac{ATS}{r^2} = \frac{49650}{(1319)^2} = .029$$





SUBJECT

OOS PARAMETRIC STUDY

DATE

7/2/71

WORK ORDER

1811-05-101

BY

L.W. BARTHOLF

CHK. BY

DATE

## F. ALLOWABLE TURBINE DISK AVERAGE TANGENTIAL STRESS FOR PRELIMINARY DESIGN.

THE BURST SPEED IS GIVEN BY:

$$N_b = N \sqrt{\frac{F_b F_{tu}}{ATS}} \quad \text{where: } F_{tu} = \text{MATERIAL ULTIMATE STRENGTH}$$

ATS = AVE. TANG. STRESS AT SPEED N

\* OR  $F_{cr}$

$F_b$  = BURST FACTOR WHICH IS A FUNCTION OF STRESS DISTRIBUTION AND MATERIAL ELONGATION.

(LONG TIME)  $N_b' \geq 1.17 N_{nom}$

(SHORT TIME)  $N_b \geq 1.20 N_{MD}$  where:  $N_{MD}$  = MECHANICAL DESIGN SPEED.  
 $N_{nom}$  = NOMINAL STEADY STATE SPEED

FOR OOS APPLICATION THE ROTORS ARE SOLID BORED AND THE MATERIAL ELONGATIONS ARE RELATIVELY GOOD, (IE > 20%) THEREFORE IT IS EXPECTED THAT A BURST FACTOR ( $F_b$ ) OF .85 WOULD NOT BE DIFFICULT TO ACHIEVE.

ALSO IT HAS BEEN SHOWN THAT A GREAT DEAL OF THE 10 HOUR LIFE REQUIREMENT WILL BE SPENT AT HIGH TEMPERATURES. THEREFORE, USING THE LONG TIME CREEP RUPTURE REQUIREMENTS THE FOLLOWING RELATIONSHIP FOR ATS TO MATERIAL CREEP RUPTURE CAN BE ESTABLISHED.

$$1.17 N_{nom} = N_{nom} \sqrt{\frac{.85 F_{cr}}{ATS_{en_{nom}}}}$$

$$\therefore ATS_{allow} = \frac{.85}{(1.17)^2} F_{cr} = .62 F_{cr} = \frac{F_{cc}}{1.61} \quad (\text{LONG TIME})$$

$$ATS_{allow} = \frac{.85}{(1.20)^2} F_{tu} = .59 F_{tu} = \frac{F_{tu}}{1.7} \quad (\text{SHORT TIME})$$



AGCS MOD-11

SUBJECT

OOS PARAMETRIC STUDY

DATE

7/2/71

WORK ORDER

1811-05-101

BY

L.K.S. &amp; LWB

CHK. BY

DATE

G. TURBINE PRELIMINARY DESIGN SIZING CRITERIAI. ESTIMATES OF APPLIED STRESS LEVELS

## A. BLADE CENTRIFUGAL STRESS:

$$\tau_{CF} = 0.97(10)^3 \underbrace{V}_{\text{FT/SEC}} \cdot \underbrace{N}_{\text{RPM}} \cdot \underbrace{h}_{\text{INCHES}} \quad (1)$$

## B. DISK AVERAGE TANGENTIAL STRESS:

$$ATS = .031 \underbrace{V}_{\text{FT/SEC}}^2 \quad (2)$$

II. ESTIMATES OF ALLOWABLE STRESSES

## A. BLADE

$$\tau_{CF} \leq \frac{F_{tu}}{2} \text{ OR } \frac{F_{cr}}{2} \quad (3)$$

## B. DISK

$$ATS \leq \frac{F_{tu}}{1.7} \text{ OR } \frac{F_{cr}}{1.61} \quad (4)$$



## H. MATERIAL PROPERTIES

LWB

CHK. BY

DATE  
6/15/71TYPICAL MATERIAL PROPERTIES FOR VARIOUS CANDIDATE  
TURBINE DISK MATERIALS

		STRENGTH, KSI					ELONG- ATION (%)
MATERIAL	TEMPERATURE	F <sub>TY</sub>	F <sub>TU</sub>	CREEP RUPTURE			
				10 HR.	100 HR.	1000 HR.	
WASPALLOY	R.T.	115	185				25
	1000°F	105	170				23
	1200°F	100	162	130	110	86	34
	1400°F	98	115	80	60	42	28
	1600°F	75	76	40	25	16	35
INCONEL 718	R.T.	172	208				21
	1000°F	154	185				18
	1200°F	148	178		105	86	19
	1400°F	107	138		44	25	25
	1600°F	48	49		—	—	88
UDIMET 700	RT.	140	204				17
	1000°F	—	—				—
	1200°F	124	180		—	102	16
	1400°F	120	150	95	79	62	33
	1600°F	92	100	60	42	29	33

REF. HIGH TEMPERATURE HIGH STRENGTH NICKEL BASE  
ALLOYS, INTERNATIONAL NICKEL CO., JUNE 1969



AERJET-GENERAL CORPORATION  
SACRAMENTO CALIFORNIA

REPORT NO.

PAGE 32 OF 69

DATE

WORK ORDER

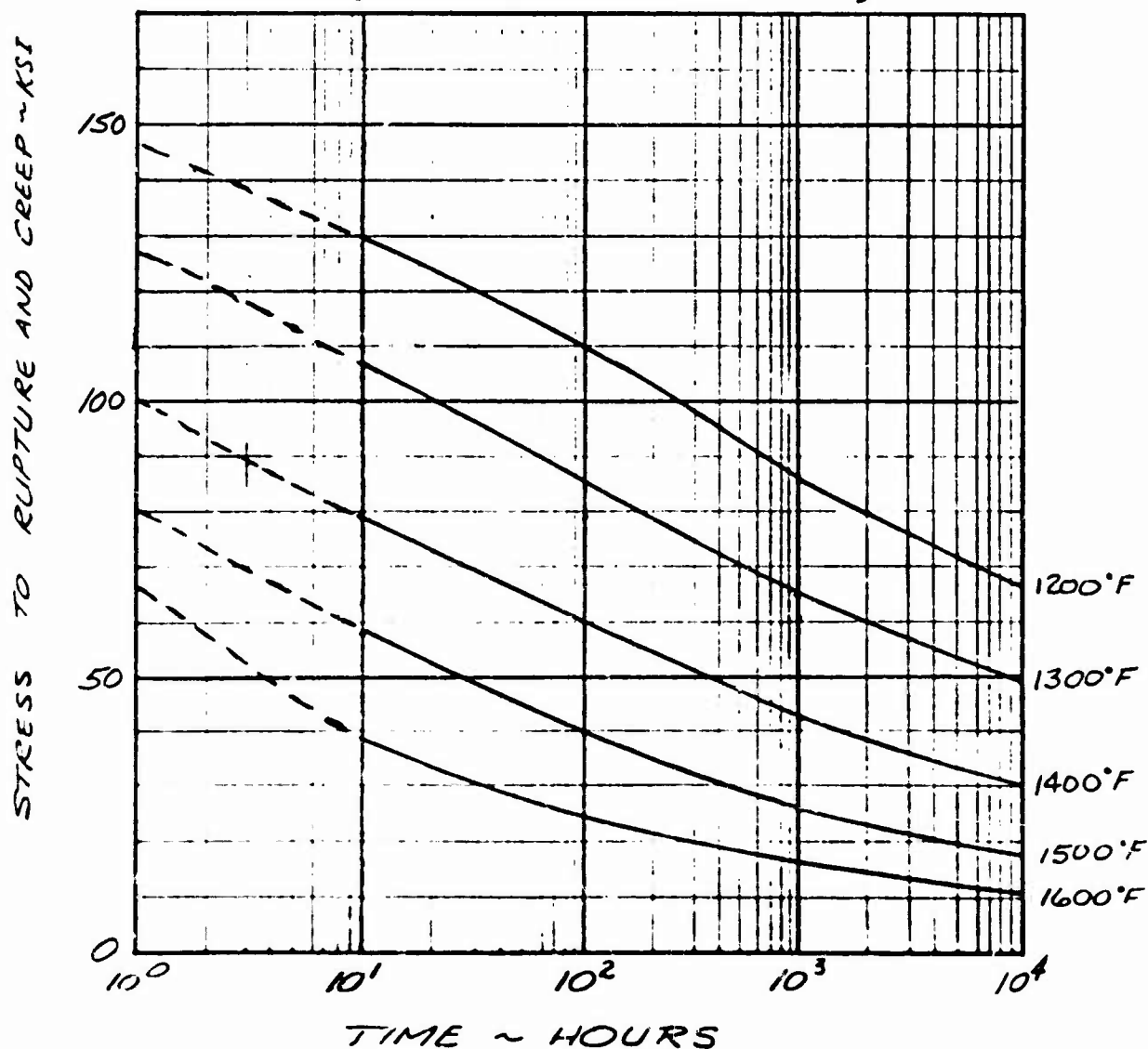
DATE

6/24/71

# 005 PARAMETRIC STUDY

FIG. 13- WASPALLOY (TYPICAL PROPERTIES)  
STRESS TO RUPTURE AND CREEP  
VS.  
TIME

(BAR - HEAT TREATMENT "A")



REF: NERVA PROGRAM MATERIALS DATA BOOK, VOLUME 1-A  
NICKEL-BASE ALLOYS, REFRACTORY METALS, OTHER  
NON-FERROUS METALS, 31 JULY 1968, PAGE 214 G



AEROJET-GENERAL CORPORATION  
SACRAMENTO • CALIFORNIA

REPORT NO

PAGE 33 OF 69

AGC 000011

SUBJECT

OOS PARAMETRIC STUDY

DATE

WORK ORDER

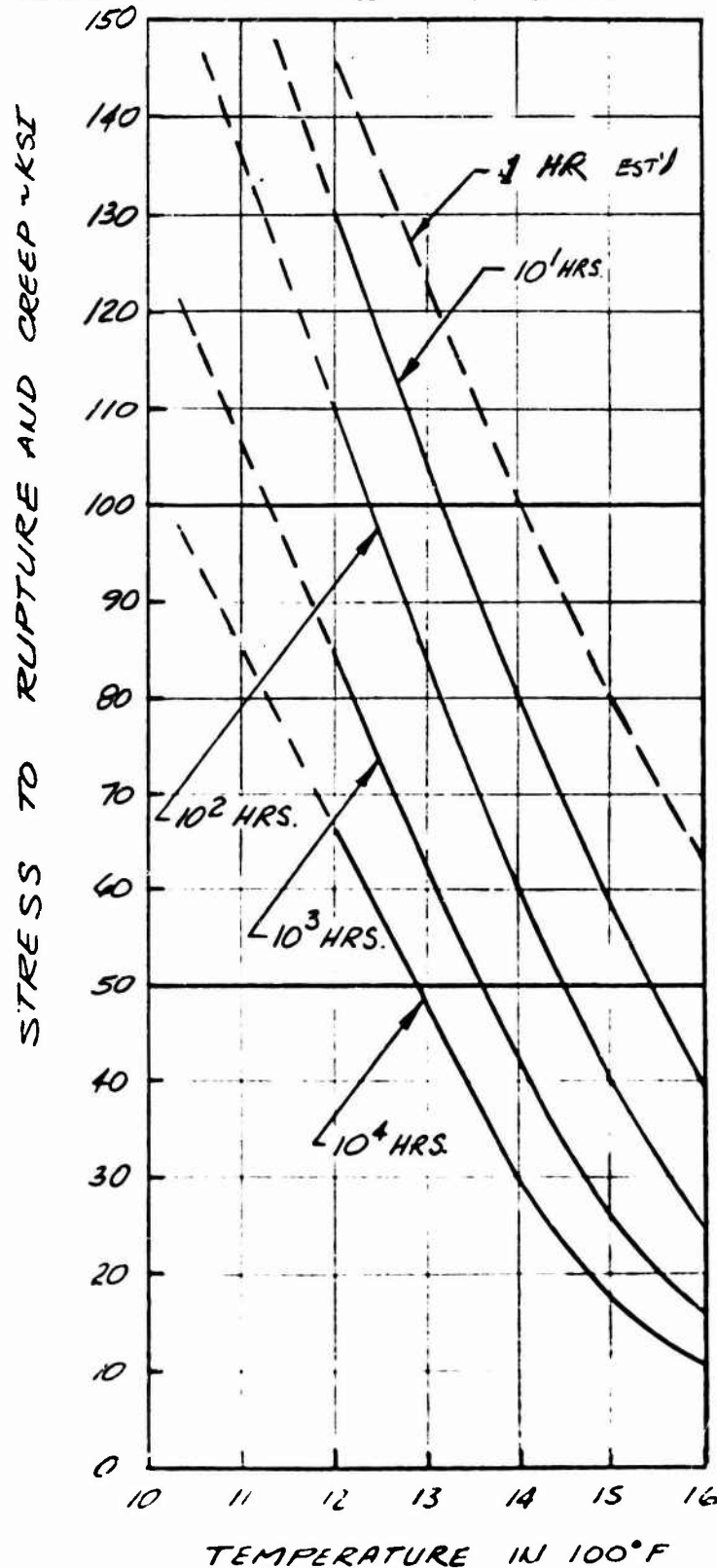
BY

CHK BY

DATE

6/24/71

FIG. 14 WASPALLOY (TYPICAL PROPERTIES)  
STRESS TO RUPTURE AND CREEP VS. TEMPERATURE



REF.: NERVA PROGRAM  
MATERIALS DATA BOOK,  
VOLUME 1-A, NICKEL  
BASE ALLOYS,  
REFRACTORY METALS,  
OTHER NON-FERROUS  
METALS, 31 JULY 1968,  
PAGE 214 F.





DATE  
7/8/71

WORK ORDER

OOS PARAMETRIC STUDY

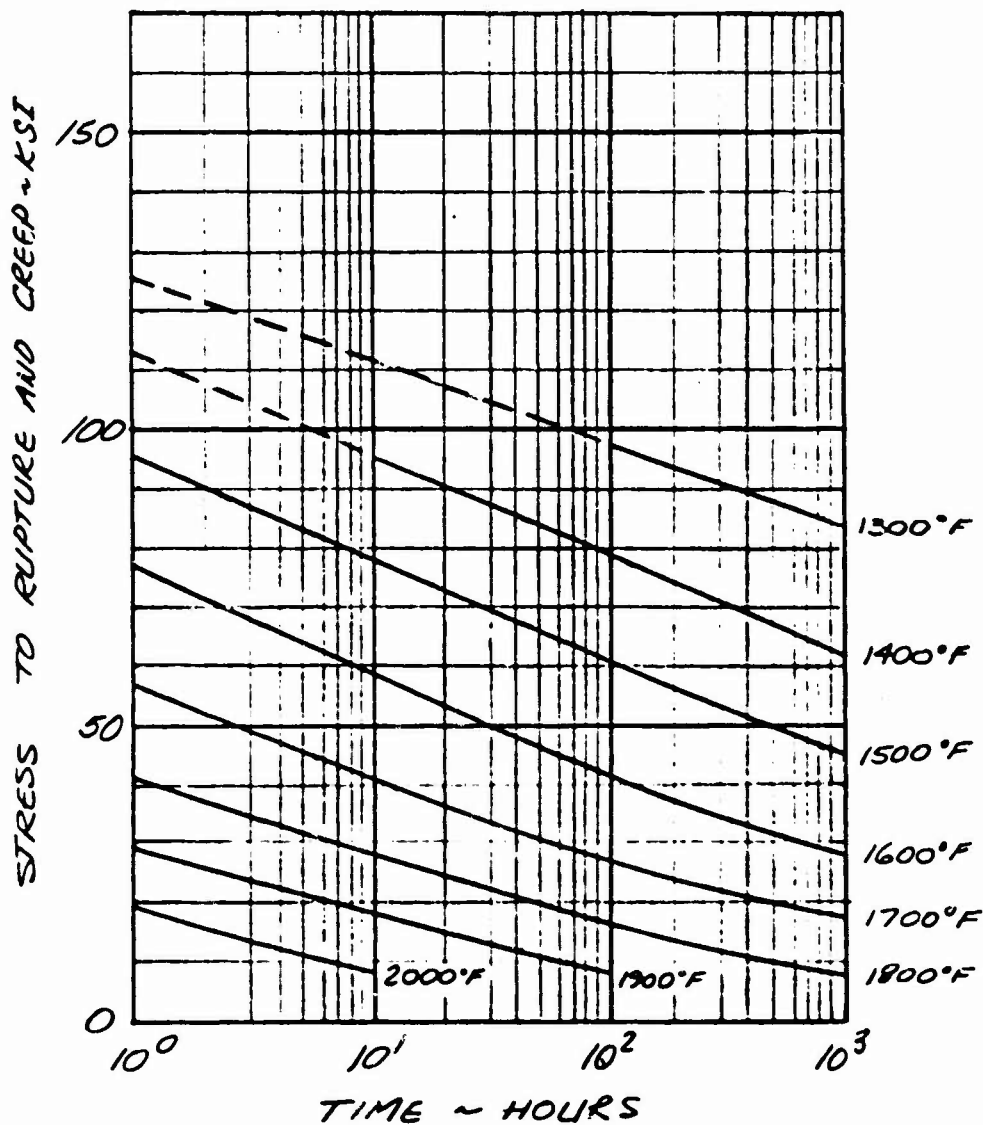
BY

CHK. BY

DATE

FIG. 15 UDIMET 700 (TYPICAL PROPERTIES)  
STRESS TO RUPTURE AND CREEP  
VS.  
TIME

(ALL FORMS-FULLY HEAT-TREATED)



REF: NERVA PROGRAM MATERIALS OF A BOOK,  
VOL. 1-A NICKEL-BASE ALLOYS, REFRACTORY  
METALS, OTHER NON FERROUS METALS,  
31 JULY 1968, PAGE 216 E.



SUBJECT

OOS PARAMETRIC STUDY

DATE

7/8/71

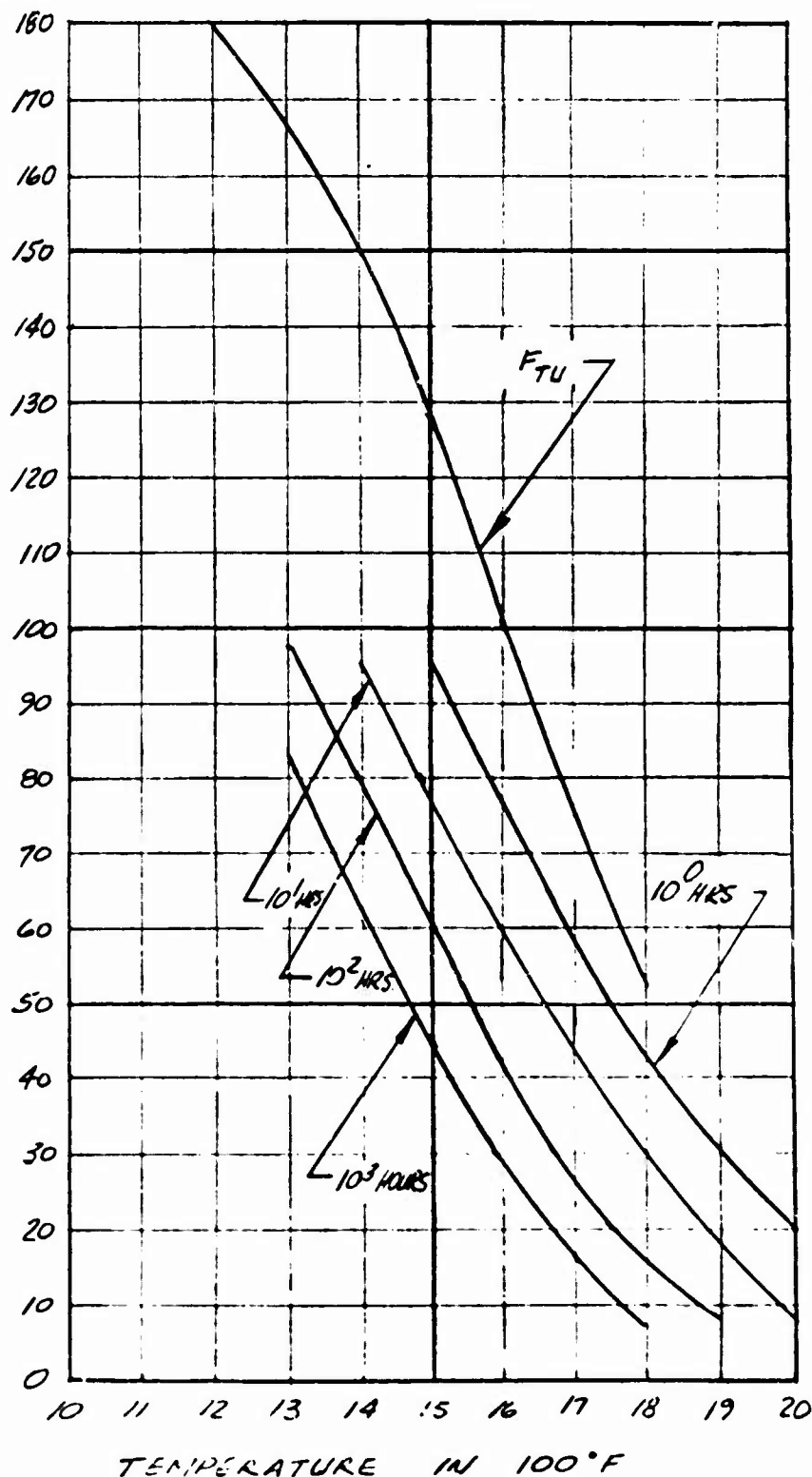
WORK ORDER

BY

CHK BY

DATE

FIG. 16 UDIMET 700 (TYPICAL PROPERTIES)  
STRESS TO RUPTURE AND CREEP VS. TEMPERATURE



REF: NERVA PROGRAM  
MATERIALS DATA  
BOOK, VOLUME I-A,  
NICKEL BASE  
ALLOYS, REFRACTORY  
METALS, OTHER  
NON FERROUS  
METALS, 31 JULY  
1968, PAGE 216 D.



AERJET-GENERAL CORPORATION  
SACRAMENTO • CALIFORNIA

REPORT NO.

PAGE 36 OF 69

1608-000-11

SUBJECT

OOS PARAMETRIC STUDY

DATE

7/2/71

WORK ORDER

1811-05-101

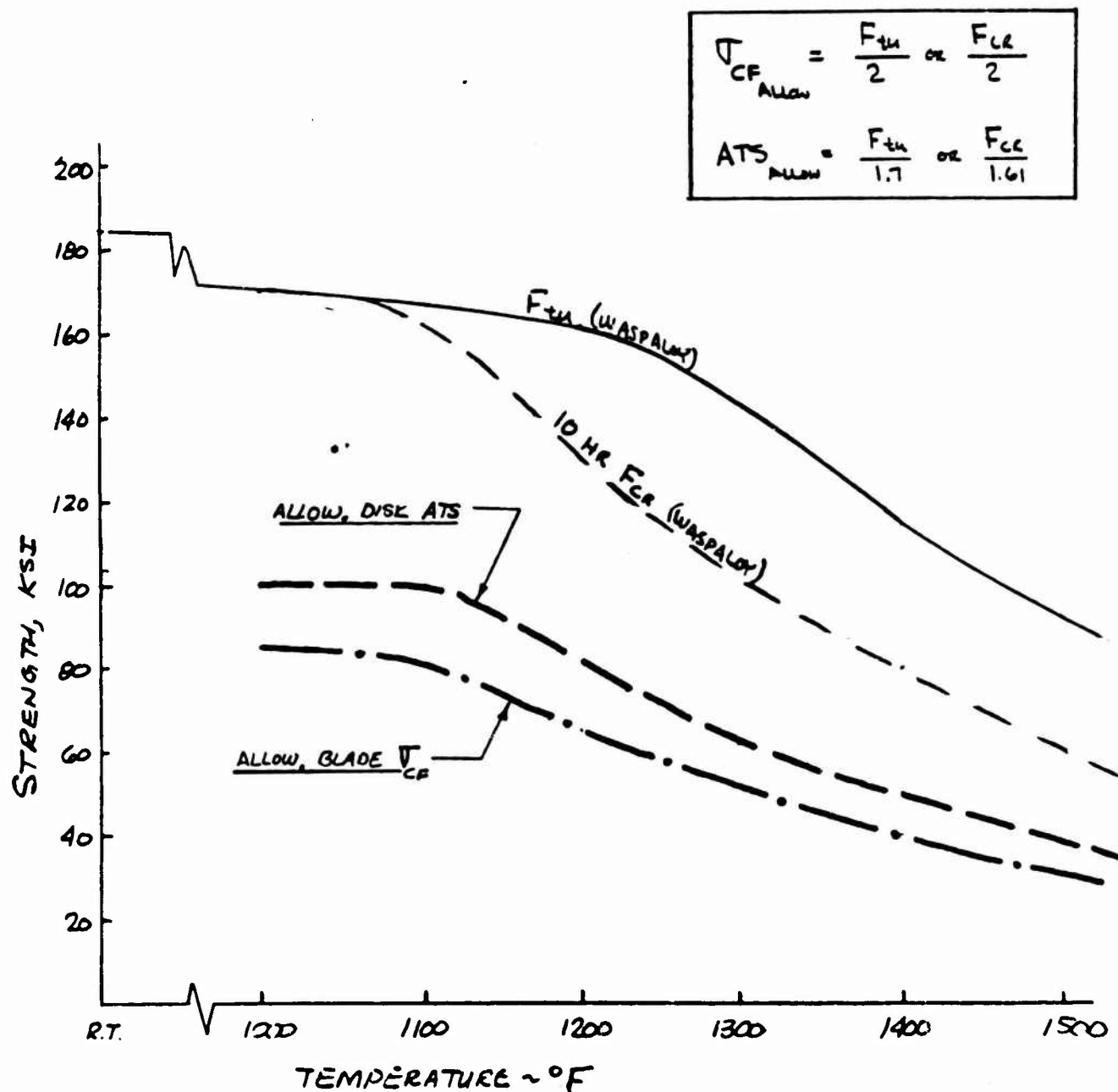
BY

L.W. BARTHOLF

CHK BY

DATE

FIG. 17 TYPICAL WASPALOY MATERIAL STRENGTH DATA





AEROJET-GENERAL CORPORATION  
SACRAMENTO • CALIFORNIA

REPORT NO.

PAGE 37 OF 69

AGCS 000-11

SUBJECT

OOS PARAMETRIC STUDY

DATE

7/2/71

WORK ORDER

1811-25-101

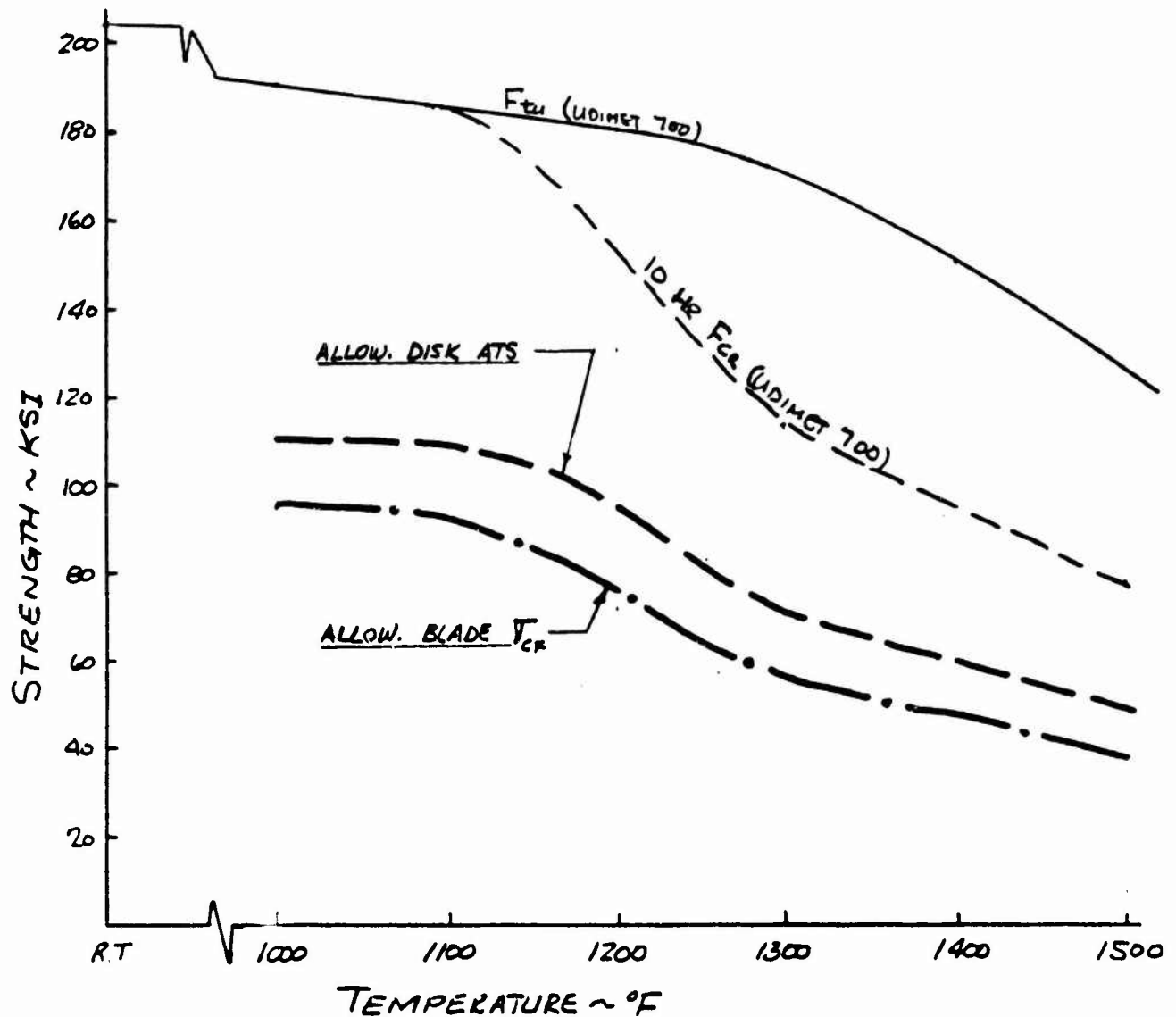
BY

L.W. BARTHOLF

CHK. BY

DATE

FIG. 18 TYPICAL UDINET 700 MATERIAL STRENGTH DATA





7/16/71

## II. TURBINE START TRANSIENT EFFECTS ON BLADE LIFE

BY

L.W. BARTHOLF

CHK BY

DATE

ESTIMATE OF THE EFFECT OF START TRANSIENT RAMP DURATION  
ON TURBINE BLADE PEAK THERMAL STRAIN

THE THERMAL SHOCK STRESS OR STRAIN IS RELATED TO THE BIOT NUMBER,  $m$ , AND THE FOURIER NUMBER,  $\tau$ , WHICH ARE DEFINED AS:

$$m = \frac{hL}{K}$$

where:  $h$  = HEAT-TRANSFER COEFFICIENT  
 $L$  = CHARACTERISTIC DIMENSION  
 $K$  = METAL CONDUCTIVITY

$$\tau = \frac{Kt}{\gamma CL^2}$$

where:  $\gamma$  = METAL DENSITY  
 $C$  = SPECIFIC HEAT  
 $t$  = RAMP DURATION

FOR OOS APPLICATIONS:

$$h_{\text{DISC RIM}} = h_{\text{BLADE}} = .032 \text{ BTU/IN}^2\text{-SEC}\cdot^{\circ}\text{F}$$

FOR WASPALCO:

$$K = .0002 \text{ BTU/SEC}\cdot\text{IN}\cdot^{\circ}\text{F}$$

$$C = .135 \text{ BTU/LB}\cdot^{\circ}\text{F}$$

$$\gamma = .296 \text{ LB/IN}^3$$



AERJET-GENERAL CORPORATION  
SACRAMENTO • CALIFORNIA

AGL 8-0000-11

REPORT NO.

PAGE 39 OF 69

SUBJECT

OOS PARAMETRIC STUDY

DATE  
7/16/71

WORK ORDER

BY

L.W. BARTHOLF

CHK. BY

DATE

TURBINE BLADE START TRANSIENT RAMP (CONT)

$$m = \frac{hL}{K} = \frac{.032}{.0002} L = 160 L$$

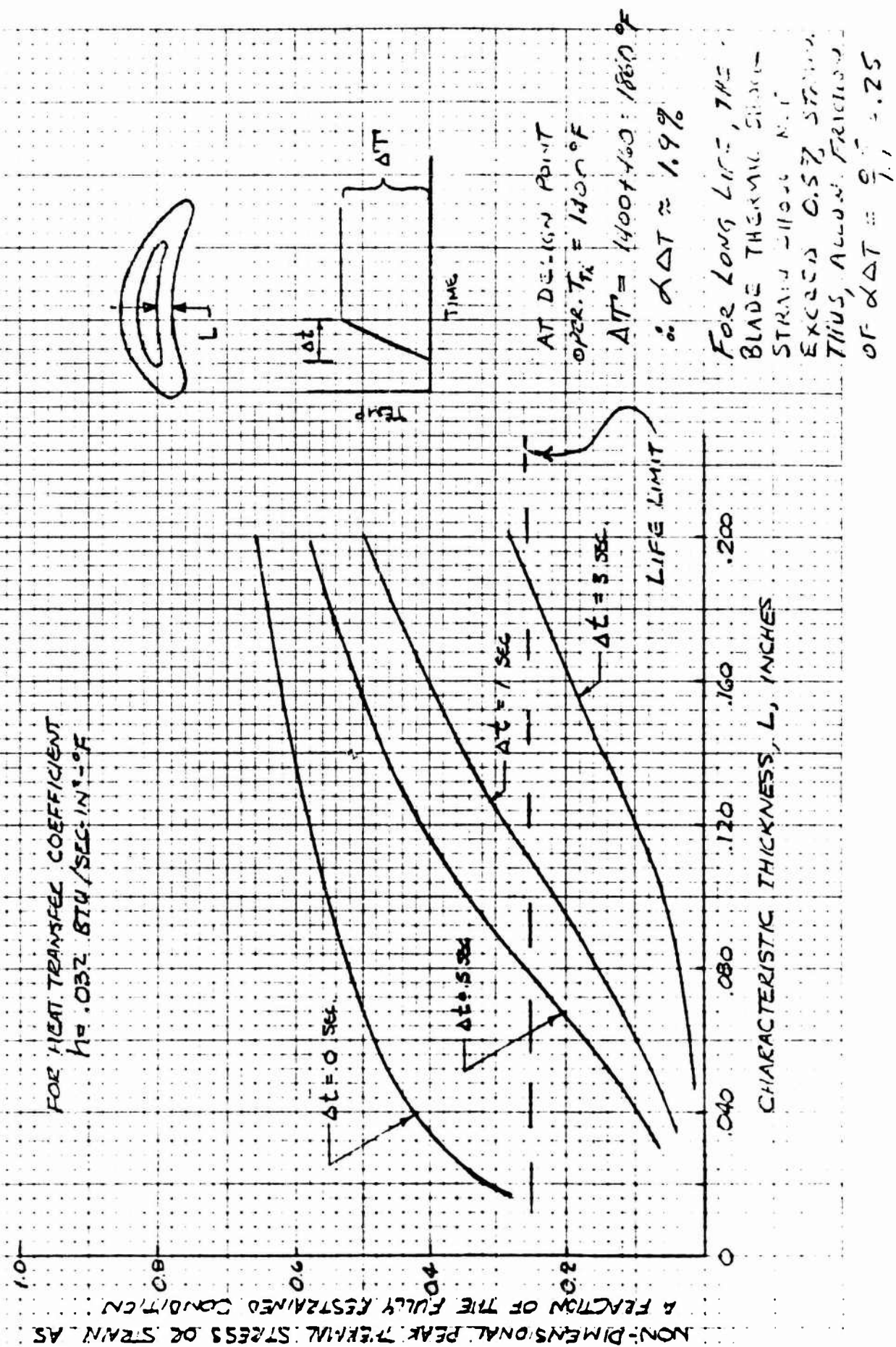
L	m
.020	3.2
.040	6.4
.060	9.6
.080	12.8
.100	16.0
.120	19.2
.140	22.4
.160	25.6
.200	32.0

$$\tau = \frac{Kt}{\gamma c L^2} = \frac{.0002 t}{.294(135) L^2} = .005 \frac{t}{L^2}$$

t (sec)	L (in)	L <sup>2</sup>	$\tau$
0	.020		0
	.040		0
	.060		0
	.100		0
	.140		0
	.160		0
	.200		0
.5 sec	.020	4 (10) <sup>-4</sup>	.6
	.040	16 (10) <sup>-4</sup>	1.6
	.060	36 (10) <sup>-4</sup>	.7
	.100	100 (10) <sup>-4</sup>	.25
	.140	196 (10) <sup>-4</sup>	.13
	.200	400 (10) <sup>-4</sup>	.06

t	$\tau$
1.0	12.5
	3.1
	1.4
	0.5
	0.25
	0.125
3.0	37
	9.1
	4.2
	1.5
	.75
	.37

FIG. 19 - TURBINE BLADE START TRANSIENT EFFECT ON PEAK THERMAL STRAIN





SUBJECT

J. DISK THERMAL SHOCK STRAINS AND CYCLIC LIFE

DATE

7/2/71

WORK ORDER

BY

L.W. BARTHOLF

CHK. BY

DATE

## THERMAL SHOCK STRESSES/STRAINS AND ASSOCIATED LOW CYCLE FATIGUE LIFE ESTIMATES FOR DISKS

THE FOLLOWING SECTION PRESENTS THE ESTIMATE OF PEAK THERMAL STRAINS FOR THE TURBINE DISKS.

SOME OF THE VARIABLES THAT WERE EXAMINED ARE:

1. FULLY INSULATED (RIM HEATING) VS PARTIALLY INSULATED (RIM PLUS SIDE HEATING).
2. EFFECT OF START TRANSIENT RAMP TIME ON THERMAL STRAIN
3. EFFECT OF RIM NUMBER ON THERMAL STRAIN & LIFE
4. EFFECT OF HEAT TRANSFER COEFFICIENT ON LIFE
5. EFFECT OF TURBINE INLET TEMPERATURE ON LIFE.

### BASIC ASSUMPTIONS:

- WASPALLOY, INCO 718, OR UDIMET 700 MATERIAL
- DISK PRE-CHILLED TO - 420°F
- FIXED DISK SIZE
- CONSTANT  $\Delta E_L$  VS  $N_f$  FOR TEMPERATURE RANGE 1000 - 1500 °F





AEROJET-GENERAL CORPORATION  
SACRAMENTO • CALIFORNIA

REPORT NO.

PAGE 42 OF 69

DATE

WORK ORDER

DATE

6/23/71

# 00S PARAMETRIC STUDY

## TURBINE DISK RIM THERMAL STRAIN ESTIMATES

THE PEAK THERMAL STRAIN IS GIVEN BY:

$\epsilon = \alpha \Delta T$  FOR UNIAXIAL STRAIN CONDITION  
IN THE FULLY SHIELDED DISK

WHERE:  $\Delta T = T_{TI} + 420$

$T_{TI}$  = TURBINE INLET TEMP, °F

$\alpha \approx (8-9)(10)^{-6}$  IN/IN/°F (INCO. 718)  
(7-8)(10)<sup>-6</sup> IN/IN/°F Waspaloy

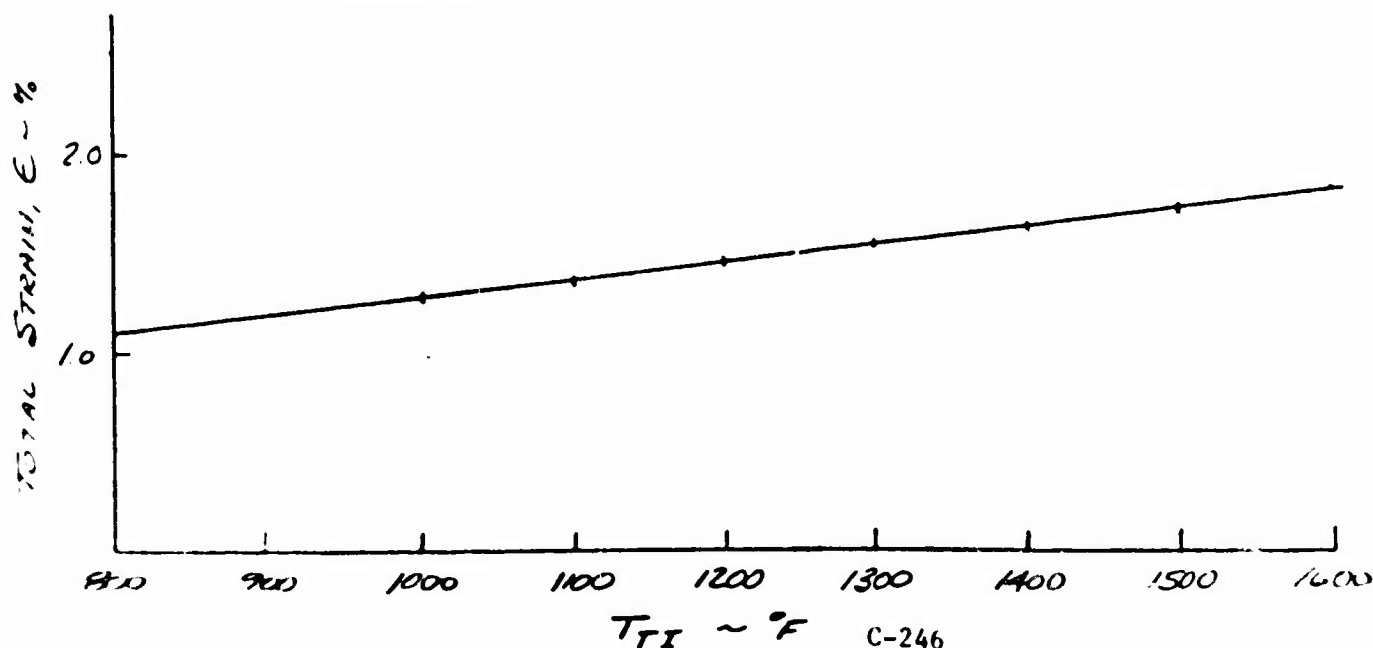
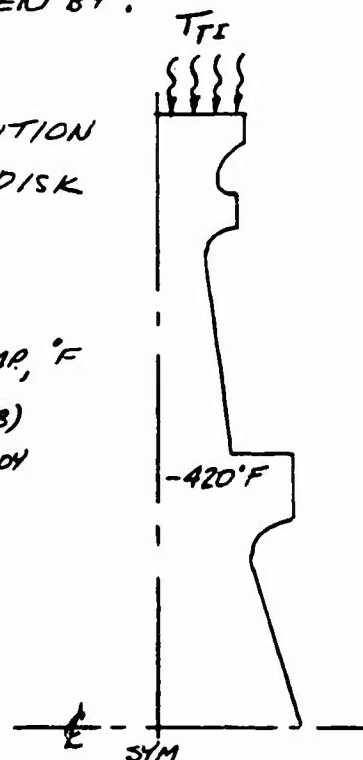
USE  $\alpha = 9(10)^{-6}$  IN/IN/°F AS A  
CONSERVATIVE VALUE.

$$\therefore \epsilon = 9(10)^{-6} (T_{TI} + 420)$$

$$\epsilon = 9(10)^{-6} T_{TI} + .0037$$

$$\epsilon_{\%} = 9(10)^{-4} T_{TI} + .37$$

FULLY RESTRAINED STEP TEMPERATURE INPUT





AEROJET-GENERAL CORPORATION  
SACRAMENTO • CALIFORNIA

REPORT NO

PAGE 43 OF 127

DATE  
7/7/71

WORK ORDER

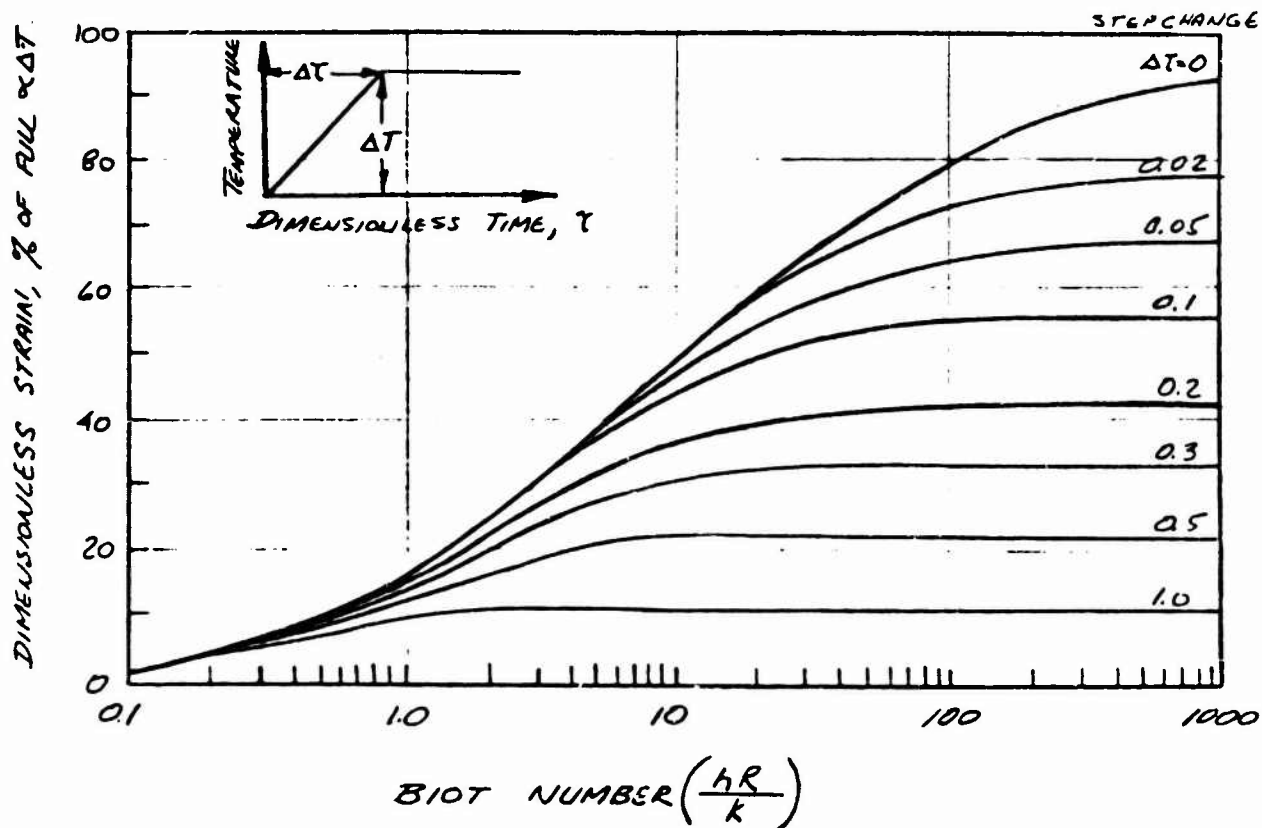
OOS PARAMETRIC STUDY

BY

CHK. BY

DATE

FIG. 20-BIOT NUMBER AND START TRANSIENT EFFECT  
ON FULL " $\alpha \Delta T$ " THERMAL STRAIN OF DISKS



REF: E. LIEBOWITZ, FRACTURE, AN ADVANCED  
TRETISE, VOLUME II, ACADEMIC PRESS,  
1969, PAGE 99.



# OOS PARAMETRIC STUDY

BY

L.W. BARTHOLF

CHK. BY

DATE

## ESTIMATE OF THE EFFECT OF START TRANSIENT RAMP DURATION ON TURBINE DISK PEAK THERMAL STRAIN.

FROM FIGURE 20 IT CAN BE SEEN THAT THE PEAK THERMAL STRAIN IS A FUNCTION OF THE DIMENSIONLESS PARAMETER  $\Delta T$ .

$$\Delta T = \left( \frac{k}{\gamma C} \right) \frac{\Delta t}{R^2}$$

where:  $k$  = THERMAL CONDUCTIVITY

$\gamma$  = WEIGHT DENSITY

$C$  = SPECIFIC HEAT

$R$  = DISK RIM RADIUS

$\Delta t$  = RAMP TIME

FOR WASPALOY:

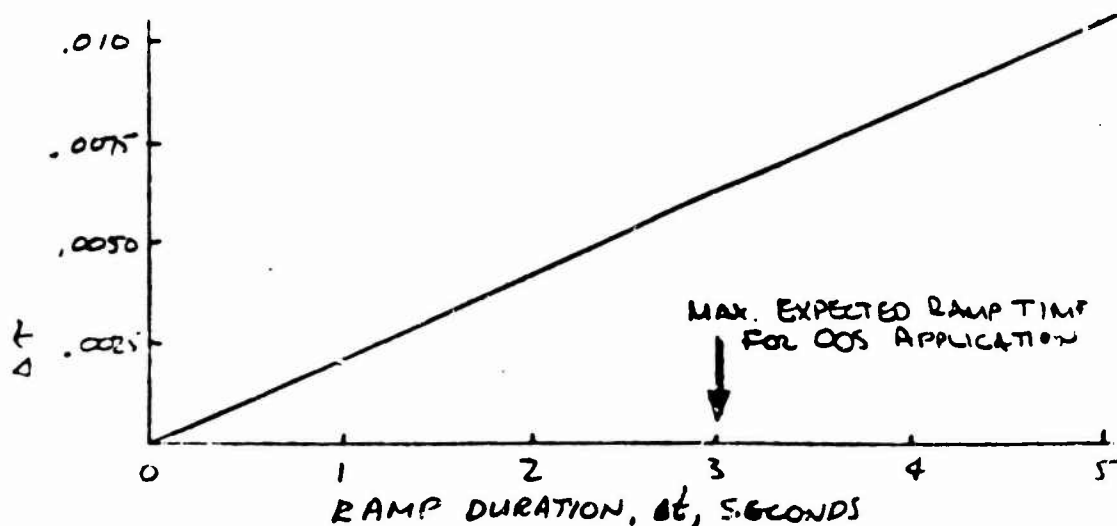
$$k = .0002 \text{ BTU/SEC-IN-F}$$

$$C = .135 \text{ BTU/LO-F}$$

$$\gamma = .296 \text{ LO/IN}^3$$

$$\therefore \Delta T = \frac{.0002}{.296(.135)} \times \frac{\Delta t}{(1.56)^2} = \underline{\underline{.002 \Delta t}}$$

THE MAXIMUM EXPECTED RAMP TIME FOR THE OOS IS ABOUT 1.3 SECONDS, WHICH RESULTS IN A  $\Delta T = .002 - .003$ . FROM FIGURE 20 IT CAN BE SEEN THAT THE PEAK THERMAL STRAIN IS NOT AFFECTED SIGNIFICANTLY BY  $\Delta T$ 'S IN THIS RANGE & FOR BIOT NUMBERS IN THE RANGE OF INTEREST FOR OOS APPLICATIONS.





SUBJECT

OOS PARAMETRIC STUDY

DATE

6/30/71

WORK ORDER

1811-US-101

BY

L.W. BARTHOLF

CHK. BY

DATE

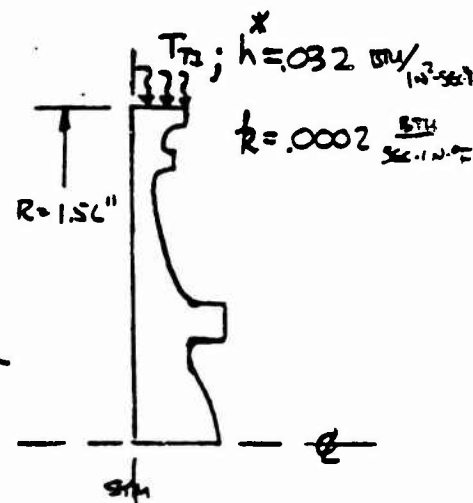
DETERMINATION OF DISK RIM PEAK THERMAL STRAIN

FOR RIM HEATING FIGURE 20 WILL BE USED WHICH SHOWS THE RELATIONSHIP BETWEEN THE BIOT NUMBER AND PERCENT OF FULLY RESTRAINED,  $\alpha \Delta T$ , STRAIN FOR AN INFINITE CYLINDER IMMERSED IN A FLUID. A STEP INPUT CHANGE IN TEMP. WILL BE USED, I.E.  $\Delta T = 0$ , SINCE THE CALCS ON PAGE 44 SHOW  $\Delta T$  TO BE VERY SMALL FOR THE MAXIMUM RAMP OF ABOUT 3 SECONDS.

$$\text{BIOT NUMBER} = \frac{hR}{k}$$

$$= \frac{.032(1.56)}{.0002}$$

$$B = 250$$



\* PER MEMO 9641: 0629,  
SEE PAGE 47.  
 $h = .59(0.059) = .032$

$$\% \Delta \epsilon'_t = .87 \alpha \Delta T \quad \text{FROM FIGURE 20.}$$

FOR A  $T_{T1}$  OF  $1400^\circ\text{F}$ ,  $\Delta T = 1400 + 400 = 1800^\circ\text{F}$   
THIS CAN RESULT IN A DIFFERENCE IN TURBINE DISK LIFE PREDICTIONS AS FOLLOWS:

$$\Delta \epsilon'_t = \alpha \Delta T = 9(10)^{-6}(1800) = .0162 \text{ in/in} = 1.62\%$$

$$\Delta \epsilon'_t = .87(1.62) = 1.41\%$$

$$N_{f, 1.62} = 250 \text{ CYCLES}$$

$$N_{f, 1.41} = 490 \text{ CYCLES}$$

$$\% \text{ CHANGE } N_f = \frac{240}{250} \times 100 = 96\%$$

IT FOLLOWS THAT ACCURATE PREDICTIONS OF THERMAL STRAINS AND TURBINE TEMPERATURES ARE REQUIRED TO PREDICT LIFE OF THE DISK.



SUBJECT

OOS PARAMETRIC STUDY

DATE

6/30/71

WORK ORDER

1811-05-10.1

BY

L.W. BARTHOLF

CHK. BY

DATE

DETERMINATION OF DISK RIM PEAK THERMAL STRAIN CONT

ANOTHER VARIABLE THAT IS HARD TO PREDICT IS THE HEAT TRANSFER COEFFICIENT. A 20% ERROR IN PREDICTING "h" RESULTS IN THE FOLLOWING CHANGE IN LIFE PREDICTION.

$$\text{BIOT NUMBER} = \frac{.8(.032)1.56}{.0002} = 200$$

$$\% \Delta E'_x = .86 \approx \Delta T$$

$$\Delta G'_x = .86(1.62) = 1.39\%$$

$$N'_x = 500 \text{ CYCLES}$$

$$\% \text{ CHANGE } N'_x = \left( \frac{10}{490} \right) \times 100 = 2\%$$

IN THE RANGE OF BIOT NUMBERS THAT ARE APPLICABLE TO OOS IT CAN BE GENERALIZED THAT THE % CHANGE IN LIFE WILL BE MUCH LESS THAN THE PERCENT CHANGE IN BIOT NUMBER.

THE CURVES ON THE FOLLOWING PAGES SHOW ESTIMATED OF TURBINE DISK TOTAL STRAIN RANGE FOR OOS APPLICATIONS AS ESTIMATED FOR A RIM HEATED CASE AND THE RIM AND SIDE HEATED CASE COMPARED TO THE FULLY RESTRAINED CONDITION FOR A STEP TEMPERATURE INPUT AND A BIOT NUMBER =  $\infty$ .



SUBJECT

OOS PARAMETRIC STUDY

DATE

WORK ORDER

BY

CHK. BY

DATE

6/23/71

TURBINE DISK SIDE THERMAL SHOCK STRAIN

ASSUME THE THERMAL STRAIN IS GIVEN BY:

$$\epsilon_y = \epsilon_x = k \alpha \Delta T \quad \text{FOR THE BI-AXIAL STRAIN CONDITION IN THE PARTIALLY SHIELDED DISK}$$

$$\epsilon_{\text{eff.}} = 2\epsilon_x$$

$$\text{WHERE: } \Delta T = T_{T_1} + 420^\circ\text{F}$$

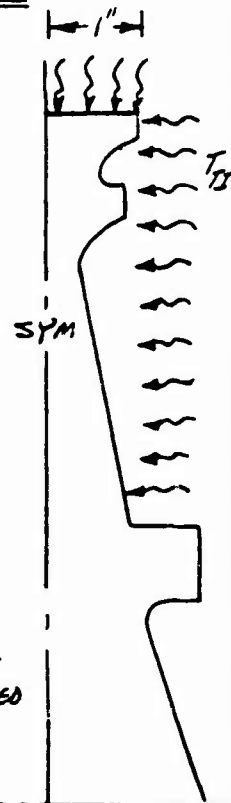
$$\alpha = 9(10)^{-6} \text{ IN./IN./}^\circ\text{F}$$

$$k = \frac{1}{1.5 + \frac{3.25}{\pi}} = \text{A NON-DIMENSIONAL PARAMETER MODIFYING THE FULLY CONSTRAINED CONDITION.}$$

$$\pi = \frac{hL}{K} = \text{BIOT NUMBER}$$

where:  $K$  = THERMAL CONDUCTIVITY  
 $L$  = CHARACTERISTIC THICKNESS  
 $h$  = HEAT TRANSFER COEFFICIENT

THE ESTIMATED HEAT TRANSFER COEFFICIENT FOR OOS TURBINES IS ABOUT 54% THAT FOR THE SSE TURBINES DUE TO THE SLIGHTLY LOWER ENVIRONMENTAL PRESSURE IN THE OOS TURBINE IN COMPARISON TO THAT OF THE SSE TURBINE. PER MEMO 9641:0629, SSOK SPACE SHUTTLE HIGH PRESSURE FUEL TPA HEAT TRANSFER ANALYSIS, FROM A. C. KOBAYASHI, TO N. P. SMITH, DATED 21 APRIL 1971. THE STEADY STATE HEAT TRANSFER COEFFICIENT ( $h$ ) FOR THE ROTOR SIDE WALL WAS .013 BTU/IN.<sup>2</sup>-SEC.-<sup>°</sup>F FOR THE SSE TURBINE. THUS, FOR THE OOS WE SHALL USE  $h = .54(.013) = .007$





AEROJET-GENERAL CORPORATION  
SACRAMENTO • CALIFORNIA

REPORT NO.

AGCS-000-11

PAGE 48 OF 69

SUBJECT

OOS PARAMETRIC STUDY

DATE

WORK ORDER

BY

CHK. BY

DATE

6/28/71

TURBINE DISK SIDE THERMAL SHOCK STRAIN (CONT'D)

$$\therefore m = \frac{.007(.1)}{.0002} = 3.5$$

$$k = \frac{1}{1.5 + \frac{3.25}{3.5}} = .41$$

$\therefore$  THEN  $\epsilon_{eff.} = 2(.41) \propto \Delta T$  WHICH IS NEARLY THE SAME CONDITION AS THE UNI-AXIAL STRAIN CONDITION FOR RIM HEATING OF THE DISK. HOWEVER, IT HAS BEEN POINTED OUT PREVIOUS TO THIS THAT SMALL CHANGES IN STRAIN RESULT IN RELATIVELY LARGE CHANGES IN LIFE. WITH THIS IN MIND THE DISTINCTION BETWEEN THE FULLY INSULATED RIM HEATED DISK AND THE PARTIALLY INSULATED RIM AND SIDE HEATED DISK WILL BE CARRIED THRU.



SUBJECT

OOS PARAMETRIC STUDY

DATE

7/1/71

WORK ORDER

1811-05-101

BY

L. W. BARTHOLF

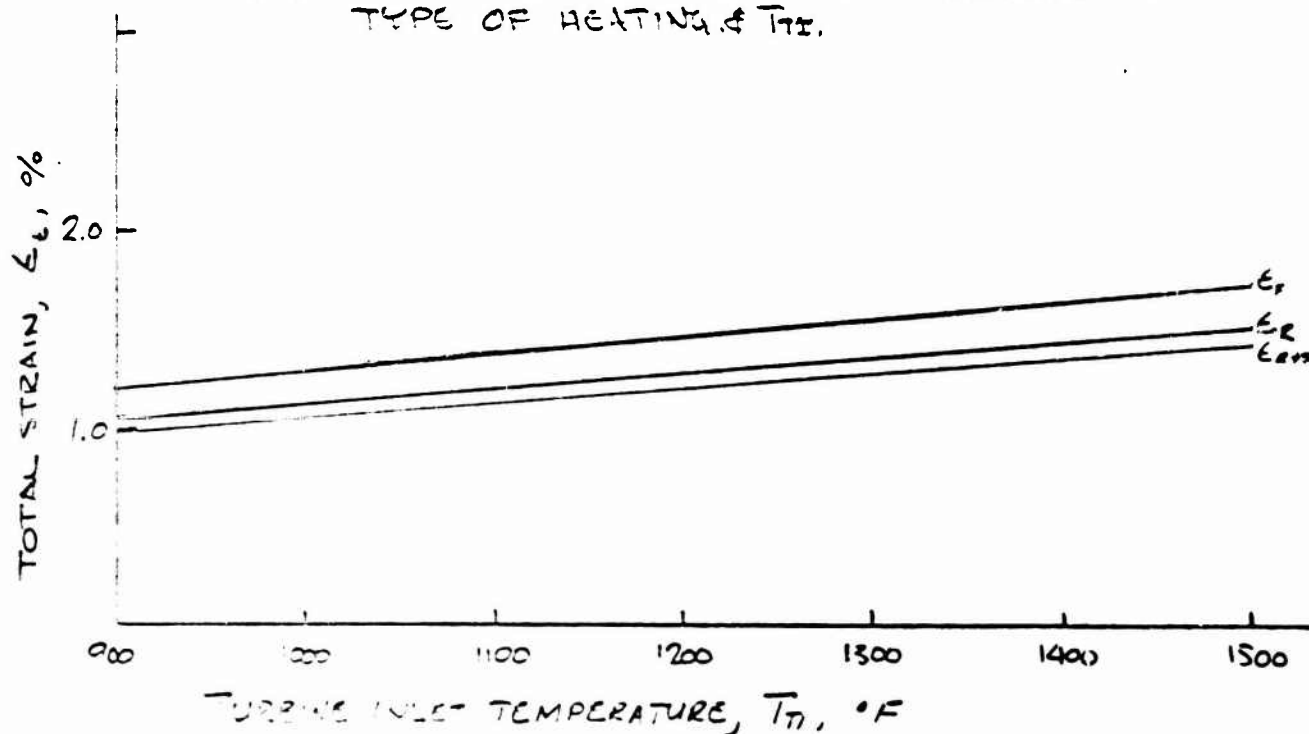
CHK BY

DATE

DETERMINATION OF DISK RIM PEAK THERMAL STRAIN (CONT)

THE THERMAL STRAINS FOR THE VARIOUS CONDITIONS ARE GIVEN BELOW.

FIG. 2/ DISK THERMAL STRAIN AS A FUNCTION OF TYPE OF HEATING &  $T_{Ti}$ .



$$\epsilon_{r+s} = 9(10)^{-4} T_{Ti} + .37$$

$$\text{(DISK RIM HEATING)} \quad \epsilon_{RIM} = .87[9(10)^{-4} T_{Ti} + .37] = .79(10)^{-4} T_{Ti} + .33$$

$$\text{(DISK RIM+SIDE HEATING)} \quad \epsilon_{RIM+SIDE} = .82[9(10)^{-4} T_{Ti} + .37] = .74(10)^{-4} T_{Ti} + .30$$



FIG. 22 - WASPALOY & INCONEL 718 LOW CYCLE FATIGUE DATA

LEGEND: — WASPALOY CALCULATED USING THE UNIVERSAL SLOPES EQUATION

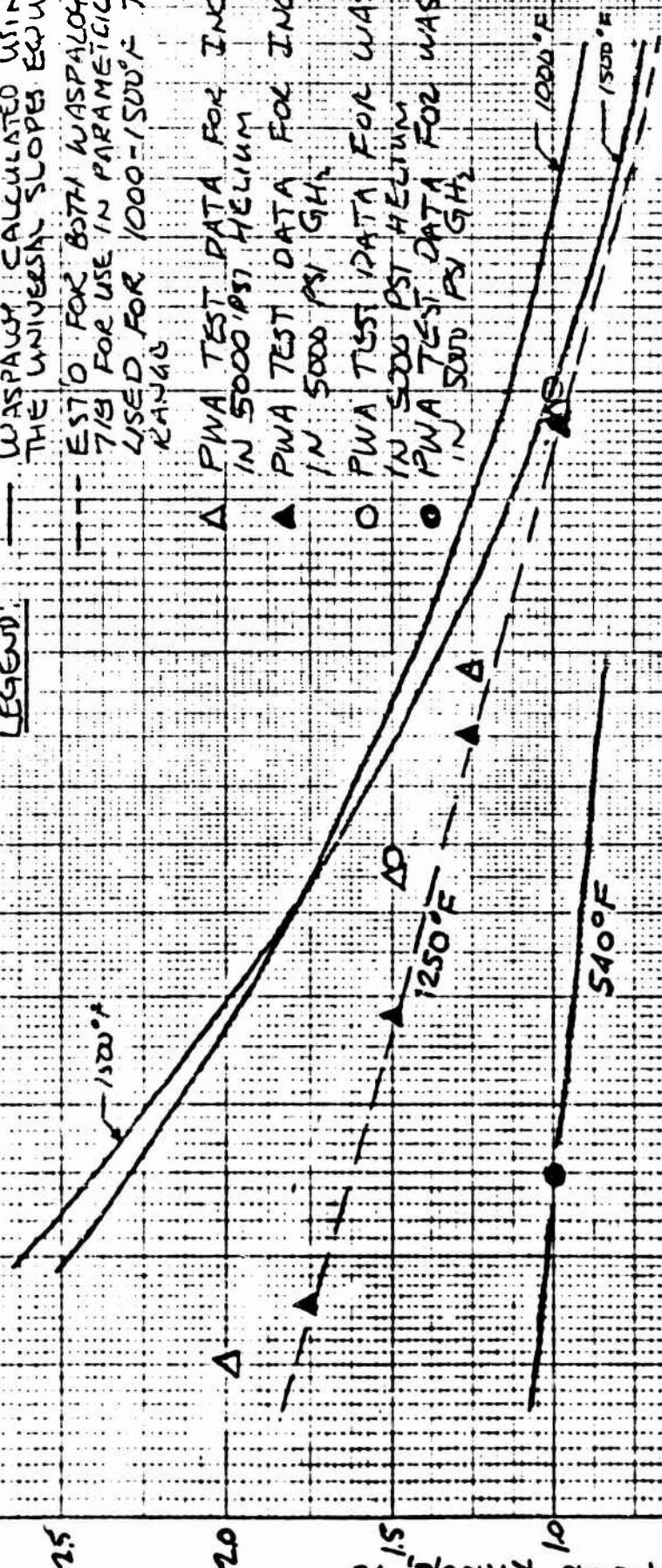
--- EST'D FOR BOTH WASPALOY & INCONEL 718 FOR USE IN PARAMETRIC STUDIES. USED FOR 1000-1500°F TEMPERATURE RANGE

△ PWA TEST DATA FOR INCO 718 @ 1200° IN 5000 PSI HELIUM

▲ PWA TEST DATA FOR INCO 718 @ 1250° IN 5000 PSI GH<sub>2</sub>

○ PWA TEST DATA FOR WASPALOY @ 540° IN 5000 PSI HELIUM

● PWA TEST DATA FOR WASPALOY @ 540° IN 5000 PSI GH<sub>2</sub>



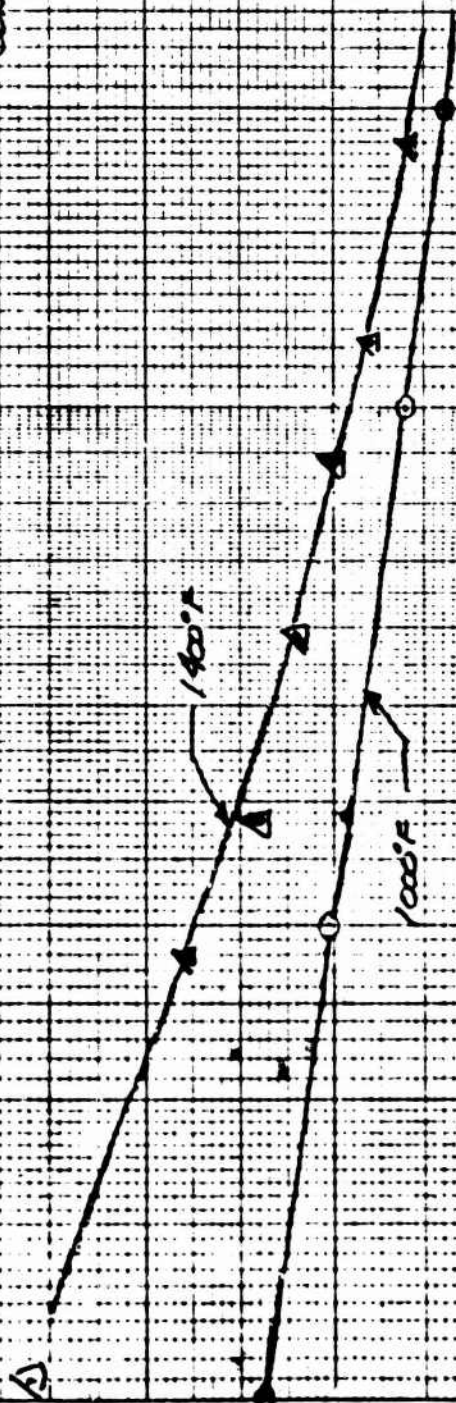
CYCLES TO FAILURE, N<sub>f</sub>

## FIG. 23- UDIMET 700 LOW CYCLE FATIGUE DATA

NOTE: NO  $G_{H_2}$  EMERITTEMENT IS  
REFLECTED IN THIS DATA.

Δ ASM TRANS., VOL. 58, 1965, P. 391.  
LOW CYCLE FATIGUE DAMAGE OF  
UDIMET 700 @ 1400°F

○ VOGEL & CARDEN, THERMAL MECH.  
FATIGUE OF SOME SUPER ALLOYS,  
PRESENTED AT 1967 NAT. METALS  
CONGRESS



TOTAL STRAIN RANGE, %

CYCLES TO FAILURE,  $N_f$





SUBJECT

## OOS PARAMETRIC STUDY

DATE

7/1/71

WORK ORDER

18'-05-101

BY

L.W. BARTHOLF

CHK. BY

DATE

TURBINE DISK SHORT TIME CYCLES TO FAILURE (WASPALLOY)  
 or  
 INEO 710

BASED ON FIGURE 22 WHERE  $\Delta E_t$  VS  $N_f$  AND PAGE 49 WHERE  $\Delta E_t$  VS  $T_{t1}$ , THE FOLLOWING CURVE IS CONSTRUCTED. FOR SHORT TIME CYCLES TO FAILURE. NO CREEP DAMAGE IS INCLUDED IN THIS CURVE. THE 1250°F CURVE WAS USED AS A REPRESENTATIVE VALUE OVER THE TEMPERATURE RANGE OF INTEREST. FOR DETERMINING CYCLES TO FAILURE

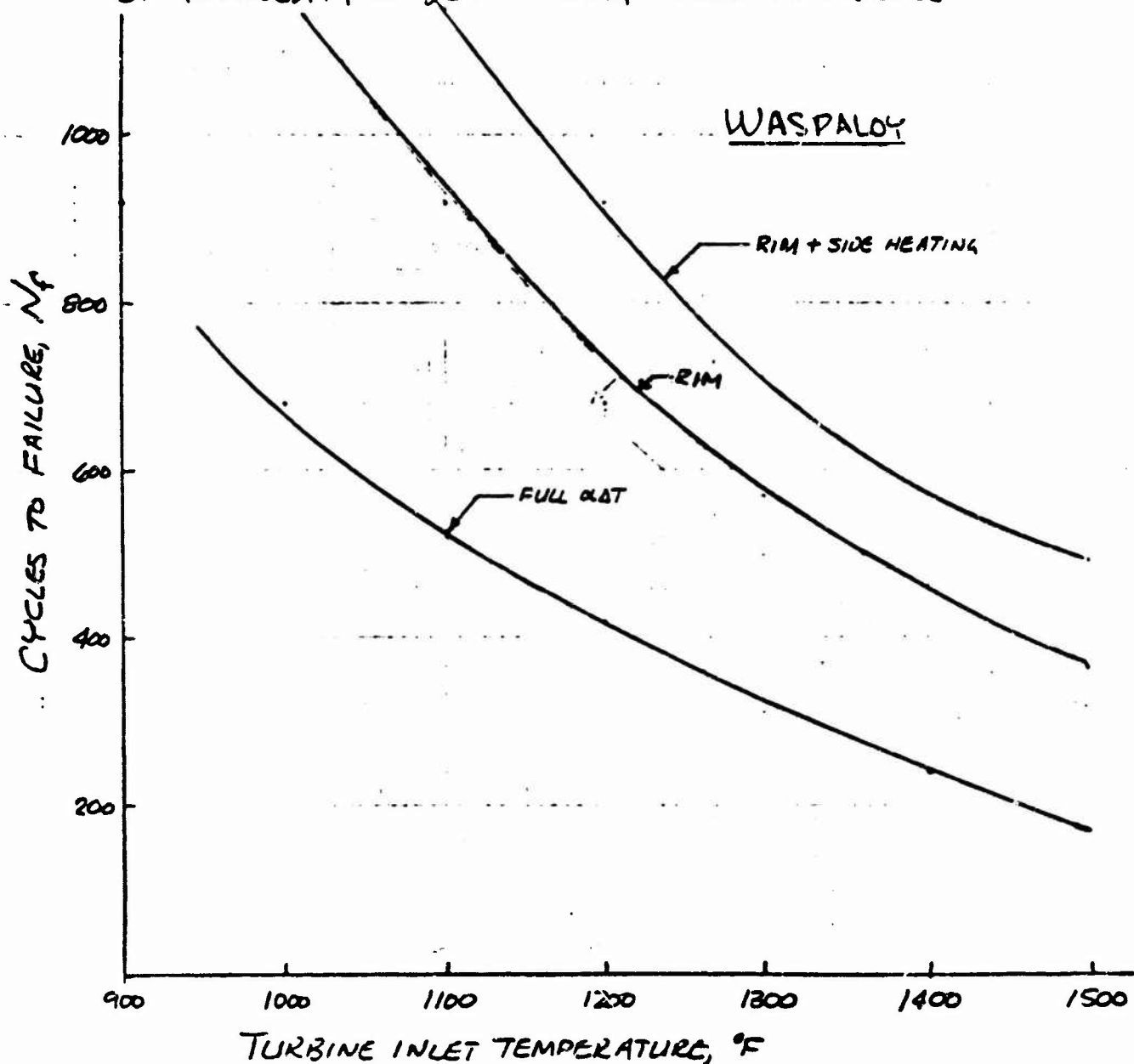


FIG. 24- DISK SHORT TIME CYCLES TO FAILURE FOR VARIOUS HEATING CONDITIONS AND  $T_{t1}$ .



SUBJECT

OOS PARAMETRIC STUDY

DATE

7/13/71

WORK ORDER

BY

L.W. BARTHOLF

CHK. BY

DATE

## TURBINE DISK SHORT TIME CYCLES TO FAILURE (UDIMET 700)

BASED ON FIGURE 23 WHERE  $\Delta E_t$  VS  $N_f$  AND PAGE 49 WHERE  $\Delta E_t$  VS  $T_{Ti}$  THE FOLLOWING CURVE IS CONSTRUCTED FOR SHORT TIME CYCLES TO FAILURE. NO CREEP DAMAGE IS INCLUDED IN THIS CURVE. THE 1400°F CURVE OF FIGURE 23 WAS USED AS A REPRESENTATIVE VALUE OVER THE TEMPERATURE RANGE OF INTEREST FOR DETERMINING CYCLES TO FAILURE.

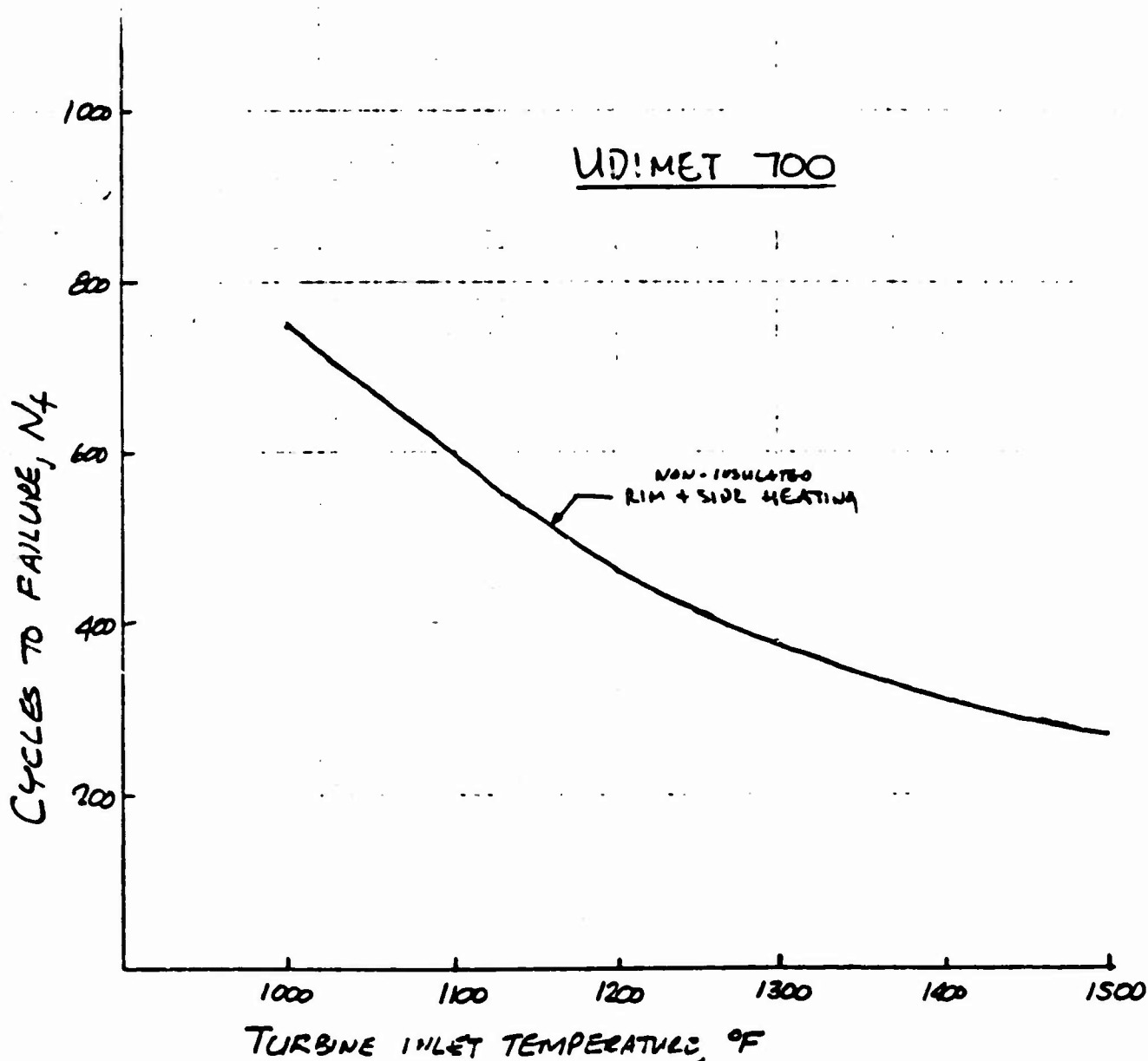


FIG. 25 DISK SHORT TIME CYCLES TO FAILURE VS  $T_{Ti}$ .



SUBJECT

K. DISK LIFE CYCLE CAPABILITIES CONSIDERING  
RUN DURATION, NUMBER OF THERMAL CYCLES AND  
TOTAL DURATION.

DATE

7/6/71

WORK ORDER

1811-05-101

BY

L.W. BAZTHOLF

CHK. BY

DATE

DISK LIFE CYCLE CAPABILITIES CONSIDERING RUN DURATION

THE FOLLOWING ANALYSIS IS USED TO ESTIMATE THE CREEP DAMAGE ASSOCIATED WITH BURN DURATION AND ASSESS THIS DAMAGE IN TERMS OF ITS EFFECT ON DISK LIFE CYCLES.

FOR A GIVEN TURBINE INLET TEMPERATURE ( $T_{Ti}$ ) THERE IS AN ALLOWABLE DISK AVERAGE TANGENTIAL STRESS (ATS) WHICH DEPENDS PARTIALLY ON THE DISK MATERIAL. FOR WASPALOY AND UDIMET 700 THE FOLLOWING APPROXIMATE RELATIONS HOLD PER FIGURES 17 & 18, FOR THE 10 HE STRESS RUPTURE

TURBINE INLET TEMP. (°F)	WASPALLOY		UDIMET 700	
	ALLOWABLE ATS (KSI)	ALLOWABLE MEAN BLADE SPEED (FT/SEC)	ALLOWABLE ATS (KSI)	ALLOWABLE MEAN BLADE SPEED (FT/SEC)
1500	36	1019	48	1245
1400	50	1270	59	1380
1300	67	1470	71	1510
1200	81	1615	94	1740
1100	100	1790	108	1860
1000	105	1795	110	1880

$$* \quad V_{\text{Allow}} = \left( \frac{\text{ATS}}{0.31} \right)^{1/2}$$



SUBJECT

OOS PARAMETRIC STUDY

DATE

WORK ORDER

1811-05-101

BY

L.K.S.

CHK BY

DATE

WASPALOY DISK ALLOWABLE MEAN BLADE SPEEDS

TEMP (°F)	MATERIAL PROPERTIES				ALLOWABLE ATS, KSI			
	0 HR F <sub>UH</sub> (KSI)	2 HR F <sub>CE</sub> (KSI)	10 HR F <sub>CE</sub> (KSI)	20 HR F <sub>CE</sub> (KSI)	F <sub>UH</sub> /1.7	F <sub>CE</sub> /1.61		
	0 HR (KSI)	2 HR (KSI)	10 HR (KSI)	20 HR (KSI)	0 HR (KSI)	2 HR (KSI)	10 HR (KSI)	20 HR (KSI)
1100	170				100	100	100	100
1200	162	140	130	124	95	87	81	77
1300	145	120	108	100	85	74	67	62
1400	115	93	80	74	69	58	50	46
1500	90	73	58	53	53	45	36	33
1600	76	57	39	34	45	35	24	21

$$\text{MEAN BLADE SPEED, } V, = \sqrt{\frac{\text{ATS}}{.031}}$$

TEMP. (°F)	ALLOWABLE MEAN BLADE SPEED, V, FT/SEC			
	LIFE = 0 HR	2 HR	10 HR	20 HR
1100	1790	1790	1790	1790
1200	1745	1670	1615	1575
1300	1655	1540	1470	1410
1400	1480	1365	1270 (1300)	1220
1500	1305	1200	1075	1030
1600	1200	1060	870	820

\* EFFECTIVE CREEP DAMAGE DURATION



SUBJECT

## OOS PARAMETRIC STUDY

DATE

7/6/71

WORK ORDER

1811-05-101

BY

L.W. BARTHOLF

CHK. BY

DATE

TO DETERMINE THE CREEP RUPTURE DAMAGE FRACTION  $(\sum t/t_r)$  FOR VARIOUS DURATION BURNS THE FOLLOWING METHOD WILL BE EMPLOYED.

GIVEN A  $T_{Ti}$  AND AN ASSOCIATED ATS THE TIME TO RUPTURE,  $t_r$ , CAN BE DETERMINED FOR VARIOUS BURN DURATIONS,  $t$ , AND THE DAMAGE FACTOR  $(t/t_r)$  EVALUATED FOR THE EXPECTED BURN DURATIONS.

FOR EXAMPLE, A RIM & SIDE HEATED DISK WITH A  $T_{Ti} = 1400^\circ\text{F}$  AND  $ATS = 49 \text{ KSI}$  FOR WASPALOY. IT CAN BE SEEN FROM FIGURE 9, THAT AFTER ABOUT 125 SECONDS THE ENTIRE DISK IS AT  $T_{Ti}$  SO THAT THE  $t_r$  @  $1400^\circ\text{F}$  AND  $49 \text{ KSI}$  IS ABOUT 400 HRS  $[1.44(10)^6 \text{ SEC}]$ . THE DAMAGE IN THE FIRST 125 SECONDS CAN BE ESTIMATED BY USING INCREMENTS OF TIME. FOR THE FIRST 75 SECONDS THE AVE. DISK METAL TEMPERATURE IS BELOW  $1200^\circ\text{F}$  AND THE ASSOCIATED TIME TO RUPTURE IS VERY HIGH (I.E.  $\approx 10^5 \text{ HRS}$ ). THE NEXT 50 SECONDS THE DISK IS AT AN AVERAGE TEMPERATURE OF ABOUT  $1300^\circ\text{F}$  AND THE ASSOCIATED TIME TO RUPTURE AT  $49 \text{ KSI}$  IS  $10^4 \text{ HRS}$   $[36(10)^6 \text{ SEC}]$ . THEREFORE THE DAMAGE FRACTION FOR A BURN GREATER THAN 125 SECONDS IS DETERMINED BY:

$$R = \sum t/t_r = \frac{75}{10^5} + \frac{50}{36(10)^6} + \frac{(t-125)}{1.44(10)^6}$$

$$= 0 + 1.4(10)^{-6} + .695(10)^{-6}(t_{\text{SEC}} - 125)$$

$$R = 1.4(10)^{-6} + .695(10)^{-6}(t_{\text{SEC}} - 125)$$

FOR MULTIPLE BURNS OF TIME,  $t$ , THE DAMAGE FRACTION,  $R'$ , IS GIVEN BY:

$$R' = N_L R \quad \text{where: } N_L = \text{NUMBER OF BURNS OF DURATION } t.$$

FOR A 1000 SECOND BURN:

$$R = 1.4(10)^{-6} + .695(10)^{-6}(875)$$

$$= 1.4(10)^{-6} + 608(10)^{-6}$$

$$R = 609(10)^{-6} \quad \text{C-260}$$



SUBJECT

OOS PARAMETRIC STUDY

DATE

6/30/71

WORK ORDER

1811-05-101

BY

L.W. BARTHOLF

CHK. BY

DATE

EFFECT OF BURN DURATION ON TURBINE DISK LIFE

THE CREEP DAMAGE ASSOCIATED WITH BURN DURATION IS EVALUATED USING A LINEAR INTERACTION THEORY AS SHOWN BELOW.

$$\sum \frac{N}{N_f} + \sum \frac{t}{t_R} = 1$$

TO DETERMINE THE SHORT TIME CYCLES (I.E. NO CREEP DAMAGE) REMAINING AFTER A SERIES OF LONG DURATION BURNS (I.E. CREEP DAMAGE) THE FOLLOWING METHOD WAS USED.

$$\frac{N_s}{N_{fs}} + \frac{N_L}{N_{fL}} + \frac{N_L t}{t_R} = 1$$

$$\text{SINCE } N_{fs} = N_{fL} = N_f$$

$$N_{S_{\text{REMAIN}}} = N_f \left[ 1 - \frac{N_L t}{t_R} - \frac{N_L}{N_f} \right]$$

$$N_{S_{\text{REMAIN}}} = N_f \left[ 1 - \frac{N_L t}{t_R} \right] - N_L$$

$N$  = NO. OF APPLIED CYCLES

$t$  = DURATION OF APPLIED CYCLES

$N_f$  = CYCLES TO FAILURE WITHOUT TIME EFFECTS (CREEP DAMAGE)

$t_R$  = DURATION TO CREEP RUPTURE WITHOUT CYCLIC FATIGUE EFFECTS





SUBJECT

OOS PARAMETER STUDY

DATE

WORK ORDER

BY

L.W. BARTHOLF

CHK. BY

DATE

6/24/71

TURBINE DISK CREEP RUPTURE DAMAGE

RIM AND SIDE HEATING (WASPALLOY MATERIAL)

TURBINE INLET TEMPERATURE (°F)	AVE. TAUG. STRESS FOR $T_{FI}$ CONDITIONS (KSI)	FIRING DURATION $t$ (SEC)	$t'$ (SEC)	$t_R$ (SEC)	$R = \epsilon \frac{t'}{t_R}$	NUMBER OF FIRINGS OF $t'$ DURATION TO FAILURE
1500	38	125	75	HIGH	0	110,000
			50	5.4(10) <sup>6</sup>	$\frac{9(10)^{-6}}{9(10)^{-6}}$	
		500	125	13.9(10) <sup>6</sup>	$9(10)^{-6}$	953
			375	.36(10) <sup>6</sup>	$\frac{1040(10)^{-6}}{1049(10)^{-6}}$	
		1000	500	.477(10) <sup>6</sup>	$1049(10)^{-6}$	410
			500	.36(10) <sup>6</sup>	$\frac{1390(10)^{-6}}{2439(10)^{-6}}$	
		2000	1000	.41(10) <sup>6</sup>	$2439(10)^{-6}$	192
			1000	.36(10) <sup>6</sup>	$\frac{2790(10)^{-6}}{5219(10)^{-6}}$	
		5000	2000	.383(10) <sup>6</sup>	$5219(10)^{-6}$	74
			3000	.36(10) <sup>6</sup>	$\frac{8330(10)^{-6}}{13549(10)^{-6}}$	
1400	49	125	75	HIGH	0	700000
			50	.36(10) <sup>6</sup>	$\frac{1.4(10)^{-6}}{1.4(10)^{-6}}$	
		500	125	.89(10) <sup>6</sup>	$1.4(10)^{-6}$	4000
			375	1.44(10) <sup>6</sup>	$\frac{260(10)^{-6}}{261(10)^{-6}}$	
		1000	500	1.92(10) <sup>6</sup>	$261(10)^{-6}$	1640
			500	1.44(10) <sup>6</sup>	$\frac{347(10)^{-6}}{608(10)^{-6}}$	
		2000	1000	1.64(10) <sup>6</sup>	$608(10)^{-6}$	765
			1000	1.44(10) <sup>6</sup>	$\frac{694(10)^{-6}}{1302(10)^{-6}}$	
		5000	2000	1.53(10) <sup>6</sup>	$1302(10)^{-6}$	295
			3000	1.44(10) <sup>6</sup>	$\frac{2090(10)^{-6}}{3382(10)^{-6}}$	



SUBJECT

OOS PARAMETER STUDY

DATE

WORK ORDER

BY

L.W. BARTHOLF

CHK. BY

DATE

6/24/71

TURBINE DISK CREEP RUPTURE DAMAGE (CON'T)  
RIM AND SIDE HEATING (WASPALLOY MATERIAL)

TURBINE INLET TEMPERATURE (°F)	AVE. TANG. STRESS FOR $T_T$ CONDITIONS (KSI)	FIRING DURATION $t$ (SEC)	$t'$ (SEC)	$t_R$ (SEC)	$R = \epsilon \frac{t'}{t_R}$	NUMBER OF FIRINGS OF $t'$ DURATION TO FAILURE
1300	62	125	75	HIGH	0	14 (10) <sup>6</sup>
			50	720 (10) <sup>6</sup>	$\frac{.07(10)^{-6}}{.07(10)^{-6}}$	
		500	125	1800 (10) <sup>6</sup>	$\frac{.07(10)^{-6}}{.07(10)^{-6}}$	14300
			375	5.4 (10) <sup>6</sup>	$\frac{.07(10)^{-6}}{5.4(10)^{-6}}$	
		1000	500	7.1 (10) <sup>6</sup>	$\frac{.07(10)^{-6}}{7.1(10)^{-6}}$	1150
			500	5.4 (10) <sup>6</sup>	$\frac{.07(10)^{-6}}{5.4(10)^{-6}}$	
		2000	1000	6.15 (10) <sup>6</sup>	$\frac{.07(10)^{-6}}{6.15(10)^{-6}}$	2870
			1000	5.4 (10) <sup>6</sup>	$\frac{.07(10)^{-6}}{5.4(10)^{-6}}$	
		5000	2000	5.7 (10) <sup>6</sup>	$\frac{.07(10)^{-6}}{5.7(10)^{-6}}$	1110
			3000	5.4 (10) <sup>6</sup>	$\frac{.07(10)^{-6}}{5.4(10)^{-6}}$	
					$\frac{.07(10)^{-6}}{9.03(10)^{-6}}$	
1200	81	125	125	HIGH	0	HIGH
		500	125	HIGH	0	17300
			375	6.5 (10) <sup>6</sup>	$\frac{.07(10)^{-6}}{6.5(10)^{-6}}$	
		1000	500	8.6 (10) <sup>6</sup>	$\frac{.07(10)^{-6}}{8.6(10)^{-6}}$	7400
			500	6.5 (10) <sup>6</sup>	$\frac{.07(10)^{-6}}{6.5(10)^{-6}}$	
		2000	1000	7.4 (10) <sup>6</sup>	$\frac{.07(10)^{-6}}{7.4(10)^{-6}}$	3460
			1000	6.5 (10) <sup>6</sup>	$\frac{.07(10)^{-6}}{6.5(10)^{-6}}$	
		5000	2000	6.9 (10) <sup>6</sup>	$\frac{.07(10)^{-6}}{6.9(10)^{-6}}$	1335
			3000	6.5 (10) <sup>6</sup>	$\frac{.07(10)^{-6}}{6.5(10)^{-6}}$	
					$\frac{.07(10)^{-6}}{7.49(10)^{-6}}$	



SUBJECT

OOS PARAMETRIC STUDY

DATE

7/6/71

WORK ORDER

181-05-101

BY

L.W. BARTHOLF

CHK. BY

DATE

THE CASE SHOWN FOR WASPALOY RIM & SIDE HEATED DISK REPRESENTS THE WORSE CONDITION FOR THE ALTERNATIVES OF MATERIALS AND TYPE OF DISK HEATING DESCRIBED IN THIS STUDY.

THAT IS: • UDIMET WILL SHOW A LOWER DAMAGE FRACTION "R"

- RIM HEATING ONLY WILL SHOW A LOWER DAMAGE FRACTION "R".

UDIMET 700 SHOWS A MUCH LOWER LOW CYCLE FATIGUE CAPABILITY THAN WASPALOY AND FOR THIS REASON MAY NOT BE AN ADEQUATE TURBINE DISK MATERIAL.



SUBJECT

OOS PARAMETER STUDY.

DATE

7/7/71

WORK ORDER

1811-05-101

BY

L.W. BARTHOLF

CHK. BY

DATE

EFFECT OF BURN DURATION ON TURBINE DISK LIFE

$$N_{S_{\text{REMAIN}}} = N_f \left[ 1 - \frac{N_L t}{t_R} \right] - N_L$$

where:  $N_{S_{\text{REMAIN}}}$  = NUMBER OF SHORT BURNS (<100 SEC) REMAINING BEFORE FAILURE

$N_f$  = NUMBER OF SHORT DURATION BURNS TO FAILURE

$N_L$  = NUMBER OF LONG DURATION BURNS

$t/t_R$  = CREEP DAMAGE FRACTION FOR THE LONG DURATION BURN.

FOR EXAMPLE TAKE A WASPALOY DISK AT A  $T_D = 1400^\circ\text{F}$  WITH RIM AND SIDE HEATING AND A 1000 SECOND BURN DURATION

$$N_f = 570$$

$$t/t_R = 608(10)^{-6}$$

$$\therefore N_{S_R} = 570 \left[ 1 - 608(10)^{-6} N_L \right] - N_L$$

$N_L$	$608(10)^{-6} N_L$	$1 - 608(10)^{-6} N_L$	WITH CREEP DAMAGE $N_{S_R}$	W/O CREEP DAMAGE $N_{S_R} = N_f - N_L$
1	$608(10)^{-6}$	.9994	568	569
10	$6080(10)^{-6}$	.9939	555	560
20	$12160(10)^{-6}$	.9878	543	550
50	$30400(10)^{-6}$	.9696	502	520



AEROJET-GENERAL CORPORATION  
SACRAMENTO • CALIFORNIA

REPORT NO.

PAGE 62 of 69

DATE

7/9/71

WORK ORDER

1811-05-101

DATE

SUBJECT

OOS PARAMETRIC STUDY

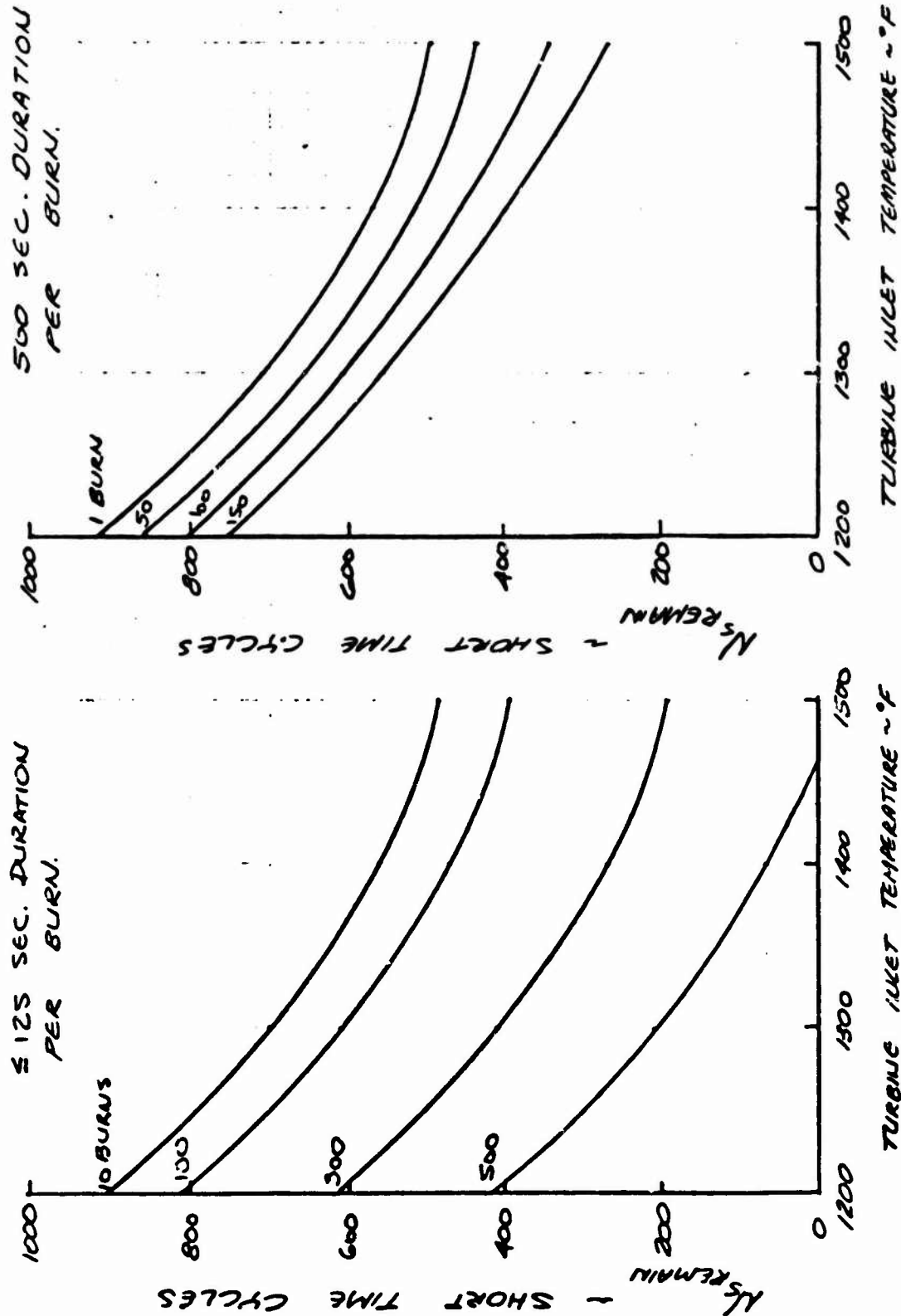
BY

G. ALDRICH

CHK BY

RIM AND SIDE HEATED TURBINE DISK LIFE CYCLES AND LIFETIME

(WASPALCOY)





SUBJECT

003 PARAMETRIC STUDY

DATE

7/8/71

WORK ORDER

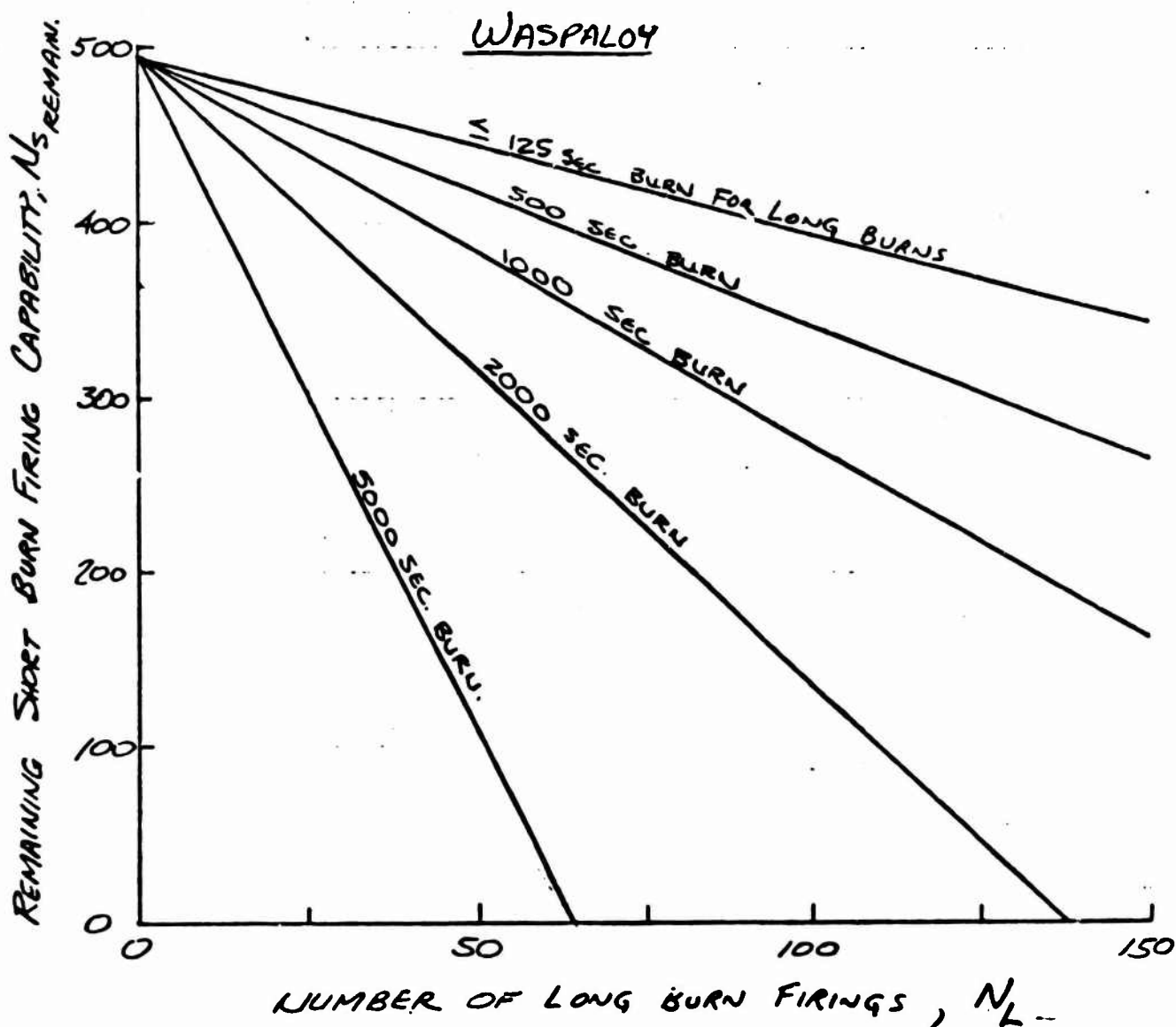
1811-05-101

BY

G. ALORICH

CHK. BY

DATE

TURBINE INLET TEMPERATURE = 1500°FRIM AND SIDE HEATING

SHORT BURN FIRINGS ARE THOSE WHOSE DURATION IS LESS THAN 125 SECONDS.



SUBJECT

OOS PARAMETRIC STUDY

DATE  
7/9/71

WORK ORDER  
1811-05-101

BY

G. ALDRICH

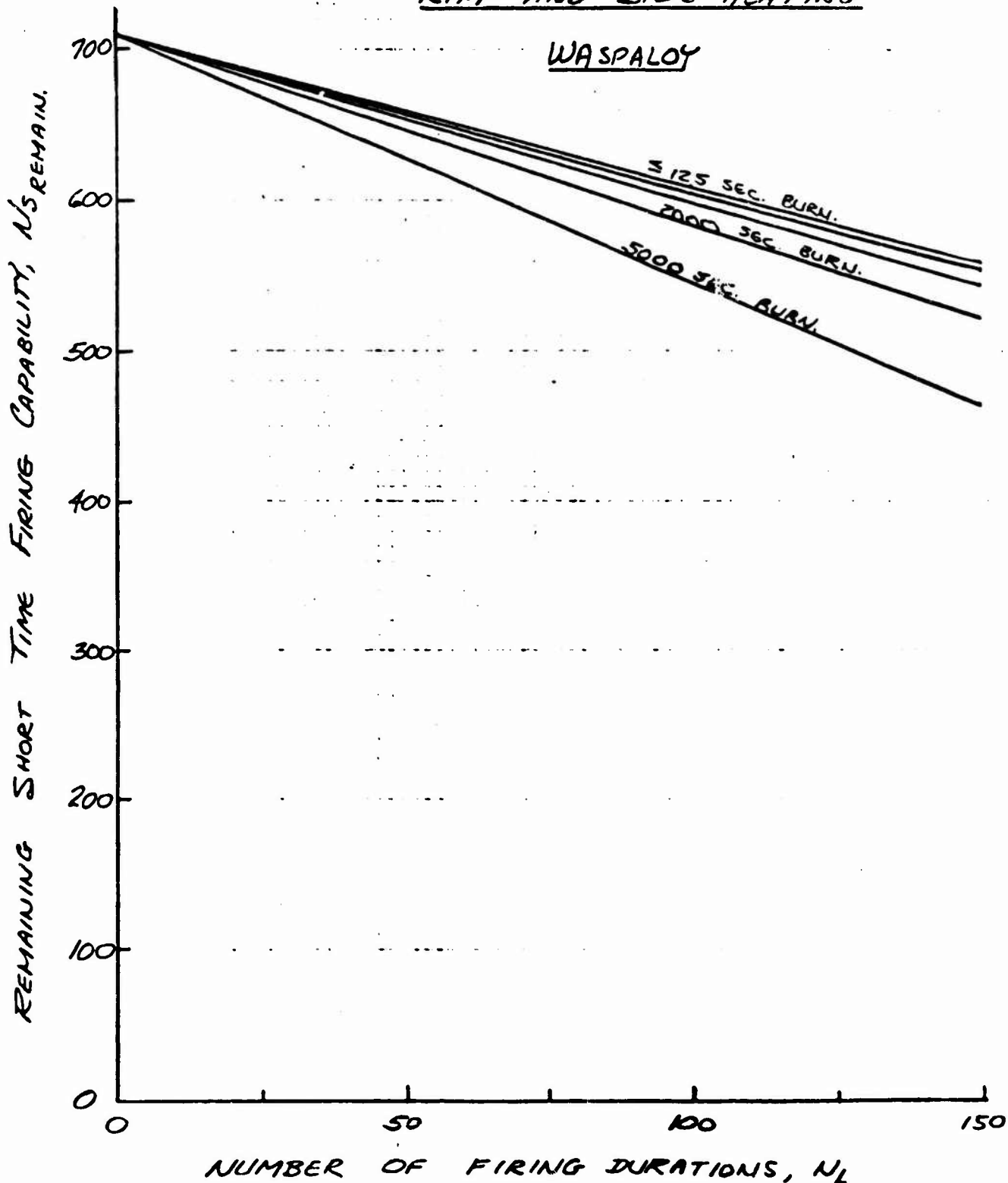
CHK. BY

DATE

TURBINE INLET TEMPERATURE = 1300°F

RIM AND SIDE HEATING

WASPALLOY





SUBJECT

OOS PARAMETRIC STUDY

DATE

7/9/71

WORK ORDER

1811-05-101

BY

G. ALORICH

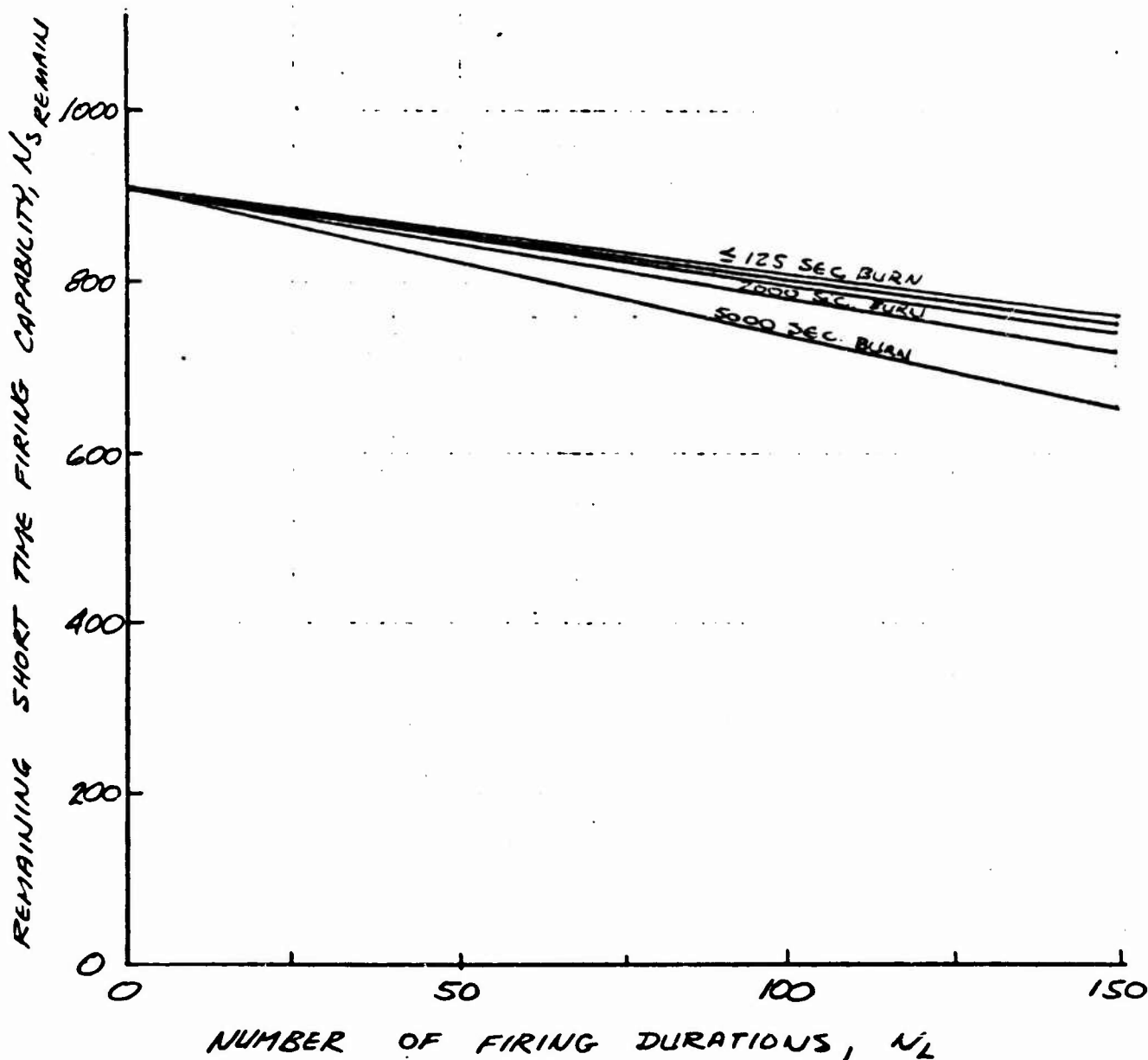
CHK. BY

DATE

TURBINE INLET TEMPERATURE = 1200°F

RIM AND SIDE HEATING

WASPALLOY







SUBJECT

OOS PARAMETRIC STUDY

DATE

7/9/71

WORK ORDER

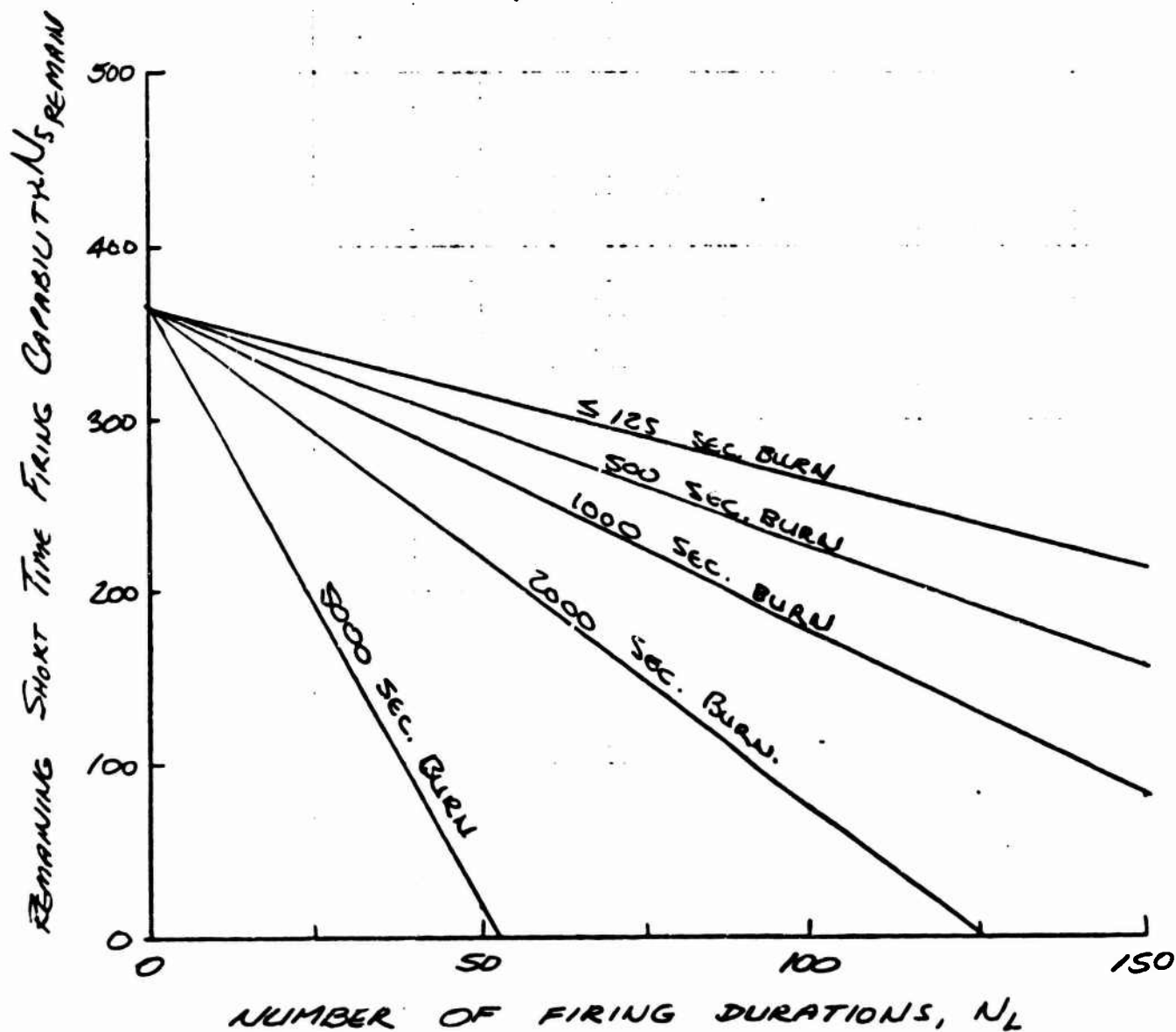
1811-05-101

BY

G. ALORICH

CHK. BY

DATE

TURBINE INLET TEMPERATURE = 1500°FRIM HEATINGWASPALLOY



SUBJECT

OOS PARAMETRIC STUDY

DATE

WORK ORDER

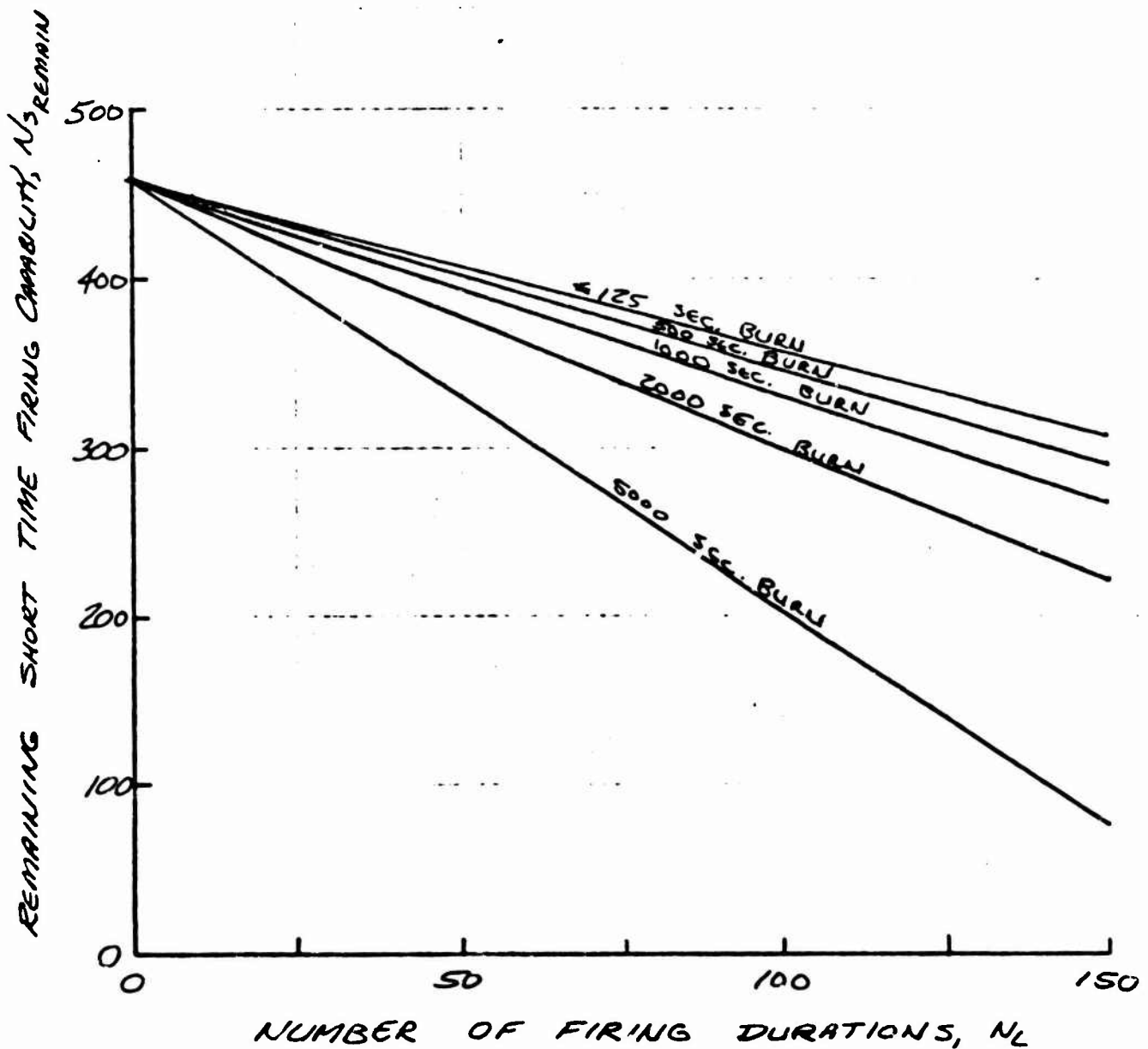
1911-05-101

BY

G. ALDRICH

CHK. BY

DATE

TURBINE INLET TEMPERATURE = 1400°FRIM HEATINGWASPALLOY



SUBJECT

OOS PARAMETRIC STUDY

DATE

7/9/71

WORK ORDER

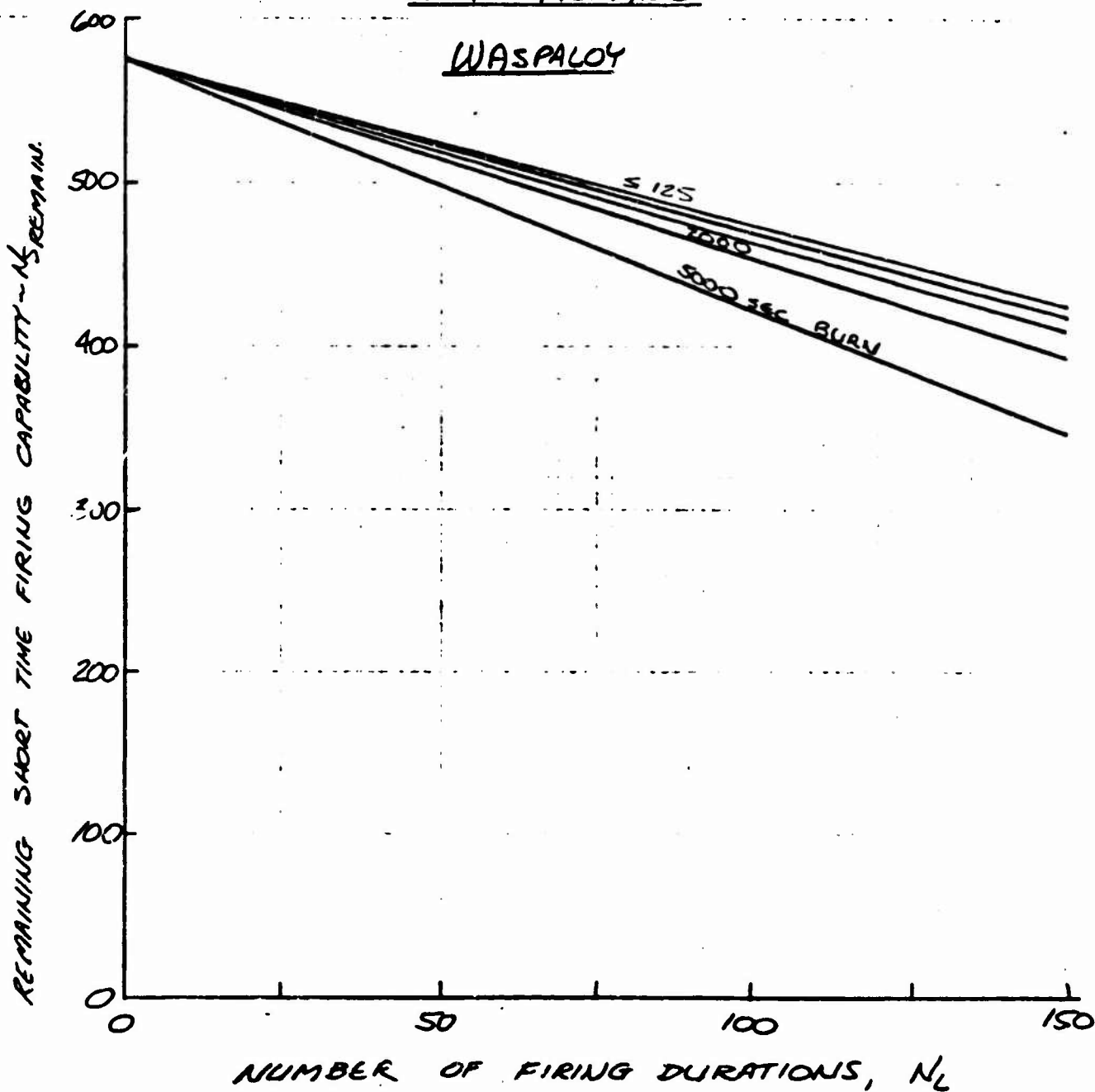
1811-05-101

BY

G. ALDRICH

CHK. BY

DATE

TURBINE INLET TEMPERATURE = 1300°FRIM HEATINGWASPALLOY



AEROJET-GENERAL CORPORATION  
SACRAMENTO • CALIFORNIA

AGCS-0800-11

REPORT NO.

PAGE 69 OF 69

SUBJECT

OOS PARAMETRIC STUDY

DATE

7/9/71

WORK ORDER

1811-05-101

BY

G. ALDRICH

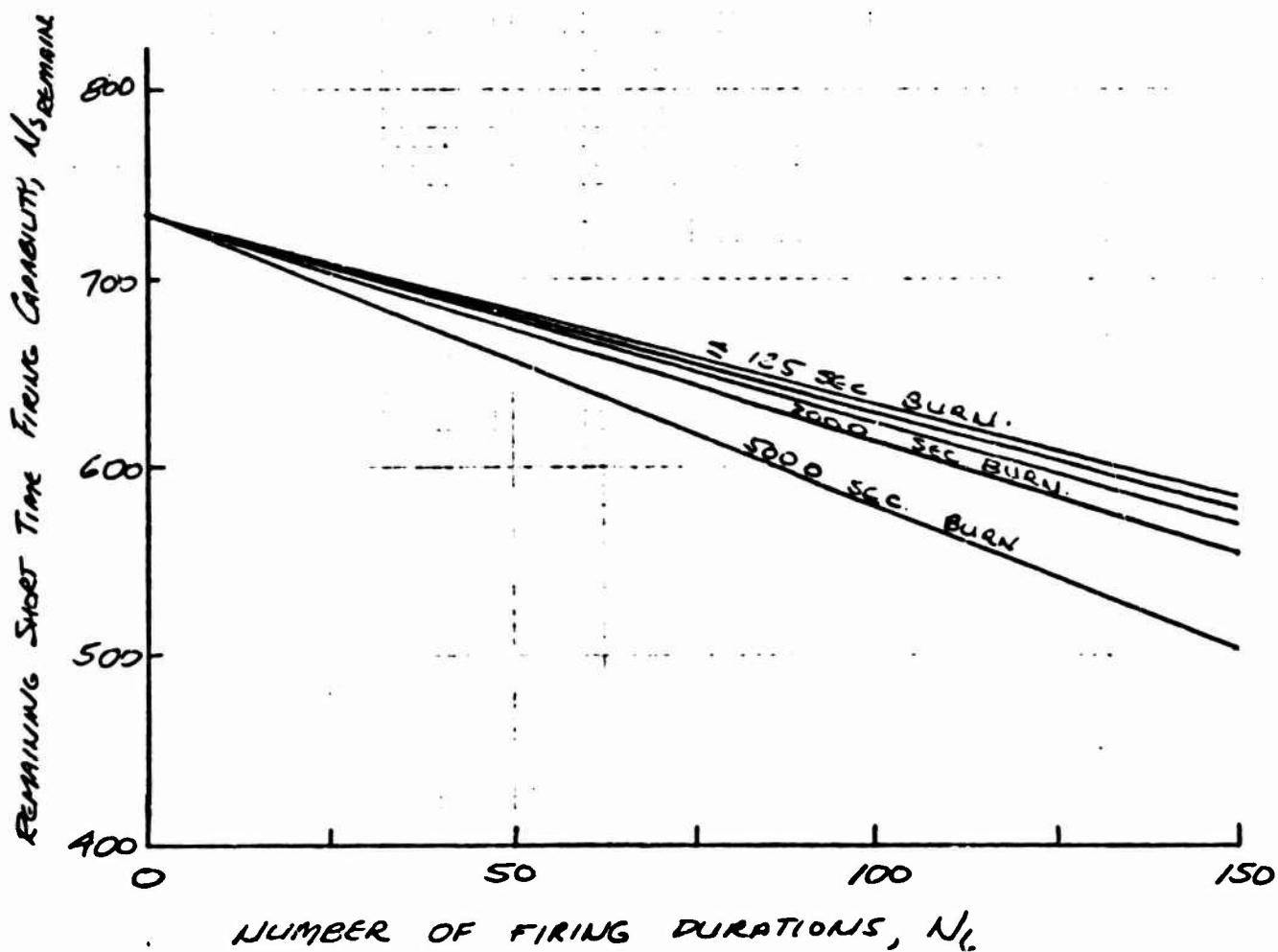
CHK. BY

DATE

TURBINE INLET TEMPERATURE - 1200°F

RIM HEATING

WASPALOX



PRELIMINARY OOS 10K FTPA AND OTPA  
CRITICAL SPEED ANALYSIS

# STRUCTURAL ENGINEERING

SA-OOS-TM-6

PRELIMINARY OOS 10<sup>K</sup> FTPA & DTPA  
CRITICAL SPEED ANALYSIS

27 SEPTEMBER 1971

PREPARED BY:

C. W. BARTHOLOMEW

APPROVED BY:

DATE

*L. H. Dwyer*  
*L. H. Dwyer*



AEROSJET LIQUID ROCKET COMPANY

SACRAMENTO, CALIFORNIA



AEROJET-GENERAL CORPORATION  
SACRAMENTO • CALIFORNIA

ALL RIGHTS RESERVED

SUBJECT		REPORT NO.	PAGE 1 of 15
		DATE	
		WORK ORDER	
BY L.W. BARTHOLF	CHK BY	DATE	

## I. INTRODUCTION:

THE FOLLOWING REPORT PRESENTS RESULTS OF PRELIMINARY CRITICAL SPEED ANALYSES OF THE OOS 10K FUEL AND OXIDIZER TURBOPUMPS.

## II. SUMMARY OF RESULTS:

BOTH THE FTFA AND THE OTFA DESIGNS ANALYZED APPEAR FEASIBLE CONSIDERING A "SOFT" MOUNTED BEARING SYSTEM.

NEITHER DESIGN APPEARS ABLE TO OPERATE SUB-CRITICAL USING A "STIFF" MOUNTED BEARING SYSTEM.

## III. DISCUSSION:

THE BASIC ASSUMPTIONS OF THIS ANALYSIS OF ALL STEEL COMPONENTS AND SUFFICIENT CLAMPING FORCE TO MAKE THE BEARING INNER RACE CHARGE OF TRANSMITTING THE BENDING MOMENT GREATER THAN THE RESULT IF NOT VALID.

COMPONENT WEIGHTS AND MATERIALS ARE INDICATED BY OTHER CONSIDERATIONS ALSO AND CANNOT BE CHANGED AT THIS TIME.

CLAMPING REQUIREMENTS LOOK REASONABLE BASED ON THIS SMALLNESS OF THE DESIGN AND THE EXPECTED LOAD PATHS.

ANALYSIS OF THE FTFA CONCEPT II WAS NOT COMPLETED DUE TO INSUFFICIENT FUNDS.



AEROJET-GENERAL CORPORATION  
SACRAMENTO CALIFORNIA

REPORT NO.

PAGE 2 OF 15

DATE  
23 SEPT. 1971

WORK ORDER  
1811-07-001

DATE

DOC 2 043

SUBJECT

OOS 10<sup>K</sup> SHAFT DYNAMICS

BY

L. W. BARTHOLO

CHK. BY

OOS 10<sup>K</sup> FTIR CRITICAL SPEED (CONCENT II)

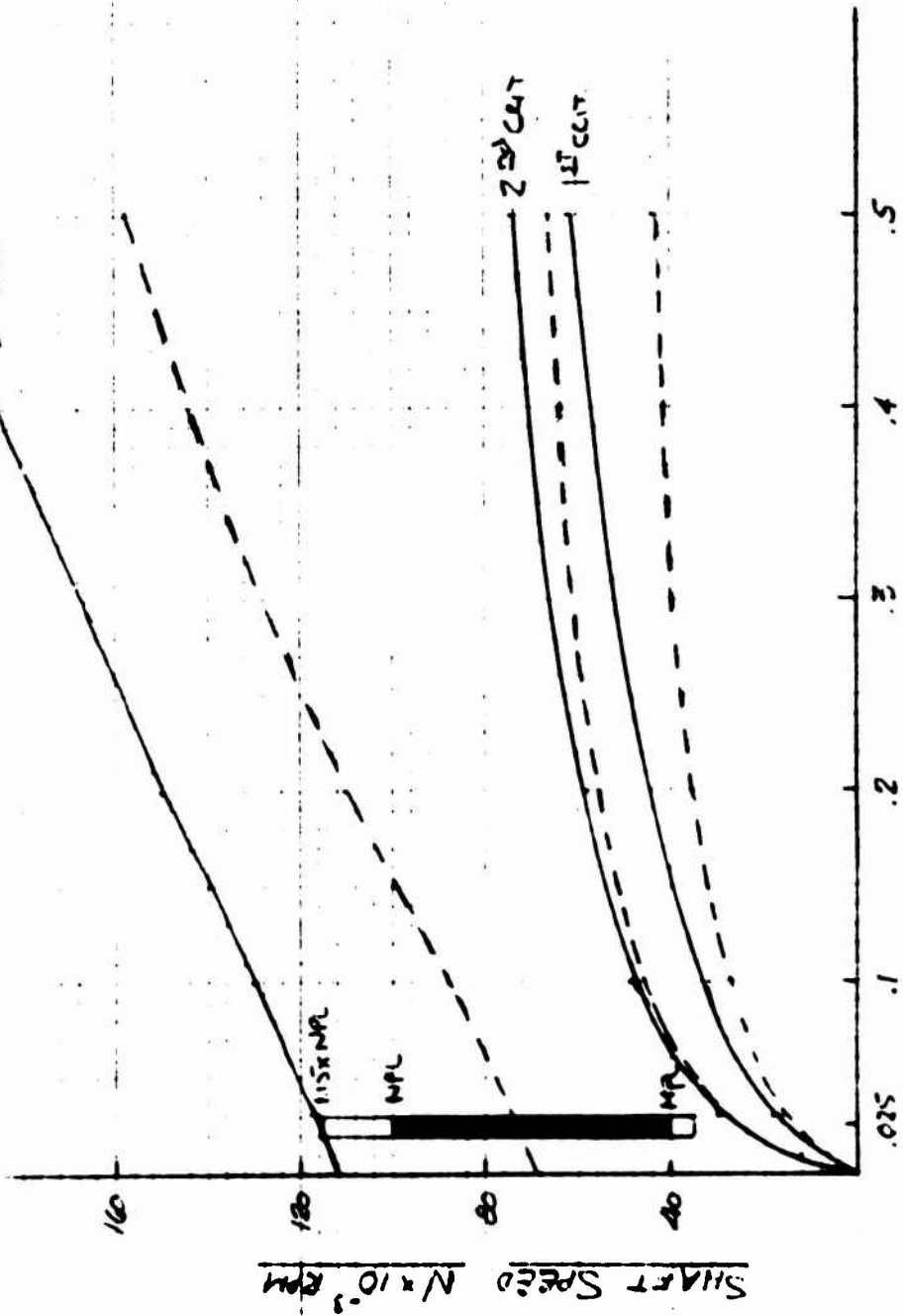
--- LATERAL VIBRATION (EXPECTED WITH STIFF MOUNTING)  
--- FLEXURAL CIRCULAR WHIRL (EXPECTED WITH SOFT MOUNTING)

3<sup>rd</sup> CRIT

2<sup>nd</sup> CRIT

1<sup>st</sup> CRIT

RADIAL STIFFNESS AT EACH BEARING,  $K \times 10^{-6}$  LB/IN







AEROJET-GENERAL CORPORATION  
SACRAMENTO CALIFORNIA

REPORT NO.

PAGE 3 OF 15

AOC 2-843

SUBJECT

COS 10K SHAFT DYNAMICS

DATE

24 SEP 77

WORK ORDER

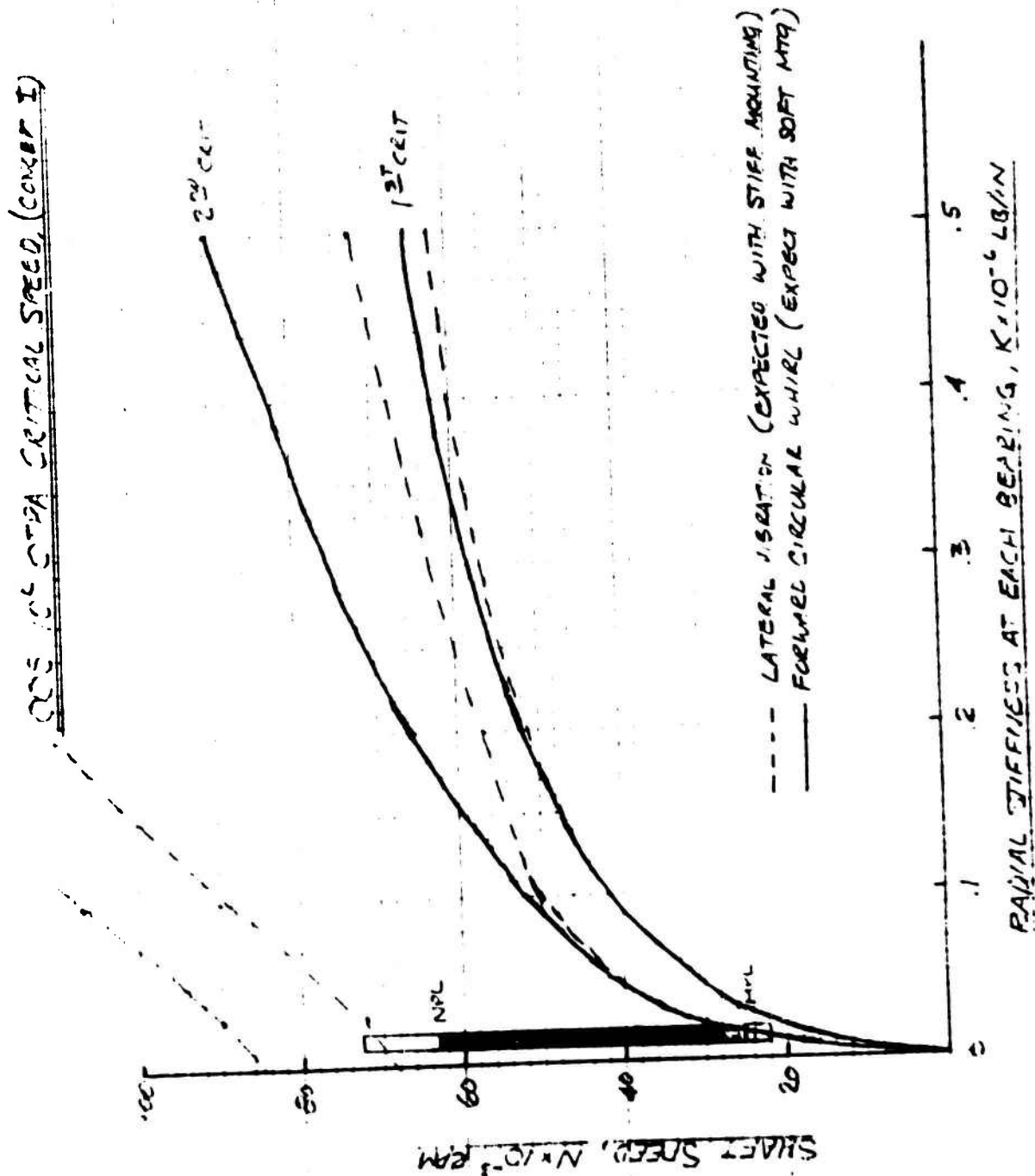
1911-07-001

DATE

BY

L W BARTHOLO

CHK. BY





AEROJET-GENERAL CORPORATION  
SACRAMENTO • CALIFORNIA

REPORT NO.

PAGE 4 OF 5

AEC 2 043

SUBJECT

005 10<sup>6</sup> SHAFT DYNAMICS

DATE  
27 SEPT. 1971

WORK ORDER  
1911-07-001

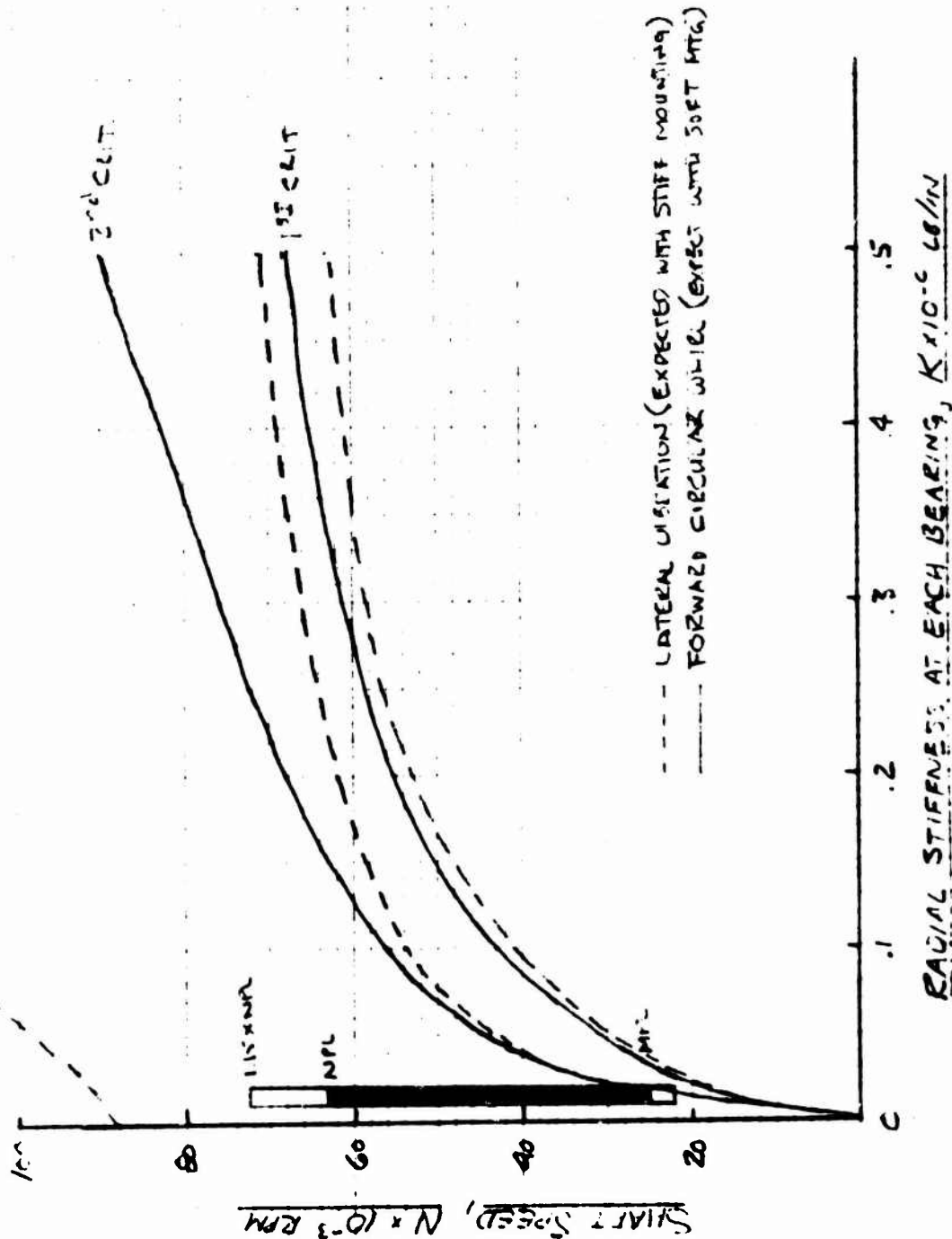
BY

L.W. BARTHOLF

CHK. BY

DATE

005 10<sup>6</sup> OPGA CRITICAL SPEED (CONCEPT II)





AERJET-GENERAL CORPORATION  
SACRAMENTO • CALIFORNIA

REPORT NO.

PAGE 5 OF 15

ALLS 000011

SUBJECT

OOS 10<sup>K</sup> SHAFT DYNAMICS

DATE

22 SEPT 1971

WORK ORDER

1811-07-001

BY

L W BARTHOLF

CHK BY

DATE

## DESIGN CRITERIA (OOS 10<sup>K</sup> FTPA)

### OPERATING SPEED RANGE

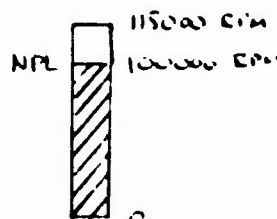
NPL = 100,000 RPM (PER DESIGNER, S. ANDRUS)

USING THE SAME RATIO OF NPL TO MPL THAT WAS APPLIED TO THE 25<sup>K</sup> DESIGN, (I.E. NPL = 80000, MPL = 32000) THE MPL SPEED FOR THE 10<sup>K</sup> DESIGN IS:

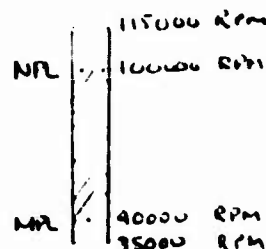
$$MPL = NPL \left( \frac{32}{80} \right) = 100000 (A) = 40000 \text{ RPM}$$

### OPERATING SPEED MARGINS:

- (1) ALL ROTOR CRITICAL SPEEDS SHALL BE 15% ABOVE THE MAX OPERATING SPEED FOR SUBCRITICAL OPERATION



- (2) FOR SUPER CRITICAL OPERATION, NO NATURAL FREQUENCIES OF THE TURBOPUMP ASSEMBLY SHALL EXIST WITHIN THE NORMAL OPERATING SPEED RANGE INCLUDING A 15% MARGIN, (I.E. 35000 TO 115,000 RPM)





AERJET-GENERAL CORPORATION  
SACRAMENTO • CALIFORNIA

4000-000011

REPORT NO.

PAGE 6 OF 5

SUBJECT

00S 10<sup>k</sup> SHAFT DYNAMICS

DATE

24 SEPT. 1971

WORK ORDER

1811-07-001

BY

L. W. BARTHOLF

CHK. BY

DATE

## DESIGN CRITERIA (00S 10<sup>k</sup> OTPA)

### OPERATING SPEED RANGE

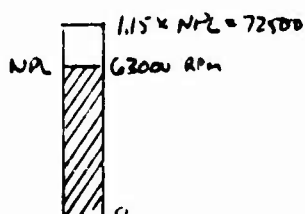
NPL = 63000 RPM (PER DESIGNER, S. ANDRUS)

USING THE SAME RATIO OF NPL TO MPL THAT WAS APPLIED TO THE 25<sup>k</sup> DESIGN, (I.E. NPL = 50000, MPL = 20000) THE MPL SPEED FOR THE 10<sup>k</sup> DESIGN IS:

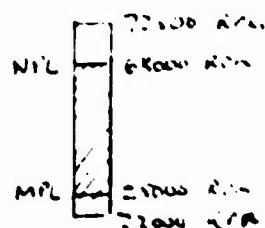
$$MPL = NPL \left( \frac{20}{50} \right) = 63000 \left( \frac{2}{5} \right) = 25200 \text{ RPM}$$

### OPERATING SPEED MARGINS: (SAME AS FTRA)

#### SUBCRITICAL



#### SUPER-CRITICAL



THE ABOVE RANGES PROVIDE A 15% MARGIN IN THE NORMAL OPERATING SPEED RANGE - IF OVERSPEED CONDITIONS CAN EXIST THE 15% MARGIN SHOULD BE APPLIED TO OVERSPEED CONDITIONS.



PROJECT

SUBJECT

OOS 10<sup>K</sup> SHAFT DYNAMICS

DATE

22 SEPT. 1971

WORK ORDER

181(-07-001

BY

L.W. BARTHOLF

CHK. BY

DATE

### RADIAL STIFFNESS AT BEARINGS:

#### STIFF MOUNTED BEARINGS (SUB-CRITICAL OPERATION)

AN ESTIMATE OF BALL BEARING RADIAL STIFFNESS FOR PRELIMINARY DESIGN IS:

$$K_R = .015(10)^6 D_{MM} \quad \text{where: } D_{MM} = \text{BEARING BORE DIAMETER IN MILLIMETERS}$$

THE OOS BEARINGS ARE 15 & 20 MM

$$\therefore K_R = .015(10)^6 (15) = .23(10)^6 \text{ LB/IN/BEARING}$$

$$K_R = .015(10)^6 (20) = .3(10)^6 \text{ LB/IN/BEARING}$$
$$.26(10)^6 \text{ LB/IN/INCH (AVERAGE)}$$

#### SOFT MOUNTED BEARINGS (SUPER-CRITICAL OPERATION)

THE ONLY LIMIT ON SOFTNESS (DEFLECTION LIMITATION DUE TO RUB POTENTIAL, PERFORMANCE LOSS OR OTHER CONSIDERATIONS) ASSOCIATED WITH SHAFT DEFLECTION.

AN ESTIMATED ALLOWABLE STIFFNESS FOR THE SYSTEM IS 10% OF THE BEARING STIFFNESS:

$$K_{R_{\text{soft}}} = .025(10)^6 \text{ LB/IN/BEARING}$$



AERJET-GENERAL CORPORATION  
SACRAMENTO • CALIFORNIA

REPORT NO

PAGE 8 OF 15

DATE  
22 SEPT 1971

WORK ORDER  
1911-07-001

DATE

SUBJECT

00S 10<sup>K</sup> SHAFT DYNAMICS

BY

L.W. BARTHOLF

CHK BY

### ESTIMATE OF WHIRL FORCING FUNCTION

ASSUME CONICAL WHIRL WITH 1 MIL (.001) DIAMETICAL CLEARANCE AT THE CENTER OF THE BEARING SET.

$$P_L = \frac{W}{g} y \quad \text{where: } W = \text{WEIGHT}$$

$$g = 386 \text{ IN/SEC}^2$$

$$y = \text{DISTANCE FROM BEARING 1 TO MASS CENTER}$$

$$y = CL$$

$$.0005 = C (1.15)$$

$$C = 435 (10)^{-6}$$

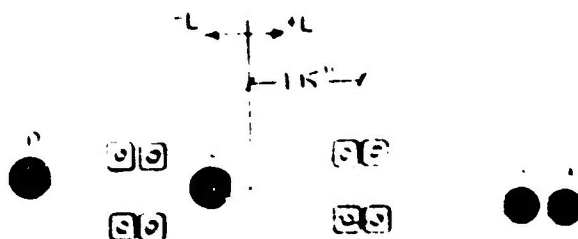
$$P_L = \frac{435 (10)^{-6}}{386} WL = 1.13 (10)^{-6} WL$$

$$P_{L_A} = 1.13 (10)^{-6} (43) (5.1) = 1.5 (10)^{-6}$$

$$P_{L_B} = 1.13 (10)^{-6} (43) (2.5) = .1 (10)^{-6}$$

$$P_{L_C} = 1.13 (10)^{-6} (17) (-3.5) = -.4 (10)^{-6}$$

$$P_{L_D} = 1.13 (10)^{-6} (12) (-2.35) = -.24 (10)^{-6}$$





AEROJET-GENERAL CORPORATION  
SACRAMENTO • CALIFORNIA

FORM 100-11

REPORT NO.

PAGE 9 OF 15

SUBJECT

OOS 10<sup>k</sup> SHAFT DYNAMICS

DATE

22 SEPT 1971

WORK ORDER

1911-07-001

BY

L.W. BARTHOLF

CHK BY

DATE

OOS 10<sup>k</sup> FTPA CRITICAL SPEED MODEL (CONCEPT II INBOARD BEARS)

$$E_{\text{STEEL}} = 29 (10)^6 \text{ PSI}$$

$$J_{\text{EFF}} = \frac{WR^2}{4g} \text{ LB-IN-SEC}^2$$

STATION	L(IN)	EI	W(LB)	J <sub>EFF</sub>	K	C	G	PI	PC	PS
701	.10	55 (10) <sup>5</sup>	.43	5 (10) <sup>4</sup>	0	2	11 (10) <sup>6</sup>	1.5 (10) <sup>7</sup>	0	0
702	.29	55 (10) <sup>5</sup>	0	0	0	↑	↑	0	↑	↑
703	.26	55 (10) <sup>5</sup>	.43	5 (10) <sup>4</sup>	0	↑	↑	1 (10) <sup>5</sup>	↑	↑
704	.60	55 (10) <sup>5</sup>	.48	0	0	↑	↑	0	↑	↑
705	.22	40 (10) <sup>5</sup>	0	0	0	↑	↑	0	↑	↑
706	.31	7 (10) <sup>5</sup>	.10	0	K	↑	↑	0	↑	↑
707	.23	7 (10) <sup>5</sup>	.10	0	0	↑	↑	0	↑	↑
708	.23	7 (10) <sup>5</sup>	.10	0	K	↑	↑	0	↑	↑
709	.19	7 (10) <sup>5</sup>	.10	0	0	↑	↑	0	↑	↑
710	.68	11 (10) <sup>5</sup>	0	0	0	↑	↑	0	↑	↑
711	.34	32 (10) <sup>5</sup>	.97	20 (10) <sup>4</sup>	0	↑	↑	-4 (10) <sup>5</sup>	↑	↑
712	.36	32 (10) <sup>5</sup>	0	0	0	↑	↑	0	↑	↑
713	.27	3 (10) <sup>5</sup>	.05	0	K	↑	↑	0	↑	↑
714	.22	3 (10) <sup>5</sup>	.05	0	0	↑	↑	0	↑	↑
715	.23	3 (10) <sup>5</sup>	.05	0	K	↑	↑	0	↑	↑
716	.32	3 (10) <sup>5</sup>	.05	0	0	↑	↑	0	↑	↑
717	.36	3 (10) <sup>5</sup>	0	0	0	↑	↑	0	↑	↑
718	.30	17 (10) <sup>5</sup>	.92	20 (10) <sup>4</sup>	0	↑	↑	-2.4 (10) <sup>5</sup>	↑	↑
719	.34	17 (10) <sup>5</sup>	.10	0	0	↑	↑	0	↑	↑
720	.61	8.7 (10) <sup>5</sup>	.10	0	0	↓	↓	0	↓	↓
721	.40	24 (10) <sup>5</sup>	.10	0	0	↓	↓	0	↓	↓
722	.55	24 (10) <sup>5</sup>	.10	0	0	2	11 (10) <sup>6</sup>	0	0	0



AEROJET-GENERAL CORPORATION  
SACRAMENTO CALIFORNIA

REPORT NO.

PAGE 10 OF 15

ALCS 000011

SUBJECT

OOS 10<sup>K</sup> SHAFT DYNAMICS

DATE

23 SEPT. 1971

WORK ORDER

1911-07-001

DATE

BY

L.W. BARTHOLF

CHK. BY

OOS 10<sup>K</sup> FTPA CRITICAL SPEED MODEL (CONCEPT II OUTBOARD BRGS)

$$E_{\text{STEEL}} = 29(10)^6 \text{ LB/IN}^2$$

$$J_{\text{EFF}} = \frac{WR^2}{4g} \quad \text{LB-IN-SEC}^2$$

STATION	U(IN)	EI	W(LB)	J <sub>EFF</sub>	K	C	G	P1	P2	P3
701 ↑ 712	SAME AS CONCEPT VI									
713	.63	64 (10) <sup>5</sup>	.4	0	0	2	11 (10) <sup>6</sup>	0	0	0
714	.57	64 (10) <sup>5</sup>	0	0	0	↑	↑	0	↑	↑
715	.27	125 (10) <sup>5</sup>	.75	20 (10) <sup>4</sup>	0	↑	↑	0	↑	↑
716	.32	125 (10) <sup>5</sup>	0	0	0	↑	↑	0	↑	↑
717	.56	3 (10) <sup>5</sup>	.1	0	K	↑	↑	0	↑	↑
718	.23	3 (10) <sup>5</sup>	.1	0	0	↑	↑	0	↑	↑
719	.25	3 (10) <sup>5</sup>	.1	0	K	↑	↑	0	↑	↑
720	.50	3 (10) <sup>5</sup>	.1	0	0	↑	↑	0	↑	↑
721	.54	3 (10) <sup>5</sup>	.2	0	0	↑	↑	0	↑	↑
722	.70	3 (10) <sup>5</sup>	.1	0	0	↓	↓	0	↓	↓
723	.50	1 (10) <sup>5</sup>	.1	0	0	2	11 (10) <sup>6</sup>	0	0	0





SUBJECT

OOS 10<sup>k</sup> SHAFT DYNAMICS

DATE

23 Sept. 1971

WORK ORDER

1511-07-001

BY

L.W. BARTHOLF

CHK. BY

DATE

OOS 10<sup>k</sup> OSPA CRITICAL SPEED MODEL (CONCEPT I, TWO STAGE PUMP)

$$E_{\text{STEEL}} = 29(10)^6 \text{ PSI}$$

$$J_{\text{EFF}} = \frac{WP^2}{4g} \quad \text{LB-IN-SEC}^2$$

STATION	L (in)	EI	W (LB)	J <sub>EFF</sub>	K	C	G	P1	P2	P3
701	.20	55 (10) <sup>5</sup>	.75	.002	0	2	11 (10) <sup>6</sup>	2 (10) <sup>6</sup>	0	0
702	.56	55 (10) <sup>5</sup>	.43	0	0	↑	↑	0	↑	↑
703	.20	35 (10) <sup>5</sup>	.10	0	0	↑	↑	↑	↑	↑
704	.32	7 (10) <sup>5</sup>	.10	0	0	↑	↑	↑	↑	↑
705	.22	7 (10) <sup>5</sup>	.10	0	0	↑	↑	↑	↑	↑
706	.24	7 (10) <sup>5</sup>	.10	0	0	↑	↑	↑	↑	↑
707	.52	7 (10) <sup>5</sup>	.10	0	0	↑	↑	↑	↑	↑
708	.58	7 (10) <sup>5</sup>	.14	0	0	↑	↑	↑	↑	↑
709	.66	7 (10) <sup>5</sup>	.14	0	0	↑	↑	↑	↑	↑
710	.76	7 (10) <sup>5</sup>	.18	0	0	↑	↑	↑	↑	↑
711	.29	4 (10) <sup>5</sup>	.10	0	0	↑	↑	↑	↑	↑
712	.79	4 (10) <sup>5</sup>	.10	0	0	↑	↑	↑	↑	↑
713	.25	4 (10) <sup>5</sup>	.10	0	0	↑	↑	↑	↑	↑
714	.26	4 (10) <sup>5</sup>	.10	0	0	↑	↑	↑	↑	↑
715	.27	4 (10) <sup>5</sup>	0	0	0	↑	↑	↑	↑	↑
716	.30	4 (10) <sup>5</sup>	.10	0	0	↑	↑	↑	↑	↑
717	.26	26 (10) <sup>5</sup>	.20	0	0	↑	↑	↑	↑	↑
718	.16	26 (10) <sup>5</sup>	.10	0	0	↑	↑	↑	↑	↑
719	.46	29 (10) <sup>5</sup>	.10	0	0	↑	↑	↑	↑	↑
720	.43	29 (10) <sup>5</sup>	.10	0	0	↑	↑	↑	↑	↑
721	.35	29 (10) <sup>5</sup>	.10	0	0	2	11 (10) <sup>6</sup>	0	0	0

# STIFFNESS MODELS

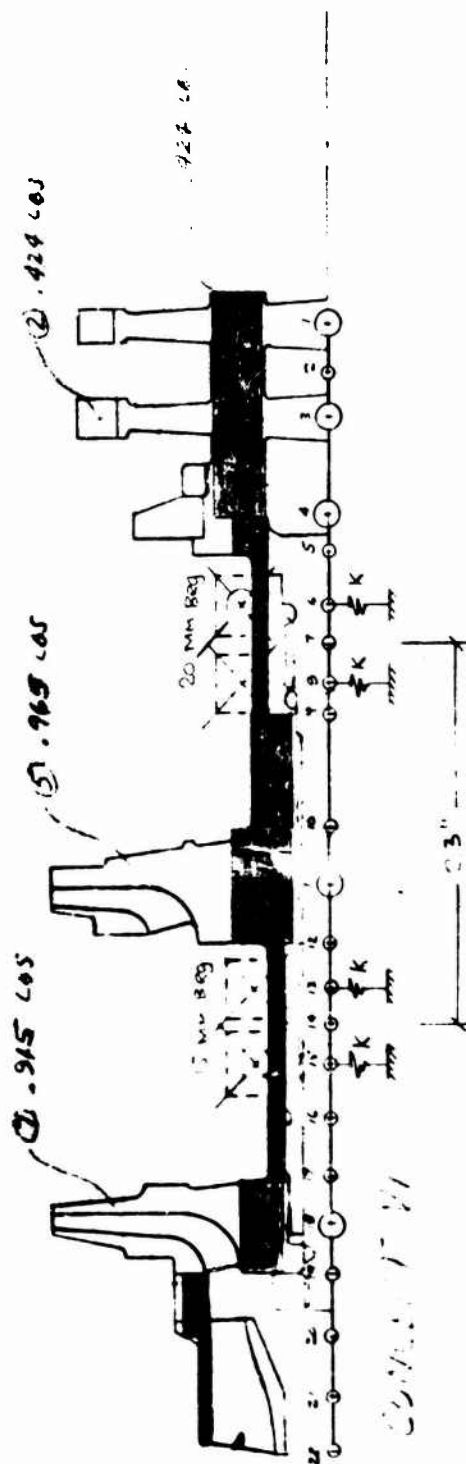
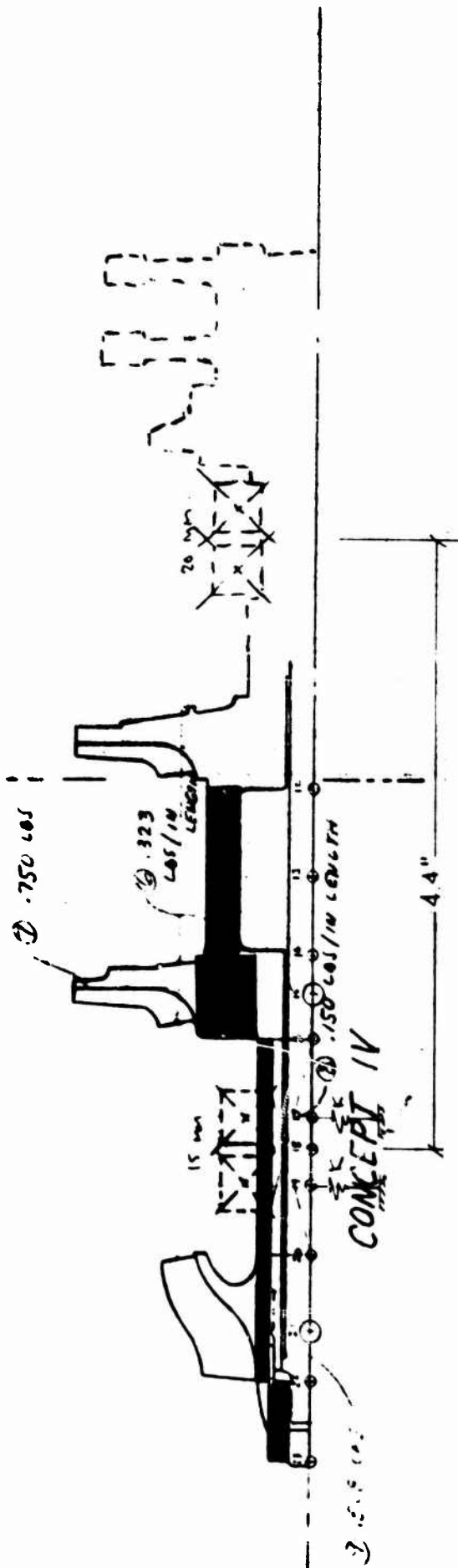
## 005 10K FUEL TURBOPUMP ROTATING WEIGHTS

(ASSUMING ALL STEEL)

W.O. 1811-07-001

$N = 100,000$  RPM

→ SAME AS CONCEPT VI



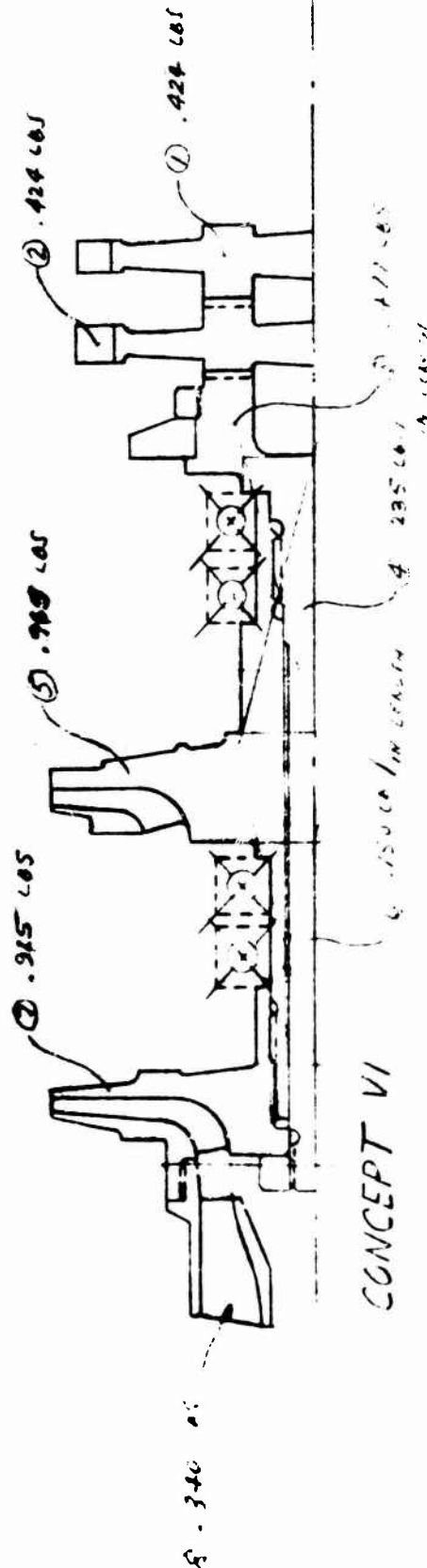
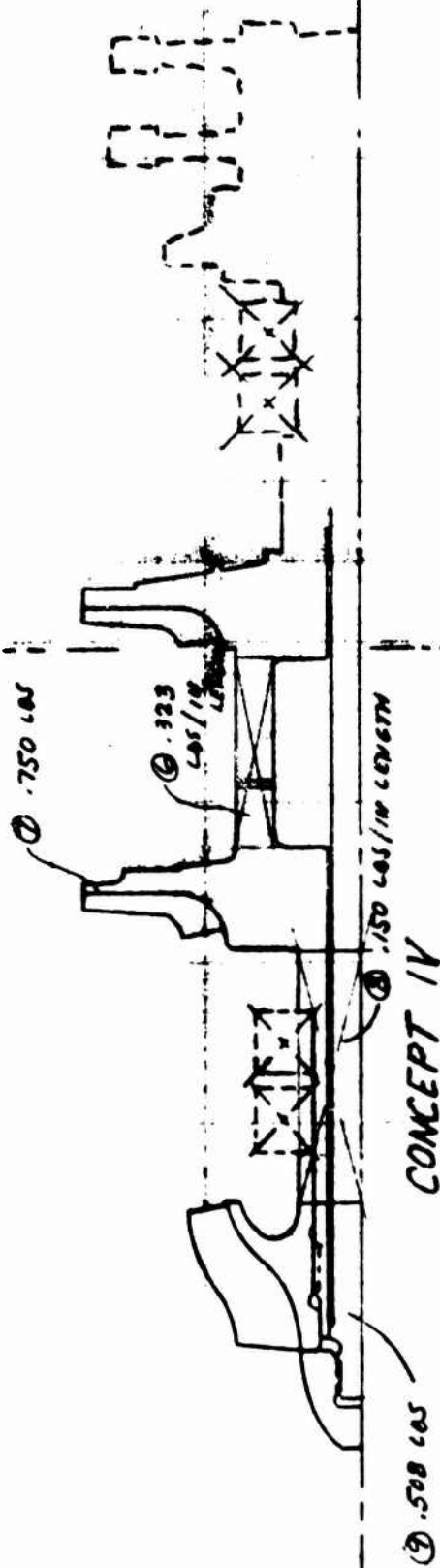
# 005. 10K FUEL TURBOPUMP ROTATING WEIGHTS

(ASSUMING A44 STEEL)

W.O. 1811-07-001

N = 100,000 RPM

— SAME AS CONCEPT III

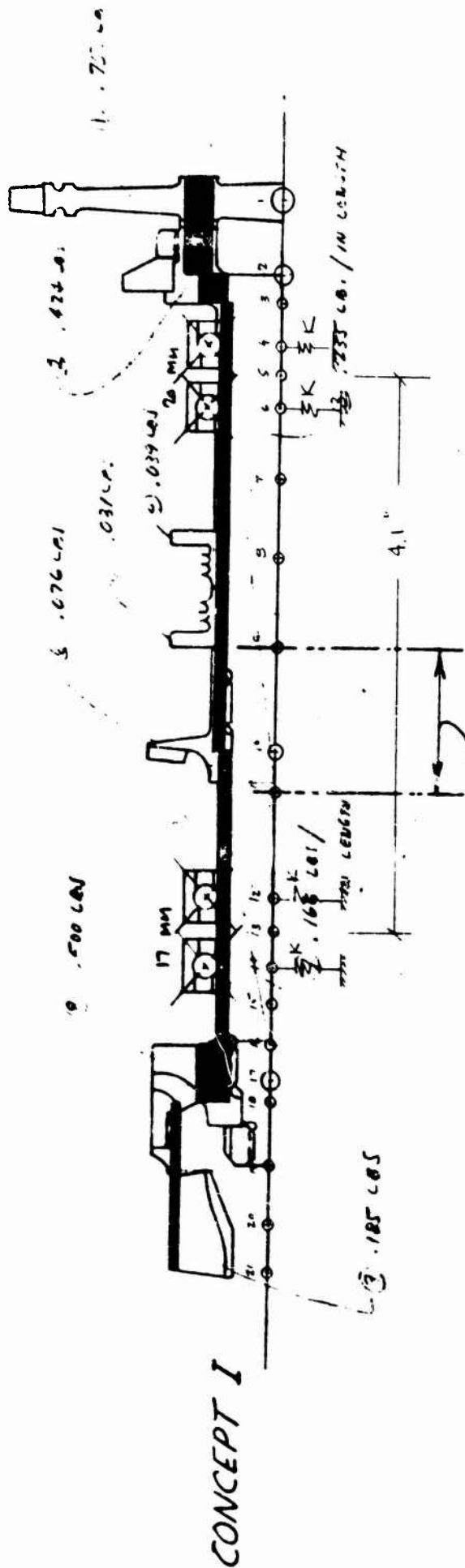


# STIFFNESS MODEL

005 10K OXID TURBOPUMP ROTATING WEIGHTS

(ASSUMING ALL STEEL)

N = 63000 RPM

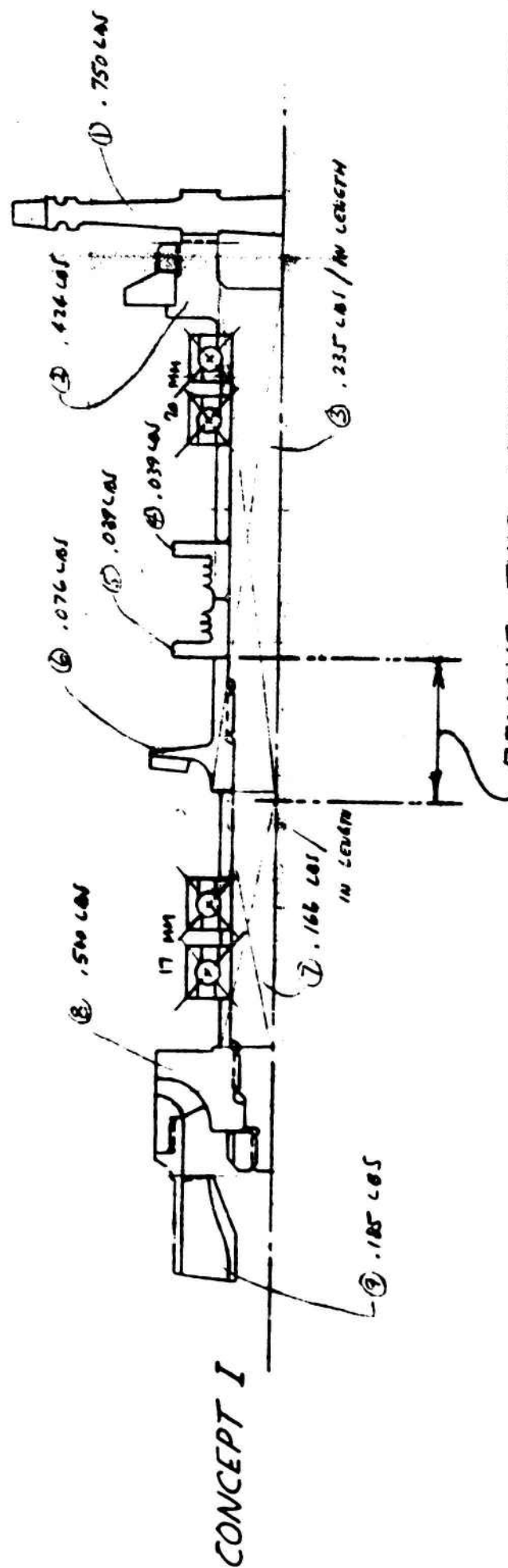


REMOVE THIS LENGTH FOR CONCEPT II

005 10K OXID TURBOPUMP ROTATING WEIGHTS

(ASSUMING ALL STEEL)

N = 63000 RPM



REMOVE THIS LENGTH FOR CONCEPT II

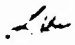
OOS COPPER CHAMBER LIFE ESTIMATES WITH  
A COMPARISON OF ZIRCONIUM COPPER AND  
NARLOY LCF STRENGTHS IN AIR AND AN INERT  
ENVIRONMENT

# STRUCTURAL ENGINEERING


REPORT NO. SA-OOS-CC-05

OOS COPPER CHAMBER LIFE ESTIMATES WITH  
A COMPARISON OF ZIRCONIUM COPPER AND NARLOY  
LCF STRENGTHS IN AIR AND AN INERT ENVIRONMENT

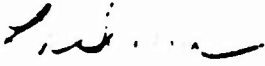
PREPARED BY:

  
L. K. Severud  
Analysis Section  
Design and Analysis Department

PREPARED BY:

  
L. W. Bartholf  
Analysis Section  
Design and Analysis Department

APPROVED BY:

  
L. K. Severud  
Analysis Section  
Design and Analysis Department

DATE 17 September 1971



AEROJET LIQUID ROCKET COMPANY

SACRAMENTO, CALIFORNIA

## TABLE OF CONTENTS

	<u>Page</u>
I. Introduction	1
II. Summary	2
III. Discussion	2
IV. Conclusions	4
V. Analysis	4
VI. Appendix	5
VII. References	6

## LIST OF FIGURES

<u>Figure</u>	<u>Title</u>	<u>Page</u>
1	ALRC Low Cycle Fatigue Experimental Results, $\Delta\epsilon_t = 2\%$	7
2	Rocketdyne, NAR Data	8
3	Life Estimates for OOS Chamber Made of Zirconium Copper	9
4	Life Estimates for OOS Chamber Made of Silver Zirconium Copper	10
5	Rocketdyne, NAR Test Schematic	11
6	Effect of Vacuum on High Temperature LCF	12
7	Effects of Vacuum (Non-Oxidizing) on High Temp. LCF	13
8	NAR Narloy and ALRC Zirconium Copper LCF Life (No Hold Time)	14
9	Comparison of NARloy and Zirconium Copper per NAR Test Data at 500°F in an Inert Environment	15
10	Zirconium Copper LCF Life	16
11	AG-ZR-CU and NARloy LCF Life	17
12	Variation of Life with Temperature for Copper Alloys (No Hold Time)	18
13	Comparison of LCF at Elevated Temperatures	19
14	LCF Trends for NARloy in Inert Environment	20
15	LCF Trends for Zirconium Copper in Inert Environment	21
16	Copper Material Properties	22



## I. INTRODUCTION

This report presents thermal fatigue life estimates for the OOS chamber considering whether it is made of silver zirconium copper or zirconium copper material. Low cycle fatigue specimen test data for the two copper alloys has been obtained from two independent sources; (1) an ALRC Space Shuttle IR&D test program and (2) an NAR, Rocketdyne contract with AFRPL (F04611-70-C-C-0014). The copper designated AG-ZR-CU is an ALRC equivalent of the North American Rockwell (NAR) Narloy.

During the Phase B ALRC Space Shuttle effort low cycle fatigue tests on various copper alloys indicated (Reference 1) as shown in Figure 1 that the zirconium copper is the superior alloy relative to the silver-zirconium or Boron deoxidized copper. Subsequently, the Rocketdyne work under contract to AFRPL (Reference 2) seemed to indicate as shown in Figure 2 that NARloy, a silver-zirconium copper, is the best fatigue resistant copper alloy. Recent investigation regarding these tests revealed that Rocketdyne's tests were run in an inert and non-oxidizing environment whereas ALRC tests were in air. Tests run in an inert environment at the Naval Research Laboratory, the General Electric Corporate Research and Development Laboratory, and the Oak Ridge National Laboratory, show significantly for a variety of structural metals a one to two order of magnitude increase in fatigue life over those of tests run in air where oxidation is taking place. Accordingly, the data presented herein is classified as to whether the environment is inert or not (i.e., Air).

The report first summarizes the estimated thermal fatigue life for the OOS chamber for various design parameters such as wall maximum metal temperature ( $T_{WG}$ ), thermal gradient ( $T_{WG} - T_{Bulk}$ ), copper alloy, and environment (air or inert). The remainder of the report pertains primarily to the analysis of the copper alloy material specimen fatigue test data and the method of estimating chamber life.

## II. SUMMARY OF RESULTS

Figures 3 and 4 present estimated thermal fatigue lives of the chamber in terms of the coolant design parameters.

## III. DISCUSSION

The first indication that the Rocketdyne tests were run in an inert environment occurred recently when it was noted upon review of their progress report (Reference 2) that their test assembly schematic, Figure 5, showed an argon purge vent. A subsequent telecon with Don Penn of AFRPL confirmed that indeed Rocketdyne's tests were in an inert environment. No mention of the test environment exists in the progress report.

Oxidation at high temperatures and even at room temperature has been found to greatly reduce fatigue life of metals tested in air relative to that of inert environment tests (References 3 and 4). Figures 6 and 7 show these effects comparing vacuum and air test results for A-286, cast Udimet 500 and high-purity nickel. Notice that zirconium copper air tested LCF life trend depicted in Figure 8 is very similar to the A-286 vacuum vs air trends in Figure 6.

In order to eliminate the test environment from the assessment as to which is the superior fatigue resistant material, both the NARloy and Zirconium copper test data for 500°F in an inert environment is presented in Figure 9. This figure shows that considering the limited data points and the scatter typical of such test data no conclusive decision regarding superiority can be made. The materials appear to be equally fatigue resistant.

The environmental effect on fatigue strengths of zirconium copper and silver-zirconium copper (NARloy) in the low cycle life range is shown in Figures 10 and 11. The differences in life are again pronounced in a fashion similar to that shown in Figure 6 for A-286.

For a given cyclic strain range the inert environment tests showed the fatigue life to be a function of temperature as shown in Figure 12. The trend of increased life with increased temperature may be explained as due to the associated reduction in yield strength (see Figure 16) and hysteresis energy described in Figure 13. The ductility as measured by reduction in area (i.e., R.A.) in elevated temperature tensile tests does not change over the temperature range where life is increasing and thus it does not explain increase life observed. Many technical papers such as References 5 through 8 have been written that correlate fatigue life to the hysteresis energy.

Through a recent telecon with Don Penn (Reference 9) of AFRPL additional fatigue data for various temperatures were obtained. Based on these data and those earlier reported in Reference 2 the plots of Figures 14 and 15 were developed. It is not uncommon to find that at the higher temperatures a plot of fatigue life versus temperature on a semi-log scale results in almost straight lines like those from 700°F to 1200°F in Figures 14 and 15. ALRC tests on ARMCO 22-13-5 and A-286 and G.E. tests on CRES 304 yielded similar trends. A plausible reason for such behavior could be that at this temperature range a significant amount of creep damage is occurring.

In summary, the general increase in life due to an inert environment could be explained in terms of the absence of oxidation. The increase in life from room temperature to 700 or 800°F may be due to the reduced hysteresis energy developed due to the lowering of the material yield strength, and the reduction in life from 800°F to higher temperatures could be due to increasing degrees of creep damage. Clearly, more test data is necessary to establish the design data necessary to chamber design. Also, the questions of what is the chamber operating environment and how close is it to the inert or air environment regarding effects on fatigue life have to be answered.

#### IV. CONCLUSIONS

- Copper chamber fatigue life estimates relative to metal temperature and gradients have been accomplished.
- A comparison of zirconium copper and silver-zirconium copper alloys regarding low cycle fatigue strengths has been made. The apparent differences in ALRC and Rocketdyne test data were attributed to the differences in test environment. ALRC tested in air whereas Rocketdyne tested in an inert environment. A comparison of zirconium copper and NARloy using 500°F inert environment test data for both shows no superiority in either material can be deduced due to the limited data points and typical data scatter.
- Test environment can have great effects on fatigue strengths and cyclic life. A non-oxidizing environment can easily increase the cyclic life by one to two orders of magnitude.
- Further material fatigue specimen data are necessary to establish optimum copper alloy choice and chamber design conditions.

#### V. RECOMMENDATIONS

A new fatigue test program for copper alloy fatigue properties should be undertaken prior to further detailed design of the OOS engine. This program should be directed toward better defining the strain, temperature, life relationships that were estimated in Figures 14 and 15 of this report. Also, perhaps some Boron De-oxidized copper alloy in addition to zirconium and Narloy alloys should be tested in an inert environment if the inert environment regarding fatigue is deemed closest to the chamber operating environment. A ROM cost of such a program is about \$75,000 based on previous test costs.



AERJET-GENERAL CORPORATION  
SACRAMENTO CALIFORNIA

REPORT NO

PAGE OF

OF

DATE  
9/16/71

WORK ORDER

ORDER

DATE

CHK BY

COPPER CHAMBER ANALYSIS

WATKINS & LKSEVERUD

LCF IN COPPER CHAMBER (NO HOLD TIMES)

$$\Delta E_t = 2 \alpha \Delta T$$

$$\Delta T = T_{wg} - T_{bulk}$$

CYCLES TO FAILURE,  $N_f$

$\Delta T$ (°F)	$T_{wg}$ (°F)	$\alpha$ (IN/IN/°F)	$\Delta E_t$ (%)	IN AIR	INERT	IN AIR	INERT
				AG-ZR-Cu	NAR NARLOY	ZR-Cu	LR-Cu
500	1000	10.4 (10) <sup>-6</sup>	1.25	1800	9000	1240	3700
	900	10.2 "	1.22	1900	12000	1270	5000
	800	10.1 "	1.21	1950	17000	1300	7100
	700	9.9 "	1.19	2050	22000	1330	9700
	600	9.8 "	1.18	2100	22000	1370	10100
	500	9.7 "	1.16	2200	18000	1400	8700
700	1000	SAME AS ABOVE	1.67	900	4000	750	1700
	900		1.63	950	5300	770	2300
	800		1.61	990	7000	790	3200
	700		1.59	1020	8500	810	3900
	600		1.57	1060	9000	830	4000
	500		1.55	1100	7000	850	3200
1000	1000	SAME AS ABOVE	2.03	540	2600	520	900
	900		2.04	560	3300	530	1200
	800		2.02	580	4200	540	1700
	700		1.98	600	4800	550	2200
	600		1.96	620	4700	560	2300
	500		1.94	640	3900	570	1700
1200	1000	SAME AS ABOVE	2.50	340	1000	370	480
	900		2.44	350	1150	380	550
	800		2.42	360	1400	390	650
	700		2.37	365	1700	400	800
	600		2.35	370	1900	405	850
	500		2.33	375	1650	410	600
1400	1000	SAME AS ABOVE	2.91	230	580	290	710
	900		2.86	240	700	295	350
	800		2.83	250	820	300	410
	700		2.77	260	1000	305	500
	600		2.74	270	1150	310	600
	500		2.71	280	1000	320	500

VII. REFERENCES

1. "Space Shuttle Main Engine Definition Study Phase B Data," AJ 550 Materials Technology Programs, DRDSE-278, Part B, NASA Contract No. NAS8-26188, Aerojet Liquid Rocket Company, Sacramento, California, 95813. 21 April 1971.
2. Rocketdyne Report R-8177-14, Monthly Report on Investigation of Thermal Fatigue in Non-Tubular Regeneratively Cooled Thrust Chambers (FO4611-70-C-0014), dated 27 April 1971.
3. Coffin, L. F., Jr., The Effect of Vacuum on the High-Temperature, Low-Cycle Fatigue Behavior of Structural Metals, General Electric Co., Report 71-C-108, April, 1971.
4. Stegman, R. L., and Shahinian, P., "Effect of Temperature on the Fatigue of Nickel at Varying Oxygen Pressures" ASTM STP-459, 1969.
5. Pimbley, W. T., and Ku, T. C., "Design for Fatigue Based on Energy Concept," ASME Publication, April 1968.
6. Feltner, C. E., and Morrow, Jo Dean, "Microplastics Strain Hysteresis Energy as a Criterion for Fatigue Fracture," Journal of Basic Engineering, Trans. ASME, vol. 83 Series D, 1961, pp. 15-22.
7. Martin, D. E., "An Energy Criterion for Low-Cycle Fatigue," Journal of Basic Engineering, Trans. ASME, vol. 83 Series D, 1961, pp. 565-571.
8. Halford, G. R., "The Energy Required for Fatigue," Journal of Materials, vol. 1, No. 1, March 1966, pp. 3-18.
9. Janser, G. R., "Material Design Property Data Sheets," ME-70-164, Aerojet Liquid Rocket Company, Sacramento, California 95813, 1 September 1970.

FIGURE 1

AIRC LOW CYCLE FATIGUE EXPERIMENTAL RESULTS,  $\Delta \epsilon_t = 2\%$

MATERIAL TESTED AT 1000°F IN AIR	CYCLES TO FAILURE	
	NO HOLD TIME	400-SEC COMP. HOLD
BORON DEOX COPPER - FINE GRAIN	981, 1382	369, 528
BORON DEOX COPPER - COARSE GRAIN	901, 1194	513, 560
ZIRCONIUM COPPER - AS BRAZED	623, 624	647, 986
ZIRCONIUM COPPER - HEAT TREAT + AGED	650, 1045	610, 676
SILVER-ZIRCONIUM COPPER - AS BRAZED	618	331
SILVER-ZIRCONIUM COPPER - HEAT TREATED	594	221



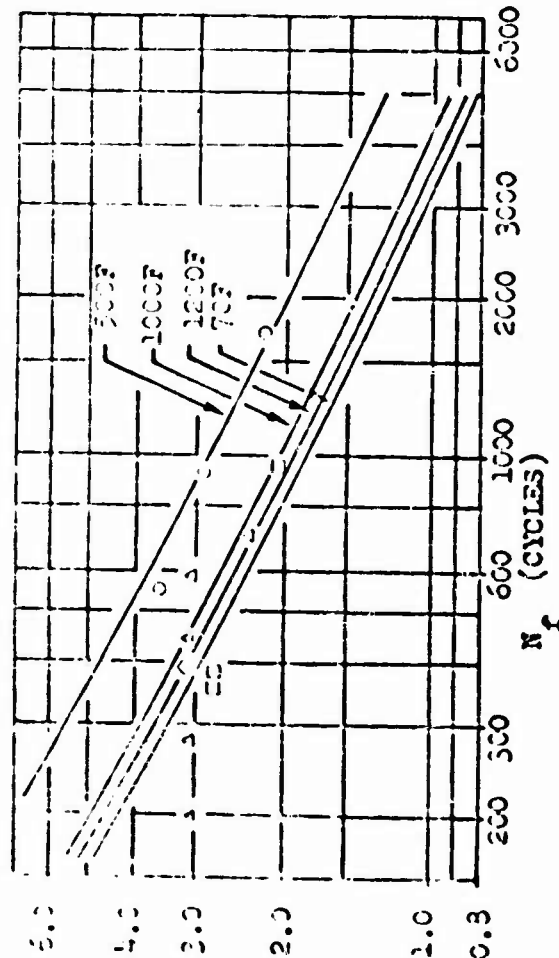
**AEROJET LIQUID ROCKET COMPANY**

SACRAMENTO, CALIFORNIA • A DIVISION OF AEROSPACE GENERAL

# ROCKETDYNE, NAR DATA

REWORKED COPPER

Alloy-2



## LEGEND

SOLID SYMBOLS  $\dot{\epsilon} = .01$  IN/IN/SEC

OPEN SYMBOLS  $\dot{\epsilon} = .1$  IN/IN/SEC

○ 700F

□ 1200F

△ 1800F

◇ 5000F

EFFECTIVE CYCLIC STRAIN RANGE

VS.

CYCLES TO FAILURE

P-8177-14

MONTHLY REPORT ON  
INVESTIGATION OF THERMAL FATIGUE IN  
NON-TUBULAR REGENERATIVELY COOLED  
THRUST CHAMBERS (FO4611-70-C-0014)  
PERIOD ENDING 15 APRIL 1971

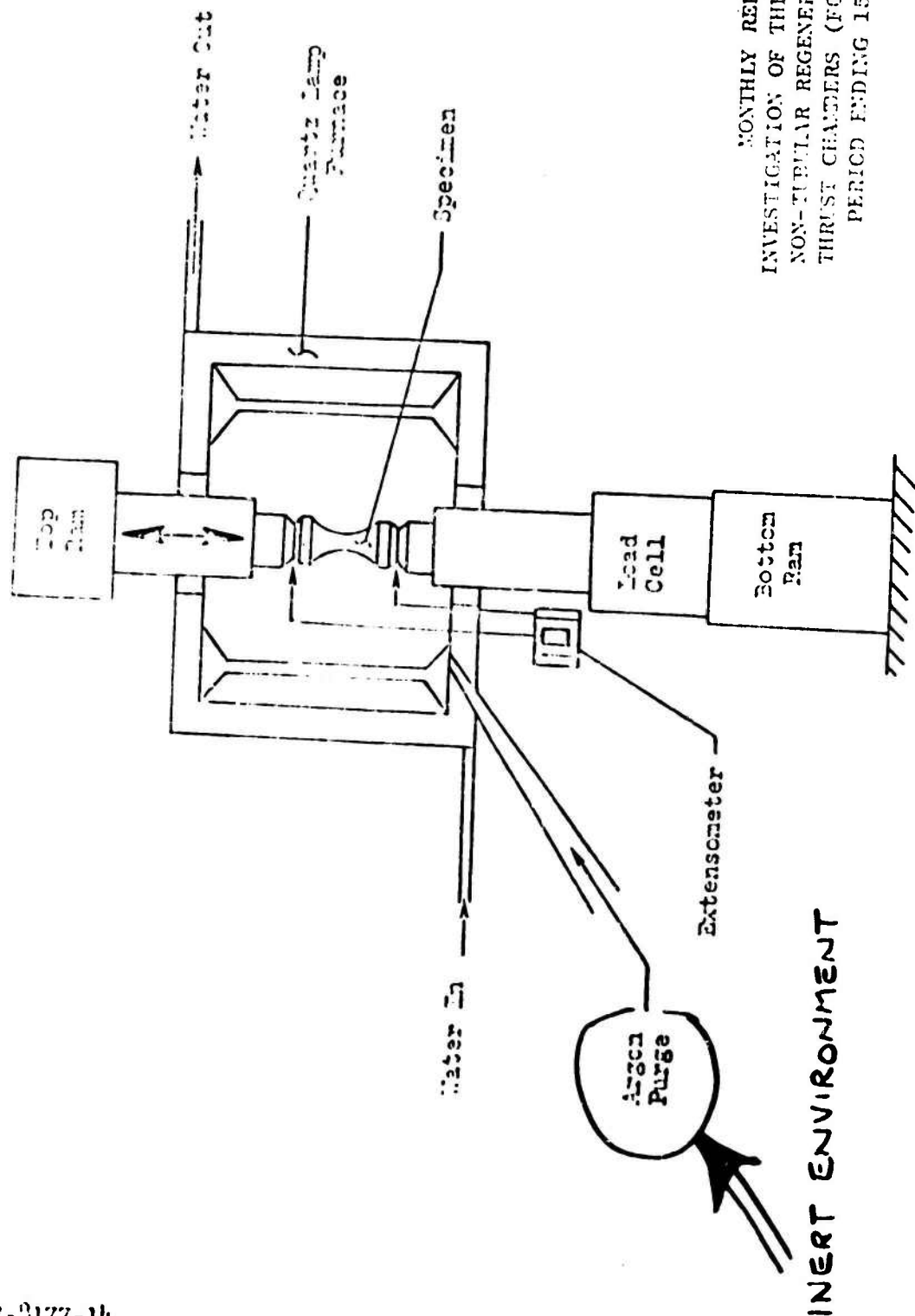
FIGURE 8. ISOTHERMAL FATIGUE TEST DATA



# ROCKETDYNE, NAR TEST SCHEMATIC

FIGURE 3

R-8177-14



R-8177-14

MONTHLY REPORT ON  
INVESTIGATION OF THERMAL FATIGUE IN  
NON-TUBULAR REGENERATIVELY COOLED  
THRUST CHAMBERS (F04611-70-C-0014)  
PERIOD ENDING 15 APRIL 1971

FIGURE 5. SCHEMATIC OF TEST ASSEMBLY



AEROJET-GENERAL CORPORATION  
SACRAMENTO • CALIFORNIA

REPORT NO

PAGE

OF

DATE

WORK ORDER

CHK BY

DATE

## FIGURE 6

### EFFECT OF VACUUM ON HIGH TEMPERATURE LCF (INERT ENVIRONMENT)

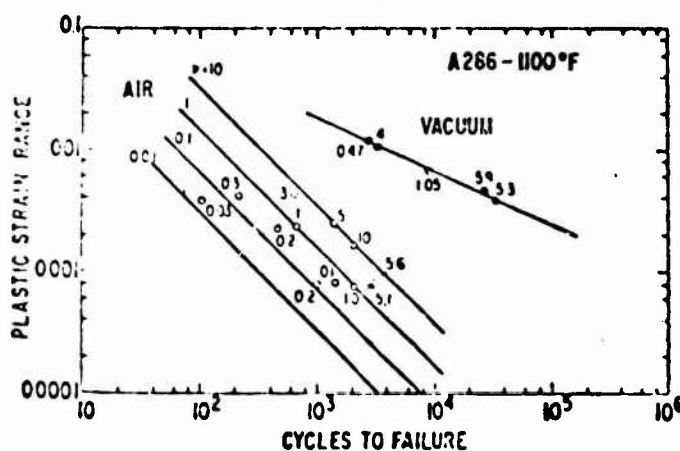


Fig. 4 Plastic strain range vs fatigue life for A286 in air and vacuum at 1100°F. Numbers adjacent to test points indicate frequency in cpm. Solid lines are regression analysis of Eq. (3).

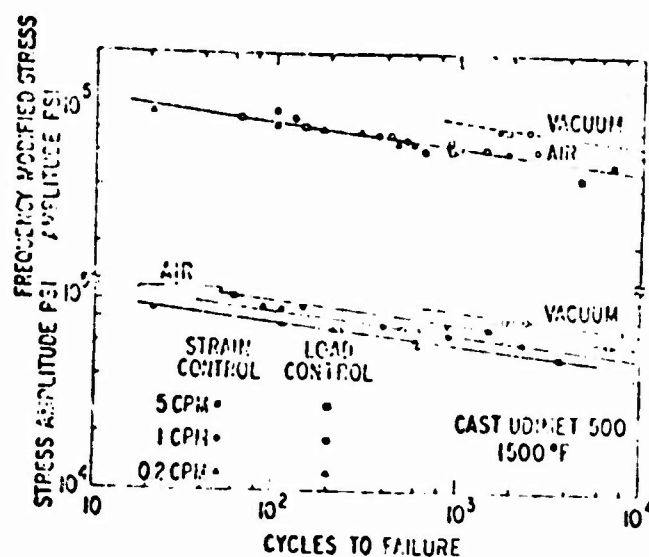


Fig. 6 Test results of stress amplitude vs fatigue life for cast Udmet 500 in air and vacuum at 1500°F (lower curve). Air tests both stress and strain control; vacuum tests stress control only. Frequency-modified stress amplitude vs fatigue life for same test results, after Eq. (10) (upper curve).

#### REFERENCE

COFFIN L.F. THE EFFECT OF VACUUM ON THE HIGH TEMPERATURE, LOW CYCLE FATIGUE BEHAVIOR OF STRUCTURAL METALS G.E. REPORT NO. TR-C-108 APRIL 1971



# FIGURE 7 EFFECTS OF VACUUM (NON-OXIDIZING) ON HIGH TEMP. L.C.F.

NICKEL

FATIGUE AT HIGH TEMPERATURE

FATIGUE AT HIGH TEMPERATURE

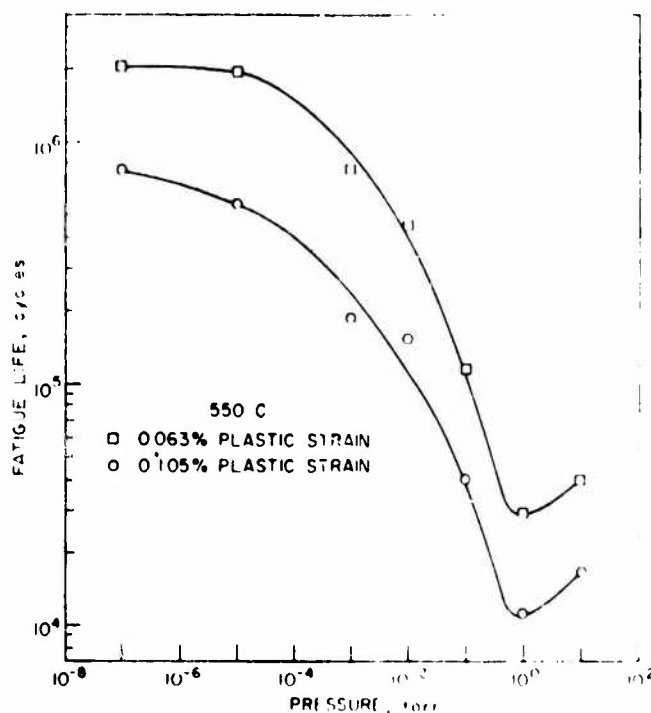
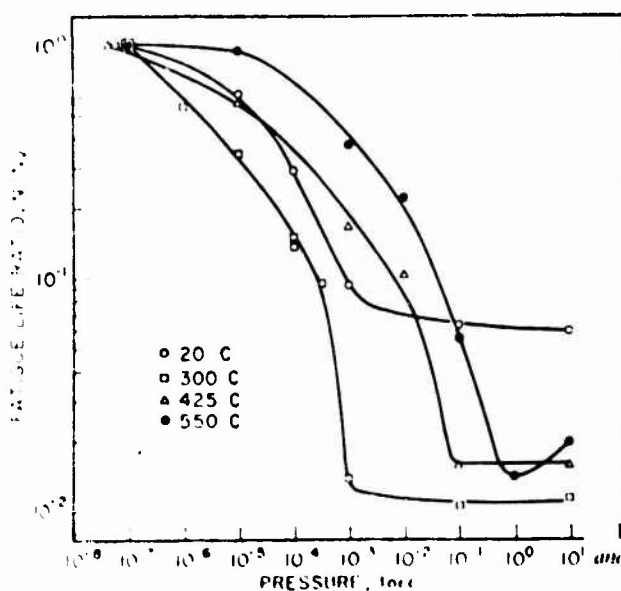


FIG. 3 - Fatigue life plotted as a function of oxygen pressure for plastic strains of 0.063 and 0.105 percent at 550 C.

FIG. 1 - Rate of fatigue life in oxygen to the life at the ultimate vacuum,  $N/N_v$ , plotted as a function of oxygen pressure at 20, 300, 425, and 550 C.

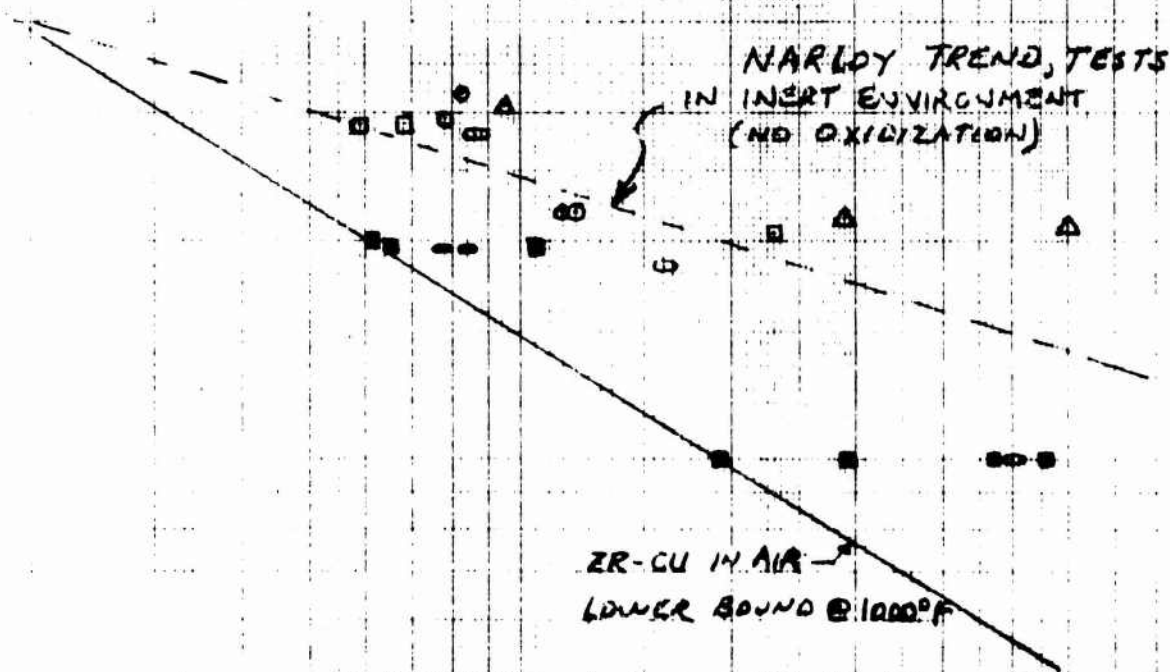
REFERENCE: ASTM STP 459, FATIGUE AT HIGH TEMPERATURE, 1969

107700 STRAIN RANGE,  $\Delta\epsilon$ , %

FIGURE 8 - NARLOY AND ALKZ ZIRCONIUM COPPER LCF LIFE

(NO HOLD TIME)

REF: L2FA



LEGEND:

NARLOY (NAK)

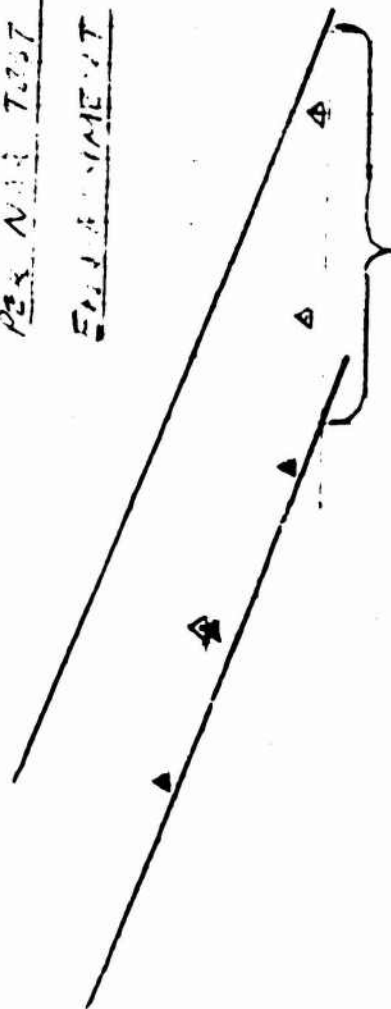
- - RT
- △ - 520°F
- - 1000°F
- ◇ - 1200°F

ZR-CU (ALKZ)

- - 1000°F
- - 1100°F

CYCLES TO FAILURE,  $N_f$

FIGURE 9 - COMPARISON OF NARLOY AND ZIRCONIUM  
PER NAR TEST DATA AT 500°F IN INERT  
ENVIRONMENT



TYPICAL MAGNITUDE OF DATA  
SCATTER IS A FACTOR OF  
4 TO 5.

LEGEND: IN INERT ENVIRONMENT  
OPEN Δ - NARLOY PER NAR @ 500°F  
CLOSED Δ - ZR-CU PER NAR @ 500°F

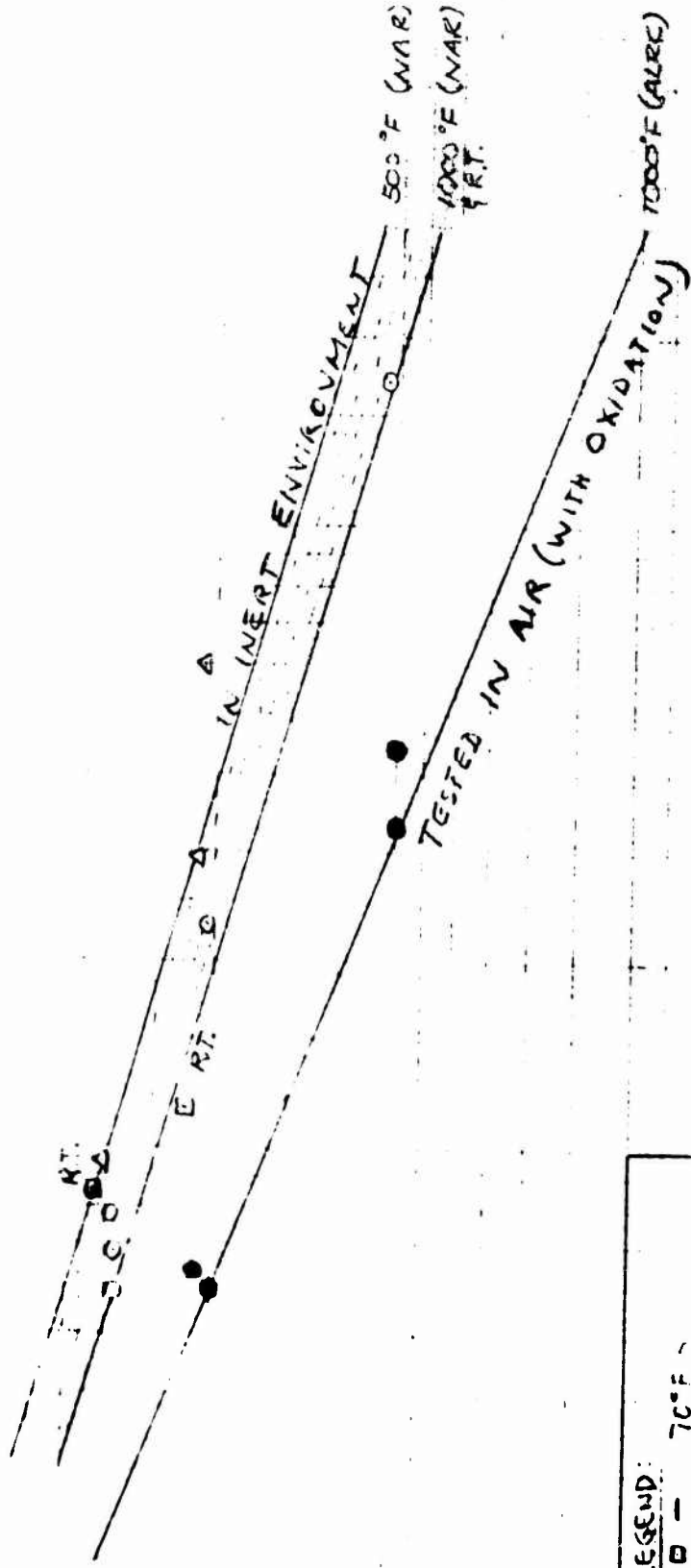
10-21-1941



CYCLES TO FAILURE 12

Figure 1 - Life

(NO HOLD TIME)  
RT: 180

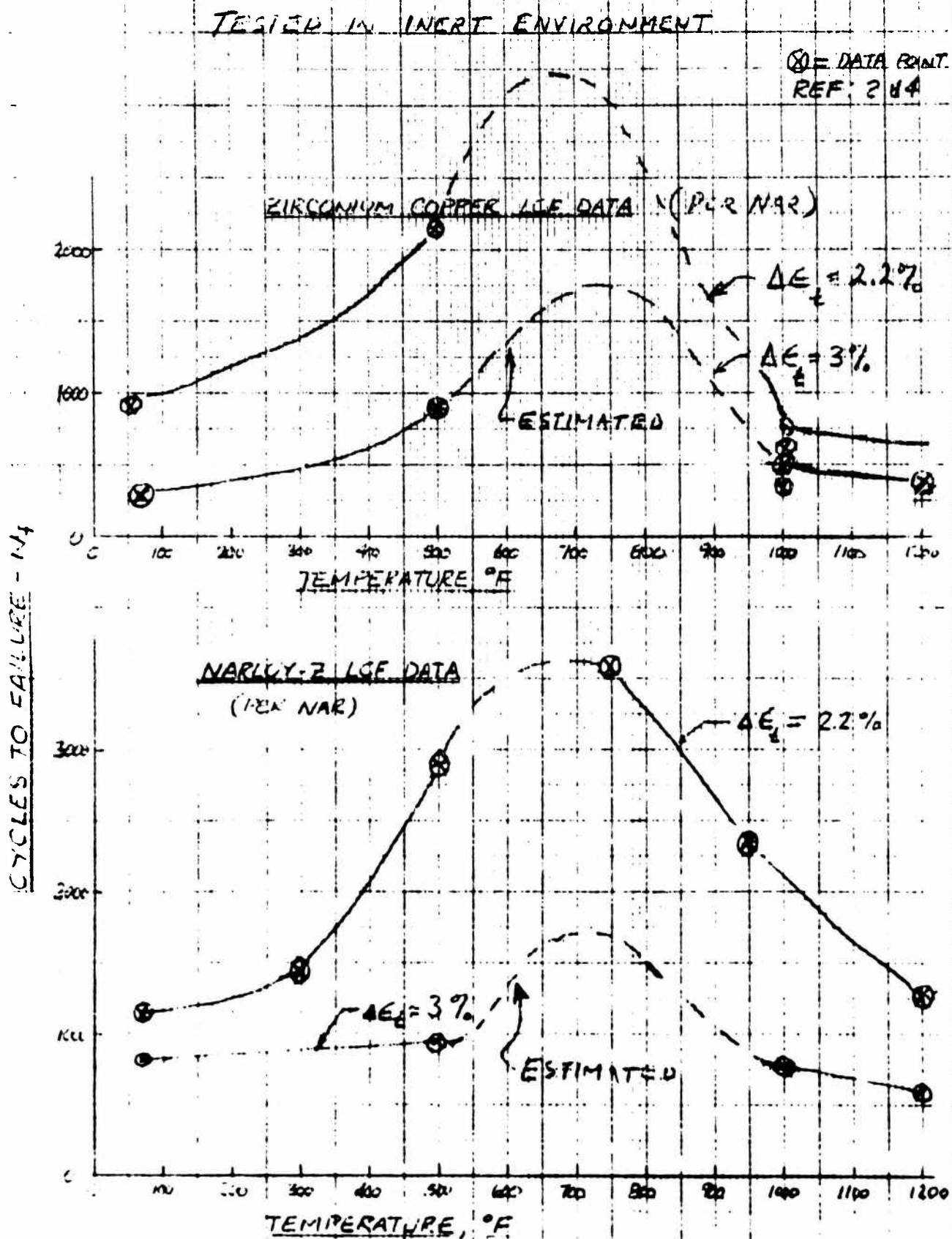


LEGEND:	
D -	70°F
L -	500°F
C -	1000°F
●	1000°F
NAR DATA	
INERT ENVIR	
ALRC DATA	
IN AIR	

Δε, TOTAL STRAIN RANGE, %

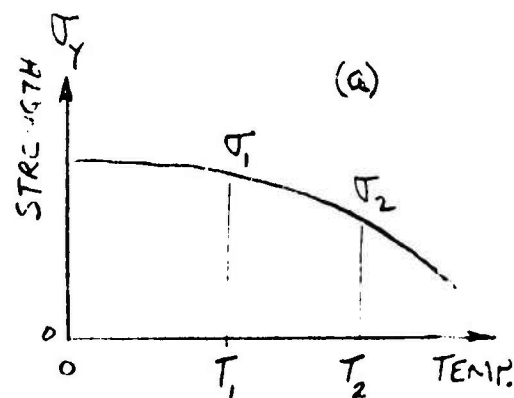
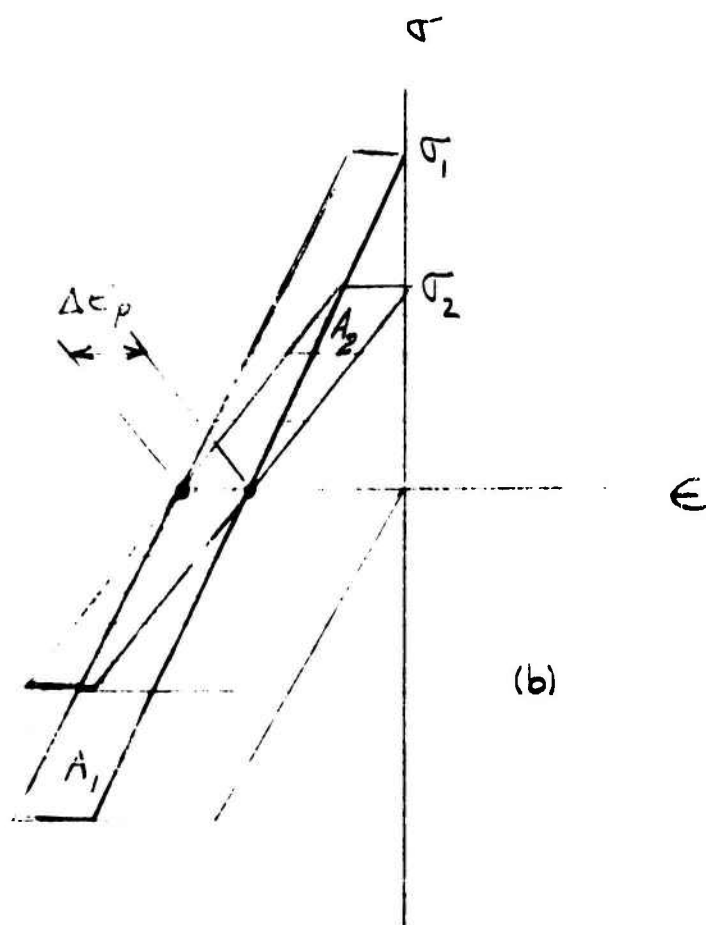
C-308

FIGURE 12 - VARIATION OF LIFE WITH TEMPERATURE FOR COPPER ALLOYS  
(NO HOLD TIME)





# FIG. 13 COMPARISON OF LCF AT ELEVATED TEMPERATURES



$$N_f \propto \frac{1}{\Delta W}, \quad N_f = \text{CYCLES TO FAILURE}$$

$$\Delta W = \text{HYSTERESIS ENERGY}$$

$\Delta W \propto A$ , AREA UNDER HYSTERESIS OF STRESS-STRAIN CURVE

$$A = \Delta \sigma \cdot \Delta \epsilon_p$$

$$\Delta W_1 \propto 2\sigma_1 \cdot \Delta \epsilon_p$$

$$\Delta W_2 \propto 2\sigma_2 \cdot \Delta \epsilon_p$$

$$\left. \begin{array}{l} \Delta W_1 \propto 2\sigma_1 \cdot \Delta \epsilon_p \\ \Delta W_2 \propto 2\sigma_2 \cdot \Delta \epsilon_p \end{array} \right\} \therefore N_{f1} = \left( \frac{\sigma_2}{\sigma_1} \right) N_{f2}$$

THUS, WITH ABSENCE OF OXIDATION AND CREEP DAMAGE AT

HIGH TEMPERATURE THE CYCLIC LIFE FOR A GIVEN STRAIN RANGE

WILL BE THE LONGEST FOR THE HIGHEST TEMPERATURE AT

WHICH THE STRESS RANGE IS SIGNIFICANTLY LOWERED.

FIGURE 14

LCF TRENDS FOR NARLOY IN INERT ENVIRONMENT

TYPICAL VALUES BASED ON DISCRETE TEST SPECIMEN DATA WITH INTERPOLATIONS AND EXTRAPOLATIONS. SCATTER FACTOR OF 4 SHOULD

BE APPLIED TO CURVE VALUES FOR PREDICTING LOWER BOUND VALUES

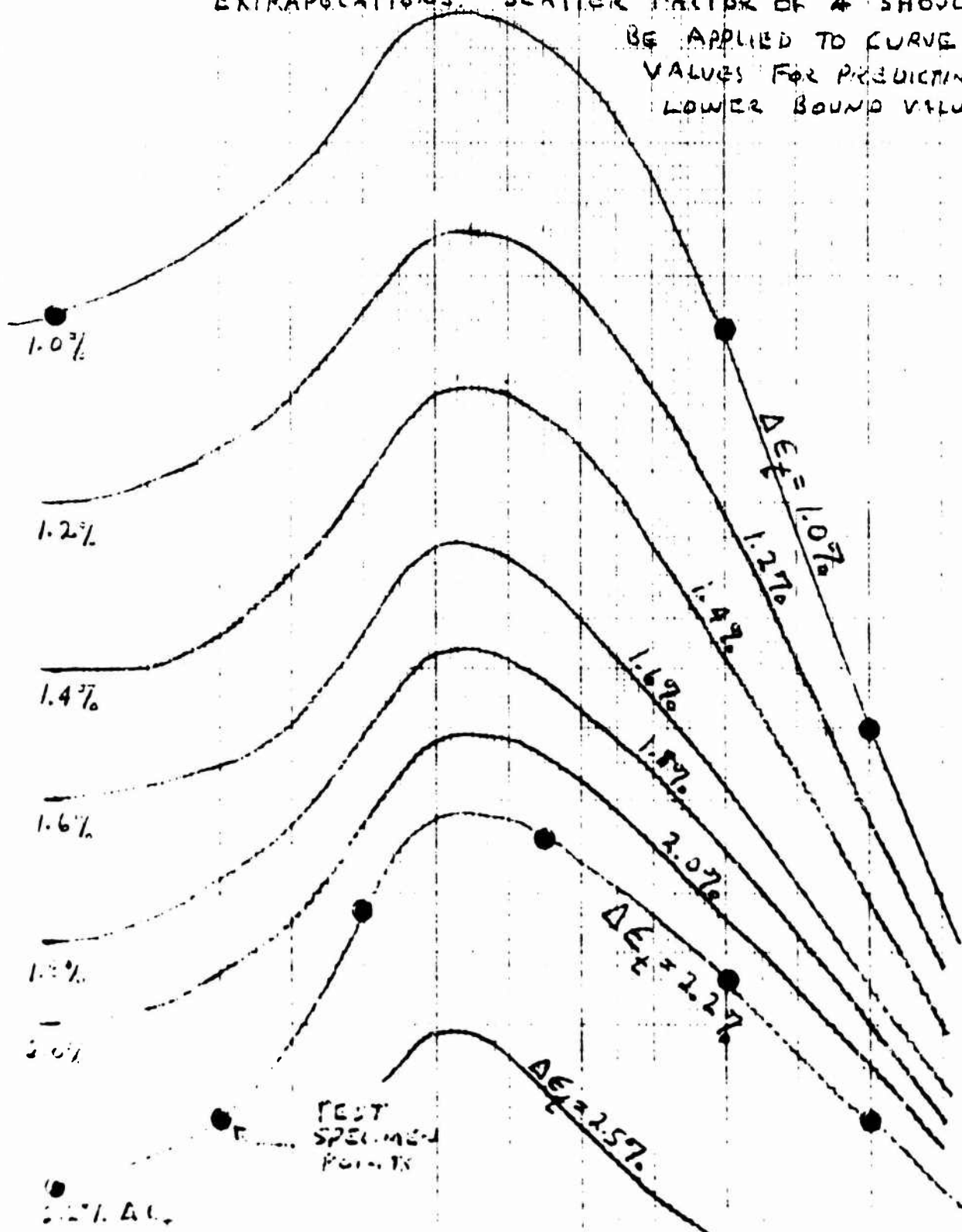


FIGURE 15

# LCF TRENDS FOR ZIRCONIUM COPPER IN INERT ENVIRONMENT

FOR ESTIMATING LOWER BOUND  
DATA A SCATTER FACTOR OF  
FOUR SHOULD BE APPLIED TO  
CURVE VALUES.

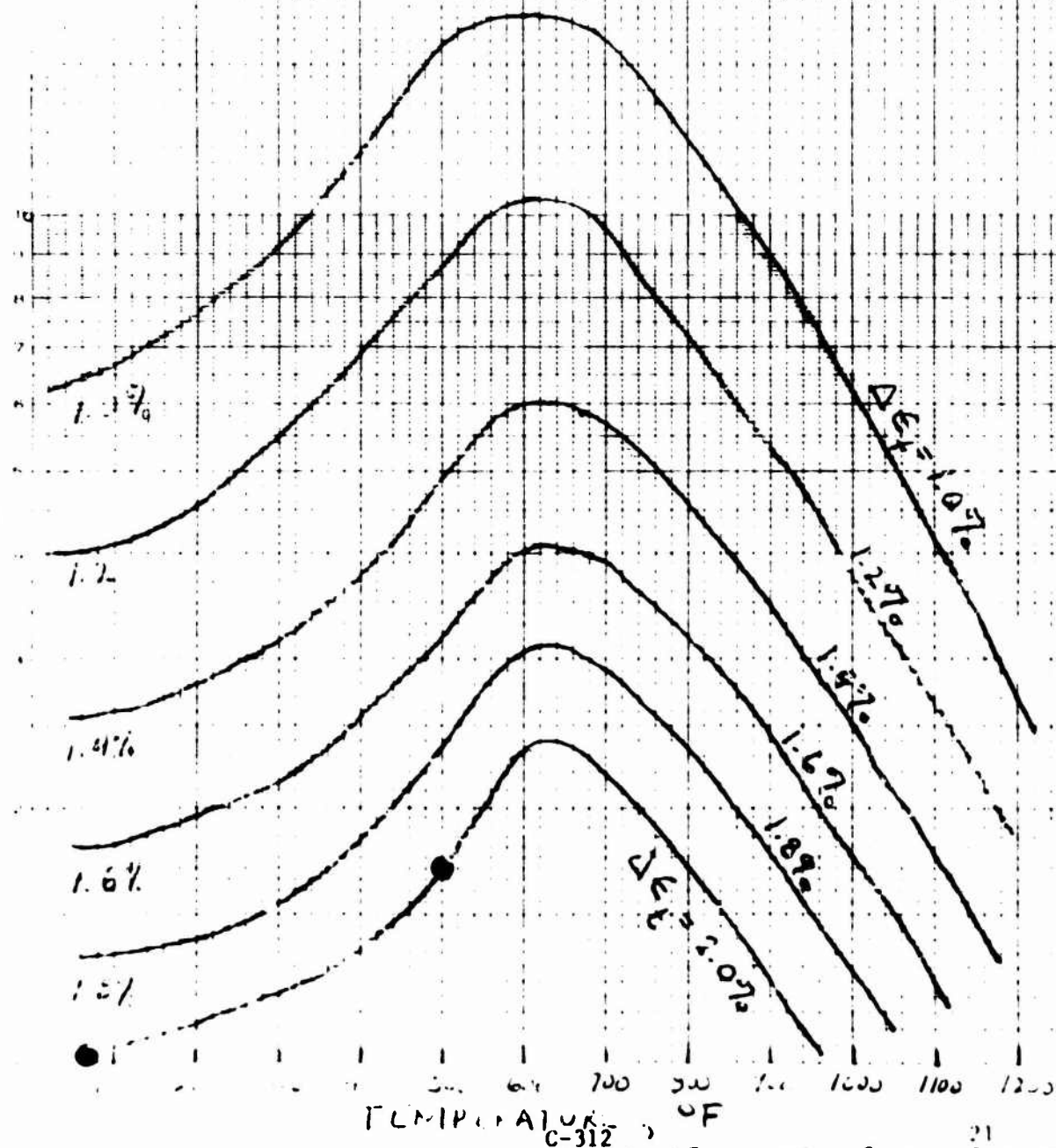
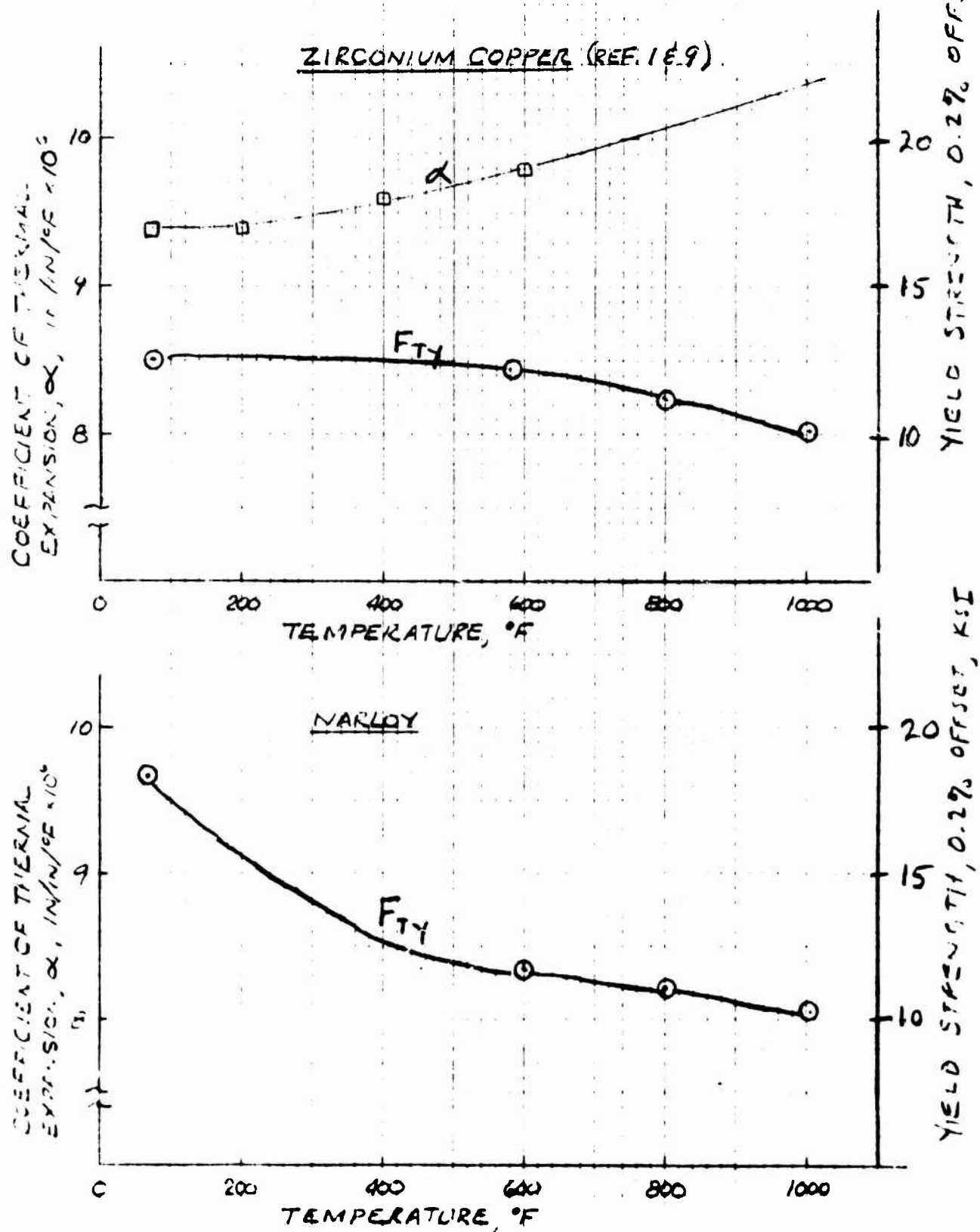


FIGURE 16- COPPER MATERIAL PROPERTIES



00S ENGINE DESIGN STUDY = 10K IN LINE ENGINE DESIGN

$P_c = 1250$  psia      MR = 6.0       $\epsilon = 356:1$       NPSH (H) = 60 F/160

I.	Thrust Chamber	Weight (lb)	% Weight
A.	Injector	12.40	
B.	Copper Thrust Chamber	23.60	
C.	Regen Tubes to $\epsilon = 356$	64.0	
D.	Igniter	12.1	50.1
II.	TPA's		
A.	Pumps, Boost Pumps and Gearbox	48.30	21.6
III.	Valves	27.20	12.20
IV.	Gas and Liquid Lines	9.70	4.30
V.	Preburner	18.70	3.40
VI.	Gimbal Assbl. and Support	7.50	3.4
	Total Calculated Weight, lb	223.5	100.0%
	Estimated Harness, Instr.		
	Support Brackets and Attach Hrdw	29.0	
	Estimated Engine Controller	35.0	

**Appendix D**

**MATERIALS**

## Combustion Components - Materials List

### Preburner

Oxidizer and Fuel Inlet Manifolds	ARMCO 22-13-5
Injector Housing	ARMCO 22-13-5
Injector Platelets	Nickel 200
Regen. Tubes	ARMCO 22-13-5

### Main Injector

FRHG Manifold and Body	ARMCO 22-13-5
Distribution Vanes	
Injector Vanes	OFHC Copper
Oxidizer Torus	ARMCO 22-13-5

### Main Combustion Chamber

Liner	Zirconium Copper
Wire Wrap	ARMCO 22-13-5
Support Cone	Inconel 718
Manifolds	ARMCO 22-13-5

### Cooled Nozzle

Tube Assembly	ARMCO 22-13-5
Manifolds	ARMCO 22-13-5

### Nozzle Extension (Alternate Concept)

	AGCarb-101
--	------------

#### Preburner - Materials

ARMCO 22-13-5, a high strength, austenitic stainless steel, has been selected as the material for the preburner assembly except for the injector face where Nickel 200 is used. ARMCO 22-13-5 was selected in preference to the higher strength, nickel base alloy, Inconel 718 due to its resistance to hydrogen embrittlement and in preference to the higher strength, embrittlement immune A-286 stainless steel due to its superior welding and brazing characteristics. The preburner fuel circuit temperature is well within the effective embrittlement temperature range.

In addition to its resistance to hydrogen embrittlement, ARMCO 22-13-5, also meets the preburner design requirements of excellent ductility and fabricability. Ductility is particularly important in the regeneratively cooled chamber which is low cycle fatigue limited. Low cycle fatigue tests conducted at ALRC on ARMCO 22-13-5 indicated that its cycle life is equivalent to that of the lower strength 300 series austenitic stainless steels and will provide the life requirements of the OOS engine.

Nickel 200 is selected as the injector material on the basis of its high thermal conductivity which is required to reduce face temperatures to within acceptable limits. Although Nickel 200 is susceptible to hydrogen embrittlement, it retains approximately 60% of its ductility in high pressure gaseous hydrogen as determined by tensile testing at ALRC. The material possesses adequate ductility since this application is tensile rather than low cycle fatigue limited due to the low temperature gradients across the thickness of the injector face. Nickel 200 possesses excellent fabrication characteristics and can readily be joined to the stainless steel portions of this assembly.



### Main Injector - Materials

ARMCO 22-13-5 stainless steel is selected as the main injector body-manifold assembly while 304L stainless steel and OFHC copper are selected as the materials for a composite vane assembly. ARMCO 22-13-5 was selected for its high strength, (typical yield strength - 70 ksi) fabricability, good low temperature ductility and resistance to hydrogen embrittlement and low thermal conductivity. The low temperature ductility is required for the body-manifold assembly which is exposed to liquid oxygen. Resistance to hydrogen embrittlement is required where the injector body comes in contact with the hydrogen rich turbine exhaust gas. Testing of alloys in high pressure gas simulating that of the turbine exhaust has been conducted at ALRC and the results indicated that the water vapor content of the hydrogen rich gas does not inhibit embrittlement. This testing also led to the selection of hydrogen embrittlement resistant 304L stainless steel and OFHC copper for the injector vanes which are exposed externally to the hydrogen rich gas.

The vane internal environment is high pressure oxygen at temperatures ranging from cryogenic at the inlet to ambient temperatures at the tip. The vane materials possess excellent ductility over the full service temperature range. OFHC copper is used for the injection vane because its high thermal conductivity enhances heat transfer through and within the vane. As a result, the thermally induced strains are minimized, and the injector is an efficient FRHG/oxidizer heat exchanger. OFHC copper is used in preference to the higher strength zirconium copper used for the injector vanes since the latter alloy places a restriction on the maximum brazing or bonding temperature that may be used in vane fabrication, and the former alloy possesses adequate strength. The oxygen distribution vanes are fabricated of 304L stainless steel; they form thermal resistances between the oxygen inlet manifold and warmer injector

### Main Combustion Chamber - Materials

The combustion chamber liner will be fabricated from oxygen free (0.001%  $O_2$  max.) zirconium copper. A copper alloy is required since the heat flux obtained in the chamber requires the use of materials of the highest thermal conductivity to prevent burn-through of the hot gas liner. Copper and its alloys are not subject to hydrogen embrittlement by the hydrogen within the chamber coolant passages. Zirconium copper is selected over other candidate alloys as the result of an extensive IR&D material test program conducted at ALRC. Since the main combustion chamber life is governed by low cycle fatigue, special emphasis was given to this type of testing. Tensile, creep and thermal conductivity tests were also conducted on the candidate copper alloys to provide needed design data. Zirconium copper provided the highest low cycle fatigue life of the alloys tested with the least sacrifice in thermal conductivity.

The brazing alloy selected for the attachment of the channel closures is a silver base alloy consisting of 65% Ag - 15 Pd and 20% Cu (Palcusil 15). The selection of this alloy was based on its excellent brazing characteristics with respect to copper alloys and its brazing temperature of 1650°F is compatible with the zirconium-copper base material. Other alloys considered for brazing of the channel closures were the gold brazing alloy (Nicoro 80) and electroless nickel. The gold alloys was not selected because it required a high brazing temperature (1750°F), which is not compatible with the zirconium copper base metal. Electroless nickel brazing alloy is selected as a back-up alloy for the Palcusil 15 since it can be readily preplaced by plating on the channel closures and minimize the risk of plugging. However electroless nickel does have the disadvantage of a high brazing temperature 1750°F. Also, joints fabricated with electroless nickel are prone to brittle nickel-phosphorous layers in the joint unless sufficient time is allowed for diffusion.

The chamber wire wrap and outlet manifold material is ARMCO 22-13-5, a high strength austenitic stainless steel. This material is selected for the manifolds primarily for its resistance to hydrogen embrittlement. It also possesses both excellent fabrication characteristics and ductility over the service temperature range. ARMCO 22-13-5 is selected as the wire wrap material since it is unique in retaining the highest strength of the non heat treatable materials after the braze cycle which joins it to the copper chamber. It also matches the coefficient of expansion of zirconium copper which is required to maintain joint contact during the brazing process.

Inconel 718 is selected as the support core on the basis of strength and fabricability characteristics. Its use is not restricted by compatibility with hydrogen in this application. Inconel 718 will be aged prior to joining to the ARMCO 22-13-5 members, since exposure the latter alloy to the thermal cycle will drastically lower its low temperature ductility.

### Cooled Nozzle - Materials

The cooled nozzle is a brazed tubular assembly whose service environment consists of exposure to high pressure hydrogen internally and exposure to propellant combustion products externally. The primary criteria for material selection are brazeability and resistance to hydrogen embrittlement. The latter requirement results from the thermal gradient within the coolant tubes which impose a localized service environment of room temperature, high pressure gaseous hydrogen, a condition for maximum embrittlement. ARMCO 22-13-5 stainless steel is selected as the tube material. Its strength is intermediate between the other embrittlement resistant candidate alloys, 347 and A-286 stainless steels, and is adequate for the nozzle. The use of the higher strength A-286 would impose additional special processing techniques due to its poor brazeability. ARMCO 22-13-5 possesses excellent brazing characteristics. Braze wet and flow studies performed at ALRC have shown its brazing characteristics are similar to those of 347 stainless steel. The hydrogen inlet manifold material is ARMCO 22-13-5 because of its strength, brazing and embrittlement characteristics.

#### Nozzle Extension - Materials

The nozzle extension material used in the alternate nozzle design is AGCarb-101, a fiber reinforced graphite composite. AGCarb is one of a relatively new class of high temperature composite materials formed from approximately 66% high strength graphite fibers bonded together with a graphite matrix. The latter is formed from the carbonization and graphitization of a special carbon-filled phenyl-aldehyde condensation resin and cool tar pitch. The strength of fibrous reinforced graphite composites typified by AGCarb-101 is two to five times the strength of normal missile grades of graphite. As with the bulk graphites, strength increases with increasing temperature to 5000°F. On a strength to weight ratio basis, AGCarb 101 offers a distinct advantage over the refractory metals at the nozzle operating temperature.

Several ALRC test programs have demonstrated that AGCarb possesses excellent resistance to thermal and mechanical shock. The corrosion rate of AGCarb in oxygen-hydrogen combustion products has been found to be negligible in nozzle extension environments when used properly.